My beautiful dissertation

My Name

January 28, 2022

Thesis submitted for the degree of
Doctor of Philosophy
in
Applied Mathematics
at The University of Adelaide
Faculty of Engineering, Computer and Mathematical Sciences
School of Mathematical Sciences

THE UNIVERSITY
of ADELAIDE

Contents

List of Tables

List of Figures

Signed Statement

I certify that this work contains no material which has been accepted for the award of any other degree or diploma in my name in any university or other tertiary institution and, to the best of my knowledge and belief, contains no material previously published or written by another person, except where due reference has been made in the text. In addition, I certify that no part of this work will, in the future, be used in a submission in my name for any other degree or diploma in any university or other tertiary institution without the prior approval of the University of Adelaide and where applicable, any partner institution responsible for the joint award of this degree.

I give consent to this copy of my thesis, when deposited in the University Library, being made available for loan and photocopying, subject to the provisions of the Copyright Act 1968.

I also give permission for the digital version of my thesis to be made available on the web, via the University's digital research repository, the Library Search and also through web search engines, unless permission has been granted by the University to restrict access for a period of time.

Signed: ..... Date: .....

Acknowledgements

Dedication

Abstract

Chapter 1 introduces

Chapter 1

Introduction & Preliminaries

A fluid queue is a two-dimensional stochastic process $\{\boldsymbol{X}(t)\} = \{(X(t), \varphi(t))\}_{t\geq 0}$. The phase process, also known as the driving process, $\{\varphi(t)\}_{t\geq 0}$, is a continuous-time Markov chain (CTMC). The level process, $\{X(t)\}_{t\geq 0}$, is a real-valued, continuous, and piecewise linear.

Stochastic fluid queues have found a variety of applications such as telecommunications (see Anick et al. (1982) as a canonical application in this area), power systems (Bean et al. 2010), risk processes (Badescu et al. 2005) and environmental modelling (Wurm 2020). Fluid queues are relatively well studied. Largely, the analysis of fluid queues falls into two categories, matrix-analytic methods (Ahn et al. 20035, Ahn & Ramaswami 2003, 2004, Bean et al. 2005*a*,*b*, 2009*a*,*b*, da Silva Soares 2005, Latouche & Nguyen 2019), and differential equation-based methods (Anick et al. 1982, Karandikar & Kulkarni 1995, Bean, Lewis, Nguyen, O'Reilly & Sunkara 2021).

More recently, Bean & O'Reilly (2014) extended fluid queues to *so-called* stochastic fluid-fluid queues. In a fluid-fluid queue there is a second level process, $\{Y(t)\}_{t\geq 0}$ which is itself driven by a fluid queue, $\{(X(t), \varphi(t))\}_{t\geq 0}$. The analysis, (Bean & O'Reilly 2014), is in principal similar to the matrix-analytic methods of (Bean et al. 2005*b*), and derives results about the second level process $\{Y(t)\}_{t\geq 0}$ in terms of the infinitesimal generator (a differential operator) of the fluid queue, $\{(X(t), \varphi(t))\}_{t\geq 0}$. For practical computation of the results of Bean & O'Reilly (2014), a matrix-discretisation of the infinitesimal generator of the fluid queue can be used. To this end, to date, two possible discretisation have been suggested. Taking a differential equations-based approach, Bean, Lewis, Nguyen, O'Reilly & Sunkara (2021) use the discontinuous Galerkin (DG) method to discretise this operator, while Bean & O'Reilly (2013) take a stochastic modelling and matrix-analytic methods approach to approximate the fluid-queue by a quasi-birth-and-death (QBD) process. Both approaches are insightful and offer different tools and perspectives with which to analyse the resulting approximations. It turns out that the latter approach is a sub-class of the former; the QBD can be viewed as the simplest DG scheme where the operator is projected onto a basis of piecewise constant functions.

In the context of approximating fluid queues, one advantage of the QBD discretisation and, equivalently, DG schemes with constant basis functions, is that they guarantee probabilities computed from the approximation are positive (Koltai 2011, Section 3.3), see also (Hesthaven & Warburton 2007) and references therein. One justification for the positivity preserving property is from the interpretation of the discretisation as a stochastic process thereby ensuring positivity. For higher order DG schemes there is no such interpretation. Moreover, higher-order DG approximation schemes may produce negative, or highly oscillatory solutions, particularly when discontinuities or steep gradients are present. Methods to navigate the problem of negative or highly oscillatory solutions have been developed, such as slope limiters, and filtering (see (Hesthaven & Warburton 2007, Section 6.5) and references therein). Slope limiting effectively alters the discretised operator in regions where oscillations are detected and lowers the order of the approximation in these regions. Filtering is a post-hoc method which looks to recover an accurate solution, given an oscillatory approximation.

1.1 Mathematical Preliminaries

1.1.1 Fluid queues

A fluid queue is a two-dimensional stochastic process $\{\boldsymbol{X}(t)\} = \{(X(t), \varphi(t))\}_{t\geq 0}$ where $\{\varphi(t)\}_{t\geq 0}$ is known as the phase or driving process, and $\{X(t)\}_{t\geq 0}$ is known as the level process or buffer. The phase process $\{\varphi(t)\}_{t\geq 0}$, is an irreducible continuous-time Markov chain (CTMC) with finite state space, which we we assume to be $\mathcal{S} = \{1, 2, \ldots, N\}$ without loss of generality, and infinitesimal generator $\boldsymbol{T} = [T_{ij}]_{i,j\in\mathcal{S}}$. We assume that $\boldsymbol{T}$ is *conservative*. Associated with states $i \in \mathcal{S}$ are real-valued *rates* $c_i \in \mathbb{R}$.

Partition the state space $\mathcal{S}$ into $\mathcal{S}_+ = \{i \in \mathcal{S} \mid c_i > 0\}$, $\mathcal{S}_- = \{i \in \mathcal{S} \mid c_i < 0\}$ and $\mathcal{S}_0 = \{i \in \mathcal{S} \mid c_i = 0\}$. We assume, without loss of generality, that the generator $\boldsymbol{T}$ is partitioned into sub-matrices

$$\boldsymbol{T} = \begin{bmatrix} \boldsymbol{T}_{++} & \boldsymbol{T}_{+-} & \boldsymbol{T}_{+0} \\ \boldsymbol{T}_{-+} & \boldsymbol{T}_{--} & \boldsymbol{T}_{-0} \\ \boldsymbol{T}_{0+} & \boldsymbol{T}_{0-} & \boldsymbol{T}_{00} \end{bmatrix},$$

where $\boldsymbol{T}_{mn} = [T_{ij}]_{i\in\mathcal{S}_m, j\in\mathcal{S}_n}$, $m, n \in \{+, -, 0\}$. Also define the diagonal matrices

$$\boldsymbol{C} = \begin{bmatrix} \boldsymbol{C}_+ & & \\ & \boldsymbol{C}_- & \\ & & \boldsymbol{0} \end{bmatrix}, \qquad \boldsymbol{C}_+ = diag(c_i, i \in \mathcal{S}_+), \qquad \boldsymbol{C}_- = diag(|c_i|, i \in \mathcal{S}_-),$$

where $diag(a_i, i \in \mathcal{I})$ denotes a diagonal matrix with entries a_i down the diagonal.

When no boundary conditions are imposed, the level process is given by

$$X(t) = X(0) + \int_{s=0}^{t} c_{\varphi(s)}\,\mathrm{d}s.$$

Sample paths of $\{X(t)\}$ are continuous and piecewise linear, with $\dfrac{\mathrm{d}}{\mathrm{d}t}X(t) = c_{\varphi}(t)$, when $X(t)$ is differentiable. Given sample paths of $\{\varphi(t)\}$, then $\{X(t)\}$ is deterministic, and in this sense, $\{\varphi(t)\}$ is the only stochastic element of the fluid queue.

Often, boundary conditions are imposed. Here, we consider a mixture of *regulated* and *reflecting* boundary conditions. Upon hitting a boundary we suppose that, with probability p_{ij}, $i, j \in \mathcal{S}$, the phase process instantaneously transitions from phase i to phase j (note that we might have $i = j$ i.e. no transition). At a lower boundary, if $j \in \mathcal{S}_0 \cup \mathcal{S}_-$, then $\dfrac{\mathrm{d}}{\mathrm{d}t}X(t) = 0$, and the phase process continues to evolve according to the sub-generator

$$\begin{bmatrix} \boldsymbol{T}_{--} & \boldsymbol{T}_{-0} \\ \boldsymbol{T}_{0-} & \boldsymbol{T}_{00} \end{bmatrix},$$

until such a time that $\varphi(t)$ transitions to a phase $k \in \mathcal{S}_+$, at which time $X(t)$ leaves the boundary. Similarly, at an upper boundary if $j \in \mathcal{S}_0 \cup \mathcal{S}_+$, then $\dfrac{\mathrm{d}}{\mathrm{d}t}X(t) = 0$ and the phase process continues to evolve according to the sub-generator

$$\begin{bmatrix} \boldsymbol{T}_{++} & \boldsymbol{T}_{+0} \\ \boldsymbol{T}_{0+} & \boldsymbol{T}_{00} \end{bmatrix},$$

until such a time that $\varphi(t)$ transitions to a phase $k \in \mathcal{S}_-$ at which time $X(t)$ leaves the boundary. Without loss of generality, we assume the lower and upper boundaries (when present) are at $x = 0$ and $x = M > 0$, respectively.

In summary, the evolution of the level can be expressed as

$$\frac{\mathrm{d}}{\mathrm{d}t}X(t) = \begin{cases} c_{\varphi(t)}, & \text{if } X(t) > 0, \\ \max\{0, c_{\varphi(t)}\}, & \text{if } X(t) = 0, \\ \min\{0, c_{\varphi(t)}\}, & \text{if } X(t) = M. \end{cases}$$

Let $\boldsymbol{f}(x,t) = \big[f_i(x,t)\big]_{i\in\mathcal{S}}$ be a row-vector function where $f_i(x,t)$ is the density of $\mathbb{P}(X(t) \le x, \varphi(t) = i)$, assuming it exists. When a differentiable density exists, the system of partial differential equation which describes the evolution of the densities $\boldsymbol{f}(x,t)$ is

$$\frac{\partial}{\partial t}\boldsymbol{f}(x,t) = \boldsymbol{f}(x,t)\boldsymbol{T} - \frac{\partial}{\partial x}\boldsymbol{f}(x,t)\boldsymbol{C}. \tag{1.1}$$

The initial condition is the initial distribution of the fluid queue, $f_i(x,0)$. Often a differentiable density function does not exist and therefore the partial differential equation

(1.1) is not well-defined. For example, for a fluid queue with a regulated boundary, if the initial distribution of the fluid queue is a point mass at any point $x_0 \geq 0$ and in phase $i \in \mathcal{S}_+ \cup \mathcal{S}_0$, then a density function $f_i(x,t)$ will not exist for any finite t. Specifically, a point mass will persist along the ray $x_0 + c_i t$, $t \geq 0$. In such situations, it is the *weak solution* to (1.1) that we seek. A weak solution satisfies

$$-\int_x \int_t \boldsymbol{f}(x,t) \frac{\partial}{\partial t} \boldsymbol{\psi}(x,t) \,\mathrm{d}t \,\mathrm{d}x = \int_x \int_t \boldsymbol{f}(x,t) \boldsymbol{T} \boldsymbol{\psi}(x,t) \,\mathrm{d}t \,\mathrm{d}x + \int_x \int_t \boldsymbol{f}(x,t) \boldsymbol{C} \frac{\partial}{\partial x} \boldsymbol{\psi}(x,t) \,\mathrm{d}t \,\mathrm{d}x, \tag{1.2}$$

for every vector of test functions, $\boldsymbol{\psi}(x,t)$, wich are smooth and have compact support.

Boundary conditions may also be imposed on (1.1).

Discretisation methods approximate the operator on the right-hand side of (1.1) by a matrix, in our case, by the generator of a QBD-RAP.

1.1.2 Fluid-fluid Queues

This subsection has been taken from Sections 2 and 3 of Bean et al. (2022) with only minor changes, such as notations, so that this chapter is consistent with the rest of the thesis. I am a co-author of the paper Bean et al. (2022). The conceptualisation of Bean et al. (2022) was originally by Vikram Sunkara, Nigel Bean and Giang Nguyen, and the original coding was done by Vikram Sunkara. I made significant contributions to Section 3 of the paper, expressing the operator-theoretic expressions to use the same partition as the approximation scheme. I contributed Sections 4.4 and 5.1. I extended the numerical experiments in Section 6 to higher orders and made all the plots in Section 6. Appendix A is also my original work. I did a significant proportion of the writing of the manuscript and addressed the reviewers comments and also developed code for the numerical experiments.

An unbounded stochastic fluid-fluid model (SFFM) is a Markov process $\{(\widehat{X}_t, \widehat{Y}_t, \varphi(t)), t \geq 0\}$, where the phase $\{\varphi(t)\}$ is a continuous-time Markov chain on a finite state space $\mathcal{S}$; $\{\widehat{X}_t\}$ is the first fluid, which varies linearly at rate $c_{\varphi(t)}$

$$\widehat{X}(t) := \widehat{X}(0) + \int_0^t c_{\varphi(s)} \,\mathrm{d}s;$$

and $\widehat{Y}_t$ is the second fluid, which varies at rate $r_{\varphi(t)}(\widehat{X}_t)$:

$$\widehat{Y}_t := \widehat{Y}(0)) + \int_0^t r_{\varphi(s)}(\widehat{X}_s) \,\mathrm{d}s.$$

Regulated boundaries may also be included for both fluids. To distinguish between unbounded and bounded processes, we use the notations $\widehat{X}(t)$ and $\widehat{Y}(t)$ to denote unbounded processes, and $X(t)$ and $Y(t)$ to denote fluid levels with a regulated lower boundary at 0.

As classic fluid processes, $\{(\widehat{X}(t), \varphi(t)), t \geq 0\}$, or unbounded analogues, are used extensively in many areas, such as insurance and environmental modelling, it is clear that stochastic fluid-fluid models have an even wider range of applicability.

We assume that $X(t), Y(t) \in [0, \infty)$ and that there is a regulated boundary at level 0 for both buffers:

$$\frac{\mathrm{d}}{\mathrm{d}t}X(t) := \max\{0, c_i\} \quad \text{if } X(t) = 0 \text{ and } \varphi(t) = i,$$
$$\frac{\mathrm{d}}{\mathrm{d}t}Y(t) := \max\{0, r_i(x)\} \quad \text{if } Y(t) = 0,\ X(t) = x \text{ and } \varphi(t) = i,$$

for $i \in \mathcal{S} = \{1, ..., N_{\mathcal{S}}\}$. Let T be the irreducible generator for the finite-state Markov chain $\{\varphi(t)\}$. We denote by $\boldsymbol{R}(x) := \mathrm{diag}(r_i(x))_{i\in\mathcal{S}}$ the diagonal fluid-rate matrix of functions for $\{Y(t)\}$.

Remark 1.1 (Notation)**.** *For future reference we require some notation regarding the elements of the model introduced above. We use the notation $\boldsymbol{u} = (u_h)_{h\in\mathcal{H}}$ to denote a row-vector, $\boldsymbol{u}$, defined by its elements, u_h, indexed by $h \in \mathcal{H}$, where $\mathcal{H}$ is some countable index set. Similarly, $\boldsymbol{u} = (\boldsymbol{u}_h)_{h\in\mathcal{H}}$, is a row-vector defined by a collection of row-vectors $\boldsymbol{u}_h$. The notation $\boldsymbol{u}_m = (u_h)_{h\in\mathcal{H}_m}$ refers to the vector containing the subset of elements corresponding to $\mathcal{H}_m \subseteq \mathcal{H}$. When the index set is empty, the resulting vector $\boldsymbol{u}_m$ is a vector of dimension 0. In cases when there are two indices, we order the elements of the vector according to the first index, then the second; i.e. $\boldsymbol{u} = (u_g^h)_{g\in\mathcal{G},h\in\mathcal{H}} = ((u_g^h)_{g\in\mathcal{G}})_{h\in\mathcal{H}}$. Here we use the convention that for a vector $\boldsymbol{u} = (u)_{h\in\mathcal{H}}$ where the elements u do not depend on the index h and H is some index set, then we repeat u h-times; i.e. $\boldsymbol{u} = (u)_{h\in\mathcal{H}} = \underbrace{(u, \ldots, u)}_{h-times}$. The notation $\boldsymbol{U} = [u_{gh}]_{g\in\mathcal{G},h\in\mathcal{H}}$ is used to denote a matrix defined by its elements, or sub-blocks, u_{gh}.*

Let $\mathcal{S}_- = \{i \in \mathcal{S} \mid c_i < 0\}$, $\mathcal{S}_+ = \{i \in \mathcal{S} \mid c_i > 0\}$, $\mathcal{S}_0 = \{i \in \mathcal{S} \mid c_i = 0\}$, $\mathcal{S}_\nabla = \{i \in \mathcal{S} \mid c_i \leq 0\}$, $\mathcal{S}_\Delta = \{i \in \mathcal{S} \mid c_i \geq 0\}$.

For the remainder of this section, we summarise the findings of (Bean & O'Reilly 2014) on the joint stationary distribution of $\{(X(t), Y(t), \varphi(t)), t \geq 0\}$. For each Markovian state $i \in \mathcal{S}$, we partition the state space of $X(t)$, $[0, \infty)$, according to the rates of change $r_i(\cdot)$ for the second fluid $\{Y(t)\}$: $[0, \infty) := \mathcal{F}_i^+ \cup \mathcal{F}_i^- \cup \mathcal{F}_i^0$, where

$$\mathcal{F}_i^+ := \{u \in \mathcal{F} : r_i(u) > 0\},\ \mathcal{F}_i^- := \{u \in \mathcal{F} : r_i(u) < 0\},\ \mathcal{F}_i^0 := \{u \in \mathcal{F} : r_i(u) = 0\}. \tag{1.3}$$

For all $i \in \mathcal{S}$, the functions $r_i(\cdot)$ are assumed to be sufficiently well-behaved that $\mathcal{F}_i^m$, $m \in \{+, -, 0\}$, is a finite union of intervals and isolated points.

We assume that the process $\{(X(t), Y(t), \varphi(t)), t \geq 0\}$ is positive recurrent, in order to guarantee the existence of the joint stationary density. Define stationary operators

$$\overline{\pi}_i(y)(\mathcal{A}) := \lim_{t\to\infty} \frac{\partial}{\partial y} \mathbb{P}\left(X(t) \in \mathcal{A}, Y(t) \leq y, \varphi(t) = i\right), \quad y > 0, \tag{1.4}$$

$$\overline{\mathbb{p}}_i(\mathcal{A}) := \lim_{t\to\infty} \mathbb{P}(X(t) \in \mathcal{A}, Y(t) = 0, \varphi(t) = i]), \tag{1.5}$$

where $\mathcal{A} \subset [0, \infty)$. Then let $\overline{\pi}(y) = (\overline{\pi}_i(y))_{i\in\mathcal{S}}$ be a vector containing the joint stationary density operators and $\overline{\mathbb{p}} = (\overline{\mathbb{p}}_i)_{i\in\mathcal{S}}$ a vector containing the joint stationary mass operators.

The determination of $\overline{\pi}(y)$ involves two important matrices of operators, $\overline{\mathbb{B}}$ and $\overline{\Psi}$. The operator $\overline{\mathbb{B}}$ is the *infinitesimal generator* of the process $\{(X(t), \varphi(t))\}$. The operator $\overline{\Psi}$ is such that $\boldsymbol{\mu}\overline{\Psi}(\mathcal{A})$ is the conditional probability of $\{Y(t)\}$ returning to level zero and doing so when $X(t) \in \mathcal{A}$, given that the initial distribution is $\boldsymbol{\mu}$.

Matrix $\overline{\mathbb{B}}$ of Operators

Since $\{(X(t), \varphi(t)), t \geq 0\}$ is a Markov process, the evolution of probability can be described by a semigroup. Let $\mathcal{M}(\mathcal{S} \times \mathbb{R}_+)$ be the set of integrable complex-valued Borel measures on the Borel σ-algebra $\mathcal{B}_{\mathcal{S}\times\mathbb{R}_+}$. For $\boldsymbol{\mu} \in \mathcal{M}(\mathcal{S} \times \mathbb{R}_+)$, we can write $\boldsymbol{\mu} = (\mu_i)_{i\in\mathcal{S}}$. The measures $\mu_i(\cdot)$ represent an initial distribution, $\mu_i(\cdot) = \mathbb{P}(X(0)) \in \cdot, \varphi(0) = i)$. Let $\{\overline{\mathbb{V}}(t)\}_{t\geq 0}$, $\overline{\mathbb{V}}(t) : \mathcal{M}(\mathcal{S} \times \mathbb{R}_+) \mapsto \mathcal{M}(\mathcal{S} \times \mathbb{R}_+)$ be the semigroup describing the evolution of probability for $\{(X(t), \varphi(t)), t \geq 0\}$ structured as a matrix of operators, $\left[\overline{\mathbb{V}}(t)\right]_{ij} = \overline{\mathbb{V}}_{ij}(t)$ where,

$$\mu_i\overline{\mathbb{V}}_{ij}(t)(\mathcal{A}) = \int_{x\in[0,\infty)} \mathrm{d}\mu_i(x)\mathbb{P}(X(t) \in \mathcal{A}, \varphi(t) = j \mid X(0)) = x, \varphi(0) = i).$$

Intuitively, the operator $\overline{\mathbb{V}}(t)$ maps an initial measure $\boldsymbol{\mu}$ on $(X(0), \varphi(0))$ to the measure $\mathbb{P}(X(t) \in \mathcal{A}, \varphi(t) = j) =: \mu_j(t)(\mathcal{A})$. The matrix of operators $\overline{\mathbb{B}} := [\overline{\mathbb{B}}_{ij}]_{i,j\in\mathcal{S}}$ is the *infinitesimal generator* of the semigroup $\{\overline{\mathbb{V}}(t)\}$ defined by

$$\overline{\mathbb{B}} = \frac{\mathrm{d}}{\mathrm{d}t}\overline{\mathbb{V}}(t)\bigg|_{t=0},$$

with domain the set of measures for which this limit exists. Specifically, the domain of $\overline{\mathbb{B}}$ is the set of measures, $\boldsymbol{\mu} = (\mu_i)_{i\in\mathcal{S}}$, for which each μ_i admits an absolutely continuous density on $(0, \infty)$, and can have a point mass at 0 if $i \in \mathcal{S}_\nabla$; call this set of measures $\mathcal{M}_0$. That is, the measures μ_i, $i \in \mathcal{S}$, such that $(\mu_i)_{i\in\mathcal{S}} \in \mathcal{M}_0$ are absolutely continuous on $(0, \infty)$ and may have point masses at 0 if $i \in \mathcal{S}_\nabla$. The measure μ_i cannot have a point mass at 0 if $i \notin \mathcal{S}_\nabla$. In the sequel we write $v_i(x)$, $x > 0$, as the density of μ_i and q_i as the point mass of μ_i at $x = 0$ (if such a point mass exists).

To use the operators $\{\overline{\mathbb{V}}(t)\}$ and $\overline{\mathbb{B}}$ to analyse the fluid-fluid model, Bean & O'Reilly (2014) explicitly track when $(X(t), \varphi(t)) \in (\mathcal{F}_i^m, i)$ for $i \in \mathcal{S}$, $m \in \{+, -, 0\}$ by partitioning the operators $\overline{\mathbb{V}}(t)$ and $\overline{\mathbb{B}}$ into $\overline{\mathbb{V}}_{ij}^{mn}$ and $\overline{\mathbb{B}}_{ij}^{mn}$, for $i, j \in \mathcal{S}$, $m, n \in \{+, -, 0\}$, where

$$\mu_i|_{\mathcal{F}_i^m} \overline{\mathbb{V}}_{ij}^{mn}(t)(\mathcal{A}) := \int_{x \in [0,\infty)} \mathrm{d}\mu_i|_{\mathcal{F}_i^m}(x) \mathbb{P}(X(t) \in \mathcal{A} \cap \mathcal{F}_j^n, \varphi(t) = j \mid X(0) = x, \varphi(0) = i),$$

and $\mu_i|_E$ is the restriction of μ_i to E. Similarly, for $\overline{\mathbb{B}}_{ij}^{mn}$, $i, j \in \mathcal{S}$, $m, n \in \{+, -, 0\}$.

We claim that numerical schemes are needed to approximate the analytic operator equations introduced in Bean & O'Reilly (2014). The DG scheme we choose to use here works by first partitioning the state space of the fluid level, $\{X(t)\}$, into a collection of intervals, $\mathcal{D}_k = [x_k, x_{k+1}]$ then, on each interval, the operator $\overline{\mathbb{B}}$ is projected onto a basis of polynomials. So, to help elucidate the connection between the operators $\{\overline{\mathbb{V}}(t)\}$, $\overline{\mathbb{B}}$ and their DG approximation counterparts, we take a slightly different approach to partitioning these operators than that taken in Bean & O'Reilly (2014). Rather than partition according to the sets $\mathcal{F}_i^m$, $i \in \mathcal{S}$, $m \in \{+, -, 0\}$, we use the same partition as that in the construction of the DG scheme. By doing so, we can directly correspond elements of the partitioned operators to their approximation counterparts. Since the partition used to construct the DG scheme is finer, then we can always reconstruct the partition in terms of the sets $\mathcal{F}_i^m$, $i \in \mathcal{S}$, $m \in \{+, -, 0\}$.

Let us first partition the space $[0, \infty)$ into $\mathcal{D}_\nabla = \{0\}$, and non-trivial intervals $\mathcal{D}_k = [x_k, x_{k+1}] \setminus \{0\}$, with $x_1 = 0$, $x_k < x_{k+1}$, $k = 1, 2, \ldots$. The symbol ∇ is used to refer to sets and quantities which are relevant to boundary at $x = 0$. For $\boldsymbol{\mu} \in \mathcal{M}_0(\mathcal{S} \times \mathbb{R}_+)$ we write $\boldsymbol{\mu} = (\mu_i^k)_{i \in \mathcal{S}, k \in \{\nabla, 1, 2, \ldots\}}$, where $\mu_i^k(\cdot) = \mu_i(\cdot \cap \mathcal{D}_k)$, $k = \nabla, 1, 2, \ldots$. We also have densities, $v_i^k(x)$, $x > 0$, associated with each measure, μ_i^k. For $i, j \in \mathcal{S}$, $k, \ell \in \{\nabla, 1, 2, \ldots\}$ define the operators

$$\mu_i^k \mathbb{V}_{ij}^{k\ell}(t)(\mathcal{A}) := \int_{x \in \mathcal{D}_k} \mathrm{d}\mu_i^k(x) \mathbb{P}(X(t) \in \mathcal{A} \cap \mathcal{D}_\ell, \varphi(t) = j \mid X(0) = x, \varphi(0) = i),$$

and the matrices of operators $\mathbb{V}^{k\ell}(t) := \left[\mathbb{V}_{ij}^{k\ell}(t)\right]_{i,j \in \mathcal{S}}$, $k, \ell \in \{\nabla, 1, 2, \ldots\}$ and write

$$\mathbb{V}(t) = \begin{bmatrix} \mathbb{V}^{\nabla,\nabla}(t) & \mathbb{V}^{\nabla,1}(t) & \mathbb{V}^{\nabla,2}(t) & \ldots \\ \mathbb{V}^{1,\nabla}(t) & \mathbb{V}^{1,1}(t) & \mathbb{V}^{1,2}(t) & \ldots \\ \mathbb{V}^{2,\nabla}(t) & \mathbb{V}^{2,1}(t) & \mathbb{V}^{2,2}(t) & \ldots \\ \vdots & \vdots & \vdots & \ddots \end{bmatrix}.$$

Now define $\mathbb{B} = \dfrac{\mathrm{d}}{\mathrm{d}t}\mathbb{V}(t)\Big|_{t=0}$ as the infinitesimal generator of $\{\mathbb{V}(t)\}$, resulting in the

tridiagonal matrix of operators

$$\mathbb{B}(t) = \begin{bmatrix} \mathbb{B}^{\nabla,\nabla}(t) & \mathbb{B}^{\nabla,1}(t) & & \\ \mathbb{B}^{1,\nabla}(t) & \mathbb{B}^{1,1}(t) & \mathbb{B}^{1,2}(t) & \\ & \mathbb{B}^{2,1}(t) & \mathbb{B}^{2,2}(t) & \ddots \\ & & \ddots & \ddots \end{bmatrix},$$

where the blocks $\mathbb{B}^{k\ell} := \left[\mathbb{B}^{k\ell}_{ij}(t)\right]_{i,j\in\mathcal{S}}$, $k, \ell \in \{\nabla, 1, 2, \dots\}$. The tridiagonal structure arises since, for $|k-\ell| \geq 2$ (where we take $\nabla = 0$ if it appears in the differences) it is impossible for $\{X(t)\}$ to move from $\mathcal{D}_k$ to $\mathcal{D}_\ell$ in an infinitesimal amount of time.

Remark 1.2 (More notation)**.** *We use a blackboard bold font with an overline above the character (e.g. $\overline{\mathbb{B}}$ and $\overline{\mathbb{V}}(t)$) to represent theoretical operators derived in (Bean & O'Reilly 2014) which are constructed using the partition in (1.3). The operators denoted with an overline play a minor role in the introductory sections of this paper, but do not appear again. We use a blackboard font sans overline (e.g. $\mathbb{V}(t)$ and $\mathbb{B}$) to represent the same operators but which are constructed with the finer partition defined by $\mathcal{D}_k$, $k = \nabla, 1, 2, \dots$. We use the letters $i, j \in \mathcal{S}$ to represent states of the phase process, letters $m, n, \in \{+, -, 0\}$ to refer to the partition in terms of the sets in Equations (1.3), and the letters $k, \ell \in \{\nabla, 1, 2, ...\}$ to refer to the finer partition into sets $\{\mathcal{D}_k\}_k$. With a slight abuse of notation, whenever we use the dummy variables k, ℓ we imply $k, \ell \in \{\nabla, 1, 2, \dots\}$, the dummy variables m, n imply $m, n \in \{+, -, 0\}$ and the dummy variables i, j imply $i, j \in \mathcal{S}$. E.g. $\mathbb{B}^{k\ell}_{ij}$ means $\mathbb{B}^{k\ell}_{ij}$, $i, j \in \mathcal{S}, k, \ell \in \{\nabla, 1, 2, \dots\}$ and $\mathbb{B}^{mn}_{ij}$ means $\mathbb{B}^{mn}_{ij}$, $i, j \in \mathcal{S}, m, n \in \{+, -, 0\}$.*

By an appropriate choice of the intervals $\{\mathcal{D}_k\}$, $k \in \{\nabla, 1, 2, \dots, \}$, the partition used in (Bean & O'Reilly 2014) can be recovered. Intuitively, we must ensure that each of the boundaries of $\mathcal{F}^m_i$, $i \in \mathcal{S}$, $m \in \{+, -, 0\}$, align with a boundary of a cell $\mathcal{D}_k = [x_k, x_{k+1}] \setminus \{0\}$. Then, each set $\mathcal{F}^m_i$, $i \in \mathcal{S}$, $m \in \{+, -, 0\}$, can be written as a union of cells, $\mathcal{D}_k$, $k = \nabla, 1, 2, \dots$, sans a collection of points which have measure zero for all measures in $\mathcal{M}_0$, and this collection of points is inconsequential for the purposes of the approximations presented here.

Formally, to recover the partition used in (Bean & O'Reilly 2014) we choose the intervals $\mathcal{D}_k$ such that $l(\mathcal{D}_k \cap \mathcal{F}^m_i) \in \{l(\mathcal{D}_k), 0\}$ for all $i \in \mathcal{S}$, $m \in \{+, -, 0\}$, $k \in \{\nabla, 1, 2, \dots\}$, for all $l \in \mathcal{M}_0$. That is, we choose $\mathcal{D}_k$ such that it is contained (up to sets of measure 0 with respect to measures in $\mathcal{M}_0$) within $\mathcal{F}^m_i$ for some $m \in \{+, -, 0\}$ and all $i \in \mathcal{S}$. We assume such a partition for the rest of the paper. For $i \in \mathcal{S}$, $m \in \{+, -, 0\}$, let $\mathcal{K}^m_i = \{k \in \{\nabla, 1, 2, \dots\} \mid l(\mathcal{D}_k \cap \mathcal{F}^m_i) = l(\mathcal{D}_k),\ l \in \mathcal{M}_0\}$, so that $\bigcup_{k\in\mathcal{K}^m_i} \mathcal{D}_k$ and $\mathcal{F}^m_i$ are equal up to a set of l-measure 0. Define $\mathcal{K}^m = \bigcup_{i\in\mathcal{S}} \mathcal{K}^m_i$, $m \in \{+, -, 0\}$.

To recover the partition defined by (1.3) we bundle together the elements of $\mathbb{V}(t)$ which correspond to $\mathcal{F}^m_i$ and $\mathcal{F}^n_j$. That is, for $m, n \in \{+, -, 0\}$, define $\mathbb{V}^{mn}_{ij}(t)$ as the matrix of

operators

$$\mathbb{V}_{ij}^{mn}(t) = \left[\mathbb{V}_{ij}^{k\ell}(t)\right]_{k\in\mathcal{K}_i^m,\ell\in\mathcal{K}_j^n}.$$

Then, for $i,j\in\mathcal{S}$, $m,n\in\{+,-,0\}$, we can write $\overline{\mathbb{V}}_{ij}^{mn}(t) = \mathbf{1}_{|\mathcal{K}_i^m|}\mathbb{V}_{ij}^{mn}(t)\mathbf{1}'_{|\mathcal{K}_j^n|}$ where $\mathbf{1}_{|\mathcal{K}_i^m|}$ and $\mathbf{1}_{|\mathcal{K}_j^n|}$ are row-vectors of 1's of length $|\mathcal{K}_i^m|$ and $|\mathcal{K}_j^n|$, respectively, and $'$ denotes the transpose. The same construction can be achieved with $\mathbb{B}$.

Let $\mathcal{S}_k^+ = \{i\in\mathcal{S} \mid r_i(x) > 0, \forall x\in\mathcal{D}_k\}$, $\mathcal{S}_k^0 = \{i\in\mathcal{S} \mid r_i(x) = 0, \forall x\in\mathcal{D}_k\}$, $\mathcal{S}_k^- = \{i\in\mathcal{S} \mid r_i(x) < 0, \forall x\in\mathcal{D}_k\}$ and $\mathcal{S}_k^\bullet = \{i\in\mathcal{S} \mid r_i(x)\neq 0, \forall x\in\mathcal{D}_k\}$ for $k\in\{\nabla,1,\ldots,K,\Delta\}$. For later reference, we need the following constructions. For $k,\ell\in\{\nabla,1,2,...\}$

$$\mathbb{B}^{k\ell} = \left[\mathbb{B}_{ij}^{k\ell}\right]_{i,j\in\mathcal{S}}, \tag{1.6}$$

for $i,j\in\mathcal{S}$

$$\mathbb{B}_{ij} = \left[\mathbb{B}_{ij}^{k\ell}\right]_{k,\ell\in\{\nabla,1,2,\ldots\}}, \tag{1.7}$$

and for $m,n\in\{+,-,0\}$

$$\mathbb{B}^{mn} = \left[\left[\mathbb{B}_{ij}^{k\ell}\right]_{i\in\mathcal{S}_k^m,j\in\mathcal{S}_\ell^n}\right]_{k\in\mathcal{K}^m,\ell\in\mathcal{K}^n}, \tag{1.8}$$

$$\mathbb{B}^{kn} = \left[\left[\mathbb{B}_{ij}^{k\ell}\right]_{i\in\mathcal{S}_k^m,j\in\mathcal{S}_\ell^n}\right]_{\ell\in\mathcal{K}^n} \text{ for } k\in\{\nabla,1,2,...\}, \tag{1.9}$$

$$\mathbb{B}^{m\ell} = \left[\left[\mathbb{B}_{ij}^{k\ell}\right]_{i\in\mathcal{S}_k^m,j\in\mathcal{S}_\ell^n}\right]_{k\in\mathcal{K}^m} \text{ for } \ell\in\{\nabla,1,2,...\}. \tag{1.10}$$

We persist with the partition $\mathcal{D}_k$, $k\in\nabla,1,2,\ldots$ throughout this paper, as this is consistent with the partition used in the DG method, and note that for all the operators defined with this partition, the partitioning used in (Bean & O'Reilly 2014) can always be recovered by the above construction.

We can write $\mu_i^k\mathbb{B}_{ij}^{k\ell}(\mathcal{A})$ in kernel form as $\displaystyle\int_{x\in\mathcal{D}_k,y\in\mathcal{A}} \mathrm{d}\mu_i^k(x)\mathbb{B}_{ij}^{k\ell}(x,dy)$. It is known that

$$\mu_i^k\mathbb{B}_{ij}^{kk}(\,\mathrm{d}y) := \int_{x\in\mathcal{D}_k} \mathrm{d}\mu_i^k(x)\mathbb{B}_{ij}^{kk}(x,\,\mathrm{d}y) = \begin{cases} v_i^k(y)T_{ij}\,\mathrm{d}y, & i\neq j,\\ v_i^k(y)T_{ii}\,\mathrm{d}y - c_i\dfrac{\mathrm{d}}{\mathrm{d}y}v_i^k(y)\,\mathrm{d}y, & i=j,\end{cases}$$

on the interior of $\mathcal{D}_k$ (Karandikar & Kulkarni 1995). Intuitively, $v_i^k(y)T_{ij}\,\mathrm{d}y$ represents the instantaneous rate of transition from phase i to j in the infinitesimal interval $\mathrm{d}y$, $v_i^k(y)T_{ii}\,\mathrm{d}y$ represents no such transition occurring, and $-c_i\dfrac{\mathrm{d}}{\mathrm{d}y}v_i^k(y)\,\mathrm{d}y$ represents the drift across the interval $\mathrm{d}y$ when the phase is i.

Translating the results of Bean & O'Reilly (2014) to use the partition $\{\mathcal{D}_k\}$ we may state that, for all $i, j \in \mathcal{S}$, $k \in \{1, 2, \dots\}$,

$$\mu_i^k \mathbb{B}_{ij}^{kk}(\mathcal{D}_k) = \int_{x \in \mathcal{D}_k} v_i^k(x) T_{ij} \, \mathrm{d}x - c_i v_i^k(x_{k+1}) \mathbb{1}_{(c_i > 0)} + c_i v_i^k(x_k) \mathbb{1}_{(c_i < 0)},$$

where $\mathbb{1}$ is the indicator function. Intuitively, the first term represents the instantaneous rate of the stochastic transitions of the phase process $\{\varphi(t)\}$, the second term represents the flux out of the right-hand edge of $\mathcal{D}_k$ which occurs when $c_i > 0$ only, and the last term represents the flux out of the left-hand edge of $\mathcal{D}_k$ which occurs when $c_i < 0$ only.

The results of Bean & O'Reilly (2014) also imply that,

$$\mu_i^k \mathbb{B}_{ii}^{k,k+1}(\mathcal{D}_{k+1}) = c_i v_i^k(x_{k+1}) \mathbb{1}_{(c_i > 0)}, \text{ for all } i \in \mathcal{S},\, k \in \{1, 2, ...\},$$
$$\mu_i^k \mathbb{B}_{ii}^{k,k-1}(\mathcal{D}_{k-1}) = -c_i v_i^k(x_k) \mathbb{1}_{(c_i < 0)}, \text{ for all } i \in \mathcal{S},\, k \in \{2, 3, ...\}.$$

Intuitively, the first equation represents the flux from $\mathcal{D}_k$ to $\mathcal{D}_{k+1}$ across the shared boundary at x_{k+1} which occurs when $c_i > 0$ only. The second expression represents the flux from $\mathcal{D}_k$ to $\mathcal{D}_{k-1}$ across the shared boundary at x_k which occurs when $c_i < 0$ only.

Bean & O'Reilly (2014) also state that, at the boundary $x = 0$, for states $i \in \mathcal{S}$ with $c_i \leq 0$ such that a point mass at 0 is possible, we have

$$\begin{aligned}
\mu_i^\nabla \mathbb{B}_{ii}^{\nabla,\nabla} &= \mu_i^\nabla(\{0\}) T_{ii}, \\
\mu_i^\nabla \mathbb{B}_{ij}^{\nabla,\nabla} &= \mu_i^\nabla(\{0\}) T_{ij},\ j \in \mathcal{S},\ c_j \leq 0, \\
\mu_i^\nabla \mathbb{B}_{ij}^{\nabla,1} &= \mu_i^\nabla(\{0\}) T_{ij},\ j \in \mathcal{S},\ c_j > 0, \\
\mu_i^1 \mathbb{B}_{ii}^{1,\nabla} &= -c_i v_i^1(0^+),\ j \in \mathcal{S},\ c_j < 0,
\end{aligned}$$

where 0^+ is the right limit at 0. Otherwise, $\mu_i^k \mathbb{B}_{ij}^{k\ell} = 0$, for $|k-\ell| \geq 2$, $i, j \in \mathcal{S}$ or $|k-\ell| = 1$, $i, j \in \mathcal{S}, i \neq j$, where we take $\nabla = 0$ if it appears in the differences, capturing the facts that the process $\{X(t)\}$ is continuous and that drift across boundaries occurs only when $\{\varphi(t)\}$ remains in the same phase.

Note that we have not presented $\mathbb{B}$ in its full detail here and refer the reader to (Bean & O'Reilly 2014) for the details. The main goal here is to show how $\mathbb{B}$ is used to construct the stationary distribution of the SFFM and to illustrate the link between the operator $\mathbb{B}$ and the DG approximation of the same object. As we shall see later, these expressions closely resemble the DG approximations to the same quantities.

Matrix $\mathbb{D}(s)$ of Operators

Let $b(t) := \int_0^t \left| r_{\varphi(z)}(X(z)) \right| \mathrm{d}z$ be the total unregulated amount of fluid that has flowed into or out of the second buffer $\{Y(t)\}$ during $[0, t]$, and let $\eta(y) := \inf\{t > 0 : b(t) = y\}$ be the first time this accumulated in-out amount hits level y. Note that at the stopping

time $\eta(y)$ it must be that $(X(\eta(y)), \varphi(\eta(y))) \in (\mathcal{F}_i^m, i)$ for some $i \in \mathcal{S}$ and $m \in \{+, -\}$, i.e. $m \neq 0$. We define the operators $\mathbb{U}_{ij}^{k\ell}(y,s) : \mathcal{M}_0(\mathcal{D}_k \cap \mathcal{F}_i^m) \mapsto \mathcal{M}_0(\mathcal{D}_\ell \cap \mathcal{F}_j^n)$, for $k \in \mathcal{K}_i^+ \cup \mathcal{K}_i^-$, $\ell \in \mathcal{K}_j^+ \cup \mathcal{K}_j^-$, and $i \in \mathcal{S}_k^\bullet$, $j \in \mathcal{S}_k^\bullet$, by

$$\begin{aligned}&\mu_i^k \mathbb{U}_{ij}^{k\ell}(y,s)(\mathcal{A})\\ &:= \int_{x \in \mathcal{D}_k} \mathrm{d}\mu_i^k(x) \mathbb{E}\left[e^{-s\eta(y)} 1\left\{\varphi(\eta(y)) = j,\ X(\eta(y)) \in \mathcal{A} \cap \mathcal{D}_\ell\right\} \mid \varphi(0) = i, X(0) = x\right].\end{aligned}$$

Then, construct the matrix of operators

$$\mathbb{U}(y,s) := \left[[\mathbb{U}_{ij}^{k\ell}(y,s)]_{i \in \mathcal{S}_k^\bullet, j \in \mathcal{S}_\ell^\bullet}\right]_{k,\ell \in \mathcal{K}^+ \cup \mathcal{K}^-}.$$

The matrix of operators $\mathbb{D}(s)$ is the infinitesimal generator of the semigroup $\{\mathbb{U}(y,s)\}_{y \geq 0}$ defined by

$$\mathbb{D}(s) = \frac{\mathrm{d}}{\mathrm{d}y} \mathbb{U}(y,s)|_{y=0},$$

whenever this limit exists.

Recalling the constructions in Equations (1.6)-(1.10) and using Lemma 4 of (Bean & O'Reilly 2014) gives the following expression for $\mathbb{D}(s)$.

Lemma 1.3. *For $y \geq 0$, $s \in \mathbb{C}$ with $Re(s) \geq 0$, $i, j \in \mathcal{S}$, $k \in \mathcal{K}_i^+ \cup \mathcal{K}_i^-$, $\ell \in \mathcal{K}_j^+ \cup \mathcal{K}_j^-$,*

$$\mathbb{D}_{ij}^{k\ell}(s) = [\mathbb{R}^k(\mathbb{B}^{k\ell} - s\mathbb{I} + \mathbb{B}^{k0}(s\mathbb{I} - \mathbb{B}^{00})^{-1}\mathbb{B}^{0\ell})]_{ij},$$

where $\mathbb{I}$ is the identity operator, and $\mathbb{R}^k := \mathrm{diag}(\mathbb{R}_i^k)_{i \in \mathcal{S}}$ is a diagonal matrix of operators $\mathbb{R}_i^k$ given by

$$\mu_i^k \mathbb{R}_i^k(\mathcal{A}) := \int_{x \in \mathcal{A} \cap \mathcal{D}_k} \frac{1}{r_i(x)} \mathrm{d}\mu_i^k(x), \quad k \in \mathcal{K}_i^+ \cup \mathcal{K}_i^-.$$

Also, construct the matrices of operators

$$\mathbb{D}^{mn} := \left[\left[\mathbb{D}_{ij}^{k\ell}\right]_{i \in \mathcal{S}_k^m, j \in \mathcal{S}_k^n}\right]_{k \in \mathcal{K}^m, \ell \in \mathcal{K}^n}.$$

Matrix $\Psi(s)$ of Operators

We denote by $\Psi(s)$ the matrix of operators with the same dimensions as $\mathbb{D}^{+-}$, recording the Laplace-Stieltjes transforms of the time for $\{Y(t)\}$ to return, for the first time, to the initial level of zero as introduced in (Bean & O'Reilly 2014) but constructed with respect to the finer partition $\{\mathcal{D}_k\}$. Define the stopping time $\zeta_Y(\{E\}) := \inf\{t > 0 : Y(t) \in E\}$

to be the first time $\{Y(t)\}$ hits the set E, then each component $\Psi_{ij}^{k\ell}(s) : \mathcal{M}_0(\mathcal{D}_k) \mapsto \mathcal{M}_0(\mathcal{D}_\ell), i, j \in \mathcal{S}$, $k \in \mathcal{K}_i^+$ and $\ell \in \mathcal{K}_j^-$, is given by

$$\mu_i^k \Psi_{ij}^{k\ell}(s)(\mathcal{A}) := \int_{x \in \mathcal{D}_k} \mathrm{d}\mu_i^k(x) \mathbb{E}\left[e^{-s\zeta_Y(\{0\})} 1\left\{\varphi(\zeta_Y(\{0\})) = j,\ X(\zeta_Y(\{0\})) \in \mathcal{A} \cap \mathcal{D}_\ell\right\} \mid X(0) = x, Y(0) = 0, \varphi$$

Bean and O'Reilly (Bean & O'Reilly 2014, Theorem 1) give the following result which characterises $\Psi(s)$.

Theorem 1.4. *For $Re(s) \geq 0$, $\Psi(s)$ satisfies the equation:*

$$\mathbb{D}^{+-}(s) + \Psi(s)\mathbb{D}^{-+}(s)\Psi(s) + \mathbb{D}^{++}(s)\Psi(s) + \Psi(s)\mathbb{D}^{--}(s) = 0.$$

Furthermore, if s is real then $\Psi(s)$ is the minimal nonnegative solution.

Stationary Distribution

Let $\Psi := \Psi(0)$. We define $\zeta_Y^n(\{0\}) := \inf\{t \geq \zeta_Y^{n-1}(\{0\}) : Y(t) = 0\}$, for $n \geq 2$, to be the sequence of hitting times to level 0 of $Y(t)$, with $\zeta_Y^1(\{0\}) := \zeta_Y(\{0\})$. Consider a discrete-time Markov process $\{X(\zeta_Y^n(\{0\})), \varphi(\zeta_Y^n(\{0\})), n \geq 1\}$, and for $i \in \mathcal{S}$, $k \in \mathcal{K}_i^-$ define the measures $\mathfrak{k}_i^k$ as follows

$$\mathfrak{k}_i^k(\mathcal{A}) := \lim_{n \to \infty} \mathbb{P}\left(X(\zeta_Y^n(\{0\})) \in \mathcal{A} \cap \mathcal{D}_k, \varphi(\zeta_Y^n(\{0\})) = i\right).$$

By (Bean & O'Reilly 2014), the vector of measures $\mathfrak{k} := (\mathfrak{k}_i^k)_{i \in \mathcal{S}_k^-, k \in \mathcal{K}^-}$ satisfies the following set of equations

$$\begin{bmatrix}\mathfrak{k} & \mathbf{0}\end{bmatrix} \left(-\begin{bmatrix}\mathbb{B}^{--} & \mathbb{B}^{-0} \\ \mathbb{B}^{0-} & \mathbb{B}^{00}\end{bmatrix}\right)^{-1} \begin{bmatrix}\mathbb{B}^{-+} \\ \mathbb{B}^{0+}\end{bmatrix} \Psi = \mathfrak{k}, \tag{1.11}$$

$$\sum_{k \in \mathcal{K}^-} \sum_{i \in \mathcal{S}_k^-} \mathfrak{k}_i^k(\mathcal{F}_i^-) = 1. \tag{1.12}$$

We reproduce Theorem 2 of (Bean & O'Reilly 2014) below, which gives the joint stationary distribution of $\{X(t), Y(t), \varphi(t)\}$. Recall that the joint stationary density operator $\mathbb{\pi}(y) = (\mathbb{\pi}_i(y))_{i \in \mathcal{S}}$ for $\{X(t), Y(t), \varphi(t)\}$ and the joint stationary mass operator $\mathbb{p} = (\mathbb{p}_i)_{i \in \mathcal{S}}$ are defined by (1.4) and (1.5), respectively. We can partition $\mathbb{\pi}$ as follows

$$\begin{aligned}\mathbb{\pi}(y) &= \begin{bmatrix}\mathbb{\pi}^+(y) & \mathbb{\pi}^-(y) & \mathbb{\pi}^0(y)\end{bmatrix} \\ &= \begin{bmatrix}\left(\mathbb{\pi}_i^k(y)\right)_{i \in \mathcal{S}_k^+, k \in \mathcal{K}^+} & \left(\mathbb{\pi}_i^k(y)\right)_{i \in \mathcal{S}_k^-, k \in \mathcal{K}^-} & \left(\mathbb{\pi}_i^k(y)\right)_{i \in \mathcal{S}_k^0, k \in \mathcal{K}^0}\end{bmatrix},\end{aligned}$$

where

$$\mathbb{\pi}_i^k(y)(\mathcal{A}) = \mathbb{\pi}_i(y)(\mathcal{A} \cap \mathcal{D}_k).$$

Similarly we can write

$$\mathbb{p} = \begin{bmatrix} \mathbb{p}^- & \mathbb{p}^0 \end{bmatrix} = \begin{bmatrix} \left(\mathbb{p}_i^k\right)_{i\in\mathcal{S}_k^-,k\in\mathcal{K}^-} & \left(\mathbb{p}_i^k\right)_{i\in\mathcal{S}_k^0,k\in\mathcal{K}^0} \end{bmatrix},$$

where $\mathbb{p}_i^k(\mathcal{A}) = \mathbb{p}_i(\mathcal{A}\cap\mathcal{D}_k)$.

Theorem 1.5. *The density $\mathbb{w}^m(y)$, for $m \in \{+,-,0\}$ and $y > 0$, and the probability mass $\mathbb{p}^m$, for $m \in \{-,0\}$, satisfy the following set of equations:*

$$\mathbb{w}^0(y) = \begin{bmatrix} \mathbb{w}^+(y) & \mathbb{w}^-(y) \end{bmatrix} \begin{bmatrix} \mathbb{B}^{+0} \\ \mathbb{B}^{-0} \end{bmatrix} \left(-\mathbb{B}^{00}\right)^{-1}, \tag{1.13}$$

$$\begin{bmatrix} \mathbb{w}^+(y) & \mathbb{w}^-(y) \end{bmatrix} = \begin{bmatrix} \mathbb{p}^- & \mathbb{p}^0 \end{bmatrix} \begin{bmatrix} \mathbb{B}^{-+} \\ \mathbb{B}^{0+} \end{bmatrix} \begin{bmatrix} e^{\mathbb{K}y} & e^{\mathbb{K}y}\Psi \end{bmatrix} \begin{bmatrix} \mathbb{R}^+ & 0 \\ 0 & \mathbb{R}^- \end{bmatrix}, \tag{1.14}$$

$$\begin{bmatrix} \mathbb{p}^- & \mathbb{p}^0 \end{bmatrix} = z \begin{bmatrix} \xi & \mathbf{0} \end{bmatrix} \left(- \begin{bmatrix} \mathbb{B}^{--} & \mathbb{B}^{-0} \\ \mathbb{B}^{0-} & \mathbb{B}^{00} \end{bmatrix} \right)^{-1}, \tag{1.15}$$

$$\sum_{m\in\{+,-,0\}} \sum_{i\in\mathcal{S}} \int_{y=0}^{\infty} \mathbb{w}_i^m(y)(\mathcal{F}_i^m)\,\mathrm{d}y + \sum_{m\in\{-,0\}} \sum_{i\in\mathcal{S}} \mathbb{p}_i^m(\mathcal{F}_i^m) = 1, \tag{1.16}$$

where $\mathbb{K} := \mathbb{D}^{++}(0) + \Psi\mathbb{D}^{(-+)}(0)$ and z is a normalising constant.

At this point we reiterate that Equations (1.13)-(1.16) are operator equations and are only amenable to numerical evaluation in the simplest of cases. Sources of this intractability come from, for example, the need to find the inverse operator $(-\mathbb{B}^{00})^{-1}$, and the need to find the solution, $\Psi(s)$, of the operator equation in Theorem 1.4. There is also the complexity of the partition of the operators defined by the sets $\mathcal{F}_i^m$, $i \in \mathcal{S}$, $m \in \{+,-,0\}$. Therefore, there is the need for approximation schemes such as the DG scheme we introduce next.

1.1.3 Matrix-exponential distributions

Here we recount some facts about matrix exponential distributions. See (Bladt & Nielsen 2017) for a more detailed exposition. A random variable, Z, is said to have a matrix-exponential distribution if it has a distribution function of the form $1 - \boldsymbol{\alpha}e^{\boldsymbol{S}x}(-\boldsymbol{S})^{-1}\boldsymbol{s}$, where $\boldsymbol{\alpha}$ is a $1 \times p$ *initial vector*, $\boldsymbol{S}$ a $p \times p$ matrix, and $\boldsymbol{s}$ a $p \times 1$ *closing vector*, and $e^{\boldsymbol{S}x} := \sum_{n=0}^{\infty} \frac{(\boldsymbol{S}x)^n}{n!}$ is the matrix exponential. The density function of Z is given by $f_Z(x) = \boldsymbol{\alpha}e^{\boldsymbol{S}x}\boldsymbol{s}$. The only restrictions on the parameters $(\boldsymbol{\alpha}, \boldsymbol{S}, \boldsymbol{s})$ are that $\boldsymbol{\alpha}e^{\boldsymbol{S}x}\boldsymbol{s}$ be a valid density function, i.e. $\boldsymbol{\alpha}e^{\boldsymbol{S}x}\boldsymbol{s} \geq 0$, for all $x \geq 0$ and $\lim_{x\to\infty} 1 - \boldsymbol{\alpha}e^{\boldsymbol{S}x}(-\boldsymbol{S})^{-1}\boldsymbol{s} = 1$. There is the possibility of an *atom* (a point mass) at 0, but here we do not consider this possibility. These condition that $\boldsymbol{\alpha}e^{\boldsymbol{S}x}\boldsymbol{s}$ be a valid density imposes some properties on

representations $(\boldsymbol{\alpha}, \boldsymbol{S}, \boldsymbol{s})$. However, in general there is no way to determine whether, given a triplet $(\boldsymbol{\alpha}, \boldsymbol{S}, \boldsymbol{s})$ whether it is a representation of a matrix-exponential distribution, or not. Nonetheless, some properties of a triplet $(\boldsymbol{\alpha}, \boldsymbol{S}, \boldsymbol{s})$ are known, such as the following, which is used in the characterisation of QBD-RAPs.

Theorem 1.6 (Theorem 4.1.3, Bladt & Nielsen (2017)). *The density function of a matrix-exponential distribution with representation $(\boldsymbol{\alpha}, \boldsymbol{S}, \boldsymbol{s})$ can be expressed in terms of real-valued constants as*

$$\begin{aligned}\psi(x) = &\sum_{j=1}^{m_1}\sum_{k=1}^{p_j} c_{jk}\frac{x^{k-1}}{(k-1)!}e^{\mu_j x} + \sum_{j=1}^{m+2}\sum_{k=1}^{q_j} d_{jk}\frac{x^{k-1}}{(k-1)!}e^{\eta_j x}\cos(\sigma_j x)\\ &+ \sum_{j=1}^{m_2}\sum_{k=1}^{q_j} e_{jk}\frac{x^{k-1}}{(k-1)!}e^{\eta_j x}\sin(\sigma_j x),\end{aligned} \tag{1.17}$$

for integers m_1, m_2, p_j, and q_j and some real constants c_{jk}, d_{jk}, e_{jk}, μ_j, η_j, and σ_j. Here μ_j, $j = 1, \ldots, m_1$ are the real eigenvalues of $\boldsymbol{S}$, while $\eta_j + i\sigma_j$, $\eta_j - i\sigma_j$, $j = 1, \ldots, m_2$ denote its complex eigenvalues, which come in conjugate pairs. Thus $m_1 + 2m_2$ is the total number of eigenvalues, while the dimension of the representation is given by $p = \sum_{j=1}^{m+1} p_j + 2\sum_{j=1}^{m_2} q_j$.

Theorem 1.7 (Theorem 4.1.4, Bladt & Nielsen (2017)). *Consider the nonvanishing terms of the matrix exponential density (1.17),* i.e., *the terms for which $c_{jk} = 0$, $d_{jk} = 0$, or $e_{jk} = 0$. Among the corresponding eigenvalues λ_j, there is a real dominating eigenvalue κ, say. That is, κ is real, $\kappa \geq Re(\lambda_j)$ for all j, and the multiplicity of κ is at least the multiplicity of every other eigenvalue with real part κ.*

Corollary 1.8 (Corollary 4.1.5, Bladt & Nielsen (2017)). *If $(\boldsymbol{\alpha}, \boldsymbol{S}, \boldsymbol{s})$ is a representation for a matrix-exponential distribution, then $\boldsymbol{S}$ has a real dominating eigenvalues.*

Theorem 1.9 (Theorem 4.1.6, Bladt & Nielsen (2017)). *Let Z be a matrix-exponentially distributed random variable with density (1.17). Then the dominant real eigenvalue κ of Theorem 1.7 is strictly negative.*

We define $dev(\boldsymbol{S})$ to be the real dominating eigenvalue of $\boldsymbol{S}$, that is $dev(\boldsymbol{S}) = \kappa$ in Theorem 1.7.

The class of matrix-exponential distribution is characterised as the class of probability distributions which have a rational Laplace transform. That is, $\int_{x=0}^{\infty} e^{-\lambda x}\boldsymbol{\alpha}e^{\boldsymbol{S}x}\boldsymbol{s}\,\mathrm{d}x$ is a ratio of two polynomial functions in λ. Matrix exponential distributions are an extension of Phase-type distributions, where for the latter, $\boldsymbol{S}$ must be a sub-generator matrix of a CTMC, $\boldsymbol{s} = -\boldsymbol{S}\boldsymbol{e}$ where $\boldsymbol{e}$ is a $1 \times p$ vector of ones, and $\boldsymbol{\alpha}$ is a discrete probability distribution.

A *representation* of a matrix exponential distribution is a triplet $(\boldsymbol{\alpha}, \boldsymbol{S}, \boldsymbol{s})$, and we write $Z \sim ME(\boldsymbol{\alpha}, \boldsymbol{S}, \boldsymbol{s})$ to denote that Z has a matrix-exponential distribution with this representation. The order of the representation is the dimension of the square matrix $\boldsymbol{S}$, i.e. if $\boldsymbol{S}$ is $p \times p$, then the matrix exponential distribution is said to be of order p. Representations of matrix-exponential distributions are not unique (Bladt & Nielsen 2017). A representation is called *minimal* when $\boldsymbol{S}$ has the smallest possible dimension. Throughout this work, we assume that the representation of any matrix exponential distribution is minimal. Let $\boldsymbol{e}_i$ be a vector with a 1 in the ith position and zeros elsewhere. We assume that $\boldsymbol{s} = -\boldsymbol{S}\boldsymbol{e}$, and that $(\boldsymbol{e}_i, \boldsymbol{S}, \boldsymbol{s})$ for $i = 1, \ldots, p$ are representations of matrix exponential distributions. It is always possible to find such a representation (Bladt & Nielsen 2017, Theorem 4.5.17, Corollary 4.5.18). As such, we abbreviate our notation $Z \sim ME(\boldsymbol{\alpha}, \boldsymbol{S}, \boldsymbol{s})$ to $Z \sim ME(\boldsymbol{\alpha}, \boldsymbol{S})$. Further, given $\boldsymbol{s} = -\boldsymbol{S}\boldsymbol{e}$ then observe that $\int_{x=0}^{\infty} e^{\boldsymbol{S}x}\boldsymbol{s}\,\mathrm{d}x = (-\boldsymbol{S})^{-1}\boldsymbol{s} = \boldsymbol{e}$.

For a given $p \times p$ matrix $\boldsymbol{S}$, denote by $\mathcal{A} \subset \mathbb{R}^p$ the space of all possible vectors $\boldsymbol{a}$ such that $(\boldsymbol{a}, \boldsymbol{S})$ is a valid representation of a (possibility defective) matrix exponential distribution.

1.1.4 QBD-RAPs

As RAPs are an extension of Markovian arrival processes to include matrix-exponential inter-arrival times, QBD-RAPs are extensions of QBDs to include matrix-exponential times between level changes. To define a QBD-RAP we first need a Batch (Marked) RAP.

Let $\mathscr{K} \subset \mathbb{Z}$ be a set of *marks*. Let N be a point process, and $Y_0 = 0 < Y_1 < Y_2 \cdots$ be event times of N. Let $\{N(t)\}$ be the counting process associated with N such that $N(t)$ returns the number of events by time t. Associated with the nth event is a mark M_n. For $i \in \mathscr{K}$, let N_i be simple point processes associated with events with marks of type i only, and let $\{N_i(t)\}_{t\geq 0}$ be the associated counting processes of events of mark i. For a matrix $\boldsymbol{B}$ let $dev(\boldsymbol{B})$ denote the real part of the dominant eigenvalue of $\boldsymbol{B}$ (the one with maximal real part). Denote by $f_{N,n}(y_1, m_1, y_2, m_2, \ldots, y_n, m_n)$ the joint density, probability mass function of the first n inter-arrival times, $Y_1, Y_2 - Y_1, \ldots, Y_n - Y_{n-1}$, and the associated marks M_n. From Bean and Nielsen (Bean & Nielsen 2010, Theorem 1) we have the following.

Theorem 1.10. *A process N is a Marked RAP if there exist matrices $\boldsymbol{S}$, $\boldsymbol{D}_i$, $i \in \mathscr{K}$, and a row vector $\boldsymbol{\alpha}$ such that $dev(\boldsymbol{S}) < 0$, $dev(\boldsymbol{S} + \boldsymbol{D}) = 0$, $(\boldsymbol{S} + \boldsymbol{D})\boldsymbol{e} = 0$, $\boldsymbol{D} = \sum_{i\in\mathscr{K}} \boldsymbol{D}_i$, and*

$$f_{N,n}(y_1, m_1, y_2, m_2, \ldots, y_n, m_n) = \boldsymbol{\alpha} e^{\boldsymbol{S}y_1}\boldsymbol{D}_{m_1} e^{\boldsymbol{S}y_2}\boldsymbol{D}_{m_2} \ldots e^{\boldsymbol{S}y_n}\boldsymbol{D}_{m_n}\boldsymbol{e}. \tag{1.18}$$

Conversely, if a point process has the property (1.18) then it is a Marked RAP.

Denote such a process $N \sim BRAP(\boldsymbol{\alpha}, \boldsymbol{S}, \boldsymbol{D}_i, i \in \mathscr{K})$.

Also from Bean & Nielsen (2010), associated with a Marked RAP is a row-vector-valued *orbit* process, $\{\boldsymbol{A}(t)\}_{t\geq 0}$,

$$\boldsymbol{A}(t) = \frac{\boldsymbol{\alpha}\left(\prod_{i=1}^{N(t)} e^{\boldsymbol{S}(Y_i - Y_{i-1})}\boldsymbol{D}_{M_i}\right) e^{\boldsymbol{S}(t-Y_{N(t)})}}{\boldsymbol{\alpha}\left(\prod_{i=1}^{N(t)} e^{\boldsymbol{S}(Y_i - Y_{i-1})}\boldsymbol{D}_{M_i}\right) e^{\boldsymbol{S}(t-Y_{N(t)})}\boldsymbol{e}}.$$

Thus, $\{\boldsymbol{A}(t)\}$ is a piecewise-deterministic Markov process where, in between events $\{\boldsymbol{A}(t)\}$ evolves deterministically according to

$$\boldsymbol{A}(t) = \frac{\boldsymbol{A}(Y^-_{N(t)})e^{\boldsymbol{S}(t-Y_{N(t)})}}{\boldsymbol{A}(Y^-_{N(t)})e^{\boldsymbol{S}(t-Y_{N(t)})}\boldsymbol{e}},$$

where $\boldsymbol{A}(Y^-_{N(t)}) = \lim_{u\to 0^+} \boldsymbol{A}(Y_{N(t)} - u)$. The process $\{\boldsymbol{A}(t)\}$ "jumps" at event times of N (the process may not always jump at these times, but typically the dynamics change discontinuously at this point). At time t the intensity with which $\{\boldsymbol{A}(t)\}$ has a jump is $\boldsymbol{A}(t)\boldsymbol{D}\boldsymbol{e}$. Upon an event the event is associated with mark i with probability $\boldsymbol{A}(t)\boldsymbol{D}_i\boldsymbol{e}/\boldsymbol{A}(t)\boldsymbol{D}\boldsymbol{e}$. Upon on an event at time t with mark i, the new position of the orbit is $\boldsymbol{A}(t) = \boldsymbol{A}(t^-)\boldsymbol{D}_i/\boldsymbol{A}(t^-)\boldsymbol{D}_i\boldsymbol{e}$. It is important to note that the jumps of the orbit process are *linear* transformations of the orbit process immediately before the time of the jump.

Marked RAPs are an extension of Marked Markovian arrival processes to include matrix-exponential inter-arrival times. For Marked MAPs, the vector $\boldsymbol{A}(t)$ is a vector of posterior probabilities of a continuous-time Markov chain.

Intuitively, $\boldsymbol{A}(t)$ encodes all of the information about the event times of the Marked RAP and associated marks up to time t that is needed to determine the future behaviour of the point process. Let $\mathcal{F}_t$ be the σ-algebra generated by $N(u), u \in [0, t]$. Then $N \mid \mathcal{F}_t \equiv N \mid \boldsymbol{A}(t) \sim BRAP(\boldsymbol{A}(t), \boldsymbol{S}, \boldsymbol{D}_i, i \in \mathscr{K})$. In words, the future of the point process after time t given all of the information about the process up to and including time t, is distributed as a Marked RAP with initial vector $\boldsymbol{A}(t)$.

Now consider a Marked RAP, $N \sim BRAP(\boldsymbol{\alpha}, \boldsymbol{S}, \boldsymbol{D}_i, i \in \{-1, 0, +1\})$. The process $\{(L(t), \boldsymbol{A}(t))\}_{t\geq 0}$ formed by letting $L(t) = N_{+1}(t) - N_{-1}(t)$ is a QBD-RAP.

1.1.5 Convergence theorems

Theorem 1.11 (Extended Continuity Theorem (Feller 1957))**.** *For $p = 1, 2, \ldots$ let U_p be a measure with Laplace transform ζ_p. If $\zeta_p(\lambda) \to \zeta(\lambda)$ for $\lambda > a \geq 0$, then ζ is the Laplace transform of a measure U and $U_p \to U$.*

Conversely, if $U_p \to U$ and the sequence $\{\zeta_p(a)\}$ is bounded, then $\zeta_p(\lambda) \to \zeta(\lambda)$ for $\lambda > a$.

Chapter 2

Approximating fluid queues with the discontinuous Galerkin method

Sections 2.1 and 2.2.1 have been taken from Sections 4 and 5 of Bean et al. (2022) with only minor changes, such as notations, so that this chapter is consistent with the rest of the thesis. I am a co-author of the paper Bean et al. (2022). The conceptualisation of Bean et al. (2022) was originally by Vikram Sunkara, Nigel Bean and Giang Nguyen, and the original coding was done by Vikram Sunkara. I made significant contributions to Section 3 of the paper, expressing the operator-theoretic expressions to use the same partition as the approximation scheme. I contributed Sections 4.4 and 5.1. I extended the numerical experiments in Section 6 to higher orders and made all the plots in Section 6. Appendix A is also my original work. I did a significant proportion of the writing of the manuscript and addressed the reviewers comments and also developed code for the numerical experiments.

2.1 Discontinuous Galerkin Approximation of the Generator of a Fluid Queue

Discontinuous Galerkin (DG) methods can be used to approximate the solutions to systems of partial differential equations (PDEs). For a more thorough description of these methods see (Hesthaven & Warburton 2007). The domain of approximation is partitioned into intervals, referred to individually as *cells* and collectively as a *mesh*. On each cell, we have a finite element approximation, which constructs a finite-dimensional smooth Sobolev space using piecewise-polynomial basis functions, and then projects the partial differential equations onto this space. This projection leads to a new system of equations, referred to as the *weak form* of the original system of PDEs. Next, we must approximate

the *flux operator* which moves probability from one cell to another, in a manner similar to the underlying principle of a finite-volume approximation. This method conserves probability, and can handle discontinuities, such as jumps and point masses. Here we construct the DG approximation to the matrix of operators $\mathbb{B}$ which we use later to construct a DG approximation to $\mathbb{D}(s)$ then $\Psi(s)$, and ultimately the stationary distribution of an SFFM.

2.1.1 The Partial Differential Equation

We start by introducing the PDE from which we will extract the approximation to the generator $\mathbb{B}$.

Let $f_i(x,t)$ be the joint density of $\{(X_t, \varphi_t)\}$:

$$f_i(x,t) := \frac{\partial}{\partial x}\mathbb{P}\left(X_t \leq x, \varphi_t = i\right), \quad x > 0,\, i \in \mathcal{S},$$

which satisfies the system of partial differential equations

$$\frac{\partial}{\partial t}f_i(x,t) = \sum_{j\in\mathcal{S}} f_j(x,t)T_{ji} - c_i\frac{\partial}{\partial x}f_i(x,t), \quad x > 0, i \in \mathcal{S}$$

subject to suitable boundary conditions (Bean & O'Reilly 2014). In matrix form,

$$\frac{\partial}{\partial t}\boldsymbol{f}(x,t) = \boldsymbol{f}(x,t)\boldsymbol{T} - \frac{\partial}{\partial x}\boldsymbol{f}(x,t)\boldsymbol{C}, \tag{2.1}$$

where $\boldsymbol{f}(x,t) = (f_i(x,t))_{i\in\mathcal{S}}$ is a row-vector. This system of PDEs is closely related to the generator $\mathbb{B}$. Write $\boldsymbol{\mu}(t)(\cdot) = (\mu_j(t)(\cdot))_{j\in\mathcal{S}}$, then, for $\mathcal{A} \subset (0,\infty)$, and assuming $\boldsymbol{\mu}(t)$ admits a density,

$$\boldsymbol{\mu}(t)(\mathcal{A}) = \int_{x\in\mathcal{A}} \boldsymbol{f}(x,t)\,\mathrm{d}x.$$

That is, $f_i(x,t)$ is the density of $\mu_i(t)$. Then $\boldsymbol{\mu}(t)$ satisfies the operator differential equation

$$\frac{\mathrm{d}}{\mathrm{d}t}\boldsymbol{\mu}(t)(\,\mathrm{d}x) = \boldsymbol{\mu}(t)\mathbb{B}(\,\mathrm{d}x) = \boldsymbol{f}(x,t)\boldsymbol{T}\,\mathrm{d}x - \frac{\partial}{\partial x}\boldsymbol{f}(x,t)\boldsymbol{C}\,\mathrm{d}x,$$

on the interior of the space $[0,\infty)$. Thus, by approximating the operator on the right-hand side of Equation (2.1) we can approximate the infinitesimal operator $\mathbb{B}$. The DG method does exactly this, by approximating the operator with a matrix.

2.1.2 Cells, Test Functions, and Weak Formulation

To begin with, consider an unbounded first fluid level $\{\widehat{X}_t, t \geq 0\}$, $\widehat{X}_t \in (-\infty, \infty)$. We will eventually truncate this space so that we have a finite dimensional approximation; however, this requires a discussion on boundary conditions which we save for later. Let $\mathcal{D}_k = [x_k, x_{k+1}]$, $k \in \mathbb{Z}$ partition the domain $(-\infty, \infty)$. We call the $\mathcal{D}_k$ *cells*.

On each cell $\mathcal{D}_k$ we choose N_k linearly independent functions $\{\phi_r^k\}_{r=1}^{N_k}$, compactly supported on $\mathcal{D}_k$ (i.e. $\phi_r^k(x) = 0$ for $x \notin \mathcal{D}_k$) to form a basis for the space W_k, in which we formulate the approximation. Here, as is standard in DG methods (Hesthaven & Warburton 2007), we take $\{\phi_r^k\}_{r=1}^{N_k}$ to be the space of polynomials of degree $N_k - 1$. It is convenient in this work to take $\{\phi_r^k\}_{r=1}^{N_k}$ as a basis of Lagrange interpolating polynomials defined by the Gauss-Lobatto quadrature points, since our approximations inherit nice properties from this (Hesthaven & Warburton 2007). However, the constructions presented here are general and any basis can be used. For the sake of illustration, the reader may think of $\{\phi_r^k\}_{r=1}^{N_k}$ as the Lagrange polynomials. On each cell $\mathcal{D}_k$ we approximate

$$f_i(x,t) \approx u_i^k(x,t) = \sum_{r=1}^{N_k} a_{i,r}^k(t)\phi_r^k(x),$$

where $a_{i,r}^k(t)$ are yet-to-be-determined time-dependent coefficients. We refer to u_i^k as the *local* approximation on $\mathcal{D}_k$, while the *global* approximation is given by $\sum_{k\in\mathbb{Z}} u_i^k$ on the whole domain. The whole approximation space is $\bigoplus_{k\in\mathbb{Z}} W_k$.

Let $\mathcal{N}_k := \{1, \ldots, N_k\}$, $k \in \mathbb{Z}$. For $k \in \mathbb{Z}$, define *local* row-vectors

$$\boldsymbol{\phi}^k(x) = (\phi_r^k(x))_{r\in\mathcal{N}_k}, \quad \boldsymbol{a}_i^k(x) = (a_{i,r}^k(x))_{r\in\mathcal{N}_k},\ i \in \mathcal{S}.$$

Note that we will always use the letter r to index the basis function within each cell.

The DG method proceeds by first considering the *weak-formulation* of the PDE, which is constructed from the *strong-form* of the PDE, Equation (2.1). In general, to construct the weak-form we need a set of test functions, say W. Now, take the strong form of the PDE, multiply it by some test function $\psi(x) \in W$, integrate with respect to x, and apply integration by parts to the derivative with respect to x, to get

$$\int_{x\in\mathbb{R}} \frac{\partial}{\partial t} f_j(x,t)\psi(x)\,\mathrm{d}x = \int_{x\in\mathbb{R}} \sum_{i\in\mathcal{S}} f_i(x,t)T_{ij}\frac{\mathrm{d}}{\mathrm{d}x}\psi(x)\,\mathrm{d}x + \int_{x\in\mathbb{R}} f_j(x,t)c_j\psi(x)\,\mathrm{d}x - [f_j(x,t)c_j\psi(x)]_{x=-\infty}^{x=\infty}, \tag{2.2}$$

for $j \in \mathcal{S}$. It is common to choose W such that $\psi(-\infty) = \psi(\infty) = 0$, in which case the last term on the right is zero. Requiring (2.2) to hold for every $\psi \in W$ gives the weak-formulation of the PDE. For a sufficiently rich set of test functions W the weak and strong forms of the PDE are equivalent. Solutions to (2.2) are known as *weak* solutions and

generalise the concept of a solution of the PDE. For example, this may allow discontinuities with respect to x in the solution – something which is ill-defined for the strong form.

For the purpose of DG, we take the set of test functions to be $W = \bigoplus_{k\in\mathbb{Z}} W^k$, the same as the set of basis functions of our solution space. Proceeding as described above, the weak formulation is

$$\int_{x\in\mathcal{D}_k} \frac{\partial}{\partial t} f_j(x,t)\phi_r^k(x)\,\mathrm{d}x = \int_{x\in\mathcal{D}_k} \sum_{i\in\mathcal{S}} f_i(x,t)T_{ij}\phi_r^k(x)\,\mathrm{d}x + \int_{x\in\mathcal{D}_k} f_j(x,t)c_j\frac{\mathrm{d}}{\mathrm{d}x}\phi_r^k(x)\,\mathrm{d}x - [f_j(x,t)c_j\phi_r^k(x)]_{x=x_k}^{x=x_{k+1}},$$

since ϕ_r^k is compactly supported on $\mathcal{D}_k$, for all $j\in\mathcal{S}$, $r\in\mathcal{N}_k$, $k\in\mathbb{Z}$. Now, note that any function $g(x)$ can be decomposed as $g(x) = g^W(x) + g^\perp(x)$ where $g^W \in W$ and $g^\perp \in W^\perp$, and $W^\perp$ is the orthogonal complement of W. Since $g^\perp$ is orthogonal to W, $\int_x g^\perp(x)\phi_r^k(x)\,\mathrm{d}x = 0$ for $r\in\mathcal{N}_k$, $k\in\mathbb{Z}$. Also, note that $\frac{\mathrm{d}}{\mathrm{d}x}\phi_r^k(x) \in W$. Using this, we can write

$$\int_{x\in\mathcal{D}_k} \frac{\partial}{\partial t}\left(f_j^W(x,t) + f_j^\perp(x,t)\right)\phi_r^k(x)\,\mathrm{d}x = \int_{x\in\mathcal{D}_k}\sum_{i\in\mathcal{S}}\left(f_i^W(x,t) + f_i^\perp(x,t)\right)T_{ij}\phi_r^k(x)\,\mathrm{d}x + \int_{x\in\mathcal{D}_k}\left(f_j^W(x,t) + f_j^\perp(x,t)\right)c_j\frac{\mathrm{d}}{\mathrm{d}x}\phi_r^k(x)\,\mathrm{d}x - [f_j(x,t)c_j\phi_r^k(x)]_{x=x_k}^{x=x_{k+1}},$$

which is equivalent to

$$\int_{x\in\mathcal{D}_k} \frac{\partial}{\partial t} f_j^W(x,t)\phi_r^k(x)\,\mathrm{d}x = \int_{x\in\mathcal{D}_k} \sum_{i\in\mathcal{S}} f_i^W(x,t)T_{ij}\phi_r^k(x)\,\mathrm{d}x + \int_{x\in\mathcal{D}_k} f_j^W(x,t)c_j\frac{\mathrm{d}}{\mathrm{d}x}\phi_r^k(x)\,\mathrm{d}x - [f_j(x,t)c_j\phi_r^k(x)]_{x=x_k}^{x=x_{k+1}}. \tag{2.3}$$

Now, $f_j^W(x,t)\in W$ so, on $\mathcal{D}_k$, it can be expressed as $\boldsymbol{a}_j^k(t)\boldsymbol{\phi}^k(x)'$, which we now substitute into (2.3) and repeat this for all test functions $\phi_r^k(x)$, $r = 1,...,N_k$, to get the following system of equations,

$$\int_{x\in\mathcal{D}_k} \frac{\mathrm{d}}{\mathrm{d}t}\boldsymbol{a}_j^k(t)\boldsymbol{\phi}^k(x)'\boldsymbol{\phi}^k(x)\,\mathrm{d}x = \int_{x\in\mathcal{D}_k}\sum_{i\in\mathcal{S}}\boldsymbol{a}_i^k(t)\boldsymbol{\phi}^k(x)'T_{ij}\boldsymbol{\phi}^k(x)\,\mathrm{d}x + \int_{x\in\mathcal{D}_k}\boldsymbol{a}_j^k(t)\boldsymbol{\phi}^k(x)'c_j\frac{\mathrm{d}}{\mathrm{d}x}\boldsymbol{\phi}^k(x)\,\mathrm{d}x - c_j[f_j(x,t)\boldsymbol{\phi}^k(x)]_{x=x_k}^{x=x_{k+1}}, \quad k\in\mathbb{Z}. \tag{2.4}$$

2.1.3 Mass, Stiffness, and Flux

For $k \in \mathbb{Z}$, define local *mass* and *stiffness* matrices $\boldsymbol{M}_k$ and $\boldsymbol{G}_k$ by

$$\boldsymbol{M}_k := \int_{x \in \mathcal{D}_k} \boldsymbol{\phi}^k(x)' \boldsymbol{\phi}^k(x) \, \mathrm{d}x, \quad \boldsymbol{G}_k := \int_{x \in \mathcal{D}_k} \boldsymbol{\phi}^k(x)' \frac{\mathrm{d}}{\mathrm{d}x} \boldsymbol{\phi}^k(x) \, \mathrm{d}x.$$

We can write (2.4) as

$$\frac{\mathrm{d}}{\mathrm{d}t} \boldsymbol{a}_j^k(t) \boldsymbol{M}_k = \sum_{i \in \mathcal{S}} \boldsymbol{a}_i^k(t) M_k T_{ij} + c_j \boldsymbol{a}_j^k(t) \boldsymbol{G}_k - c_j [f_j(x,t) \boldsymbol{\phi}^k(x)]_{x=x_k}^{x=x_{k+1}}. \tag{2.5}$$

It remains to approximate the *flux*, $f_j(x,t)$ at the cell edges x_k, $k \in \mathbb{Z}$, so that we may evaluate the terms $[f_j(x,t)\phi_r^k(x)]_{x=x_k}^{x=x_{k+1}}$, $r = 1, ..., N_k$, $k \in \mathbb{Z}$. This is the key for DG – it joins the local approximations on each cell $\mathcal{D}_k$, into a global approximation on the whole domain of approximation. The flux is the instantaneous rate (with respect to time) at which density moves across the boundaries x_k, $k \in \mathbb{Z}$. There are different choices for the flux, and we refer the reader to (Cockburn 1999, Hesthaven & Warburton 2007), and references therein, for some discussion of the topic. Here, we choose the *upwind* scheme, which, as we shall see, closely resembles the flux terms from the generator $\mathbb{B}$. The approximate flux, also known as the *numerical flux*, is given by

$$f_j^*(x,t) = sign(c_j) \lim_{\varepsilon \to 0^+} u_j(x - \varepsilon c_j, t),$$

at each $x = x_k$, $k \in \mathbb{Z}$. Intuitively, the upwind flux takes the value of the density immediately on the upwind side of each x_k.

Denote by x^- and x^+ the left and right limits at x, respectively. Assume first $c_j > 0$, then

$$\begin{aligned}
-c_j [f_j(x,t)\phi_r^k(x)]_{x=x_k}^{x=x_{k+1}} &\approx -c_j [f_j^*(x,t)\phi_r^k(x)]_{x=x_k}^{x=x_{k+1}} \\
&= -c_j f_j^*(x_{k+1},t)\phi_r^k(x_{k+1}) + c_j f_j^*(x_k,t)\phi_r^k(x_k) \\
&= -c_j u_j(x_{k+1}^-,t)\phi_r^k(x_{k+1}) + c_j u_j(x_k^-,t)\phi_r^k(x_k) \\
&= -c_j u_j^k(x_{k+1}^-,t)\phi_r^k(x_{k+1}) + c_j u_j^{k-1}(x_k^-,t)\phi_r^k(x_k) \\
&= -c_j \boldsymbol{a}_j^k(t)\boldsymbol{\phi}^k(x_{k+1}^-)'\phi_r^k(x_{k+1}) + c_j \boldsymbol{a}_j^{k-1}(t)\boldsymbol{\phi}^{k-1}(x_k^-)'\phi_r^k(x_k).
\end{aligned}$$

In matrix form,

$$\begin{aligned}
-c_j [f_j(x,t)\boldsymbol{\phi}^k(x)]_{x=x_k}^{x=x_{k+1}} &\approx -c_j [f_j^*(x,t)\boldsymbol{\phi}^k(x)]_{x=x_k}^{x=x_{k+1}} \\
&= -c_j \boldsymbol{a}_j^k(t)\boldsymbol{\phi}^k(x_{k+1}^-)'\boldsymbol{\phi}^k(x_{k+1}) + c_j \boldsymbol{a}_j^{k-1}(t)\boldsymbol{\phi}^{k-1}(x_k^-)'\boldsymbol{\phi}^k(x_k) \\
&= c_j \boldsymbol{a}_j^k(t) F_j^{k,k} + c_j \boldsymbol{a}_j^{k-1}(t) F_j^{k-1,k},
\end{aligned}$$

where, for $j \in \mathcal{S}$ with $c_j > 0$, we define $\boldsymbol{F}_j^{k,k} := -\boldsymbol{\phi}^k(x_{k+1}^-)'\boldsymbol{\phi}^k(x_{k+1})$, $k \in \mathbb{Z}$ and $\boldsymbol{F}_j^{k-1,k} := \boldsymbol{\phi}^{k-1}(x_k^-)'\boldsymbol{\phi}^k(x_k)$, $k \in \mathbb{Z}$.

Now proceed similarly for $c_j < 0$ to get the approximation

$$\begin{aligned} -c_j[f_j(x,t)\boldsymbol{\phi}^k(x)]_{x=x_k}^{x=x_{k+1}} &\approx -c_j[f_j^*(x,t)\boldsymbol{\phi}^k(x)]_{x=x_k}^{x=x_{k+1}} \\ &= -c_j\boldsymbol{a}_j^{k+1}(t)\boldsymbol{\phi}^{k+1}(x_{k+1}^+)'\boldsymbol{\phi}^k(x_{k+1}) + c_j\boldsymbol{a}_j^k(t)\boldsymbol{\phi}^k(x_k^+)'\boldsymbol{\phi}^k(x_k) \\ &= c_j\boldsymbol{a}_j^{k+1}(t)\boldsymbol{F}_j^{k+1,k} + c_j\boldsymbol{a}_j^k(t)\boldsymbol{F}_j^{k,k}, \end{aligned}$$

where, for $j \in \mathcal{S}$ with $c_j < 0$, we define $\boldsymbol{F}_j^{k+1,k} := -\boldsymbol{\phi}^{k+1}(x_{k+1}^+)'\boldsymbol{\phi}^k(x_{k+1})$, $k \in \mathbb{Z}$, and $\boldsymbol{F}_j^{k,k} := \boldsymbol{\phi}^k(x_k^+)'\boldsymbol{\phi}^k(x_k)$, $k \in \mathbb{Z}$.

The matrices $\boldsymbol{F}_j^{k-1,k}$, $\boldsymbol{F}_j^{k,k}$, and $\boldsymbol{F}_j^{k+1,k}$ are the local flux matrices. For convenience, we also define the matrices $\boldsymbol{F}_j^{k,k+1} = 0$ for $c_j < 0$ and $\boldsymbol{F}_j^{k,k-1} = 0$ for $c_j > 0$, $k \in \mathbb{Z}$.

To write this out as a *global* system, define the row-vectors

$$\boldsymbol{a}^k(t) = (\boldsymbol{a}_i^k(t))_{i\in\mathcal{S}}, \quad \boldsymbol{a}(t) = (\boldsymbol{a}^k(t))_{k\in\mathbb{Z}},$$

and the block-diagonal matrix

$$\widetilde{\boldsymbol{M}} = \begin{bmatrix} \ddots & & \\ & \boldsymbol{I}_{N_\mathcal{S}} \otimes \boldsymbol{M}_k & \\ & & \ddots \end{bmatrix},$$

where $N_\mathcal{S} = |\mathcal{S}|$, $\otimes$ is the Kronecker product, and the block-tridiagonal matrix

$$\widetilde{\mathfrak{B}} = \begin{bmatrix} \ddots & \ddots & \ddots & & \\ & \widetilde{\mathfrak{B}}^{k,k-1} & \widetilde{\mathfrak{B}}^{k,k} & \widetilde{\mathfrak{B}}^{k,k+1} & \\ & & \ddots & \ddots & \ddots \end{bmatrix},$$

where, for $k \in \mathbb{Z}$,

$$\widetilde{\mathfrak{B}}^{kk} = \begin{bmatrix} T_{11}\boldsymbol{M}_k + c_1(\boldsymbol{F}_1^{kk} + \boldsymbol{G}_k) & T_{12}\boldsymbol{M}_k & T_{1N_\mathcal{S}}\boldsymbol{M}_k \\ T_{21}\boldsymbol{M}_k & & \\ \vdots & \ddots & \vdots \\ & & T_{N_\mathcal{S}-1,N_\mathcal{S}}\boldsymbol{M}_k \\ T_{N_\mathcal{S}1}\boldsymbol{M}_k & T_{N_\mathcal{S},N_\mathcal{S}-1}\boldsymbol{M}_k & T_{N_\mathcal{S},N_\mathcal{S}}\boldsymbol{M}_k + c_{N_\mathcal{S}}(\boldsymbol{F}_{N_\mathcal{S}}^{kk} + \boldsymbol{G}_k) \end{bmatrix},$$

$$\widetilde{\mathfrak{B}}^{k,k+1} = \begin{bmatrix} c_1\boldsymbol{F}_1^{k,k+1} & & \\ & \ddots & \\ & & c_{N_\mathcal{S}}\boldsymbol{F}_{N_\mathcal{S}}^{k,k+1} \end{bmatrix},$$

$$\widetilde{\mathfrak{B}}^{k,k-1} = \begin{bmatrix} c_1 \boldsymbol{F}_1^{k,k-1} & & \\ & \ddots & \\ & & c_{N_{\mathcal{S}}} \boldsymbol{F}_{N_{\mathcal{S}}}^{k,k-1} \end{bmatrix}.$$

The matrices $\widetilde{\mathfrak{B}}^{k\ell}$ are defined by sub-blocks; denote these sub-blocks by $\widetilde{\mathfrak{B}}_{ij}^{k\ell}$:

$$\widetilde{\mathfrak{B}}_{ij}^{kk} = \begin{cases} T_{ij}\boldsymbol{M}_k + c_i(\boldsymbol{F}_i^{kk} + \boldsymbol{G}_k) & i = j, \\ T_{ij}\boldsymbol{M}_k & i \neq j, \end{cases}$$

$$\widetilde{\mathfrak{B}}_{ij}^{k\ell} = \begin{cases} c_i \boldsymbol{F}_i^{k\ell} & i = j, \\ 0 & i \neq j, \end{cases} \quad \ell \in \{k-1, k\}.$$

The global system of equations is

$$\frac{\mathrm{d}}{\mathrm{d}t}\boldsymbol{a}(t)\widetilde{\boldsymbol{M}} = \boldsymbol{a}(t)\widetilde{\mathfrak{B}}. \tag{2.6}$$

2.1.4 Boundary conditions

To enable computation, this numerical approximation has to take place on a finite interval, which means we must consider a bounded domain and specify boundary conditions. Recall from Section 1.1.2 that we wish to impose a regulated boundary at $x = 0$. To apply the DG method, we must truncate the state space of the first fluid at some finite interval upper bound, $[0, \mathcal{I}]$, for some $\mathcal{I} < \infty$, and specify the boundary behaviour at $x = \mathcal{I}$. Here we consider $\mathcal{I}$ to be a regulated boundary. Let us denote the doubly-bounded fluid level by $\overline{X}_t$. Ultimately, we wish to approximate a fluid-fluid queue where the first fluid level, X_t, is bounded below at 0, only. Thus, the first step in the approximation scheme is to approximate X_t by $\overline{X}_t$. The truncation of X_t to $\overline{X}_t$ will result in an artificial point mass at the upper bound, which we have to address properly. It is important to choose an $\mathcal{I}$ sufficiently large to control the error induced by the artificial upper bound, however, with larger $\mathcal{I}$ there comes increased computational burden. We shall further comment on this in Section **??**, where we report our numerical experiments.

Let $[0, \mathcal{I}]$ be the domain of the approximation, where $\mathcal{I} < \infty$, and assume there is a regulated boundary for $\{\overline{X}_t\}$ at $x = \mathcal{I}$. We partition the space $[0, \mathcal{I}]$ into $\mathcal{D}_\nabla = \{0\}$, $\mathcal{D}_\Delta = \{\mathcal{I}\}$, and K non-trivial intervals, $\mathcal{D}_k = [x_k, x_{k+1}] \setminus \{\{0\} \cup \{\mathcal{I}\}\}$, $x_k < x_{k+1}$, $k = 1, ..., K$, $x_1 = 0$, $x_{K+1} = \mathcal{I}$ and define $h_k := x_{k+1} - x_k$. The notation Δ refers to quantities and sets which are relevant to the boundary at $\mathcal{I}$.

For states with $c_i \leq 0$, there is the possibility of point mass accumulating at the boundary at 0. Denote these point masses by $q_{\nabla,i}(t)$ for $i \in \mathcal{S}_\nabla$. For states with $c_i > 0$ there is no possibility of a point mass at 0. Similarly, for $c_i \geq 0$ there is the possibility of a point mass at $\mathcal{I}$. Denote these point masses by $q_{\Delta,i}(t)$, for $i \in \mathcal{S}_\Delta$. For states

with $c_i < 0$ there is no possibility of a point mass at $\mathcal{I}$. Let $\boldsymbol{q}_\nabla(t) = (q_{\nabla,i}(t))_{i\in\mathcal{S}_\nabla}$ and $\boldsymbol{q}_\Delta(t) = (q_{\Delta,i}(t))_{i\in\mathcal{S}_\Delta}$ and $\boldsymbol{f}_m(x,t) = (f_i(x,t))_{i\in\mathcal{S}_m}$, $m \in \{+,-,0\}$.

Let us first consider the boundary at $X_t = 0$. Bean & O'Reilly (2014) show the following boundary conditions describe the evolution of probability/density of a stochastic fluid model with a regulated boundary at 0;

$$\frac{\mathrm{d}}{\mathrm{d}t}\boldsymbol{q}_\nabla(t) = \boldsymbol{q}_\nabla(t)T_{\nabla\nabla} - \boldsymbol{f}_\nabla(0,t)C_\nabla, \tag{2.7}$$

$$\boldsymbol{q}_\nabla(t)T_{\nabla+} = \boldsymbol{f}_+(0,t)C_+. \tag{2.8}$$

Equation (2.7) states that point mass moves between phases according to the sub-generator matrix $T_{\nabla\nabla}$, and that the flux of probability density into the point masses is $-\boldsymbol{f}_\nabla(0,t)C_\nabla$. Substituting the DG approximation for $\boldsymbol{f}_\nabla(0,t)$ into (2.7) gives, for $j \in \mathcal{S}_\nabla$,

$$\frac{\mathrm{d}}{\mathrm{d}t}q_{\nabla,j}(t) = \sum_{i\in\mathcal{S}_\nabla} q_{\nabla,i}(t)T_{ij} - \boldsymbol{a}_j^1(t)\boldsymbol{\phi}^1(0)'c_j.$$

Equation (2.8) describes the flux of probability mass to density upon a transition from a phase in $\mathcal{S}_\nabla$ to a phase in $\mathcal{S}_+$. Thus, the flux into the left-hand edge of $\mathcal{D}_1$ in phase $j \in \mathcal{S}_+$ is, $\sum_{i\in\mathcal{S}_\nabla} q_{\nabla,i}(t)T_{ij}$. Therefore, we can now evaluate

$$\begin{aligned}
-c_j[f_j(x,t)\boldsymbol{\phi}^1(x)]_{x=0}^{x=x_1} &= -c_j f_j(x_1,t)\boldsymbol{\phi}^1(x_1) + c_j f_j(0,t)\boldsymbol{\phi}^1(0)\\
&\approx -c_j(f_j^*(x_1,t)\boldsymbol{\phi}^1(x_1) + \sum_{i\in\mathcal{S}_\nabla} q_{\nabla,i}(t)T_{ij}\boldsymbol{\phi}^1(0)\\
&= c_j\boldsymbol{a}_j^1(t)F_j^{1,1} + \sum_{i\in\mathcal{S}_\nabla} q_{\nabla,i}(t)T_{ij}\boldsymbol{\phi}^1(0),
\end{aligned}$$

for $i \in \mathcal{S}_+$. Thus, the DG approximation of the flux into point masses $q_{\nabla,j}(t)$ is $-\boldsymbol{a}_j^1(t)\boldsymbol{\phi}^1(0)'c_j$, $j \in \mathcal{S}_-$, the rate of transition of point mass within $\boldsymbol{q}_\nabla(t)$ is $T_{\nabla\nabla}$, and the DG approximation of the transition of point mass to density is $\sum_{i\in\mathcal{S}_\nabla} q_{\nabla,i}(t)T_{ij}\boldsymbol{\phi}^1(0)$, $j \in \mathcal{S}_+$.

Similarly, for the boundary at $X_t = \mathcal{I}$ the boundary conditions are

$$\begin{aligned}
\frac{\mathrm{d}}{\mathrm{d}t}\boldsymbol{q}_\Delta(t) &= \boldsymbol{q}_\Delta(t)T_{\Delta\Delta} + \boldsymbol{f}_\Delta(\mathcal{I},t)C_\Delta,\\
\boldsymbol{q}_\Delta(t)T_{\Delta-} &= -\boldsymbol{f}_-(\mathcal{I},t)C_-.
\end{aligned}$$

Using the same arguments as above,

$$\frac{\mathrm{d}}{\mathrm{d}t}q_{\Delta,j}(t) = \sum_{i\in\mathcal{S}_\Delta} q_{\Delta,i}(t)T_{ij} + \boldsymbol{a}_j^K(t)\boldsymbol{\phi}^K(\mathcal{I})'c_j,$$

$$-c_j[f_j(x,t)\boldsymbol{\phi}^K(x)]_{x=x_K}^{x=\mathcal{I}} \approx c_j \boldsymbol{a}_j^K(t) F_j^{K,K} + \sum_{i\in\mathcal{S}_\Delta} q_{\Delta,i}(t) T_{ij} \boldsymbol{\phi}^K(\mathcal{I}),$$

for $j \in \mathcal{S}_\Delta$. Thus, the DG approximation of the flux into the point mass $q_{\Delta,j}(t)$ is $\boldsymbol{a}_j^K(t)\boldsymbol{\phi}^K(0)' c_j$, $j \in \mathcal{S}_+$, the rate of transition of point mass within $\boldsymbol{q}_\Delta(t)$ is $T_{\Delta\Delta}$, and the DG approximation of the transition of point mass to density is $\sum_{i\in\mathcal{S}_\Delta} q_{\Delta,i}(t) T_{ij} \boldsymbol{\phi}^K(\mathcal{I})$, $j \in \mathcal{S}_-$.

To include this behaviour in the DG generator we truncate the doubly-infinite matrix $\widetilde{\mathfrak{B}}$ at $k = 1$ and $k = K$, then append $|\mathcal{S}_\nabla|$ rows and columns to the top and left, and $|\mathcal{S}_\Delta|$ rows and columns to the bottom and right. These represent the point masses $\boldsymbol{q}_\nabla(t)$ and $\boldsymbol{q}_\Delta(t)$, respectively. Given the discussion above, the truncated matrix is

$$\widehat{\mathfrak{B}} = \begin{bmatrix} \boldsymbol{T}_{\nabla\nabla} & \widetilde{\mathfrak{B}}^{\nabla 1} & & & & & \\ \widetilde{\mathfrak{B}}^{1\nabla} & \widetilde{\mathfrak{B}}^{11} & \widetilde{\mathfrak{B}}^{12} & & & & \\ & \widetilde{\mathfrak{B}}^{21} & \widetilde{\mathfrak{B}}^{22} & \widetilde{\mathfrak{B}}^{23} & & & \\ & & \ddots & \ddots & \ddots & & \\ & & \widetilde{\mathfrak{B}}^{K-1,K-2} & \widetilde{\mathfrak{B}}^{K-1,K-1} & \widetilde{\mathfrak{B}}^{K-1,K} & & \\ & & & \widetilde{\mathfrak{B}}^{K,K-1} & \widetilde{\mathfrak{B}}^{K,K} & \widetilde{\mathfrak{B}}^{K,\Delta} & \\ & & & & \widetilde{\mathfrak{B}}^{\Delta,K} & \boldsymbol{T}_{\Delta\Delta} \end{bmatrix},$$

where $\widetilde{\mathfrak{B}}^{\nabla 1} := \boldsymbol{T}_{\nabla+} \otimes \boldsymbol{\phi}^1(0)$, $\widetilde{\mathfrak{B}}^{1\nabla} := -\mathrm{diag}(c_i \mathbb{1}_{(c_i<0)})_{i\in\mathcal{S}} \otimes \boldsymbol{\phi}^1(0)'$, $\widetilde{\mathfrak{B}}^{\Delta K} := \boldsymbol{T}_{\Delta-} \otimes \boldsymbol{\phi}^K(\mathcal{I})$ and $\widetilde{\mathfrak{B}}^{K,\Delta} := \mathrm{diag}(c_i \mathbb{1}_{(c_i>0)})_{i\in\mathcal{S}} \otimes \boldsymbol{\phi}^K(\mathcal{I})'$, and $\otimes$ is the Kronecker product. Where we have used the same sub-block notation as we have for $\widetilde{\mathfrak{B}}$.

After the addition of the boundary conditions, the system of ODEs (2.6) can now be written as

$$\frac{\mathrm{d}}{\mathrm{d}t}\begin{bmatrix}\boldsymbol{q}_\nabla(t) & \boldsymbol{a}(t) & \boldsymbol{q}_\Delta(t)\end{bmatrix} = \begin{bmatrix}\boldsymbol{q}_\nabla(t) & \boldsymbol{a}(t) & \boldsymbol{q}_\Delta(t)\end{bmatrix} \widehat{\mathfrak{B}}\widehat{\boldsymbol{M}}^{-1}, \tag{2.9}$$

where $\widehat{\boldsymbol{M}} = \begin{bmatrix} \boldsymbol{I}_{|\mathcal{S}_\nabla|} & & & & \\ & \boldsymbol{I}_{N_S} \otimes \boldsymbol{M}_1 & & & \\ & & \ddots & & \\ & & & \boldsymbol{I}_{N_S} \otimes \boldsymbol{M}_K & \\ & & & & \boldsymbol{I}_{|\mathcal{S}_\Delta|} \end{bmatrix}$. Define $\boldsymbol{B} = \widehat{\mathfrak{B}}\widehat{\boldsymbol{M}}^{-1}$, with the sub-block as we used for $\widetilde{\mathfrak{B}}$.

Regarding our notational convention, the matrices in fraktur fonts (e.g. $\mathfrak{B}$) are intermediary constructions that are not directly referred to for the rest of the paper (but do appear again in the appendix). We use regular mathematics fonts to represent DG approximations to operators, i.e. $\boldsymbol{B}$ is a DG approximation to $\mathbb{B}$ and $\boldsymbol{\Psi}$ is an approximation to Ψ.

We prove the following result in AppendixC.

Corollary 2.1. *The approximate generator* $\boldsymbol{B}$ *conserves probability. That is, for all* $t \geq 0$*,*

$$\sum_{i\in\mathcal{S}_\nabla} q_{\nabla,i}(t) + \sum_{i\in\mathcal{S}_\Delta} q_{\Delta,i}(t) + \sum_{i\in\mathcal{S}} \int_{x\in[0,\mathcal{I}]} u_i(x,t)\,\mathrm{d}x$$
$$= \sum_{i\in\mathcal{S}_\nabla} q_{\nabla,i}(0) + \sum_{i\in\mathcal{S}_\Delta} q_{\Delta,i}(0) + \sum_{i\in\mathcal{S}} \int_{x\in[0,\mathcal{I}]} u_i(x,0)\,\mathrm{d}x.$$

2.1.5 Putting it all together

Recall that the ultimate goal for our DG approximation is to approximate the operator $\mathbb{B}$. We have that $\boldsymbol{B}^{k\ell}$ is an approximation to $\mathbb{B}^{k\ell}$, $k,\ell \in \{\nabla, 1, ..., K, \Delta\}$.

Given we have now truncated the space and added boundaries, let us define $\mathcal{M}_{0,\mathcal{I}}$ as the set of measures, μ_i, which admit an absolutely continuous density on $(0,\mathcal{I})$, may have a point mass at $x = 0$ if $i \in \mathcal{S}_\nabla$, and another at $x = \mathcal{I}$ if $i \in \mathcal{S}_\Delta$. The set $\mathcal{M}_{0,\mathcal{I}}$ is the domain of the operator $\mathbb{B}$ truncated to the interval $[0,\mathcal{I}]$ with regulated boundaries at $x = 0$ and $x = \mathcal{I}$. Also, redefine $\mathcal{K}_i^m = \{k \in \{\nabla, 1, ..., K, \Delta\} \mid l(\mathcal{D}_k \cap \mathcal{F}_i^m) = l(\mathcal{D}_k)\}$ for $i \in \mathcal{S}, m \in \{+,-,0\}$ for all $l \in \mathcal{M}_{0,\mathcal{I}}$.

Approximations $\boldsymbol{B}_{ij}^{mn}$, $\boldsymbol{B}_{ij}$, and $\boldsymbol{B}^{mn}$ to $\mathbb{B}_{ij}^{mn}$, $\mathbb{B}_{ij}$, and $\mathbb{B}^{mn}$, $i,j \in \mathcal{S}$, $m,n \in \{+,-,0\}$, are constructed from the block-matrices $\boldsymbol{B}_{ij}^{k\ell}$, $i,j \in \mathcal{S}$, $k,\ell \in \{\nabla, 1, \ldots, K, \Delta\}$, as

$$\boldsymbol{B}_{ij}^{mn} = \left[\boldsymbol{B}_{ij}^{k\ell}\right]_{k\in\mathcal{K}_i^m,\ell\in\mathcal{K}_j^n}, \quad i,j \in \mathcal{S},\ m,n \in \{+,-,0\},$$
$$\boldsymbol{B}_{ij} = \left[\boldsymbol{B}_{ij}^{k\ell}\right]_{k,\ell\in\{\nabla,1,\ldots,K,\Delta\}}, \ i,j \in \mathcal{S},$$
$$\boldsymbol{B}^{mn} = \left[\left[\boldsymbol{B}_{ij}^{k\ell}\right]_{i\in\mathcal{S}_k^m, j\in\mathcal{S}_\ell^n}\right]_{k\in\mathcal{K}^m,\ell\in\mathcal{K}^n}, \ m,n \in \{+,-,0\}.$$

2.2 Application to an SFFM

Given our approximation $\boldsymbol{B}$ to the generator $\mathbb{B}$ we now follow the recipe from (Bean & O'Reilly 2014), replacing the actual generator $\mathbb{B}$ with its approximation $\boldsymbol{B}$, to construct approximations, $\boldsymbol{\pi}$ and $\boldsymbol{p}$, to the stationary operators, $\mathbb{\pi}$ and $\mathbb{p}$.

It may be convenient to think of our approximations in terms of approximations of kernels. Recall that the operators in (Bean & O'Reilly 2014) can be thought of in terms of kernels. That is, for some function $\boldsymbol{g} = (g_i(x))_{i\in\mathcal{S}}$, we can write $\boldsymbol{\mu}\mathbb{B}\boldsymbol{g}' = \sum_{k,\ell\in\{\nabla,1,\ldots,K,\Delta\}} \sum_{i,j\in\mathcal{S}} \int_{x,y} \mathrm{d}\mu_i(x)\mathbb{B}_{ij}^{k\ell}(x,\mathrm{d}y)g_j(y)$ where $\mathbb{B}_{ij}^{k\ell}(x,\mathrm{d}y)$ is the kernel of the operator $\mathbb{B}_{ij}^{k\ell}$.

Let $\boldsymbol{a}^\nabla(t) := \boldsymbol{q}_\nabla(t)$ and $\boldsymbol{a}^\Delta(t) := \boldsymbol{q}_\Delta(t)$, and define basis functions $\boldsymbol{\phi}^\nabla(x) = \phi_1^\nabla(x) = \delta(x)$ and $\boldsymbol{\phi}^\Delta(x) = \phi_1^\Delta(x) = \delta(x-\mathcal{I})$, where δ is the Dirac delta function, $N_\nabla = N_\Delta = 1$,

and $\mathcal{N}_\nabla = \mathcal{N}_\Delta = \{1\}$. Also define $\widehat{M}_\nabla = I_{|\mathcal{S}_\nabla|}$ and $\widehat{M}_\Delta = I_{|\mathcal{S}_\Delta|}$ and row-vectors

$$\boldsymbol{\phi}(x) = (\boldsymbol{\phi}^k(x))_{k\in\{\nabla,1,\ldots,K,\Delta\}}, \quad \boldsymbol{a}_i(t) = (\boldsymbol{a}_i^k(t))_{k\in\{\nabla,1,\ldots,K,\Delta\}},\ i \in \mathcal{S}.$$

To pose the approximation $\mathbb{B}$ in kernel form let $\boldsymbol{a}_i\boldsymbol{\phi}(x)' \in W$, $i \in \mathcal{S}$ be the initial density of the process, and $\boldsymbol{\phi}(x)\boldsymbol{b}_i' \in W$, $i \in \mathcal{S}$ be a test function. Observe that, from our DG construction earlier and the definition of $\widehat{\boldsymbol{M}}$,

$$\sum_{i,j\in\mathcal{S}} \int_{x,y\in[0,\mathcal{I}]} \boldsymbol{a}_i\boldsymbol{\phi}(x)'\boldsymbol{\phi}(x)\,\mathrm{d}x\widehat{\boldsymbol{M}}^{-1}\boldsymbol{B}_{ij}\boldsymbol{\phi}(y)'\boldsymbol{\phi}(y)\boldsymbol{b}_j\,\mathrm{d}y = \sum_{i,j\in\mathcal{S}} \boldsymbol{a}_i\boldsymbol{B}_{ij}\widehat{\boldsymbol{M}}\boldsymbol{b}_j.$$

Thus, we can think of

$$\boldsymbol{\phi}(x)\widehat{\boldsymbol{M}}^{-1}\boldsymbol{B}_{ij}\boldsymbol{\phi}(y)'\,\mathrm{d}y,$$

as an approximation to the kernel $\mathbb{B}_{ij}(x,\,\mathrm{d}y)$. This concept can be extended to all the approximations of operators considered in this work.

2.2.1 Approximating the operator $\mathbb{R}$

Recall the operator $\mathbb{R}^k$ from Lemma 1.3. Essentially, the operator $\mathbb{R}^k$ takes an initial measure $\boldsymbol{\mu}^k$ and multiplies each element by $1/|r_i(x)|$ on cells $\mathcal{D}_k$ where $r_i(x) \neq 0$. In the context of DG the initial distribution is given by $\boldsymbol{a}_i\boldsymbol{\phi}(x)' \in W$, $i \in \mathcal{S}$. Thus, for $k \in \{\nabla, 1, ..., K, \Delta\}$ such that $r_i(x) \neq 0$ on $\mathcal{D}_k$, we have

$$\boldsymbol{a}_i^k\boldsymbol{\phi}^k(x)'\mathbb{R}_i^k = \frac{\boldsymbol{a}_i^k\boldsymbol{\phi}^k(x)'}{|r_i(x)|}.$$

Decompose the right-hand side into a component which lies in W and another orthogonal to W:

$$\frac{\boldsymbol{a}_i^k\boldsymbol{\phi}^k(x)'}{|r_i(x)|} = \boldsymbol{\rho}_i^k\boldsymbol{\phi}^k(x)' + g_i^\perp(x),$$

where $\boldsymbol{\rho}_i^k\boldsymbol{\phi}^k(x)' \in W$, $g_i^\perp \in W^\perp$. Now, multiply by test functions $\{\phi_r^k(x)\}_{r=1}^{N_k}$ and integrate over $[0,\mathcal{I}]$:

$$\begin{aligned}\boldsymbol{a}_i^k \int_{x\in[0,\mathcal{I}]} \frac{\boldsymbol{\phi}^k(x)'\boldsymbol{\phi}^k(x)}{|r_i(x)|}\mathrm{d}x &= \boldsymbol{\rho}_i^k \int_{x\in[0,\mathcal{I}]} \boldsymbol{\phi}^k(x)'\boldsymbol{\phi}^k(x)\,\mathrm{d}x + \int_{x\in[0,\mathcal{I}]} g_i^\perp(x)\boldsymbol{\phi}^k(x)\,\mathrm{d}x \\ &= \boldsymbol{\rho}_i^k \int_{x\in[0,\mathcal{I}]} \boldsymbol{\phi}^k(x)'\boldsymbol{\phi}^k(x)\,\mathrm{d}x = \boldsymbol{\rho}_i^k\boldsymbol{M}_k,\end{aligned}$$

since $g_i(x)^\perp \in W^\perp$. Define the matrix $\boldsymbol{M}_k^r := \int_{x\in[0,\mathcal{I}]} \frac{\boldsymbol{\phi}^k(x)'\boldsymbol{\phi}^k(x)}{|r_i(x)|}\mathrm{d}x$, then $\boldsymbol{a}_i^k\boldsymbol{M}_k^r = \boldsymbol{\rho}_i^k M_k$, which implies $\boldsymbol{\rho}_i^k = \boldsymbol{a}_i^k\boldsymbol{M}_k^r\boldsymbol{M}_k^{-1}$. Thus, we have the approximation

$$\boldsymbol{a}_i^k\boldsymbol{\phi}^k(x)'\mathbb{R}_i^k = \frac{\boldsymbol{a}_i^k\boldsymbol{\phi}^k(x)'}{|r_i(x)|} \approx \boldsymbol{a}_i^k\boldsymbol{M}_k^r\boldsymbol{M}_k^{-1}\boldsymbol{\phi}^k(x)'.$$

Since $\boldsymbol{a}_i^k$ is arbitrary, we see that we approximate $\mathbb{R}_i^k$ by $\boldsymbol{R}_i^k = \boldsymbol{M}_k^r \boldsymbol{M}_k^{-1}$, and $\mathbb{R}^k$ by $\boldsymbol{R}^k = \operatorname{diag}(\boldsymbol{R}_i^k)_{i\in\mathcal{S}_k^\bullet}$.

In practice, we implement a Gauss-Lobatto quadrature approximation to compute the elements of $\boldsymbol{M}_k^r$.

2.2.2 Approximating the operator D and the DG Riccati equation

Recalling Lemma 1.3 and replacing the operators $\mathbb{R}^k$ and $\mathbb{B}^{\ell m}$, by their approximations we have the following approximation to $\mathbb{D}^{mn}(s)$

$$\boldsymbol{D}^{mn}(s) = \left[\boldsymbol{R}^m \left(\boldsymbol{B}^{mn} - s\boldsymbol{I} + \boldsymbol{B}^{m0}\left(\boldsymbol{B}^{00} - s\boldsymbol{I}\right)^{-1}\boldsymbol{B}^{0n}\right)\right], \quad m,n \in \{+,-\}.$$

Let $\boldsymbol{\phi}^k(x)\boldsymbol{M}_k^{-1}\boldsymbol{\Psi}_{ij}^{k\ell}(s)\boldsymbol{\phi}^\ell(y)'\,\mathrm{d}y$, $i,j \in \mathcal{S}$, $k \in \mathcal{K}_i^+, \ell \in \mathcal{K}_j^-$ be a finite-dimensional approximation of the operator kernel $\Psi_{ij}^{k\ell}(s)(x,\,\mathrm{d}y)$, where $\boldsymbol{\Psi}_{ij}^{k\ell}(s)$ is a matrix of constants for a given s. Construct an approximation to $\Psi(s)(x,\,\mathrm{d}y)$ by

$$\boldsymbol{\phi}^+(x)\widehat{\boldsymbol{M}}_+^{-1}\boldsymbol{\Psi}(s)\boldsymbol{\phi}^-(y)'\,\mathrm{d}y = \left[\left[\boldsymbol{\phi}^k(x)M_k^{-1}\boldsymbol{\Psi}_{ij}^{k\ell}(s)\boldsymbol{\phi}^\ell(y)'\,\mathrm{d}y\right]_{i\in\mathcal{S}_k^+, j\in\mathcal{S}_\ell^-}\right]_{k\in\mathcal{K}^+,\ell\in\mathcal{K}^-},$$

where $\boldsymbol{\phi}^+(x) = (\boldsymbol{\phi}^k(x))_{i\in\mathcal{S}_k^+,k\in\mathcal{K}^+}$ and $\boldsymbol{\phi}^-(y) = (\boldsymbol{\phi}^k(y))_{i\in\mathcal{S}_k^-,k\in\mathcal{K}^-}$ are row-vectors, $\boldsymbol{\Psi}(s)$ is a matrix of constants for a given s with the same size as $\boldsymbol{D}^{+-}$, and $\widehat{\boldsymbol{M}}_m$, $m \in \{+,-,0\}$ is a block diagonal matrix $\widehat{\boldsymbol{M}}_m = \operatorname{diag}\left((\boldsymbol{M}_k)_{i\in\mathcal{S}_k^m}\right)_{k\in\mathcal{K}^m}$, $m \in \{+,-,0\}$. Now replace the theoretical kernels in Theorem 1.4 by their DG approximations to get

$$\begin{aligned}
&\boldsymbol{\phi}^+(x)\widehat{\boldsymbol{M}}_+^{-1}\boldsymbol{D}^{+-}(s)\boldsymbol{\phi}^-(y)'\,\mathrm{d}y \\
&+ \int_{z_1,z_2} \boldsymbol{\phi}^+(x)\widehat{\boldsymbol{M}}_+^{-1}\boldsymbol{\Psi}(s)\boldsymbol{\phi}^-(z_1)'\boldsymbol{\phi}^-(z_1)\widehat{\boldsymbol{M}}_-^{-1}\boldsymbol{D}^{-+}(s)\boldsymbol{\phi}^+(z_2)\boldsymbol{\phi}^+(z_2)\widehat{\boldsymbol{M}}_+^{-1}\boldsymbol{\Psi}(s)\boldsymbol{\phi}^-(y)'\,\mathrm{d}z_1\,\mathrm{d}z_2\,\mathrm{d}y \\
&+ \int_{z_1} \boldsymbol{\phi}^+(x)\widehat{\boldsymbol{M}}_+^{-1}\boldsymbol{D}^{++}(s)\boldsymbol{\phi}^+(z_1)'\boldsymbol{\phi}^+(z_1)\widehat{\boldsymbol{M}}_+^{-1}\boldsymbol{\Psi}(s)\boldsymbol{\phi}^-(y)'\,\mathrm{d}z_1\,\mathrm{d}y \\
&+ \int_{z_1} \boldsymbol{\phi}^+(x)\widehat{\boldsymbol{M}}_+^{-1}\boldsymbol{\Psi}(s)\boldsymbol{\phi}^-(z_1)'\boldsymbol{\phi}^-(z_1)\widehat{\boldsymbol{M}}_-^{-1}\boldsymbol{D}^{--}(s)\boldsymbol{\phi}^-(y)'\,\mathrm{d}z_1\,\mathrm{d}y = 0.
\end{aligned}$$

Multiplying on the left by $\boldsymbol{\phi}^+(x)'$ and on the right by $\boldsymbol{\phi}^-(y)$, integrating over both x and y, then post-multiplying by $\widehat{\boldsymbol{M}}_-^{-1}$ gives the following matrix Ricatti equation

$$\boldsymbol{D}^{+-}(s) + \boldsymbol{\Psi}(s)\boldsymbol{D}^{-+}(s)\boldsymbol{\Psi}(s) + \boldsymbol{D}^{++}(s)\boldsymbol{\Psi}(s) + \boldsymbol{\Psi}(s)\boldsymbol{D}^{--}(s) = 0. \tag{2.10}$$

Thus, we may find $\boldsymbol{\Psi}(s)$ by solving (2.10), using one of the methods in (Bean et al. 2009*a*). Here, we use the Newtons method.

Given the stochastic interpretation of $\Psi(0)$ we know that $\nu\Psi(0)([0,\infty)) = 1$ for every vector of measures ν such that $\nu([0,\infty)\mathbf{1} = 1$, when an SFFM is recurrent. It appears that this result carries over to the matrix $\mathbf{\Psi}(0)$ giving the property that $\int_{y\in[0,\mathcal{I}]} \mathbf{\Psi}(0)\boldsymbol{\phi}^-(y)'\,\mathrm{d}y = \mathbf{1}$. However, we have only observed this numerically and have no proof of this property.

2.2.3 Putting it all together: constructing an approximation to the stationary distribution

We find an approximation to the stationary distribution by replacing the theoretical operators in Theorem 1.5 with their approximations. Table 2.1 defines the notation we use for the DG approximations to stationary operators.

Exact operator	Operator indices	Approximation notation	Approximations
$\mathbb{f}_i^k$	$i \in \mathcal{S}_k^-$, $k \in \mathcal{K}^-$	$\boldsymbol{\xi}_i^k := (\xi_{i,r}^k)_{r\in\mathcal{N}_k}$	$\mathbb{f}_i^k(\,\mathrm{d}x) \approx \boldsymbol{\xi}_i^k\boldsymbol{\phi}^k(x)'\,\mathrm{d}x$,
$\mathbb{p}_i^k$	$i \in \mathcal{S}_k^- \cup \mathcal{S}_k^0$, $k \in \bigcup_{m\in\{-,0\}} \mathcal{K}_m$	$\boldsymbol{p}_i^k := (p_{i,r}^k)_{r\in\mathcal{N}_k}$	$\mathbb{p}_i^k(\,\mathrm{d}x) \approx \boldsymbol{p}_i^k\boldsymbol{\phi}^k(x)'\,\mathrm{d}x$
$\mathbb{\pi}_i^k(y)$	$i \in \mathcal{S}$, $k \in \{\nabla, 1, \ldots, K, \Delta\}$	$\boldsymbol{\pi}_i^k(y) := (\pi_{i,r}^k(y))_{r\in\mathcal{N}_k}$	$\mathbb{\pi}_i^k(y)(\,\mathrm{d}x) \approx \boldsymbol{\pi}_i^k(y)\boldsymbol{\phi}^k(x)'\,\mathrm{d}x$

Table 2.1: Notation for the approximation of the stationary operators of an SFFM. The first column contains the operators which we are approximating, the second column contains indices for which the operators are defined, the third column defines the notation we use for the coefficients of the approximation, and the last column defines how the coefficients and basis functions are used to approximate the operators.

With the notation in Table 2.1 define row-vectors

$$\begin{aligned}
\boldsymbol{\xi}^k &:= (\boldsymbol{\xi}_i^k)_{i\in\mathcal{S}_k^-}, \quad k \in \mathcal{K}_i^-,\\
\boldsymbol{\xi} &:= (\boldsymbol{\xi}^k)_{k\in\mathcal{K}^-},\\
\boldsymbol{p}^{k,m} &:= (\boldsymbol{p}_i^k)_{i\in\mathcal{S}_k^m}, \quad k \in \mathcal{K}^m,\, m \in \{-,0\},\\
\boldsymbol{p}^m &:= (\boldsymbol{p}^{k,m})_{k\in\mathcal{K}^m}, \quad m \in \{-,0\},\\
\boldsymbol{p} &:= (\boldsymbol{p}^m)_{m\in\{-,0\}},\\
\boldsymbol{\pi}^{k,m}(y) &:= (\boldsymbol{\pi}_i^k(y))_{i\in\mathcal{S}_k^m}, \quad k \in \{\nabla, 1, \ldots, K, \Delta\},\, m \in \{+,-,0\},\\
\boldsymbol{\pi}^m(y) &:= (\boldsymbol{\pi}^{k,m}(y))_{k\in\mathcal{K}^m}, \quad m \in \{+,-,0\},\\
\boldsymbol{\pi}(y) &:= (\boldsymbol{\pi}^m(y))_{m\in\{+,-,0\}}.
\end{aligned}$$

Proceeding similarly to the derivation of the Ricatti equation (2.10), we can argue that the coefficients $\boldsymbol{\xi}$ are the solution to the matrix system

$$\begin{aligned}\begin{bmatrix}\boldsymbol{\xi} & \mathbf{0}\end{bmatrix}\left(-\begin{bmatrix}\boldsymbol{B}^{--} & \boldsymbol{B}^{-0}\\ \boldsymbol{B}^{0-} & \boldsymbol{B}^{00}\end{bmatrix}\right)^{-1}\begin{bmatrix}\boldsymbol{B}^{-+}\\ \boldsymbol{B}^{0+}\end{bmatrix}\boldsymbol{\Psi}(0) &= \boldsymbol{\xi},\\ \int_{x\in[0,\mathcal{I}]}\boldsymbol{\xi}\begin{bmatrix}\boldsymbol{\phi}^{-}(x)'\\ \boldsymbol{\phi}^{0}(x)'\end{bmatrix}\mathrm{d}x\mathbf{1} &= 1.\end{aligned}$$

Essentially, we replace the theoretical operators in (1.11) and (1.12) with their DG counterparts.

Similarly, the coefficients $\boldsymbol{p}$ are given by

$$\begin{bmatrix}\boldsymbol{p}^{-} & \boldsymbol{p}^{0}\end{bmatrix} = z\begin{bmatrix}\boldsymbol{\xi} & \mathbf{0}\end{bmatrix}\left(-\begin{bmatrix}\boldsymbol{B}^{--} & \boldsymbol{B}^{-0}\\ \boldsymbol{B}^{0-} & \boldsymbol{B}^{00}\end{bmatrix}\right)^{-1}, \tag{2.11}$$

where z is a normalising constant. The coefficients $\boldsymbol{\pi}(y)$ are given by

$$\boldsymbol{\pi}^{0}(y) = \begin{bmatrix}\boldsymbol{\pi}^{+}(y) & \boldsymbol{\pi}^{-}(y)\end{bmatrix}\begin{bmatrix}\boldsymbol{B}^{+0}\\ \boldsymbol{B}^{-0}\end{bmatrix}\left(-\boldsymbol{B}^{00}\right)^{-1}, \tag{2.12}$$

$$\begin{bmatrix}\boldsymbol{\pi}^{+}(y) & \boldsymbol{\pi}^{-}(y)\end{bmatrix} = \begin{bmatrix}\boldsymbol{p}^{-} & \boldsymbol{p}^{0}\end{bmatrix}\begin{bmatrix}\boldsymbol{B}^{-+}\\ \boldsymbol{B}^{0+}\end{bmatrix}\begin{bmatrix}e^{\boldsymbol{K}y} & e^{\boldsymbol{K}y}\boldsymbol{\Psi}(0)\end{bmatrix}\begin{bmatrix}\boldsymbol{R}^{+} & 0\\ 0 & \boldsymbol{R}^{-}\end{bmatrix}, \tag{2.13}$$

$$\sum_{i\in\mathcal{S}}\sum_{k\in\{\nabla,1,\ldots,K,\Delta\}}\int_{y=0}^{\infty}\int_{x\in[0,\mathcal{I}]}\boldsymbol{\pi}_i^k(y)\boldsymbol{\phi}^k(x)'\,\mathrm{d}x\,\mathrm{d}y \tag{2.14}$$

$$+\sum_{i\in\mathcal{S}}\sum_{\ell\in\{-,0\}}\sum_{k\in\mathcal{K}_i^\ell}\int_{x\in[0,\mathcal{I}]}\boldsymbol{p}_i^k\boldsymbol{\phi}^k(x)'\,\mathrm{d}x = 1, \tag{2.15}$$

where $\boldsymbol{K} := \boldsymbol{D}^{++}(0) + \boldsymbol{\Psi}(0)\boldsymbol{D}^{(-+)}(0)$, and z is a normalising constant.

To assist the reader in understanding these constructions and the notation we provide an explicitly worked toy-example in Appendix B.

2.3 A stochastic interpretation of the simplest DG scheme

2.4 Oscillations and slope limiting

Chapter 3

A stochastic modelling approach to approximating fluid queues

In this chapter we develop a new discretisation of a fluid queue using a *quasi-birth-and-death process with rational arrival process components* (QBD-RAP). In the following chapter, Chapter 4 we prove the scheme converges weakly. To improve upon the discretisation of Bean & O'Reilly (2013), we argue that the shift from QBD to QBD-RAP is necessary. The QBD construction of Bean & O'Reilly (2013) uses Erlang distributions to approximate the deterministic time that the fluid queue spends in an interval on the event that the phase is constant – it is well known that the Erlang distribution is the distribution with the smallest variance in the class of Phase-type distributions of a given order Aldous & Shepp (1987), and in this sense is the best approximation to the deterministic behaviour we want to capture.

By choosing a matrix-exponential distribution with sufficiently small variance, the QBD-RAP approximation can be made arbitrarily accurate. Due to its stochastic interpretation, the QBD-RAP discretisation ensures solutions are positive, even when discontinuities are present. Unlike slope limiters and post-hoc filtering, for the QBD-RAP the positivity preserving nature is a property of the discretised operator.

The structure of this chapter is as follows. Section 3.1 motivates the idea using the QBD approximation of Bean & O'Reilly (2014). Sections 3.2 and 3.3 describe the modelling of certain events of the fluid queue with matrix exponential distributions to ultimately construct the behaviour of the QBD-RAP on the event that the QBD-RAP remains in a given level. Section 3.4 describes the dynamics of the construction and also constructs the level process of the QBD-RAP. Section 3.5 deals with modelling boundary behaviour. Section 3.6 describes how to model initial conditions of the fluid queue. Section 3.7 introduces the concept of a *closing operator* which maps the state space of the QBD-RAP to estimates of the density of the fluid queue.

3.1 Inspiration and motivation

The inspiration for our approach stems from the QBD-based discretisation of Bean & O'Reilly (2013). A QBD can be seen as a two dimensional CTMC, $\{(L(t), \phi(t))\}_{t\geq 0}$, where $\{L(t)\}$ is the discrete level, and $\{\phi(t)\}$ is the phase. Bean & O'Reilly (2013) discretise the state space of the fluid into small intervals of width Δ; denote these by $\mathcal{D}_k = [k\Delta, (k+1)\Delta]$. Their approximation captures the dynamics of the phase process exactly, but discretises the level process of the fluid queue. Their approximation supposes that when $L(t) = k$, $\phi(t) = i$, then $X(t) \approx k\Delta$, $\phi(t) = i$.

When in level k and phase i, the approximation sees events at rate $|T_{ii}| + |c_i|\Delta$. Upon an event, with probability $T_{ij}/(|T_{ii}| + |c_i|\Delta)$ a change of phase from i to j is observed and the approximation remains in level k; with probability $|c_i|\Delta/(|T_{ii}| + |c_i|\Delta)$ a change of level occurs, to $k+1$ if $c_i > 0$ and $k-1$ if $c_i < 0$. The generator of their QBD approximation (for an unbounded fluid queue) is

$$\boldsymbol{B} = \begin{bmatrix} \ddots & \ddots & \ddots & \\ \boldsymbol{B}_{-1}(\Delta) & \boldsymbol{B}_0(\Delta) & \boldsymbol{B}_{+1}(\Delta) & \\ & \boldsymbol{B}_{-1}(\Delta) & \boldsymbol{B}_0(\Delta) & \boldsymbol{B}_{+1}(\Delta) \\ & & \ddots & \ddots & \ddots \end{bmatrix}$$

$$\boldsymbol{B}_0 = \boldsymbol{T} - \boldsymbol{C}\Delta, \qquad \boldsymbol{B}_{-1} = \begin{bmatrix} \boldsymbol{0} & & \\ & \boldsymbol{C}_-\Delta & \\ & & \boldsymbol{0} \end{bmatrix}, \qquad \boldsymbol{B}_{+1} = \begin{bmatrix} \boldsymbol{C}_+\Delta & & \\ & \boldsymbol{0} & \\ & & \boldsymbol{0} \end{bmatrix}. \tag{3.1}$$

Bean and O'Reilly then take $\Delta \to 0$ and show that the approximation converges weakly to the fluid queue. It seems that this is the best we can do if we want to keep the interpretation of the approximation as a QBD. We now elaborate on this point.

For a given Δ, the discretisation of Bean and O'Reilly supposes that, when the phase is i and on the event of no change of phase, the sojourn time in a given level has an exponential distribution with rate $|c_i|\Delta$. However, the corresponding sojourn time of the fluid queue is deterministic: given $X(t) = x \in \mathcal{D}_k$, then $\{X(t)\}$ will leave $\mathcal{D}_k$ in exactly $((k+1)\Delta - x)/|c_i|$ units of time if $c_i > 0$, and $(x - k\Delta)/|c_i|$ units of time if $c_i < 0$, on the event that the phase does not change before this time. We can extend the QBD model of Bean and O'Reilly to model this determinism more accurately by supposing that the sojourn times in each interval have Erlang distributions (rather than exponential). However, we effectively realise the same QBD approximation as the original, but on a finer discretisation. For example, using Erlang distributions of order 2 we would get a

generator of the QBD approximation

$$\boldsymbol{B} = \begin{bmatrix} \ddots & \ddots & \ddots & \\ \boldsymbol{B}_{-1}(\Delta) & \boldsymbol{B}_0(\Delta) & \boldsymbol{B}_{+1}(\Delta) & \\ & \boldsymbol{B}_{-1}(\Delta) & \boldsymbol{B}_0(\Delta) & \boldsymbol{B}_{+1}(\Delta) \\ & \ddots & \ddots & \ddots \end{bmatrix}$$

$$\boldsymbol{B}_0 = \boldsymbol{T} \otimes I_2 - \begin{bmatrix} \begin{bmatrix} -\Delta/2 & \Delta/2 \\ 0 & -\Delta/2 \end{bmatrix} \otimes \boldsymbol{C}_+ & & \\ & \begin{bmatrix} -\Delta/2 & 0 \\ \Delta/2 & -\Delta/2 \end{bmatrix} \otimes C_- & \\ & & \mathbf{0} \end{bmatrix}, \tag{3.2}$$

$$\boldsymbol{B}_{-1} = \begin{bmatrix} \mathbf{0} & & \\ & \boldsymbol{C}_- \otimes \begin{bmatrix} 0 & \Delta/2 \\ 0 & 0 \end{bmatrix} & \\ & & \mathbf{0} \end{bmatrix}, \quad \boldsymbol{B}_{+1} = \begin{bmatrix} \boldsymbol{C}_+ \otimes \begin{bmatrix} 0 & 0 \\ \Delta/2 & 0 \end{bmatrix} & & \\ & \mathbf{0} & \\ & & \mathbf{0} \end{bmatrix}. \tag{3.3}$$

But this is the same discretisation we would get if we were to use intervals of width $\Delta/2$ in the QBD approximation of Bean & O'Reilly (2013), with the rows/columns reordered. Indeed, this appears to be the best we can do with a QBD approximation as the Erlang distribution is known to be the least variable Phase-type distribution for a given order (Aldous & Shepp 1987) and therefore gives the closest approximation to the deterministic behaviour we are trying to approximate. This necessitates the extension to QBD-RAPs, whereby we can find more concentrated distributions than any Phase-type and retain enough stochastic interpretation and matrix-analytic tools.

Here, the construction of the approximating QBD-RAP is developed intuitively, from a stochastic modelling perspective. The key observation is that, given $\{\varphi(t)\}$ is constant, then $\{X(t)\}$ moves deterministically. Upon discretising the state space of the level process into intervals of width Δ, then, given $X(t)$, the distribution of time it takes for $\{X(t)\}$ to leave a given interval on the event that $\{\varphi(t)\}$ remains in the same phase, is deterministic. We model this deterministic behaviour approximately by concentrated matrix exponential distributions (matrix exponential distributions with low-variance) (Élteto et al. 2006, Horváth et al. 2016, Élteto et al. 2006, Horváth et al. 2020, Mészáros & Telek 2021). We construct a level process for the QBD-RAP and correspond it to a discretisation the level process of the fluid queue. This is similar to Bean & O'Reilly (2013) where the level process of their QBD corresponds a discretisation of the fluid level. Unlike Bean & O'Reilly (2013), however, here we do not take $\Delta \to 0$. Rather, we suppose that the variance of the concentrated matrix exponential distributions we use to approximate deterministic events gets small.

It turns out that the corresponding orbit process $\{\boldsymbol{A}(t)\}$ can be seen to "track", approximately, how far $X(t)$ is from the left of a given interval when the phase is in $\mathcal{S}_+$, or how far from the right of the interval $X(t)$ is when the phase is in $\mathcal{S}_-$. This leaves us with two problems. 1) on a transition from $\mathcal{S}_+$ to $\mathcal{S}_-$ or $\mathcal{S}_-$ to $\mathcal{S}_+$ how must $\boldsymbol{A}(t)$ jump to retain this information about where $X(t)$ is within a given interval. 2) how to use the orbit position at time t, $\boldsymbol{A}(t)$, to obtain an approximation for the density of $X(t)$. Answers to both problems can be derived from the *residual time* of a matrix exponential distribution. Let us now formalise these concepts some more.

3.2 Time to exit an interval

Consider the partition of the state space of the level of a fluid queue, $[0, M]$ into K intervals of width $\Delta = M/(K+1)$, specifically $\mathcal{D}_{k,i} = [k\Delta, (k+1)\Delta)$ if $i \in \mathcal{S}_+$ and $\mathcal{D}_{k,i} = (k\Delta, (k+1)\Delta]$ if $i \in \mathcal{S}_-$, $k = 0, \ldots, K+1$. The distinction between $\mathcal{D}_{k,i}$ for $i \in \mathcal{S}_+$ and $\mathcal{S}_-$ is a technical one and will be discussed later. For now, one reason we might want to specify the discretisation in this way, is that it ensures the stochastic process

$$\left\{ \sum_{k \in \mathcal{K}} \sum_{i \in \mathcal{S}} k 1(X(t) \in \mathcal{D}_{k,i}) \right\}_{t \geq 0} \tag{3.4}$$

is right-continuous with left limits (cádlág). The expression (3.4) is the discrete process of the fluid-queue which the level process of the QBD-RAP will approximate. Let $y_k = k\Delta$, $k = 0, \ldots, K+1$ and $\mathcal{D}_k = [y_k, y_{k+1}]$. We now look to model the behaviour of $\{X(t)\}$ on an interval $\mathcal{D}_k$ over the time $[t, t+u]$ given information about the phase process over this time.

3.2.1 Modelling the residual time to exit on no change of phase

We first consider no change of phase in $[t, t+u]$. Suppose that $\varphi(t) = i \in \mathcal{S}_+$ and $X(t) = x \in \mathcal{D}_{k,i}$. Observe that on the event that there is no change of phase, $\varphi(t+s) = i$, $s \in [0, u]$, and at time $t+s$ the level of the fluid queue is given by $X(t+s) = x + c_i s$, $s \in [0, u]$. Further, for $u > (y_{k+1} - x)/c_i$ the level process $\{X(t)\}$ leaves the interval $\mathcal{D}_{k,i}$ at exactly time $t + (y_{k+1} - x)/c_i$. Similarly, for $i \in \mathcal{S}_-$, $\{X(t)\}$ leaves the interval $\mathcal{D}_{k,i}$ at exactly time $t + (x - y_k)/|c_i|$ on the event that there is no change of phase on $[t, t+u]$ for $u > (x - y_k)/|c_i|$.

To approximate the deterministic behaviour observed above, consider a matrix-exponential distribution $Z \sim ME(\boldsymbol{\alpha}, \boldsymbol{S}, \boldsymbol{s})$ with mean Δ and low variance. As we shall see later, the assumption that Z has low variance will allow us to claim that Z can be used to approximate deterministic behaviour. Let $Z_i \sim ME(\boldsymbol{\alpha}, \boldsymbol{S}_i, \boldsymbol{s}_i)$ where $\boldsymbol{S}_i = |c_i|\boldsymbol{S}$, $\boldsymbol{s}_i = -\boldsymbol{S}_i \boldsymbol{e}$, $i \in \mathcal{S}$. The random variable Z_i has mean $\Delta/|c_i|$.

Suppose first that $X(t) = y_k$ and $\varphi(t) = i \in \mathcal{S}_+$, so that $X(t)$ will leave $\mathcal{D}_{k,i}$ in exactly $\Delta/|c_i|$ units of time on the event that the phase process of the QBD-RAP remains in i for at least this amount of time. A sensible approximation for this deterministic event is to choose the value of the orbit process at time t to be $\boldsymbol{\alpha}$, $\boldsymbol{A}(t) = \boldsymbol{\alpha}$. With this choice, the distribution of time until the next event of the QBD-RAP, on the event that the phase process remains constant will be the distribution of Z_i. Observe,

$$\begin{aligned}\mathbb{P}(Z_i \in ((\Delta-\varepsilon)/|c_i|, (\Delta+\varepsilon)/|c_i|)) &= \mathbb{P}(Z \in (\Delta-\varepsilon, \Delta+\varepsilon)) \\ &\geq 1 - \frac{\mathrm{Var}(Z)}{\varepsilon^2},\end{aligned}$$

since, by Chebyshev's inequality, $\mathbb{P}(Z \in (\Delta-\varepsilon, \Delta+\varepsilon)) \geq 1 - \dfrac{\mathrm{Var}(Z)}{\varepsilon^2}$. Choosing $\varepsilon = \mathrm{Var}(Z)^{1/3}$, then

$$\mathbb{P}(R_i(u) \in ((\Delta-\varepsilon)/|c_i| - u, (\Delta+\varepsilon)/|c_i|)) \geq 1 - \mathrm{Var}(Z)^{1/3} \approx 1,$$

when $\mathrm{Var}(Z)$ is small. Hence, when the variance of Z (equivalently Z_i) is low, then with high probability the time until the next event of the QBD-RAP, given the phase process remains constant will occur at approximately $\Delta/|c_i|$.

Now, let $R_i(u)$ be the residual time, $R_i(u) = (Z_i - u)1\{Z_i - u > 0\}$, $i \in \mathcal{S}$. After $u \in [0, \Delta/|c_i|)$ amount of time has elapsed, on the event that $\varphi(t+s) = i$, for all $s \in [0, u)$, then $X(t+u) = y_k + c_i u$. If the phase remains i for a further $\Delta/|c_i| - u$ amount of time, then $\{X(t)\}$ will leave $\mathcal{D}_{k,i}$ at exactly this time. Also at time $t+u$, given $Z_i > u$, the distribution of the residual time, $R_i(u)$, has density

$$f_{R_i(u)}(r) = \frac{\boldsymbol{\alpha} e^{\boldsymbol{S}_i(u+r)}\boldsymbol{s}_i}{\boldsymbol{\alpha} e^{\boldsymbol{S}_i u}\boldsymbol{e}} = \boldsymbol{A}(t+u)e^{\boldsymbol{S}_i r}\boldsymbol{s}_i.$$

Here, the event $Z_i > u$ approximates the event $X(t+u) \in \mathcal{D}_{k,i}$ and we want the residual time, $R_i(u)$, to approximate the time until $\{X(t)\}$ leaves $\mathcal{D}_{k,i}$. That is, we want $R_i(u)$ to approximate a deterministic random variable at $\Delta/|c_i| - u$. To this end, we observe that for $\varepsilon > 0$ and $u < (\Delta-\varepsilon)/|c_i|$, then

$$\begin{aligned}&\mathbb{P}(R_i(u) \in ((\Delta-\varepsilon)/|c_i| - u, (\Delta+\varepsilon)/|c_i| - u)) \\ &= \mathbb{P}(Z_i \in ((\Delta-\varepsilon)/|c_i|, (\Delta+\varepsilon)/|c_i|)) \\ &= \mathbb{P}(Z \in (\Delta-\varepsilon, \Delta+\varepsilon)) \\ &\geq 1 - \frac{\mathrm{Var}(Z)}{\varepsilon^2}.\end{aligned}$$

Choosing $\varepsilon = \mathrm{Var}(Z)^{1/3}$, then

$$\mathbb{P}(R_i(u) \in ((\Delta-\varepsilon)/|c_i| - u, (\Delta+\varepsilon)/|c_i|)) \geq 1 - \mathrm{Var}(Z)^{1/3} \approx 1,$$

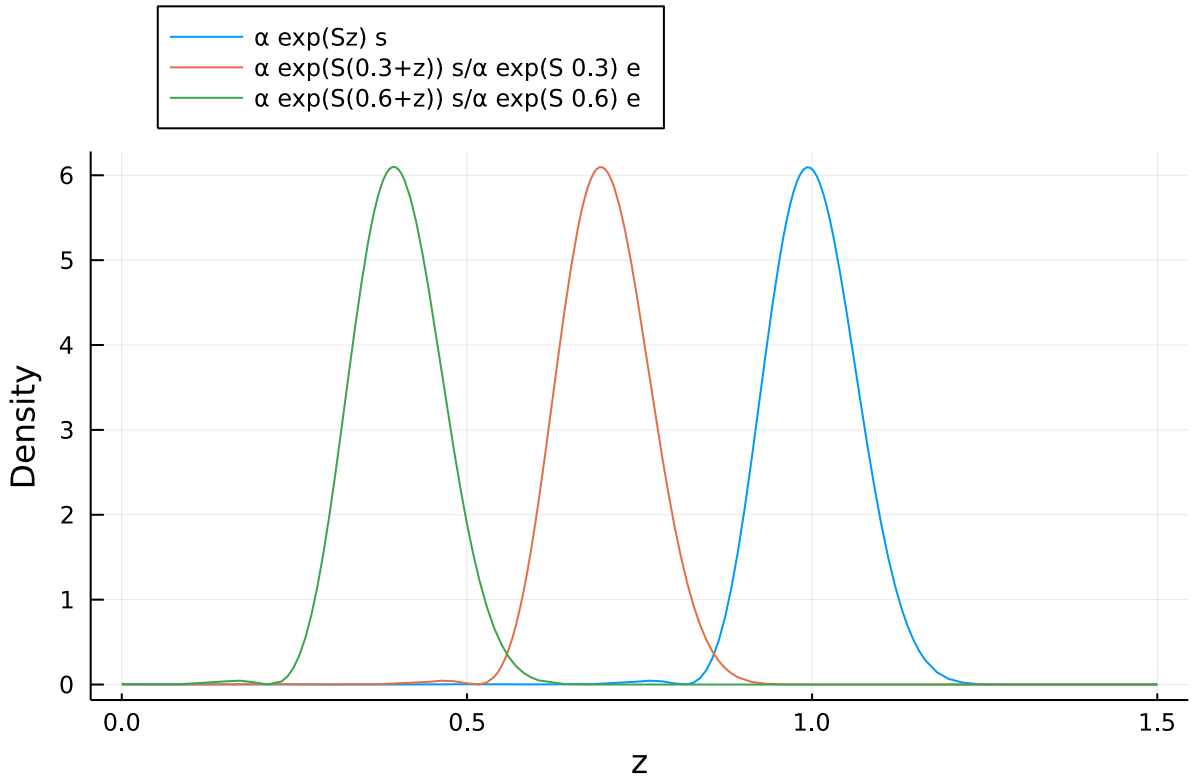

Figure 3.1: The density function for a *concentrated matrix exponential of order 21* from (Horváth et al. 2020) (blue) and corresponding density functions of the residual lives, $R_{0.3}$ (red), $R_{0.6}$ (blue). Observe how the density function of the Z_i (blue) to approximate a point mass at $\Delta = 1$, while the density functions of $R_{0.3}$ (red) and $R_{0.6}$ (blue) approximate point masses at 0.7 and 0.4, respectively.

when $\mathrm{Var}(Z)$ is small. That is, when the variance of Z (equivalently Z_i) is low, the residual time $R_i(u)$ will be concentrated around $\Delta/|c_i| - u$, as required. Figure 3.1 gives an example of a density function for a Z_i with mean $\Delta = 1$ and $c_i = 1$, as well as the density function of $R_i(0.3)$ conditional on $Z_i > 0.3$ and $R_i(0.6)$ conditional on $Z_i > 0.6$, for comparison. Observe that the density of the residual life $R_i(0.3)$ conditional on $Z_i > 0.3$ is concentrated around $\Delta - 0.3 = 0.7$ and, similarly the density of the residual life $R_i(0.6)$ conditional in $Z_i > 0.6$ is concentrated around $\Delta - 0.6 = 0.4$.

For notational convenience, define the row-vector-valued function $\boldsymbol{k}(t) : \mathbb{R} \to \mathcal{A}$,

$$\boldsymbol{k}(t) = \frac{\boldsymbol{\alpha} e^{\boldsymbol{S}t}}{\boldsymbol{\alpha} e^{\boldsymbol{S}t} \boldsymbol{e}}, \tag{3.5}$$

and the operator $\boldsymbol{K}(t) : \mathcal{A} \to \mathbb{R}$, $t \geq 0$,

$$\boldsymbol{a}\boldsymbol{K}(t) = \frac{\boldsymbol{a}e^{\boldsymbol{S}t}}{\boldsymbol{a}e^{\boldsymbol{S}t}\boldsymbol{e}}, \tag{3.6}$$

for any $a \in \mathcal{A}$.

We interpret the position of the orbit $\boldsymbol{A}(t+u) = \boldsymbol{k}(|c_i|u)$ as corresponding to the fact that $X(t+u)$ is $|c_i|u$ units from the left-hand boundary of the interval $\mathcal{D}_{k,i}$. This gives a heuristic argument as to how we can model the sojourn times in a given interval $\mathcal{D}_{k,i}$ on the event that the phase does not change.

We can apply analogous arguments to heuristically develop a model for the sojourn time of the fluid queue in an interval, $\mathcal{D}_{k,i}$, $i \in \mathcal{S}_-$, on the event that the phase does not change, given the fluid is $X(t) = y_{k+1}$. For $i \in \mathcal{S}_-$, the orbit position $\boldsymbol{A}(t+u) = \boldsymbol{k}(|c_i|u)$ is interpreted as corresponding to $X(t)$ being $|c_i|u$ units from the right-hand boundary of the interval $\mathcal{D}_{k,i}$, y_{k+1}.

3.2.2 On a change of phase from $i \in \mathcal{S}_+$ to $j \in \mathcal{S}_+$

Let E be the event that, at time t the orbit of the QBD-RAP is $\boldsymbol{A}(t) = \boldsymbol{\alpha}$, the phase process is $\varphi(t) = i \in \mathcal{S}_+$, and there are no events of the QBD-RAP before time $t+u$. On the event E the orbit position at time $t+u$ will be

$$\boldsymbol{A}(t+u) = \boldsymbol{k}(|c_i|u) = \frac{\boldsymbol{\alpha}e^{\boldsymbol{S}_i u}}{\boldsymbol{\alpha}e^{\boldsymbol{S}_i u}\boldsymbol{e}}. \tag{3.7}$$

Correspondingly, on the event that at time t the level process of the fluid queue is $X(t) = y_k$, the phase is $\varphi(t) = i$ and there are no change of phase by time $t+u$, then $X(t+u) = y_k + c_i u$. That is, $X(t+u)$ is $c_i u$ units from the left-hand edge of $\mathcal{D}_k$.

If, at time $t+u$ there is a change of phase from $i \in \mathcal{S}_+$ to $j \in \mathcal{S}_+$, then we need to map the orbit position $\boldsymbol{A}(t+u^-) = \boldsymbol{k}(|c_i|u)$ to an orbit position which corresponds to the being $c_i u$ units from the left-hand edge of $\mathcal{D}_k$ in phase j. Call this mapping $\boldsymbol{D}(i,j)(\cdot)$. As noted in Section 1.1.4, the mapping must be linear, $\boldsymbol{D}(i,j)(\boldsymbol{a}) = \boldsymbol{a}\boldsymbol{D}(i,j)$, $\boldsymbol{a} \in \mathcal{A}$, for some matrix $\boldsymbol{D}(i,j)$. The matrix $\boldsymbol{D}(i,j)$ is a modelling choice.

So that the process is a QBD-RAP, the matrix $\boldsymbol{D}(i,j)$ must have the property that, for any $\boldsymbol{a} \in \mathcal{A}$, $(\boldsymbol{a}\boldsymbol{D}(i,j), \boldsymbol{S})$ is a representation of a matrix exponential distribution. We would also like the matrix $\boldsymbol{D}(i,j)$ to have the property $\boldsymbol{D}(i,j)\boldsymbol{e} = \boldsymbol{e}$ as this will mean that the rate at which a change of phase from i to j of the QBD-RAP occurs proportional to

$$\boldsymbol{A}(t+u)\boldsymbol{D}(i,j)\boldsymbol{e} = 1,$$

which is constant and therefore the distribution of time until a change from phase i to j is exponential. We can use this to show, for certain models, the distribution of the phase

process of the fluid queue and the distribution of the phase process of the QBD-RAP share the same distribution.

An orbit position which corresponds to the level process of the QBD-RAP beign $c_i u$ units to the right of y_k in phase $j \in \mathcal{S}_+$ is

$$\boldsymbol{A}(t+u) = \frac{\boldsymbol{\alpha} e^{\boldsymbol{S}_j(|c_i|u/|c_j|)}}{\boldsymbol{\alpha} e^{\boldsymbol{S}_j(|c_i|u/|c_j|)u}\boldsymbol{e}}.$$

To see this, consider the event that at time t the orbit process of the QBD-RAP is $\boldsymbol{A}(t) = \boldsymbol{\alpha}$, the phase process is $\varphi(t) = j \in \mathcal{S}_+$, and there are no events of the QBD-RAP before time $t + |c_i|u/|c_j|$. On this event, the orbit position at time $t + u$ will be

$$\boldsymbol{A}(t+u) = \frac{\boldsymbol{\alpha} e^{\boldsymbol{S}_j(|c_i|u)/|c_j|}}{\boldsymbol{\alpha} e^{\boldsymbol{S}_j(|c_i|u/|c_j|)u}\boldsymbol{e}}.$$

Correspondingly, on the event that at time t the level process of the fluid queue is $X(t) = y_k$, the phase is $\varphi(t) = j$ and there are no change of phase by time $t + |c_i|u/|c_j|$, then $X(t+u) = y_k + c_j|c_i|u/|c_j| = y_k + c_i u$. That is, $X(t+u)$ is $c_i u$ units from the left-hand edge of $\mathcal{D}_k$.

Now, observe

$$\frac{\boldsymbol{\alpha} e^{\boldsymbol{S}_j(|c_i|u/|c_j|)}}{\boldsymbol{\alpha} e^{\boldsymbol{S}_j(|c_i|u/|c_j|)u}\boldsymbol{e}} = \frac{\boldsymbol{\alpha} e^{\boldsymbol{S}_i u}}{\boldsymbol{\alpha} e^{\boldsymbol{S}_i u}\boldsymbol{e}} = \boldsymbol{k}(|c_i|u),$$

which is exactly (3.7), the orbit position on the event E. Hence, it is sensible to choose $\boldsymbol{D}(i,j) = \boldsymbol{I}$.

Moreover, the residual time $R_j(|c_i|u/|c_j|)$ has density

$$f_{R_j(|c_i|u/|c_j|)}(r) = \frac{\boldsymbol{\alpha} e^{\boldsymbol{S}_i u}}{\boldsymbol{\alpha} e^{\boldsymbol{S}_i u}\boldsymbol{e}} e^{\boldsymbol{S}_j r}\boldsymbol{s}_j,$$

and

$$\begin{aligned}
&\mathbb{P}(R_j(|c_i|u/|c_j|) \in ((\Delta - |c_i|u - \varepsilon)/|c_j|, (\Delta - |c_i|u + \varepsilon)/|c_j|)) \\
&= \mathbb{P}(Z_j \in ((\Delta - \varepsilon)/|c_j|, (\Delta + \varepsilon)/|c_j|)) && (3.8)\\
&= \mathbb{P}(Z \in (\Delta - \varepsilon, \Delta + \varepsilon)) && (3.9)\\
&\geq 1 - \mathrm{Var}(Z)^{1/3} \approx 1. && (3.10)
\end{aligned}$$

Hence, when the variance of Z is low, the residual time, $R_j(|c_i|u/|c_j|)$, is concentrated around $(\Delta - |c_i|u)/|c_j|$, as required.

Analogous arguments suggest that the same applies for changes of phase from $i \in \mathcal{S}_-$ to $j \in \mathcal{S}_-$.

3.2.3 On a change of phase from $i \in \mathcal{S}_+$ to $j \in \mathcal{S}_-$

Now suppose $X(t) = y_k$, $\varphi(t) = i \in \mathcal{S}_+$, and the phase remains in state i until there is a change of phase from $i \in \mathcal{S}_+$ to $j \in \mathcal{S}_-$ at time $t + u$, $u \in [0, \Delta/|c_i|)$. As before, we need to find a matrix $\boldsymbol{D}(i, j)$ to map the orbit position on the event E when there is a change of phase from $i \in \mathcal{S}_+$ to $j \in \mathcal{S}_-$ at time $t + u$, from

$$\boldsymbol{A}(t + u^-) = \boldsymbol{k}(|c_i|u^-),$$

to

$$\boldsymbol{A}(t + u) = \frac{\boldsymbol{k}(u^-)\boldsymbol{D}(i, j)}{\boldsymbol{k}(u^-)\boldsymbol{D}(i, j)\boldsymbol{e}} = \frac{\boldsymbol{\alpha} e^{\boldsymbol{S}_i u}\boldsymbol{D}(i, j)}{\boldsymbol{\alpha} e^{\boldsymbol{S}_i u}\boldsymbol{D}(i, j)\boldsymbol{e}}$$

in such a way that the orbit position after the jump corresponds, in some way, to the fluid level being a distance of $|c_i|u$ from y_k in phase j.

Again, the matrix $\boldsymbol{D}(i, j)$ is a modelling choice. We first discuss how we might choose the matrix $\boldsymbol{D}(i, j)$ for when the matrix-exponential Z is a phase-type distribution.

The Phase-type case If $Z \sim ME(\boldsymbol{\alpha}, \boldsymbol{S})$ is chosen to be a phase-type distribution then Z has the interpretation as the distribution of time until absorption of a finite-state continuous-time Markov chain with transient states $\{1, \ldots, p\}$ and a single absrobing state. The sub-generator matrix describing the dynamics of the Markov chain on transient states is $\boldsymbol{S}$, and $\boldsymbol{\alpha}$ is an initial probability distribution over the transient states. Let $\{J(t)\}$ be the Markov chain associated with the phase-type distribution.

In the discussions above, we have relied on the relationship between the event E and the orbit position $\boldsymbol{k}(|c_i|u)$. The relationship allows us to associate this orbit position with the level of the fluid queue. For phase-type distributions the vector $\boldsymbol{k}(|c_i|u)$ is the vector of posterior probabilities $[\mathbb{P}(J(u) = k \mid E)]_{k\in\{1,\ldots,p\}}$. We can use this vector of posterior probabilities in the same way as we do for matrix-exponential distributions and QBD-RAPs. However, the orbit interpretation forgoes the presence of the phase process $\{J(t)\}$. Here, we will use the phase process $\{J(t)\}$ to derive a choice of $\boldsymbol{D}(i, j)$.

Recall the position of the orbit process can be used to determine the residual time. This idea can be replicated when we are given the phase of the phase-type rather than the value of the orbit process. Given the phase of the phase-type distribution is $k \in \{1, ..., p\}$, the distribution of the residual time is

$$\mathbb{P}(R_i \leq r \mid \text{phase} = k) = 1 - \boldsymbol{e}_k e^{\boldsymbol{S}_i r}\boldsymbol{e}.$$

Notice that this is independent of the time since the phase-type distribution was initialised. We call the time since the phase-type distribution was initialised the *age*. As noted by Hautphenne et al. (2017), the distribution of the age given the phase of the phase-type is $k \in \{1, ..., p\}$ depends on the sampling scheme which determines the observation time. Here, on the event that at time t the phase of the QBD-RAP is i, a change of phase occurs

after an exponential amount of time with rate $-T_{ii}$. Proposition 4.1, Hautphenne et al. (2017) states that the distribution function of the age, given the phase of the phase-type is k and the process is observed after an exponential time with rate $-T_{ii}$ is

$$\mathbb{P}(\text{age} \leq u \mid \text{phase} = k) = 1 - \frac{\boldsymbol{\alpha} e^{(\boldsymbol{S}_i + T_{ii}\boldsymbol{I})u}(-(\boldsymbol{S}_i + T_{ii}\boldsymbol{I}))^{-1}\boldsymbol{e}_k}{\boldsymbol{\alpha}(-(\boldsymbol{S}_i + T_{ii}\boldsymbol{I}))^{-1}\boldsymbol{e}_k}.$$

Let $\widehat{\boldsymbol{S}}_i(T_{ii}) = diag(\boldsymbol{\nu})^{-1}\boldsymbol{S}_i' diag(\boldsymbol{\nu})$, where $\boldsymbol{\nu} = \boldsymbol{\alpha}(-(\boldsymbol{S}_i + T_{ii}\boldsymbol{I}))^{-1}/(\boldsymbol{\alpha}(-(\boldsymbol{S}_i + T_{ii}\boldsymbol{I}))^{-1}\boldsymbol{e})$. Algebraic manipulations show

$$1 - \frac{\boldsymbol{\alpha} e^{(\boldsymbol{S}_i + T_{ii}\boldsymbol{I})u}(-(\boldsymbol{S}_i + T_{ii}\boldsymbol{I}))^{-1}\boldsymbol{e}_k}{\boldsymbol{\alpha}(-(\boldsymbol{S}_i + T_{ii}\boldsymbol{I}))^{-1}\boldsymbol{e}_k} = 1 - \boldsymbol{e}_k' e^{(\widehat{\boldsymbol{S}}_i(T_{ii}) + T_{ii}\boldsymbol{I})u}\boldsymbol{e}, \tag{3.11}$$

which is of Phase-type.

Recall that in the matrix-exponential case we associated the value of the orbit process $\boldsymbol{k}(|c_i|u)$ with being $|c_i|u$ units to the right of y_k. In contrast, for the phase-type case if we use the phase process $\{J(t)\}$ to inform our modelling of the fluid queue (as opposed to the value of the orbit process), then we associate phase $k \in \{1, ..., p\}$ of $\{J(t)\}$ with being a *random* distance to the right of y_k where this distance has distribution

$$1 - \boldsymbol{e}_k' e^{(\widehat{\boldsymbol{S}}_i(T_{ii}) + T_{ii}\boldsymbol{I})u}\boldsymbol{e}. \tag{3.12}$$

Therefore, on the event E, upon a change from of phase of the QBD-RAP from $i \in \mathcal{S}_+$ to $j \in \mathcal{S}_-$ at time $t + u$, it seems reasonable to want the distribution of time until the next event of the QBD-RAP to be

$$1 - \boldsymbol{e}_k' e^{(\widehat{\boldsymbol{S}}_i(T_{ii}) + T_{ii}\boldsymbol{I})|c_j|u/|c_i| + T_{jj}Iu}\boldsymbol{e}. \tag{3.13}$$

The factor $|c_j|u/|c_i|$ arises as a conversion between the speed at which the fluid level moves in phase j compared to phase i. The rate T_{jj} in the exponent is the rate at which the next change of phase occurs.

While this does achieve what we want, it is not quite satisfactory for the purpose of our approximation scheme due to dependence on the sample path of $\{\varphi(t)\}$. Specifically, the evolution of the QBD-RAP from time $t+u$ until the next event depends on the phase immediately before the change of phase at time $t + u$, $\varphi(t + u^-) = i$. This increases the size of the approximating QBD-RAP as we need a separate model for each $\varphi(t+u^-) \in \mathcal{S}_+$. Furthermore, we have not yet considered how to model any further changes from $\mathcal{S}_-$ to $\mathcal{S}_+$ or beyond, which further complicates matters.

A solution is to suppose that, rather than observing the phase-type random variable at an exponential time with rate $-T_{ii}$, we instead observe the process uniformly randomly on the lifetime of length Z_i. Let $\boldsymbol{\Pi} = diag\,(\boldsymbol{\pi})$, where $\left[\pi_k\right]_{k\in\{1,\ldots,p\}} =: \boldsymbol{\pi} = \boldsymbol{\alpha}(-\boldsymbol{S})^{-1}/m$ and $m = \boldsymbol{\alpha}(-\boldsymbol{S})^{-1}\boldsymbol{e}$. There is a time-reverse representation of a Phase-type distribution

given by $(\widetilde{\boldsymbol{\alpha}}, \widetilde{\boldsymbol{S}}, \widetilde{\boldsymbol{s}})$, where $\widetilde{\boldsymbol{\alpha}} = m\boldsymbol{s}'\boldsymbol{\Pi}$, $\widetilde{\boldsymbol{S}} = \boldsymbol{\Pi}^{-1}\boldsymbol{S}'\boldsymbol{\Pi}$ and $\widetilde{\boldsymbol{s}} = \boldsymbol{\Pi}^{-1}\boldsymbol{\alpha}'/m$ (Asmussen 2008, Page 91). In the case where the phase is observed randomly on the lifetime of Z_i, the distribution function of the age, given the phase is k is (Hautphenne et al. 2017, Lemma 3.1)

$$\mathbb{P}(\text{age} \leq u \mid \text{phase} = k) = 1 - \frac{\boldsymbol{\alpha} e^{\boldsymbol{S}_i u}(-\boldsymbol{S}_i)^{-1}\boldsymbol{e}_k}{\boldsymbol{\alpha}(-\boldsymbol{S}_i)^{-1}\boldsymbol{e}_k} = 1 - \boldsymbol{e}_k e^{\widetilde{\boldsymbol{S}}_i u}\boldsymbol{e}. \tag{3.14}$$

With this interpretation, we may associate phase $k \in \{1, ..., p\}$ of $\{J(t)\}$ with being a *random* distance, with distribution (3.14), to the right of y_k.

Therefore, on the event E and on a change of phase from $i \in \mathcal{S}_+$ to $j \in \mathcal{S}_-$ at time $t+u$, a reasonable model for the time until the next event of the QBD-RAP has distribution

$$1 - \boldsymbol{e}_k e^{\widetilde{\boldsymbol{S}}_i u|c_j|/|c_i| + T_{jj}\boldsymbol{I}u}\boldsymbol{e} = 1 - \boldsymbol{e}_k e^{\widetilde{\boldsymbol{S}}_j u + T_{jj}\boldsymbol{I}u}\boldsymbol{e}. \tag{3.15}$$

This suggests that, at a jump from $\mathcal{S}_+$ to $\mathcal{S}_-$, the state of $\{J(t)\}$ does not change, but begins to evolve according to the time-reverse generator at an appropriate speed. Since the time-reverse of $\widetilde{\boldsymbol{S}}$ is $\boldsymbol{S}$, then upon a jump back to $\mathcal{S}_+$ from $\mathcal{S}_-$, the phase of the phase-type random variable remains k but begins to evolve according to $\mathcal{S}$. This suggests that we use the representation $(\boldsymbol{\alpha}, \boldsymbol{S})$ when in phases in $\mathcal{S}_+$, and use the time-reverse representation $(\widetilde{\boldsymbol{\alpha}}, \widetilde{\boldsymbol{S}})$ when in phases in $\mathcal{S}_-$. The matrices $\boldsymbol{D}(i,j) = \boldsymbol{I}$ for all $i, j \in \mathcal{S}$.

With this construction, and choosing $Z \sim Erlang(p, \Delta/p)$, we recover the discretisation of Bean & O'Reilly (2013) with discretisation parameter Δ/p.

The matrix-exponential case For matrix exponential distributions we cannot rely on the phase process $\{J(t)\}$ as we did in the phase-type case. Recall that we want to find a matrix $\boldsymbol{D}(i,j)$ to map the orbit position on the event E when there is a change of phase from $i \in \mathcal{S}_+$ to $j \in \mathcal{S}_-$ at time $t+u$, from $\boldsymbol{A}(t+u^-) = \boldsymbol{k}(|c_i|u)$, to

$$\boldsymbol{A}(t+u) = \frac{\boldsymbol{k}(|c_i|u)\boldsymbol{D}(i,j)}{\boldsymbol{k}(|c_i|u)\boldsymbol{D}(i,j)\boldsymbol{e}} = \frac{\boldsymbol{\alpha} e^{\boldsymbol{S}_i u}\boldsymbol{D}(i,j)}{\boldsymbol{\alpha} e^{\boldsymbol{S}_i u}\boldsymbol{D}(i,j)\boldsymbol{e}}$$

in such a way that the orbit position after the jump corresponds, in some way, to the fluid level being a distance of $|c_i|u$ from y_k in phase j.

Given our interpretation of the orbit position, $\boldsymbol{k}(x)$, a solution would be find a linear map which takes $\boldsymbol{k}(x)$ and maps it directly to

$$\boldsymbol{k}(\Delta - x) = \frac{\boldsymbol{\alpha} e^{\boldsymbol{S}(\Delta - x)}}{\boldsymbol{\alpha} e^{\boldsymbol{S}(\Delta - x)}\boldsymbol{e}}.$$

However, we have been unsuccessful in finding such a mapping. The main hurdle being that the map must be linear. Instead, we approximate as follows.

Recall that we use $R_i(u)$ to approximate the distance of the fluid level to the left of y_{k+1}. Suppose we are given $R_i(u) = r$ which corresponds, approximately, to the fluid level being $|c_i|r$ units to the left of y_{k+1}. The position of the orbit process which corresponds to a distance of $|c_i|r$ to the left of y_{k+1} in phase j is $\boldsymbol{k}(|c_i|r)$. Hence, on $R_i(u) = r$, the event E and on the event that a change of phase from $i \in \mathcal{S}_+$ to $j \in \mathcal{S}_-$ occurs at time $t + u$, the orbit position should jump from $\boldsymbol{k}(|c_i|u)$ to $\boldsymbol{k}(|c_i|r)$. However, at time $t + u$, $R_i(u)$ is a random variable about the future of the process and therefore not known, so instead, we take the expected initial vector

$$\mathbb{E}\left[\boldsymbol{k}(|c_i|R_i(u))\right] = \int_{r=0}^{\infty} \frac{\boldsymbol{\alpha} e^{\boldsymbol{S}_i u}}{\boldsymbol{\alpha} e^{\boldsymbol{S}_i u}\boldsymbol{e}} e^{\boldsymbol{S}_i r}\boldsymbol{s}_i \boldsymbol{k}(|c_i|r)\,\mathrm{d}r = \frac{\boldsymbol{\alpha} e^{\boldsymbol{S}_i u}}{\boldsymbol{\alpha} e^{\boldsymbol{S}_i u}\boldsymbol{e}} \int_{r=0}^{\infty} e^{\boldsymbol{S}_i r}\boldsymbol{s}_i \frac{\boldsymbol{\alpha} e^{\boldsymbol{S}_i r}}{\boldsymbol{\alpha} e^{\boldsymbol{S}_i r}\boldsymbol{e}}\,\mathrm{d}r.$$

After a change of variables $x = |c_i|r$ we get

$$\frac{\boldsymbol{\alpha} e^{\boldsymbol{S}_i u}}{\boldsymbol{\alpha} e^{\boldsymbol{S}_i u}\boldsymbol{e}} \int_{x=0}^{\infty} e^{\boldsymbol{S}x}|c_i|\boldsymbol{s}\frac{\boldsymbol{\alpha} e^{\boldsymbol{S}x}}{\boldsymbol{\alpha} e^{\boldsymbol{S}x}\boldsymbol{e}}\,\mathrm{d}x/|c_i| = \boldsymbol{A}(t + u^-) \int_{x=0}^{\infty} e^{\boldsymbol{S}x}\boldsymbol{s}\frac{\boldsymbol{\alpha} e^{\boldsymbol{S}x}}{\boldsymbol{\alpha} e^{\boldsymbol{S}x}\boldsymbol{e}}\,\mathrm{d}x,$$

since at time $t + u^-$, the orbit position is $\boldsymbol{A}(t + u^-) = \boldsymbol{\alpha} e^{\boldsymbol{S}_i u}/\boldsymbol{\alpha} e^{\boldsymbol{S}_i u}\boldsymbol{e}$. Thus, we find

$$\boldsymbol{D}(i, j) = \int_{x=0}^{\infty} e^{\boldsymbol{S}x}\boldsymbol{s}\boldsymbol{k}(x)\,\mathrm{d}x =: \boldsymbol{D}.$$

Observe that $\boldsymbol{D}\boldsymbol{e} = \int_{x=0}^{\infty} e^{\boldsymbol{S}x}\boldsymbol{s}\boldsymbol{k}(x)\,\mathrm{d}x\boldsymbol{e} = \int_{x=0}^{\infty} e^{\boldsymbol{S}x}\boldsymbol{s}\,\mathrm{d}x = \boldsymbol{e}$, since $\boldsymbol{k}(x)\boldsymbol{e} = 1$ for all $x \geq 0$. Further, since $\mathcal{A}$ is closed and convex (Bladt & Nielsen 2017), then $(\boldsymbol{a}\boldsymbol{D}, \boldsymbol{S}, \boldsymbol{s})$ is a representation of a matrix exponential distribution for any $\boldsymbol{a} \in \mathcal{A}$.

We pose the choice of the matrix $\boldsymbol{D}$ as a modelling choice. Other choices are possible, for example, $\boldsymbol{D} = \int_{x=0}^{\Delta} e^{\boldsymbol{S}x}\boldsymbol{s}\boldsymbol{k}(x)\,\mathrm{d}x + \int_{x=\Delta}^{\infty} e^{\boldsymbol{S}x}\boldsymbol{s}\boldsymbol{\alpha}\,\mathrm{d}x$, or $\boldsymbol{D} = \int_{x=0}^{\Delta} \boldsymbol{v}(x)\boldsymbol{k}(x)\,\mathrm{d}x$, where $\boldsymbol{v}(x)$ is a *closing operator* as introduced later in Section 3.7, are other possible choices. It may also be possible to construct other matrices $\boldsymbol{D}$, perhaps via geometric arguments.

Computing $\boldsymbol{D}$ In practice, we use the class of concentrated matrix exponential distributions (CMEs) found numerically in (Horváth et al. 2020). For this class of CMEs, we take the index p to be the order of the representation. Moreover, we take p to be odd. The justification for considering representations of odd orders only is that the variance of CME representations of orders $2p$ and $2p-1$ are relatively similar and therefore have similar abilities to represent the delta function (Horváth et al. 2020). Hence, if we construct a QBD-RAP approximation with a representation of order $2p$ we expect it to perform only marginally better than an approximation constructed with representations of order $2p - 1$. However, the computational cost of the latter is lower, so we opt for the order $2p - 1$ representation.

For a given CME with odd order, p, and representation $(\boldsymbol{\alpha}, \boldsymbol{S})$, the matrix $\boldsymbol{S}$ has one real eigenvalue, and $p-1$ complex eigenvalues and all eigenvalues have the same real part.

We numerically evaluate the matrix $\boldsymbol{D}$ where

$$\boldsymbol{D} = \int_{t=0}^{\infty} e^{\boldsymbol{S}t}\boldsymbol{s} \cdot \boldsymbol{k}(t)\,\mathrm{d}t$$

using a trapezoidal rule as follows. For the CMEs considered here, the vector function $\boldsymbol{k}(t)$ is periodic with period $\rho = 2\pi/\omega$ where $\omega = min_i(|\Im(\lambda_i)|)$, λ_i are the eigenvalues of $\boldsymbol{S}$ and $\Im(z)$ is the imaginary component of a complex number z. Let $\boldsymbol{f}(t) = e^{\boldsymbol{S}t}\boldsymbol{s}$. Then $\boldsymbol{f}(t)e^{-\lambda t}$ where $\lambda = \Re(\lambda_i)$ is the real part of the eigenvalues of $\boldsymbol{S}$ (they all share the same real part), is also periodic with the same period. Hence we can simplify the integral to a finite one;

$$\begin{aligned}
\boldsymbol{D} &= \int_{t=0}^{\infty} \boldsymbol{f}(t) \cdot \boldsymbol{k}(t)\,\mathrm{d}t \\
&= \sum_{k=0}^{\infty} \int_{k\rho}^{(k+1)\rho} e^{\lambda t}e^{-\lambda t}\boldsymbol{f}(t) \cdot \boldsymbol{k}(t)\,\mathrm{d}t \\
&= \sum_{k=0}^{\infty} \int_{0}^{\rho} e^{\lambda(k\rho+t)}e^{-\lambda(k\rho+t)}\boldsymbol{f}(k\rho+t) \cdot \boldsymbol{k}(k\rho+t)\,\mathrm{d}t. \qquad (3.16)
\end{aligned}$$

By periodicity, then $e^{-\lambda(k\rho+t)}\boldsymbol{f}(k\rho+t) \cdot \boldsymbol{k}(k\rho+t) = e^{-\lambda t}\boldsymbol{f}(t) \cdot \boldsymbol{k}(t)$, hence (3.16) is equal to

$$\sum_{k=0}^{\infty}(e^{\lambda\rho})^k \int_{0}^{\rho} e^{\lambda t}e^{-\lambda t}\boldsymbol{f}(t) \cdot \boldsymbol{k}(t)\,\mathrm{d}t = \frac{1}{1-e^{\lambda\rho}}\int_{0}^{\rho} \boldsymbol{f}(t) \cdot \boldsymbol{k}(t)\,\mathrm{d}t, \qquad (3.17)$$

where the sum converges as it is a geometric series and $\lambda < 0$, $\rho > 0$.

To approximate (3.17) numerically, we first partition $[0, \rho)$ into N equal-width intervals $[t_n, t_{n+1})$, where $t_n = (n-1)\rho/N$, $n = 1, 2, ..., N+1$. On $[t_n, t_{n+1})$ we approximate the orbit $\boldsymbol{k}(t)$ by a constant $\boldsymbol{k}(t) \approx \boldsymbol{k}_n := \frac{1}{2}(\boldsymbol{k}(t_n) + \boldsymbol{k}(t_{n+1}))$, $t \in [t_n, t_{n+1})$. Substituting this approximation into the expression for $\boldsymbol{D}$ gives

$$\begin{aligned}
\boldsymbol{D} &\approx \frac{1}{1-e^{\lambda\rho}}\sum_{n=1}^{N}\int_{t_n}^{t_{n+1}} \boldsymbol{f}(t) \cdot \boldsymbol{k}_n\,\mathrm{d}t \\
&= \frac{1}{1-e^{\lambda\rho}}\sum_{n=1}^{N}\left[e^{\boldsymbol{S}t_{n+1}} - e^{\boldsymbol{S}t_n}\right]\boldsymbol{e} \cdot \boldsymbol{k}_n.
\end{aligned}$$

This approximation preserves the property that $\boldsymbol{D}\boldsymbol{e} = \boldsymbol{e}$.

Computationally efficient expressions for $e^{\boldsymbol{S}t}\boldsymbol{e}$ and $\boldsymbol{k}(t)$ are provided in (Horváth et al. 2020).

3.2.4 Upon exiting $\mathcal{D}_{k,i}$

Suppose that upon exiting $\mathcal{D}_{k,i}$ at time t the phase is $\varphi(t) = i \in \mathcal{S}_+$. At this time $X(t) = y_{k+1}$ which is the left-hand endpoint of $\mathcal{D}_{k+1,i}$. Hence, we restart the model of the sojourn time with the initial condition $\boldsymbol{A}(t) = \boldsymbol{\alpha}$. Similarly, upon exiting $\mathcal{D}_{k,i}$ at time t in phase $\varphi(t) = i \in \mathcal{S}_-$, then $X(t) = y_k$, which is the right-hand endpoint of $\mathcal{D}_{k,i}$, and so we restart the model of the sojourn time with the initial condition $\boldsymbol{A}(t) = \boldsymbol{\alpha}$.

3.3 The association of $j \in \mathcal{S}_0$ with $\mathcal{S}_+$ or $\mathcal{S}_-$

Let $X(0) = y_\ell$ and consider the event where $\{\varphi(t)\}$ transitions from $j_0 \to j_1 \to j_2$ where $j_0 \in \mathcal{S}_+$, $j_1 \in \mathcal{S}_0$ and $j_2 \in \mathcal{S}_-$, before there is a change of level, i.e.

$$\varphi(t) = \begin{cases} j_0 & t \in [0, t_1)\,, \\ j_1 & t \in [t_1, t_2)\,, \\ j_2 & t \in [t_2, t_3)\,, \end{cases}$$

and $X(t) \in \mathcal{D}_\ell$, $t \in [0, t_3)$. On approximating this event, the initial orbit position is $\boldsymbol{A}(0) = \boldsymbol{\alpha}$. The corresponding sample path of the orbit process on $t \in [0, t_3)$, is

$$\boldsymbol{A}(t) = \begin{cases} \dfrac{\boldsymbol{\alpha} e^{(\boldsymbol{S}_{j_0} + T_{j_0 j_0}\boldsymbol{I})t}}{\boldsymbol{\alpha} e^{(\boldsymbol{S}_{j_0} + T_{j_0 j_0}\boldsymbol{I})t}\boldsymbol{e}} & t \in [0, t_1)\,, \\ \dfrac{\boldsymbol{\alpha} e^{(\boldsymbol{S}_{j_0} + T_{j_0 j_0}\boldsymbol{I})t_1}\boldsymbol{D}(j_0, j_1) e^{T_{j_1 j_1}(t - t_1)}}{\boldsymbol{\alpha} e^{(\boldsymbol{S}_{j_0} + T_{j_0 j_0}\boldsymbol{I})t_1}\boldsymbol{D}(j_0, j_1) e^{T_{j_1 j_1}(t - t_1)}\boldsymbol{e}} & t \in [t_1, t_2)\,, \\ \dfrac{\boldsymbol{\alpha} e^{(\boldsymbol{S}_{j_0} + T_{j_0 j_0}\boldsymbol{I})t_1}\boldsymbol{D}(j_0, j_1) e^{T_{j_1 j_1}(t_2 - t_1)}\boldsymbol{D}(j_1, j_2) e^{(\boldsymbol{S}_{j_2} + T_{j_2 j_2}\boldsymbol{I})(t - t_2)}}{\boldsymbol{\alpha} e^{(\boldsymbol{S}_{j_0} + T_{j_0 j_0}\boldsymbol{I})t_1}\boldsymbol{D}(j_0, j_1) e^{T_{j_1 j_1}(t_2 - t_1)}\boldsymbol{D}(j_1, j_2) e^{(\boldsymbol{S}_{j_2} + T_{j_2 j_2}\boldsymbol{I})(t - t_2)}\boldsymbol{e}} & t \in [t_2, t_3)\,, \end{cases}$$

$$= \begin{cases} \dfrac{\boldsymbol{\alpha} e^{\boldsymbol{S}_{j_0} t}}{\boldsymbol{\alpha} e^{\boldsymbol{S}_{j_0} t}\boldsymbol{e}} & t \in [0, t_1)\,, \\ \dfrac{\boldsymbol{\alpha} e^{\boldsymbol{S}_{j_0} t_1}\boldsymbol{D}(j_0, j_1)}{\boldsymbol{\alpha} e^{\boldsymbol{S}_{j_0} t_1}\boldsymbol{D}(j_0, j_1)\boldsymbol{e}} & t \in [t_1, t_2)\,, \\ \dfrac{\boldsymbol{\alpha} e^{\boldsymbol{S}_{j_0} t_1}\boldsymbol{D}(j_0, j_1)\boldsymbol{D}(j_1, j_2) e^{\boldsymbol{S}_{j_2}(t - t_2)}}{\boldsymbol{\alpha} e^{\boldsymbol{S}_{j_0} t_1}\boldsymbol{D}(j_0, j_1)\boldsymbol{D}(j_1, j_2) e^{\boldsymbol{S}_{j_2}(t - t_2)}\boldsymbol{e}} & t \in [t_2, t_3)\,, \end{cases}$$

for some matrices $\boldsymbol{D}(j_0, j_1)$ and $\boldsymbol{D}(j_2, j_1)$. Notice that $\{\boldsymbol{A}(t)\}$ is constant on $t \in [t_1, t_2)$. The matrix product $\boldsymbol{D}(j_0, j_1)\boldsymbol{D}(j_1, j_2)$ is there to capture the change in direction due to the change from $\mathcal{S}_+$ to $\mathcal{S}_-$. Hence $\boldsymbol{D}(j_0, j_1)\boldsymbol{D}(j_1, j_2)$ should be equal to $\boldsymbol{D}$. These types of sample paths are the reason we need to associate states $j_1 \in \mathcal{S}_0$ with either $\mathcal{S}_+$ or $\mathcal{S}_-$.

Associating j_1 with $\mathcal{S}_+$, amounts to choosing $\boldsymbol{D}(j_0, j_1) = \boldsymbol{I}$ and $\boldsymbol{D}(j_1, j_2) = \boldsymbol{D}$; associating j_1 with $\mathcal{S}_-$, amounts to choosing $\boldsymbol{D}(j_0, j_1) = \boldsymbol{D}$ and $\boldsymbol{D}(j_1, j_2) = \boldsymbol{I}$.

There are some consequences to this choice. Let $k_2 \in \mathcal{S}_+$. Consider an event where the phase process of the fluid queue transitions from $j_0 \to j_1 \to k_2$ and there is no change of level. If j_1 is associated with $\mathcal{S}_+$, then $\boldsymbol{D}(j_0, j_1) = \boldsymbol{D}(j_1, k_2) = \boldsymbol{I}$ and the corresponding orbit process, given $\boldsymbol{A}(0) = \boldsymbol{\alpha}$, is

$$\boldsymbol{A}(t) = \begin{cases} \dfrac{\boldsymbol{\alpha} e^{\boldsymbol{S}_{j_0} t}}{\boldsymbol{\alpha} e^{\boldsymbol{S}_{j_0} t} \boldsymbol{e}} & t \in [0, t_1)\,, \\ \dfrac{\boldsymbol{\alpha} e^{\boldsymbol{S}_{j_0} t_1}}{\boldsymbol{\alpha} e^{\boldsymbol{S}_{j_0} t_1} \boldsymbol{e}} & t \in [t_1, t_2)\,, \\ \dfrac{\boldsymbol{\alpha} e^{\boldsymbol{S}_{j_0} t_1} e^{\boldsymbol{S}_{k_2}(t-t_2)}}{\boldsymbol{\alpha} e^{\boldsymbol{S}_{j_0} t_1} e^{\boldsymbol{S}_{k_2}(t-t_2)} \boldsymbol{e}} & t \in [t_2, t_3)\,. \end{cases}$$

Notice that there is no matrix $\boldsymbol{D}$ in this expression.

Compare this to if j_1 is associated with $\mathcal{S}_-$. In this case $\boldsymbol{D}(j_0, j_1) = \boldsymbol{D}(j_1, k_2) = \boldsymbol{D}$ and the corresponding orbit process of the approximation, given $\boldsymbol{A}(0) = \boldsymbol{\alpha}$ and there are no change of level in $[t_1, t_3)$, is

$$\boldsymbol{A}(t) = \begin{cases} \dfrac{\boldsymbol{\alpha} e^{\boldsymbol{S}_{j_0} t}}{\boldsymbol{\alpha} e^{\boldsymbol{S}_{j_0} t} \boldsymbol{e}} & t \in [0, t_1)\,, \\ \dfrac{\boldsymbol{\alpha} e^{\boldsymbol{S}_{j_0} t_1} \boldsymbol{D}}{\boldsymbol{\alpha} e^{\boldsymbol{S}_{j_0} t_1} \boldsymbol{D} \boldsymbol{e}} & t \in [t_1, t_2)\,, \\ \dfrac{\boldsymbol{\alpha} e^{\boldsymbol{S}_{j_0} t_1} \boldsymbol{D} \boldsymbol{D} e^{\boldsymbol{S}_{k_2}(t-t_2)}}{\boldsymbol{\alpha} e^{\boldsymbol{S}_{j_0} t_1} \boldsymbol{D} \boldsymbol{D} e^{\boldsymbol{S}_{k_2}(t-t_2)} \boldsymbol{e}} & t \in [t_2, t_3)\,. \end{cases}$$

Ideally $\boldsymbol{D}^2 = \boldsymbol{I}$, however this is not the case here. Recall that a jump according to $\boldsymbol{D}$ corresponds to approximating the residual life by an expectation. With this interpretation as an approximation, it suggests that we might want to minimise the number of jumps according to $\boldsymbol{D}$ which occur. Therefore, for $j_1 \in \mathcal{S}_0$, if transitions $\mathcal{S}_+ \to j_1 \to \mathcal{S}_+$ occur with high probability compared to transition $\mathcal{S}_- \to j_1 \to \mathcal{S}_-$, then this suggests we might want to associate j_1 with $\mathcal{S}_+$. Which association is chosen will depend on the parameters of the fluid queue and on which aspects of the model we wish to approximate. Although this advice is based on intuition only, numerical results in Section TBC suggest that it is reasonable.

Augmented state-space schemes

Another way to approach the problem is to augment the state space of the phase process by duplicating $\mathcal{S}_0$ and associating one copy of $\mathcal{S}_0$ with $\mathcal{S}_+$ and one copy of $\mathcal{S}_0$ with $\mathcal{S}_-$. Let $\{\varphi^*(t)\}$ be the augmented CTMC with state space $\mathcal{S}^*$ and generator $\boldsymbol{T}^*$. Let $\mathcal{S}_+$ and $\mathcal{S}_-$ be as before and $\mathcal{S}_{m0} = \{(m, i) \mid i \in \mathcal{S}_m\}$, $m \in \{+, -\}$, then $\mathcal{S}^* = \mathcal{S}_+ \cup \mathcal{S}_- \cup \mathcal{S}_{+0} \cup \mathcal{S}_{-0}$.

The generator of $\varphi^*(t)$ can be written as

$$\boldsymbol{T}^* = \begin{bmatrix} \boldsymbol{T}_{++} & \boldsymbol{T}_{+0} & \boldsymbol{T}_{+-} & 0 \\ \boldsymbol{T}_{0+} & \boldsymbol{T}_{00} & \boldsymbol{T}_{0-} & 0 \\ \boldsymbol{T}_{-+} & 0 & \boldsymbol{T}_{--} & \boldsymbol{T}_{-0} \\ \boldsymbol{T}_{0+} & 0 & \boldsymbol{T}_{0-} & \boldsymbol{T}_{00} \end{bmatrix}.$$

Also define a fluid level $\{X^*(t)\}$ using $\{\varphi^*(t)\}$, with rates $c_i^* = c_i$ for $i \in \mathcal{S}_+ \cup \mathcal{S}_-$ and $c_{(m,i)}^* = 0$ for $(m,i) \in \mathcal{S}_{+0} \cup \mathcal{S}_{-0}$. The process $\{\varphi(t)\}$ is imbedded within $\{\varphi^*(t)\}$ and is recovered by marginalising over $\mathcal{S}_{+0}$ and $\mathcal{S}_{-0}$. On the event $X^*(0) = X(0)$, the fluid levels $X^*(t)$ and $X(t)$ match exactly. Hence, by approximating $\{(X^*(t), \varphi^*(t))\}$, we can recover an approximation to $\{(X(t), \varphi(t))\}$. This construction removes the problem of having to choose how to associate states $j \in \mathcal{S}_0$ with either $\mathcal{S}_+$ or $\mathcal{S}_-$

The generator for the QBD-RAP approximation to the augmented fluid process (ignoring boundaries) is

$$\boldsymbol{B} = \begin{bmatrix} \ddots & \ddots & \ddots & & \\ & \boldsymbol{B}_{-1} & \boldsymbol{B}_0 & \boldsymbol{B}_{+1} & \\ & & \boldsymbol{B}_{-1} & \boldsymbol{B}_0 & \boldsymbol{B}_{+1} \\ & & & \ddots & \ddots & \ddots \end{bmatrix},$$

where,

$$\boldsymbol{B}_0 = \begin{bmatrix} \boldsymbol{C}_+ \otimes \boldsymbol{S} + \boldsymbol{T}_{++} \otimes \boldsymbol{I} & \boldsymbol{T}_{+0} \otimes \boldsymbol{I} & \boldsymbol{T}_{+-} \otimes \boldsymbol{D} & \boldsymbol{0} \\ \boldsymbol{T}_{0+} \otimes \boldsymbol{I} & \boldsymbol{T}_{00} \otimes \boldsymbol{I} & \boldsymbol{T}_{0-} \otimes \boldsymbol{D} & \boldsymbol{0} \\ \boldsymbol{T}_{-+} \otimes \boldsymbol{D} & \boldsymbol{0} & \boldsymbol{C}_- \otimes \boldsymbol{S} + \boldsymbol{T}_{--} \otimes \boldsymbol{I} & \boldsymbol{T}_{-0} \otimes \boldsymbol{I} \\ \boldsymbol{T}_{0+} \otimes \boldsymbol{D} & \boldsymbol{0} & \boldsymbol{T}_{0-} \otimes \boldsymbol{I} & \boldsymbol{T}_{00} \otimes \boldsymbol{I} \end{bmatrix},$$

$$\boldsymbol{B}_{-1} = \begin{bmatrix} \boldsymbol{0} & & & \\ & \boldsymbol{0} & & \\ & & \boldsymbol{C}_- \otimes (\boldsymbol{s}\boldsymbol{\alpha}) & \\ & & & \boldsymbol{0} \end{bmatrix}, \qquad \boldsymbol{B}_{+1} = \begin{bmatrix} \boldsymbol{C}_+ \otimes (\boldsymbol{s}\boldsymbol{\alpha}) & & & \\ & \boldsymbol{0} & & \\ & & \boldsymbol{0} & \\ & & & \boldsymbol{0} \end{bmatrix}.$$

With this construction, jumps according to the matrix $\boldsymbol{D}$ occur only on transitions from $\mathcal{S}_m \to \mathcal{S}_n$, or $\mathcal{S}_m \to \mathcal{S}_{0m} \to \mathcal{S}_n$, $m, n \in \{+.-\}$, $m \neq n$.

3.4 The dynamics of the QBD-RAP approximation

We now have all the elements we need to describe the dynamics of the QBD-RAP approximation. Since the phase dynamics are a CTMC, we choose to use an alternate notation

to the standard presented in Section 1.1.4. Let $\{\boldsymbol{Y}(t)\}_{t\geq 0} = \{(L(t), \boldsymbol{A}(t), \phi(t))\}_{t\geq 0}$ be the QBD-RAP approximation of a fluid queue, where $\{L(t)\}$ is the level, $\{\boldsymbol{A}(t)\}$ is the orbit process and $\{\phi(t)\}$ is the phase process. We use this representation to make explicit how the approximation captures the phase dynamics of the fluid queue.

We will show later that $\phi(t)$ captures the phase dynamics of the fluid queue exactly, provided the phase process is independent of the fluid level $\{X(t)\}$. The level $L(t) = \ell$ approximates which band $\mathcal{D}_\ell$ that $X(t)$ is in at time t, and the orbit $\boldsymbol{A}(t)$ can be use to obtain an approximation of where $X(t)$ is within the interval $\mathcal{D}_\ell$.

We now proceed to describe the evolution of the orbit and phase processes, before introducing the level variable later.

The orbit process and phase dynamics On $\phi(t) = i$, between event epochs, the process $\{\boldsymbol{A}(t)\}$ evolves deterministically according to the differential equation

$$\frac{\mathrm{d}}{\mathrm{d}t}\boldsymbol{A}(t) = \boldsymbol{A}(t)(\boldsymbol{S}_i - \boldsymbol{A}(t)(\boldsymbol{S}_i + T_{ii}\boldsymbol{I}_p)\boldsymbol{e})\boldsymbol{I}_p. \tag{3.18}$$

Let $\boldsymbol{a} \in \mathcal{A}$ be an arbitrary vector in $\mathcal{A}$. On the event that no events occur before time $t + u$, $\boldsymbol{A}(u) = \boldsymbol{a} \in \mathcal{A}$ and $\phi(u) = i$, the solution to (3.18) states that $\boldsymbol{A}(t + u)$ evolves deterministically according to

$$\boldsymbol{A}(t+u) = \frac{\boldsymbol{a}e^{(\boldsymbol{S}_i + T_{ii}\boldsymbol{I}_p)t}}{\boldsymbol{a}e^{(\boldsymbol{S}_i + T_{ii}\boldsymbol{I}_p)t}\boldsymbol{e}} = \frac{\boldsymbol{a}e^{\boldsymbol{S}_i t}}{\boldsymbol{a}e^{\boldsymbol{S}_i t}\boldsymbol{e}}.$$

At time t an event occurs at rate

$$\boldsymbol{A}(t)(\boldsymbol{S}_i - T_{ii}\boldsymbol{I}_p)\boldsymbol{e} = \boldsymbol{A}(t)\boldsymbol{s}_i - T_{ii}.$$

More precisely, an event corresponding to a change in phase for $\phi(t)$ occurs at rate $-\boldsymbol{A}(t)T_{ii}\boldsymbol{e} = -T_{ii}$ and an event corresponding to a *change of level* occurs at rate $-\boldsymbol{A}(t)\boldsymbol{S}_i\boldsymbol{e} = \boldsymbol{A}(t)\boldsymbol{s}_i$. Later, we will make clear why we say that the latter event corresponds to a change of level. Upon an event occurring at time t, with probability $-T_{ii}/(-T_{ii} + \boldsymbol{A}(t^-)\boldsymbol{s}_i)$ the event corresponds to a change of phase and with probability $\boldsymbol{A}(t^-)\boldsymbol{s}_i/(-T_{ii} + \boldsymbol{A}(t^-)\boldsymbol{s}_i)$ the event corresponds a change of level.

Upon an event corresponding to a change of level occurring at time t the process $\{\boldsymbol{A}(t)\}$ jumps to $\boldsymbol{A}(t) = \boldsymbol{\alpha}$.

Upon an event corresponding to a change of phase from i to $j \neq i$ occurring at time t, there are two possibilities; either $sign(c_i) = sign(c_j)$, or $sign(c_i) \neq sign(c_j)$. As discussed earlier, for states $i \in \mathcal{S}_0$ we must specify some association with either $\mathcal{S}_+$ or $\mathcal{S}_-$. Here we choose the augmented state space approach and duplicate $\mathcal{S}_0$ and associate one copy with $i \in \mathcal{S}_+$ and one copy with $\mathcal{S}_-$; call these $\mathcal{S}_{+0}$ and $\mathcal{S}_{-0}$, respectively. We take $sign(c_i) = +$ for $i \in \mathcal{S}_{+0}$ and $sign(c_i) = -$ for $i \in \mathcal{S}_{-0}$.

Upon an event corresponding to a change of phase from i to $j \neq i$ occurring at time t, in the case $sign(c_i) = sign(c_j)$, at the time of the event $\boldsymbol{A}(t)$ is unchanged but immediately begins to evolve according to (3.18) with i replaced by j, while $\{\phi(t)\}$ jumps from $\phi(t^-) = i$ to $\phi(t) = j$.

Upon an event corresponding to a change of phase from i to $j \neq i$ occurring at time t, in the case $sign(c_i) \neq sign(c_j)$, the process $\{\boldsymbol{A}(t)\}$ jumps to

$$\boldsymbol{A}(t) = \frac{\boldsymbol{A}(t^-)T_{ij}\boldsymbol{D}}{\boldsymbol{A}(t^-)T_{ij}\boldsymbol{D}\boldsymbol{e}} = \frac{\boldsymbol{A}(t^-)T_{ij}\boldsymbol{D}}{T_{ij}} = \boldsymbol{A}(t^-)\boldsymbol{D}$$

and then immediately proceeds to evolve according to (3.18) with i replaced by j, and $\{\phi(t)\}$ jumps from $\phi(t^-) = i$ to $\phi(t) = j$.

The two scenarios, $sign(c_i) \neq sign(c_j)$ and $sign(c_i) = sign(c_j)$, can be written succinctly by stating that, at the time of an event corresponding to a change of phase from i to j, $\{\boldsymbol{A}(t)\}$ jumps to $\boldsymbol{A}(t)\boldsymbol{D}^{1(sign(c_i)\neq sign(c_j))}$ and begins to evolve according to (3.18) with i replaced by j, meanwhile $\{\phi(t)\}$ jumps from $\phi(t^-) = i$ to $\phi(t) = j$.

The following result states that $\{\phi(t)\}$ has the same distribution as $\{\varphi(t)\}$ when the fluid queue is unbounded, the latter being the phase process of the fluid queue.

Theorem 3.1. *Let Θ_i be the time at which the first jump of the phase process of the unbounded QBD-RAP, $\{\phi(t)\}$, occurs, given $\phi(0) = i$. For any initial orbit $\boldsymbol{a} \in \mathcal{A}$, then Θ_i has an exponential distribution with rate parameter $|T_{ii}|$. Furthermore, given $\phi(t)$ leaves state i, it jumps to state j with probability $T_{ij}/|T_{ii}|$. Hence $\phi(t)$ and $\varphi(t)$ have the same probability law.*

Proof. Let $\{\tau_n\}_{n\geq 0}$ with $\tau_0 = 0$ and τ_n the time of the n-th change of level of the QBD-RAP. Consider partitioning $\{\Theta_i > t\}$ with respect to $\{\tau_{n-1} < t \leq \tau_n\}$, $n = 1, 2, \ldots$. For $n = 1$ we can write

$$\mathbb{P}(\Theta_i > t, \tau_0 < t \leq \tau_1 \mid \boldsymbol{A}(0) = \boldsymbol{a}) = \boldsymbol{a}e^{(\boldsymbol{S}_i + T_{ii}\boldsymbol{I}_p)t}\boldsymbol{e}$$

and since $T_{ii}\boldsymbol{I}_p$ commutes with $\boldsymbol{S}_i$ and $e^{T_{ii}t}$ is a scalar, then this is equal to

$$\boldsymbol{a}e^{\boldsymbol{S}_i t}e^{T_{ii}\boldsymbol{I}_p t}\boldsymbol{e} = \boldsymbol{a}e^{\boldsymbol{S}_i t}\boldsymbol{e}e^{T_{ii}t} = \mathbb{P}(\tau_0 < t \leq \tau_1)e^{T_{ii}t}.$$

For $n > 1$, by partitioning on the times of the first $n-1$ level changes, $\tau_1, \ldots, \tau_n$, we get

$$\begin{aligned}
&\mathbb{P}(\Theta_i > t, \tau_{n-1} < t \leq \tau_n \mid \boldsymbol{A}(0) = \boldsymbol{a}) \\
&= \int_{t_1=0}^{t}\int_{t_2=t_1}^{t}\cdots\int_{t_{n-1}=t_{n-2}}^{t} \mathbb{P}(\Theta_i > t, t \leq \tau_n, \tau_{n-1} \in \mathrm{d}t_{n-1}, \ldots \tau_2 \in \mathrm{d}t_2, \tau_1 \in \mathrm{d}t_1 \mid \boldsymbol{A}(0) = \boldsymbol{a}) \\
&= \int_{t_1=0}^{t}\int_{t_2=t_1}^{t}\cdots\int_{t_{n-1}=t_{n-2}}^{t} \boldsymbol{a}e^{(\boldsymbol{S}_i + T_{ii}\boldsymbol{I}_p)t_1}\boldsymbol{s}_i \left(\prod_{k=2}^{n-1}\boldsymbol{\alpha}e^{(\boldsymbol{S}_i + T_{ii}\boldsymbol{I}_p)(t_k - t_{k-1})}\boldsymbol{s}_i\right)
\end{aligned}$$

$$\times \boldsymbol{\alpha} e^{(\boldsymbol{S}_i + T_{ii}\boldsymbol{I}_p)(t-t_{n-1})}\boldsymbol{e}\,\mathrm{d}t_{n-1}\,\mathrm{d}t_{n-2}\ldots\,\mathrm{d}t_1.$$

Since $T_{ii}\boldsymbol{I}_p$ commutes with $\boldsymbol{S}_i$, $e^{T_{ii}t_k}$, $k = 1, ..., n-1$ are scalars, and $t_1 + (t_2 - t_1) + \ldots + (t_{n-1} - t_{n-2}) + (t - t_{n-1}) = t$, then this is equal to

$$\int_{t_1=0}^{t}\int_{t_2=t_1}^{t}\ldots\int_{t_{n-1}=t_{n-2}}^{t}\boldsymbol{a}e^{\boldsymbol{S}_i t_1}\boldsymbol{s}_i\left(\prod_{k=2}^{n-1}\boldsymbol{\alpha}e^{\boldsymbol{S}_i(t_k-t_{k-1})}\boldsymbol{s}_i\right)\boldsymbol{\alpha}e^{\boldsymbol{S}_i(t-t_{n-1})}\boldsymbol{e}\times e^{T_{ii}t}\,\mathrm{d}t_{n-1}\,\mathrm{d}t_{n-2}\ldots\,\mathrm{d}t_1$$
$$= \mathbb{P}(\tau_{n-1} < t \leq \tau_n)e^{T_{ii}t}.$$

Hence, by the law of total probability,

$$\begin{aligned}\mathbb{P}(\Theta_i > t) &= \sum_{n=1}^{\infty}\mathbb{P}(\Theta_i > t, \tau_{n-1} < t \leq \tau_n)\\ &= \sum_{n=1}^{\infty}\mathbb{P}(\tau_{n-1} < t \leq \tau_n)e^{T_{ii}t}\\ &= e^{T_{ii}t},\end{aligned}$$

and therefore Θ_i has an exponential distribution with rate $|T_{ii}|$.

Upon leaving state i at time t, $\phi(t)$ transitions to state j with probability

$$\frac{\left(\dfrac{\boldsymbol{A}(t)\boldsymbol{D}^{1(sign(c_i)\neq sign(c_j))}T_{ij}\boldsymbol{e}}{\sum_{j\in\mathcal{S}}\boldsymbol{A}(t)\boldsymbol{D}^{1(sign(c_i)\neq sign(c_j))}T_{ij}\boldsymbol{e} + \boldsymbol{A}(t)\boldsymbol{s}_i}\right)}{\left(\dfrac{\sum_{j\in\mathcal{S}}\boldsymbol{A}(t)\boldsymbol{D}^{1(sign(c_i)\neq sign(c_j))}T_{ij}\boldsymbol{e}}{\sum_{j\in\mathcal{S}}\boldsymbol{A}(t)\boldsymbol{D}^{1(sign(c_i)\neq sign(c_j))}T_{ij}\boldsymbol{e} + \boldsymbol{A}(t)\boldsymbol{s}_i}\right)} = \frac{\boldsymbol{A}(t)\boldsymbol{e}T_{ij}}{\sum_{j\in\mathcal{S}}\boldsymbol{A}(t)\boldsymbol{e}T_{ij}} = \frac{T_{ij}}{-T_{ii}}.$$

Therefore the process $\{\phi(t)\}$ is has the same probability law as $\{\varphi(t)\}$. □

Remark 3.2. *The same result can be shown for a regulated boundary. For boundary conditions which interact with the phase dynamics, such as a reflecting boundary, the result does not hold. The cause is the fact that the phase dynamics are level dependent – we may see a forced change of phase upon a boundary being hit – and the QBD-RAP can only approximate the level process of the fluid queue. However, until a boundary is hit (by either the fluid queue or QBD-RAP) then the phase processes match. We show later that, in the limit as the variance of the the matrix exponential distribution used in the construction of the QBD-RAP goes to zero, then the dynamics of the level process of the fluid queue, $X(t)$, are captured by the QBD-RAP, and boundary behaviour which interacts with the phase dynamics can be captured too.*

Since the phase processes $\{\phi(t)\}$ and $\{\varphi(t)\}$ have the same law when boundaries are not present, henceforth, we shall assume $\{\phi(t)\}$ and $\{\varphi(t)\}$ are coupled when possible (they share the same sample path). Specifically, in Section 4.2, we will analyse the QBD-RAP on the event that it remains in the same level, ℓ, say, and we compare this to the fluid queue on the event that the level remains in the band $\mathcal{D}_\ell$. No boundary behaviour is involved in this calculation, so we treat $\{\phi(t)\}$ and $\{\varphi(t)\}$ as coupled and use the latter notation. When we must distinguish the two processes, we use $\phi(t)$ for the phase of the QBD-RAP and $\varphi(t)$ for the phase of the fluid.

The level process To event epochs of $\{(\boldsymbol{A}(t), \varphi(t))\}_{t\geq 0}$ we associate marks $\{-1, 0, +1\}$ in the following way.

- To events epochs corresponding to a change of phase of $\varphi(t)$ we associate the mark 0.
- To event epochs at time t which correspond to a change in level and for which $\varphi(t^-) = i \in \mathcal{S}_-$ we associate the mark -1.
- To event epochs at time t which correspond to a change in level and for which $\varphi(t^-) = i \in \mathcal{S}_+$ we associate the mark $+1$.

Now define $N_+(t)$ ($N_-(t)$) as the simple point process which counts the number of event epochs with marks $+1$ (-1) which have occurred in the time up to and including time t. The level process of the QBD-RAP is given by $L(t) = N_+(t) - N_-(t)$. The process $\{(L(t), \boldsymbol{A}(t), \varphi(t))\}_{t\geq 0}$ forms a QBD with RAP components.

One way to specify the QBD with RAP components, $\{(L(t), \boldsymbol{A}(t), \varphi(t))\}$, is to describe its generator:

$$\boldsymbol{B} = \begin{bmatrix} \ddots & \ddots & \ddots & & \\ & \boldsymbol{B}_{-1} & \boldsymbol{B}_0 & \boldsymbol{B}_{+1} & \\ & & \boldsymbol{B}_{-1} & \boldsymbol{B}_0 & \boldsymbol{B}_{+1} \\ & & & \ddots & \ddots & \ddots \end{bmatrix},$$

where,

$$\boldsymbol{B} = \begin{bmatrix} \boldsymbol{B}_{++} & \boldsymbol{B}_{+-} \\ \boldsymbol{B}_{-+} & \boldsymbol{B}_{--} \end{bmatrix}$$

$$\boldsymbol{B}_{-1} = \begin{bmatrix} \mathbf{0} & & & \\ & \mathbf{0} & & \\ & & \boldsymbol{C}_- \otimes (\boldsymbol{s}\boldsymbol{\alpha}) & \\ & & & \mathbf{0} \end{bmatrix}, \qquad \boldsymbol{B}_{+1} = \begin{bmatrix} \boldsymbol{C}_+ \otimes (\boldsymbol{s}\boldsymbol{\alpha}) & & & \\ & \mathbf{0} & & \\ & & \mathbf{0} & \\ & & & \mathbf{0} \end{bmatrix},$$

and

$$\boldsymbol{B}_{++} = \begin{bmatrix} \boldsymbol{C}_+ \otimes \boldsymbol{S} + \boldsymbol{T}_{++} \otimes \boldsymbol{I} & \boldsymbol{T}_{+0} \otimes \boldsymbol{I} \\ \boldsymbol{T}_{0+} \otimes \boldsymbol{I} & \boldsymbol{T}_{00} \otimes \boldsymbol{I} \end{bmatrix}, \boldsymbol{B}_{+-} = \begin{bmatrix} \boldsymbol{T}_{+-} \otimes \boldsymbol{D} & \boldsymbol{0} \\ \boldsymbol{T}_{0-} \otimes \boldsymbol{D} & \boldsymbol{0} \end{bmatrix},$$
$$\boldsymbol{B}_{-+} = \begin{bmatrix} \boldsymbol{T}_{-+} \otimes \boldsymbol{D} & \boldsymbol{0} \\ \boldsymbol{T}_{0+} \otimes \boldsymbol{D} & \boldsymbol{0} \end{bmatrix}, \boldsymbol{B}_{--} = \begin{bmatrix} \boldsymbol{C}_- \otimes \boldsymbol{S} - \boldsymbol{T}_{--} \otimes \boldsymbol{I} & \boldsymbol{T}_{-0} \otimes \boldsymbol{I} \\ \boldsymbol{T}_{0-} \otimes \boldsymbol{I} & \boldsymbol{T}_{00} \otimes \boldsymbol{I} \end{bmatrix}.$$

3.5 Boundary conditions

In the study and practical application of fluid queues, regulated, reflecting, sticky, or a mixture of these boundary conditions may be imposed. We now present the intuition as to how one may include such boundary conditions in the QBD-RAP approximation scheme.

Without loss of generality, assume that there is a boundary for the fluid level at $y_0 = 0$. This boundary can only be hit from above in phases $i \in \mathcal{S}_-$. Suppose that, upon hitting the boundary in phase $i \in \mathcal{S}_-$, the phase jumps from i to $j \in \mathcal{S}$ with probability p_{ij}. If $j \in \mathcal{S}_- \cup \mathcal{S}_0$ the process remains at the boundary and the phase process evolves among states in $\mathcal{S}_- \cup \mathcal{S}_0$ until the first transition to a state in $\mathcal{S}_+$, at which point the level $\{X(t)\}$ immediately leaves the boundary – we will call this a *sticky* boundary. If $j \in \mathcal{S}_+$ the process immediately leaves the boundary – we will call this a refecting boundary. We collect the probabilities p_{ij} into the matrices $\boldsymbol{P}_{-+} = [p_{ij}]_{i\in\mathcal{S}_-, j\in\mathcal{S}_+}$, $\boldsymbol{P}_{-0} = [p_{ij}]_{i\in\mathcal{S}_-, j\in\mathcal{S}_0}$, and $\boldsymbol{P}_{--} = [p_{ij}]_{i\in\mathcal{S}_-, j\in\mathcal{S}_-}$.

Adjacent to the boundary at $y_0 = 0$ is the band $\mathcal{D}_0 = [0, \Delta]$ which corresponds to level 0 for the QBD-RAP. We denote the boundary of the QBD-RAP as level -1, which corresponds to $\{0\}$ for the fluid queue. Modelling the behaviour of the fluid queue at boundaries can be broken down into three components. 1) Modelling the time and phase when the fluid level hits the boundary. 2) Modelling the phase whilst the fluid level remains at the boundary. 3) Modelling the fluid level and phase at the exit from the boundary.

We claim that the event $\{L(t) = \ell, \phi(t) = i\}$ models the event $\{X(t) \in \mathcal{D}_{\ell,i}, \varphi(t) = i\}$, and further that instants u with $L(u^-) \neq L(u), \phi(u) = i$ model the events $\{X(u^-) \in \mathcal{D}_{\ell,i}, X(u) \notin \mathcal{D}_{\ell,i}, \varphi(u) = i\}$. With this in mind, we suppose that when the QBD-RAP is in level 0 in phase $i \in \mathcal{S}_-$ and there is a change of level, this corresponds to approximating the event that the fluid level $\{X(t)\}$ hits the boundary at 0. We refer to this as the QBD-RAP hitting the boundary also. We show later that, using matrix exponentials with sufficiently small variance in the construction of the QBD-RAP, then the distribution of time until the QBD-RAP first hits the boundary closely models the time until the fluid level hits the boundary. This addresses component 1).

For a sticky lower boundary at 0, given the fluid level reaches zero at time u in phase $i \in \mathcal{S}_-$, then the phase transitions to some phase $j \in \mathcal{S}_- \cup \mathcal{S}_0$ with probability p_{ij}, and the

distribution of the phase $\varphi(t)$ (on the event that the process has not left the boundary at or before time t) is given by the elements of the vector

$$p_{ij}\boldsymbol{e}_j \exp\left(\begin{bmatrix} \boldsymbol{T}_{--} & \boldsymbol{T}_{-0} \\ \boldsymbol{T}_{0-} & \boldsymbol{T}_{00} \end{bmatrix}(t-u)\right).$$

The distribution for the time until $\{X(t)\}$ leaves $x=0$ for the first time after u is

$$1 - p_{ij}\boldsymbol{e}_j \exp\left(\begin{bmatrix} \boldsymbol{T}_{--} & \boldsymbol{T}_{-0} \\ \boldsymbol{T}_{0-} & \boldsymbol{T}_{00} \end{bmatrix}(t-u)\right)\boldsymbol{e}.$$

Therefore, in the case of a sticky boundary, we can capture the behaviour of the process at the boundary exactly. For a reflecting boundary there is no time spent at the boundary. This addresses component 2) of the modelling problem.

For both sticky and reflecting boundaries, given the QBD-RAP is in the correct phase at the instant upon which it hits the boundary, then upon exiting the boundary the phase can be captured exactly too. For a sticky boundary, given the fluid/QBD-RAP hits the boundary in phase $i \in \mathcal{S}_-$ at time t, it then jumps to phase $j \in \mathcal{S}_+ \cup \mathcal{S}_0$ and exits the boundary in phase $k \in \mathcal{S}_+$ at time $(t-u)$ with density

$$p_{ij}\boldsymbol{e}_j \exp\left(\begin{bmatrix} \boldsymbol{T}_{--} & \boldsymbol{T}_{-0} \\ \boldsymbol{T}_{0-} & \boldsymbol{T}_{00} \end{bmatrix}(t-u)\right)\begin{bmatrix} \boldsymbol{T}_{-+} \\ \boldsymbol{T}_{0+} \end{bmatrix}\boldsymbol{e}_k.$$

For a reflecting boundary, given the boundary is hit in phase $i \in \mathcal{S}_-$, the phase upon leaving the boundary is $j \in \mathcal{S}_+$ with probability p_{ij}. Upon leaving the boundary, the appropriate orbit position for the QBD-RAP is $\boldsymbol{\alpha}$, as this corresponds to the fluid level $X=0$.

To summarise, at time t the rate at which probability mass accumulates at the sticky boundary in phase $j \in \mathcal{S}_- \cup \mathcal{S}_0$ and level -1, upon hitting the boundary in phase $i \in \mathcal{S}_-$ and level 0, is

$$c_i p_{ij} \boldsymbol{A}(t)\boldsymbol{s}.$$

The rate at which density from phase $i \in \mathcal{S}_-$ and level 0 transitions to density in phase $j \in \mathcal{S}_+$ and level 0 upon hitting a boundary is

$$c_i p_{ij} \boldsymbol{A}(t)\boldsymbol{s},$$

and upon this transition, the orbit jumps to $\boldsymbol{\alpha}$. The rate at which mass leaves the sticky boundary from phase $i \in \mathcal{S}_- \cup \mathcal{S}_0$ and level -1 into phases $j \in \mathcal{S}_+$ and level 0 is

$$T_{ij},$$

and upon leaving the boundary the orbit is $\boldsymbol{\alpha}$.

This information can be inscribed in the generator of the QBD-RAP. For example, using the augmented state-space scheme to account for phases $\mathcal{S}_0$, the generator of the QBD-RAP described above has boundary conditions included as

$$\left[\begin{array}{cc|cccc|c} \boldsymbol{T}_{--} & \boldsymbol{T}_{0-} & \boldsymbol{T}_{-+}\otimes\boldsymbol{\alpha} & \mathbf{0} & \mathbf{0} & \mathbf{0} & \\ \boldsymbol{T}_{-0} & \boldsymbol{T}_{00} & \boldsymbol{T}_{0+}\otimes\boldsymbol{\alpha} & \mathbf{0} & \mathbf{0} & \mathbf{0} & \\ \hline \mathbf{0} & \mathbf{0} & & & & & \\ \mathbf{0} & \mathbf{0} & & & & & \\ (\boldsymbol{C}_-\boldsymbol{P}_{--})\otimes\boldsymbol{s} & (\boldsymbol{C}_-\boldsymbol{P}_{-0})\otimes\boldsymbol{s} & & \multicolumn{2}{c}{\check{\boldsymbol{B}}_0} & & \boldsymbol{B}_{+1} & \\ \mathbf{0} & \mathbf{0} & & & & & & \ddots \\ \hline & & & \multicolumn{2}{c}{\boldsymbol{B}_{-1}} & & \boldsymbol{B}_0 & \\ & & & & & \ddots & & \ddots \end{array}\right],$$

where

$$\check{\boldsymbol{B}}_0 = \left[\begin{array}{ccccc} \boldsymbol{C}_+\otimes\boldsymbol{S}+\boldsymbol{T}_{++}\otimes\boldsymbol{I} & \boldsymbol{T}_{+0}\otimes\boldsymbol{I} & \boldsymbol{T}_{+-}\otimes\boldsymbol{D} & & \\ \boldsymbol{T}_{0+}\otimes\boldsymbol{I} & \boldsymbol{T}_{00}\otimes\boldsymbol{I} & \boldsymbol{T}_{0-}\otimes\boldsymbol{D} & & \\ (\boldsymbol{C}_-\boldsymbol{P}_{-+})\otimes\boldsymbol{s}\boldsymbol{\alpha}+\boldsymbol{T}_{-+}\otimes\boldsymbol{D} & & \boldsymbol{C}_-\otimes\boldsymbol{S}+\boldsymbol{T}_{--}\otimes\boldsymbol{I} & \boldsymbol{T}_{-0}\otimes\boldsymbol{I} & \\ \boldsymbol{T}_{0+}\otimes\boldsymbol{D} & & \boldsymbol{T}_{0-}\otimes\boldsymbol{I} & \boldsymbol{T}_{00}\otimes\boldsymbol{I} & \end{array}\right].$$

The top-left block represents the point masses due to the sticky boundary. The bottom-left block is the transition of density into point masses due to the sticky boundary. The top-right block is the transition of point masses into density as the process leaves the boundary. The term $(\boldsymbol{C}_-\boldsymbol{P}_{-+})\otimes\boldsymbol{s}\boldsymbol{\alpha}$ in $\check{\boldsymbol{B}}_0$ incorporates the reflecting boundary behaviour.

Upper boundaries can be included in an analogous manner.

The orbit process $\{\boldsymbol{A}(t)\}$ is not required to model the behaviour at the sticky boundary. However, we suppose that $\boldsymbol{A}(t) = 1$ at the boundaries. This choice is arbitrary but allows us to generalise some notation later when we are describing the evolution of the QBD-RAP. Further, for boundaries at $y_0 = 0$ and $y_{K+1} = (K+1)\Delta$, we let the level process take the value $L(t) = -1$ at the lower boundary, and $L(t) = K+1$ at the upper boundary. Denote the set of levels (including boundary levels) by $\mathcal{K} = \{-1, 0, \ldots, K, K+1\}$.

Remark 3.3. *It may be possible to extend the QBD-RAP approximation to model jumps into and out of the boundary, provided that the jumps into/out of the boundary happen at an intensity which can be described by a matrix exponential distribution.*

Furthermore, it may be possible to model more general boundary behaviours which can be approximated by a limit of matrix exponentials. For example, a boundary condition where the fluid queue spends a deterministic time at the boundary.

3.6 Initial conditions

We argued earlier that we can think of the orbit $\boldsymbol{k}(x)$ as corresponding to the fluid being a distance of x from the left boundary of an interval when $i \in \mathcal{S}_+$, or from the

right boundary of an interval when $i \in \mathcal{S}_-$. With this interpretation, an approximation to the initial condition $\boldsymbol{X}(0) = (X(0), \varphi(0)) = (x_0, i)$, $x_0 \in \mathcal{D}_{\ell,i}$, $i \in \mathcal{S}_+ \cup \mathcal{S}_{+0}$ is to set the initial orbit to $\boldsymbol{k}(x_0 - y_\ell)$. Similarly, an approximation to the initial condition $\boldsymbol{X}(0) = (x_0, i)$, $x_0 \in \mathcal{D}_{\ell,i}, x_0 \neq y_{\ell+1}$, $i \in \mathcal{S}_- \cup \mathcal{S}_{-0}$ is to set the initial orbit position to $\boldsymbol{k}(y_{\ell+1} - x_0)$.

We use the notation $\boldsymbol{a}_{\ell,i}(x_0) = \boldsymbol{a}_{\ell,+}(x_0) = \boldsymbol{k}(x_0 - y_\ell)$ for the initial orbit position corresponding to x_0 when the initial phase is $i \in \mathcal{S}_+$ and $x_0 \in \mathcal{D}_{\ell,i}$. Similarly, for $i \in \mathcal{S}_-$ and $x_0 \in \mathcal{D}_{\ell,i}$ define the notation $\boldsymbol{a}_{\ell,i}(x_0) = \boldsymbol{a}_{\ell,-}(x_0) = \boldsymbol{k}(y_{\ell+1} - x_0)$.

More generally, given an initial measure $\mu_i(\cdot) := \mathbb{P}(X(0) \in \cdot, \varphi(0) = i)$, an approximation to this initial condition is to set the orbit to $\displaystyle\int_{x \in \mathcal{D}_{\ell,i}} \boldsymbol{a}_{\ell,i}(x)\, \mathrm{d}\mu_i$, for $i \in \mathcal{S}$, $\ell \in \mathcal{K} \setminus \{-1, K+1\}$.

Initial conditions for phases $i \in \mathcal{S}_0$ While the augmented state-space scheme described above is a convergent one, the analysis of the QBD-RAP scheme is *greatly* simplified if we allow initial conditions which allocate 0 probability to phases in $i \in \mathcal{S}_{+0} \cup \mathcal{S}_{-0}$ only. To see why initial mass in $\mathcal{S}_{+0} \cup \mathcal{S}_{-0}$ might introduce further complexity, consider a sample path with $\varphi(0) = k \in \mathcal{S}_{+0}$ and $\boldsymbol{A}(0) = \boldsymbol{a} \in \mathcal{A}$. On $\varphi(u) \in \mathcal{S}_{+0}$, for all $u \in [0, t)$, then $\boldsymbol{A}(u) = \boldsymbol{a}$ is constant. Upon the phase leaving $\mathcal{S}_{+0}$, at time t, say, the phase will either jump to $\mathcal{S}_+$ or $\mathcal{S}_-$. If $\varphi(t)$ jumps to $i \in \mathcal{S}_+$, the orbit process at time t will be $\boldsymbol{A}(t) = \boldsymbol{a}$ and the process evolve from time t as if it has started in phase $i \in \mathcal{S}_+$ with initial orbit $\boldsymbol{a}$ – there are no major issues in this case. If, however, $\varphi(t)$ jumps to $i \in \mathcal{S}_-$, then the orbit process will jump to $\boldsymbol{A}(t) = \boldsymbol{aD}$ at time t. From time t onward the QBD-RAP process will evolve as if it has started in phase $i \in \mathcal{S}_-$ with initial orbit $\boldsymbol{aD}$. With the way we have structured the proof of convergence, we then have to complete two analyses of the QBD-RAP process – one for the initial condition $\boldsymbol{a}$ and another for the initial condition $\boldsymbol{aD}$.

A solution to this problem is to augment a set of ephemeral states to the QBD-RAP which capture the initial sojourn in $\mathcal{S}_0$ only. Suppose we wish to approximate a fluid queue with the initial condition μ_k where μ_k has mass 1. Let us denote the set of ephemeral states by $\mathcal{S}_0^{*,k}$ and each state in $\mathcal{S}_0^{*,k}$ by i^*. Each state $i^* \in \mathcal{S}_0^{*,k}$ is a copy of $i \in \mathcal{S}_0$, and, in $\mathcal{S}_0^{*,k}$ the phase process has the same phase dynamics as it does in $\mathcal{S}_0$. At time 0, we start the QBD-RAP in the ephemeral set of states $\mathcal{S}_0^{*,k}$ in phase $k^* \in \mathcal{S}_0^{*,k}$. While in $\mathcal{S}_0^{*,k}$, the phase process evolves according to the generator $\boldsymbol{T}_{00}$. Upon exiting the ephemeral set $\mathcal{S}_0^{*,k}$ at time t, say, the QBD-RAP process jumps to $L(t) = \ell$, $\boldsymbol{A}(t) = \int_{\mathcal{D}_{\ell,i}} \boldsymbol{a}_{\ell,i}(x)\, \mathrm{d}\mu_k$, $\varphi(t) = i$, where $\ell \in \mathcal{K}$, $i \in \mathcal{S}_+ \cup \mathcal{S}_-$.

Notice that we have not mentioned anything about the level or orbit process during the sojourn in $\mathcal{S}_0^{*,k}$. This is because all information about the level and phase during this time is contained within the initial condition μ_k, and the only thing that changes is the phase.

To include the ephemeral states within the generator of the QBD-RAP we can do the following,

$$\left[\begin{array}{c|cccc} \boldsymbol{T}_{00} & \boldsymbol{B}^{*,k}_{-1} & \boldsymbol{B}^{*,k}_{0} & \boldsymbol{B}^{*,k}_{1} & \dots \\ \hline & \check{\boldsymbol{B}}_0 & \check{\boldsymbol{B}}_{+1} & & \\ & \check{\boldsymbol{B}}_{-1} & \check{\boldsymbol{B}}_0 & \boldsymbol{B}_{+1} & \\ & & \boldsymbol{B}_{-1} & \boldsymbol{B}_0 & \ddots \\ & & & \ddots & \ddots \end{array}\right],$$

where

$$\boldsymbol{B}^{*,k}_{-1} = \begin{bmatrix} \boldsymbol{T}_{0-}\mu_k(\{0\}) & \boldsymbol{0} \end{bmatrix} \qquad \boldsymbol{B}^{*,k}_{\ell} = \begin{bmatrix} \boldsymbol{T}_{0+} \otimes \boldsymbol{a}^{+}_{\ell} & \boldsymbol{0} & \boldsymbol{T}_{0-} \otimes \boldsymbol{a}^{-}_{\ell} & \boldsymbol{0} \end{bmatrix},$$

$$\check{\boldsymbol{B}}_0 = \begin{bmatrix} \boldsymbol{T}_{--} & \boldsymbol{T}_{-0} \\ \boldsymbol{T}_{0-} & \boldsymbol{T}_{00} \end{bmatrix}, \qquad \check{\boldsymbol{B}}_{+1} = \begin{bmatrix} \boldsymbol{T}_{-+} \otimes \boldsymbol{\alpha} & \boldsymbol{0} & \boldsymbol{0} & \boldsymbol{0} \\ \boldsymbol{T}_{0+} \otimes \boldsymbol{\alpha} & \boldsymbol{0} & \boldsymbol{0} & \boldsymbol{0} \end{bmatrix},$$

$$\check{\boldsymbol{B}}_{-1} = \begin{bmatrix} \boldsymbol{0} & \boldsymbol{0} \\ \boldsymbol{0} & \boldsymbol{0} \\ (\boldsymbol{C}_{-}\boldsymbol{P}_{--}) \otimes \boldsymbol{s} & (\boldsymbol{C}_{-}\boldsymbol{P}_{-0}) \otimes \boldsymbol{s} \\ \boldsymbol{0} & \boldsymbol{0} \end{bmatrix},$$

and

$$\boldsymbol{a}^{r}_{\ell} = \int_{\mathcal{D}_{\ell,r}} \boldsymbol{a}_{\ell,r}(x)\,\mathrm{d}\mu_k,\ \ell \in \mathcal{K} \setminus \{-1, K+1\},\ r \in \{+,-\}.$$

In general, we need to augment a set of states $\mathcal{S}^{*,k}_0$ to the QBD-RAP for each initial phase, $k \in \mathcal{S}_0$ such that μ_k has positive mass.

3.7 At time t – closing operators

The level process $\{L(t)\}$ of the QBD-RAP approximates the process

$$\left\{\sum_{k\in\mathcal{K}}\sum_{i\in\mathcal{S}} k1(X(t) \in \mathcal{D}_{k,i})\right\}_{t\geq 0}. \tag{3.19}$$

This may be of interest in its own right. However, for some applications, this approximation may be too coarse – the level process tells us nothing about where in the intervals $\mathcal{D}_{k,i}$ the fluid queue might be.

We now describe how the orbit position $\boldsymbol{A}(t)$ can be used to approximate the density of the level of the fluid queue $X(t)$. This reconstruction is entirely post-hoc in the sense that it does not affect the dymaics of the QBD-RAP itself. For any time t we only take

the information contained in $\mathbb{E}[\boldsymbol{A}(t)1(L(t)=\ell,\varphi(t)=i)]$ and rewrite it in a descriptive way.

Suppose that the QBD-RAP is in level $L(t)=\ell$, phase $\phi(t)=j\in\mathcal{S}_+$, and the orbit is $\boldsymbol{A}(t)=\boldsymbol{a}$. If the QBD-RAP remains in phase j, the QBD-RAP approximation will transition out of level ℓ in the infinitesimal time interval $t+\,\mathrm{d}u$ with density $\boldsymbol{a}e^{|c_j|\boldsymbol{S}u}|c_j|\boldsymbol{s}\,\mathrm{d}u$. At the time of the change of level we estimate the position of $X(t+u)$ by $X(t+u)\approx y_{\ell+1}$. Tracing this back to time t, we estimate the position of $X(t)$ as $X(t)\approx y_{\ell+1}-|c_j|u$. Reverse engineering this logic, the approximation to the density of $X(t)\in\,\mathrm{d}x$ is $\boldsymbol{a}e^{|c_j|\boldsymbol{S}(y_{\ell+1}-x)/|c_j|}|c_j|\boldsymbol{s}\,\mathrm{d}x/|c_j|$, since $\mathrm{d}x=|c_j|\,\mathrm{d}u$ where $\mathrm{d}x$ is an infinitesimal interval in space and $\mathrm{d}u$ is an infinitesimal interval with respect to time.

Similarly, for $j\in\mathcal{S}_-$, if the QBD-RAP remains in phase j then the QBD-RAP approximation will transition out of level ℓ in the infinitesimal time interval $t+\,\mathrm{d}u$ with density $\boldsymbol{a}e^{|c_j|\boldsymbol{S}u}|c_j|\boldsymbol{s}\,\mathrm{d}u$. At the time of the transition of level, we estimate the position of $X(t+u)$ by $X(t+u)\approx y_\ell$. Tracing this back to time t, we estimate the position of $X(t)$ as $X(t)\approx y_\ell+|c_j|u$. Reverse engineering this logic, the approximation to the density $X(t)\in\,\mathrm{d}x$ is $\boldsymbol{a}e^{|c_j|\boldsymbol{S}(x-y_\ell)/|c_j|}|c_j|\boldsymbol{s}\,\mathrm{d}x/|c_j|$, since $\mathrm{d}x=|c_j|\,\mathrm{d}u$.

For phases $j\in\mathcal{S}_0$, if phase j is associated with $\mathcal{S}_+$, we use the same approximation as if $j\in\mathcal{S}_+$, and if phase $j\in\mathcal{S}_0$ is associated with $\mathcal{S}_-$, we use the same approximation as if $j\in\mathcal{S}_-$.

This reasoning leads to an approximation of the distribution of the fluid at time t, $\mathbb{P}(\boldsymbol{X}(t)\in(\,\mathrm{d}x,j)\mid\boldsymbol{X}(0)=(x_0,i))$, as

$$\int_{\boldsymbol{a}\in\mathcal{A}}\mathbb{P}(\boldsymbol{Y}(t)\in(\ell,\,\mathrm{d}\boldsymbol{a},j)\mid\boldsymbol{Y}(0)=\boldsymbol{y}_0)\boldsymbol{a}e^{\boldsymbol{S}z}\boldsymbol{s}\,\mathrm{d}x, \tag{3.20}$$

where $x\in\mathcal{D}_{\ell,j}$, $x_0\in\mathcal{D}_{\ell_0,i}$, $\boldsymbol{y}_0=(\ell_0,\boldsymbol{a}_{\ell_0,i}(x_0),i)$, and

$$z=\begin{cases}x-y_\ell & i\in\mathcal{S}_-,\\ y_{\ell+1}-x & i\in\mathcal{S}_+.\end{cases}$$

While the estimate (3.20) is appealing, it is, however, defective – it does not integrate to 1 for any finite-dimensional matrix exponential distribution. To see this, compute

$$\begin{aligned}&\sum_{\ell\in\mathcal{K}}\sum_{j\in\mathcal{S}}\int_{z\in\mathcal{D}_{\ell,j}}\int_{\boldsymbol{a}\in\mathcal{A}}\mathbb{P}(\boldsymbol{Y}(t)\in(\ell,\,\mathrm{d}\boldsymbol{a},j)\mid\boldsymbol{Y}(0)=\boldsymbol{y}_0)\boldsymbol{a}e^{\boldsymbol{S}z}\boldsymbol{s}\,\mathrm{d}z\\&=\sum_{\ell\in\mathcal{K}}\sum_{j\in\mathcal{S}}\int_{\boldsymbol{a}\in\mathcal{A}}\mathbb{P}(\boldsymbol{Y}(t)\in(\ell,\,\mathrm{d}\boldsymbol{a},j)\mid\boldsymbol{Y}(0)=\boldsymbol{y}_0)(1-\boldsymbol{a}e^{\boldsymbol{S}\Delta}\boldsymbol{e})\\&<1,\end{aligned}$$

since $\boldsymbol{a}e^{\boldsymbol{S}u}\boldsymbol{e}>0$ for any $u>0$. For an orbit position $\boldsymbol{A}(t)=\boldsymbol{a}$, the amount of mass missing from each level and phase is

$$\mathbb{P}(\boldsymbol{Y}(t)\in(\ell,\,\mathrm{d}\boldsymbol{a},j)\mid\boldsymbol{Y}(0)=\boldsymbol{y}_0)\boldsymbol{a}e^{\boldsymbol{S}\Delta}\boldsymbol{e}\,\mathrm{d}x.$$

The problem is that the triple $(\boldsymbol{a}, \boldsymbol{S}, \boldsymbol{s})$ defines a distribution on $x \in [0, \infty)$, however, it only makes sense to take $x \in [0, \Delta)$ in the approximation scheme.

To partially rectify this we can instead approximate $\mathbb{P}(\boldsymbol{X}(t) \in (\,\mathrm{d}x, j) \mid \boldsymbol{X}(0) = (x_0, i))$ by

$$\int_{\boldsymbol{a} \in \mathcal{A}} \mathbb{P}(\boldsymbol{Y}(t) \in (\ell,\, \mathrm{d}\boldsymbol{a}, j) \mid \boldsymbol{Y}(0) = \boldsymbol{y}_0) \boldsymbol{a}\boldsymbol{u}_{\ell,j}(x)\,\mathrm{d}x, \tag{3.21}$$

where

$$\boldsymbol{a}\boldsymbol{u}_{\ell,j}(x) = \begin{cases} \boldsymbol{a}\left(e^{\boldsymbol{S}(y_{\ell+1}-x)}\boldsymbol{s} + e^{\boldsymbol{S}(2\Delta-(y_{\ell+1}-x))}\boldsymbol{s}\right), & j \in \mathcal{S}_+, \\ \boldsymbol{a}\left(e^{\boldsymbol{S}(x-y_\ell)}\boldsymbol{s} + e^{\boldsymbol{S}(2\Delta-(x-y_\ell))}\boldsymbol{s}\right), & j \in \mathcal{S}_-. \end{cases} \tag{3.22}$$

Intuitively, we take the density function $\boldsymbol{a}e^{\boldsymbol{S}x}\boldsymbol{s}$ on $x \in [0, 2\Delta)$, and 'fold' it back on itself around Δ, to create a density function on $[0, \Delta)$,

$$\boldsymbol{a}e^{\boldsymbol{S}x}\boldsymbol{s} + \boldsymbol{a}e^{\boldsymbol{S}(2\Delta-x)}\boldsymbol{s},\ x \in [0, \Delta).$$

The missing mass is now proportional to

$$\boldsymbol{a}e^{\boldsymbol{S}2\Delta}\boldsymbol{e},$$

which is less than the quantity $\boldsymbol{a}e^{\boldsymbol{S}\Delta}\boldsymbol{e}$ from the approximation scheme (3.20). There is nothing special about the choice of truncating the distribution at 2Δ in this construction, and we could choose any truncation value greater than Δ.

A third option is to approximate $\mathbb{P}(\boldsymbol{X}(t) \in (\,\mathrm{d}x, j) \mid \boldsymbol{X}(0) = (x_0, i))$ by

$$\int_{\boldsymbol{a} \in \mathcal{A}} \mathbb{P}(\boldsymbol{Y}(t) \in (\ell,\, \mathrm{d}\boldsymbol{a}, j) \mid \boldsymbol{Y}(0) = (\ell_0, \boldsymbol{a}_{\ell_0,i}(x_0), i)) \boldsymbol{a}\boldsymbol{v}_{\ell,j}(x)\,\mathrm{d}x, \tag{3.23}$$

where

$$\boldsymbol{a}\boldsymbol{v}_{\ell,j}(x) = \begin{cases} \boldsymbol{a}\left(e^{\boldsymbol{S}(y_{\ell+1}-x)} + e^{\boldsymbol{S}(2\Delta-(y_{\ell+1}-x))}\right)\left[I - e^{\boldsymbol{S}2\Delta}\right]^{-1}\boldsymbol{s}, & j \in \mathcal{S}_+, \\ \boldsymbol{a}\left(e^{\boldsymbol{S}(x-y_\ell)} + e^{\boldsymbol{S}(2\Delta-(x-y_\ell))}\right)\left[I - e^{\boldsymbol{S}2\Delta}\right]^{-1}\boldsymbol{s}, & j \in \mathcal{S}_-. \end{cases} \tag{3.24}$$

Here, we take the density function $\boldsymbol{a}e^{\boldsymbol{S}x}\boldsymbol{s}$, defined on $[0, \infty)$, and map it to a density function on $[0, \Delta)$ by $\Delta - |(x \mod 2\Delta) - \Delta|$. The resulting density function is

$$\begin{aligned} v(x) &= \sum_{m=0}^{\infty} \boldsymbol{a}\left(e^{\boldsymbol{S}(x+2\Delta m)} + e^{\boldsymbol{S}(2\Delta-x+2\Delta m)}\right)\boldsymbol{s} \\ &= \boldsymbol{a}\left(e^{\boldsymbol{S}x} + e^{\boldsymbol{S}(2\Delta-x)}\right)\sum_{m=0}^{\infty} e^{\boldsymbol{S}2\Delta m}\boldsymbol{s} \end{aligned}$$

$$= \boldsymbol{a}\left(e^{\boldsymbol{S}x} + e^{\boldsymbol{S}(2\Delta - x)}\right)\left[I - e^{S2\Delta}\right]^{-1}\boldsymbol{s}.$$

The difference between the approximation schemes is the way in which the vector $\boldsymbol{a}$ is used. We generalise this idea with the concept of *closing operators* which is a linear operator $\boldsymbol{v}(x) : \mathcal{A} \to \mathbb{R}$, for each $x \in [0, \Delta)$. For example, the closing operator in Equations (3.20) is the operator $\boldsymbol{v}(x)$, $x \in [0, \Delta)$ such that for any $\boldsymbol{a} \in \mathcal{A}$,

$$\boldsymbol{a}\boldsymbol{v}(x) = \boldsymbol{a}e^{\boldsymbol{S}x}\boldsymbol{s}. \tag{3.25}$$

Similarly, in (3.21)

$$\boldsymbol{a}\boldsymbol{v}(x) = \boldsymbol{a}\left(e^{\boldsymbol{S}x}\boldsymbol{s} + e^{\boldsymbol{S}(2\Delta - x)}\boldsymbol{s}\right), \tag{3.26}$$

and in (3.23)

$$\boldsymbol{a}\boldsymbol{v}(x) = \boldsymbol{a}\left(e^{\boldsymbol{S}x}\boldsymbol{s} + e^{\boldsymbol{S}(2\Delta - x)}\right)\left[I - e^{S2\Delta}\right]^{-1}\boldsymbol{s}. \tag{3.27}$$

We will use the notation

$$\boldsymbol{v}_{\ell,j}(x) = \begin{cases} \boldsymbol{v}(y_{\ell+1} - x) & j \in \mathcal{S}_+ \cup \mathcal{S}_{0+}, \\ \boldsymbol{v}(x - y_\ell) & j \in \mathcal{S}_- \cup \mathcal{S}_{0-}. \end{cases} \tag{3.28}$$

The operator $\boldsymbol{v}(x)$ is a choice which forms part of the definition of the approximation scheme. As we shall see, given certain properties of $\boldsymbol{v}(x)$, we can prove that the approximation scheme converges, and ensures positivity. In the cases above, all the closing operators (3.25)-(3.26) lead to an approximation which converges and, due to their interpretation as probability densities, ensure positivity.

Comments on linearity and normalisation We considered taking the closing operators to be

$$\boldsymbol{a}\boldsymbol{v}(x) = \frac{\boldsymbol{a}\left(e^{\boldsymbol{S}x}\boldsymbol{s} + e^{\boldsymbol{S}(2\Delta - x)}\boldsymbol{s}\right)}{1 - \boldsymbol{a}e^{\boldsymbol{S}2\Delta}\boldsymbol{e}}, \tag{3.29}$$

which also ensures that the solution always preserves mass (the result of integrating (3.29) over $[0, \Delta)$ is 1). However, (3.29) is not a linear operator. The importance of this fact is that for a linear operator,

$$\mathbb{E}[\boldsymbol{A}(t)\boldsymbol{v}(x)] = \mathbb{E}[\boldsymbol{A}(t)]\boldsymbol{v}(x),$$

thus, the computation of $\mathbb{E}[\boldsymbol{A}(t)\boldsymbol{v}(x)]$ can be achieved by first computing $\mathbb{E}[\boldsymbol{A}(t)]$ and then applying $\boldsymbol{v}(x)$ to the result. In this sense, $\mathbb{E}[\boldsymbol{A}(t)]$ contains all of the information about the history of the process up to time t needed to compute $\mathbb{E}[\boldsymbol{A}(t)\boldsymbol{v}(x)]$. This is much the same as in RAPs and QBD-RAPs where $\mathbb{E}[\boldsymbol{A}(t)]$ is all that is required to compute probabilities about the future of the processes from time t onwards.

When $\boldsymbol{v}(x)$ is not linear then, in general,

$$\mathbb{E}[\boldsymbol{A}(t)\boldsymbol{v}(x)] \neq \mathbb{E}[\boldsymbol{A}(t)]\boldsymbol{v}(x).$$

For example, with (3.29),

$$\mathbb{E}[\boldsymbol{A}(t)\boldsymbol{v}(x)] = \int_{\boldsymbol{a}\in\mathcal{A}} \mathbb{P}(\boldsymbol{A}(t) \in \mathrm{d}\boldsymbol{a}) \frac{\boldsymbol{a}\left(e^{\boldsymbol{S}x}\boldsymbol{s} + e^{\boldsymbol{S}(2\Delta - x)}\boldsymbol{s}\right)}{1 - \boldsymbol{a}e^{\boldsymbol{S}2\Delta}\boldsymbol{e}}. \tag{3.30}$$

While the calculation in (3.30) is theoretically possible, practically it is not. The seemingly innocuous integral over $\boldsymbol{a} \in \mathcal{A}$ actually amounts to an integral over all possible sample paths of the QBD-RAP (i.e. all possible event times of the QBD-RAP before time t) and in general, there is no 'nice' way to do this computation.

In the linear case, computation of

$$\mathbb{E}[\boldsymbol{A}(t)] = \int_{\boldsymbol{a}\in\mathcal{A}} \mathbb{P}(\boldsymbol{A}(t) \in \mathrm{d}\boldsymbol{a})\boldsymbol{a},$$

amounts to a matrix-exponential calculation.

In practice we may use

$$\frac{\mathbb{E}\left[\boldsymbol{A}(t)\right]\left(e^{\boldsymbol{S}x}\boldsymbol{s} + e^{\boldsymbol{S}(2\Delta - x)}\boldsymbol{s}\right)}{1 - \mathbb{E}\left[\boldsymbol{A}(t)\right]e^{\boldsymbol{S}2\Delta}\boldsymbol{e}} \tag{3.31}$$

as a normalised version of (3.26), and this seems to work well. However, this is not the same as using the closing operator (3.29).

3.8 Approximating Fluid-fluid queues

Chapter 4

Convergence of the QBD-RAP before the first orbit restart epoch

This chapter details a convergence of the approximation scheme constructed in Chapter 3 on the event the first *orbit restart epoch* is yet to occur. Unless the QBD-RAP hits a boundary and is immediately reflected, an orbit restart epoch corresponds to a change of level. If the process hits a boundary and is immediately reflected, then there is no change of level, but the orbit process does 'restart' at this time. We will define orbit restart epochs more precisely, later. From the stochastic interpretation in Chapter 3, the orbit restart epochs approximate the hitting times of the fluid queue on the points $\{y_\ell\}$ when the fluid level is not at a boundary, or the exit times of the boundaries when sticky boundaries are present and the fluid queue is at the boundary. Thus, this chapter proves a convergence of the QBD-RAP scheme to the fluid queue in each of the sets $\{0\}, \mathcal{D}_0, \mathcal{D}_1, \ldots, \mathcal{D}_K, \{y_{K+1}\}$.

In Chapter 5, we use the main results of this chapter to prove further convergence results for the QBD-RAP scheme, and ultimately provide a global result. Conceptually Chapter 5 stitches together the convergence on each of the sets $\{0\}, \mathcal{D}_0, \mathcal{D}_1, \ldots, \mathcal{D}_K, \{y_{K+1}\}$ proved in this chapter to claim the global convergence. Chapters 4 and 5 differ somewhat in their proof techniques: Chapter 4 relies more heavily on concentrated-matrix-exponential-specific arguments whereas Chapter 5 uses more traditional arguments such as the Markov property, time-homogeneity and the law of total probability. We now detail the QBD-RAP scheme with which we will work throughout this chapter, and detail the structure of the chapter.

Recall that the QBD-RAP is constructed using *matrix exponential distributions* to model, approximately, the sojourn time of the fluid queue in a given interval. This chapter shows a type of convergence under the assumption that the variance of the matrix exponential distribution(s) used in the construction tends to 0. The result applies to any sequence of matrix exponential distributions such that the variance tends to zero. The generality of the result is necessitated by the fact that, in practice, we use the class of *concentrated matrix exponential distributions* found numerically in (Horváth et al. 2020),

for which there are relatively few known properties.

In this chapter we work exclusively with the *augmented state space model* to model phases with rates $c_i = 0$ as described in Section 3.3.

Further, to model an initial condition, $\varphi(0) = k \in \mathcal{S}_0$, we use the ephemeral set of phases $\mathcal{S}_0^{*,k}$ as described in Section 3.6. Approximating the initial condition $\varphi(0) = k \in \mathcal{S}_0$ in this way greatly simplifies some results in this chapter. In Appendix C we provide results which prove the convergence of the approximation without the need to model the initial condition $\varphi(0) = k \in \mathcal{S}_0$ by an ephemeral set of phases. Appendix C relies on the fact that $\boldsymbol{a}_{\ell_0,i}(\Delta - x_0)$ and $\boldsymbol{a}_{\ell_0,i}(x_0)\boldsymbol{D}$ are 'close', in some sense, then leverages the results of this chapter to prove various bounds which ultimately show convergence. Beyond that, Appendix C provides limited further insight into the QBD-RAP process, it is also long and somewhat tedious, hence why it is in an appendix.

In this chapter we analyse the distribution of the QBD-RAP scheme up to the first orbit restart epoch. The structure of the analysis is to first partition the distribution of the QBD-RAP at time t (where t is before the first orbit restart epoch) on the number of changes of phase from $\mathcal{S}_+ \cup \mathcal{S}_{+0}$ to $\mathcal{S}_-$ or $\mathcal{S}_- \cup \mathcal{S}_{-0}$ to $\mathcal{S}_+$. We will refer to changes of phase from $\mathcal{S}_+ \cup \mathcal{S}_{+0}$ to $\mathcal{S}_-$ as *up-down* transitions and changes of phase from $\mathcal{S}_- \cup \mathcal{S}_{-0}$ to $\mathcal{S}_+$ as *down-up* transitions. Next, for each term in the partition we take the Laplace transform with respect to time. This is convenient as it enables algebraic manipulations such that we can separate the Laplace transforms into one term solely about the orbit process of the QBD-RAP and one expression about the phase process and associated rates. Once we have established a convenient algebraic form, we then turn our attention to bounds and convergence, establishing bounds for the difference between the Laplace transforms of the QBD-RAP just described and corresponding Laplace transforms of the fluid queue. Thus, we establish a convergence result for the Laplace transforms with respect to time for each of the distributions in the partition. We then wish to 'undo' the partitioning on the event of a given number of up-down and down-up transitions before the first orbit restart epoch to establish a convergence result for the Laplace transform on the event that the first orbit restart epoch is yet to occur.

The main steps of the convergence result of this chapter are listed below.

1. Define the partition on the number of up-down and down-up transitions and the collections sample paths of the QBD-RAP and fluid queue with which we will work. Describe the distributions of the processes on theses sample paths and compute their Laplace transforms with respect to time. (Sections 4.1, 4.2 and 4.3).

2. Show error bounds for the difference between the Laplace transforms of the QBD-RAP and the fluid queue for each term in the partition. (Section 4.4).

3. Show a geometric domination condition so that we may apply the Dominated Convergence Theorem to 'undo' the partitioning and hence prove convergence of the Laplace transforms. (Section **??**).

First we give some preliminaries and some technical assumptions we will use in the proofs.

Preliminaries

Suppose we have a sequence, $\{Z^{(p)}\}_{p\geq 1}$, of matrix exponential random variables with, $Z^{(p)} \sim ME(\boldsymbol{\alpha}^{(p)}, \boldsymbol{S}^{(p)}, \boldsymbol{s}^{(p)})$, such that $\text{Var}\left(Z^{(p)}\right) \to 0$ as $p \to \infty$. For notational convenience we suppose that p is the order of the representation $(\boldsymbol{\alpha}^{(p)}, \boldsymbol{S}^{(p)}, \boldsymbol{s}^{(p)})$, but strictly speaking, this is not necessary. We use the superscript (p) to denote dependence on the underlying choice of matrix exponential distribution that is used in the construction of the QBD-RAP scheme. To simplify notation, we may omit the superscript (p) when it is not necessary. In the following we show error bounds for an arbitrary parameter $\varepsilon > 0$. However, keep in mind the ultimate intention is to show convergence, for which we choose this parameter to be $\varepsilon^{(p)} = \text{Var}\left(Z^{(p)}\right)^{1/3}$. Other notations that have been defined, which are functions of $Z^{(p)}$ and therefore also implicitly depend on p, are $\boldsymbol{\alpha}^{(p)}$, $\boldsymbol{S}^{(p)}$, $\boldsymbol{s}^{(p)}$, $\boldsymbol{S}_i^{(p)}$, $\boldsymbol{s}_i^{(p)}$, $\boldsymbol{D}^{(p)}$, $\mathcal{A}^{(p)}$, $\boldsymbol{Y}^{(p)}(t) = (L^{(p)}(t), \boldsymbol{A}^{(p)}(t), \phi^{(p)}(t))$, $\boldsymbol{Y}_{\boldsymbol{\alpha}}^{(p)}(t)$, $\boldsymbol{y}_0^{(p)}$.

In the following we show various results which involve integrating a function g, or a sequence of functions $g_1, g_2, \ldots$. We make the following assumptions about such functions,

Assumptions 4.1. *Let g be a function $g : [0,\infty) \to [0,\infty)$ which is*
(i) non-negative,

$$g(x) \geq 0 \text{ for all } x \geq 0,$$

(ii) bounded,

$$g(x) \leq G < \infty \text{ for all } x \geq 0,$$

(iii) integrable,

$$\int_{x=0}^{\infty} g(x)\,\mathrm{d}x \leq \widehat{G} < \infty,$$

(iv) and Lipschitz continuous

$$|g(x) - g(u)| \leq L|x-u| \text{ for all } x,\, u \geq 0,\, 0 < L < \infty. \tag{4.1}$$

We also need a sequence of closing operators which we denote by $\boldsymbol{v}^{(p)}$. For the convergence results, we require the following properties of the closing operators $\boldsymbol{v}^{(p)}(x)$, $x \in [0,\Delta)$.

Properties 4.2. *Let $\{\boldsymbol{v}^{(p)}(x)\}_{p\geq 1}$ be a sequence of closing operators such that they may be decomposed into $\boldsymbol{v}^{(p)}(x) = \boldsymbol{w}^{(p)}(x) + \widetilde{\boldsymbol{w}}^{(p)}(x)$, where;*
(i) for $x \in [0,\Delta), u, v \geq 0$,

$$\boldsymbol{\alpha}^{(p)} e^{\boldsymbol{S}^{(p)}(u+v)} (-\boldsymbol{S}^{(p)})^{-1} \widetilde{\boldsymbol{w}}^{(p)}(x) \leq \boldsymbol{\alpha}^{(p)} e^{\boldsymbol{S}^{(p)}u} (-\boldsymbol{S}^{(p)})^{-1} \widetilde{\boldsymbol{w}}^{(p)}(x).$$

(ii) for $x \in [0, \Delta), u \geq 0$,

$$\boldsymbol{\alpha}^{(p)} e^{\boldsymbol{S}^{(p)} u} (-\boldsymbol{S}^{(p)})^{-1} \widetilde{\boldsymbol{w}}^{(p)}(x) = \widetilde{G}_{\boldsymbol{v}}^{(p)} \to 0, \quad as\ p \to \infty.$$

(iii) for $x \in [0, \Delta), u \geq 0$,

$$\boldsymbol{\alpha}^{(p)} e^{\boldsymbol{S}^{(p)} u} (-\boldsymbol{S}^{(p)})^{-1} \boldsymbol{w}^{(p)}(x) \leq \boldsymbol{\alpha}^{(p)} e^{\boldsymbol{S}^{(p)} u} \boldsymbol{e} G_{\boldsymbol{v}},$$

for some $0 \leq G_{\boldsymbol{v}} < \infty$ *independent of* p *for* $p > p_0$ *where* $p_0 < \infty$.
(iv) for $\boldsymbol{a} \in \mathcal{A}$, $u \geq 0$,

$$\int_{x \in [0,\Delta)} \boldsymbol{a}^{(p)} e^{\boldsymbol{S}^{(p)} u} \boldsymbol{v}^{(p)}(x)\, \mathrm{d}x \leq \boldsymbol{a}^{(p)} e^{\boldsymbol{S}^{(p)} u} \boldsymbol{e}.$$

(v) Let g *be a function satisfying the Assumptions 4.1. For* $u \leq \Delta - \varepsilon^{(p)}$, $v \in [0, \Delta)$, *then*

$$\left| \int_{x=0}^{\infty} \frac{\boldsymbol{\alpha}^{(p)} e^{\boldsymbol{S}^{(p)}(u+x)}}{\boldsymbol{\alpha}^{(p)} e^{\boldsymbol{S}^{(p)} u} \boldsymbol{e}} \boldsymbol{v}^{(p)}(v) g(x)\, \mathrm{d}x - g(\Delta - u - v) 1(u + v \leq \Delta - \varepsilon^{(p)}) \right| = |r_{\boldsymbol{v}}^{(p)}(u, v)|,$$

where

$$\int_{u=0}^{\Delta} \left| r_{\boldsymbol{v}}^{(p)}(u, v) \right| \mathrm{d}u \leq R_{\boldsymbol{v},1}^{(p)} \to 0$$

and

$$\int_{v=0}^{\Delta} \left| r_{\boldsymbol{v}}^{(p)}(u, v) \right| \mathrm{d}v \leq R_{\boldsymbol{v},2}^{(p)} \to 0$$

as $\mathrm{Var}(Z^{(p)}) \to 0$.

In Appendix D we provide results which show that the closing operators (3.25) - (3.27) satisfy Properties 4.2.

Though it is a slight abuse of notation, for convenience, let us write

$$\mathbb{P}(\boldsymbol{Y}(t) \in (\ell,\, \mathrm{d}x, j) \mid \boldsymbol{Y}(0) = \boldsymbol{y}_0)$$

in place of

$$\int_{\boldsymbol{a} \in \mathcal{A}} \mathbb{P}(\boldsymbol{Y}(t) \in (\ell,\, \mathrm{d}\boldsymbol{a}, j) \mid \boldsymbol{Y}(0) = \boldsymbol{y}_0) \boldsymbol{a} \boldsymbol{v}_{\ell,j}(x)\, \mathrm{d}x \tag{4.2}$$

where $\boldsymbol{v}_{\ell,j}(x)$ is a closing operator. Expression (4.2) is an approximation to

$$\mathbb{P}(\boldsymbol{X}(t) \in (\, \mathrm{d}x, j) \mid \boldsymbol{X}(0) = (x_0, i)), \tag{4.3}$$

$x \in \mathcal{D}_{\ell,j}$, $x_0 \in \mathcal{D}_{\ell_0,i}$. Further, let us write

$$\mathbb{P}(\boldsymbol{Y}(t) \in (\ell, E, j) \mid \boldsymbol{Y}(0) = \boldsymbol{y}_0)$$

in place of

$$\int_{x\in E}\int_{\boldsymbol{a}\in\mathcal{A}} \mathbb{P}(\boldsymbol{Y}(t)\in(\ell,\,\mathrm{d}\boldsymbol{a},j)\mid \boldsymbol{Y}(0)=\boldsymbol{y}_0)\boldsymbol{a}\boldsymbol{v}_{\ell,j}(x)\,\mathrm{d}x \tag{4.4}$$

for some measurable set $E\subseteq\mathcal{D}_{\ell,j}$.

Ultimately, in Chapter 5, we will apply the Extended Continuity Theorem for Laplace transforms (Feller 1957, Chapter XIII, Theorem 2a) to claim convergence. The Extended Continuity Theorem for Laplace transforms requires us to show convergence of the Laplace transform pointwise with respect to the transform parameter, λ, on the set $\lambda\in\mathbb{R}$, $\lambda>0$. Therefore, we can fix $\lambda\in\mathbb{R}$, $\lambda>0$ in the following.

4.1 The distribution of the QBD-RAP

In this chapter we are interested in the QBD-RAP up to the first orbit restart epoch, which we denote by $\tau_1^{(p)}$, which is the random (stopping) time at which the QBD-RAP changes level, or hits the boundary, or exits a boundary, for the first time. More precisely,

$$\tau_1^{(p)}=\inf\left\{t>0\mid L^{(p)}(t)\neq L^{(p)}(0),\text{ or }(L^{(p)}(t),\boldsymbol{A}^{(p)}(t),\varphi(t))\text{ hits a boundary}\right\}.$$

At this time, the orbit process of the QBD-RAP is restarted at the initial value $\boldsymbol{A}^{(p)}(\tau_1^{(p)})=\boldsymbol{\alpha}^{(p)}$, unless the QBD-RAP hits a boundary and is absorbed, in which case the orbit process is restarted at the value $\boldsymbol{A}^{(p)}(\tau_1^{(p)})=1$.*

Consider the initial condition $\boldsymbol{y}_0^{(p)}=(L^{(p)}(0),\boldsymbol{A}^{(p)}(0),\varphi(0))=(\ell_0,\boldsymbol{a}_{\ell_0,i}^{(p)}(x_0),i)$, where $\ell_0\in\mathcal{K}\backslash\{-1,K+1\}$, and $i\in\mathcal{S}$. The value $\boldsymbol{y}_0$ is the approximation to the initial condition $\boldsymbol{X}(0)=(x_0,i)$. We are interested in the quantity, $f^{\ell_0,(p)}(t)(x,j;x_0,i)\,\mathrm{d}x$ given by

$$\begin{aligned}&\int_{\boldsymbol{a}\in\mathcal{A}^{(p)}}\mathbb{P}\Big(\boldsymbol{A}^{(p)}(t)\in\,\mathrm{d}\boldsymbol{a},t<\tau_1^{(p)},\varphi(t)=j\mid\boldsymbol{Y}^{(p)}(0)=\boldsymbol{y}_0^{(p)}\Big)\boldsymbol{a}\boldsymbol{v}_{\ell_0,j}^{(p)}(x)\,\mathrm{d}x\\&=(\boldsymbol{e}_i\otimes\boldsymbol{a}_{\ell_0,i}^{(p)}(x_0))e^{\boldsymbol{B}^{(p)}t}(\boldsymbol{e}_j\otimes\boldsymbol{v}_{\ell_0,j}^{(p)}(x))\,\mathrm{d}x,\end{aligned}\tag{4.5}$$

which is the QBD-RAP approximation to the distribution

$$\mathbb{P}(\boldsymbol{X}(t)\in(\,\mathrm{d}x,j),t<\tau_1^X\mid\boldsymbol{X}(0)=(x_0,i)).$$

For now consider $\varphi(0)=i\in\mathcal{S}_+\cup\mathcal{S}_-$. As we shall see, certain Laplace transform expressions for phases $i\in\mathcal{S}_0^*$ with rate $c_i=0$ can be written as a linear combination of certain Laplace transforms of phases in $\mathcal{S}_+\cup\mathcal{S}_-$.

*Recall from the discussion in Section 3.5 in the paragraph above Remark 3.3, that the orbit process is not actually required to model the behaviour at the boundary. We set it to be $\boldsymbol{A}(t)=1$ for all times t when the QBD-RAP is at the boundary for notational convenience.

Now, introduce a partition on the number of up-down and down-up transitions of the sample paths. Denote by $\{\Sigma_m\}_{m\geq 1}$ the sequence of (stopping) times at which $\{\varphi(t)\}$ has an up-down transition (i.e. jumps from $\mathcal{S}_+ \cup \mathcal{S}_{+0}$ to $\mathcal{S}_-$) for the mth time. Denote by $\{\Gamma_m\}_{m\geq 1}$ the sequence of (stopping) times at which $\{\varphi(t)\}$ has a down-up transition (i.e. jumps from $\mathcal{S}_- \cup \mathcal{S}_{-0}$ to $\mathcal{S}_+$) for the mth time. More precisely, for sample paths with $\varphi(0) \in \mathcal{S}_+$, let $\Gamma_0 = 0$, then for $m \geq 1$,

$$\Sigma_m := \inf\{t > \Gamma_{m-1} \mid \varphi(t) \in \mathcal{S}_-\}, \tag{4.6}$$
$$\Gamma_m := \inf\{t > \Sigma_m \mid \varphi(t) \in \mathcal{S}_+\}. \tag{4.7}$$

Similarly, for sample paths with $\varphi(0) \in \mathcal{S}_-$, let $\Sigma_0 = 0$, then for $m \geq 1$,

$$\Gamma_m := \inf\{t > \Sigma_{m-1} \mid \varphi(t) \in \mathcal{S}_+\}, \tag{4.8}$$
$$\Sigma_m := \inf\{t > \Gamma_m \mid \varphi(t) \in \mathcal{S}_-\}. \tag{4.9}$$

For times t such that $\Gamma_m \leq t < \Sigma_{m+1}$, then $\varphi(t) \in \mathcal{S}_+ \cup \mathcal{S}_{+0}$. For times t such that $\Sigma_{m+1} \leq t < \Gamma_{m+1}$, then $\varphi(t) \in \mathcal{S}_- \cup \mathcal{S}_{-0}$.

With these stopping times, partition the sample paths of the QBD-RAP by the number of up-down and down-up transition which occur as follows. For $x_0 \in \mathcal{D}_{\ell_0,i}$, $x \in \mathcal{D}_{\ell_0,j}$, $t \geq 0$, $\ell_0 \in \{0,\ldots,K\}$, $m \geq 0$, and for $i \in \mathcal{S}_+$, $j \in \mathcal{S}_+ \cup \mathcal{S}_{+0}$, let $f^{\ell_0,(p)}_{m,+,+}(t)(x,j;x_0,i)$, be

$$\begin{aligned}
&\int_{\boldsymbol{a}\in\mathcal{A}^{(p)}} \mathbb{P}\Big(\boldsymbol{A}^{(p)}(t) \in \mathrm{d}\boldsymbol{a}, \varphi(t) = j, t < \tau_1^{(p)}, \Gamma_m \leq t < \Sigma_{m+1} \mid \boldsymbol{Y}^{(p)}(0) = \boldsymbol{y}_0^{(p)}\Big)\boldsymbol{a}\boldsymbol{v}^{(p)}_{\ell_0,j}(x) \\
&= \int_{\sigma_1=0}^{t} (\boldsymbol{e}_i \otimes \boldsymbol{a}^{(p)}_{\ell_0,i}(x_0)) e^{\boldsymbol{B}^{(p)}_{++}\sigma_1}\boldsymbol{B}^{(p)}_{+-} \int_{\gamma_1=\sigma_1}^{t} e^{\boldsymbol{B}^{(p)}_{--}(\gamma_1-\sigma_1)}\boldsymbol{B}^{(p)}_{-+} \ldots \int_{\gamma_m=\sigma_m}^{t} e^{\boldsymbol{B}^{(p)}_{--}(\gamma_m-\sigma_m)}\boldsymbol{B}^{(p)}_{-+} \\
&\quad \times e^{\boldsymbol{B}^{(p)}_{++}(t-\gamma_m)}\Big(\boldsymbol{e}_j \otimes \boldsymbol{v}^{(p)}_{\ell_0,j}(x)\Big)\,\mathrm{d}\gamma_m\,\mathrm{d}\sigma_m \ldots \mathrm{d}\gamma_1\,\mathrm{d}\sigma_1.
\end{aligned} \tag{4.10}$$

Analogously, for $i \in \mathcal{S}_+$, $j \in \mathcal{S}_- \cup \mathcal{S}_{-0}$, let

$$\begin{aligned}
&f^{\ell_0,(p)}_{m+1,+,-}(t)(x,j;x_0,i) \\
&= \int_{\boldsymbol{a}\in\mathcal{A}^{(p)}} \mathbb{P}\Big(\boldsymbol{A}^{(p)}(t) \in \mathrm{d}\boldsymbol{a}, \varphi(t) = j, t < \tau_1^{(p)}, \Sigma_{m+1} \leq t < \Gamma_{m+1} \mid \boldsymbol{Y}^{(p)}(0) = \boldsymbol{y}_0^{(p)}\Big)\boldsymbol{a}\boldsymbol{v}^{(p)}_{\ell_0,j}(x) \\
&= \int_{\sigma_1=0}^{t} (\boldsymbol{e}_i \otimes \boldsymbol{a}^{(p)}_{\ell_0,i}(x_0)) e^{\boldsymbol{B}^{(p)}_{++}\sigma_1}\boldsymbol{B}^{(p)}_{+-} \int_{\gamma_1=\sigma_1}^{t} e^{\boldsymbol{B}^{(p)}_{--}(\gamma_1-\sigma_1)}\boldsymbol{B}^{(p)}_{-+} \ldots \int_{\sigma_{m+1}=\gamma_m}^{t} e^{\boldsymbol{B}^{(p)}_{++}(\sigma_{m+1}-\gamma_m)} \\
&\quad \times \boldsymbol{B}^{(p)}_{+-} e^{\boldsymbol{B}^{(p)}_{--}(t-\sigma_{m+1})}\Big(\boldsymbol{e}_j \otimes \boldsymbol{v}^{(p)}_{\ell_0,j}(x)\Big)\,\mathrm{d}\sigma_1\,\mathrm{d}\gamma_1 \ldots \mathrm{d}\sigma_m\,\mathrm{d}\gamma_m\,\mathrm{d}\sigma_{m+1}
\end{aligned} \tag{4.11}$$

for $i \in \mathcal{S}_-$, $j \in \mathcal{S}_+ \cup \mathcal{S}_{+0}$ let

$$f^{\ell_0,(p)}_{m+1,-,+}(t)(x,j;x_0,i)$$

$$= \int_{\boldsymbol{a}\in\mathcal{A}^{(p)}} \mathbb{P}\Big(\boldsymbol{A}^{(p)}(t) \in \mathrm{d}\boldsymbol{a}, \varphi(t) = j, t < \tau_1^{(p)}, \Gamma_{m+1} \le t < \Sigma_{m+1} \mid \boldsymbol{Y}^{(p)}(0) = \boldsymbol{y}_0^{(p)}\Big)\boldsymbol{a}\boldsymbol{v}_{\ell_0,j}^{(p)}(x)$$
$$= \int_{\gamma_1=0}^{t} (\boldsymbol{e}_i \otimes \boldsymbol{a}_{\ell_0,i}^{(p)}(x_0)) e^{\boldsymbol{B}_{--}^{(p)}\gamma_1} \boldsymbol{B}_{-+}^{(p)} \int_{\sigma_1=\gamma_1}^{t} e^{\boldsymbol{B}_{++}^{(p)}(\sigma_1-\gamma_1)} \boldsymbol{B}_{+-}^{(p)} \cdots \int_{\gamma_{m+1}=\sigma_m}^{t} e^{\boldsymbol{B}_{--}^{(p)}(\gamma_{m+1}-\sigma_m)}$$
$$\times \boldsymbol{B}_{-+}^{(p)} e^{\boldsymbol{B}_{++}^{(p)}(t-\gamma_{m+1})} \Big(\boldsymbol{e}_j \otimes \boldsymbol{v}_{\ell_0,j}^{(p)}(x)\Big)\, \mathrm{d}\gamma_1\, \mathrm{d}\sigma_1 \ldots \mathrm{d}\gamma_m\, \mathrm{d}\sigma_m\, \mathrm{d}\gamma_{m+1} \tag{4.12}$$

and for $i \in \mathcal{S}_-, j \in \mathcal{S}_- \cup \mathcal{S}_{-0}$ let

$$f_{m,-,-}^{\ell_0,(p)}(t)(x,j;x_0,i)$$
$$= \int_{\boldsymbol{a}\in\mathcal{A}^{(p)}} \mathbb{P}\Big(\boldsymbol{A}^{(p)}(t) \in \mathrm{d}\boldsymbol{a}, \varphi(t) = j, t < \tau_1^{(p)}, \Sigma_m \le t < \Gamma_{m+1} \mid \boldsymbol{Y}^{(p)}(0) = \boldsymbol{y}_0^{(p)}\Big)\boldsymbol{a}\boldsymbol{v}_{\ell_0,j}^{(p)}(x)$$
$$= \int_{\gamma_1=0}^{t} (\boldsymbol{e}_i \otimes \boldsymbol{a}_{\ell_0,i}^{(p)}(x_0)) e^{\boldsymbol{B}_{--}^{(p)}\gamma_1} \boldsymbol{B}_{-+}^{(p)} \int_{\sigma_1=\gamma_1}^{t} e^{\boldsymbol{B}_{++}^{(p)}(\sigma_1-\gamma_1)} \boldsymbol{B}_{+-}^{(p)} \cdots \int_{\sigma_m=\gamma_m}^{t} e^{\boldsymbol{B}_{++}^{(p)}(\sigma_m-\gamma_m)} \boldsymbol{B}_{+-}^{(p)}$$
$$\times e^{\boldsymbol{B}_{--}^{(p)}(t-\sigma_m)} \Big(\boldsymbol{e}_j \otimes \boldsymbol{v}_{\ell_0,j}^{(p)}(x)\Big)\, \mathrm{d}\sigma_m\, \mathrm{d}\gamma_m \ldots \mathrm{d}\sigma_1\, \mathrm{d}\gamma_1. \tag{4.13}$$

Now, for $q, r \in \{+,-\}$, $q \neq r$, define

$$f_{q,q}^{\ell_0,(p)}(t)(x,j;x_0,i) := \sum_{m=0}^{\infty} f_{m,q,q}^{\ell_0,(p)}(t)(x,j;x_0,i) \qquad i \in \mathcal{S}_q,\ j \in \mathcal{S}_q \cup \mathcal{S}_{q0},$$
$$f_{q,r}^{\ell_0,(p)}(t)(x,j;x_0,i) := \sum_{m=1}^{\infty} f_{m,q,r}^{\ell_0,(p)}(t)(x,j;x_0,i) \qquad i \in \mathcal{S}_q,\ j \in \mathcal{S}_0 \cup \mathcal{S}_{r0},$$

so that

$$f^{\ell_0,(p)}(t)(x,j;x_0,i) = \begin{cases} f_{q,q}^{\ell_0,(p)}(t)(x,j;x_0,i) & i \in \mathcal{S}_q,\ j \in \mathcal{S}_q \cup \mathcal{S}_{q0}, \\ f_{q,r}^{\ell_0,(p)}(t)(x,j;x_0,i) & i \in \mathcal{S}_q,\ j \in \mathcal{S}_r \cup \mathcal{S}_{r0}. \end{cases} \tag{4.14}$$

Recall, in this chapter, we suppose the QBD-RAP approximation uses ephemeral states $\mathcal{S}_0^{*,k}$ to model the fluid queue whenever the phase starts in $k \in \mathcal{S}_0$. In general, for $k \in \mathcal{S}_0^{*,k}$, $r \in \{+,-\}$, $m \ge 0$, we define

$$f_{m,0,r}^{\ell_0,(p)}(t)(x,j;x_0,k) := \sum_{q\in\{+,-\}} \sum_{i\in\mathcal{S}_q} \int_{t_0=0}^{t} \boldsymbol{e}_k e^{\boldsymbol{T}_{00}t_0} \boldsymbol{T}_{0i} f_{m+1(q\neq r),q,r}^{\ell_0,(p)}(t-t_0)(x,j;x_0,i)\, \mathrm{d}t_0. \tag{4.15}$$

Upon taking the Laplace transform of (4.15) the convolutions become products, so the Laplace transform of $f_{m,0,r}^{\ell_0}(t)(x,j;x_0,k)$ is a linear combination of the Laplace transforms of (4.10)-(4.13). Thus, once we show convergence for the Laplace transforms of (4.10)-(4.13) we get convergence of the Laplace transform for starting in $\mathcal{S}_0^{*,k}$ too.

4.2 The distribution of the fluid queue

Let τ_1^X be the minimum of the time at which $\{X(t)\}$ hits a boundary, or exits a boundary, of exits $\mathcal{D}_{\ell_0}$, where $X(0) = x_0 \in \mathcal{D}_{\ell_0}$. More precisely,

$$\tau_1^X = \min \left\{ \begin{array}{c} \inf\{t > 0 \mid X(t) = y_\ell, \ell \in \mathcal{K}\}, \\ \inf\{t > 0 \mid X(t) \neq 0, X(0) = 0\}, \\ \inf\{t > 0 \mid X(t) \neq y_{K+1}, X(0) = y_{K+1}\} \end{array} \right\}.$$

Consider the measures on the σ-algebra generated by $\mathcal{D}_{\ell_0,j}$ given by

$$\mu^{\ell_0}(t)(\cdot, j; x_0, i) := \mathbb{P}(\boldsymbol{X}(t) \in (\cdot, j), t < \tau_1^X \mid \boldsymbol{X}(0) = (x_0, i)), \tag{4.16}$$

$\ell_0 \in \mathcal{K} \setminus \{-1, K+1\}$, $x_0 \in \mathcal{D}_{\ell_0,i}, i, j \in \mathcal{S}, t \geq 0$. In words, this is the distribution of the fluid queue at time t on the event that the fluid level remains within $\mathcal{D}_{\ell_0}$ up to and including time t and is in phase j at time t, given that is started at $X(0) = x_0 \in \mathcal{D}_{\ell_0,i}$ in phase i.

I do not know of any simple expression for (4.16). There are expressions for the Laplace transform of (4.16) with respect to time. One is in terms of the of first return matrices $\Psi(\lambda)$ and $\Xi(\lambda)$ (Bean et al. 2009*b*). Here we opt for another expression for the Laplace transform which is obtained by partitioning as follows.

As before, we use the sequence of up-down transition times, $\{\Sigma_m\}_{m\geq 1}$, and the sequence of down-up transition times, $\{\Gamma_m\}_{m\geq 1}$, to partition sample paths. The events $\{\Gamma_m \leq t < \Sigma_{m+1}\}$, and $\{\Sigma_{m+1} \leq t < \Gamma_{m+1}\}$, $m \geq 0$, partition the sample paths of (4.16) into periods where the fluid is either non-decreasing or non-increasing, respectively; see Figure 4.1.

For $m \geq 0$, $i \in \mathcal{S}_+$, $j \in \mathcal{S}_+ \cup \mathcal{S}_{+0}$ define

$$\mu^{\ell_0}_{m,+,+}(t)(\cdot, j; x_0, i) = \mathbb{P}(\boldsymbol{X}(t) \in (\cdot, j), t < \tau_1^X, \Gamma_m \leq t < \Sigma_{m+1} \mid \boldsymbol{X}(0) = (x_0, i)), \tag{4.17}$$

for $i \in \mathcal{S}_+$, $j \in \mathcal{S}_- \cup \mathcal{S}_{-0}$ define

$$\mu^{\ell_0}_{m+1,+,-}(t)(\cdot, j; x_0, i) = \mathbb{P}(\boldsymbol{X}(t) \in (\cdot, j), t < \tau_1^X, \Sigma_{m+1} \leq t < \Gamma_{m+1} \mid \boldsymbol{X}(0) = (x_0, i)), \tag{4.18}$$

for $i \in \mathcal{S}_-$, $j \in \mathcal{S}_+ \cup \mathcal{S}_{+0}$ define

$$\mu^{\ell_0}_{m+1,-,+}(t)(\cdot, j; x_0, i) = \mathbb{P}(\boldsymbol{X}(t) \in (\cdot, j), t < \tau_1^X, \Gamma_{m+1} \leq t < \Sigma_{m+1} \mid X(0) = (x_0, i)), \tag{4.19}$$

and for $i \in \mathcal{S}_-$, $j \in \mathcal{S}_- \cup \mathcal{S}_{-0}$ define

$$\mu^{\ell_0}_{m,-,-}(t)(\cdot, j; x_0, i) = \mathbb{P}(\boldsymbol{X}(t) \in (\cdot, j), t < \tau_1^X, \Sigma_m \leq t < \Gamma_{m+1} \mid \boldsymbol{X}(0) = (x_0, i)). \tag{4.20}$$

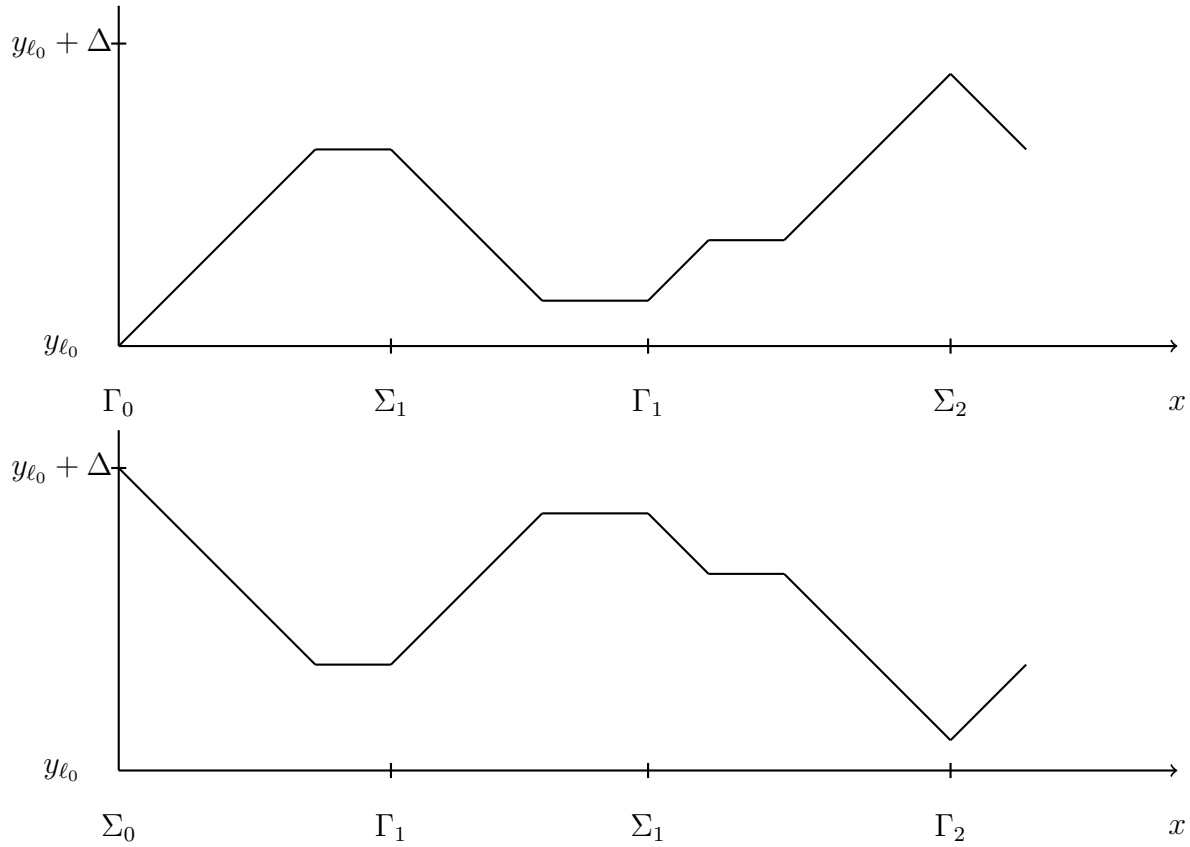

Figure 4.1: Sample paths and times of up-down and down-up transitions for $\varphi(0) \in \mathcal{S}_+$ (top) and $\varphi(0) \in \mathcal{S}_-$ (bottom).

Furthermore, for $q, r \in \{+,-\}$, $q \neq r$, let

$$\mu^{\ell_0}_{q,q}(t)(\cdot, j; x_0, i) := \sum_{m=0}^{\infty} \mu^{\ell_0}_{m,q,q}(t)(\cdot, j; x_0, i) \qquad i \in \mathcal{S}_q,\ j \in \mathcal{S}_q \cup \mathcal{S}_{q0}, \tag{4.21}$$

$$\mu^{\ell_0}_{q,r}(t)(\cdot, j; x_0, i) := \sum_{m=1}^{\infty} \mu^{\ell_0}_{m,q,r}(t)(\cdot, j; x_0, i) \qquad i \in \mathcal{S}_q,\ j \in \mathcal{S}_r \cup \mathcal{S}_{r0}. \tag{4.22}$$

Then we can write (4.16) as

$$\mu^{\ell_0}(t)(\cdot, j; x_0, i) = \begin{cases} \mu^{\ell_0}_{q,q}(t)(\cdot, j; x_0, i) & i \in \mathcal{S}_q,\ j \in \mathcal{S}_q \cup \mathcal{S}_{q0}, \\ \mu^{\ell_0}_{q,r}(t)(\cdot, j; x_0, i) & i \in \mathcal{S}_q,\ j \in \mathcal{S}_r \cup \mathcal{S}_{r0}, \end{cases} \tag{4.23}$$

For states $k \in \mathcal{S}_0$, and $q \in \{+,-\}$, $r \in \{+,-\}$, $m \geq 0$, then

$$\mu^{\ell_0}_{m,0,r}(t)(x, j; x_0, k) := \sum_{q \in \{+,-\}} \sum_{i \in \mathcal{S}_q} \int_{t_0=0}^{t} \boldsymbol{e}_k e^{\boldsymbol{T}_{00} t_0} \boldsymbol{T}_{0i} \mu^{\ell_0}_{m+1(q \neq r),q,r}(t - t_0)(x, j; x_0, i)\, \mathrm{d}t_0. \tag{4.24}$$

4.3 Laplace transforms with respect to time

In this section we take the Laplace transform with respect to time of the densities $f^{\ell_0,(p)}_{m,q,r}(t)(x, j; x_0, k)$, and measures $\mu^{\ell_0}_{m,q,r}(t)(x, j; x_0, k)$, $q \in \{+,-,0\}$, $r \in \{+,-\}$. The Laplace transform is convenient as it allows us to manipulate the expressions for the QBD-RAP into one component related to the orbit process and one component related the phase process and the rates c_i, $i \in \mathcal{S}$.

The following matrices play a key role in the analysis of fluid queues (see, for example, Bean et al. (2009*b*), da Silva Soares (2005)). Here, they appear in the Laplace transforms of the QBD-RAP and the fluid queue. Define matrices

$$\begin{aligned}
\boldsymbol{Q}_{+0}(\lambda) &= \boldsymbol{C}_+^{-1} \boldsymbol{T}_{+0} \left[\lambda \boldsymbol{I} - \boldsymbol{T}_{00}\right]^{-1}, \\
\boldsymbol{Q}_{-0}(\lambda) &= \boldsymbol{C}_-^{-1} \boldsymbol{T}_{-0} \left[\lambda \boldsymbol{I} - \boldsymbol{T}_{00}\right]^{-1}, \\
\boldsymbol{Q}_{++}(\lambda) &= \boldsymbol{C}_+^{-1} \left(\boldsymbol{T}_{++} - \lambda \boldsymbol{I} + \boldsymbol{T}_{+0} \left[\lambda \boldsymbol{I} - \boldsymbol{T}_{00}\right]^{-1} \boldsymbol{T}_{0+}\right), \\
\boldsymbol{Q}_{+-}(\lambda) &= \boldsymbol{C}_+^{-1} \left(\boldsymbol{T}_{+-} + \boldsymbol{T}_{+0} \left[\lambda \boldsymbol{I} - \boldsymbol{T}_{00}\right]^{-1} \boldsymbol{T}_{0-}\right), \\
\boldsymbol{Q}_{--}(\lambda) &= \boldsymbol{C}_-^{-1} \left(\boldsymbol{T}_{--} - \lambda \boldsymbol{I} + \boldsymbol{T}_{-0} \left[\lambda \boldsymbol{I} - \boldsymbol{T}_{00}\right]^{-1} \boldsymbol{T}_{0-}\right), \\
\boldsymbol{Q}_{-+}(\lambda) &= \boldsymbol{C}_-^{-1} \left(\boldsymbol{T}_{-+} + \boldsymbol{T}_{-0} \left[\lambda \boldsymbol{I} - \boldsymbol{T}_{00}\right]^{-1} \boldsymbol{T}_{0+}\right),
\end{aligned}$$

and matrix functions,

$$\boldsymbol{H}^{++}(\lambda, x) = \left[h^{++}_{ij}(\lambda, x)\right]_{i \in \mathcal{S}_+, j \in \mathcal{S}_+ \cup \mathcal{S}_{+0}} := e^{\boldsymbol{Q}_{++}(\lambda) x} \left[\boldsymbol{C}_+^{-1} \quad \boldsymbol{Q}_{+0}(\lambda)\right], \tag{4.25}$$

$$\boldsymbol{H}^{--}(\lambda,x) = \left[h_{ij}^{--}(\lambda,x)\right]_{i\in\mathcal{S}_-,j\in\mathcal{S}_-\cup\mathcal{S}_{-0}} := e^{\boldsymbol{Q}_{--}(\lambda)x}\left[\boldsymbol{C}_-^{-1} \quad \boldsymbol{Q}_{-0}(\lambda)\right], \tag{4.26}$$

$$\boldsymbol{H}^{+-}(\lambda,x) = \left[h_{ij}^{+-}(\lambda,x)\right]_{i\in\mathcal{S}_+,j\in\mathcal{S}_-} := e^{\boldsymbol{Q}_{++}(\lambda)x}\boldsymbol{Q}_{+-}(\lambda), \tag{4.27}$$

$$\boldsymbol{H}^{-+}(\lambda,x) = \left[h_{ij}^{-+}(\lambda,x)\right]_{i\in\mathcal{S}_-,j\in\mathcal{S}_+} := e^{\boldsymbol{Q}_{--}(\lambda)x}\boldsymbol{Q}_{-+}(\lambda), \tag{4.28}$$

for $x,\lambda \geq 0$. The function $h_{ij}^{++}(\lambda,x)$ ($h_{ij}^{--}(\lambda,x)$) is the Laplace transform with respect to time of the time taken for the fluid level to shift by an amount x whilst remaining in phases in $\mathcal{S}_+\cup\mathcal{S}_{+0}$ ($\mathcal{S}_-\cup\mathcal{S}_{-0}$), given the phase was initially $i\in\mathcal{S}_+$ ($i\in\mathcal{S}_-$) (Bean et al. 2005*b*). The function $h_{ij}^{+-}(\lambda,x)$ ($h_{ij}^{-+}(\lambda,x)$) is the Laplace transform with respect to time of the time taken for the fluid level, $\{X(t)\}$ to shift by an amount x whilst remaining in phases in $\mathcal{S}_+\cup\mathcal{S}_{+0}$ ($\mathcal{S}_-\cup\mathcal{S}_{-0}$), after which time the phase instantaneously changes to $j\in\mathcal{S}_-$ ($\mathcal{S}_+$), given the phase was initially $i\in\mathcal{S}_+$ ($\mathcal{S}_-$) (Bean et al. 2005*b*).

Consider taking the Laplace transform with respect to time of (4.17);

$$\begin{aligned}\int_{t=0}^{\infty} e^{-\lambda t}\mu_{m,+,+}^{\ell_0}(t)(\cdot,j;x_0,i)\,\mathrm{d}t &= \int_{t=0}^{\infty} e^{-\lambda t}\mu_{m,+,+}^{\ell_0}(t)(\cdot,j;x_0,i)\,\mathrm{d}t \\ &= \widehat{\mu}_{m,+,+}^{\ell_0}(\lambda)(\cdot,j;x_0,i)\end{aligned} \tag{4.29}$$

where we use $\widehat{\mu}_{m,+,+}^{\ell_0}(\lambda)(\cdot,j;x_0,i)$ to denote the Laplace transform with respect to time of (4.17). Throughout, we use the hat $\widehat{\ }$ notation to denote Laplace transforms with respect to time.

From the stochastic interpretations of the Laplace transforms (4.25)-(4.28) given in (Bean et al. 2005*b*) and summarised above, the Laplace transforms with respect to time, $\widehat{\mu}_{m,+,+}^{\ell_0}(\lambda)(x,j;x_0,i)$, of (4.17) are given by

$$\widehat{\mu}_{0,+,+}^{\ell_0}(\lambda)(x,j;x_0,i)\,\mathrm{d}x = h_{ij}^{++}(\lambda,x-x_0)1(x\geq x_0)\,\mathrm{d}x,$$

for $m=0$, and

$$\begin{aligned}&\int_{x_1=0}^{\Delta-(x_0-y_{\ell_0})} \boldsymbol{e}_i\boldsymbol{H}^{+-}(\lambda,\Delta-(x_0-y_{\ell_0})-x_1) \\ &\left[\prod_{r=1}^{m-1}\int_{x_{2r}=0}^{\Delta-x_{2r-1}} \boldsymbol{H}^{-+}(\lambda,\Delta-x_{2r}-x_{2r-1})\,\mathrm{d}x_{2r-1}\int_{x_{2r+1}=0}^{\Delta-x_{2r}} \boldsymbol{H}^{+-}(\lambda,\Delta-x_{2r+1}-x_{2r})\,\mathrm{d}x_{2r}\right] \\ &\int_{x_{2m}=0}^{\Delta-x_{2m-1}} \boldsymbol{H}^{-+}(\lambda,\Delta-x_{2m-1}-x_{2m})\,\mathrm{d}x_{2m-1}\boldsymbol{H}^{++}(\lambda,\Delta-x_{2m}-(y_{\ell_0+1}-x))\boldsymbol{e}_j \\ &1(\Delta-x_{2m}-(y_{\ell_0+1}-x)\geq 0)\,\mathrm{d}x_{2m}\,\mathrm{d}x\end{aligned} \tag{4.30}$$

for $m\geq 1$. Figure 4.2 shows an example of the sample paths to which these Laplace transforms correspond. Analogously, we can write down similar expressions for the Laplace transforms with respect to time of (4.17)-(4.20) (omitted).

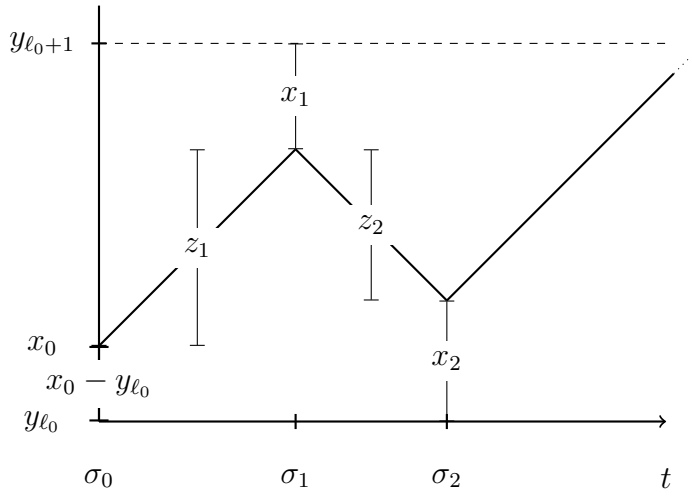

Figure 4.2: Sample paths corresponding to the Laplace transforms (4.30). $z_1 = \Delta - x_1 - (x - y_{\ell_0})$, $z_2 = \Delta - x_2 - x_1$.

Now consider taking the Laplace transform with respect to time of (4.10);

$$\begin{aligned}\int_{t=0}^{\infty} e^{-\lambda t} f_{m,+,+}^{\ell_0,(p)}(t)(x,j;x_0,i)\,\mathrm{d}t &= \int_{t=0}^{\infty} e^{-\lambda t} f_{m,+,+}^{\ell_0,(p)}(t)(x,j;x_0,i)\,\mathrm{d}t \\ &= \widehat{f}_{m,+,+}^{\ell_0,(p)}(\lambda)(x,j;x_0,i) \end{aligned} \tag{4.31}$$

where we use $\widehat{f}_{m,+,+}^{\ell_0,(p)}(\lambda)(x,j;x_0,i)$ to denote the Laplace transform with respect to time of (4.10). Notice that (4.10) is a convolution. Hence, the Laplace transform with respect to time of (4.10) is

$$\begin{aligned}&\widehat{f}_{m,+,+}^{\ell_0,(p)}(\lambda)(x,j;x_0,i) \\ &= (\boldsymbol{e}_i \otimes \boldsymbol{a}_{\ell_0,i}^{(p)}(x_0)) \int_{t_1=0}^{\infty} e^{-\lambda t_1} e^{\boldsymbol{B}_{++}^{(p)} t_1}\,\mathrm{d}t_1 \boldsymbol{B}_{+-}^{(p)} \int_{t_2=0}^{\infty} e^{-\lambda t_2} e^{\boldsymbol{B}_{--}^{(p)} t_2}\,\mathrm{d}t_2 \boldsymbol{B}_{-+}^{(p)} \\ &\cdots \int_{t_{2m}=0}^{\infty} e^{-\lambda t_{2m}} e^{\boldsymbol{B}_{--}^{(p)} t_{2m}}\,\mathrm{d}t_{2m} \boldsymbol{B}_{-+}^{(p)} \int_{t=0}^{\infty} e^{-\lambda t} e^{\boldsymbol{B}_{++}^{(p)} t}\,\mathrm{d}t \left(\boldsymbol{e}_j \otimes \boldsymbol{v}_{\ell_0,j}^{(p)}(x)\right). \end{aligned} \tag{4.32}$$

Analogous expressions can be computed for the Laplace transforms with respect to time of (4.11)-(4.13).

In Corollary D.4 in Appendix D, we show the following relation

$$\begin{aligned}&\left[\boldsymbol{I}_{p|\mathcal{S}_m|} \quad \boldsymbol{0}_{p|\mathcal{S}_m|\times p|\mathcal{S}_0|}\right] \int_{t=0}^{\infty} e^{-\lambda t} e^{\boldsymbol{B}_{mm}^{(p)} t}\,\mathrm{d}t \boldsymbol{B}_{mn}^{(p)} \\ &= \int_{x=0}^{\infty} \boldsymbol{H}^{mn}(\lambda,x) \otimes e^{\boldsymbol{S}^{(p)} x} \boldsymbol{D}^{(p)}\,\mathrm{d}x \left[\boldsymbol{I}_{p|\mathcal{S}_n|} \quad \boldsymbol{0}_{p|\mathcal{S}_n|\times p|\mathcal{S}_0|}\right], \end{aligned} \tag{4.33}$$

for $m, n \in \{+, -\}$, $m \neq n$. Before we can apply this result, observe that, since $i \in \mathcal{S}_+$, we can write the initial vector in (4.32) as

$$\begin{aligned}(\boldsymbol{e}_i)_{1\times|\mathcal{S}_+\cup\mathcal{S}_{+0}|} \otimes \boldsymbol{a}^{(p)}_{\ell_0,i}(x_0) &= \left[(\boldsymbol{e}_i)_{1\times|\mathcal{S}_+|} \quad \boldsymbol{0}_{1\times|\mathcal{S}_{+0}|}\right] \otimes \boldsymbol{a}^{(p)}_{\ell_0,i}(x_0) \\ &= \left[(\boldsymbol{e}_i)_{1\times|\mathcal{S}_+|} \otimes \boldsymbol{a}^{(p)}_{\ell_0,i}(x_0) \quad \boldsymbol{0}_{1\times p|\mathcal{S}_{+0}|}\right] \\ &= \left((\boldsymbol{e}_i)_{1\times|\mathcal{S}_+|} \otimes \boldsymbol{a}^{(p)}_{\ell_0,i}(x_0)\right)\left[\boldsymbol{I}_{p|\mathcal{S}_+|} \quad \boldsymbol{0}_{p|\mathcal{S}_+|\times p|\mathcal{S}_{+0}|}\right]. \end{aligned} \tag{4.34}$$

With this observation, applying (4.33) to the first integral in (4.32) transforms the expression to

$$\begin{aligned}&(\boldsymbol{e}_i \otimes \boldsymbol{a}^{(p)}_{\ell_0,i}(x_0)) \int_{x_1=0}^{\infty} \left(\boldsymbol{H}^{+-}(\lambda, x_1) \otimes e^{\boldsymbol{S}^{(p)}x}\boldsymbol{D}^{(p)}\right) \mathrm{d}x_1 \left[\boldsymbol{I}_{p|\mathcal{S}_-|} \quad \boldsymbol{0}_{p|\mathcal{S}_-|\times p|\mathcal{S}_0|}\right] \\ &\int_{t_2=0}^{\infty} e^{-\lambda t_2} e^{\boldsymbol{B}^{(p)}_{--}t_2}\,\mathrm{d}t_2 \boldsymbol{B}^{(p)}_{-+} \cdots \int_{t_{2m}=0}^{\infty} e^{-\lambda t_{2m}} e^{\boldsymbol{B}^{(p)}_{--}t_{2m}}\,\mathrm{d}t_{2m}\boldsymbol{B}^{(p)}_{-+} \int_{t=0}^{\infty} e^{-\lambda t} e^{\boldsymbol{B}^{(p)}_{++}t}\,\mathrm{d}t \\ &\left(\boldsymbol{e}_j \otimes \boldsymbol{v}^{(p)}_{\ell_0,j}(x)\right). \end{aligned} \tag{4.35}$$

We may now apply (4.33) to the second integral, after which we can apply (4.33) to the third integral and so on. Ultimately, after applying (4.33) to all the integrals in (4.32), we get

$$\begin{aligned}&(\boldsymbol{e}_i \otimes \boldsymbol{a}^{(p)}_{\ell_0,i}(x_0)) \left(\int_{x_1=0}^{\infty} \boldsymbol{H}^{+-}(\lambda, x_1) \otimes e^{\boldsymbol{S}^{(p)}x_1}\boldsymbol{D}^{(p)}\,\mathrm{d}x_1\right) \\ &\left[\prod_{r=1}^{m-1} \left(\int_{x_{2r}=0}^{\infty} \boldsymbol{H}^{-+}(\lambda, x_{2r}) \otimes e^{\boldsymbol{S}^{(p)}x_{2r}}\boldsymbol{D}^{(p)}\,\mathrm{d}x_{2r}\right)\right. \\ &\left.\left(\int_{x_{2r+1}=0}^{\infty} \boldsymbol{H}^{+-}(\lambda, x_{2r+1}) \otimes e^{\boldsymbol{S}^{(p)}x_{2r+1}}\boldsymbol{D}^{(p)}\,\mathrm{d}x_{2r+1}\right)\right] \\ &\left(\int_{x_{2m}=0}^{\infty} \boldsymbol{H}^{-+}(\lambda, x_{2m}) \otimes e^{\boldsymbol{S}^{(p)}x_{2m}}\boldsymbol{D}^{(p)}\,\mathrm{d}x_{2m}\right) \\ &\left(\int_{x_{2m+1}=0}^{\infty} \boldsymbol{H}^{++}(\lambda, x_{2m+1}) \otimes e^{\boldsymbol{S}^{(p)}x_{2m+1}}\,\mathrm{d}x_{2m+1}\right)\left(\boldsymbol{e}_j \otimes \boldsymbol{v}^{(p)}_{\ell_0,j}(x)\right) \\ &= \int_{x_1=0}^{\infty} \cdots \int_{x_{2m+1}=0}^{\infty} \boldsymbol{e}_i \boldsymbol{M}^m_{++}(\lambda, x_1, \ldots, x_{2m+1})\boldsymbol{e}_j \\ &\times \boldsymbol{a}^{(p)}_{\ell_0,i}(x_0)\boldsymbol{N}^{2m+1,(p)}(\lambda, x_1, \ldots, x_{2m+1})\boldsymbol{v}^{(p)}_{\ell_0,j}(x)\,\mathrm{d}x_{2m+1}\ldots\,\mathrm{d}x_1, \end{aligned} \tag{4.36}$$

by the Mixed Product Rule, where we define matrices

$$\boldsymbol{M}^m_{++}(\lambda, x_1, \ldots, x_{2m+1}) = \prod_{r=1}^{m} \boldsymbol{H}^{+-}(\lambda, x_{2r-1})\boldsymbol{H}^{-+}(\lambda, x_{2r})\boldsymbol{H}^{++}(\lambda, x_{2m+1}),$$

for $m \geq 0$, and

$$\boldsymbol{N}^{n,(p)}(\lambda, x_1, \ldots, x_n) = \prod_{r=1}^{n-1} e^{\boldsymbol{S}^{(p)} x_r} \boldsymbol{D}^{(p)} e^{\boldsymbol{S}^{(p)} x_n},$$

for $n \geq 1$. By convention, we take a product over an empty set to be 1. The relation (4.33) is key to our analysis. It allows us to factorise the integrand of the Laplace transform (4.36) into one factor solely related to the orbit process $\{\boldsymbol{A}^{(p)}(t)\}$,

$$\boldsymbol{a}^{(p)}_{\ell_0,i}(x_0) \boldsymbol{N}^{2m+1,(p)}(\lambda, x_1, \ldots, x_{2m+1}) \boldsymbol{v}^{(p)}_{\ell_0,j}(x)$$

and another factor solely related to the fluid queue,

$$\boldsymbol{e}_i \boldsymbol{M}^m_{++}(\lambda, x_1, \ldots, x_{2m+1}) \boldsymbol{e}_j.$$

Further, if we define matrices

$$\boldsymbol{M}^m_{-+}(\lambda, x_1, \ldots, x_{2m}) = \prod_{r=1}^{m-1} \boldsymbol{H}^{-+}(\lambda, x_{2r-1}) \boldsymbol{H}^{+-}(\lambda, x_{2r}) \boldsymbol{H}^{-+}(\lambda, x_{2m-1}) \boldsymbol{H}^{++}(\lambda, x_{2m}),$$
$$\boldsymbol{M}^m_{+-}(\lambda, x_1, \ldots, x_{2m}) = \prod_{r=1}^{m-1} \boldsymbol{H}^{+-}(\lambda, x_{2r-1}) \boldsymbol{H}^{-+}(\lambda, x_{2r}) \boldsymbol{H}^{+-}(\lambda, x_{2m-1}) \boldsymbol{H}^{--}(\lambda, x_{2m}),$$

for $m \geq 1$, and

$$\boldsymbol{M}^m_{--}(\lambda, x_1, \ldots, x_{2m+1}) = \prod_{r=1}^{m} \boldsymbol{H}^{-+}(\lambda, x_{2r-1}) \boldsymbol{H}^{+-}(\lambda, x_{2r}) \boldsymbol{H}^{--}(\lambda, x_{2m+1}),$$

for $m \geq 1$, then analogous expressions can be shown for the Laplace transforms of (4.11)-(4.13) in terms of these matrices. For $m \geq 0$,

$$\begin{aligned}
\widehat{f}^{\ell_0,(p)}_{m+1,-,+}(\lambda)(x, j; x_0, i) &= \int_{x_1=0}^{\infty} \cdots \int_{x_{2m+2}=0}^{\infty} \boldsymbol{e}_i \boldsymbol{M}^{m+1}_{-+}(\lambda, x_1, \ldots, x_{2m+2}) \boldsymbol{e}_j \\
&\quad \times \boldsymbol{a}^{(p)}_{\ell_0,i}(x_0) \boldsymbol{N}^{2m+2,(p)}(\lambda, x_1, \ldots, x_{2m+2}) \boldsymbol{v}^{(p)}_{\ell_0,j}(x) \, \mathrm{d}x_{2m+2} \ldots \mathrm{d}x_1, \\
\widehat{f}^{\ell_0,(p)}_{m+1,+,-}(\lambda)(x, j; x_0, i) &= \int_{x_1=0}^{\infty} \cdots \int_{x_{2m+2}=0}^{\infty} \boldsymbol{e}_i \boldsymbol{M}^{m+1}_{+-}(\lambda, x_1, \ldots, x_{2m+2}) \boldsymbol{e}_j \\
&\quad \times \boldsymbol{a}^{(p)}_{\ell_0,i}(x_0) \boldsymbol{N}^{2m+1,(p)}(\lambda, x_1, \ldots, x_{2m+1}) \boldsymbol{v}^{(p)}_{\ell_0,j}(x) \, \mathrm{d}x_{2m+2} \ldots \mathrm{d}x_1, \\
\widehat{f}^{\ell_0,(p)}_{m,-,-}(\lambda)(x, j; x_0, i) &= \int_{x_1=0}^{\infty} \cdots \int_{x_{2m+1}=0}^{\infty} \boldsymbol{e}_i \boldsymbol{M}^{m}_{--}(\lambda, x_1, \ldots, x_{2m+1}) \boldsymbol{e}_j \\
&\quad \times \boldsymbol{a}^{(p)}_{\ell_0,i}(x_0) \boldsymbol{N}^{2m+1,(p)}(\lambda, x_1, \ldots, x_{2m+1}) \boldsymbol{v}^{(p)}_{\ell_0,j}(x) \, \mathrm{d}x_{2m+1} \ldots \mathrm{d}x_1.
\end{aligned}$$

In general, for $k \in \mathcal{S}_0^*$, $q \in \{+,-\}$, $r \in \{+,-\}$, $m \geq 0$,

$$\widehat{f}^{\ell_0}_{m,0,r}(\lambda)(x,j;x_0,k) := \sum_{q\in\{+,-\}} \sum_{i\in\mathcal{S}_q} \boldsymbol{e}_k \left[\lambda \boldsymbol{I} - \boldsymbol{T}_{00}\right]^{-1} \boldsymbol{T}_{0i} \widehat{f}^{\ell_0}_{m+1(q\neq r),q,r}(\lambda)(x,j;x_0,i), \quad (4.37)$$

and

$$\widehat{\mu}^{\ell_0}_{m,0,r}(\lambda)(x,j;x_0,k) := \sum_{q\in\{+,-\}} \sum_{i\in\mathcal{S}_q} \boldsymbol{e}_k \left[\lambda \boldsymbol{I} - \boldsymbol{T}_{00}\right]^{-1} \boldsymbol{T}_{0i} \widehat{\mu}^{\ell_0}_{m+1(q\neq r),q,r}(\lambda)(x,j;x_0,i). \quad (4.38)$$

In Section 4.4 wish to establish that $\widehat{f}^{\ell_0,(p)}_{m,q,r}(\lambda)(x,j;x_0,k) \to \widehat{\mu}^{\ell_0}_{m,q,r}(\lambda)(x,j;x_0,k)$, $q \in \{+,-,0\}$, $r \in \{+,-\}$. To do so we use the fact that the functions $h^{qq}_{ij}(\lambda,x)$, $h^{qr}_{ij}(\lambda,x)$, $q,r \in \{+,-\}$, $i \in \mathcal{S}_q, j \in \mathcal{S}_r \cup \mathcal{S}_{r0}$ and $\lambda > 0$ satisfy the Assumptions 4.1 as functions of x. To this end, we observe the following bounds, which follow from the stochastic interpretation of the functions. Let $c_{min} = \min_{i\in\mathcal{S}_-\cup\mathcal{S}_+} |c_i|$ (recall that we fix $\lambda \in \mathbb{R}, \lambda > 0$). For all $\lambda > 0$, there is some $0 \leq G < \infty$ such that, for $q,r \in \{+,-\}$, $q \neq r$,

$$\begin{aligned} &0 \leq h^{qq}_{ij}(\lambda,x) \leq \max\{1/c_{min}, 1\} \leq G,\ i \in \mathcal{S}_q, j \in \mathcal{S}_q \cup \mathcal{S}_{q0}, \\ &0 \leq h^{qr}_{ij}(\lambda,x) \leq \max_{k,\ell} [\boldsymbol{Q}_{qr}(0)]_{k,\ell} \leq G,\ i \in \mathcal{S}_q,\ j \in \mathcal{S}_r. \end{aligned}$$

Furthermore, there exists some $0 \leq \widehat{G} < \infty$ such that,

$$\begin{aligned} \int_{x=0}^{\infty} h^{qq}_{ij}(\lambda,x)\,\mathrm{d}x \leq \int_{x=0}^{\infty} h^{qq}_{ij}(0,x)\,\mathrm{d}x = \left[-\boldsymbol{Q}_{qq}(0)^{-1}\boldsymbol{C}_q \quad -\boldsymbol{Q}_{qq}(0)^{-1}\boldsymbol{Q}_{q0}(0)\right]_{ij} \leq \widehat{G}, \\ \int_{x=0}^{\infty} h^{qr}_{ij}(\lambda,x)\,\mathrm{d}x \leq \int_{x=0}^{\infty} h^{qr}_{ij}(0,x)\,\mathrm{d}x = \left[-\boldsymbol{Q}_{qq}(0)^{-1}\boldsymbol{Q}_{qr}(0)\right]_{ij} \leq \widehat{G}. \end{aligned}$$

Moreover, since $h^{qq}_{ij}(\lambda,x)$ and $h^{qr}_{ij}(\lambda,x)$, are matrix exponential functions with exponent which is a sub-generator matrix, then for every $\lambda > 0$, $h^{qq}_{ij}(\lambda,x)$ and $h^{qr}_{ij}(\lambda,x)$ is Lipschitz continuous with respect to x on $x \in [0,\infty)$. Therefore, there exists some $0 < L < \infty$ such that $\left|h^{qq}_{ij}(\lambda,x) - h^{qq}_{ij}(\lambda,y)\right| \leq L|x-y|$ and $\left|h^{qr}_{ij}(\lambda,x) - h^{qr}_{ij}(\lambda,y)\right| \leq L|x-y|$.

4.4 Convergence on fixed number of up-down/down-up transitions

The main result of this chapter is the following theorem.

Theorem 4.3. *Let $\psi : \mathbb{R} \to \mathbb{R}$, be bounded, $|\psi| \leq F$. As $p \to \infty$, for $m \geq 1$, $q \in \{+,-,0\}$, $r \in \{+,-\}$, and for $m = 0$, $q = 0$, $r \in \{+,-\}$, and for $m = 0$, $q = r$, $q,r \in \{+,-\}$, then*

$$\int_{x\in\mathcal{D}_{\ell_0}} \widehat{f}^{\ell_0,(p)}_{m,q,r}(\lambda)(x,j;x_0,k)\psi(x)\,\mathrm{d}x \to \int_{x\in\mathcal{D}_{\ell_0}} \widehat{\mu}^{\ell_0}_{m,q,r}(\lambda)(x,j;x_0,k)\psi(x)\,\mathrm{d}x. \quad (4.39)$$

The proof of Theorem 4.3 is at the end of this section as it is the result of numerous other sub-results, which we now proceed to show. Notice that the convergence in Theorem 4.3 is a weak result as we integrate the spatial variable, x, against test functions ψ. This is necessary due to the discontinuity at $x = x_0$ in terms with $m = 0$.

Let $\Delta = \mathbb{E}[Z]$ be the mean of a matrix exponential random variable, Z. The convergence results rely on the fact that integrating a function, g say, against the density function of a matrix exponential random variable conditional on the ME-life-time surviving until some time $u < \Delta - \varepsilon$, approximates integrating said function against a Kronecker delta situated at $\Delta - u$, provided the variance of the ME is sufficiently low.

The next result is used in the proof of Theorem 4.3 to prove convergence on the event that there are no up-down or down-up transitions before, τ_1, the first orbit restart epoch.

Lemma 4.4. *Let $\psi : [0, \Delta) \to \mathbb{R}$ be bounded, $\psi(x) \leq F$. Then, for $x_0 \in \mathcal{D}_{\ell_0,i}$, $x \in \mathcal{D}_{\ell_0,j}$, $\ell_0 \in \mathcal{K} \setminus \{-1, K+1\}$, $\lambda > 0$, $q \in \{+, -\}$,*

$$\left| \int_{x \in \mathcal{D}_{\ell_0,j}} \widehat{f}^{\ell_0,(p)}_{0,q,q}(\lambda)(x, j; x_0, i)\psi(x - y_{\ell_0}) \,\mathrm{d}x - \int_{x \in \mathcal{D}_{\ell_0,j}} \mu^{\ell_0}_{0,q,q}(\lambda)(x, j; x_0, i)\psi(x - y_{\ell_0}) \,\mathrm{d}x \right| \leq \left(R^{(p)}_{\boldsymbol{v},2} + \varepsilon^{(p)} G \right) F. \tag{4.40}$$

Proof. Let us write $x_0 = y_{\ell_0} + u$, for $u \in [0, \Delta)$. Recalling

$$\widehat{f}^{\ell_0,(p)}_{0,+,+}(\lambda)(v, j; y_{\ell_0} + u, i) = \int_{x_1=0}^{\infty} \frac{\boldsymbol{\alpha}^{(p)} e^{\boldsymbol{S}^{(p)}(u+x_1)}}{\boldsymbol{\alpha}^{(p)} e^{\boldsymbol{S}^{(p)} u} \boldsymbol{e}} \boldsymbol{v}^{(p)}_{\ell_0,j}(x) h^{++}_{ij}(\lambda, x_1) \,\mathrm{d}x_1,$$

and

$$\widehat{\mu}^{\ell_0}_{0,+,+}(\lambda)(v, j; y_{\ell_0} + u, i) = h^{++}_{ij}(\lambda, \Delta - u - x) 1(u + x < \Delta),$$

then (4.40) is equal to

$$\begin{aligned}
&\left| \int_{x \in \mathcal{D}_{\ell_0,j}} \int_{x_1=0}^{\infty} \frac{\boldsymbol{\alpha}^{(p)} e^{\boldsymbol{S}^{(p)}(u+x_1)}}{\boldsymbol{\alpha}^{(p)} e^{\boldsymbol{S}^{(p)} u} \boldsymbol{e}} \boldsymbol{v}^{(p)}_{\ell_0,j}(x) h^{++}_{ij}(\lambda, x_1) \,\mathrm{d}x_1 \psi(x - y_{\ell_0}) \,\mathrm{d}x \right. \\
&\quad \left. - \int_{x \in \mathcal{D}_{\ell_0,j}} h^{++}_{ij}(\lambda, \Delta - u - x) 1(\Delta - u - x \geq 0) \psi(x - y_{\ell_0}) \,\mathrm{d}x \right| \\
&\leq \int_{x \in \mathcal{D}_{\ell_0,j}} \left| \int_{x_1=0}^{\infty} \frac{\boldsymbol{\alpha}^{(p)} e^{\boldsymbol{S}^{(p)}(u+x_1)}}{\boldsymbol{\alpha} e^{\boldsymbol{S}^{(p)} u} \boldsymbol{e}} \boldsymbol{v}^{(p)}_{\ell_0,j}(x) h^{++}_{ij}(\lambda, x_1) \,\mathrm{d}x_1 \right. \\
&\quad \left. - h^{++}_{ij}(\lambda, \Delta - u - x) 1(u + x < \Delta) \right| F \,\mathrm{d}x \\
&\leq \int_{x \in \mathcal{D}_{\ell_0,j}} \left| \int_{x_1=0}^{\infty} \frac{\boldsymbol{\alpha}^{(p)} e^{\boldsymbol{S}^{(p)}(u+x_1)}}{\boldsymbol{\alpha}^{(p)} e^{\boldsymbol{S}^{(p)} u} \boldsymbol{e}} \boldsymbol{v}^{(p)}_{\ell_0,j}(x) h^{++}_{ij}(\lambda, x_1) \,\mathrm{d}x_1 \right.
\end{aligned}$$

$$- h_{ij}^{++}(\lambda, \Delta - u - x)1(u + x < \Delta - \varepsilon)\Big| F \,\mathrm{d}x$$

$$+ \int_{x \in \mathcal{D}_{\ell_0,j}} \left| h_{ij}^{++}(\lambda, \Delta - u - x)1(\Delta - \varepsilon \leq u + x < \Delta) \right| F \,\mathrm{d}x, \tag{4.41}$$

by the triangle inequality and since ψ is bounded. By Property 4.2(v), then

$$\left| \int_{x_1=0}^{\infty} \frac{\boldsymbol{\alpha}^{(p)} e^{\boldsymbol{S}^{(p)}(u+x_1)}}{\boldsymbol{\alpha}^{(p)} e^{\boldsymbol{S}^{(p)}u}\boldsymbol{e}} \boldsymbol{v}_{\ell_0,j}^{(p)}(x) h_{ij}^{++}(\lambda, x_1) \,\mathrm{d}x_1 - h_{ij}^{++}(\lambda, \Delta - u - x)1(u + x < \Delta - \varepsilon) \right| \mathrm{d}x$$
$$\leq \left| r_{\boldsymbol{v}}(u, x) \right|. \tag{4.42}$$

Hence, (4.41) is less than or equal to

$$\int_{x \in \mathcal{D}_{\ell_0,j}} |r_{\boldsymbol{v}}^{(p)}(u, x)| F \,\mathrm{d}x + \int_{x \in \mathcal{D}_{\ell_0,j}} \left| h_{ij}^{++}(\lambda, \Delta - u - x)1(\Delta - \varepsilon \leq u + x < \Delta) \right| F \,\mathrm{d}x$$
$$\leq R_{\boldsymbol{v},2}^{(p)} F + \varepsilon G F,$$

since $|h_{ij}^{++}| \leq G$. Thus, we have shown (4.40) for $q = +$.

Using analogous arguments we can show (4.40) for $q = -$. □

Upon choosing $\varepsilon^{(p)} = \mathrm{Var}(Z^{(p)})^{1/3}$, then the bounds in (4.40) tend to 0.

Next, we proceed to show results needed to prove convergence on the event that there are one or more up-down or down-up transitions before the first orbit restart epoch. The expressions arising from the QBD-RAP which we wish to show converge have the form

$$\left| \int_{x_1=0}^{\infty} g_1(x_1) \boldsymbol{k}(x_0) e^{\boldsymbol{S}x_1} \,\mathrm{d}x_1 \boldsymbol{D} \left[\prod_{k=2}^{n-1} \int_{x_k=0}^{\infty} g_k(x_k) e^{\boldsymbol{S}x_k} \,\mathrm{d}x_k \boldsymbol{D} \right] \int_{x_n=0}^{\infty} g_n(x_n) e^{\boldsymbol{S}x_n} \,\mathrm{d}x_n \boldsymbol{v}(x), \right. \tag{4.43}$$

where $n \geq 2$, $\boldsymbol{v}(x)$ is a closing operator with the Properties 4.2, $\{g_k\}$ are functions satisfying Assumptions 4.1 and $\boldsymbol{k}(x_0) = \boldsymbol{\alpha} e^{\boldsymbol{S}x_0} / \boldsymbol{\alpha} e^{\boldsymbol{S}x_0} \boldsymbol{e}$.

We now introduce some notation we will use in the sequel. Define $w_n(x_0, x)$ to be the expression (4.43). Define the column vectors

$$\mathcal{I}_{m,k}(u_k) = \left[\prod_{\ell=m}^{k-1} \int_{x_\ell=0}^{\infty} g_\ell(x_\ell) e^{\boldsymbol{S}x_\ell} \,\mathrm{d}x_\ell \boldsymbol{D} \right] \int_{x_k=0}^{\infty} g_k(x_k) e^{\boldsymbol{S}x_k} \,\mathrm{d}x_k e^{\boldsymbol{S}u_k} \boldsymbol{s} \tag{4.44}$$

for $m, k \in \{1, 2, \dots\}$, $m \leq k$, where a product over an empty set is equal to 1. Notice that $\mathcal{I}_{m,k}(u_k)$ can be written as

$$\mathcal{I}_{m,k}(u_k) = \int_{x_m=0}^{\infty} g_m(x_m) e^{\boldsymbol{S}x_m} \,\mathrm{d}x_m \boldsymbol{D} \mathcal{I}_{m+1,k}(u_k). \tag{4.45}$$

Define the row vectors

$$\mathcal{J}_{k+1,k+1}(u_k, x_{k+1}) := g_{k+1}(x_{k+1}) \frac{\boldsymbol{\alpha} e^{\boldsymbol{S}u_k}}{\boldsymbol{\alpha} e^{\boldsymbol{S}u_k} \boldsymbol{e}} e^{\boldsymbol{S}x_{k+1}}, \tag{4.46}$$

and

$$\mathcal{J}_{k+1,n}(u_k, x_{k+1}) := g_{k+1}(x_{k+1}) \frac{\boldsymbol{\alpha} e^{\boldsymbol{S}u_k}}{\boldsymbol{\alpha} e^{\boldsymbol{S}u_k} \boldsymbol{e}} e^{\boldsymbol{S}x_{k+1}} \boldsymbol{D} \left[\prod_{m=k+2}^{n-1} \int_{x_m=0}^{\infty} g_m(x_m) e^{\boldsymbol{S}x_m} \, \mathrm{d}x_m \boldsymbol{D} \right] \times \int_{x_n=0}^{\infty} g_n(x_n) e^{\boldsymbol{S}x_n} \, \mathrm{d}x_n \tag{4.47}$$

for $k, n \in \{0, 1, 2, \dots\}$, $k+1 < n$. The vectors $\mathcal{J}_{k+1,n}(u_k, x_{k+1})$ can also be written recursively,

$$\mathcal{J}_{k+1,n}(u_k, x_{k+1}) = \mathcal{J}_{k+1,n-1}(u_k, x_{k+1}) \boldsymbol{D} \int_{x_n=0}^{\infty} g_n(x_n) e^{\boldsymbol{S}x_n} \, \mathrm{d}x_n. \tag{4.48}$$

Also define $\boldsymbol{D}(b) = \displaystyle\int_{u=0}^{b} e^{\boldsymbol{S}u} \boldsymbol{s} \frac{\boldsymbol{\alpha} e^{\boldsymbol{S}u}}{\boldsymbol{\alpha} e^{\boldsymbol{S}u} \boldsymbol{e}} \mathrm{d}u$.

We prove that (4.43) converges by writing it as

$$\int_{x_1=0}^{\infty} g_1(x_1) \boldsymbol{k}(x_0) e^{\boldsymbol{S}x_1} \, \mathrm{d}x_1 \boldsymbol{D}(\Delta - \varepsilon) \left[\prod_{k=2}^{n-1} \int_{x_k=0}^{\infty} g_k(x_k) e^{\boldsymbol{S}x_k} \, \mathrm{d}x_k \boldsymbol{D}(\Delta - \varepsilon) \right] \times \int_{x_n=0}^{\infty} g_n(x_n) e^{\boldsymbol{S}x_n} \, \mathrm{d}x_n \boldsymbol{v}(x) + \sum_{k=1}^{n-1} \int_{x_{k+1}=0}^{\infty} \int_{u_k=\Delta-\varepsilon}^{\infty} \boldsymbol{k}(x_0) \mathcal{I}_{1,k}(u_k) \mathcal{J}_{k+1,n}(u_k, x_{k+1}) \boldsymbol{v}(x). \tag{4.49}$$

We show that each of the terms in the last summation in (4.49) is bounded by something which can be made arbitrarily small upon choosing the variance of the distribution $(\boldsymbol{\alpha}, \boldsymbol{S})$ to be sufficiently small. Then we show that the difference between the first term in (4.49) and the corresponding expression for the fluid queue is also bounded by something which can be made arbitrarily small. The decomposition in (4.49) is advantageous since in the first term, the matrices $\boldsymbol{D}(\Delta - \varepsilon)$ are the integrals $\displaystyle\int_{u=0}^{\Delta-\varepsilon} e^{\boldsymbol{S}u} \boldsymbol{s} \frac{\boldsymbol{\alpha} e^{\boldsymbol{S}u}}{\boldsymbol{\alpha} e^{\boldsymbol{S}u} \boldsymbol{e}} \mathrm{d}u$, so the variable of integration never exceeds $\Delta - \varepsilon$. As a result, we can use Chebyshev's inequality to bound the denominator in the integrand of $\boldsymbol{D}(\Delta - \varepsilon)$ near 1.

Our next result shows a bound for the terms in the last summation in (4.49).

Recall the row vector function $\boldsymbol{k}(x) : [0, \infty) \to \mathcal{A} \subset \mathbb{R}^p$,

$$\boldsymbol{k}(x) = \frac{\boldsymbol{\alpha} e^{\boldsymbol{S}x}}{\boldsymbol{\alpha} e^{\boldsymbol{S}x} \boldsymbol{e}}.$$

Corollary 4.5. *Let $g_1, g_2, \dots,$ be functions satisfying the Assumptions 4.1 and let $\boldsymbol{v}(x)$ be a closing operator with the Properties 4.2, then, for $k, n \in \{1, 2, \dots\}$, $k+1 \leq n$,*

$$\begin{aligned}&\int_{x_{k+1}=0}^{\infty}\int_{u_k=\Delta-\varepsilon}^{\infty} \boldsymbol{k}(x_0)\mathcal{I}_{1,k}(u_k)\mathcal{J}_{k+1,n}(u_k, x_{k+1})\boldsymbol{v}(x)\\ &\leq \frac{1}{\boldsymbol{\alpha}e^{\boldsymbol{S}x_0}\boldsymbol{e}}\left(\left(2\varepsilon + \frac{\mathrm{Var}(Z)}{\varepsilon}\right)G^2\widehat{G}^{n-2}G_{\boldsymbol{v}} + G\widehat{G}^n\widetilde{G}_{\boldsymbol{v}}\right) =: |r_1(n)|. \end{aligned} \tag{4.50}$$

The structure of the proof is as follows. First, recall that we can decompose $\boldsymbol{v}(x) = \boldsymbol{w}(x) + \widetilde{\boldsymbol{w}}(x)$, by Properties 4.2, hence we can decompose the left-hand side of (4.50) into

$$\begin{aligned}&\int_{x_{k+1}=0}^{\infty}\int_{u_k=\Delta-\varepsilon}^{\infty} \boldsymbol{k}(x_0)\mathcal{I}_{1,k}(u_k)\mathcal{J}_{k+1,n}(u_k, x_{k+1})\boldsymbol{w}(x)\\ &+ \int_{x_{k+1}=0}^{\infty}\int_{u_k=\Delta-\varepsilon}^{\infty} \boldsymbol{k}(x_0)\mathcal{I}_{1,k}(u_k)\mathcal{J}_{k+1,n}(u_k, x_{k+1})\widetilde{\boldsymbol{w}}(x). \end{aligned} \tag{4.51}$$

Next, we bound $\boldsymbol{k}(x_0)\mathcal{I}_{1,k}(u_k)$ and $\mathcal{J}_{k+1,n}(u_k, x_{k+1})\boldsymbol{w}(x)$. With these two bounds we can derive a bound for the first term in (4.51). A bound on the second term of (4.51) follows from the bound on $\boldsymbol{k}(x_0)\mathcal{I}_{1,n-1}(u_{n-1})$ along with Properties 4.2(i) and 4.2(ii) of $\widetilde{\boldsymbol{w}}$.

Proof. Step 1: Decompose the left-hand side of (4.50) as (4.51). Referring to the Properties 4.2, we can decompose the closing operator $\boldsymbol{v}(x) = \boldsymbol{w}(x) + \widetilde{\boldsymbol{w}}(x)$, and therefore, due to the linearity of the decomposition, we can decompose (4.50) as (4.51).

Step 2: Show the following bound.

$$\boldsymbol{k}(x_0)\mathcal{I}_{1,k}(u_k) \leq \frac{1}{\boldsymbol{\alpha}e^{\boldsymbol{S}x_0}\boldsymbol{e}}G\widehat{G}^{k-1}\boldsymbol{\alpha}e^{\boldsymbol{S}u_k}\boldsymbol{e}. \tag{4.52}$$

Recall the definition of $\boldsymbol{D} := \displaystyle\int_{u=0}^{\infty} e^{\boldsymbol{S}u}\boldsymbol{s}\frac{\boldsymbol{\alpha}e^{\boldsymbol{S}u}}{\boldsymbol{\alpha}e^{\boldsymbol{S}u}\boldsymbol{e}}\mathrm{d}u$ and substitute it into the left-hand side of (4.52),

$$\begin{aligned}\boldsymbol{k}(x_0)\mathcal{I}_{1,k}(u_k) &= \boldsymbol{k}(x_0)\int_{x_1=0}^{\infty} g_1(x_1)e^{\boldsymbol{S}x_1}\,\mathrm{d}x_1\boldsymbol{D}\mathcal{I}_{2,k}(u_k)\\ &= \boldsymbol{k}(x_0)\int_{x_1=0}^{\infty} g_1(x_1)e^{\boldsymbol{S}x_1}\,\mathrm{d}x_1\int_{u_1=0}^{\infty} e^{\boldsymbol{S}u_1}\boldsymbol{s}\frac{\boldsymbol{\alpha}e^{\boldsymbol{S}u_1}}{\boldsymbol{\alpha}e^{\boldsymbol{S}u_1}\boldsymbol{e}}\mathrm{d}u_1\mathcal{I}_{2,k}(u_k). \end{aligned} \tag{4.53}$$

Since $|g_1| \leq G$, then (4.53) is less than or equal to

$$\boldsymbol{k}(x_0)\int_{x_1=0}^{\infty} Ge^{\boldsymbol{S}x_1}\,\mathrm{d}x_1\int_{u_1=0}^{\infty} e^{\boldsymbol{S}u_1}\boldsymbol{s}\frac{\boldsymbol{\alpha}e^{\boldsymbol{S}u_1}}{\boldsymbol{\alpha}e^{\boldsymbol{S}u_1}\boldsymbol{e}}\mathrm{d}u_1\mathcal{I}_{2,k}(u_k). \tag{4.54}$$

Computing the integral with respect to x_1 in (4.54) gives

$$G\boldsymbol{k}(x_0)(-\boldsymbol{S})^{-1}\int_{u_1=0}^{\infty} e^{\boldsymbol{S}u_1}\boldsymbol{s}\frac{\boldsymbol{\alpha}e^{\boldsymbol{S}u_1}}{\boldsymbol{\alpha}e^{\boldsymbol{S}u_1}\boldsymbol{e}}\,\mathrm{d}u_1\mathcal{I}_{2,k}(u_k)$$
$$=\frac{G}{\boldsymbol{\alpha}e^{\boldsymbol{S}x_0}\boldsymbol{e}}\int_{u_1=0}^{\infty}\boldsymbol{\alpha}e^{\boldsymbol{S}(x_0+u_1)}\boldsymbol{e}\frac{\boldsymbol{\alpha}e^{\boldsymbol{S}u_1}}{\boldsymbol{\alpha}e^{\boldsymbol{S}u_1}\boldsymbol{e}}\,\mathrm{d}u_1\mathcal{I}_{2,k}(u_k), \tag{4.55}$$

since $(-\boldsymbol{S})^{-1}$ and $e^{\boldsymbol{S}t}$ commute, $\boldsymbol{s}=-\boldsymbol{S}\boldsymbol{e}$ and $e^{\boldsymbol{S}(t+u)}=e^{\boldsymbol{S}t}e^{\boldsymbol{S}u}$. Since $\boldsymbol{\alpha}e^{\boldsymbol{S}(x_0+u_1)}\boldsymbol{e}\leq\boldsymbol{\alpha}e^{\boldsymbol{S}u_1}\boldsymbol{e}$, then (4.55) is less than or equal to

$$G\frac{1}{\boldsymbol{\alpha}e^{\boldsymbol{S}x_0}\boldsymbol{e}}\int_{u_1=0}^{\infty}\boldsymbol{\alpha}e^{\boldsymbol{S}u_1}\boldsymbol{e}\frac{\boldsymbol{\alpha}e^{\boldsymbol{S}u_1}}{\boldsymbol{\alpha}e^{\boldsymbol{S}u_1}\boldsymbol{e}}\,\mathrm{d}u_1\mathcal{I}_{2,k}(u_k)=G\frac{1}{\boldsymbol{\alpha}e^{\boldsymbol{S}x_0}\boldsymbol{e}}\int_{u_1=0}^{\infty}\boldsymbol{\alpha}e^{\boldsymbol{S}u_1}\,\mathrm{d}u_1\mathcal{I}_{2,k}(u_k),$$

where we have cancelled the terms $\boldsymbol{\alpha}e^{\boldsymbol{S}u_1}\boldsymbol{e}$ on the numerator and denominator.[†]

Now integrate with respect to u_1 and use the facts that $(-\boldsymbol{S})^{-1}$ and $e^{\boldsymbol{S}x}$ commute, and $\boldsymbol{s}=-\boldsymbol{S}\boldsymbol{e}$, to get

$$G\frac{1}{\boldsymbol{\alpha}e^{\boldsymbol{S}x_0}\boldsymbol{e}}\boldsymbol{\alpha}(-\boldsymbol{S})^{-1}\mathcal{I}_{2,k}(u_k) \tag{4.56}$$
$$=G\frac{1}{\boldsymbol{\alpha}e^{\boldsymbol{S}x_0}\boldsymbol{e}}\boldsymbol{\alpha}(-\boldsymbol{S})^{-1}\int_{x_2=0}^{\infty}g_2(x_2)e^{\boldsymbol{S}x_2}\,\mathrm{d}x_2\int_{u_2=0}^{\infty}e^{\boldsymbol{S}u_2}\boldsymbol{s}\frac{\boldsymbol{\alpha}e^{\boldsymbol{S}u_2}}{\boldsymbol{\alpha}e^{\boldsymbol{S}u_2}\boldsymbol{e}}\,\mathrm{d}u_2\mathcal{I}_{3,k}(u_k)$$
$$=G\frac{1}{\boldsymbol{\alpha}e^{\boldsymbol{S}x_0}\boldsymbol{e}}\int_{x_2=0}^{\infty}g_2(x_2)\boldsymbol{\alpha}e^{\boldsymbol{S}x_2}\,\mathrm{d}x_2\int_{u_2=0}^{\infty}e^{\boldsymbol{S}u_2}\boldsymbol{e}\frac{\boldsymbol{\alpha}e^{\boldsymbol{S}u_2}}{\boldsymbol{\alpha}e^{\boldsymbol{S}u_2}\boldsymbol{e}}\,\mathrm{d}u_2\mathcal{I}_{3,k}(u_k) \tag{4.57}$$

Since $\boldsymbol{\alpha}e^{\boldsymbol{S}x_2}e^{\boldsymbol{S}u_2}\boldsymbol{e}\leq\boldsymbol{\alpha}e^{\boldsymbol{S}u_2}\boldsymbol{e}$, then (4.57) is less than or equal to

$$G\frac{1}{\boldsymbol{\alpha}e^{\boldsymbol{S}x_0}\boldsymbol{e}}\int_{x_2=0}^{\infty}g_2(x_2)\,\mathrm{d}x_2\int_{u_2=0}^{\infty}\boldsymbol{\alpha}e^{\boldsymbol{S}u_2}\boldsymbol{e}\frac{\boldsymbol{\alpha}e^{\boldsymbol{S}u_2}}{\boldsymbol{\alpha}e^{\boldsymbol{S}u_2}\boldsymbol{e}}\,\mathrm{d}u_2\mathcal{I}_{3,k}(u_k)$$
$$=G\frac{1}{\boldsymbol{\alpha}e^{\boldsymbol{S}x_0}\boldsymbol{e}}\int_{x_2=0}^{\infty}g_2(x_2)\,\mathrm{d}x_2\int_{u_2=0}^{\infty}\boldsymbol{\alpha}e^{\boldsymbol{S}u_2}\boldsymbol{e}\,\mathrm{d}u_2\mathcal{I}_{3,k}(u_k), \tag{4.58}$$

where we have cancelled the terms $\boldsymbol{\alpha}e^{\boldsymbol{S}u_2}\boldsymbol{e}$ on the numerator and denominator.[‡]

Now, since $\displaystyle\int_{x_2=0}^{\infty}g_2(x_2)\,\mathrm{d}x_2\leq\widehat{G}$, then (4.58) is less than or equal to

$$G\frac{1}{\boldsymbol{\alpha}e^{\boldsymbol{S}x_0}\boldsymbol{e}}\widehat{G}\int_{u_2=0}^{\infty}\boldsymbol{\alpha}e^{\boldsymbol{S}u_2}\,\mathrm{d}u_2\mathcal{I}_{3,k}(u_k)=G\frac{1}{\boldsymbol{\alpha}e^{\boldsymbol{S}x_0}\boldsymbol{e}}\widehat{G}\boldsymbol{\alpha}(-\boldsymbol{S})^{-1}\mathcal{I}_{3,k}(u_k). \tag{4.59}$$

[†]The cancellation of terms is important as, for $u_1>\Delta$, then $\boldsymbol{\alpha}^{(p)}e^{\boldsymbol{S}^{(p)}u_1}\boldsymbol{e}$ becomes small as $p\to\infty$.

[‡]As I mentioned in the previous footnote, this is important as, for $u_k>\Delta$, then $\boldsymbol{\alpha}^{(p)}e^{\boldsymbol{S}^{(p)}u_k}\boldsymbol{e}$ becomes small as $p\to\infty$. Deriving a bound in such a way that this cancellation occurs was one of the main challenges I encountered with this proof – in retrospect it is somewhat obvious once we accept that g_1 is bounded and g_k, $k>1$, are integrable.

Repeating the arguments which got us from (4.56) to (4.59) another $k-2$ times gives the result.

Step 3: Show the bound

$$\mathcal{J}_{k+1,n}(u_k, x_{k+1})\boldsymbol{w}(x) \leq g_{k+1}(x_{k+1})\widehat{G}^{n-k-2}GG_{\boldsymbol{v}}. \tag{4.60}$$

The argument is much the same as that we used to bound (4.52).

Starting with the left-hand side, upon substituting $\boldsymbol{D}$,

$$\begin{aligned}
&\mathcal{J}_{k+1,n}(u_k, x_{k+1})\boldsymbol{w}(x) \\
&= \mathcal{J}_{k+1,n-1}(u_k, x_{k+1})\boldsymbol{D}\int_{x_n=0}^{\infty} g_n(x_n)e^{\boldsymbol{S}x_n}\,\mathrm{d}x_n\boldsymbol{w}(x) \\
&= \mathcal{J}_{k+1,n-1}(u_k, x_{k+1})\int_{u_{n-1}=0}^{\infty} e^{\boldsymbol{S}u_{n-1}}\boldsymbol{s}\frac{\boldsymbol{\alpha}e^{\boldsymbol{S}u_{n-1}}}{\boldsymbol{\alpha}e^{\boldsymbol{S}u_{n-1}}\boldsymbol{e}}\,\mathrm{d}u_{n-1}\int_{x_n=0}^{\infty} g_n(x_n)e^{\boldsymbol{S}x_n}\,\mathrm{d}x_n\boldsymbol{w}(x) \\
&\leq \mathcal{J}_{k+1,n-1}(u_k, x_{k+1})\int_{u_{n-1}=0}^{\infty} e^{\boldsymbol{S}u_{n-1}}\boldsymbol{s}\frac{\boldsymbol{\alpha}e^{\boldsymbol{S}u_{n-1}}}{\boldsymbol{\alpha}e^{\boldsymbol{S}u_{n-1}}\boldsymbol{e}}\,\mathrm{d}u_{n-1}\int_{x_n=0}^{\infty} Ge^{\boldsymbol{S}x_n}\,\mathrm{d}x_n\boldsymbol{w}(x),
\end{aligned} \tag{4.61}$$

since $|g_n| \leq G$. By Property 4.2(*iii*) of $\boldsymbol{w}(x)$, $\boldsymbol{\alpha}e^{\boldsymbol{S}u_{n-1}}\int_{x_n=0}^{\infty} e^{\boldsymbol{S}x_n}\boldsymbol{w}(x)\,\mathrm{d}x_n \leq \boldsymbol{\alpha}e^{\boldsymbol{S}u_{n-1}}\boldsymbol{e}G_{\boldsymbol{v}}$, hence (4.61) is less than or equal to

$$\begin{aligned}
&\mathcal{J}_{k+1,n-1}(u_k, x_{k+1})\int_{u_{n-1}=0}^{\infty} e^{\boldsymbol{S}u_{n-1}}\boldsymbol{s}\frac{\boldsymbol{\alpha}e^{\boldsymbol{S}u_{n-1}}\boldsymbol{e}}{\boldsymbol{\alpha}e^{\boldsymbol{S}u_{n-1}}\boldsymbol{e}}\,\mathrm{d}u_{n-1}GG_{\boldsymbol{v}} \\
&= \mathcal{J}_{k+1,n-1}(u_k, x_{k+1})\int_{u_{n-1}=0}^{\infty} e^{\boldsymbol{S}u_{n-1}}\boldsymbol{s}\,\mathrm{d}u_{n-1}GG_{\boldsymbol{v}}
\end{aligned} \tag{4.62}$$

where the terms $\boldsymbol{\alpha}e^{\boldsymbol{S}u_{n-1}}\boldsymbol{e}$ cancel from the numerator and denominator.[§]

Computing the integral with respect to u_{n-1} in (4.62), gives

$$\begin{aligned}
\mathcal{J}_{k+1,n-1}(u_k, x_{k+1})\boldsymbol{e}GG_{\boldsymbol{v}} = \mathcal{J}_{k+1,n-2}(u_k, x_{k+1})&\int_{u_{n-2}=0}^{\infty} e^{\boldsymbol{S}u_{n-2}}\boldsymbol{s}\frac{\boldsymbol{\alpha}e^{\boldsymbol{S}u_{n-2}}}{\boldsymbol{\alpha}e^{\boldsymbol{S}u_{n-2}}\boldsymbol{e}}\,\mathrm{d}u_{n-2} \\
&\times\int_{x_{n-1}=0}^{\infty} g_{n-1}(x_{n-1})e^{\boldsymbol{S}x_{n-1}}\,\mathrm{d}x_{n-1}\boldsymbol{e}GG_{\boldsymbol{v}}.
\end{aligned} \tag{4.63}$$

Since $\boldsymbol{\alpha}e^{\boldsymbol{S}(x_{n-1}+u_{n-2})}\boldsymbol{e} \leq \boldsymbol{\alpha}e^{\boldsymbol{S}(u_{n-2})}\boldsymbol{e}$, then (4.63) is less than or equal to

$$\mathcal{J}_{k+1,n-2}(u_k, x_{k+1})\int_{u_{n-2}=0}^{\infty} e^{\boldsymbol{S}u_{n-2}}\boldsymbol{s}\frac{\boldsymbol{\alpha}e^{\boldsymbol{S}u_{n-2}}\boldsymbol{e}}{\boldsymbol{\alpha}e^{\boldsymbol{S}u_{n-2}}\boldsymbol{e}}\,\mathrm{d}u_{n-2}\int_{x_{n-1}=0}^{\infty} g_{n-1}(x_{n-1})\,\mathrm{d}x_{n-1}GG_{\boldsymbol{v}}$$

[§]Once again, this cancellation is important. In this case Property 4.2(*iii*) of $\boldsymbol{w}(x)$ and that g_n is bounded which are key the deriving an expression where this term cancels.

$$= \mathcal{J}_{k+1,n-2}(u_k, x_{k+1}) \int_{u_{n-2}=0}^{\infty} e^{\boldsymbol{S}u_{n-2}} \boldsymbol{s}\, \mathrm{d}u_{n-2} \int_{x_{n-1}=0}^{\infty} g_{n-1}(x_{n-1})\, \mathrm{d}x_{n-1} G G_{\boldsymbol{v}} \tag{4.64}$$

where $\boldsymbol{\alpha} e^{\boldsymbol{S}u_{n-2}} \boldsymbol{e}$ cancels in the numerator and denominator.¶ Since $\int_{x_{n-1}=0}^{\infty} g_{x_{n-1}}\, \mathrm{d}x_{n-1} \leq \widehat{G}$, then (4.64) is less than or equal to

$$\mathcal{J}_{k+1,n-2}(u_k, x_{k+1}) \int_{u_{n-2}=0}^{\infty} e^{\boldsymbol{S}u_{n-2}} \boldsymbol{s}\, \mathrm{d}u_{n-2} \widehat{G} G G_{\boldsymbol{v}} = \mathcal{J}_{k+1,n-2}(u_k, x_{k+1}) \boldsymbol{e} \widehat{G} G G_{\boldsymbol{v}}. \tag{4.65}$$

This is of the same form as the left-hand side of (4.63), hence repeating the same arguments which took us from (4.63) to (4.65) another $n-k-3$ more times gives

$$\begin{aligned}
\mathcal{J}_{k+1,n}(u_k, x_{k+1}) \boldsymbol{w}(x) &\leq \mathcal{J}_{k+1,k+1}(u_k, x_{k+1}) \boldsymbol{e} \widehat{G}^{n-k-2} G G_{\boldsymbol{v}} \\
&= g_{k+1}(x_{k+1}) \frac{\boldsymbol{\alpha} e^{\boldsymbol{S}(u_k + x_{k+1})}}{\boldsymbol{\alpha} e^{\boldsymbol{S}u_k} \boldsymbol{e}} \boldsymbol{e} \widehat{G}^{n-k-2} G G_{\boldsymbol{v}} \\
&\leq g_{k+1}(x_{k+1}) \widehat{G}^{n-k-2} G G_{\boldsymbol{v}}.
\end{aligned}$$

Step 4: Combine the bounds on $\boldsymbol{k}(x_0)\mathcal{I}_{1,k}(u_k)$ and $\mathcal{J}_{k+1,n}(u_k, x_{k+1})\boldsymbol{w}(x)$ to bound the first term in (4.51).

First consider $k+1 < n$. With the bounds (4.52) and (4.60), the first term of (4.51) is less than or equal to

$$\begin{aligned}
&\frac{1}{\boldsymbol{\alpha} e^{\boldsymbol{S}x_0} \boldsymbol{e}} G \widehat{G}^{k-1} \int_{x_{k+1}=0}^{\infty} \int_{u_k=\Delta-\varepsilon}^{\infty} \boldsymbol{\alpha} e^{\boldsymbol{S}u_k} \boldsymbol{e} g_{k+1}(x_{k+1})\, \mathrm{d}u_k\, \mathrm{d}x_{k+1} \widehat{G}^{n-k-2} G G_{\boldsymbol{v}} \\
&\leq \frac{1}{\boldsymbol{\alpha} e^{\boldsymbol{S}x_0} \boldsymbol{e}} G \widehat{G}^{k-1} \int_{u_k=\Delta-\varepsilon}^{\infty} \boldsymbol{\alpha} e^{\boldsymbol{S}u_k} \boldsymbol{e}\, \mathrm{d}u_k \widehat{G} \widehat{G}^{n-k-2} G G_{\boldsymbol{v}}.
\end{aligned} \tag{4.66}$$

Now, observe that

$$\begin{aligned}
\int_{u_k=\Delta-\varepsilon}^{\infty} \boldsymbol{\alpha} e^{\boldsymbol{S}u_k} \boldsymbol{e}\, \mathrm{d}u_k &= \int_{u_k=\Delta-\varepsilon}^{\Delta+\varepsilon} \mathbb{P}(Z > u_k)\, \mathrm{d}u_k + \int_{u_k=\Delta+\varepsilon}^{\infty} \mathbb{P}(Z > u_k)\, \mathrm{d}u_k \\
&\leq \int_{u_k=\Delta-\varepsilon}^{\Delta+\varepsilon} \mathrm{d}u_k + \int_{u_k=\Delta+\varepsilon}^{\infty} \frac{\mathrm{Var}(Z)}{(u_k - \Delta)^2}\, \mathrm{d}u_k \\
&= 2\varepsilon + \frac{\mathrm{Var}(Z)}{\varepsilon},
\end{aligned} \tag{4.67}$$

where we have used Chebyshev's inequality to bound the tail probability,

$$\mathbb{P}(Z > u_k) \leq \mathbb{P}(|Z - \Delta| > |u_k - \Delta|) \leq \frac{\mathrm{Var}(Z)}{(u_k - \Delta)^2},$$

¶In this case the fact that the g_k are integrable helps us cancel these terms.

for $u_k \geq \Delta + \varepsilon$. Hence, (4.66) is less than or equal to

$$\frac{1}{\boldsymbol{\alpha} e^{\boldsymbol{S}x_0}\boldsymbol{e}} G\widehat{G}^{k-1}\left(2\varepsilon + \frac{\mathrm{Var}(Z)}{\varepsilon}\right)\widehat{G}^{n-k-1}GG_{\boldsymbol{v}}.$$

Now consider $k+1=n$. By the bound (4.52), the first term of (4.51) is less than or equal to

$$\frac{1}{\boldsymbol{\alpha} e^{\boldsymbol{S}x_0}\boldsymbol{e}} G\widehat{G}^{k-1}\int_{x_{k+1}=0}^{\infty}\int_{u_k=\Delta-\varepsilon}^{\infty}\boldsymbol{\alpha}e^{\boldsymbol{S}u_k}\boldsymbol{e}g_{k+1}(x_{k+1})\frac{\boldsymbol{\alpha}e^{\boldsymbol{S}(u_k+x_{k+1})}}{\boldsymbol{\alpha}e^{\boldsymbol{S}u_k}\boldsymbol{e}}\boldsymbol{w}(x)\,\mathrm{d}u_k\,\mathrm{d}x_{k+1}. \tag{4.68}$$

Since $g_{k+1} \leq G$, and upon integrating over x_{k+1}, then (4.68) is less than or equal to

$$\frac{1}{\boldsymbol{\alpha} e^{\boldsymbol{S}x_0}\boldsymbol{e}} G^2\widehat{G}^{k-1}\int_{u_k=\Delta-\varepsilon}^{\infty}\boldsymbol{\alpha}e^{\boldsymbol{S}u_k}(-\boldsymbol{S})^{-1}\boldsymbol{w}(x)\,\mathrm{d}u_k \leq \frac{1}{\boldsymbol{\alpha} e^{\boldsymbol{S}x_0}\boldsymbol{e}} G^2\widehat{G}^{k-1}\int_{u_k=\Delta-\varepsilon}^{\infty}\boldsymbol{\alpha}e^{\boldsymbol{S}u_k}\boldsymbol{e}G_{\boldsymbol{v}}\,\mathrm{d}u_k, \tag{4.69}$$

where we have used Property 4.2(*iii*) to get the upper bound on the right-hand side of (4.69). Using (4.67) again, then (4.69) is less than or equal to

$$\frac{1}{\boldsymbol{\alpha} e^{\boldsymbol{S}x_0}\boldsymbol{e}} G\widehat{G}^{n-2}GG_{\boldsymbol{v}}\left(2\varepsilon + \frac{\mathrm{Var}\,(Z)}{\varepsilon}\right). \tag{4.70}$$

Thus, we have shown the desired bound.

Step 5: Bound the second term in (4.51).

To bound the second term in (4.51) we instead bound

$$\begin{aligned}&\int_{x_{k+1}=0}^{\infty}\int_{u_k=0}^{\infty}\boldsymbol{k}(x_0)\mathcal{I}_{1,k}(u_k)\mathcal{J}_{k+1,n}(u_k,x_{k+1})\widetilde{\boldsymbol{w}}(x)\\ =&\int_{x_{k+1}=0}^{\infty}\int_{u=0}^{\infty}\mathcal{I}_{1,n}(u)\frac{\boldsymbol{\alpha}e^{\boldsymbol{S}u}}{\boldsymbol{\alpha}e^{\boldsymbol{S}u}\boldsymbol{e}}\int_{x_n=0}^{\infty}g_n(x_n)e^{\boldsymbol{S}x_n}\,\mathrm{d}x_n\widetilde{\boldsymbol{w}}(x)\end{aligned} \tag{4.71}$$

which is the same as the second term in (4.51) except that in (4.71) the integral is over a larger interval. Using the bound in (4.52), then (4.71) is less than or equal to

$$\frac{1}{\boldsymbol{\alpha} e^{\boldsymbol{S}x_0}\boldsymbol{e}} G\widehat{G}^{n-1}\int_{u=0}^{\infty}\boldsymbol{\alpha}e^{\boldsymbol{S}u}\boldsymbol{e}\frac{\boldsymbol{\alpha}e^{\boldsymbol{S}u}}{\boldsymbol{\alpha}e^{\boldsymbol{S}u}\boldsymbol{e}}\mathrm{d}u\int_{x_n=0}^{\infty}g_n(x_n)e^{\boldsymbol{S}x_n}\,\mathrm{d}x_n\widetilde{\boldsymbol{w}}(x).$$

Integrating over u gives

$$\frac{1}{\boldsymbol{\alpha} e^{\boldsymbol{S}x_0}\boldsymbol{e}} G\widehat{G}^{n-1}\boldsymbol{\alpha}(-\boldsymbol{S})^{-1}\int_{x_n=0}^{\infty}g_n(x_n)e^{\boldsymbol{S}x_n}\,\mathrm{d}x_n\widetilde{\boldsymbol{w}}(x)$$

$$\leq \frac{1}{\boldsymbol{\alpha} e^{\boldsymbol{S}x_0}\boldsymbol{e}} G\widehat{G}^{n-1}\boldsymbol{\alpha}(-\boldsymbol{S})^{-1}\int_{x_n=0}^{\infty} g_n(x_n)\,\mathrm{d}x_n\widetilde{\boldsymbol{w}}(x),$$

where the inequality holds by Property 4.2(i). Integrating over x_n, gives

$$\frac{1}{\boldsymbol{\alpha} e^{\boldsymbol{S}x_0}\boldsymbol{e}} G\widehat{G}^{n}\boldsymbol{\alpha}(-\boldsymbol{S})^{-1}\widetilde{\boldsymbol{w}}(x) = \frac{1}{\boldsymbol{\alpha} e^{\boldsymbol{S}x_0}\boldsymbol{e}} G\widehat{G}^{n}\widetilde{G}_{\boldsymbol{v}}, \tag{4.72}$$

by Property 4.2(ii).

Combining all the bounds proves the result. □

Next we wish to prove a bound on the difference between the first term in (4.49) and $g^*_{1,n}(x_0,x)$, where we define expressions of the form

$$\begin{aligned} g^*_{2,n}(u_1,x) := \int_{u_2=0}^{\Delta-u_1} g_2(\Delta-u_2-u_1)\,\mathrm{d}u_1 \ldots \int_{u_{n-1}=0}^{\Delta-u_{n-2}} g_{n-1}(\Delta-u_{n-1}-u_{n-2})\,\mathrm{d}u_{n-2} \\ g_n(\Delta-x-u_{n-1})1(\Delta-x-u_{n-1}\geq 0)\,\mathrm{d}u_{n-1}, \end{aligned} \tag{4.73}$$

and

$$g^*_{1,n}(x_0,x) := \int_{u_1=0}^{\Delta-x_0} g_1(\Delta-u_1-x_0)g^*_{2,n}(u_1,x)\,\mathrm{d}u_1. \tag{4.74}$$

The expression $g^*_{1,n}$ is of a similar form as $\widehat{\mu}^{\ell_0}_{n,q,r}(\lambda)$ except that the functions in $\widehat{\mu}^{\ell_0}_{n,q,r}(\lambda)$ are matrices. Since the functions in $\widehat{\mu}^{\ell_0}_{n,q,r}(\lambda)$ are matrices, then $\widehat{\mu}^{\ell_0}_{n,q,r}(\lambda)$ can be written as a linear combination of terms with the form $g^*_{1,n}$.

The idea of the proof is to first show a bound for the difference between the first term in (4.49) and the expression $g^{*,\varepsilon}_{1,n}(x_0,x)$ given by

$$\begin{aligned} &\int_{u_1=0}^{\Delta-\varepsilon-x_0} g_1(\Delta-u_1-x_0)\int_{u_2=0}^{\Delta-\varepsilon-u_1} g_2(\Delta-u_2-u_1)\,\mathrm{d}u_1 \\ &\quad\ldots\int_{u_{n-1}=0}^{\Delta-\varepsilon-u_{n-2}} g_{n-1}(\Delta-u_{n-1}-u_{n-2})\,\mathrm{d}u_{n-2}g_n(\Delta-x-u_{n-1})1(\Delta-x-u_{n-1}\geq\varepsilon). \end{aligned} \tag{4.75}$$

We then establish a bound on the difference between $g^{*,\varepsilon}_{1,n}(x_0,x)$ and $g^*_{1,n}(x_0,x)$ which can be made arbitrarily small by choosing ε sufficiently small.

Recall that the first term in (4.49) looks like

$$\int_{x_1=0}^{\infty} g_1(x_1)\boldsymbol{k}(x_0)e^{\boldsymbol{S}x_1}\,\mathrm{d}x_1\boldsymbol{D}(\Delta-\varepsilon)\left[\prod_{k=2}^{n-1}\int_{x_k=0}^{\infty} g_k(x_k)e^{\boldsymbol{S}x_k}\,\mathrm{d}x_k\boldsymbol{D}(\Delta-\varepsilon)\right]$$

$$\times \int_{x_n=0}^{\infty} g_n(x_n) e^{\boldsymbol{S}x_n} \,\mathrm{d}x_n \boldsymbol{v}(x) \tag{4.76}$$

which, upon substituting $\boldsymbol{D}(\Delta-\varepsilon) = \int_{u=0}^{\Delta-\varepsilon} e^{\boldsymbol{S}u}\boldsymbol{s}\frac{\boldsymbol{\alpha}e^{\boldsymbol{S}u}}{\boldsymbol{\alpha}e^{\boldsymbol{S}u}\boldsymbol{e}}\mathrm{d}u$, can be written as

$$\int_{u_1=0}^{\Delta-\varepsilon}\int_{x_1=0}^{\infty} \frac{\boldsymbol{\alpha}e^{\boldsymbol{S}(x_0+x_1+u_1)}\boldsymbol{s}}{\boldsymbol{\alpha}e^{\boldsymbol{S}x_0}\boldsymbol{e}} g_1(x_1)\,\mathrm{d}x_1 \left[\prod_{k=2}^{n-1}\int_{u_k=0}^{\Delta-\varepsilon}\int_{x_k=0}^{\infty} \frac{\boldsymbol{\alpha}e^{\boldsymbol{S}(u_{k-1}+x_k+u_k)}\boldsymbol{s}}{\boldsymbol{\alpha}e^{\boldsymbol{S}u_{k-1}}\boldsymbol{e}} g_k(x_k)\,\mathrm{d}x_k\,\mathrm{d}u_{k-1}\right]$$
$$\times \int_{x_n=0}^{\infty} \frac{\boldsymbol{\alpha}e^{\boldsymbol{S}(u_{n-1}+x_n)}}{\boldsymbol{\alpha}e^{\boldsymbol{S}u_{n-1}}\boldsymbol{e}}\boldsymbol{v}(x) g_n(x_n)\,\mathrm{d}x_n\,\mathrm{d}u_{n-1}. \tag{4.77}$$

The last integral in (4.77) is close to $g_n(\Delta - x - u_{n-1})$ by Property 4.2(v).

Also, appearing in (4.77) are integrals of the form

$$\int_{x_\ell=0}^{\infty} \frac{\boldsymbol{\alpha}e^{\boldsymbol{S}(u_{\ell-1}+x_\ell+u_\ell)}\boldsymbol{s}}{\boldsymbol{\alpha}e^{\boldsymbol{S}u_{\ell-1}}\boldsymbol{e}} g_\ell(x_\ell)\,\mathrm{d}x_\ell. \tag{4.78}$$

Intuitively, if the variance of Z is sufficiently small and if $u_{\ell-1} \leq \Delta - \varepsilon$ where Δ is the expected value of Z, then the distribution of Z will be concentrated around Δ and the integral in (4.78) should be approximately equal to $g_\ell(\Delta - u_\ell - u_{\ell-1})$. Our first step towards showing a bound for the difference between the first term in (4.49) and the expression $g^{*,\varepsilon}_{1,n}(x_0, x)$ is to prove this intuition. We start with a result about with a simpler integral than that in (4.78), from which the result we require follows as a Corollary.

Lemma 4.6. *Let g be a function satisfying Assumptions 4.1, then, for $u \leq \Delta - \varepsilon$,*

$$\int_{x=0}^{\infty} g(x)\,\boldsymbol{\alpha}e^{\boldsymbol{S}(x+u)}\boldsymbol{s}\,\mathrm{d}x = g(\Delta - u) + r_2, \tag{4.79}$$

where

$$|r_2| \leq 2G\frac{\mathrm{Var}(Z)}{\varepsilon^2} + 2L\varepsilon.$$

The proof follows closely that of (Horváth et al. 2020, Appendix A, Theorem 4). The idea of the proof is to recognise that (assuming the variance of Z is small) the largest contribution to the integral on the left-hand side of (4.79) will come from integrating over the interval $x \in (\Delta - u - \varepsilon, \Delta - u + \varepsilon)$. Since g is non-negative and bounded, then the rest of the integral is bounded by

$$\int_{\substack{x\in[0,\infty)\\ x\notin(\Delta-u-\varepsilon,\Delta-u+\varepsilon)}} G\boldsymbol{\alpha}e^{\boldsymbol{S}(x+u)}\boldsymbol{s}\,\mathrm{d}x,$$

which can be shown to be small by Chebyshev's inequality provided the variance of Z is small.

Proof. With a change of variables,

$$\begin{aligned}
&\left|\int_{x=0}^{\infty} g(x)\,\boldsymbol{\alpha}e^{\boldsymbol{S}(x+u)}\boldsymbol{s}\,\mathrm{d}x - g(\Delta-u)\right| \\
&= \left|\int_{x=u}^{\infty} g(x-u)\,\boldsymbol{\alpha}e^{\boldsymbol{S}x}\boldsymbol{s}\,\mathrm{d}x - g(\Delta-u)\right| \\
&= \left|\int_{x=u}^{\infty} g(x-u)\,\boldsymbol{\alpha}e^{\boldsymbol{S}x}\boldsymbol{s}\,\mathrm{d}x - \int_{x=u}^{\infty} g(\Delta-u)\,\boldsymbol{\alpha}e^{\boldsymbol{S}x}\boldsymbol{s}\,\mathrm{d}x - g(\Delta-u)\left(1-\boldsymbol{\alpha}e^{\boldsymbol{S}u}\boldsymbol{e}\right)\right|.
\end{aligned}$$

By the triangle inequality this is less than or equal to

$$\begin{aligned}
&\left|\int_{x=u}^{\infty} \left(g(x-u)-g(\Delta-u)\right)\boldsymbol{\alpha}e^{\boldsymbol{S}x}\boldsymbol{s}\,\mathrm{d}x\right| + \left|g(\Delta-u)\left(1-\boldsymbol{\alpha}e^{\boldsymbol{S}u}\boldsymbol{e}\right)\right| \\
&= \left|\int_{x=u}^{\infty} \left(g(x-u)-g(\Delta-u)\right)\boldsymbol{\alpha}e^{\boldsymbol{S}x}\boldsymbol{s}\,\mathrm{d}x\right| + \left|\int_{x=0}^{u} g(\Delta-u)\,\boldsymbol{\alpha}e^{\boldsymbol{S}x}\boldsymbol{s}\,\mathrm{d}x\right| \\
&\leq d_1 + d_2
\end{aligned}$$

where

$$\begin{aligned}
d_1 &= \left|\int_{x=0}^{u} g(\Delta-u)\,\boldsymbol{\alpha}e^{\boldsymbol{S}x}\boldsymbol{s}\,\mathrm{d}x\right| + \left|\int_{x=u}^{\Delta-\varepsilon} \left(g(x-u)-g(\Delta-u)\right)\boldsymbol{\alpha}e^{\boldsymbol{S}x}\boldsymbol{s}\,\mathrm{d}x\right| \\
&\quad + \left|\int_{x=\Delta+\varepsilon}^{\infty} \left(g(x-u)-g(\Delta-u)\right)\boldsymbol{\alpha}e^{\boldsymbol{S}x}\boldsymbol{s}\,\mathrm{d}x\right|, \\
d_2 &= \left|\int_{x=\Delta-\varepsilon}^{\Delta+\varepsilon} \left(g(x-u)-g(\Delta-u)\right)\boldsymbol{\alpha}e^{\boldsymbol{S}x}\boldsymbol{s}\,\mathrm{d}x\right|.
\end{aligned}$$

By the triangle inequality for integrals, d_2 is less than or equal to

$$\begin{aligned}
\int_{x=\Delta-\varepsilon}^{\Delta+\varepsilon} \left|g(x-u)-g(\Delta-u)\right|\boldsymbol{\alpha}e^{\boldsymbol{S}x}\boldsymbol{s}\,\mathrm{d}x &\leq \int_{x=\Delta-\varepsilon}^{\Delta+\varepsilon} 2L\varepsilon\boldsymbol{\alpha}e^{\boldsymbol{S}x}\boldsymbol{s}\,\mathrm{d}x \\
&= 2L\varepsilon\mathbb{P}(Z\in(\Delta-\varepsilon,\Delta+\varepsilon)) \\
&\leq 2L\varepsilon,
\end{aligned}$$

where we have used the Lipschitz property of g from Assumption 4.1(iv) in the first line.

Applying the triangle inequality to d_1,

$$\begin{aligned}
d_1 \leq &\int_{x=u}^{\Delta-\varepsilon} \left|g(x-u)-g(\Delta-u)\right|\boldsymbol{\alpha}e^{\boldsymbol{S}x}\boldsymbol{s}\,\mathrm{d}x + \int_{x=\Delta+\varepsilon}^{\infty} \left|g(x-u)-g(\Delta-u)\right|\boldsymbol{\alpha}e^{\boldsymbol{S}x}\boldsymbol{s}\,\mathrm{d}x \\
&+ \left|\int_{x=0}^{u} g(\Delta-u)\,\boldsymbol{\alpha}e^{\boldsymbol{S}x}\boldsymbol{s}\,\mathrm{d}x\right|
\end{aligned}$$

$$\leq 2G\left(\int_{x=u}^{\Delta-\varepsilon}\boldsymbol{\alpha}e^{\boldsymbol{S}x}\boldsymbol{s}\,\mathrm{d}x+\int_{x=\Delta+\varepsilon}^{\infty}\boldsymbol{\alpha}e^{\boldsymbol{S}x}\boldsymbol{s}\,\mathrm{d}x+\int_{x=0}^{u}\boldsymbol{\alpha}e^{\boldsymbol{S}x}\boldsymbol{s}\,\mathrm{d}x\right)=2G\mathbb{P}\left(|Z-\Delta|>\varepsilon\right),$$

where the second inequality holds since $|g\left(x\right)|\leq G$. By Chebyshev's inequality,

$$2G\mathbb{P}\left(|Z-\Delta|>\varepsilon\right)\leq 2G\frac{\mathrm{Var}\left(Z\right)}{\varepsilon^2}. \tag{4.80}$$

Hence, there is some r_2 such that

$$\left|\int_{x=0}^{\infty}g\left(x\right)\boldsymbol{\alpha}e^{\boldsymbol{S}(x+u)}\boldsymbol{s}\,\mathrm{d}x-g\left(\Delta-u\right)\right|=|r_2|\leq 2G\frac{\mathrm{Var}(Z)}{\varepsilon^2}+2L\varepsilon,$$

and this completes the proof. □

Corollary 4.7. *Let g be a function satisfying the Assumptions 4.1. For $u\leq\Delta-\varepsilon$, $v\geq 0$,*

$$\int_{x=0}^{\infty}\frac{\boldsymbol{\alpha}e^{\boldsymbol{S}(x+u+v)}\boldsymbol{s}}{\boldsymbol{\alpha}e^{\boldsymbol{S}u}\boldsymbol{e}}g(x)\,\mathrm{d}x=g(\Delta-u-v)1(u+v\leq\Delta-\varepsilon)+r_3(u+v), \tag{4.81}$$

where

$$|r_3(u+v)|\leq\begin{cases}3G\delta+2L\varepsilon & u+v\leq\Delta-\varepsilon,\\ G & u+v\in(\Delta-\varepsilon,\Delta+\varepsilon),\\ G\dfrac{\delta}{1-\delta} & u+v\geq\Delta+\varepsilon.\end{cases},$$

where $\delta=\dfrac{\mathrm{Var}(Z)}{\varepsilon^2}$.

Proof. First consider $u+v\leq\Delta-\varepsilon$. Observe that, since $u\leq\Delta-\varepsilon$, Chebyshev's inequality gives

$$\begin{aligned}\boldsymbol{\alpha}e^{\boldsymbol{S}u}\boldsymbol{e}&=\mathbb{P}\left(Z>u\right)\\&\geq\mathbb{P}\left(|Z-\Delta|\leq\varepsilon\right)\\&\geq 1-\frac{\mathrm{Var}\left(Z\right)}{\varepsilon^2}\\&=:1-\delta,\end{aligned}$$

thus we have a bound for the denominator in the integrand on the left-hand side of (4.81).

Now, since $1-\delta\leq\boldsymbol{\alpha}e^{\boldsymbol{S}u}\boldsymbol{e}\leq 1$, then

$$\int_{x=0}^{\infty}\boldsymbol{\alpha}e^{\boldsymbol{S}(x+u+v)}\boldsymbol{s}g(x)\,\mathrm{d}x\leq\int_{x=0}^{\infty}\frac{\boldsymbol{\alpha}e^{\boldsymbol{S}(x+u+v)}\boldsymbol{s}}{\boldsymbol{\alpha}e^{\boldsymbol{S}u}\boldsymbol{e}}g(x)\,\mathrm{d}x\leq\frac{1}{1-\delta}\int_{x=0}^{\infty}\boldsymbol{\alpha}e^{\boldsymbol{S}(x+u+v)}\boldsymbol{s}g(x)\,\mathrm{d}x.$$

By Lemma 4.6

$$g(\Delta-u-v)+r_2 \le \int_{x=0}^{\infty} \frac{\boldsymbol{\alpha} e^{\boldsymbol{S}(x+u+v)}\boldsymbol{s}}{\boldsymbol{\alpha} e^{\boldsymbol{S}u}\boldsymbol{e}} g(x)\,\mathrm{d}x \le \frac{g(\Delta-u-v)+r_2}{1-\delta}.$$

Multiplying by $1-\delta$, then subtracting $g(\Delta-u-v)$ and adding $\displaystyle\int_{x=0}^{\infty} \frac{\boldsymbol{\alpha} e^{\boldsymbol{S}(x+u+v)}\boldsymbol{s}}{\boldsymbol{\alpha} e^{\boldsymbol{S}u}\boldsymbol{e}} g(x)\,\mathrm{d}x\delta$ gives

$$\begin{aligned}
&r_2(1-\delta)-g(\Delta-u-v)\delta+\int_{x=0}^{\infty} \frac{\boldsymbol{\alpha} e^{\boldsymbol{S}(x+u+v)}\boldsymbol{s}}{\boldsymbol{\alpha} e^{\boldsymbol{S}u}\boldsymbol{e}} g(x)\,\mathrm{d}x\delta \\
&\le \int_{x=0}^{\infty} \frac{\boldsymbol{\alpha} e^{\boldsymbol{S}(x+u+v)}\boldsymbol{s}}{\boldsymbol{\alpha} e^{\boldsymbol{S}u}\boldsymbol{e}} g(x)\,\mathrm{d}x - g(\Delta-u-v) \\
&\le r_2+\int_{x=0}^{\infty} \frac{\boldsymbol{\alpha} e^{\boldsymbol{S}(x+u+v)}\boldsymbol{s}}{\boldsymbol{\alpha} e^{\boldsymbol{S}u}\boldsymbol{e}} g(x)\,\mathrm{d}x\delta.
\end{aligned}$$

The last line is bounded above by

$$r_2+\int_{x=0}^{\infty} \frac{\boldsymbol{\alpha} e^{\boldsymbol{S}(x+u+v)}\boldsymbol{s}}{\boldsymbol{\alpha} e^{\boldsymbol{S}u}\boldsymbol{e}} g(x)\,\mathrm{d}x\delta \le r_2+G\delta.$$

The first line is bounded below by

$$r_2(1-\delta)-g(\Delta-u-v)\delta+\int_{x=0}^{\infty} \frac{\boldsymbol{\alpha} e^{\boldsymbol{S}(x+u+v)}\boldsymbol{s}}{\boldsymbol{\alpha} e^{\boldsymbol{S}u}\boldsymbol{e}} g(x)\,\mathrm{d}x\delta \ge r_2(1-\delta)-g(\Delta-u-v)\delta.$$

Therefore,

$$\int_{x=0}^{\infty} \frac{\boldsymbol{\alpha} e^{\boldsymbol{S}(x+u+v)}\boldsymbol{s}}{\boldsymbol{\alpha} e^{\boldsymbol{S}u}\boldsymbol{e}} g(x)\,\mathrm{d}x = g(\Delta-u-v)+r_3, \tag{4.82}$$

where

$$\begin{aligned}
|r_3| &\le \max\left(|r_2|(1-\delta)+g(\Delta-u-v)\delta, |r_2|+G\delta\right) \\
&\le |r_2|+G\delta \\
&\le 3G\delta+2L\varepsilon,
\end{aligned} \tag{4.83}$$

as required.

For $u+v\in(\Delta-\varepsilon,\Delta+\varepsilon)$,

$$\int_{x=0}^{\infty} \frac{\boldsymbol{\alpha} e^{\boldsymbol{S}(x+u+v)}\boldsymbol{s}}{\boldsymbol{\alpha} e^{\boldsymbol{S}u}\boldsymbol{e}} g(x)\,\mathrm{d}x \le G\mathbb{P}(Z>u+v \mid Z>u) \le G. \tag{4.84}$$

For $u+v \geq \Delta+\varepsilon$,

$$\int_{x=0}^{\infty} \frac{\boldsymbol{\alpha} e^{\boldsymbol{S}(x+u+v)}\boldsymbol{s}}{\boldsymbol{\alpha} e^{\boldsymbol{S}u}\boldsymbol{e}} g(x)\,\mathrm{d}x \leq G\frac{\mathbb{P}(Z>u+v)}{\mathbb{P}(Z>u)} \leq G\frac{\mathrm{Var}(Z)/\varepsilon^2}{1-\mathrm{Var}(Z)/\varepsilon^2}. \tag{4.85}$$

□

The error term $r_3^{(p)}$ depends on p, as it is defined by $Z^{(p)}$ and $\varepsilon^{(p)}$, but we have omitted the superscript p here. Choosing $\varepsilon = \mathrm{Var}(Z^{(p)})^{1/3}$ then, outside the vanishingly small interval $u \in (\Delta-\varepsilon^{(p)}, \Delta+\varepsilon^{(p)})$, the error term $|r_3^{(p)}(u)|$ is bounded by $O\left(\mathrm{Var}\left(Z^{(p)}\right)^{1/3}\right)$, which tends to 0 as $p\to\infty$. On $u \in (\Delta-\varepsilon^{(p)}, \Delta+\varepsilon^{(p)})$ the error term $|r_3^{(p)}(u)|$ is bounded by a constant which does not tend to 0 as $p\to\infty$. However, when we integrate a bounded function against $r_3^{(p)}(u)$, then the resulting integral tends to 0, i.e. for $|\psi(x)| \leq F$, $M < \infty$, $\displaystyle\int_0^M \psi(u)|r_3^{(p)}(u)|\,\mathrm{d}u \leq F\Delta(3G\delta^{(p)}+2L\varepsilon) + 2GF\varepsilon^{(p)} + (M-\Delta)GF\delta^{(p)}/(1-\delta^{(p)}) = O\left(\mathrm{Var}\left(Z^{(p)}\right)^{1/3}\right) \to 0$ as $p\to\infty$. This is the context in which we apply Corollary 4.7 and thus the error bound is sufficient.

We are now in a position to prove the desired bound on the difference between the first term in (4.49) and $g_{1,n}^*(x_0,x)$.

Lemma 4.8. *Let $g_1, g_2, \ldots,$ be functions satisfying the Assumptions 4.1 and let $\boldsymbol{v}(x)$ be a closing operator with the Properties 4.2. Then, for $n \geq 2$,*

$$\begin{aligned}
&\int_{x_1=0}^{\infty} g_1(x_1)\boldsymbol{k}(x_0)e^{\boldsymbol{S}x_1}\,\mathrm{d}x_1 \boldsymbol{D}(\Delta-\varepsilon)\left[\prod_{k=2}^{n-1}\int_{x_k=0}^{\infty} g_k(x_k)e^{\boldsymbol{S}x_k}\,\mathrm{d}x_k\right]\boldsymbol{D}(\Delta-\varepsilon)\\
&\qquad\times\int_{x_n=0}^{\infty} g_n(x_n)e^{\boldsymbol{S}x_n}\,\mathrm{d}x_n\boldsymbol{v}(x)\\
&= g_{1,n}^*(x_0,x) + r_4(n) + r_5(n),
\end{aligned} \tag{4.86}$$

where

$$\begin{aligned}
|r_4(n)| &= O\left(\max\left\{\delta, \varepsilon, \frac{\delta}{1-\delta}, R_{\boldsymbol{v},1}\right\}\right),\\
|r_5(n)| &\leq \varepsilon^{n-1}G^{n-1}
\end{aligned}$$

Proof. Rewriting the left-hand side of (4.86) as in (4.77), then we see that we can apply Corollary 4.7 to all the integrals over x_k, $k=1,\ldots,n-1$ and use Property 4.2(v) of $\boldsymbol{v}(x)$ for the integral over x_n, to get

$$\int_{u_1=0}^{\Delta-\varepsilon}\left[g_1(\Delta-u_1-x_0)1(u_1+x_0\leq\Delta-\varepsilon) + r_3(u_1+x_0)\right]$$

$$
\begin{aligned}
&\times \int_{u_2=0}^{\Delta-\varepsilon} [g_2(\Delta-u_2-u_1)1(u_2+u_1\le\Delta-\varepsilon)+r_3(u_2+u_1)]\,\mathrm{d}u_1\\
&\dots\int_{u_{n-1}=0}^{\Delta-\varepsilon} [g_{n-1}(\Delta-u_{n-1}-u_{n-2})1(u_{n-1}+u_{n-2}\le\Delta-\varepsilon)+r_3(u_{n-1}+u_{n-2})]\,\mathrm{d}u_{n-2}\\
&\times [g_n(\Delta-u_{n-1}-x)1(u_{n-1}+x\le\Delta-\varepsilon)+r_{\boldsymbol{v}}(u_{n-1},x)]\,\mathrm{d}u_{n-1}\\
&= g_{1,n}^{*,\varepsilon}(x_0,x)+r_4(n)
\end{aligned}
$$

where $r_4(n)$ is an error term. The leading terms of $r_4(n)$ are of the form

$$
\begin{aligned}
&\int_{u_1=0}^{\Delta-\varepsilon-x_0} g_1(\Delta-u_1-x_0)\int_{u_2=0}^{\Delta-\varepsilon-u_1} g_2(\Delta-u_2-u_1)\,\mathrm{d}u_1\\
&\quad\dots\int_{u_{k-1}=0}^{\Delta-\varepsilon-u_{k-2}} g_{k-1}(\Delta-u_{k-1}-u_{k-2})\,\mathrm{d}u_{k-2}\int_{u_k=0}^{\Delta-\varepsilon} r_3(u_k+u_{k-1})\,\mathrm{d}u_{k-1}\\
&\quad\times\int_{u_{k+1}=0}^{\Delta-\varepsilon-u_k} g_{k+1}(\Delta-u_{k+1}-u_k)\,\mathrm{d}u_k\dots\int_{u_{n-1}=0}^{\Delta-\varepsilon-u_{n-2}} g_{n-1}(\Delta-u_{n-1}-u_{n-2})\,\mathrm{d}u_{n-2}\\
&\quad\times g_n(\Delta-u_{n-1}-x)1(u_{n-1}+x\le\Delta-\varepsilon)\,\mathrm{d}u_{n-1}
\end{aligned}
\tag{4.87}
$$

or

$$
\begin{aligned}
&\int_{u_1=0}^{\Delta-\varepsilon-x_0} g_1(\Delta-u_1-x_0)\int_{u_2=0}^{\Delta-\varepsilon-u_1} g_2(\Delta-u_2-u_1)\,\mathrm{d}u_1\\
&\dots\int_{u_{n-1}=0}^{\Delta-\varepsilon-u_{n-2}} g_{n-1}(\Delta-u_{n-1}-u_{n-2})\,\mathrm{d}u_{n-2}r_{\boldsymbol{v}}(u_{n-1},x)\,\mathrm{d}u_{n-1},
\end{aligned}
\tag{4.88}
$$

whichever is larger. Since $|g_\ell|\le G$, $\ell\ge 1$, then (4.88) and (4.87) are less than or equal to

$$
G^{k-1}\Delta^{k-2}\int_{u_{k-1}=0}^{\Delta-\varepsilon}\int_{u_k=0}^{\Delta-\varepsilon} r_3(u_k+u_{k-1})\,\mathrm{d}u_k\,\mathrm{d}u_{k-1}G^{n-k}\Delta^{n-k-1},
$$

and

$$
G^{n-1}\Delta^{n-2}\int_{u_{n-1}=0}^{\Delta-\varepsilon} r_{\boldsymbol{v}}(u_{n-1},x)\,\mathrm{d}u_{n-1},
$$

respectively.

Recall that we have a bound on $|r_3|$ which is piecewise constant. Breaking up the integral of $|r_3|$ above into three intervals over which the bound is constant and using the triangle inequality, then

$$
\left|\int_{u_{k-1}=0}^{\Delta-\varepsilon}\int_{u_k=0}^{\Delta-\varepsilon} r_3(u_k+u_{k-1})\,\mathrm{d}u_k\,\mathrm{d}u_{k-1}\right|
$$

$$\leq \int_{u_{k-1}=0}^{\Delta-\varepsilon} \left[\int_{u_k=u_{k-1}}^{\Delta-\varepsilon} |r_3(u_k)| \, \mathrm{d}u_k + \int_{u_k=\Delta-\varepsilon}^{\min(\Delta+\varepsilon, \Delta-\varepsilon+u_{k-1})} |r_3(u_k)| \, \mathrm{d}u_k \right.$$
$$\left. + \int_{u_k=\Delta+\varepsilon}^{\Delta-\varepsilon+u_{k-1}} |r_3(u_k)| \, \mathrm{d}u_k 1(u_{k-1} > 2\varepsilon) \right] \mathrm{d}u_{k-1}. \tag{4.89}$$

Using the piecewise upper bounds on $|r_3|$ then, in the square brackets in (4.89), the first integral is less than or equal to

$$(\Delta - \varepsilon - u_{k-1})(3G\Delta + 2L\varepsilon),$$

the second integral is less than or equal to

$$\int_{u_k=\Delta-\varepsilon}^{\Delta+\varepsilon} |r_3(u_k)| \, \mathrm{d}u_k \leq 2\varepsilon G$$

and the third integral is less than or equal to

$$G\frac{\delta}{1-\delta}(u_{k-1} - 2\varepsilon)1(u_{k-1} > 2\varepsilon).$$

With these bounds (4.89) is less than or equal to

$$\left[\int_{u_{k-1}=0}^{\Delta-\varepsilon} (\Delta - \varepsilon - u_{k-1})(3G\delta + 2L\varepsilon) + 2\varepsilon G + G\frac{\delta}{1-\delta}(u_{k-1} - 2\varepsilon)1(u_{k-1} > 2\varepsilon) \right] \mathrm{d}u_{k-1}$$
$$\leq \frac{1}{2}\Delta^2(3G\delta + 2L\varepsilon) + 2\Delta\varepsilon G + \frac{1}{2}\Delta^2 G\frac{\delta}{1-\delta}$$
$$= O\left(\delta, \varepsilon, \frac{\delta}{1-\delta}\right).$$

Thus, (4.87) is, at worst, $O\left(\delta, \varepsilon, \dfrac{\delta}{1-\delta}\right)$.

As for (4.88), by Property 4.2(v),

$$\int_{u_{n-1}=0}^{\Delta-\varepsilon} |r_{\boldsymbol{v}}(u_{n-1}, x)| \, \mathrm{d}u_{n-1} \leq R_{\boldsymbol{v},1},$$

hence (4.88) is $O(R_{\boldsymbol{v},1})$.

Therefore, the error term $|r_4(n)| = O\left(\max\left\{\delta, \varepsilon, \dfrac{\delta}{1-\delta}, R_{\boldsymbol{v},1}\right\}\right)$.

Now,

$$\begin{aligned}
&\left|g_{1,n}^{*,\varepsilon}(x_0,x)-g_{1,n}^{*}(x_0,x)\right| \\
&=\int_{u_1=\Delta-\varepsilon-x_0}^{\Delta-x_0} g_1(\Delta-u_1-x_0)\int_{u_2=\Delta-\varepsilon-u_1}^{\Delta-u_1} g_2(\Delta-u_2-u_1)\,\mathrm{d}u_1 \\
&\quad\ldots\int_{u_{n-1}=\Delta-\varepsilon-u_{n-2}}^{\Delta-u_{n-2}} g_{n-1}(\Delta-u_{n-1}-u_{n-2})\,\mathrm{d}u_{n-2}g_n(\Delta-x-u_{n-1}) \\
&\quad\times 1(\Delta-x-u_{n-1}\geq 0)\,\mathrm{d}u_{n-1} \\
&\leq\int_{u_1=\Delta-\varepsilon-x_0}^{\Delta-x_0} G\int_{u_2=\Delta-\varepsilon-u_1}^{\Delta-u_1} G\,\mathrm{d}u_1\ldots\int_{u_{n-1}=\Delta-\varepsilon-u_{n-2}}^{\Delta-u_{n-2}} G\,\mathrm{d}u_{n-2}G\,\mathrm{d}u_{n-1} \\
&=\varepsilon^{n-1}G^n,
\end{aligned}$$

where the inequality holds since $|g_\ell|$ are bounded. Therefore, the left-hand side of (4.86) is equal to

$$g_{1,n}^{*,\varepsilon}(x_0,x)+r_4(n)+r_5(n),$$

where $r_5(n)=g_{1,n}^{*}(x_0,x)-g_{1,n}^{*,\varepsilon}(x_0,x)\leq\varepsilon^{n-1}G^n$. □

Combining the results obtained so far in this chapter we have a bound on the difference between $w_n(x_0,x)$ and $g_{1,n}^{*}(x_0,x)$ which we state formally as the following corollary.

Corollary 4.9. *Let $g_1,g_2,\ldots,$ be functions satisfying Assumptions 4.1 and let $\boldsymbol{v}(x)$, $x\in[0,\Delta)$, be a closing operator with Properties 4.2. Then, for $n\geq 2$, $x_0\in[0,\Delta)$,*

$$\left|w_n(x_0,x)-g_{1,n}^{*}(x_0,x)\right|\leq(n-1)|r_1(n)|+|r_4(n)|+|r_5(n)|, \tag{4.90}$$

Proof. Substitute the expression for $w_n(x_0,x)$ in (4.49) into the left-hand side of (4.90), apply the triangle inequality and Corollary 4.5 and Lemma 4.8 to get the result. □

A direct corollary is the following.

Corollary 4.10. *Let $g_1,g_2,\ldots,$ be functions satisfying Assumptions 4.1, $\psi:[0,\Delta)\to\mathbb{R}$ be bounded, $|\psi|\leq F$, and let $\boldsymbol{v}(x)$, $x\in[0,\Delta)$, be a closing operator with Properties 4.2. Then, for $n\geq 2$, $x_0\in[0,\Delta)$,*

$$\left|\int_{x=0}^{\Delta} w_n(x_0,x)\psi(x)-g_{1,n}^{*}(x_0,x)\psi(x)\,\mathrm{d}x\right|\leq((n-1)|r_1(n)|+|r_4(n)|+|r_5(n)|)\Delta F. \tag{4.91}$$

Proof. The left-hand side of (4.91) is less than or equal to

$$\int_{x=0}^{\Delta} \left| w_n(x_0, x) - g^*_{1,n}(x_0, x) \right| |\psi(x)| \, \mathrm{d}x. \tag{4.92}$$

Applying Corollary 4.9, and since $|\psi| \leq F$, then (4.92) is less than or equal to

$$\int_{x=0}^{\Delta} ((n-1)|r_1(n)| + |r_4(n)| + |r_5(n)|)F \, \mathrm{d}x = ((n-1)|r_1(n)| + |r_4(n)| + |r_5(n)|)\Delta F$$

which is the desired result. □

We have assumed throughout this section that the functions g and $\{g_k\}$ are scalar functions, however, we are ultimately interested in expressions of the form (4.36), which contain matrix functions. Conveniently, the matrix-function expression (4.36) can be written as a linear combination of the scalar case. Hence, we can obtain a bound for the matrix-function case from the scalar case, which we state in the following result.

Lemma 4.11. *Let $\boldsymbol{G}_k(x)$, $k \in \{1, 2, ...\}$, be matrix functions with dimensions $N_k \times N_{k+1}$, and let $\psi : [0, \Delta) \to \mathbb{R}$ be bounded, $|\psi| \leq F$. Further, suppose $[\boldsymbol{G}_k(x)]_{ij}$, $i \in \{1, ..., N_k\}$, $j \in \{1, ..., N_{k+1}\}$, $k \in \{1, 2, ...\}$ satisfy Assumptions 4.1. Then,*

$$\begin{aligned}
&\Bigg| \int_{x=0}^{\Delta} \int_{x_1=0}^{\infty} \boldsymbol{G}_1(x_1) \otimes \boldsymbol{k}(x_0) e^{\boldsymbol{S}x_1} \boldsymbol{D}(x_1) \, \mathrm{d}x_1 \left[\prod_{k=2}^{n-1} \int_{x_k=0}^{\infty} \boldsymbol{G}_k(x_k) \otimes e^{\boldsymbol{S}x_k} \, \mathrm{d}x_k \boldsymbol{D} \right] \\
&\qquad \int_{x_n=0}^{\infty} \boldsymbol{G}_n(x_n) \otimes e^{\boldsymbol{S}x_n} \, \mathrm{d}x_n \boldsymbol{v}(x) \psi(x) \, \mathrm{d}x \\
&- \int_{x=0}^{\Delta} \int_{u_1=0}^{\Delta - x_0} \boldsymbol{G}_1(\Delta - u_1 - x_0) \left[\prod_{k=2}^{n-1} \int_{u_k=0}^{\Delta - u_{k-1}} \boldsymbol{G}_k(\Delta - u_k - u_{k-1}) \, \mathrm{d}u_{k-1} \right] \\
&\qquad \boldsymbol{G}_n(\Delta - x - u_{n-1}) 1(\Delta - x - u_{n-1} \geq 0) \, \mathrm{d}u_{n-1} \psi(x) \, \mathrm{d}x \Bigg| \\
&\leq ((n-1)|r_1(n)| + |r_4(n)| + |r_5(n)|)\Delta F \prod_{k=2}^{n} N_k,
\end{aligned} \tag{4.93}$$

where the inequality is an element-wise inequality. Moreover, choosing $\varepsilon = \mathrm{Var}(Z)$, then, for each n, the bound (4.93) is $\mathcal{O}(\mathrm{Var}(Z)^{1/3})$.

Proof. By the Mixed Product Rule the (i, j)th element of the first term on the left-hand side of (4.93) is

$$\int_{x=0}^{\Delta} \int_{x_1=0}^{\infty} \cdots \int_{x_n=0}^{\infty} \left[\boldsymbol{G}_1(x_1) \ldots \boldsymbol{G}_n(x_n) \right]_{i,j} \boldsymbol{k}(x_0) e^{\boldsymbol{S}x_1} \boldsymbol{D} \ldots e^{\boldsymbol{S}x_{n-1}} \boldsymbol{D}$$

$$
\begin{aligned}
&e^{\boldsymbol{S}x_n}\,\mathrm{d}x_n\ldots\,\mathrm{d}x_1\boldsymbol{v}(x)\psi(x)\,\mathrm{d}x\\
&=\int_{x=0}^{\Delta}\int_{x_1=0}^{\infty}\cdots\int_{x_n=0}^{\infty}\sum_{j_1=1}^{N_2}[\boldsymbol{G}_1(x_1)]_{i,j_1}\sum_{j_2=1}^{N_3}[\boldsymbol{G}_2(x_2)]_{j_1,j_2}\cdots\sum_{j_{n-1}=1}^{N_n}[\boldsymbol{G}_n(x_n)]_{j_{n-1},j}\\
&\quad\boldsymbol{k}(x_0)e^{\boldsymbol{S}x_1}\boldsymbol{D}\ldots e^{\boldsymbol{S}x_{n-1}}\boldsymbol{D}e^{\boldsymbol{S}x_n}\,\mathrm{d}x_n\ldots\,\mathrm{d}x_1\boldsymbol{v}(x)\psi(x)\,\mathrm{d}x,
\end{aligned}
\tag{4.94}
$$

from which we see that (4.94) is a linear combination of the scalar function case in Corollary 4.10. Applying the bound for the scalar case, Corollary 4.10, to each term in the linear combination then summing the bounds obtained gives the bound (4.93).

The fact that the error bound is $\mathcal{O}(\mathrm{Var}(Z)^{1/3})$ follows by substituting $\varepsilon=\mathrm{Var}(Z)^{1/3}$ into each term and observing that each term is at most $\mathcal{O}(\mathrm{Var}(Z)^{1/3})$. □

Finally, we are in a position to prove the main result of this section.

Proof of Theorem 4.3. Cases $q=r\in\{+,-\}$ and $m=0$. Lemma 4.4 bounds the absolute difference

$$
\left|\int_{x\in\mathcal{D}_{\ell_0}}\widehat{f}^{\ell_0,(p)}_{0,r,r}(\lambda)(x,j;x_0,k)\psi(x)\,\mathrm{d}x-\int_{x\in\mathcal{D}_{\ell_0}}\widehat{\mu}^{\ell_0}_{0,r,r}(\lambda)(x,j;x_0,k)\psi(x)\,\mathrm{d}x\right|.
$$

Since the bounds from Lemma 4.4 are $\mathcal{O}(\mathrm{Var}(Z^{(p)})^{1/3})$ then, as we take $p\to\infty$, the bounds becomes arbitrarily small which gives the required convergence.

Cases $q,r\in\{+,-\}$, and $m\geq 1$. Given the properties of the functions $h^{u,v}_{ij}$, $u,v\in\{+,-\}$, then $\int_{x\in\mathcal{D}_{\ell_0}}\widehat{f}^{\ell_0,(p)}_{0,q,r}(\lambda)(x,j;x_0,k)\psi(x)\,\mathrm{d}x$ satisfies the assumptions of Lemma 4.11. To see this, let q' be the opposite sign to q, i.e. $q'\in\{+,-\}$, $q\neq q'$. Then, in Equation (4.93), take $n=2m+1(q=r)$, $\boldsymbol{G}_1(x_1)=\boldsymbol{e}_i\boldsymbol{H}^{qq'}(\lambda,x_1)$, $\boldsymbol{G}_{2k}(x_{2k})=\boldsymbol{H}^{q'q}(\lambda,x_{2k})$, $\boldsymbol{G}_{2k+1}(x_{2k})=\boldsymbol{H}^{qq'}(\lambda,x_{2k+1})$, $k=1,\ldots,m-1$; if $q\neq r$ then take $\boldsymbol{G}_{2m}(x_{2m})=\boldsymbol{H}^{rr}(x_{2m})\boldsymbol{e}_j$, otherwise, take $\boldsymbol{G}_{2m}(x_{2m})=\boldsymbol{H}^{q'r}(x_{2m})$ and $\boldsymbol{G}_{2m+1}=\boldsymbol{H}^{rr}(\lambda,x_{2m+1})\boldsymbol{e}_j$. Thus, Lemma 4.11, establishes a bound on (4.39) which is $\mathcal{O}(\mathrm{Var}(Z^{(p)})^{1/3})$, thus taking $p\to\infty$ gives the stated convergence.

Cases $q=0$, $r\in\{+,-\}$ and $m\geq 0$. Since

$$
\widehat{f}^{\ell_0}_{m,0,r}(\lambda)(x,j;x_0,k)=\sum_{q\in\{+,-\}}\sum_{i\in\mathcal{S}_q}\boldsymbol{e}_k\left[\lambda\boldsymbol{I}-\boldsymbol{T}_{00}\right]^{-1}\boldsymbol{T}_{0i}\widehat{f}^{\ell_0}_{m+1(r\neq q),q,r}(\lambda)(x,j;x_0,i),
\tag{4.95}
$$

is a linear combination of terms which are treated in the two cases above, then (4.95) converges to

$$
\widehat{\mu}^{\ell_0}_{m,0,r}(\lambda)(x,j;x_0,k)=\sum_{q\in\{+,-\}}\sum_{i\in\mathcal{S}_q}\boldsymbol{e}_k\left[\lambda\boldsymbol{I}-\boldsymbol{T}_{00}\right]^{-1}\boldsymbol{T}_{0i}\widehat{\mu}^{\ell_0}_{m+1(r\neq q),q,r}(\lambda)(x,j;x_0,i),
\tag{4.96}
$$

as required. □

4.5 Convergence before the first orbit restart epoch

Recall that the goal in this chapter is to show a convergence of

$$\widehat{f}^{\ell_0,(p)}_{q,r}(\lambda)(x,j;x_0,i) \to \widehat{\mu}^{\ell_0}_{q,r}(\lambda)(x,j;x_0,i),$$

where

$$\widehat{f}^{\ell_0,(p)}(\lambda)(x,j;x_0,i) = \int_{t=0}^{\infty} \sum_{m=0}^{\infty} e^{-\lambda t} f^{\ell_0,(p)}_{m+1(p\neq q),q,r}(t)(x,j;x_0,k)\,\mathrm{d}t.$$

Since $f^{\ell_0,(p)}_{m+1(p\neq q),q,r}$ are positive, as is $e^{-\lambda t}$, then we can use the Fubini-Tonelli Theorem to justify a swap of the integral and infinite sum to get

$$\widehat{f}^{\ell_0,(p)}(\lambda)(x,j;x_0,i) = \sum_{m=0}^{\infty} \widehat{f}^{\ell_0,(p)}_{m+1(p\neq q),q,r}(\lambda)(x,j;x_0,k). \tag{4.97}$$

Similarly, we can write

$$\widehat{\mu}^{\ell_0}(\lambda)(x,j;x_0,i) = \sum_{m=0}^{\infty} \widehat{\mu}^{\ell_0}_{m+1(p\neq q),q,r}(\lambda)(x,j;x_0,k).$$

The previous section proved that the Laplace transforms

$$\widehat{f}^{\ell_0,(p)}_{m,q,r}(\lambda)(x,j;x_0,k) \to \widehat{\mu}^{\ell_0}_{m,q,r}(\lambda)(x,j;x_0,k),$$

for $q \in \{+,-,+0,-0\}$, $r \in \{+,-\}$. Thus, all we need to show is that, upon taking the limit of (4.97), we can swap the limit and the summation. Here we apply the Dominated Convergence Theorem to justify the swap. To this end, we show a domination condition in Lemma 4.12 below.

Recall $c_{min} = \min_{i\in\mathcal{S}_+\cup\mathcal{S}_-} |c_i|$, and let E^λ be an independent exponential random variable with rate λ. In the following we use the stochastic interpretation of the Laplace transform of a probability distribution with non-negative support and real, non-negative parameter λ. For a random variable W with distribution function $F_W(w) = \mathbb{P}(W < w)$, then $\int_{w=0}^{\infty} e^{-\lambda w}\,\mathrm{d}F_W(w) = \mathbb{P}(W < E^\lambda)$. That is, the Laplace transform with parameter $\lambda > 0$ is the probability that W occurs before E^λ, an independent random exponential time with rate λ, occurs.

Lemma 4.12. *For all $M \geq 0$, $x \in \mathcal{D}_{\ell_0,j}$, $x_0 \in \mathcal{D}_{\ell_0,i}$, $\ell_0 \in \mathcal{K}$, $\lambda > 0$, $q \in \{+,-,0\}$, $r \in \{+,-\}$, $i \in \mathcal{S}_q$, $j \in \mathcal{S}_r \cup \mathcal{S}_{r0}$,*

$$\sum_{m=M+1}^{\infty} \left| \int_{x\in\mathcal{D}_{\ell_0}} \widehat{f}^{\ell_0,(p)}_{m,q,r}(\lambda)(x,j;x_0,i)\psi(x)\,\mathrm{d}x - \int_{x\in\mathcal{D}_{\ell_0}} \widehat{\mu}^{\ell_0}_{m,q,r}(\lambda)(x,j;x_0,i)\psi(x)\,\mathrm{d}x \right| \leq r_6^M \tag{4.98}$$

where

$$r_6^M = F(\Delta G + \widehat{G}) \left(\frac{q}{q+\lambda}\right)^{2M+2} \left(1 - \left(\frac{q}{q+\lambda}\right)^2\right)^{-1}.$$

Note that the bound r_6^M is independent of p.

We prove the result for $q = r = +$ only, with the proof for the other cases following analogously. Essentially, this result follows from noting the probabilistic interpretation of the Laplace transforms $\widehat{f}^{\ell_0}_{m,+,+}(\lambda)(x, j; x_0, i)$, as the probability that,

- there are m up-down and down-up transitions,
- the orbit process $\{\boldsymbol{A}(t)\}$ evolves accordingly,
- and an independent exponential random variable with rate λ, E^λ, has not yet occurred,
- before the first orbit restart epoch.

We obtain an upper bound by ignoring the behaviour of the orbit process $\{\boldsymbol{A}(t)\}$, then, by a uniformisation argument, we bound the probability that there are m up-down and down-up transitions before E^λ occurs, by the event that there are m independent exponential events before an E^λ occurs.

Similarly, the stochastic interpretation of the Laplace transforms $\widehat{\mu}^{\ell_0}_{m,+,+}(\lambda)(x, j; x_0, i)$, is the probability that,

- there are m up-down and down-up transitions,
- the fluid level $X(t)$ remains in $\mathcal{D}_{\ell_0}$,
- and an independent exponential random variable with rate λ, E^λ, has not yet occurred,
- before the first orbit restart epoch.

We obtain an upper bound by removing the requirement that the fluid level $X(t)$ remain in $\mathcal{D}_{\ell_0}$, then applying the same uniformisation argument as we do for $\widehat{f}^{\ell_0}_{m,+,+}(\lambda)(x, j; x_0, i)$.

Proof. The same arguments and results apply for all p, so let us drop the dependence on p.

Consider $i \in \mathcal{S}_+, j \in \mathcal{S}_+ \cup \mathcal{S}_{+0}$. By the triangle inequality,

$$\sum_{m=M+1}^{\infty} \left| \int_{x \in \mathcal{D}_{\ell_0}} \widehat{f}^{\ell_0}_{m,+,+}(\lambda)(x, j; x_0, i)\psi(x)\,\mathrm{d}x - \int_{x \in \mathcal{D}_{\ell_0}} \widehat{\mu}^{\ell_0}_{m,+,+}(\lambda)(x, j; x_0, i)\psi(x)\,\mathrm{d}x \right|$$

$$\leq \sum_{m=M+1}^{\infty} \int_{x\in\mathcal{D}_{\ell_0}} \widehat{f}^{\ell_0}_{m,+,+}(\lambda)(x,j;x_0,i)|\psi(x)|\,\mathrm{d}x + \sum_{m=M+1}^{\infty} \int_{x\in\mathcal{D}_{\ell_0}} \widehat{\mu}^{\ell_0}_{m,+,+}(\lambda)(x,j;x_0,i)|\psi(x)|\,\mathrm{d}x,$$

since all terms are non-negative.

Consider $\int_{x\in\mathcal{D}_{\ell_0}} \widehat{f}^{\ell_0}_{m,+,+}(\lambda)(x,j;x_0,i)|\psi(x)|\,\mathrm{d}x$, which is given by

$$\begin{aligned}
&\int_{x\in\mathcal{D}_{\ell_0}} \boldsymbol{e}_i \left[\prod_{r=1}^{m}\int_{x_{2r-1}=0}^{\infty} \boldsymbol{H}^{+-}(\lambda,x_{2r-1})\int_{x_{2r}=0}^{\infty}\boldsymbol{H}^{-+}(\lambda,x_{2r})\right]\int_{x_{2m+1}=0}^{\infty}\boldsymbol{H}^{++}(\lambda,x_{2m+1})\boldsymbol{e}_j \\
&\boldsymbol{a}_{\ell_0,i}(x_0)\boldsymbol{N}^{2m+1}(\lambda,x_1,\ldots,x_{2m+1})\boldsymbol{v}_{\ell_0,j}(x)\,\mathrm{d}x_{2m+1}\ldots\,\mathrm{d}x_1\psi(x)\,\mathrm{d}x \\
\leq &\int_{x\in\mathcal{D}_{\ell_0}} \boldsymbol{e}_i \left[\prod_{r=1}^{m}\int_{x_{2r-1}=0}^{\infty} \boldsymbol{H}^{+-}(\lambda,x_{2r-1})\int_{x_{2r}=0}^{\infty}\boldsymbol{H}^{-+}(\lambda,x_{2r})\right]\int_{x_{2m+1}=0}^{\infty}\boldsymbol{H}^{++}(\lambda,x_{2m+1})\boldsymbol{e}_j \\
&\boldsymbol{a}_{\ell_0,i}(x_0)\boldsymbol{N}^{2m+1}(\lambda,x_1,\ldots,x_{2m+1})\boldsymbol{v}_{\ell_0,j}(x)\,\mathrm{d}x_{2m+1}\ldots\,\mathrm{d}x_1\,\mathrm{d}xF \qquad (4.99)
\end{aligned}$$

since $|\psi|\leq F$. To bound the last-line of (4.99) we first observe that for $\boldsymbol{a}\in\mathcal{A}$,

$$\begin{aligned}
\boldsymbol{a}\int_{x\in\mathcal{D}_{\ell_0}} \boldsymbol{D}e^{\boldsymbol{S}x_{2m+1}}\boldsymbol{v}_{\ell_0,j}(x) &= \boldsymbol{a}\int_{x\in\mathcal{D}_{\ell_0}}\int_{u=0}^{\infty} e^{\boldsymbol{S}u}\boldsymbol{s}\frac{\boldsymbol{\alpha}e^{\boldsymbol{S}u}}{\boldsymbol{\alpha}e^{\boldsymbol{S}u}\boldsymbol{e}}e^{\boldsymbol{S}x_{2m+1}}\boldsymbol{v}_{\ell_0,j}(x)\,\mathrm{d}u\,\mathrm{d}x \\
&\leq \boldsymbol{a}\int_{u=0}^{\infty} e^{\boldsymbol{S}u}\boldsymbol{s}\frac{\boldsymbol{\alpha}e^{\boldsymbol{S}u}}{\boldsymbol{\alpha}e^{\boldsymbol{S}u}\boldsymbol{e}}e^{\boldsymbol{S}x_{2m+1}}\boldsymbol{e}\,\mathrm{d}u \\
&= \boldsymbol{a}\boldsymbol{D}e^{\boldsymbol{S}x_{2m+1}}\boldsymbol{e}\,\mathrm{d}u, \qquad (4.100)
\end{aligned}$$

where the inequality holds from Property 4.2(iv). By definition, the last-line of (4.99) is

$$\begin{aligned}
&\int_{x\in\mathcal{D}_{\ell_0}} \boldsymbol{a}_{\ell_0,i}(x_0)\boldsymbol{N}^{2m+1}(\lambda,x_1,\ldots,x_{2m+1})\boldsymbol{v}_{\ell_0,j}(x)\,\mathrm{d}x_{2m+1}\ldots\,\mathrm{d}x_1 \\
&= \int_{x\in\mathcal{D}_{\ell_0}} \boldsymbol{a}_{\ell_0,i}(x_0)e^{\boldsymbol{S}x_1}\boldsymbol{D}e^{\boldsymbol{S}x_2}\boldsymbol{D}\ldots e^{\boldsymbol{S}x_{2m}}\boldsymbol{D}e^{\boldsymbol{S}x_{2m+1}}\boldsymbol{v}_{\ell_0,j}(x). \qquad (4.101)
\end{aligned}$$

Now, using (4.100), then (4.101) is less than or equal to

$$\begin{aligned}
&\boldsymbol{a}_{\ell_0,i}(x_0)e^{\boldsymbol{S}x_1}\boldsymbol{D}e^{\boldsymbol{S}x_2}\boldsymbol{D}\ldots e^{\boldsymbol{S}x_{2m}}\boldsymbol{D}e^{\boldsymbol{S}x_{2m+1}}\boldsymbol{e} \\
&= \boldsymbol{a}_{\ell_0,i}(x_0)e^{\boldsymbol{S}x_1}\boldsymbol{D}e^{\boldsymbol{S}x_2}\boldsymbol{D}\ldots e^{\boldsymbol{S}x_{2m}}\int_{u=0}^{\infty} e^{\boldsymbol{S}u}\frac{\boldsymbol{\alpha}e^{\boldsymbol{S}u}}{\boldsymbol{\alpha}e^{\boldsymbol{S}u}\boldsymbol{e}}\,\mathrm{d}u e^{\boldsymbol{S}x_{2m+1}}\boldsymbol{e} \\
&\leq \boldsymbol{a}_{\ell_0,i}(x_0)e^{\boldsymbol{S}x_1}\boldsymbol{D}e^{\boldsymbol{S}x_2}\boldsymbol{D}\ldots e^{\boldsymbol{S}x_{2m}}\int_{u=0}^{\infty} e^{\boldsymbol{S}u}\frac{\boldsymbol{\alpha}e^{\boldsymbol{S}u}}{\boldsymbol{\alpha}e^{\boldsymbol{S}u}\boldsymbol{e}}\,\mathrm{d}u\boldsymbol{e}
\end{aligned}$$

$$= \boldsymbol{a}_{\ell_0,i}(x_0)e^{\boldsymbol{S}x_1}\boldsymbol{D}e^{\boldsymbol{S}x_2}\boldsymbol{D}\ldots e^{\boldsymbol{S}x_{2m}}\boldsymbol{e}.$$

Repeating m more times gives the bound $\boldsymbol{a}_{\ell_0,i}(x_0)\boldsymbol{e} = 1$. Hence, we have the bound

$$\boldsymbol{a}_{\ell_0,i}(x_0)e^{\boldsymbol{S}x_1}\boldsymbol{D}e^{\boldsymbol{S}x_2}\boldsymbol{D}\ldots e^{\boldsymbol{S}x_{2m}}\boldsymbol{D}e^{\boldsymbol{S}x_{2m+1}}\boldsymbol{e} \leq 1.$$

Therefore, (4.99) is less than or equal to

$$\boldsymbol{e}_i\left[\prod_{r=1}^{m}\int_{x_{2r-1}=0}^{\infty}\boldsymbol{H}^{+-}(\lambda,x_{2r-1})\int_{x_{2r}=0}^{\infty}\boldsymbol{H}^{-+}(\lambda,x_{2r})\right]\int_{x_{2m+1}=0}^{\infty}\boldsymbol{H}^{++}(\lambda,x_{2m+1})\boldsymbol{e}_j \mathrm{d}x_{2m+1}\ldots\mathrm{d}x_1F. \tag{4.102}$$

Now, for any row-vector of non-negative numbers $\boldsymbol{b}$, since the elements of $\boldsymbol{H}^{++}$ are non-negative and integrable, then

$$\boldsymbol{b}\int_{x_{2m+1}=0}^{\infty}\boldsymbol{H}^{++}(\lambda,x_{2m+1})\,\mathrm{d}x_{2m+1}\boldsymbol{e}_j \leq \boldsymbol{b}\boldsymbol{e}_j\widehat{G} \leq \boldsymbol{b}\boldsymbol{e}\widehat{G}.$$

Observing that

$$\boldsymbol{e}_i\left[\prod_{r=1}^{m}\int_{x_{2r-1}=0}^{\infty}\boldsymbol{H}^{+-}(\lambda,x_{2r-1})\int_{x_{2r}=0}^{\infty}\boldsymbol{H}^{-+}(\lambda,x_{2r})\right]\mathrm{d}x_{2m}\ldots\mathrm{d}x_1$$

is a vector of row-vector non-negative numbers, then (4.102) is less than or equal to

$$\boldsymbol{e}_i\left[\prod_{r=1}^{m}\int_{x_{2r-1}=0}^{\infty}\boldsymbol{H}^{+-}(\lambda,x_{2r-1})\int_{x_{2r}=0}^{\infty}\boldsymbol{H}^{-+}(\lambda,x_{2r})\right]\boldsymbol{e}\,\mathrm{d}x_{2m}\ldots\mathrm{d}x_1\widehat{G}F \tag{4.103}$$

The stochastic interpretation of the ith element of the vector $\boldsymbol{H}^{+-}(\lambda,x)\boldsymbol{e}$ is that it is the probability density of an up-down transition at the time when the in-out fluid has increased by $\mathrm{d}x$ and before an exponential random variable with rate λ occurs, given the phase is initially i. There may be multiple changes of phase within $\mathcal{S}_+ \cup \mathcal{S}_{+0}$ before the first up-down transition. The first change of phase occurs at rate (with respect to the in-out level) $-T_{ii}/|c_i|$ and this is the lowest in-out fluid level at which it may be possible to see an up-down transition. Consider a uniformised version of the in-out fluid process with uniformisation parameter $q = \max\limits_{i\in\mathcal{S}\setminus\mathcal{S}_0} -T_{ii}/|c_i|$. Then the first event of the phase process of the uniformised version of the in-out fluid process occurs at rate q and occurs at, or before, the first change of phase of the uniformised process. Therefore, the first uniformisation event occurs at, or before, the first up-down transition of the uniformised version of the in-out process. Hence, the first uniformisation event occurs at, or before, the first up-down transition of the original process (since they are versions

of each other). This gives the bound $\boldsymbol{H}^{+-}(\lambda,x)\boldsymbol{e} \leq qe^{-(\lambda+q)x}\boldsymbol{e}$ where the inequality is understood elementwise. Similarly, for $\boldsymbol{H}^{-+}(\lambda,x)\boldsymbol{e} \leq qe^{-(\lambda+q)x}\boldsymbol{e}$.

From the stochastic interpretation above, (4.103) is less than or equal to

$$\begin{aligned}
&\boldsymbol{e}_i\boldsymbol{H}^{+-}(\lambda,x_1)\,\mathrm{d}x_1\int_{x_2=0}^{\infty}\boldsymbol{H}^{-+}(\lambda,x_2)\boldsymbol{e}\,\mathrm{d}x_2\ldots\int_{x_{2m}=0}^{\infty}qe^{(-q-\lambda)x_{2m}}\,\mathrm{d}x_{2m}\widehat{G}F\\
&\leq\int_{x_1=0}^{\infty}qe^{(-q-\lambda)x_1}\,\mathrm{d}x_1\int_{x_2=0}^{\infty}qe^{(-q-\lambda)x_2}\,\mathrm{d}x_2\ldots\int_{x_{2m}=0}^{\infty}qe^{(-q-\lambda)x_{2m}}\,\mathrm{d}x_{2m}\widehat{G}F\\
&=\left(\frac{q}{q+\lambda}\right)^{2m}\widehat{G}F. \qquad (4.104)
\end{aligned}$$

Hence,

$$\begin{aligned}
\sum_{m=M+1}^{\infty}\int_{x\in\mathcal{D}_{\ell_0}}\widehat{f}^{\ell_0}_{m,+,+}(\lambda)(x,j;x_0,i)|\psi(x)|\,\mathrm{d}x &\leq\widehat{G}F\sum_{m=M+1}^{\infty}\left(\frac{q}{q+\lambda}\right)^{2m}\int_{x\in\mathcal{D}_{\ell_0}}|\psi(x)|\,\mathrm{d}x\\
&\leq\widehat{G}F\left(\frac{q}{q+\lambda}\right)^{2M+2}\left(1-\left(\frac{q}{q+\lambda}\right)^{2}\right)^{-1}\Delta F. \qquad (4.105)
\end{aligned}$$

Now consider $\widehat{\mu}^{\ell_0}_{m,+,+}(\lambda)(x,j;x_0,i)$ which is given by

$$\begin{aligned}
&\int_{x_1=0}^{\Delta-(x_0-y_{\ell_0})}\boldsymbol{e}_i\boldsymbol{H}^{+-}(\lambda,\Delta-(x_0-y_{\ell_0})-x_1)\int_{x_2=0}^{\Delta-x_1}\boldsymbol{H}^{-+}(\lambda,\Delta-x_2-x_1)\,\mathrm{d}x_1\\
&\quad\cdots\int_{x_{2m}=0}^{\Delta-x_{m-1}}\boldsymbol{H}^{-+}(\lambda,\Delta-x_{2m-1}-x_{2m})\,\mathrm{d}x_{2m-1}\boldsymbol{H}^{++}(\lambda,\Delta-x_{2m}-(y_{\ell_0+1}-x))\boldsymbol{e}_j\,\mathrm{d}x_{2m}\\
&=\int_{x_1=(x_0-y_{\ell_0})}^{\Delta}\boldsymbol{e}_i\boldsymbol{H}^{+-}(\lambda,\Delta-x_1)\int_{x_2=x_1}^{\Delta}\boldsymbol{H}^{-+}(\lambda,\Delta-x_2)\,\mathrm{d}x_1\ldots\\
&\int_{x_{2m}=x_{2m-1}}^{\Delta}\boldsymbol{H}^{-+}(\lambda,\Delta-x_{2m})\boldsymbol{H}^{++}(\lambda,\Delta-x_{2m}-x_{2m-1}-(y_{\ell_0+1}-x))\boldsymbol{e}_j\,\mathrm{d}x_{2m-1}\,\mathrm{d}x_{2m}. \qquad (4.106)
\end{aligned}$$

Using the bound $\boldsymbol{H}^{++}(\lambda,x_{m+1})\leq G$ elementwise, then (4.106) is less than or equal to

$$\begin{aligned}
&\int_{x_1=(x_0-y_{\ell_0})}^{\Delta}\boldsymbol{e}_i\boldsymbol{H}^{+-}(\lambda,\Delta-x_1)\int_{x_2=x_1}^{\Delta}\boldsymbol{H}^{-+}(\lambda,\Delta-x_2)\,\mathrm{d}x_1\\
&\quad\cdots\int_{x_{2m}=x_{2m-1}}^{\Delta}\boldsymbol{H}^{-+}(\lambda,\Delta-x_{2m})\,\mathrm{d}x_{2m-1}\,\mathrm{d}x_{2m}\boldsymbol{e}G. \qquad (4.107)
\end{aligned}$$

The expression (4.107) differs from (4.103) only by a constant factor and that the integrals in the (4.107) are finite, hence we may bound it in the same way. Therefore,

$$\sum_{m=M+1}^{\infty} \int_{x\in\mathcal{D}_{\ell_0}} \widehat{\mu}^{\ell_0}_{m,+,+}(\lambda)(x,j;x_0,i)|\psi(x)|\,\mathrm{d}x \le G\left(\frac{q}{q+\lambda}\right)^{2M+2}\left(1-\left(\frac{q}{q+\lambda}\right)^{2}\right)^{-1}\Delta F.$$

Analogous arguments show the same bounds for any $i,j\in\mathcal{S}$. □

Combining the domination in Lemma 4.12 and the convergence in Theorem 4.3 via the Dominated Convergence Theorem gives the following result.

Lemma 4.13. *For all $x\in\mathcal{D}_{\ell_0,j}$, $x_0\in\mathcal{D}_{\ell_0,i}$, $i,j\in\mathcal{S}$, $\ell_0\in\mathcal{K}$, $\lambda>0$,*

$$\left|\int_{x\in\mathcal{D}_{\ell_0}} \widehat{f}^{\ell_0,(p)}(\lambda)(x,j;x_0,i)\psi(x)\,\mathrm{d}x - \int_{x\in\mathcal{D}_{\ell_0}} \widehat{\mu}^{\ell_0}(\lambda)(x,j;x_0,i)\psi(x)\,\mathrm{d}x\right| \to 0 \qquad (4.108)$$

as $p\to\infty$.

Remark 4.14. *For a fixed $\lambda>0$, convergence of*

$$\left|\widehat{f}^{\ell_0,(p)}(\lambda)(x,j;x_0,i) - \widehat{\mu}^{\ell_0}(\lambda)(x,j;x_0,i)\right| \qquad (4.109)$$

actually holds pointwise for each $\ell_0\in\mathcal{K}\setminus\{-1,K+1\}$, and each $i,j\in\mathcal{S}$, $x_0\in\mathcal{D}_{\ell_0,i}$, $x\in\mathcal{D}_{\ell_0,j}$ except at the set of points where $x=x_0$. Specifically, the lack of pointwise convergence at this point occurs due to terms with the index $m=0$, that is, terms where there are no changes of phase from $\mathcal{S}_+\to\mathcal{S}_-$ or $\mathcal{S}_-\to\mathcal{S}_+$. On these sample paths the relevant Laplace transforms of the fluid queue are discontinuous at this point. For example,

$$\widehat{\mu}^{\ell_0}_{0,+,+}(\lambda)(x,j;x_0,i)\,\mathrm{d}x = h^{++}_{ij}(\lambda,x-x_0)1(x\ge x_0)\,\mathrm{d}x,$$

is discontinuous at $x=x_0$.

4.6 Convergence at the time of the first orbit restart epoch

We conclude this chapter with a statement about a convergence of the QBD-RAP to the fluid queue at the time of the first orbit restart epoch, $\tau_1^{(p)}$.

Corollary 4.15. *Recall* $\boldsymbol{y}_0^{(p)} = (\ell_0, \boldsymbol{a}_{\ell_0,j}^{(p)}(x_0), i)$. *For* $\ell_0 \in \mathcal{K}$ $x_0 \in \mathcal{D}_{\ell_0,i}$, $i \in \mathcal{S}_+ \cup \mathcal{S}_- \cup \mathcal{S}_0^*$,

$$\begin{aligned}&\mathbb{P}(L^{(p)}(\tau_1^{(p)}) = \ell(\ell_0, j), \varphi(\tau_1^{(p)}) = j, \tau_1^{(p)} \leq E^\lambda \mid \boldsymbol{Y}^{(p)}(0) = \boldsymbol{y}_0^{(p)})\\ &\to \mathbb{P}(\boldsymbol{X}(\tau_1^X) = (y_{\ell+1(j\in\mathcal{S}_-)}, j), \tau_1^X \leq E^\lambda \mid \boldsymbol{X}(0) = (x_0, i))\end{aligned} \tag{4.110}$$

where $\ell(\ell_0, j)$ *can take values*

$$\ell(\ell_0, j) = \begin{cases} \ell_0 - 1 & \ell_0 \in \{0, 1, \ldots, K+1\},\ j \in \mathcal{S}_- \\ \ell_0, & \ell_0 = 0, j \in \mathcal{S}_+,\ \textit{or}\ \ell_0 = K, j \in \mathcal{S}_-, \\ \ell_0 + 1 & \ell_0 \in \{-1, 0, 1, \ldots, K\},\ j \in \mathcal{S}_+. \end{cases} \tag{4.111}$$

Proof. The proof follows the same structure as the proof of Theorem 4.3 however, changes are required in all the results used in the proof, as here we do not need to integrate a function ψ. We give an outline of the proof only.

At a boundary we can model the fluid queue exactly, hence (4.110) holds for $\ell_0 = -1$ and $\ell_0 = K + 1$.

Now consider $i \in \mathcal{S}_+, j \in \mathcal{S}_+$. Partition the probability (4.110) on the times $\{\Sigma_n\}_{n\geq 1}$ and $\{\Gamma_n\}_{n\geq 1}$ and, specifically, partition on the event that there are exactly m events $\{\Sigma_n\}_{n=1}^m$ and exactly m events $\{\Gamma_n\}_{n=1}^m$. The resulting partitioned probabilities are

$$\begin{aligned}&\int_{x_1=0}^\infty \left(\boldsymbol{e}_i \boldsymbol{H}^{+-}(\lambda, x_1) \otimes \boldsymbol{a}_{\ell_0,i}^{(p)}(x_0) e^{\boldsymbol{S}^{(p)} x_1} \boldsymbol{D}^{(p)}\right) \mathrm{d}x_1\\ &\left[\prod_{r=1}^{m-1} \int_{x_{2r}=0}^\infty \left(\boldsymbol{H}^{-+}(\lambda, x_{2r}) \otimes e^{\boldsymbol{S}^{(p)} x_{2r}} \boldsymbol{D}^{(p)}\right) \mathrm{d}x_{2r}\right.\\ &\left.\int_{x_{2r+1}=0}^\infty \left(\boldsymbol{H}^{+-}(\lambda, x_{2r+1}) \otimes e^{\boldsymbol{S}^{(p)} x_{2r+1}} \boldsymbol{D}^{(p)}\right) \mathrm{d}x_{2r+1}\right]\\ &\int_{x_{2m}=0}^\infty \left(\boldsymbol{H}^{-+}(\lambda, x_{2m}) \otimes e^{\boldsymbol{S}^{(p)} x_{2m}} \boldsymbol{D}^{(p)}\right) \mathrm{d}x_{2m}\\ &\int_{x_{2m+1}=0}^\infty \left(\boldsymbol{H}^{++}(\lambda, x_{2m+1}) \boldsymbol{e}_j \otimes e^{\boldsymbol{S}^{(p)} x_{2m+1}} \boldsymbol{s}^{(p)}\right) \mathrm{d}x_{2m+1}.\end{aligned} \tag{4.112}$$

To show that the terms (4.112) converge to

$$\mathbb{P}(\boldsymbol{X}(\tau_1^X) = (y_{\ell_0+1}, j), \tau_1^X \leq E^\lambda, \Sigma_m \leq \tau_1^X < \Gamma_{m+1}, \mid \boldsymbol{X}(0) = (x_0, i)) \tag{4.113}$$

we can use the bounds from Corollary 4.7 and Corollary 4.9. For $m = 0$ we recognise (4.112) as the same form as that appearing in Corollary 4.7 upon choosing $v = 0$. For $m \geq 1$, choose the closing operator to be $\boldsymbol{v}(x) = e^{\boldsymbol{S}x}\boldsymbol{s}$ and set $x = 0$ in Corollary 4.9. Now take the bound from Corollary 4.9 and extend it to the case of matrix functions in

the same way we extended Corollary 4.10 to the matrix case in Lemma 4.11. In this way, we have a bound for (4.112) which tends to 0 as $p \to \infty$.

What remains is a domination condition so that we may apply the Dominated Convergence Theorem to claim that the sum over the number of up-down and down-up transition converges (i.e. the sum over m in (4.112) converges). After algebraic manipulation, (4.112) is

$$\begin{aligned}&\boldsymbol{e}_i \left[\prod_{r=1}^{m} \int_{x_{2r-1}=0}^{\infty} \boldsymbol{H}^{+-}(\lambda, x_{2r-1}) \int_{x_{2r}=0}^{\infty} \boldsymbol{H}^{-+}(\lambda, x_{2r})\right] \int_{x_{2m+1}=0}^{\infty} \boldsymbol{H}^{++}(\lambda, x_{2m+1}) \boldsymbol{e}_j \\ &\boldsymbol{a}_{\ell_0,i}(x_0) \boldsymbol{N}^{2m}(\lambda, x_1, \ldots, x_{2m}) \boldsymbol{D} e^{\boldsymbol{S} x_{2m+1}} \boldsymbol{s} \, \mathrm{d}x_{2m+1} \ldots \, \mathrm{d}x_1 \end{aligned} \tag{4.114}$$

Now, since $[\boldsymbol{H}^{++}(\lambda, x_{2m+1})]_{ij} \leq G$ and

$$\boldsymbol{e}_i \left[\prod_{r=1}^{m} \int_{x_{2r-1}=0}^{\infty} \boldsymbol{H}^{+-}(\lambda, x_{2r-1}) \int_{x_{2r}=0}^{\infty} \boldsymbol{H}^{-+}(\lambda, x_{2r})\right]$$

is a row-vector of positive numbers, then (4.114) is less than or equal to

$$\begin{aligned}&\boldsymbol{e}_i \left[\prod_{r=1}^{m} \int_{x_{2r-1}=0}^{\infty} \boldsymbol{H}^{+-}(\lambda, x_{2r-1}) \int_{x_{2r}=0}^{\infty} \boldsymbol{H}^{-+}(\lambda, x_{2r})\right] \int_{x_{2m+1}=0}^{\infty} \boldsymbol{e} G \\ &\boldsymbol{a}_{\ell_0,i}(x_0) \boldsymbol{N}^{2m}(\lambda, x_1, \ldots, x_{2m}) \boldsymbol{D} e^{\boldsymbol{S} x_{2m+1}} \boldsymbol{s} \, \mathrm{d}x_{2m+1} \ldots \, \mathrm{d}x_1.\end{aligned}$$

Integrating with respect to x_{2m+1} gives

$$\begin{aligned}&\boldsymbol{e}_i \left[\prod_{r=1}^{m} \int_{x_{2r-1}=0}^{\infty} \boldsymbol{H}^{+-}(\lambda, x_{2r-1}) \int_{x_{2r}=0}^{\infty} \boldsymbol{H}^{-+}(\lambda, x_{2r})\right] \boldsymbol{e} G \\ &\boldsymbol{a}_{\ell_0,i}(x_0) \boldsymbol{N}^{2m}(\lambda, x_1, \ldots, x_{2m}) \boldsymbol{D} \boldsymbol{e} \, \mathrm{d}x_{2m} \ldots \, \mathrm{d}x_1 \\ \leq\ &\boldsymbol{e}_i \left[\prod_{r=1}^{m} \int_{x_{2r-1}=0}^{\infty} \boldsymbol{H}^{+-}(\lambda, x_{2r-1}) \int_{x_{2r}=0}^{\infty} \boldsymbol{H}^{-+}(\lambda, x_{2r})\right] \boldsymbol{e} G \, \mathrm{d}x_{2m} \ldots \, \mathrm{d}x_1\end{aligned} \tag{4.115}$$

the last inequality holds since, $\boldsymbol{D}\boldsymbol{e} = \boldsymbol{e}$, and $\boldsymbol{a}_{\ell_0,i}(x_0)\boldsymbol{N}^{2m}(\lambda, x_1, \ldots, x_{2m})\boldsymbol{e} \leq 1$, as we claimed previously in the discussion after (4.102) in the proof of Lemma 4.12. Equation (4.115) is of a similar form to (4.103) (they differ only by a constant), hence the same arguments used to bound (4.103) can be applied to get the desired domination result.

Ultimately, we can apply the Dominated Convergence Theorem to prove that the sum of the partitioned probabilities (4.112) converges as $p \to \infty$. The sum of the limits is

$$\mathbb{P}(\boldsymbol{X}(\tau_1^X) = (y_{\ell_0+1}, j), \tau_1 \leq E^\lambda \mid \boldsymbol{X}(0) = (x_0, i)).$$

The results for all other cases of $i, j \in \mathcal{S}$ follow analogously. □

Chapter 5

Global convergence results

In this chapter we prove some results which stem from the main results of Chapter 4. We consider the discrete-time embedded processes formed by observing the QBD-RAP at the orbit restart epochs and by observing the fluid queue at the hitting times of the level process at the of points $\{y_\ell\}$, which are the boundaries of the intervals $\{\mathcal{D}_\ell\}$. In Corollary 5.2 we prove that the transition probability of the embedded process of the QBD-RAP converge those of the embedded process of the fluid queue. In Corollary 5.3 we prove that distribution of the sojourn time of the QBD-RAP in a given level converges to distribution of the sojourn time of the fluid queue in the corresponding interval. In Section 5.2.4, we state global results on the weak convergence (in space and time) of the QBD-RAP approximation scheme to the fluid queue.

In this chapter we work with the augmented state space scheme to model phases with rates $c_i = 0$ as described in Section 3.3. The results of this chapter rely on results of Chapter 4 and therefore apply to the QBD-RAP scheme which uses ephemeral states to model a fluid queue which starts in a phase with rate 0, as described in Section 3.6. However, supplementing the results of Chapter 4 with the results from Appendix C and using the same arguments from this chapter with only slight modifications, then the results of this chapter can be extended to the augmented state-space QBD-RAP scheme without the initial ephemeral phases.

5.1 Convergence of an embedded process

In this section we consider the embedded process formed by observing the QBD-RAP at the orbit restart epochs. Let $\{\tau_n^{(p)}\}_{n\geq 0, n\in\mathbb{Z}}$, $\tau_0^{(p)} = 0$, and

$$\tau_n^{(p)} = \inf\left\{t \geq \tau_{n-1}^{(p)} \mid L^{(p)}(t) \neq L^{(p)}(\tau_{n-1}^{(p)})\right\},$$

be orbit restart epochs. These are the (stopping) times at which $\{L^{(p)}(t)\}$, the level process of the QBD-RAP, changes, or the boundary is hit, or, if the process is at the boundary, the

process leaves the boundary. To simplify notation, we may drop the superscript p where it is not explicitly needed. Further, let $\{\boldsymbol{Y}_{\boldsymbol{\alpha}}^{(p)}(n)\}_{n\geq 0,n\in\mathbb{Z}} = \{(L^{(p)}(\tau_n^{(p)}), \varphi(\tau_n^{(p)}))\}_{n\geq 0,n\in\mathbb{Z}}$ be the level and phase of the discrete-time process embedded at the orbit restart epochs, $\{\tau_n^{(p)}\}_{n\geq 0}$. The subscript $\boldsymbol{\alpha}$ refers to the fact that $\boldsymbol{A}^{(p)}(\tau_n^{(p)}) = \boldsymbol{\alpha}^{(p)}$ for $n \geq 1$. The process $\{\boldsymbol{Y}_{\boldsymbol{\alpha}}^{(p)}(n)\}_{n\geq 0}$ is a discrete-time Markov chain, which is time-homogeneous for $n \geq 1$.

Let $\{\tau_n^X\}_{n\geq 0}$, be the sequence of (stopping) times with $\tau_0^X = 0$, and

$$\tau_{n+1}^X = \min\left\{\begin{array}{c}\inf\left\{t > \tau_n^X \mid X(t) = y_\ell, \ell \in \mathcal{K}\right\},\\ \inf\left\{t > \tau_n^X \mid X(t) \neq 0, X(0) = 0\right\},\\ \inf\left\{t > \tau_n^X \mid X(t) \neq y_{K+1}, X(0) = y_{K+1}\right\}\end{array}\right\},$$

for $n \geq 0$. For $n \geq 1$, τ_n^X is the time at which $X(t)$ either changes band, or hits a boundary, or leaves a boundary, for the nth time. The embedded process $\{\boldsymbol{X}(\tau_n)\}$ is a discrete-time Markov chain which is time-homogeneous for $n \geq 1$.

We have the following result on the convergence of the embedded processes $\{\boldsymbol{Y}_{\boldsymbol{\alpha}}^{(p)}(n)\}$ and $\{\boldsymbol{X}(\tau_n^X)\}$, which we will utilise later to prove a global result.

Corollary 5.1. *For $\ell_0 \in \mathcal{K}$, $x_0 \in \mathcal{D}_{\ell_0,i}$, $i \in \mathcal{S}$, for $n = 0$, then*

$$\begin{aligned}&\mathbb{P}(\boldsymbol{Y}_{\boldsymbol{\alpha}}^{(p)}(1) = (\ell(\ell_0, j), j), \tau_1^{(p)} \leq E^\lambda \mid \boldsymbol{Y}^{(p)}(0) = (\ell_0, \boldsymbol{a}_{\ell_0,i}^{(p)}(x_0), i))\\ &\to \mathbb{P}(\boldsymbol{X}(\tau_1^X) = (y_{\ell(\ell_0,j)+1(j\in\mathcal{S}_-)}, j), \tau_1^X \leq E^\lambda \mid \boldsymbol{X}(0) = (x_0, i)),\end{aligned} \tag{5.1}$$

and for $n \geq 1$, then,

$$\begin{aligned}&\mathbb{P}(\boldsymbol{Y}_{\boldsymbol{\alpha}}^{(p)}(n+1) = (\ell(\ell_0, j), j), \tau_{n+1}^{(p)} \leq E^\lambda \mid \boldsymbol{Y}_{\boldsymbol{\alpha}}^{(p)}(n) = (\ell_0, i), \tau_n^{(p)} \leq E^\lambda)\\ &\to \mathbb{P}(\boldsymbol{X}(\tau_{n+1}^X) = (y_{\ell(\ell_0,j)+1(j\in\mathcal{S}_-)}, j), \tau_{n+1}^X \leq E^\lambda \mid \boldsymbol{X}(\tau_n^X) = (y_{\ell_0+1(i\in\mathcal{S}_-)}, i), \tau_n^X \leq E^\lambda).\end{aligned} \tag{5.2}$$

where $\ell(\ell_0, j)$ can take values

$$\ell(\ell_0, j) = \begin{cases}\ell_0 - 1, & \ell_0 \in \{0, 1, \ldots, K+1\},\ j \in \mathcal{S}_-\\ \ell_0, & \ell_0 = 0, j \in \mathcal{S}_+,\ \text{or } \ell_0 = K, j \in \mathcal{S}_-,\\ \ell_0 + 1, & \ell_0 \in \{-1, 0, 1, \ldots, K\},\ j \in \mathcal{S}_+.\end{cases} \tag{5.3}$$

Proof. The convergence for $\ell_0 \in \{-1, K+1\}$ holds trivially as the QBD-RAP and fluid queue have the same behaviour at the sticky boundary.

The case for $n = 0$ is a direct result of Corollary 4.15.

All that is left is to prove (5.2). For $n \geq 1$, consider the transition probabilities of the embedded process from the QBD-RAP,

$$\mathbb{P}(\boldsymbol{Y}_{\boldsymbol{\alpha}}^{(p)}(n+1) = (\ell(\ell_0, j), j), \tau_{n+1}^{(p)} \leq E^\lambda \mid \boldsymbol{Y}_{\boldsymbol{\alpha}}^{(p)}(n) = (\ell_0, i), \tau_n^{(p)} \leq E^\lambda)$$

$$= \mathbb{P}(\boldsymbol{Y}_{\boldsymbol{\alpha}}^{(p)}(1) = (\ell(\ell_0, j), j), \tau_1^{(p)} \leq E^\lambda \mid \boldsymbol{Y}^{(p)}(0) = (\ell_0, \boldsymbol{\alpha}, i)), \tag{5.4}$$

since the QBD-RAP is time-homogeneous and the exponential random variable E^λ is memoryless. Applying Corollary 4.15 to (5.4) then

$$\begin{aligned} &\mathbb{P}(\boldsymbol{Y}_{\boldsymbol{\alpha}}^{(p)}(n+1) = (\ell(\ell_0, j), j), \tau_{n+1}^{(p)} \leq E^\lambda \mid \boldsymbol{Y}_{\boldsymbol{\alpha}}^{(p)}(n) = (\ell_0, i), \tau_n^{(p)} \leq E^\lambda) \\ &\to \mathbb{P}(\boldsymbol{X}(\tau_1^X) = (y_{\ell(\ell_0,j)+1(j\in\mathcal{S}_-)}, j), \tau_1^X \leq E^\lambda \mid \boldsymbol{X}(0) = (y_{\ell_0+1(i\in\mathcal{S}_-)}, i)). \end{aligned} \tag{5.5}$$

Since the fluid queue is time-homogeneous, and E^λ memoryless, then (5.5) is equal to

$$\begin{aligned} &\mathbb{P}(\boldsymbol{X}(\tau_1^X) = (y_{\ell(\ell_0,j)+1(j\in\mathcal{S}_-)}, j), \tau_1^X \leq E^\lambda \mid \boldsymbol{X}(\tau_1^X) = (y_{\ell_0+1(i\in\mathcal{S}_-)}, i)) \\ &= \mathbb{P}(\boldsymbol{X}(\tau_{n+1}^X) = (y_{\ell(\ell_0,j)+1(j\in\mathcal{S}_-)}, j), \tau_{n+1}^X \leq E^\lambda \mid \boldsymbol{X}(\tau_n^X) = (y_{\ell_0+1(i\in\mathcal{S}_-)}, i), \tau_n^X \leq E^\lambda), \end{aligned} \tag{5.6}$$

which proves the result. □

A direct corollary of Corollary 5.1 is the convergence of the transition probabilities of the embedded process.

Corollary 5.2. *For $\ell_0 \in \mathcal{K}$, $x_0 \in \mathcal{D}_{\ell_0,i}$, $i \in \mathcal{S}$, for $n = 0$, then*

$$\begin{aligned} &\mathbb{P}(\boldsymbol{Y}_{\boldsymbol{\alpha}}^{(p)}(1) = (\ell(\ell_0, j), j) \mid \boldsymbol{Y}^{(p)}(0) = (\ell_0, \boldsymbol{a}_{\ell_0,i}^{(p)}(x_0), i)) \\ &\to \mathbb{P}(\boldsymbol{X}(\tau_1^X) = (y_{\ell(\ell_0,j)+1(j\in\mathcal{S}_-)}, j) \mid \boldsymbol{X}(0) = (x_0, i)). \end{aligned} \tag{5.7}$$

and for $n \geq 1$,

$$\begin{aligned} &\mathbb{P}(\boldsymbol{Y}_{\boldsymbol{\alpha}}^{(p)}(n+1) = (\ell(\ell_0, j), j) \mid \boldsymbol{Y}_{\boldsymbol{\alpha}}^{(p)}(n) = (\ell_0, i)) \\ &\to \mathbb{P}(\boldsymbol{X}(\tau_{n+1}^X) = (y_{\ell(\ell_0,j)+1(j\in\mathcal{S}_-)}, j) \mid \boldsymbol{X}(\tau_n) = (y_{\ell_0+1(i\in\mathcal{S}_-)}, i)). \end{aligned} \tag{5.8}$$

Proof. Since $\tau_1^{(p)} < \infty$ almost surely, as is τ_1^X, then taking $\lambda \to 0$ in Corollary 5.1 yields the result. □

Corollary 5.2 states that the transition probabilities of the embedded processes converge. Thus, the finite-dimensional distributions of $\{\boldsymbol{Y}_{\boldsymbol{\alpha}}^{(p)}(n)\}$ converge, and if the space $\mathcal{K} \times \mathcal{S}$ is finite, then the sequence of distributions of $\{\boldsymbol{Y}_{\boldsymbol{\alpha}}^{(p)}(n)\}$ is tight. Thus, we can establish the convergence in distribution of $\{\boldsymbol{Y}_{\boldsymbol{\alpha}}^{(p)}(n)\}$ and $\{\boldsymbol{X}(\tau_n^X)\}$.

Another direct corollary of Corollary 4.15 is the convergence in distribution of the random variables $\{\tau_1^{(p)}\}_{p\geq 1}$ to τ_1^X.

Corollary 5.3. *The random variables $\{\tau_1^{(p)}\}_{p\geq 1}$ converge in distribution to τ_1^X.*

Proof. By Corollary 4.15 the probabilities

$$\begin{aligned}&\mathbb{P}(\boldsymbol{Y}_{\alpha}^{(p)}(1) = (\ell(\ell_0, j), j), \tau_1^{(p)} \leq E^{\lambda} \mid \boldsymbol{Y}^{(p)}(0) = \boldsymbol{y}_0)\\ &\to \mathbb{P}(\boldsymbol{X}(\tau_1^X) = (y_{\ell(\ell_0,j)+1(j\in\mathcal{S}_-)}, j), \tau_1^{(p)} \leq E^{\lambda} \mid \boldsymbol{X}(0) = (x_0, i)).\end{aligned}$$

By the law of total probability and the convergence above,

$$\begin{aligned}&\mathbb{P}(\tau_1^{(p)} \leq E^{\lambda} \mid \boldsymbol{Y}^{(p)}(0) = \boldsymbol{y}_0)\\ &= \sum_{\ell\in\{\ell_0-1,\ell_0,\ell_0+1\}\cap\mathcal{K}} \sum_{j\in\mathcal{S}} \mathbb{P}(\boldsymbol{Y}_{\alpha}^{(p)}(1) = (\ell, j), \tau_1^{(p)} \leq E^{\lambda} \mid \boldsymbol{Y}^{(p)}(0) = \boldsymbol{y}_0)\\ &\to \sum_{\ell\in\{\ell_0,\ell_0+1\}\cap\{0,1,\ldots,K+1\}} \sum_{j\in\mathcal{S}} \mathbb{P}(\boldsymbol{X}(\tau_1^X) = (y_\ell, j), \tau_1^{(p)} \leq E^{\lambda} \mid \boldsymbol{X}(0) = (x_0, i)).\\ &= \mathbb{P}(\tau^X \leq E^{\lambda} \mid \boldsymbol{X}(0) = (x_0, i)). \qquad (5.9)\end{aligned}$$

Thus, the Laplace transform of $\tau_1^{(p)}$ converges to the Laplace transform of τ_1^X. By the Continuity Theorem for Laplace transforms (Feller 1957, Chapter XIII, Theorem 2a), then $\{\tau_1^{(p)}\}$ converges in distribution to τ_1^X. □

5.2 Convergence of the QBD-RAP scheme

This section is dedicated to proving a global convergence results of the QBD-RAP approximation scheme to the fluid queue. Ultimately, we prove the weak convergence (in space and time) of the QBD-RAP approximation scheme to the distribution of the fluid queue. The structure of the argument is to first show a convergence result for the Laplace transform with respect to time of the distributions of the QBD-RAP and fluid queue at the nth orbit restart epoch. We then prove a convergence result of the QBD-RAP and fluid queue between the nth and $n+1$th orbit restart epoch. Summing over the number of orbit restart epochs, n, and via the Dominated Convergence Theorem, we claim a convergence of the Laplace transforms with respect to time of the QBD-RAP approximation and fluid queue. Lastly, we apply the Extended Continuity Theorem for Laplace transforms (Feller 1957, Chapter XIII, Theorem 2a) to claim a weak convergence (in space and time) of the QBD-RAP approximation scheme to the fluid queue.

5.2.1 At the nth orbit restart epoch

For $n \geq 1$, consider the Laplace transform

$$\begin{aligned}&\int_{t=0}^{\infty} e^{-\lambda t}\mathbb{P}(\boldsymbol{Y}_{\boldsymbol{\alpha}}^{(p)}(n) = (\ell, j_n), \tau_n^{(p)} \in \mathrm{d}t \mid \boldsymbol{Y}^{(p)}(0) = \boldsymbol{y}_0^{(p)})\,\mathrm{d}t\\ &= \mathbb{P}(\boldsymbol{Y}_{\boldsymbol{\alpha}}^{(p)}(n) = (\ell, j_n), \tau_n^{(p)} \leq E^{\lambda} \mid \boldsymbol{Y}^{(p)}(0) = \boldsymbol{y}_0^{(p)}), \qquad (5.10)\end{aligned}$$

which is the Laplace transform of the time until the nth orbit restart epoch of the QBD-RAP on the event that the level and phase at the nth orbit restart epoch are ℓ and j_n, respectively, given that the initial level and phases are ℓ_0 and i, respectively, and the initial orbit is $\boldsymbol{a}^{(p)}_{\ell_0,i}(x_0)$. Partitioning on the time of the first orbit restart epoch, τ_1, and the level and phase at this time, then (5.10) is equal to

$$\sum_{j_1\in\mathcal{S}}\sum_{\ell_1\in\{\ell_0+1,\ell_0,\ell_0-1\}\cap\mathcal{K}} \mathbb{P}(\boldsymbol{Y}^{(p)}_{\boldsymbol{\alpha}}(n)=(\ell,j_n),\tau^{(p)}_n\le E^\lambda \mid \boldsymbol{Y}^{(p)}_{\boldsymbol{\alpha}}(1)=(\ell_1,j_1),\tau^{(p)}_1\le E^\lambda)$$
$$\times\,\mathbb{P}(\boldsymbol{Y}^{(p)}_{\boldsymbol{\alpha}}(1)=(\ell_1,j_1),\tau^{(p)}_1\le E^\lambda \mid \boldsymbol{Y}(0)=\boldsymbol{y}^{(p)}_0). \tag{5.11}$$

An application of Corollary 4.15 to the expression on the second line of (5.11) states,

$$\lim_{p\to\infty}\mathbb{P}(\boldsymbol{Y}^{(p)}_{\boldsymbol{\alpha}}(1)=(\ell_1,j_1),\tau^{(p)}_1\le E^\lambda \mid \boldsymbol{Y}^{(p)}(0)=\boldsymbol{y}^{(p)}_0)$$
$$\to\mathbb{P}(\boldsymbol{X}(\tau^X_1)=(y_{\ell+1(j_1\in\mathcal{S}_-)},j_1),\tau^X_1\le E^\lambda \mid \boldsymbol{X}(0)=(x_0,i)) \tag{5.12}$$

for $i\in\mathcal{S}$, $j_1\in\mathcal{S}_+\cup\mathcal{S}_-$, $\ell_0\in\mathcal{K}$, $x_0\in\mathcal{D}_{\ell_0}$.

We now turn our attention to the first factor in the summands of (5.11). For a given $j_1\in\mathcal{S}_+\cup\mathcal{S}_-$ and $\ell_1\in\mathcal{K}$, consider

$$\mathbb{P}(\boldsymbol{Y}^{(p)}_{\boldsymbol{\alpha}}(n)=(\ell,j_n),\tau^{(p)}_n\le E^\lambda \mid \boldsymbol{Y}^{(p)}_{\boldsymbol{\alpha}}(1)=(\ell_1,j_1),\tau^{(p)}_1\le E^\lambda)$$
$$=\mathbb{P}(\boldsymbol{Y}^{(p)}_{\boldsymbol{\alpha}}(n-1)=(\ell,j_n),\tau^{(p)}_{n-1}\le E^\lambda \mid \boldsymbol{Y}(0)=(\ell_1,\boldsymbol{\alpha},j_1)) \tag{5.13}$$

by the time-homogeneous property of the QBD-RAP and the memoryless property of the exponential distribution.

Let

$$\mathcal{P}^n_{\ell_0,\ell_n}=\left\{(\ell_1,\ldots,\ell_{n-1})\in\mathcal{K}^{n-1}\,\middle|\,\begin{array}{l}\ell_{r-1}=\ell_r=0 \text{ or } \ell_{r-1}=\ell_r=K\\ \text{or } |\ell_{r-1}-\ell_r|=1, r=1,\ldots,n\end{array}\right\}. \tag{5.14}$$

The set $\mathcal{P}^n_{\ell_0,\ell}$ contains all the possible values which $\{L(\tau_m)\}_{m=2}^{n-1}$ may take on a sample path which starts in level ℓ_0, ends in level ℓ and has n orbit restart epochs.

Thus, by partitioning on the phases and the levels at the times τ_m, $m=2,\ldots,n-1$,and using the strong Markov property of the QBD-RAP, then (5.13) is

$$\sum_{\substack{j_2,\ldots,j_{n-1}\in\mathcal{S}\\(\ell_2,\ldots,\ell_{n-1})\in\mathcal{P}^{n-1}_{\ell_1,\ell}}}\prod_{m=2}^{n}\mathbb{P}(\boldsymbol{Y}^{(p)}_{\boldsymbol{\alpha}}(m)=(\ell_m,j_m),\tau^{(p)}_m\le E^\lambda \mid \boldsymbol{Y}^{(p)}_{\boldsymbol{\alpha}}(m-1)=(\ell_{m-1},j_{m-1}),$$
$$\tau^{(p)}_{m-1}\le E^\lambda)$$
$$=\sum_{\substack{j_2,\ldots,j_{n-1}\in\mathcal{S}\\(\ell_2,\ldots,\ell_{n-1})\in\mathcal{P}^{n-1}_{\ell_1,\ell}}}\prod_{m=2}^{n}\mathbb{P}(\boldsymbol{Y}^{(p)}_{\boldsymbol{\alpha}}(1)=(\ell_m,j_m),\tau^{(p)}_1\le E^\lambda \mid \boldsymbol{Y}^{(p)}(0)=(\ell_{m-1},\boldsymbol{\alpha},j_{m-1})), \tag{5.15}$$

by the time-homogeneity property of the QBD-RAP and the memoryless property of E^λ and where we define $\ell_n = \ell$ for notational convenience. We can apply Corollary 4.15 to the factors of the summands in (5.15) and conclude

$$\begin{aligned}&\mathbb{P}(\boldsymbol{Y}_{\boldsymbol{\alpha}}^{(p)}(1) = (\ell_m, j_m), \tau_1^{(p)} \leq E^\lambda \mid \boldsymbol{Y}^{(p)}(0) = (\ell_{m-1}, \boldsymbol{\alpha}, j_{m-1}))\\ &\to \mathbb{P}(\boldsymbol{X}(\tau_1^X) = (y_{\ell_m + 1(j_m \in \mathcal{S}_-)}, j_m), \tau_1^X \leq E^\lambda \mid \boldsymbol{X}(0) = (y_{\ell_{m-1}+1(j_{m-1}\in\mathcal{S}_-)}, j_{m-1})). \quad (5.16)\end{aligned}$$

By the time-homogeneous property of the fluid queue and the memoryless property of the exponential distribution, (5.16) is equal to

$$\begin{aligned}&\mathbb{P}(\boldsymbol{X}(\tau_m^X) = (y_{\ell_m+1(j_m\in\mathcal{S}_-)}, j_m), \tau_m^X \leq E^\lambda \mid \boldsymbol{X}(\tau_{m-1}) = (y_{\ell_{m-1}+1(j_{m-1}\in\mathcal{S}_-)}, j_{m-1}),\\ &\tau_{m-1}^X \leq E^\lambda). \quad (5.17)\end{aligned}$$

Thus, returning to (5.15) and taking the limit as $p \to \infty$,

$$\begin{aligned}&\lim_{p\to\infty} \sum_{\substack{j_2,\ldots,j_{n-1}\in\mathcal{S}\\(\ell_2,\ldots,\ell_{n-1})\in\mathcal{P}_{\ell_1,\ell}^{n-1}}} \prod_{m=2}^{n} \mathbb{P}(\boldsymbol{Y}_{\boldsymbol{\alpha}}^{(p)}(1) = (\ell_m, j_m), \tau_1^{(p)} \leq E^\lambda \mid \boldsymbol{Y}^{(p)}(0) = (\ell_{m-1}, \boldsymbol{\alpha}, j_{m-1}))\\ &= \sum_{\substack{j_2,\ldots,j_{n-1}\in\mathcal{S}\\(\ell_2,\ldots,\ell_{n-1})\in\mathcal{P}_{\ell_1,\ell}^{n-1}}} \prod_{m=2}^{n} \lim_{p\to\infty} \mathbb{P}(\boldsymbol{Y}_{\boldsymbol{\alpha}}^{(p)}(1) = (\ell_m, j_m), \tau_1^{(p)} \leq E^\lambda \mid \boldsymbol{Y}^{(p)}(0) = (\ell_{m-1}, \boldsymbol{\alpha}, j_{m-1})),\end{aligned} \quad (5.18)$$

where we may swap the limit and the sums as they are finite, and we can swap the limit and the product since all the limits exist and the product is finite. Substituting the limits (5.17) into (5.18) gives

$$\begin{aligned}&\sum_{\substack{j_2,\ldots,j_{n-1}\in\mathcal{S}\\(\ell_2,\ldots,\ell_{n-1})\in\mathcal{P}_{\ell_1,\ell}^{n-1}}} \prod_{m=2}^{n} \mathbb{P}(\boldsymbol{X}(\tau_m^X) = (y_{\ell_m+1(j_m\in\mathcal{S}_-)}, j_m), \tau_m^X \leq E^\lambda \mid\\ &\qquad \boldsymbol{X}(\tau_{m-1}^X) = (y_{\ell_{m-1}+1(j_{m-1}\in\mathcal{S}_-)}, j_{m-1}), \tau_{m-1}^X \leq E^\lambda),\\ &= \mathbb{P}(\boldsymbol{X}(\tau_n^X) = (y_{\ell+1(j_n\in\mathcal{S}_-)}, j_n), \tau_n^X \leq E^\lambda \mid \boldsymbol{X}(0) = (y_{\ell_1+1(j_1\in\mathcal{S}_-)}, j_1), \tau_1^X \leq E^\lambda), \quad (5.19)\end{aligned}$$

by the strong Markov property of the fluid queue and the Law of total probability.

Returning now to (5.11) and taking the limit as $p \to \infty$,

$$\begin{aligned}&\lim_{p\to\infty} \sum_{j_1\in\mathcal{S}} \sum_{\ell_1\in\{\ell_0+1,\ell_0,\ell_0-1\}\cap\mathcal{K}} \mathbb{P}(\boldsymbol{Y}_{\boldsymbol{\alpha}}^{(p)}(n) = (\ell, j_n), \tau_n^{(p)} \leq E^\lambda \mid \boldsymbol{Y}_{\boldsymbol{\alpha}}^{(p)}(1) = (\ell_1, j_1), \tau_1^{(p)} \leq E^\lambda)\\ &\mathbb{P}(\boldsymbol{Y}_{\boldsymbol{\alpha}}^{(p)}(1) = (\ell_1, j_1), \tau_1^{(p)} \leq E^\lambda \mid \boldsymbol{Y}^{(p)}(0) = \boldsymbol{y}_0^{(p)})\end{aligned}$$

$$
\begin{aligned}
&= \sum_{j_1 \in \mathcal{S}} \sum_{\ell_1 \in \{\ell_0+1, \ell_0-1\} \cap \mathcal{K}} \lim_{p\to\infty} \mathbb{P}(\boldsymbol{Y}_{\boldsymbol{\alpha}}^{(p)}(n) = (\ell, j_n), \tau_n^{(p)} \leq E^\lambda \mid \boldsymbol{Y}_{\boldsymbol{\alpha}}^{(p)}(1) = (\ell_1, j_1), \tau_1^{(p)} \leq E^\lambda) \\
&\quad \lim_{p\to\infty} \mathbb{P}(\boldsymbol{Y}_{\boldsymbol{\alpha}}^{(p)}(1) = (\ell_1, j_1), \tau_1^{(p)} \leq E^\lambda \mid \boldsymbol{Y}^{(p)}(0) = \boldsymbol{y}_0^{(p)}) \\
&= \sum_{j_1 \in \mathcal{S}} \sum_{\ell_1 \in \{\ell_0+1, \ell_0-1\} \cap \mathcal{K}} \mathbb{P}(\boldsymbol{X}(\tau_n^X) = (y_{\ell+1(j_n \in \mathcal{S}_-)}, j_n), \tau_n^X \leq E^\lambda \mid \boldsymbol{X}(\tau_1^X) = (y_{\ell_1+1(j_1 \in \mathcal{S}_-)}, j_1), \\
&\qquad \tau_1^X \leq E^\lambda) \mathbb{P}(\boldsymbol{X}(\tau_1^X) = (y_{\ell_1+1(j_1 \in \mathcal{S}_-)}, j_1), \tau_1^X \leq E^\lambda \mid \boldsymbol{X}(0) = (x_0, i)) \\
&= \mathbb{P}(\boldsymbol{X}(\tau_n^X) = (y_{\ell+1(j_n \in \mathcal{S}_-)}, j_n), \tau_n^X \leq E^\lambda \mid \boldsymbol{X}(0) = (x_0, i)) \qquad (5.20)
\end{aligned}
$$

where the swapping of limits and sums in the first equality is justified as the sums are finite, the swapping limits and products in the first equality is justified as the product is finite and all limits exist, and the last inequality is the Law of total probability.

Hence, we have proved the following result

Lemma 5.4. *For all $\ell, \ell_0 \in \mathcal{K}$, $i, j_n \in \mathcal{S}$, $x_0 \in \mathcal{D}_{\ell_0,i}$, $n \geq 1$, then, as $p \to \infty$,*

$$
\begin{aligned}
&\mathbb{P}(\boldsymbol{Y}_{\boldsymbol{\alpha}}^{(p)}(n) = (\ell, j_n), \tau_n^{(p)} \leq E^\lambda \mid \boldsymbol{Y}^{(p)}(0) = \boldsymbol{y}_0^{(p)}), \\
&\to \mathbb{P}(\boldsymbol{X}(\tau_n^X) = (y_{\ell+1(j_n \in \mathcal{S}_-)}, j_n), \tau_n^X \leq E^\lambda \mid \boldsymbol{X}(0) = (x_0, i)). \qquad (5.21)
\end{aligned}
$$

Lemma 5.4 is what is required to proceed with the proof of convergence of the QBD-RAP scheme. However, at this point we also point out the following corollary, which may be of interest in other contexts.

Corollary 5.5. *The random variables $\{\tau_n^{(p)}\}_{p\geq 1}$ converge in distribution to τ_n^X.*

Proof. The proof follows the same arguments as the proof of Corollary 5.3. In Lemma 5.4 sum over ℓ and j_n, then apply the Extended Continuity Theorem (Feller 1957, Chapter XIII, Theorem 2a). □

5.2.2 Between the nth and $n+1$th orbit restart epochs

In the last section we proved a convergence of the QBD-RAP to the fluid queue *at* the nth orbit restart epoch. However, we ultimately want to make a convergence statement about the QBD-RAP scheme at any time. The next step is therefore to show a convergence of the QBD-RAP to the fluid queue between the nth and $n+1$th orbit restart epoch, after which we sum over n to prove a convergence result independent of the number of orbit restart epochs.

Let $\mathcal{T}_n^{(p)} = (\tau_n^{(p)}, \tau_{n+1}^{(p)}]$ and $\mathcal{T}_n^X = (\tau_n^X, \tau_{n+1}^X]$. Consider the Laplace transform

$$
\int_{t=0}^{\infty} e^{-\lambda t} \int_{x \in \mathcal{D}_{\ell,j}} \mathbb{P}(\boldsymbol{Y}^{(p)}(t) = (\ell, \mathrm{d}x, j), t \in \mathcal{T}_n^{(p)} \mid \boldsymbol{Y}^{(p)}(0) = \boldsymbol{y}_0^{(p)}) \psi(x) \, \mathrm{d}t, \qquad (5.22)
$$

where $\psi : \mathbb{R} \to \mathbb{R}$ is a bounded function.

Partitioning (5.22) on the time of the nth orbit restart epoch and the phase and level at this time gives

$$\begin{aligned}
&\int_{t=0}^{\infty} e^{-\lambda t} \int_{x\in\mathcal{D}_{\ell,j}} \int_{u_n=0}^{t} \sum_{j_n\in\mathcal{S}} \mathbb{P}(\boldsymbol{Y}^{(p)}(t) = (\ell,\, \mathrm{d}x, j), t \in (u_n, \tau_{n+1}^{(p)}] \mid \boldsymbol{Y}_{\boldsymbol{\alpha}}^{(p)}(n) = (\ell, j_n),\\
&\quad \tau_n^{(p)} = u_n)\psi(x)\mathbb{P}(\boldsymbol{Y}_{\boldsymbol{\alpha}}^{(p)}(n) = (\ell, j_n), \tau_n^{(p)} \in \mathrm{d}u_n \mid \boldsymbol{Y}^{(p)}(0) = \boldsymbol{y}_0^{(p)})\,\mathrm{d}t\\
&= \sum_{j_n\in\mathcal{S}} \int_{x\in\mathcal{D}_{\ell,j}} \int_{t=0}^{\infty} e^{-\lambda t}\mathbb{P}(\boldsymbol{Y}^{(p)}(t) = (\ell,\, \mathrm{d}x, j), t \in \mathcal{T}_0^{(p)} \mid \boldsymbol{Y}(0) = (\ell, \boldsymbol{\alpha}, j_n))\,\mathrm{d}t\psi(x)\\
&\quad \mathbb{P}(\boldsymbol{Y}_{\boldsymbol{\alpha}}^{(p)}(n) = (\ell, j_n), \tau_n^{(p)} \le E^{\lambda} \mid \boldsymbol{Y}^{(p)}(0) = \boldsymbol{y}_0^{(p)}) \qquad (5.23)
\end{aligned}$$

by the time homogenous property of the QBD-RAP, the memoryless property of the exponential distribution, and the convolution theorem of Laplace transforms. The swap of integrals and sums is justified by the Fubini-Tonelli Theorem. We recognise the probability

$$\mathbb{P}(\boldsymbol{Y}_{\boldsymbol{\alpha}}^{(p)}(n) = (\ell, j_n), \tau_n^{(p)} \le E^{\lambda} \mid \boldsymbol{Y}^{(p)}(0) = \boldsymbol{y}_0^{(p)}) \qquad (5.24)$$

as that appearing in Lemma 5.4, hence (5.24) converges to

$$\mathbb{P}(\boldsymbol{X}(\tau_n^X) = (y_{\ell+1(j_n\in\mathcal{S}_-)}, j_n), \tau_n^X \le E^{\lambda} \mid \boldsymbol{X}(0) = (x_0, i)) \qquad (5.25)$$

as $p \to \infty$.

Now consider the expression

$$\int_{x\in\mathcal{D}_{\ell,j}} \int_{t=0}^{\infty} e^{-\lambda t}\mathbb{P}(\boldsymbol{Y}^{(p)}(t) = (\ell,\, \mathrm{d}x, j), t \in \mathcal{T}_0^{(p)} \mid \boldsymbol{Y}(0) = (\ell, \boldsymbol{\alpha}, j_n))\,\mathrm{d}t\psi(x) \qquad (5.26)$$

which appears as part of (5.23). We can rewrite (5.26) as

$$\begin{aligned}
&\int_{x\in\mathcal{D}_{\ell,j}} \int_{t=0}^{\infty} e^{-\lambda t}\mathbb{P}(\boldsymbol{Y}^{(p)}(t) = (\ell,\, \mathrm{d}x, j), t \in \mathcal{T}_0^{(p)} \mid \boldsymbol{Y}_{\boldsymbol{\alpha}}^{(p)}(0) = (\ell, j_n))\,\mathrm{d}t\psi(x)\\
&= \int_{x\in\mathcal{D}_{\ell,j}} \widehat{f}^{\ell,(p)}(\lambda)(x, j; y_{\ell+1(j_n\in\mathcal{S}_-)}, j_n)\psi(x)\,\mathrm{d}x \qquad (5.27)
\end{aligned}$$

Applying Theorem 4.3, then (5.27) converges to

$$\begin{aligned}
&\int_{x\in\mathcal{D}_{\ell,j}} \widehat{\mu}^{\ell}(\lambda)(x, j; y_{\ell+1(j_n\in\mathcal{S}_-)}, j_n)\psi(x)\,\mathrm{d}x\\
&= \int_{x\in\mathcal{D}_{\ell,j}} \int_{t=0}^{\infty} e^{-\lambda t}\mathbb{P}(\boldsymbol{X}(t) \in (\,\mathrm{d}x, j), t \in \mathcal{T}_0^X \mid \boldsymbol{X}(0) = (y_{\ell+1(j_n\in\mathcal{S}_-)}, j_n))\psi(x). \qquad (5.28)
\end{aligned}$$

Since the fluid queue is time-homogeneous and E^λ memoryless, then (5.28) is equal to

$$\int_{x\in\mathcal{D}_{\ell,j}}\int_{t=0}^{\infty} e^{-\lambda t}\mathbb{P}(\boldsymbol{X}(t)\in(\,\mathrm{d}x,j),t\in\mathcal{T}_n^X\mid \boldsymbol{X}(\tau_n^X)=(y_{\ell+1(j_n\in\mathcal{S}_-)},j_n),\tau_n^X\le E^\lambda)\psi(x). \tag{5.29}$$

Therefore, we have shown (5.26) converges to (5.29) as $p\to\infty$.

Returning to the right-hand side of (5.23) and taking the limit as $p\to\infty$,

$$\begin{aligned}
&\lim_{p\to\infty}\sum_{j_n\in\mathcal{S}}\int_{x\in\mathcal{D}_{\ell,j}}\int_{t=0}^{\infty} e^{-\lambda t}\mathbb{P}(\boldsymbol{Y}^{(p)}(t)=(\ell,\,\mathrm{d}x,j),t\in\mathcal{T}_0^{(p)}\mid \boldsymbol{Y}(0)=(\ell,\boldsymbol{\alpha},j_n))\,\mathrm{d}t\psi(x)\\
&\qquad \mathbb{P}(\boldsymbol{Y}_{\boldsymbol{\alpha}}^{(p)}(n)=(\ell,j_n),\tau_n^{(p)}\le E^\lambda\mid \boldsymbol{Y}^{(p)}(0)=\boldsymbol{y}_0^{(p)}). \qquad (5.30)\\
&=\sum_{j_n\in\mathcal{S}}\int_{x\in\mathcal{D}_{\ell,j}}\int_{t=0}^{\infty} e^{-\lambda t}\mathbb{P}(\boldsymbol{X}(t)\in(\,\mathrm{d}x,j),t\in\mathcal{T}_n^X\mid \boldsymbol{X}(\tau_n^X)=(y_{\ell+1(j_n\in\mathcal{S}_-)},j_n),\tau_n^X\le E^\lambda)\\
&\quad \psi(x)\mathbb{P}(\boldsymbol{X}(\tau_n^X)=(y_{\ell+1(j_n\in\mathcal{S}_-)},j_n),\tau_n^X\le E^\lambda\mid \boldsymbol{X}(0)=(x_0,i))\\
&=\int_{t=0}^{\infty} e^{-\lambda t}\int_{x\in\mathcal{D}_{\ell,j}}\mathbb{P}(\boldsymbol{X}(t)\in(\,\mathrm{d}x,j),t\in\mathcal{T}_n^X\mid X(0)=x_0,\varphi(0)=i)\psi(x)\,\mathrm{d}t, \qquad (5.31)
\end{aligned}$$

where the first equality holds since the sum is finite and the limits exist, and the second equality holds from the law of total probability.

Hence, we have shown the following result

Lemma 5.6. *For $\ell,\ell_0\in\mathcal{K}$, $i,j\in\mathcal{S}$, $n\ge 0$, then, as $p\to\infty$,*

$$\begin{aligned}
&\int_{t=0}^{\infty} e^{-\lambda t}\int_{x\in\mathcal{D}_{\ell,j}}\mathbb{P}(\boldsymbol{Y}^{(p)}(t)=(\ell,\,\mathrm{d}x,j),t\in\mathcal{T}_n^{(p)}\mid \boldsymbol{Y}(0)=\boldsymbol{y}_0)\psi(x)\,\mathrm{d}t\\
&\to\int_{t=0}^{\infty} e^{-\lambda t}\int_{x\in\mathcal{D}_{\ell,j_n}}\mathbb{P}(\boldsymbol{X}(t)\in(\,\mathrm{d}x,j),t\in\mathcal{T}_n^X\mid \boldsymbol{X}(0)=(x_0,i))\psi(x)\,\mathrm{d}x\,\mathrm{d}t. \qquad (5.32)
\end{aligned}$$

5.2.3 A domination condition

Our aim is to prove convergence of

$$\begin{aligned}
&\int_{t=0}^{\infty} e^{-\lambda t}\int_{x\in\mathcal{D}_{\ell,j}}\mathbb{P}(\boldsymbol{Y}^{(p)}(t)=(\ell,\,\mathrm{d}x,j)\mid \boldsymbol{Y}(0)=\boldsymbol{y}_0)\psi(x)\,\mathrm{d}t\\
&=\int_{t=0}^{\infty} e^{-\lambda t}\int_{x\in\mathcal{D}_{\ell,j}}\sum_{n=0}^{\infty}\mathbb{P}(\boldsymbol{Y}^{(p)}(t)=(\ell,\,\mathrm{d}x,j),t\in\mathcal{T}_n^{(p)}\mid \boldsymbol{Y}(0)=\boldsymbol{y}_0)\psi(x)\,\mathrm{d}t\\
&=\sum_{n=0}^{\infty}\int_{t=0}^{\infty} e^{-\lambda t}\int_{x\in\mathcal{D}_{\ell,j}}\mathbb{P}(\boldsymbol{Y}^{(p)}(t)=(\ell,\,\mathrm{d}x,j),t\in\mathcal{T}_n^{(p)}\mid \boldsymbol{Y}(0)=\boldsymbol{y}_0)\psi(x)\,\mathrm{d}t \qquad (5.33)
\end{aligned}$$

where the swap of the intergals and sums is justified by the Fubini-Tonelli Theorem. Now, (5.33) is an infinite sum of terms appearing in Lemma 5.6. Hence, upon taking the limit of (5.33), if we can justify the swap of the sum and the limit, we will obtain the desired result. To this end, we now show a domination condition in Corollary 5.9 so that we may apply the Dominated Convergence Theorem.

Lemma 5.7. *For all $i \in \mathcal{S}_+ \cup \mathcal{S}_-$, and $n \geq 2$,*

$$\mathbb{P}(\tau_n \leq E^\lambda \mid \phi(\tau_{n-1}) = i, \tau_{n-1} \leq E^\lambda) \leq b, \tag{5.34}$$

where

$$b = \min\left\{1 - e^{-q(\Delta+\varepsilon)}\left[1 - e^{q\varepsilon - \lambda\Delta/|c_{min}|}\right] + \frac{\mathrm{Var}(Z)}{\varepsilon^2} + |r_2|, \frac{q}{q+\lambda}\right\}$$

and

$$|r_2| \leq 2G\frac{\mathrm{Var}\,(Z)}{\varepsilon^2} + 2L\varepsilon.$$

Note that b and r_1 depend on p which has been suppressed to simplify notation. When explicitly needed, we use a superscript p to denote this dependence.

Proof. For the QBD-RAP, orbit restart epochs can only occur when $i \in \mathcal{S}_+ \cup \mathcal{S}_-$.

Suppose that the phase at time τ_{n-1} is $i \in \mathcal{S}_+$ and that at time τ_{n-1} the QBD-RAP is not at a boundary. The arguments for an initial phase $i \in \mathcal{S}_-$ are analogous. For an orbit restart epochs to occur, either;

1. the QBD-RAP remains in phase i until the orbit restart epoch occurs, or
2. the QBD-RAP changes phase before there is an orbit restart epoch, after which the orbit restart epoch occurs eventually.

Hence, for sample paths which contribute to the Laplace transform, one of two things must happen, either;

1. the phase remains i until there is an orbit restart epoch and E^λ does not occur before the orbit restart epoch, or,
2. the phase changes before there is an orbit restart epoch and E^λ does not occur before the orbit restart epoch.

The probability of 1 is

$$\int_{x=0}^{\infty} \boldsymbol{\alpha} e^{\boldsymbol{S}x} \boldsymbol{s} e^{(T_{ii}-\lambda)x/|c_i|}\,\mathrm{d}x = e^{(T_{ii}-\lambda)\Delta/|c_i|} + r_2, \tag{5.35}$$

by Lemma 4.6.

The probability of 2 is

$$\int_{x=0}^{\infty} \boldsymbol{\alpha} e^{\boldsymbol{S}x} \boldsymbol{e} e^{(T_{ii}-\lambda)x/|c_i|}(-T_{ii}/|c_i|)\,\mathrm{d}x = \int_{x=0}^{\Delta+\varepsilon} \boldsymbol{\alpha} e^{\boldsymbol{S}x} \boldsymbol{e} e^{(T_{ii}-\lambda)x/|c_i|}(-T_{ii}/|c_i|)\,\mathrm{d}x + \int_{x=\Delta+\varepsilon}^{\infty} \boldsymbol{\alpha} e^{\boldsymbol{S}x} \boldsymbol{e} e^{(T_{ii}-\lambda)x/|c_i|}(-T_{ii}/|c_i|)\,\mathrm{d}x. \quad (5.36)$$

Now, since $\boldsymbol{\alpha} e^{\boldsymbol{S}x} \boldsymbol{e} \leq 1$ for $x \leq \Delta + \varepsilon$ then the first term on the right-hand side of (5.36) is less than or equal to

$$\int_{x=0}^{\Delta+\varepsilon} e^{(T_{ii}-\lambda)/|c_i|x}(-T_{ii}/|c_i|)\,\mathrm{d}x \leq \int_{x=0}^{\Delta+\varepsilon} e^{T_{ii}/|c_i|x}(-T_{ii}/|c_i|)\,\mathrm{d}x = 1 - e^{T_{ii}/|c_i|(\Delta+\varepsilon)}.$$

By Chebyshev's inequality, $\boldsymbol{\alpha} e^{\boldsymbol{S}x} \boldsymbol{e} \leq \dfrac{\mathrm{Var}(Z)}{\varepsilon^2}$ for $x > \Delta + \varepsilon$, hence the second term on the right-hand side of (5.36) is less than or equal to

$$\int_{x=\Delta+\varepsilon}^{\infty} \frac{\mathrm{Var}(Z)}{\varepsilon^2} e^{(T_{ii}-\lambda)x/|c_i|}(-T_{ii}/|c_i|)\,\mathrm{d}x \leq \frac{\mathrm{Var}(Z)}{\varepsilon^2}.$$

Putting these together, then the right-hand side of (5.36) is less than or equal to

$$1 - e^{T_{ii}(\Delta+\varepsilon)/|c_i|} + \frac{\mathrm{Var}(Z)}{\varepsilon^2}. \quad (5.37)$$

Combining (5.35) and (5.37), then $\mathbb{P}(\tau_n \leq E^\lambda \mid \phi(\tau_{n-1}) = i, \tau_{n-1} \leq E^\lambda)$ is less than or equal to

$$\begin{aligned} & e^{(T_{ii}-\lambda)\Delta/|c_i|} + |r_2| + 1 - e^{T_{ii}(\Delta+\varepsilon)/|c_i|} + \frac{\mathrm{Var}(Z)}{\varepsilon^2} \\ &= 1 - e^{T_{ii}(\Delta+\varepsilon)/|c_i|}\left[1 - e^{(-T_{ii}\varepsilon-\lambda\Delta)/|c_i|}\right] + \frac{\mathrm{Var}(Z)}{\varepsilon^2} + |r_2| \\ &= 1 - e^{-q(\Delta+\varepsilon)}\left[1 - e^{q\varepsilon-\lambda\Delta/|c_{min}|}\right] + \frac{\mathrm{Var}(Z)}{\varepsilon^2} + |r_2|, \end{aligned} \quad (5.38)$$

since $-T_{ii}/|c_i| \leq q$ and $\lambda\Delta/|c_i| \leq \lambda\Delta/c_{min}$ for all $i \in \mathcal{S}_+ \cup \mathcal{S}_-$.

Now consider the QBD-RAP at a boundary. To leave the boundary there must be at-least one change of phase before E^λ. By a uniformisation argument, the probability of at-least one change of phase before E^λ is less than or equal to $q/(q+\lambda)$. □

Lemma 5.8. *For $n \geq 2$, $i \in \mathcal{S}_+ \cup \mathcal{S}_-$,*

$$\mathbb{P}(\tau_n \leq E^\lambda \mid \phi(\tau_1) = i, \tau_1 \leq E^\lambda) \leq b^{n-1}. \quad (5.39)$$

Proof. The proof is by induction.

For the base case, set $n = 2$ and apply Lemma 5.7.

Now, assume the induction hypothesis $\mathbb{P}(\tau_{n-1} \leq E^\lambda \mid \phi(\tau_1) = i, \tau_1 \leq E^\lambda) \leq b^{n-2}$ for arbitrary $n \geq 3$.

Since $\{\tau_{n-1} \leq E^\lambda\}$ is a subset of $\{\tau_n \leq E^\lambda\}$, then

$$\mathbb{P}(\tau_n \leq E^\lambda \mid \phi(\tau_1) = i, \tau_1 \leq E^\lambda) = \mathbb{P}(\tau_n \leq E^\lambda, \tau_{n-1} \leq E^\lambda \mid \phi(\tau_1) = i, \tau_1 \leq E^\lambda). \quad (5.40)$$

Now partition (5.40) on the phase at time τ_{n-1},

$$\begin{aligned}
&\sum_{j_{n-1} \in \mathcal{S}} \mathbb{P}(\tau_n \leq E^\lambda, \tau_{n-1} \leq E^\lambda, \phi(\tau_{n-1}) = j_{n-1} \mid \phi(\tau_1) = i, \tau_1 \leq E^\lambda) \\
&= \sum_{j_{n-1} \in \mathcal{S}} \mathbb{P}(\tau_n \leq E^\lambda \mid \phi(\tau_{n-1}) = j_{n-1}, \tau_{n-1} \leq E^\lambda) \\
&\qquad \times \mathbb{P}(\phi(\tau_{n-1}) = j_{n-1}, \tau_{n-1} \leq E^\lambda \mid \phi(\tau_1) = i, \tau_1 \leq E^\lambda), \qquad (5.41)
\end{aligned}$$

by the strong Markov property of the QBD-RAP and the fact that $\boldsymbol{A}(\tau_{n-1}) = \boldsymbol{\alpha}$.

By Lemma 5.7 (5.41) is less than or equal to

$$\begin{aligned}
&\sum_{j_{n-1} \in \mathcal{S}} b\mathbb{P}(\phi(\tau_{n-1}) = j_{n-1}, \tau_{n-1} \leq E^\lambda \mid \phi(\tau_1) = i, \tau_1 \leq E^\lambda) \\
&= b\mathbb{P}(\tau_{n-1} \leq E^\lambda \mid \phi(\tau_1) = i, \tau_1 \leq E^\lambda) \\
&\leq b \cdot b^{n-2}, \qquad (5.42)
\end{aligned}$$

by the induction hypothesis, and this completes the proof. □

Corollary 5.9. *For $\boldsymbol{y}_0 = (\ell_0, \boldsymbol{a}_{\ell_0,i}(x_0), i)$, $\lambda > 0$, $\ell_0, \ell \in \mathcal{K}$, $i, j \in \mathcal{S}$ and any bounded function $\psi \leq F$, then*

$$\left| \int_{t=0}^{\infty} e^{-\lambda t} \int_{x \in \mathcal{D}_{\ell,j}} \mathbb{P}(\boldsymbol{Y}(t) \in (\ell, \mathrm{d}x, j), t \in \mathcal{T}_n \mid \boldsymbol{Y}(0) = \boldsymbol{y}_0) \psi(x) \, \mathrm{d}t \right| \leq \frac{F b^{n-1}}{\lambda}. \quad (5.43)$$

Proof. First, since $|\psi(x)| \leq F$, then the left-hand side of (5.43) is less than or equal to

$$\begin{aligned}
&\int_{t=0}^{\infty} e^{-\lambda t} \int_{x \in \mathcal{D}_{\ell,j}} \mathbb{P}(\boldsymbol{Y}(t) \in (\ell, \mathrm{d}x, j), t \in \mathcal{T}_n \mid \boldsymbol{Y}(0) = \boldsymbol{y}_0) F \, \mathrm{d}t \\
&= \int_{t=0}^{\infty} e^{-\lambda t} \mathbb{P}(\boldsymbol{Y}(t) \in (\ell, \mathcal{D}_{\ell,j}, j), t \in \mathcal{T}_n \mid \boldsymbol{Y}(0) = \boldsymbol{y}_0) F \, \mathrm{d}t. \qquad (5.44)
\end{aligned}$$

Partitioning on the time of the 1st orbit restart epoch, τ_1, and the phase and level at time τ_1, then (5.44) is equal to

$$\int_{t=0}^{\infty} e^{-\lambda t} \int_{u_1=0}^{t} \sum_{\substack{j_1 \in \mathcal{S} \\ \ell_1 \in \{\ell_0+1, \ell_0, \ell_0-1\} \cap \mathcal{K}}} \mathbb{P}(\boldsymbol{Y}(t) \in (\ell, \mathcal{D}_{\ell,j}, j), t \in \mathcal{T}_n \mid \boldsymbol{Y}_{\boldsymbol{\alpha}}(1) = (\ell_1, j_1), \tau_1 = u_1)$$

$$\begin{aligned}
&\mathbb{P}(\boldsymbol{Y}_{\boldsymbol{\alpha}}(1) = (\ell_1, j_1), \tau_1 \in \mathrm{d}u_1 \mid \boldsymbol{Y}(0) = \boldsymbol{y}_0)F\,\mathrm{d}t \\
&= \int_{t=0}^{\infty} e^{-\lambda t} \int_{u_1=0}^{t} \sum_{\substack{j_1 \in \mathcal{S} \\ \ell_1 \in \{\ell_0+1, \ell_0, \ell_0-1\} \cap \mathcal{K}}} \mathbb{P}(\boldsymbol{Y}(t) \in (\ell, \mathcal{D}_{\ell,j}, j), t - u_1 \in \mathcal{T}_{n-1} \mid \boldsymbol{Y}(0) = (\ell_1, \boldsymbol{\alpha}, j_1)) \\
&\mathbb{P}(\boldsymbol{Y}_{\boldsymbol{\alpha}}(1) = (\ell_1, j_1), \tau_1 \in \mathrm{d}u_1 \mid \boldsymbol{Y}(0) = \boldsymbol{y}_0)F\,\mathrm{d}t, \qquad (5.45)
\end{aligned}$$

by the time-homogeneous property of the QBD-RAP. By the convolution theorem for Laplace transforms, (5.45) is equal to

$$\begin{aligned}
&\sum_{\substack{j_1 \in \mathcal{S} \\ \ell_1 \in \{\ell_0+1, \ell_0, \ell_0-1\} \cap \mathcal{K}}} \int_{t=0}^{\infty} e^{-\lambda t} \mathbb{P}(\boldsymbol{Y}(t) \in (\ell, \mathcal{D}_{\ell,j}, j), t \in \mathcal{T}_{n-1} \mid \boldsymbol{Y}(0) = (\ell_1, \boldsymbol{\alpha}, j_1))\,\mathrm{d}t \\
&\quad \int_{u_1=0}^{\infty} e^{-\lambda u_1} \mathbb{P}(\boldsymbol{Y}_{\boldsymbol{\alpha}}(1) = (\ell_1, j_1), \tau_1 \in \mathrm{d}u_1 \mid \boldsymbol{Y}(0) = \boldsymbol{y}_0)F \\
&= \sum_{\substack{j_1 \in \mathcal{S} \\ \ell_1 \in \{\ell_0+1, \ell_0, \ell_0-1\} \cap \mathcal{K}}} \int_{t=0}^{\infty} e^{-\lambda t} \mathbb{P}(\boldsymbol{Y}(t) \in (\ell, \mathcal{D}_{\ell,j}, j), t \in \mathcal{T}_{n-1} \mid \boldsymbol{Y}(0) = (\ell_1, \boldsymbol{\alpha}, j_1))\,\mathrm{d}t \\
&\quad \mathbb{P}(\boldsymbol{Y}_{\boldsymbol{\alpha}}(1) = (\ell_1, j_1), \tau_1 \leq E^{\lambda} \mid \boldsymbol{Y}(0) = \boldsymbol{y}_0)F. \qquad (5.46)
\end{aligned}$$

The expression

$$\begin{aligned}
&\int_{t=0}^{\infty} e^{-\lambda t} \mathbb{P}(\boldsymbol{Y}(t) \in (\ell, \mathcal{D}_{\ell,j}, j), t \in \mathcal{T}_n \mid \boldsymbol{Y}(0) = (\ell_1, \boldsymbol{\alpha}, j_1))\,\mathrm{d}t \\
&\leq \int_{t=0}^{\infty} e^{-\lambda t} \mathbb{P}(\tau_n \leq t \mid \boldsymbol{Y}(0) = (\ell_1, \boldsymbol{\alpha}, j_1))\,\mathrm{d}t \\
&\leq b^{n-1} \int_{t=0}^{\infty} e^{-\lambda t}\,\mathrm{d}t \\
&= b^{n-1} \frac{1}{\lambda}, \qquad (5.47)
\end{aligned}$$

by Lemma 5.8.

Using the bound (5.47) in (5.46) gives

$$\sum_{j_1 \in \mathcal{S}} \sum_{\ell_1 \in \{\ell_0+1, \ell_0-1\} \cap \mathcal{K}} b^{n-1} \frac{1}{\lambda} \mathbb{P}(\boldsymbol{Y}_{\boldsymbol{\alpha}}(1) = (\ell_1, j_1), \tau_1 \leq E^{\lambda} \mid \boldsymbol{Y}(0) = \boldsymbol{y}_0)F \leq b^{n-1} \frac{1}{\lambda} F, \quad (5.48)$$

by the law of total probability. This concludes the proof. □

5.2.4 Global convergence

Finally, we combine the convergence result of Lemma 5.6 and the domination condition from Corollary 5.9 via the Dominated Convergence Theorem to claim convergence of the

Laplace transform of the QBD-RAP given by

$$\int_{t=0}^{\infty} e^{-\lambda t} \int_{x\in\mathcal{D}_{\ell,j}} \mathbb{P}(\boldsymbol{Y}^{(p)}(t) = (\ell,\, \mathrm{d}x, j) \mid \boldsymbol{Y}^{(p)}(0) = \boldsymbol{y}_0^{(p)})\psi(x)\,\mathrm{d}t. \tag{5.49}$$

Partitioning (5.49) on the number of orbit restart epochs by time t gives

$$\begin{aligned}
&\int_{t=0}^{\infty} e^{-\lambda t} \int_{x\in\mathcal{D}_{\ell,j}} \sum_{n=0}^{\infty} \mathbb{P}(\boldsymbol{Y}^{(p)}(t) \in (\ell,\, \mathrm{d}x, j), t \in \mathcal{T}_n^{(p)} \mid \boldsymbol{Y}^{(p)}(0) = \boldsymbol{y}_0^{(p)})\,\mathrm{d}t\psi(x) \\
&= \sum_{n=0}^{\infty} \int_{t=0}^{\infty} e^{-\lambda t} \int_{x\in\mathcal{D}_{\ell,j}} \mathbb{P}(\boldsymbol{Y}^{(p)}(t) \in (\ell,\, \mathrm{d}x, j), t \in \mathcal{T}_n^{(p)} \mid \boldsymbol{Y}^{(p)}(0) = \boldsymbol{y}_0^{(p)})\,\mathrm{d}t\psi(x).
\end{aligned} \tag{5.50}$$

We can justify the swap of the sum and integrals since

$$\begin{aligned}
&\int_{t=0}^{\infty} e^{-\lambda t} \int_{x\in\mathcal{D}_{\ell,j}} \sum_{n=0}^{\infty} \mathbb{P}(\boldsymbol{Y}^{(p)}(t) \in (\ell,\, \mathrm{d}x, j), t \in \mathcal{T}_n^{(p)} \mid \boldsymbol{Y}^{(p)}(0) = \boldsymbol{y}_0^{(p)})\,\mathrm{d}t|\psi(x)| \\
&\leq \int_{t=0}^{\infty} e^{-\lambda t} \int_{x\in\mathcal{D}_{\ell,j}} \sum_{n=0}^{\infty} \mathbb{P}(\boldsymbol{Y}^{(p)}(t) \in (\ell,\, \mathrm{d}x, j), t \in \mathcal{T}_n^{(p)} \mid \boldsymbol{Y}^{(p)}(0) = \boldsymbol{y}_0^{(p)})\,\mathrm{d}tF \\
&\leq \int_{t=0}^{\infty} e^{-\lambda t}\,\mathrm{d}tF \\
&\leq \frac{1}{\lambda}F < \infty
\end{aligned}$$

so the Fubini-Tonelli Theorem applies.

By Lemma (5.6), each term in the sum (5.50) converges. Furthermore, for $n \geq 1$, each term is dominated by $\left(b^{(p)}\right)^{n-1} F/\lambda$, from Corollary 5.9. The dominating terms $\left(b^{(p)}\right)^{n-1} F/\lambda$ depend on p and may not be summable. However, for p sufficiently large, there exists a $p_0 < \infty$ and a B with $B < 1$ such that $b^{(p)} < B$ for all $p > p_0$. Hence we can apply the Dominated Convergence Theorem to (5.50) and claim that

$$\begin{aligned}
&\lim_{p\to\infty} \sum_{n=0}^{\infty} \int_{x\in\mathcal{D}_{\ell,j}} \int_{t=0}^{\infty} e^{-\lambda t} \mathbb{P}(\boldsymbol{Y}^{(p)}(t) \in (\ell,\, \mathrm{d}x, j), t \in \mathcal{T}_n^{(p)} \mid \boldsymbol{Y}^{(p)}(0) = \boldsymbol{y}_0^{(p)})\,\mathrm{d}t\psi(x) \\
&= \sum_{n=0}^{\infty} \int_{t=0}^{\infty} e^{-\lambda t} \int_{x\in\mathcal{D}_{\ell,j}} \mathbb{P}(\boldsymbol{X}(t) \in (\,\mathrm{d}x, j), t \in \mathcal{T}_n^{X} \mid \boldsymbol{X}(0) = (x_0, i))\psi(x)\,\mathrm{d}t.
\end{aligned} \tag{5.51}$$

where we have used Lemma 5.6. Swapping the sum and integrals and by the law of total probability, then (5.51) is equal to

$$\int_{t=0}^{\infty} e^{-\lambda t} \int_{x\in\mathcal{D}_{\ell,j}} \sum_{n=0}^{\infty} \mathbb{P}(\boldsymbol{X}(t) \in (\,\mathrm{d}x, j), t \in \mathcal{T}_n^{X} \mid \boldsymbol{X}(0) = (x_0, i))\psi(x)\,\mathrm{d}t$$

$$= \int_{t=0}^{\infty} e^{-\lambda t} \int_{x \in \mathcal{D}_{\ell,j}} \mathbb{P}(\boldsymbol{X}(t) \in (\,\mathrm{d}x, j) \mid \boldsymbol{X}(0) = (x_0, i))\psi(x)\,\mathrm{d}t.$$

The swap of the sum and integrals is justfied as

$$\begin{aligned}
&\int_{t=0}^{\infty} e^{-\lambda t} \int_{x \in \mathcal{D}_{\ell,j}} \sum_{n=0}^{\infty} \mathbb{P}(\boldsymbol{X}(t) \in (\,\mathrm{d}x, j), t \in \mathcal{T}_n^X \mid \boldsymbol{X}(0) = (x_0, i))|\psi(x)|\,\mathrm{d}t \\
&\leq \int_{t=0}^{\infty} e^{-\lambda t} \int_{x \in \mathcal{D}_{\ell,j}} \sum_{n=0}^{\infty} \mathbb{P}(\boldsymbol{X}(t) \in (\,\mathrm{d}x, j), t \in \mathcal{T}_n^X \mid \boldsymbol{X}(0) = (x_0, i))\,\mathrm{d}tF \\
&\leq \int_{t=0}^{\infty} e^{-\lambda t}\,\mathrm{d}tF \\
&= \frac{1}{\lambda}F < \infty
\end{aligned} \tag{5.52}$$

so the Fubini-Tonelli Theorem applies.

Thus, we have shown the following result.

Lemma 5.10. *For all $\ell_0, \ell \in \mathcal{K}$, $i, j \in \mathcal{S}$, $x_0 \in \mathcal{D}_{\ell_0,i}$, as $p \to \infty$,*

$$\begin{aligned}
&\int_{t=0}^{\infty} e^{-\lambda t} \int_{x \in \mathcal{D}_{\ell,j}} \mathbb{P}(\boldsymbol{Y}^{(p)}(t) = (\ell,\, \mathrm{d}x, j) \mid \boldsymbol{Y}^{(p)}(0) = \boldsymbol{y}_0^{(p)})\psi(x)\,\mathrm{d}t \\
&\to \int_{t=0}^{\infty} e^{-\lambda t} \int_{x \in \mathcal{D}_{\ell,j}} \mathbb{P}(\boldsymbol{X}(t) \in (\,\mathrm{d}x, j) \mid \boldsymbol{X}(0) = (x_0, i))\psi(x)\,\mathrm{d}t.
\end{aligned}$$

Lemma 5.10 establishes a convergence for a given interval $\mathcal{D}_\ell$, $\ell \in \mathcal{K}$, and phase $j \in \mathcal{S}$. We now formally extend this to a global result. To do so, we find it convenient to re-write the problem in terms of expectations.

Let $\mathcal{R}(L(t), \boldsymbol{A}(t), \varphi(t))$ be the random variable with density function $\boldsymbol{A}(t)\boldsymbol{v}_{L(t),\varphi(t)}(x)$, $x \in \mathcal{D}_{L(t),\varphi(t)}$, then

$$\begin{aligned}
&\int_{t=0}^{\infty} e^{-\lambda t} \mathbb{E}\left[\psi(\mathcal{R}(L(t), \boldsymbol{A}(t), \varphi(t)), \varphi(t)) \mid \boldsymbol{Y}(0) = \boldsymbol{y}_0\right] \mathrm{d}t \\
&= \int_{t=0}^{\infty} e^{-\lambda t} \int_{\boldsymbol{a} \in \mathcal{A}} \sum_{\substack{\ell \in \mathcal{K} \\ j \in \mathcal{S}}} \int_{x \in \mathcal{D}_{\ell,j}} \mathbb{P}(\boldsymbol{Y}(t) \in (\ell,\, \mathrm{d}\boldsymbol{a}, j) \mid \boldsymbol{Y}(0) = \boldsymbol{y}_0)\boldsymbol{a}\boldsymbol{v}_{\ell,j}(x)\psi(x)\,\mathrm{d}x\,\mathrm{d}t \\
&= \int_{t=0}^{\infty} e^{-\lambda t} \sum_{\substack{\ell \in \mathcal{K} \\ j \in \mathcal{S}}} \int_{x \in \mathcal{D}_{\ell,j}} \mathbb{P}(\boldsymbol{Y}(t) \in (\ell,\, \mathrm{d}x, j) \mid \boldsymbol{Y}(0) = \boldsymbol{y}_0)\psi(x)\,\mathrm{d}t,
\end{aligned} \tag{5.53}$$

and the terms in the last line are those in Lemma 5.10.

Corollary 5.11. *Let $\psi : \mathbb{R} \times \mathcal{S} \to \mathbb{R}$ be an arbitrary, bounded function with $|\psi(\cdot)| \leq F$. For each $i \in \mathcal{S}$, $\ell_0 \in \mathcal{K}$, $x_0 \in \mathcal{D}_{\ell_0,i}$,*

$$\int_{t=0}^{\infty} e^{-\lambda t} \mathbb{E}\left[\psi(\mathcal{R}(L^{(p)}(t), \boldsymbol{A}^{(p)}(t), \varphi(t)), \varphi(t)) \mid \boldsymbol{Y}^{(p)}(0) = \boldsymbol{y}_0^{(p)}\right] \mathrm{d}t$$
$$\to \int_{t=0}^{\infty} e^{-\lambda t} \mathbb{E}\left[\psi(\boldsymbol{X}(t)) \mid \boldsymbol{X}(0) = (x_0, i)\right] \mathrm{d}t.$$

Proof. Consider the left-hand side

$$\begin{aligned}
&\int_{t=0}^{\infty} e^{-\lambda t} \mathbb{E}\left[\psi(\mathcal{R}(L^{(p)}(t), \boldsymbol{A}^{(p)}(t), \varphi(t)), \varphi(t)) \mid \boldsymbol{Y}^{(p)}(0) = \boldsymbol{y}_0^{(p)}\right] \mathrm{d}t \\
&= \int_{t=0}^{\infty} e^{-\lambda t} \sum_{\ell \in \mathcal{K}} \sum_{j \in \mathcal{S}} \mathbb{E}\left[\psi(\mathcal{R}(\ell, \boldsymbol{A}^{(p)}(t), j), j) 1(L^{(p)}(t) = \ell, \varphi(t) = j)) \mid \boldsymbol{Y}^{(p)}(0) = \boldsymbol{y}_0^{(p)}\right] \mathrm{d}t \\
&= \sum_{\ell \in \mathcal{K}} \sum_{j \in \mathcal{S}} \int_{t=0}^{\infty} e^{-\lambda t} \mathbb{E}\left[\psi(\mathcal{R}(\ell, \boldsymbol{A}^{(p)}(t), j), j) 1(L^{(p)}(t) = \ell, \varphi(t) = j)) \mid \boldsymbol{Y}^{(p)}(0) = \boldsymbol{y}_0^{(p)}\right] \mathrm{d}t,
\end{aligned} \tag{5.54}$$

where the swap of the summations and integrals is on the last line justified since ψ is bounded and by the Fubini-Tonelli Theorem. By Lemma 5.10, for each $\ell \in \mathcal{K}$, $j \in \mathcal{S}$, the terms

$$\int_{t=0}^{\infty} e^{-\lambda t} \mathbb{E}\left[\psi(\mathcal{R}(\ell, \boldsymbol{A}^{(p)}(t), j), j) \, \mathrm{d}x 1(L^{(p)}(t) = \ell, \varphi(t) = j)) \mid \boldsymbol{Y}^{(p)}(0) = \boldsymbol{y}_0^{(p)}\right] \mathrm{d}t$$

converge to

$$\int_{t=0}^{\infty} e^{-\lambda t} \mathbb{E}\left[\psi(\boldsymbol{X}(t)) 1(\boldsymbol{X}(t) \in (\mathcal{D}_{\ell_j}, j)) \mid \boldsymbol{X}(0) = (x_0, i)\right] \mathrm{d}t.$$

If $\mathcal{K}$ is finite, we are done upon taking the limit of (5.54) as $p \to \infty$ and swapping the limit and the sums.

If $\mathcal{K}$ is countably infinite, then for a given $k \in \mathcal{K}$, since ψ is bounded,

$$\begin{aligned}
&\left| \sum_{j \in \mathcal{S}} \int_{t=0}^{\infty} e^{-\lambda t} \mathbb{E}\left[\psi(\mathcal{R}(\ell, \boldsymbol{A}^{(p)}(t), j), \varphi(t)) 1(L^{(p)}(t) = \ell, \varphi(t) = j)) \mid \boldsymbol{Y}^{(p)}(0) = \boldsymbol{y}_0^{(p)}\right] \mathrm{d}t \right| \\
&\leq F \sum_{j \in \mathcal{S}} \int_{t=0}^{\infty} e^{-\lambda t} \mathbb{E}\left[1(L^{(p)}(t) = \ell, \varphi(t) = j)) \mid \boldsymbol{Y}^{(p)}(0) = \boldsymbol{y}_0^{(p)}\right] \mathrm{d}t
\end{aligned}$$

$$\leq F \int_{t=0}^{\infty} e^{-\lambda t} \mathbb{P}(\boldsymbol{Y}^{(p)}(t) \in (\ell, \mathcal{D}_{\ell,j}, j) \mid \boldsymbol{Y}^{(p)}(0) = \boldsymbol{y}_0^{(p)}) \, \mathrm{d}t$$
$$\leq F \mathbb{P}(\tau^{(p)}_{|\ell-\ell_0|} \leq E^{\lambda} \mid \boldsymbol{Y}^{(p)}(0) = \boldsymbol{y}_0^{(p)}), \tag{5.55}$$

since, to be in level ℓ after starting in level ℓ_0, there must be at least $|\ell_0 - \ell|$ orbit restart epochs. By Lemma 5.8 then (5.55) is bounded by $\left(b^{(p)}\right)^{|\ell-\ell_0|-1}$ for $|\ell - \ell_0| \geq 2$ and by 1 otherwise. Now, choose p_0 sufficiently large so that $b^{(p)} < B < 1$ for all $p > p_0$. Therefore, for all $p > p_0$, the terms in (5.54) are dominated by $F \min\{B^{|\ell-\ell_0|-1}, 1\}$. Moreover,

$$\begin{aligned} F \sum_{\ell \in \mathcal{K}} \min\{B^{|\ell-\ell_0|-1}, 1\} &\leq 2 \sum_{n=1}^{\infty} B^{n-1} + 1 \\ &= \frac{2}{1-B} + 1 \\ &< \infty, \end{aligned}$$

hence the dominating terms are summable. Hence, we may apply the Dominated Convergence Theorem to swap the necessary limits and sums, from which the result follows. □

The Extended Continuity Theorem for Laplace transforms (Feller 1957, Chapter XIII, Theorem 2a) can now be used to claim that the QBD-RAP approximation scheme converges weakly (in space and time) to the fluid queue.

Theorem 5.12. *For all $\boldsymbol{y}_0^{(p)} = (\ell, \boldsymbol{a}^{(p)}_{\ell_0,i}(x_0), i)$, $\ell_0 \in \mathcal{K}$, $x_0 \in \mathcal{D}_{\ell_0,i}$, $i \in \mathcal{S}$, and any bounded function $\psi : \mathbb{R} \times \mathcal{S} \to \mathbb{R}$, then*

$$\mathbb{E}\left[\psi(\mathcal{R}(L^{(p)}(t), \boldsymbol{A}^{(p)}(t), \varphi(t)), \varphi(t)) \mid \boldsymbol{Y}^{(p)}(0) = \boldsymbol{y}_0^{(p)}\right] \to \mathbb{E}\left[\psi(\boldsymbol{X}(t)) \mid \boldsymbol{X}(0) = (x_0, i)\right]$$

weakly in t as $p \to \infty$.

Proof. Combine the Extended Continuity Theorem for Laplace transforms (Feller 1957, Chapter XIII, Theorem 2a) with the convergence of Laplace transforms in Corollary 5.11. □

Ideally, we would like to obtain a point-wise convergence result in the variable t. However, to date, this has eluded me. Although

$$\mathbb{E}\left[\psi(\boldsymbol{X}(t)) \mid \boldsymbol{X}(0) = (x_0, i)\right]$$

is a continuous function of t (it is a Feller semigroup), and, for $p < \infty$,

$$\mathbb{E}\left[\psi(\mathcal{R}(L^{(p)}(t), \boldsymbol{A}^{(p)}(t), \varphi(t)), \varphi(t)) \mid \boldsymbol{Y}^{(p)}(0) = \boldsymbol{y}_0^{(p)}\right]$$

is continuous in t, the limit

$$\lim_{p\to\infty} \mathbb{E}\left[\psi(\mathcal{R}(L^{(p)}(t), \boldsymbol{A}^{(p)}(t), \varphi(t)), \varphi(t)) \mid \boldsymbol{Y}^{(p)}(0) = \boldsymbol{y}_0^{(p)}\right]$$

need not be continuous in t. Nonetheless, we can claim that

$$\mathbb{E}\left[\psi(\mathcal{R}(L^{(p)}(t), \boldsymbol{A}^{(p)}(t), \varphi(t)), \varphi(t)) \mid \boldsymbol{Y}^{(p)}(0) = \boldsymbol{y}_0^{(p)}\right] \to \mathbb{E}\left[\psi(\boldsymbol{X}(t)) \mid \boldsymbol{X}(0) = (x_0, i)\right]$$

for almost all $t \geq 0$. At such values of t, since ψ is arbitrary and bounded, then the Portmanteau Theorem (Billingsley 1999, Theorem 2.1) states that the QBD-RAP approximation scheme converges in distribution to the fluid queue.

A sufficient condition to upgrade the convergence from weak to point-wise (in the variable t) is to show that for $t \geq 0$

$$\sup_p \mathbb{E}\left[\psi(\mathcal{R}(L^{(p)}(t), \boldsymbol{A}^{(p)}(t), \varphi(t)), \varphi(t)) \mid \boldsymbol{Y}^{(p)}(0) = \boldsymbol{y}_0^{(p)}\right] \leq M(t) < \infty$$

and the sequence $\mathbb{E}\left[\psi(\mathcal{R}(L^{(p)}(t), \boldsymbol{A}^{(p)}(t), \varphi(t)), \varphi(t)) \mid \boldsymbol{Y}^{(p)}(0) = \boldsymbol{y}_0^{(p)}\right]$ is eventually equicontinuous in t. That is, for every $\varepsilon > 0$ there exists a $\delta(t, \varepsilon) > 0$ and an $p_0(t, \varepsilon)$ such that $|t - u| < \delta(t, \varepsilon)$ implies that

$$\left|\mathbb{E}\left[\psi(\mathcal{R}(L^{(p)}(t), \boldsymbol{A}^{(p)}(t), \varphi(t)), \varphi(t)) \mid \boldsymbol{Y}^{(p)}(0) = \boldsymbol{y}_0^{(p)}\right]\right.$$
$$\left. - \mathbb{E}\left[\psi(\mathcal{R}(L^{(p)}(u), \boldsymbol{A}^{(p)}(u), \varphi(u)), \varphi(u)) \mid \boldsymbol{Y}^{(p)}(0) = \boldsymbol{y}_0^{(p)}\right]\right| < \varepsilon$$

for all $p \geq p_0(t, \varepsilon)$.

5.3 Extension to arbitrary (but fixed) discretisation structures

To conclude this chapter we include some remarks on how to extend the convergence results to arbitrary discretisation structures.

Throughout, we have assumed that all intervals are of width Δ, i.e. $|y_{\ell+1} - y_\ell| = \Delta$, and that on every interval the dynamics of the fluid queue are modelled based on the same matrix exponential representation $(\boldsymbol{\alpha}, \boldsymbol{S}, \boldsymbol{s})$. These assumptions are, in fact, not necessary, but they do serve to simplify the presentation slightly. The convergence results can be extended to use different sequences of matrix exponential representations on each interval, provided that for each sequence of matrix exponential distributions, the variance

tends to 0. Moreover, we can extend the results to intervals of arbitrary width, provided that the width of the intervals is not arbitrarily small. Here we describe how one would prove such results.

The arguments which prove Theorem 4.3 are independent of all other levels/intervals, i.e. the hypotheses of the Theorem depend only on the interval $\mathcal{D}_{\ell_0}$, and the sequence of matrix exponential distributions used to model the behaviour of the fluid queue on this interval, and not on any other interval. Thus, Lemma 4.3 holds independently on each interval, as does Corollary 4.15.

Let the width of an interval $\mathcal{D}_{\ell_0}$ be $\Delta_{\ell_0} = y_{\ell_0+1} - y_{\ell_0}$ and suppose that sequence of matrix exponential random variables used to model the dynamics of the fluid queue on the interval $\mathcal{D}_{\ell_0}$ is $Z_{\ell_0}^{(p)}$. Regarding the domination condition in Lemma 5.7, we can extend it the following version,

Lemma 5.13. *Assume* $\inf_{\ell_0} \Delta_{\ell_0} > 0$ *and* $\sup_{\ell_0} \mathrm{Var}(Z_{\ell_0}) < \infty$. *Then, for all* $i \in \mathcal{S}_+ \cup \mathcal{S}_-$, $\ell_0 \in \mathcal{K} \setminus \{-1, K+1\}$, *and* $n \geq 2$,

$$\mathbb{P}(\tau_n^{(p)} \leq E^\lambda \mid \boldsymbol{Y}_{\boldsymbol{\alpha}}^{(p)}(n-1) = (\ell_0, i), \tau_{n-1}^{(p)} \leq E^\lambda) \leq b_{\ell_0}^{(p)}, \tag{5.56}$$

where

$$b_{\ell_0}^{(p)} = 1 - e^{-q(\Delta_{\ell_0} + \varepsilon_{\ell_0}^{(p)})} \left[1 - e^{q\varepsilon_{\ell_0}^{(p)} - \lambda\Delta_{\ell_0}/|c_{min}|}\right] + \frac{\mathrm{Var}(Z_{\ell_0}^{(p)})}{\left(\varepsilon^{(p)}\right)^2} + |r_{1,\ell_0}^{(p)}|$$

and

$$|r_{1,\ell_0}^{(p)}| \leq 2G \frac{\mathrm{Var}\left(Z_{\ell_0}^{(p)}\right)}{\left(\varepsilon_{\ell_0}^{(p)}\right)^2} + 2L\varepsilon_{\ell_0}^{(p)}.$$

Hence, for all $i \in \mathcal{S}_+ \cup \mathcal{S}_-$, *and* $n \geq 2$,

$$\mathbb{P}(\tau_n^{(p)} \leq E^\lambda \mid \phi^{(p)}(\tau_{n-1}^{(p)}) = i, \tau_{n-1}^{(p)} \leq E^\lambda) \leq b^{(p)}, \tag{5.57}$$

where

$$b^{(p)} = \max\left\{\sup_{\ell_0} b_{\ell_0}^{(p)}, \frac{q}{\lambda + q}\right\}.$$

Proof. For the proof of (5.56) follow the same arguments as in the proof of Lemma 5.7. The bound in (5.57) follows by the assumptions in the statement of the result, since

$$\begin{aligned}
&\mathbb{P}(\tau_n^{(p)} \leq E^\lambda \mid \phi^{(p)}(\tau_{n-1}^{(p)}) = i, \tau_{n-1}^{(p)} \leq E^\lambda) \\
&\leq \sup_{\ell_0} \mathbb{P}(\tau_n^{(p)} \leq E^\lambda \mid \boldsymbol{Y}_{\boldsymbol{\alpha}}^{(p)}(n-1) = (\ell_0, i), \tau_{n-1}^{(p)} \leq E^\lambda) \\
&\leq \max\left\{\sup_{\ell_0} b_{\ell_0}^{(p)}, \frac{q}{\lambda + q}\right\}.
\end{aligned}$$

□

Given Lemma 5.13, then an equivalent of Lemma 5.8 remains true, the proof of which follows verbatim except with the use of Lemma 5.7 replaced by Lemma 5.13. Corollary 5.9 remains true without modification. Lemma 5.10 and Corollary 5.11 remain true without modification provided that $\lim_{p\to\infty} \mathrm{Var}(Z_\ell^{(p)}) \to 0$ for all ℓ.

Remark 5.14. *I suspect that the convergence results can also be extended to approximating so-called* multi-layer fluid queues*, as described in Bean & O'Reilly (2008).*

Chapter 6

Numerical investigations

We have now established multiple methods for approximating fluid queues which are suitable for approximating the performance measures for fluid-fluid queues derived in Bean & O'Reilly (2014). In this chapter we numerically investigate various aspects of the approximation schemes. Throughout, we compare the QBD-RAP scheme (from Chapter 3), the discontinuous Galerkin method (as described in Chapter 2), and the spatially-coherent uniformisation as described in Bean & O'Reilly (2013), which we will refer to a just the *uniformisation scheme*. Recall that, due to their stochastic interpretation, the uniformisation and QBD-RAP schemes are positivity preserving.

Where possible, we implement the discontinuous Galerkin method with and without a slope-limiter implemented (Cockburn 1999), (Hesthaven & Warburton 2007, Section 5.6.2) (see also Section 2.4). The slope limiter avoids oscillations and negative solutions. However, we note that in the context of approximating the operator Ψ for a fluid-fluid queue, it is not obvious how one might apply the concept of slope-limiting, other than to post-process the solution with a limiter or filter. Even when slope limiting is possible, the resultant approximation is at best linear around discontinuities. Moreover, there is a computational cost in applying a limiter. However, high-order accuracy of the DG scheme is maintained away from the discontinuities (Cockburn 1999), (Hesthaven & Warburton 2007, Section 5.6.2).

The main focus of our numerical experiments is on the convergence properties as the number of basis functions is increased. For simplicity, the number of basis functions is kept constant across all cells. We refer to the number of basis functions on a cell as the *dimension*. For discontinuous Galerkin method, increasing the dimension of the scheme means increasing the number of polynomial basis functions used to approximate the solution within each cell. E.g. if we use 3 basis functions in the discontinuous Galerkin method, we approximate the solution by a quadratic on each cell. For the QBD-RAP scheme, increasing the dimension of the scheme means increasing the order of the CME distribution used to construct the scheme. To make a comparable equivalent for the uniformisation scheme with a fixed cell size we divide each cell into smaller sub-cells over

which we approximate the solution. I.e. for a dimension p uniformisation scheme we divide each cell into p sub-cells. Equivalently, we may think of a dimension p uniformisation scheme as using p piecewise constant functions to approximate the solution on each cell. For all schemes (DG, QBD-RAP and uniformisation), if we construct and order p approximation, there are K cells, and N phases then the resulting approximation to the generator $\mathbb{B}$ is a matrix of dimension pKN. In this sense each approximation scheme leads to matrices of the same size (although not necessarily the same number of non-zero elements).

To keep the content of this chapter contained, we do not investigate all aspects of the schemes. For each numerical experiment we keep the cell size fixed for the DG and QBD-RAP schemes. As part of deriving a discontinuous Galerkin scheme, one needs to choose the *numerical flux* which is used to approximate the transition of density from one cell to the next (Hesthaven & Warburton 2007). We investigate schemes with an upwind flux only. For schemes which require us to integrate over time we do not investigate the stability of the schemes with respect to the t-step-size of the time-integration or time-integration scheme itself (where required). Instead, we fix the time-integration step size for each numerical experiment at a suitably small value to obey a certain stability criterion (a CFL-like condition, (Hesthaven & Warburton 2007, Section 4.8)). Moreover, we always implement the strong stability preserving Runge-Kutta method of order 4 with 5 stages (Spiteri & Ruuth 2002), (Hesthaven & Warburton 2007, Section 5.7) (see also Appendix A.1), which claims to introduce no more oscillations into the solution as we integrate over time. Where a slope limiter is implemented, we implement the *Generalised MUSCL* limiter (Cockburn 1999), (Hesthaven & Warburton 2007, Section 5.6.2) (see also Section 2.4). We do not investigate filtering for the DG scheme (see (Hesthaven & Warburton 2007, Section 5.6.1) and references therein).

The performance of the discontinuous Galerkin method has been well-studied in some contexts Cockburn (1999), (Hesthaven & Warburton 2007, Section 5.5), and it is well-known that the discontinuous Galerkin method performs remarkably well on problems with smooth solutions. Here, we mostly focus on investigating the numerical performance of the methods on problems with non-smooth solutions, the purpose of this is to emphasise the positivity-preserving properties of the QBD-RAP method. In the stochastic modelling community it is very common to have problems with discontinuities, such as a non-smooth initial conditions. Even if a fluid-queue is initialised with a smooth initial density, the boundary dynamics may induce transient discontinuities or non-smooth behaviour into the problem (see, for example, Section 6.4, below). A very specific set of conditions must hold for the initial density and point masses for the distribution to remain continuous as it evolves over time (Bean & O'Reilly 2014, Bean et al. 2020). Limiting distributions of fluid queues are smooth, however. Further, it is possible that discontinuities are present in the performance measures of fluid-fluid queues (see, for example, Section 6.5).

As we shall see, if the solution is smooth, then the Galerkin method is highly-effective

and displays rapid convergence to the solution as the number of polynomial basis functions is increased. However, when the solution is non-smooth oscillations and negative approximations may occur when using the discontinuous Galerkin method, leading to nonsense solutions. In these cases, the QBD-RAP approximation performs relatively well compared to the other positivity preserving schemes investigated.

The structure of this chapter is as follows. In Section 6.1 we compute approximations to various initial conditions for the different methods and observe their performance at approximating the initial condition, which allows us to instrument the performance of the reconstruction methods without considering a specific model or any dynamics of the problem. In Section 6.2 we investigate a simple travelling wave problem with various initial conditions. For this problem the dynamics are deterministic, which allows us to instrument the ability of the schemes to approximate the flow of probability across cells without any stochastic dynamics. Next, we investigate a simple fluid queue with two phases. Section 6.3 investigates the ability of the methods to approximate the stationary distribution of the model, Section 6.4 investigates the ability of the schemes to approximate the transient distribution of the fluid queue for two initial conditions, and Section 6.5 investigates the ability of the methods to approximate the first hitting time of the fluid level on the boundary of the interval $[0, 1]$. Section 6.6 approximates the distribution of $\{(X(t), \varphi(t))\}$ at the time at which $\{Y(t)\}$ first returns to 0 for two simple fluid-fluid queue models.

6.1 Function approximation/reconstruction

We start our investigation by looking at how well the methods perform at approximating an initial condition. By approximating the initial condition only, we aim to instrument the performance of the approximation schemes without any dynamics.

For the discontinuous Galerkin method, this we project the initial condition on to the set of polynomial functions which define the scheme, for the spatially-coherent uniformisation scheme, we look at the sub-cell averages of the initial condition, and for the QBD-RAP scheme, we compute the initial vector for the approximation, then reconstructing the solutions as described in Sections 3.6 and 3.7. For the purposes of approximation and reconstruction for the QBD-RAP scheme we must orientate the initial condition in a positive or negative direction; here, we suppose that the initial conditions belong to a positive phase. First we investigate three closing vectors we can use for the reconstruction for the QBD-RAP, from which we find that the closing operator in (3.27). From the investigation, we decide to use the closing vector (3.27) throughout the rest of the chapter.

For this investigation we consider approximating initial conditions over a single cell of width $\Delta = 1$. To numerically evaluate integrals arising in the approximation step (inner products and cell averages) we use a trapezoidal rule with 10,001 function evaluations.

Similarly, we use 10,001 function evaluations to approximate L^p norms, and also as a finite set of points over which to compute the KS statistics.

6.1.1 QBD-RAP closing operators

The three closing operators we investigate are the following. The unnormalised closing vector in Equation (3.25). A normalised version of the closing operator in Equation (3.26), with the normalised version given by (3.29). We refer to the closing vector in (3.29) as the *naive normalised* closing vector. Technically we have not yet proved that the *naive normalised* closing vector leads to a convergent approximation scheme, though it clearly appears to converge. The third closing vector we investigate is that in Equation (3.27) and we refer to this as the *normalised closing operator*.

Example 6.1. First consider approximating the initial condition with density function $2 \times 1(x < 0.5)$. In the left-hand side of Figure 6.1 we plot the Kolmogorov-Smirnov error between the true CDF and the CDF constructed via the QBD-RAP approximation with the three different closing vectors. Interestingly, in this case, the unnormalised error outperforms the other two reconstructions at low orders. It just so happens that, in this case, the error due to truncation of the unnormalised reconstruction destructively interferes with other errors to cause the error to be lower at low orders for the unnormalised scheme. Figure 6.1 also shows that the naive normalised and normalised reconstructions perform very similarly – this is the case throughout much of this subsection. The difference between the naive normalised and normalised reconstructions is how they treat mass in the tail of a matrix exponential distribution (from 2Δ onward). Intuitively, there should be very little mass in the tail of the distribution as we are using concentrated matrix exponential distributions in the reconstruction.

If we instead look at the L^2 error between the true PDF and the reconstructions in Figure 6.1, then we see that the unnormalised reconstruction performs the poorest. Figure 6.1 also suggests the naive normalised and normalised reconstruction are very similar.

Example 6.2. Now consider approximating the initial density $f(x) = 1$. Observing Figure 6.2 of the KS error and L^2 error of the PDF we now see that the normalised reconstructions outperform the unnormalised reconstruction. This suggests that, in this case, the 'folding' of closing operator about Δ has greatly increased the ability of the reconstruction to approximate this initial distribution.

Some insight is gained by looking at Figure 6.3 where we plot the reconstructed PDFs for the unnormalised and normalised closing operators for dimension 1, 3, 5 and 7, as well as the true PDF. Observing Figure 6.3 notice that the unnormalised reconstruction fails to capture the density at the left of each of the plots. This feature is due to a significant amount of mass being lost due to the truncation. In comparison, the reconstruction with the normalised closing operator is much better in this region due to the 'folding'

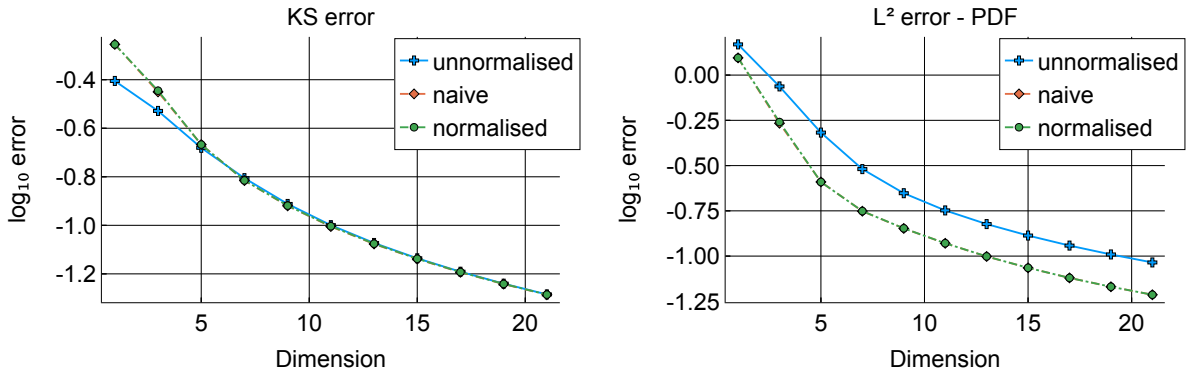

Figure 6.1: KS error between the true CDF, $2x1(x < 0.5) + 1(x \geq 0.5)$, and the approximations (left) and L^2 error between the true PDF, $2 \times 1(x < 0.5)$, and the approximations (right) for the three closing vectors considered; unnormalised (blue solid line with crosses), naive normalised (orange dashed line with diamonds) and normalised (green dash-dotted line with circles). The naive normalised (orange) an normalised closing vectors are coincident.

around Δ in the construction of the closing operator. The 'folding' in the normalised closing operator manifest itself as more mass at the left of these plots compared to the unnormalised reconstructions.

Figure 6.3 also show that both closing operators do not approximate the initial condition well at the right-hand side of the interval. Perhaps there is a different reconstruction method or yet another closing operator which could alleviate this issue.

Example 6.3. Next we consider approximating the initial distribution with density $-6x^2 + 6x$. Observing the left-hand panel of Figure 6.4, which plots the KS error against the dimension of the reconstruction for the three closing operators, we once again see that the reconstruction using the unnormalised closing operator performs the worst, while the performance of the two normalised reconstructions is indistinguishable. However, if we instead look at the right-hand panel of Figure 6.4, which plots the L^2 error between the reconstructed PDF and the true PDF, then the unnormalised closing operator performs better than the two normalised ones for dimension 5 and above.

The fact that the unnormalised closing operator outperforms the two normalised ones can be explained by the 'folding' of the normalised operators around Δ. In Figure 6.5 we plot the unnormalised and normalised reconstructions along with the true PDF, $-6x^2+6x$. In Figure 6.5 at the left of the plots, we observe that the normalised reconstructions overestimate the density function, whereas the unnormalised reconstruction looks to be doing better. The 'folding' in the normalised closing operator manifest itself as more mass at the left of these plots compared to the unnormalised reconstructions.

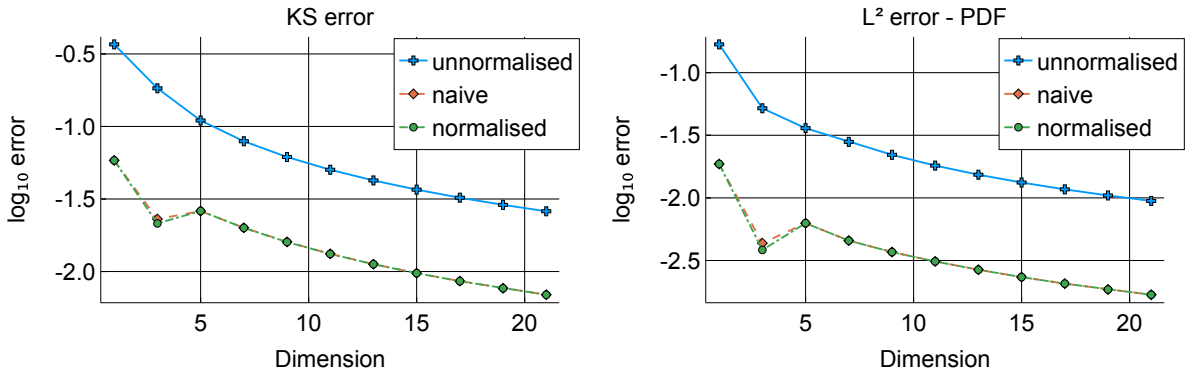

Figure 6.2: KS error between the true CDF, x, and the approximation (left) and L^2 error between the true PDF and the approximation (right) for the three closing vectors considered; unnormalised (blue solid line with crosses), naive normalised (orange dashed line with diamonds) and normalised (green dash-dotted line with circles). The naive normalised (orange) an normalised closing vectors are coincident.

Example 6.4. Lastly, we consider approximating the initial distribution with PDF $3e^{-3x}/(1-e^{-3})$. This density function is at a maximum at the left of the region. Considering what we have learnt so far about the unnormalised operator underestimating in this region, we expect that the unnormalised closing operator will perform relatively poorly in this case. Indeed, observing Figures 6.6 we see that this is the case; the normalised reconstructions perform relatively well compared to the unnormalised reconstruction, as measured by both error metrics (KS statistic and L^2 norm on the PDF). If we observed plots of the PDFs (omitted), we would once again see that this is due to the loss of mass at the left-hand side of the region due to the truncation.

Given the evidence above we choose to use the normalised closing operator to reconstruct solutions. Further, unlike the naive normalised operator, the normalised operator is theoretically justified in that we proved the closing operator leads to a convergent scheme and is linear.

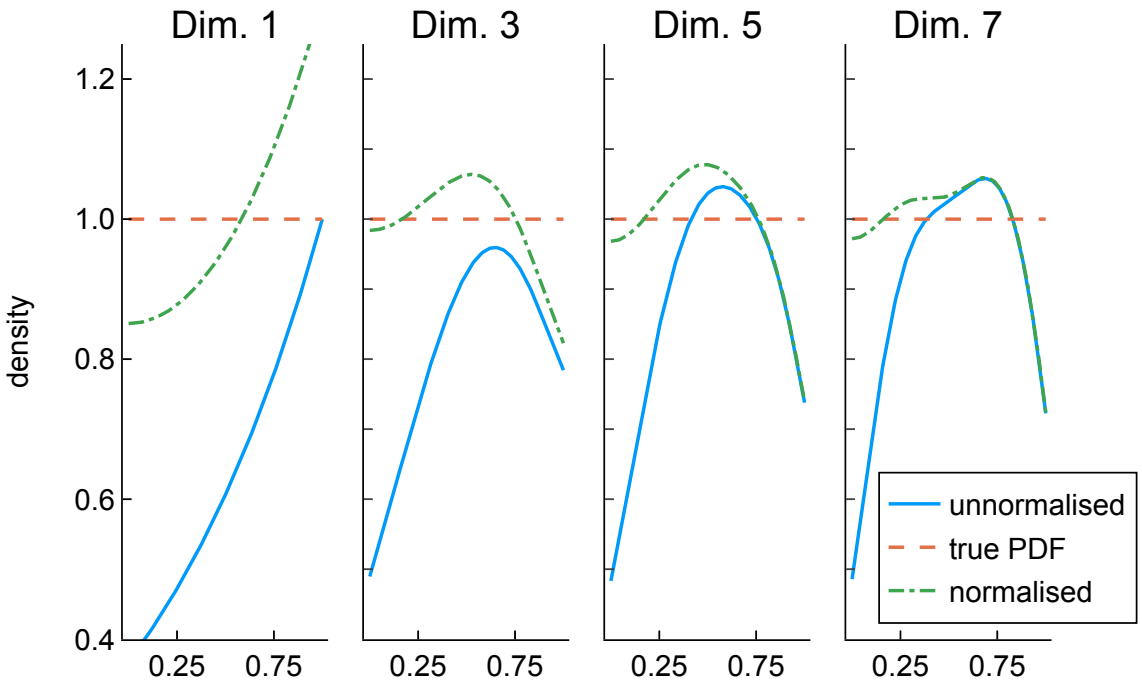

Figure 6.3: Reconstructed PDFs using the unnormalised closing operator (blue solid line), normalised closing operator (green dash-dotted line), for various dimensions, and the true PDF which is $f(x) = 1$ (orange dashed line).

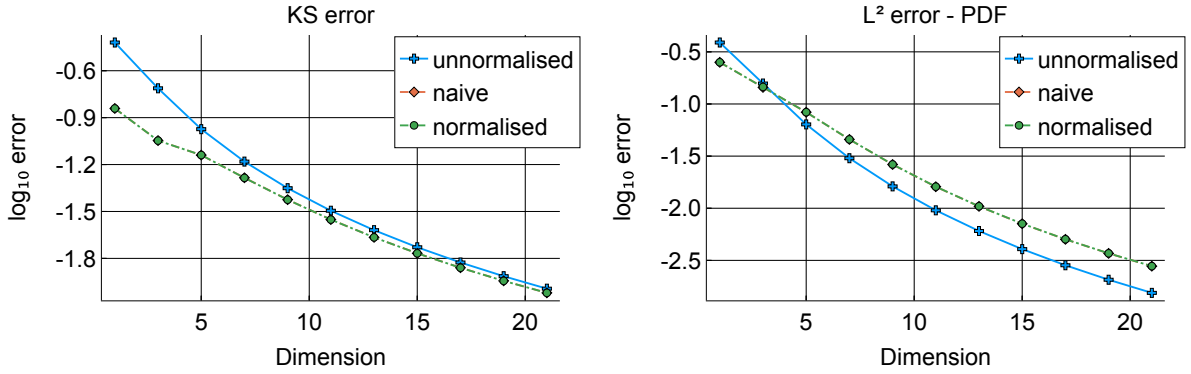

Figure 6.4: KS error between the true CDF, $-2x^3+3x^2$, and the approximation (left) and L^2 error between the true PDF $-6x^2+6x$ and the approximation (right), for the three closing vectors considered; unnormalised (blue solid line with crosses), naive normalised (orange dashed line with diamonds) and normalised (green dash-dotted line with circles). The naive normalised (orange) an normalised closing vectors are coincident.

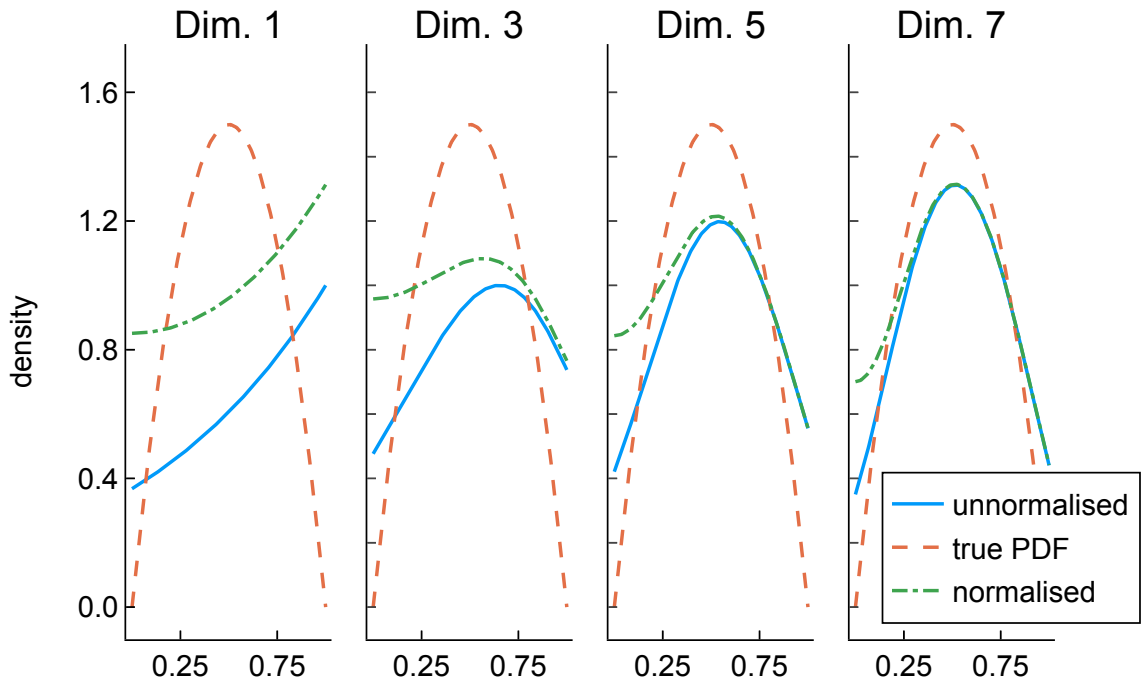

Figure 6.5: Reconstructed PDFs using the unnormalised closing operator (blue solid line), normalised closing operator (green dash-dotted line), for various orders, and the true PDF which is $f(x) = -6x^2 + 6x$ (orange dashed line).

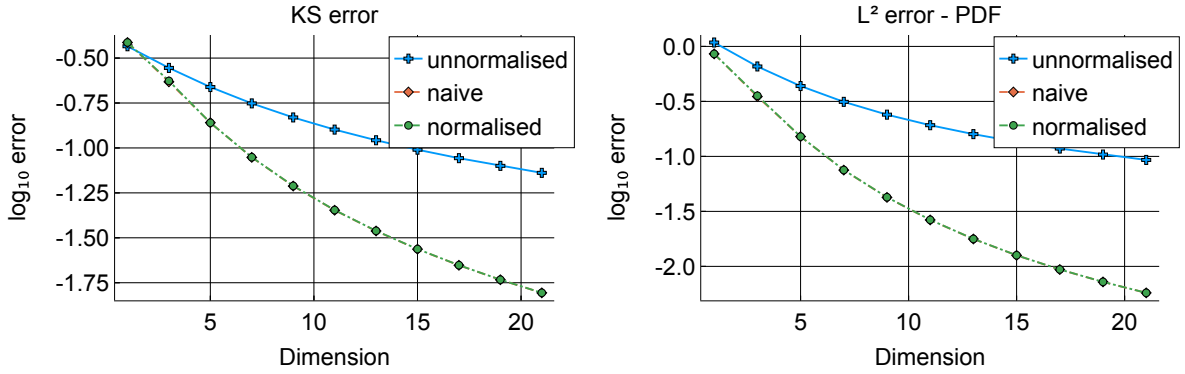

Figure 6.6: KS error between the true CDF, $(1 - e^{-3x})/(1 - e^{-3})$, and the approximation (left) and L^2 error between the true PDF and the approximation for the three closing vectors considered; unnormalised (blue solid line with crosses), naive normalised (orange dashed line with diamonds) and normalised (green dash-dotted line with circles). The naive normalised (orange) and normalised closing vectors are coincident.

6.1.2 Comparison of methods

Here we compare the ability of the QBD-RAP, uniformisation, and DG methods to reconstruct initial conditions.

Example 6.5. First we consider the initial condition with CDF $1(x \geq 0.5)$, that is, a point mass at 0.5. This distribution does not have a PDF, so we compare the CDFs only. In Figure 6.7 we plot the KS metric (left) and L^1 metric (right) between the true CDF and the reconstructed approximations. Observing the KS metric, it appears that none of the methods converge and the KS error sits around 0.5. This reflects the fact that convergence in distribution implies point-wise convergence of the CDFs except, perhaps, at points of discontinuity. None of the methods appear to converge at the discontinuity at $x = 0.5$. Observing the L^1 error between the true CDF and reconstructed approximation (which is the area between the two CDFs) we now see that the methods appear to show the convergent behaviour we expect. Here, the uniformisation method appears to perform the best, while the QBD-RAP method performs the worst. The rate of convergence of the QBD-RAP method appears to be similar to the rate of convergence of the DG scheme.

Perhaps it is no surprise that the uniformisation method performs best. In the uniformisation method as we increase the order we partition the cell $[0, 1]$ into smaller sub-cells, and use constant functions on each sub-cell to approximate the initial distribution. As such, the uniformisation method can produce a piecewise continuous, linear approximation to the CDF. In contrast, both the DG and QBD-RAP methods result in a smooth approximation to the CDF. Given the initial distribution is far from smooth (it's a point mass), then we might expect that the uniformisation method will perform relatively well.

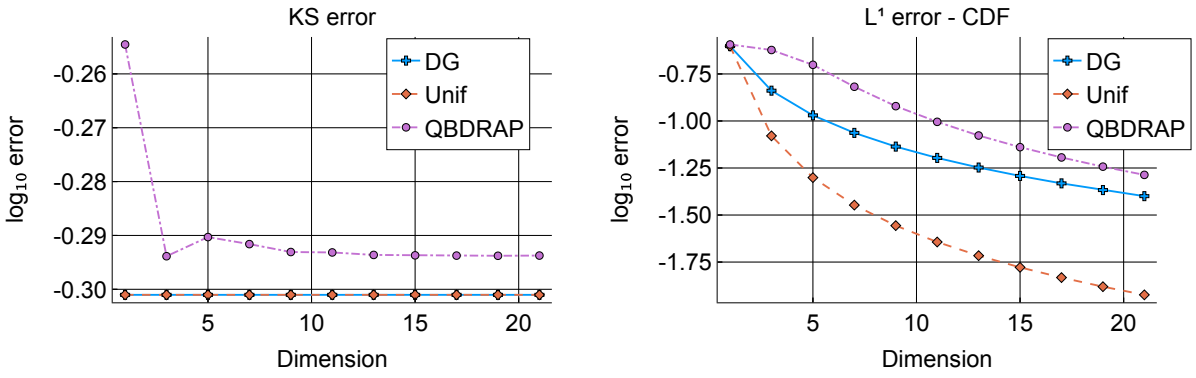

Figure 6.7: KS error between the true CDF, $1(x \geq 0.5)$, and the approximations (left) and L^1 error between the true CDF and the approximations for the DG method (blue solid line with crosses), uniformisation method (orange dashed line with diamonds) and QBD-RAP method (purple dashed line with circles).

In Figure 6.8 we plot approximated CDFs from the DG, uniformisation and QBD-RAP methods alongside the true CDF. The DG method displays undesirable features for an approximation to a CDF – it is not monotonically increasing, at some points it is negative and at some points it is above 1. On the other hand, although the QBD-RAP method converges slowest, it displays good properties in that it results in a monotonically increasing CDF, starting at 0 and ending at 1. The uniformisation scheme approximates the CDF exceptionally well.

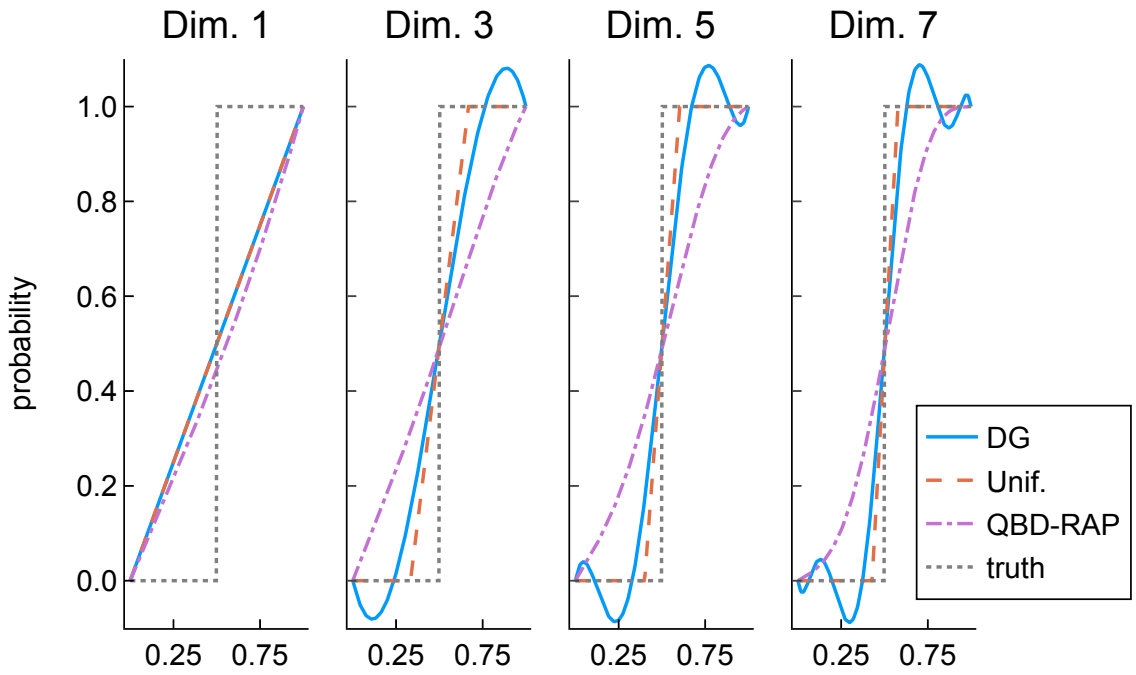

Figure 6.8: Reconstructed CDFs using the DG (blue solid line), uniformisation (orange dashed line) and QBD-RAP (purple dashed line) methods. The true distribution function is $1(x \geq 0.5)$ (grey dotted line).

Example 6.6. Now consider approximating the initial distribution with PDF $1(x \leq 0.5)$. Figure 6.9 plots the KS error (left) and L^2 error between the true and approximate PDFs (right). Figure 6.9 suggests that all methods converge at a similar rate for this problem. Here, the QBD-RAP method performs worst, the uniformisation method second, and the DG method the best. However, once again the DG method exhibits undesirable properties (plots not shown) – the approximation to the CDF is at some points above 1 and is not monotonic (although these violations do not appear to be as severe in this case as they were for the example above).

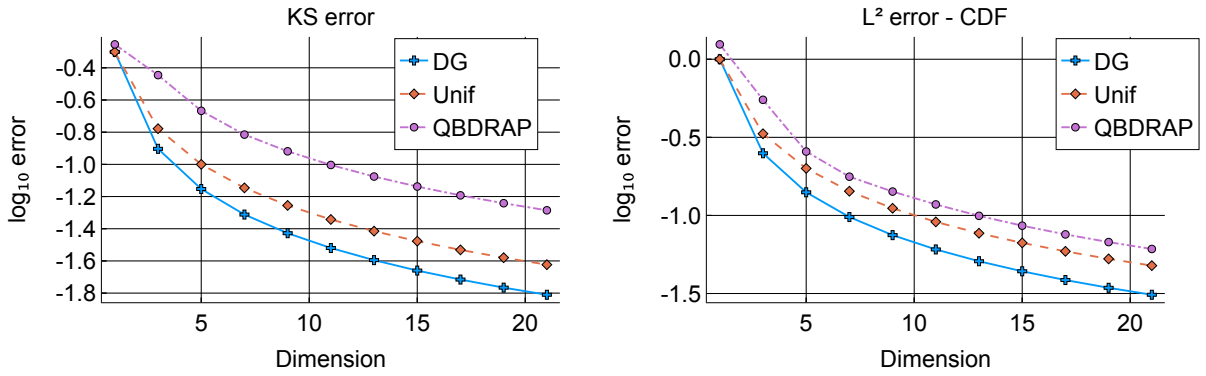

Figure 6.9: KS error between the true CDF and the approximations (left) and L^2 error between the true PDF, $1(x \geq 0.5)$, and the approximations for the DG method (blue solid line with crosses), uniformisation method (orange dashed line with diamonds) and QBD-RAP method (purple dashed line with circles).

Example 6.7. So far we have considered two problems which exhibit discontinuities. At the other extreme we now consider an initial distribution with density $-6x^2 + 6x$. In Figure 6.10 we plot the KS error and the L^2 error between the true and approximated PDFs. Since the DG method projects the initial condition onto a polynomial basis, then, for an order 3 approximation and above, the DG method can approximate the initial condition exactly. This is reflected in Figure 6.10, where the blue curve drops sharply from dimension 1 to 3, then plateaus. Due to numerical integration errors, for example in the evaluation of the integral in the L^2 norm, and due to machine arithmetic, the errors for the DG scheme are not 0. Regarding the other two methods, they too appear to be convergent at approximately the same rate, with the uniformisation method performing better for the KS error, but very similarly in terms of the L^2 error.

Example 6.8. Consider now the initial distribution with PDF $cos(4\pi(x + 0.5)) + 1$. Figure 6.11 shows the errors. Both the KS error (left) and L^2 norm between the true and approximated PDFs (right) tell a similar story; for sufficiently high order, the DG method approximates the initial condition very well. The uniformisation method performs second best, while the QBD-RAP method is slowest to converge.

In conclusion, we have observed that the DG method performs well with respect to the error metrics considered, but can display oscillations and result in CDFs which are not non-decreasing. On the other hand, the uniformisation and QBD-RAP schemes result in non-decreasing approximations to the CDFs, but can converge slower with respect to the error metrics considered, with the QBD-RAP scheme often converging the slowest.

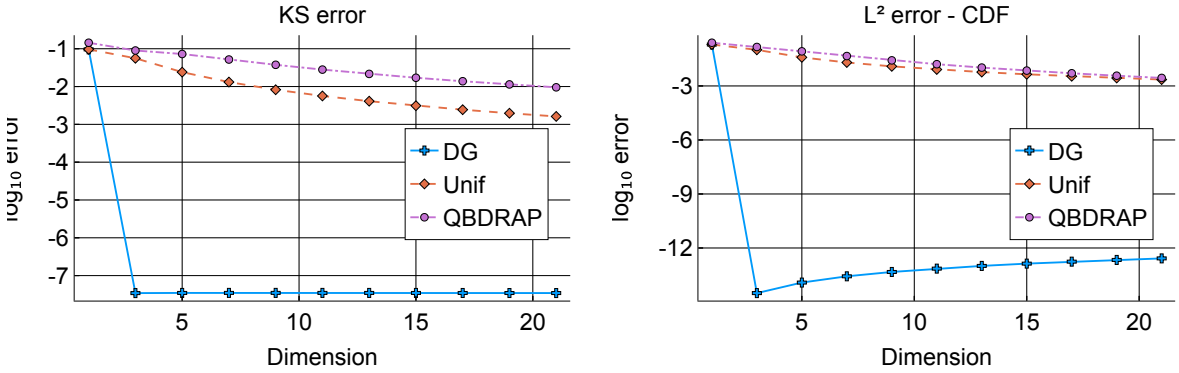

Figure 6.10: KS error between the true CDF and the approximations (left) and L^2 error between the true PDF, $-6z^2 + 6x$, and the approximations for the DG method (blue solid line with crosses), uniformisation method (orange dashed line with diamonds) and QBD-RAP method (purple dashed line with circles).

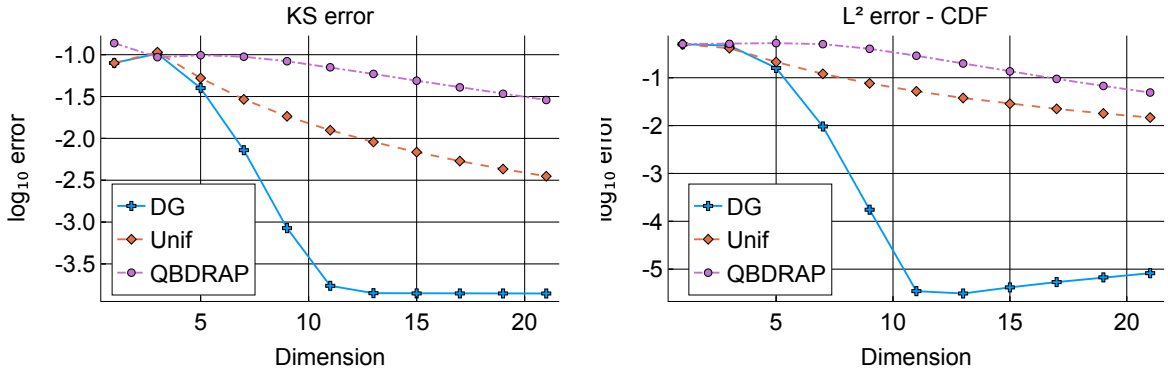

Figure 6.11: KS error between the true CDF and the approximations (left) and L^2 error between the true PDF, $cos(4\pi(x + 0.5)) + 1$, and the approximations for the DG method (blue solid line with crosses), uniformisation method (orange dashed line with diamonds) and QBD-RAP method (purple dashed line with circles).

6.2 Travelling wave

Here we investigate the performance the different schemes for approximating transient distributions of one-dimensional travelling wave problems with various initial conditions. Consider a (trivial) fluid queue with one phase, generator $\boldsymbol{T} = [0]$ and rate $c = 1$. The PDE (if/when it exists) which describes this system is

$$\frac{\partial}{\partial t} f(x,t) = -\frac{\partial}{\partial x} f(x,t),$$

where $f(x,t)$ is the density at time t. Given an initial condition, $f(x,0)$, solutions to this problem are given by

$$f(x,t) = f(x-t,0)$$

so the solution at time t is just a shift in the initial condition t units to the right. We suppose that the fluid queue is bounded, with a lower boundary $x = 0$ and upper boundary $x = 10$. This example is convenient as it has a known solution and no stochastic dynamics, hence we can instrument the ability of the schemes to approximate the flow of mass, without any stochastic dynamics.

We use the QBD-RAP, uniformisation and DG schemes to discretise the solution in space. We discretise the interval $[0, 10]$ into 10 cell, each of width 1. We use $10,001$ points to approximate the integrals which appear in the construction of the initial conditions, to approximate the integrals appearing in the error metrics, and also as a set of discrete points on which evaluate the CDFs to approximate the KS metric. We use the SSPRK4 method to integrate over time with a t-step size of 0.005, and we evolve the system until time $t = 4$.* For the DG method we also implement the Generalised MUSCL slope limiter to stabilise the integration (Cockburn 1999), (Hesthaven & Warburton 2007, Section 5.6.2) (see also Section 2.4).

To investigate the performance of the methods without the need to reconstruct the function within each cell we use the cell-wise error metric obtained by computing

$$\begin{aligned}&\sum_{\ell=1}^{10} |\mathbb{P}(X(4) \in \mathcal{D}_{\ell,1}, \varphi(4) = 1 \mid X(0) = 0.5, \varphi(0) = 1) - p(4,\ell,1)| \\ &+ |\mathbb{P}(X(4) \in \{10\}, \varphi(4) = 1 \mid X(0) = 0.5, \varphi(0) = 1) - p(4,11,1)| \end{aligned} \tag{6.1}$$

where

$$\mathbb{P}(X(4) \in \mathcal{D}_{\ell,1}, \varphi(4) = 1 \mid X(0) = 0.5, \varphi(0) = 1) \tag{6.2}$$

for $\ell = 1, \ldots, K$, and

$$\mathbb{P}(X(4) \in \{10\}, \varphi(4) = 1 \mid X(0) = 0.5, \varphi(0) = 1) \tag{6.3}$$

*The t-step size must be chosen to ensure that numerical integration over time is stable up to dimension 21, adhering to a CFL-like condition (Hesthaven & Warburton 2007, Section 4.8).

is the mass at the boundary and where $p(4, \ell, 1)$ is an approximation to $\mathbb{P}(X(4) \in \mathcal{D}_{\ell,1}, \varphi(4) = 1 \mid X(0) = 0.5, \varphi(0) = 1)$, and $p(4, 11, 1)$ is an approximation to $\mathbb{P}(X(4) \in \{10\}, \varphi(4) = 1 \mid X(0) = 0.5, \varphi(0) = 1)$.

Example 6.9. First consider the initial condition with PDF $1(x < 1)$. The level of the fluid queue is uniformly distributed over the first cell. For the DG and uniformisation methods, the initial condition can be represented exactly, whereas, for the QBD-RAP method, it cannot. Thus, in this case, there is no discretisation error in constructing the initial condition for the DG and uniformisation methods. At time $t = 4$, the solution is $f(x, 4) = 1(x \in [4, 5))$. The projections related to the DG and uniformisation methods can represent this solution exactly too, hence we might expect these methods to work well here.

We plot the cell-wise error metric in Figure 6.12 and observe that the DG method appears to converge fastest, followed by the QBD-RAP method, then the uniformisation method, and the DG scheme with a slope limiter does not appear to converge. The DG scheme with a slope limiter has detected oscillations in the approximate solution and reduced the scheme to linear where oscillations are detected, thereby decreasing the accuracy of the scheme to linear where oscillations are present.

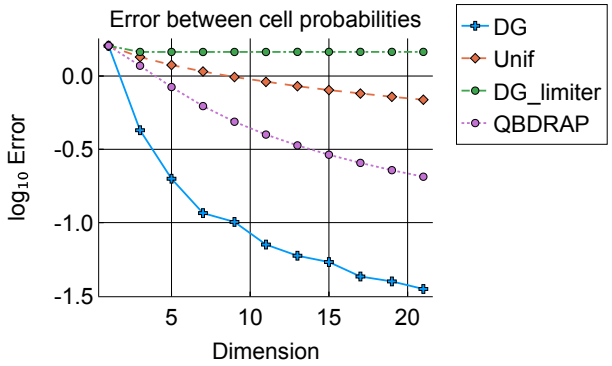

Figure 6.12: Cell-wise error defined in (6.1) for the travelling wave in Example 6.9. Plotted are the cell-wise errors for the DG method (blue solid line), DG method with Generalised MUSCL limiter (green dashed line), uniformisation method (orange dashed line) and QBD-RAP method (purple dotted line) versus the dimension of the approximation.

Figure 6.13 plots the KS error between the approximated and true CDFs and L^2 error between the approximated and true PDFs. Comparing Figure 6.12 with Figure 6.13, each method seems to show a similar rate of decay for error metrics with and without reconstruction.

Returning to Figure 6.13, the DG method with the MUSCL limiter does not appear to converge with these error metrics for this problem (due to the limiter reducing the

approximation to linear near the discontinuity), while the other two positivity preserving methods, the uniformisation and QBD-RAP schemes, both appear to be converging with the QBD-RAP method converging faster. With these error metrics, the DG method appears to be converging fastest. However, if we observe the approximations resulting from the DG method (Figure 6.14 top-row), we find them to be unsatisfactory due to oscillations and negative values.

Figure 6.14 plots the density functions reconstructed using the DG, uniformisation, DG with MUSCL limiter and QBD-RAP methods for various dimension schemes. In the first row we observe that the DG method (sans limiter) produces an approximation to the PDF with negative values when the dimension is greater than 1. In the third row of Figure 6.14 we observe that, with the limiter, the DG approximation does not change significantly after order 3. This is due the fact that the DG method is at best linear in the presence of oscillations. In the second row of Figure 6.14 is the solution approximated using the uniformisation method, and in the last row is the solution approximated using the QBD-RAP method.

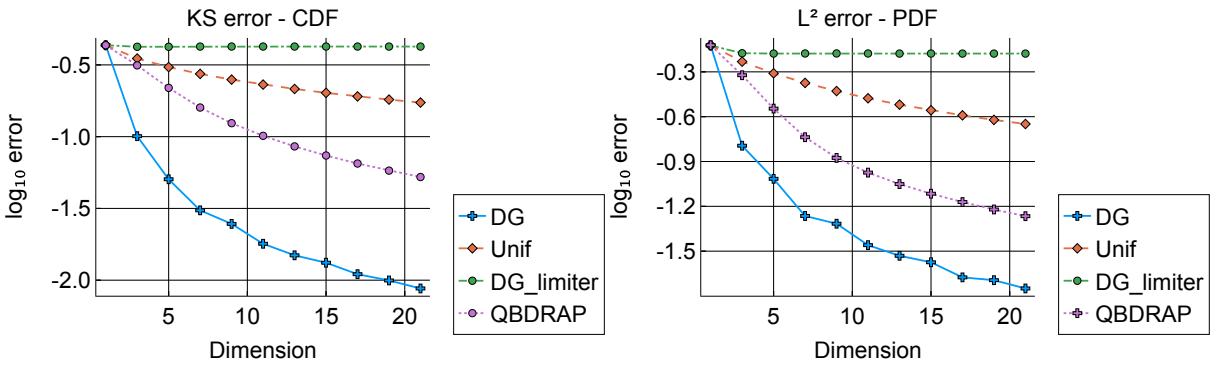

Figure 6.13: KS error (left) and L^2 error of the PDFs for the travelling eave problem in Example 6.9 using the approximations from the DG method (blue solid line with crosses), DG method with the MUSCL limiter (green dash-dotted line with crosses), uniformisation method (orange dashed line with diamonds) and QBD-RAP method (purple dotted line with circles).

This is a particularly interesting example. It shows that, for the DG method, even though there is no discretisation error for the initial condition, we use a strong stability preserving time-integration method, and the projection off which the DG method is based can represent the transient distribution at time $t = 4$ exactly, there is still the possibility of badly behaved solutions as in the top row of Figure 6.14.

Example 6.10. Another interesting example occurs with the initial condition with CDF $1(x \geq 0.5)$, i.e. a point mass at 0.5. The exact solution at time $t = 4$ is therefore a point

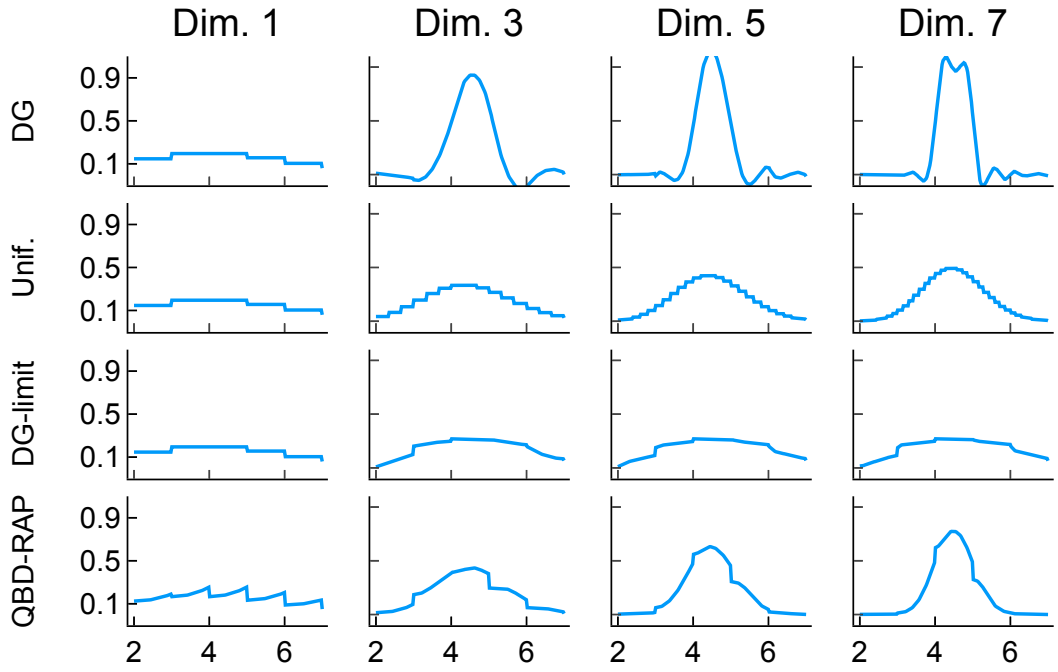

Figure 6.14: Reconstructed PDFs using the DG (top row), uniformisation (second row), DG with MUSCL limiter (third row) and QBD-RAP (bottom row) methods, for order 1, 3, 5, and 7 (columns) for the travelling eave problem in Example 6.9. The true density function is $1(4 \leq x < 5)$.

mass at 4.5. No PDF exists for the true distribution, so instead we compare the CDFs. Moreover, when we analysed reconstruction of this initial condition we saw that using the KS metric may be uninformative. Instead, for this example, we measure errors by looking at the L^1 error between the CDFs (the area between the CDFs) and the cell-wise error from (6.2)-(6.1).

Figure 6.15 (left) plots the L^1 error between the true and approximated CDFs. The L^1 metric tells a similar story to the previous analysis: the DG method with the limiter does not converge as order increases, the other two positivity preserving methods (the uniformisation and QBD-RAP methods) appear to converge, with the QBD-RAP method converging faster, while the DG method appears to converge the fastest. However, if we plot the approximations to the CDFs from the DG method (not shown) we would once again see an oscillating, non-monotonic function. Another interesting observation is to compare the performance of the uniformisation and QBD-RAP methods with respect to the L^1 metric on the CDFs in Figure 6.15 (left) to that in Figure 6.7 (right). Recall, in Figure 6.7 we investigated the ability of the different approximation methods to represent the initial distribution with CDF $1(x \geq 0.5)$, which is the initial condition of the problem

we are considering here. In Figure 6.7 (right) the uniformisation method out-performed the QBD-RAP method at reconstructing the initial condition. However, in Figure 6.15 (left) we see that the QBD-RAP method out-performs the uniformisation method. This suggests that the QBD-RAP method is better able to resolve movement of mass across the domain when integrating over time, compared to the uniformisation method.

Figure 6.15 (right) plots the cell-based error metric in (6.1). Once again, the DG method with MUSCL limiter does not appear to converge. The uniformisation and QBD-RAP method both appear to converge, with the QBD-RAP method converging faster. Most interestingly though is the DG method. It is unclear whether this method will converge in this case as the errors in the plot are not obviously decreasing. Moreover, with this metric, the QBD-RAP method out-performs the DG method when the dimension is large enough. Furthermore, the DG method can result in negative estimates of the cell probabilities in (6.2) and (6.3) (plots not shown).

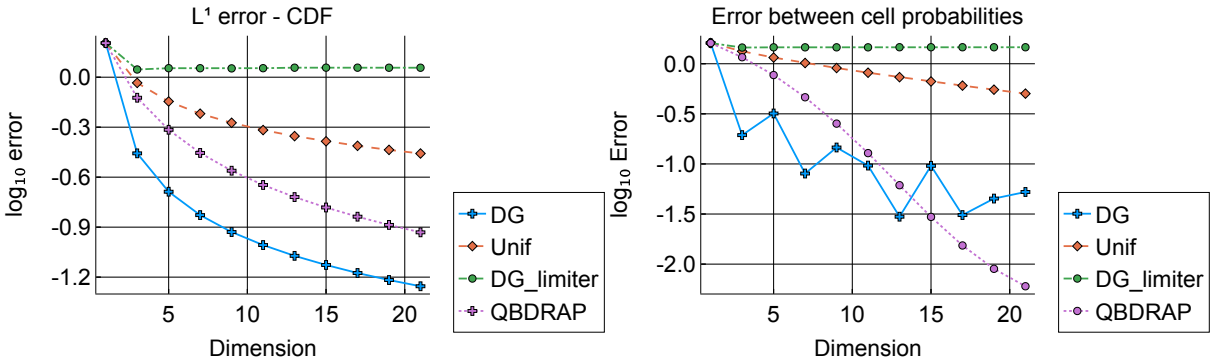

Figure 6.15: L^1 error between the true CDF and the approximations (left) and the cell-wise error metric in (6.1) for the travelling wave problem in Example 6.10 where approximation were constructed via the DG method (blue solid line with crosses), DG method with the MUSCL limiter (green dash-dotted line with crosses), uniformisation method (orange dashed line with diamonds) and QBD-RAP method (purple dotted line with circles).

Example 6.11. Now consider an initial distribution which is truncated Gaussian with mean parameter 2.5 and standard deviation parameter 0.5, and truncated at the boundaries, 0 and 10;

$$\mu([0,x)) := \mathbb{P}(X(0) \leq x, \varphi(0) = 1) = \frac{\Phi((x-2.5)/0.5)1(0 \leq x < 10.0)}{\Phi(7.5/0.5) - \Phi(-2.5/0.5)} + 1(10 \leq x), \tag{6.4}$$

where $\Phi(x)$ is the CDF of the standard normal distribution.

At time $t = 4$ the distribution is truncated Gaussian with mean parameter 6.5, standard deviation parameter 0.5, and is truncated below at 4.0 and above at 10, and there is also a small mass at the upper boundary;

$$\mathbb{P}(X(4) \leq x, \varphi(4) = 1 \mid X(0) \sim \mu, \varphi(0) = 1) = \frac{\Phi((x - 6.5)/0.5)1(4.0 \leq x)}{\Phi(7.5/0.5) - \Phi(-2.5/0.5)} + 1(10 \leq x). \tag{6.5}$$

At time $t = 4$ the mass at the boundary is approximately 1.28×10^{-12} and there is a small discontinuity at $x = 4$ where the CDF jumps from 0 to $\sim 2.87 \times 10^{-7}$, due to the truncation of the initial distribution at 0.

Since the discontinuity at $x = 4$ is small (much smaller than numerical integration errors in the evaluation of the error metrics), and the distribution is otherwise smooth, we expect that the DG method will perform well for this example. Figures 6.16 and 6.17 confirms that this is indeed the case. For all three metrics the error obtained by the DG method rapidly decreases to a point where it is swamped by other numerical errors. This is characteristic of the DG method for the smooth problems we investigate throughout this chapter. For low order DG schemes there are regions where the approximated PDF is negative, however, as the order of the DG scheme increases, these regions disappear. Interestingly, even though this is a relatively smooth problem, the DG method with MUSCL limiter does not perform well. It must be that the initial and transient distributions are 'sufficiently pointy' that oscillations in the numerical solutions occur and the limiter reduces the order of the scheme to linear. Both the uniformisation and QBD-RAP schemes perform similarly to previous examples. Comparing the cell-wise error plots in Figure 6.16 with the higher-resolution error metrics in Figure 6.17, all the approximation schemes show a similar rate of decay of errors as a function of the dimension of the approximation.

Example 6.12. We now want to look at how the methods might handle a mass at the boundary. We introduce an ephemeral second phase into the model with phase transition rate $T_{22} = -1$, and fluid rate $c_2 = 0$. The generator is therefore

$$T = \begin{bmatrix} 0 & 0 \\ 1 & -1 \end{bmatrix}.$$

We suppose that the initial condition is a point mass at the boundary in phase 2, i.e.

$$\mathbb{P}(X(0) \leq x, \varphi(0) = 2) = 1(0 \leq x).$$

With this initial condition, the transient distribution at time $t = 4$ is

$$\begin{aligned} &\mathbb{P}(X(4) \leq x, \varphi(4) = 1 \mid X(0) = 0, \varphi(0) = 2) \\ &= e^{T_{22}4} \left(e^{-T_{22}x} - 1\right) 1(4 < x) + (1 - e^{T_{22}4}) 1(4 \geq x) \end{aligned}$$

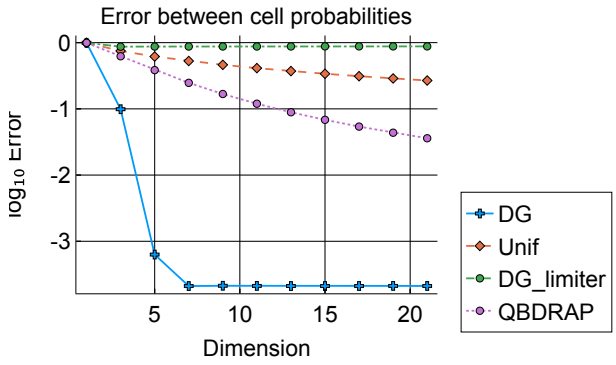

Figure 6.16: Cell-wise error defined in (6.1) for the travelling wave problem in Example 6.11. Plotted are the cell-wise errors for the DG method (blue solid line), DG method with Generalised MUSCL limiter (green dashed line), uniformisation method (orange dashed line) and QBD-RAP method (purple dotted line) versus the dimension of the approximation.

$$= e^{-4}\left(e^{4x} - 1\right) 1(4 < x) + (1 - e^{-4})1(4 \geq x) \tag{6.6}$$

and

$$\mathbb{P}(X(4) \leq x, \varphi(4) = 2 \mid X(0) = 0, \varphi(0) = 2) = e^{-4}1(0 \leq x). \tag{6.7}$$

The PDF at $t = 4$ is discontinuous at $x = 4$, which is at the edge of a cell. For this problem, all methods can represent the initial condition exactly.

Figure 6.18 plots the cell-wise error metric and Figure 6.19 plots the KS error (right) and the L^2 error between of the PDFs. Once again, the cell-wise error metrics in Figure 6.18 show similar characteristics to the finer-resolution error metrics in Figure 6.19. Observing Figures 6.18 and 6.19, the DG method with MUSCL limiter does not perform well, which might be expected due to the discontinuity in the transient distribution at $x = 4$ in Phase 1. The uniformisation and QBD-RAP methods appear to converge, with the QBD-RAP method converging faster. The DG method converges fastest, however, produces approximations with negative and oscillatory solutions as we might expect given the discontinuity. A selection of approximations to the transient PDF are shown in Figure 6.20.

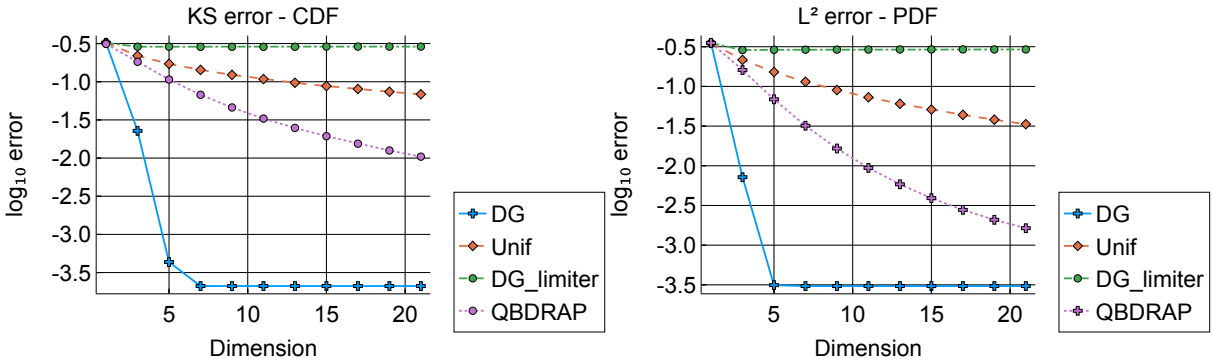

Figure 6.17: KS error (left) and L^2 error for the PDFs for Example 6.11 where approximations were constructed via the DG method (blue solid line with crosses), DG method with the MUSCL limiter (green dash-dotted line with crosses), uniformisation method (orange dashed line with diamonds) and QBD-RAP method (purple dotted line with circles).

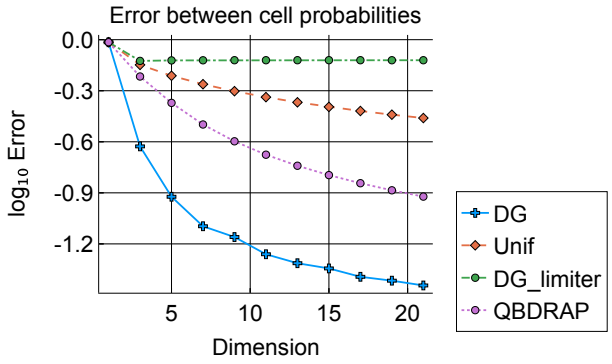

Figure 6.18: Cell-wise error for the travelling wave problem in Example 6.12. Plotted are the cell-wise errors for the DG method (blue solid line), DG method with Generalised MUSCL limiter (green dashed line), uniformisation method (orange dashed line) and QBD-RAP method (purple dotted line) versus the dimension of the approximation.

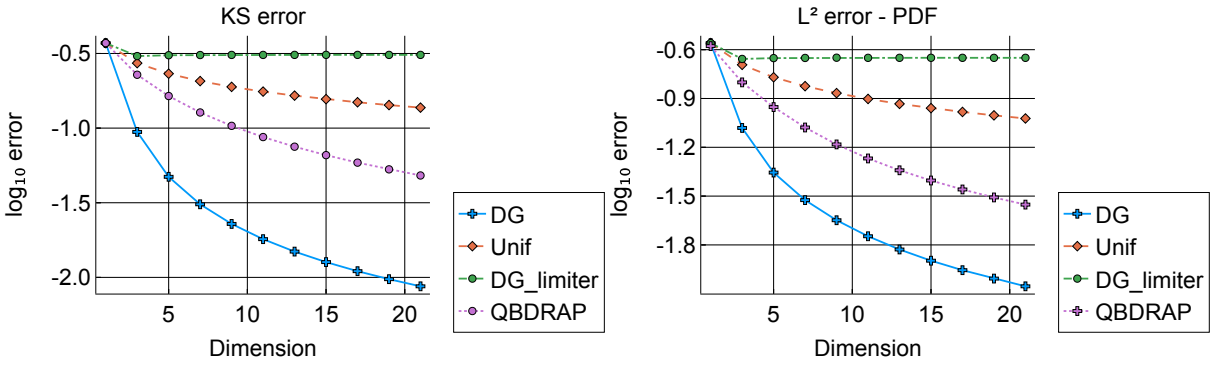

Figure 6.19: KS error (left) and L^2 error of the PDFs for the travelling wave problem in Example 6.12 where approximations were constructed via the DG method (blue solid line with crosses), DG method with the MUSCL limiter (green dash-dotted line with crosses), uniformisation method (orange dashed line with diamonds) and QBD-RAP method (purple dotted line with circles).

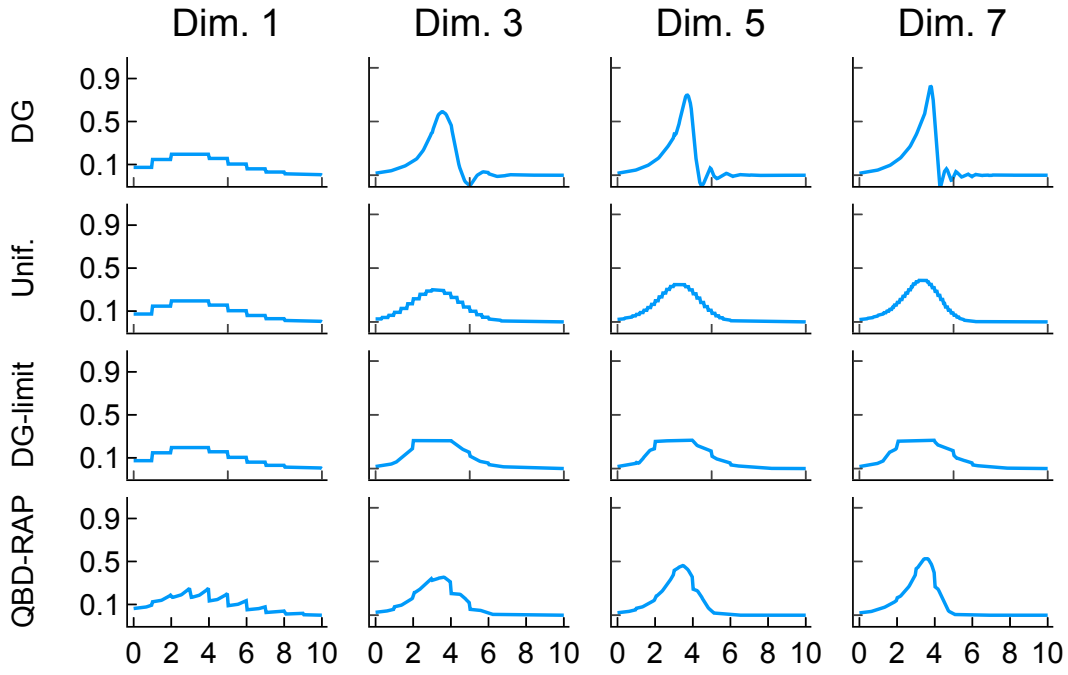

Figure 6.20: Approximate PDFs for Example 6.12 using the DG (top row), uniformisation (second row), DG with MUSCL limiter (third row) and QBD-RAP (bottom row) methods, with dimensions 1, 3, 5, and 7 (columns). The true density function is $e^{-4}e^{x}1(x < 4)$.

6.3 Stationary distributions

We briefly turn our attention to stationary distributions of fluid queues. Since the stationary distribution is smooth we expect that the DG method will work well here. The stationary distribution is convenient as we can evaluate them analytically Sonenberg (2017) and do not require us to approximate initial conditions or integrate over time. Hence, analysing the performance of the approximation methods with the stationary distribution allows us to instrument the ability of the methods to capture the stochastic dynamics, without numerical integration in time.

Here we analyse a simple model which is based on Example 2 in (Bean et al. 2009*b*), except here we add a lower boundary to the model (no lower boundary is specified in Example 2 of (Bean et al. 2009*b*) as it is inconsequential to their analysis).

Model 6.13. *Consider a fluid queue where the driving process is a CTMC with state space* $\mathcal{S} = \{1, 2, 3, 4\}$*, generator*

$$\boldsymbol{T} = \begin{bmatrix} -1.1 & 1.1 \\ 1 & -1 \end{bmatrix},$$

and there are associated rates $c_1 = 1, c_2 = -1$*, and boundaries at* $x = 0$ *and* $x = 10$*. We specify two types of behaviour at the boundary.*

Upon hitting the lower boundary, the process transitions from phase 2 *to phase* j *with probability* p_{2j} *where*

$$\begin{bmatrix} p_{21} & p_{22} \end{bmatrix} = \begin{bmatrix} 1 & 0 \end{bmatrix}.$$

Upon hitting the upper boundary, the process transitions from phase 1 *to phase* j *with probability* p_{1j} *where*

$$\begin{bmatrix} p_{11} & p_{12} \end{bmatrix} = \begin{bmatrix} 0 & 1 \end{bmatrix}.$$

Thus, upon hitting the boundary, the fluid queue immediately transitions to the other phase and is reflected.

The model was discretised using the DG, uniformisation and QBD-RAP methods using ten cells of width 1. We compute the coefficients for the stationary distribution in the following way. Suppose that a given discretisation method results in an approximation to the generator of the fluid queue as a matrix $\boldsymbol{B}$. Then the stationary coefficients are found by solving

$$\boldsymbol{b}\boldsymbol{B} = 0, \tag{6.8}$$

$$\text{such that } \boldsymbol{b}\boldsymbol{1} = 1, \tag{6.9}$$

for the coefficients $\boldsymbol{b}$.

Model 6.13. Figure 6.21 plots KS errors between the true stationary CDF and the approximations (left) and the L^2 error between the true stationary PDF and the approximations. Clearly the DG method is superior here as its error rapidly decreases to a point where is become insignificant compared to other numerical errors. The QBD-RAP method and uniformisation method both appear to be converging, with the errors for the QBD-RAP method decreasing faster.

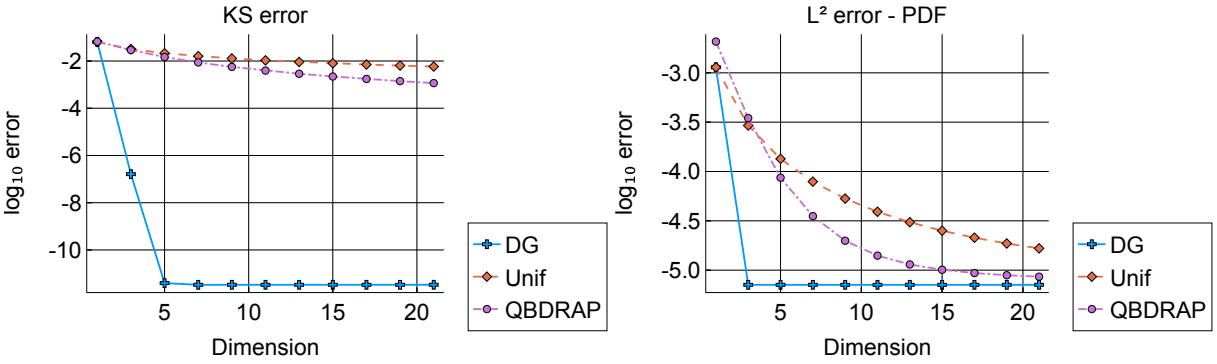

Figure 6.21: KS error (left) and L^2 error of the PDFs for Model 6.13 using the DG method (blue solid line with crosses), uniformisation method (orange dashed line with diamonds) and QBD-RAP method (purple dotted line with circles).

6.4 Transient distributions

Once again we consider Model 6.13 and use the same spatial discretisation as described in Section 6.3 (ten cells with width $\Delta = 1$). Two initial conditions are considered, a point mass at 0 in phase 1, and the initial distribution with PDF

$$\frac{1}{2}e^{-x}/(1-e^{-10}) \tag{6.10}$$

in phases 1 and 2, with no mass at the boundaries. We numerically integrate over time until time $t = 2.0$ using the SSPRK4 method with t-step size 0.005.[†] We apply the DG method with, and without, the Generalised MUSCL slope limiter.

To obtain a *ground truth* 5,000,000 realisations of the fluid queue were simulated until $t = 2$, then the empirical CDF and the masses within each cell and at the boundaries were computed from the simulations. We do not attempt to numerically approximate the true PDF via simulation. We then compute the KS and L^1 error metrics between the

[†]Once again, the t-step size must be chosen to ensure that numerical integration over time is stable up to dimension 21, adhering to a CFL-like condition (Hesthaven & Warburton 2007, Section 4.8).

approximated CDF and simulated CDF, as well as the cell-wise error metric, given as follows.

$$\begin{aligned}&\sum_{j\in\{1,2\}}\sum_{\ell=1}^{10}|\mathbb{P}_{sim}(X(2)\in\mathcal{D}_{\ell,j},\varphi(2)=j\mid X(0)=0.5,\varphi(0)=1)-p(2,\ell,j)|\\&+|\mathbb{P}_{sim}(X(2)\in\{10\},\varphi(2)=4\mid X(0),\varphi(0))-p(2,11,4)|\\&+|\mathbb{P}_{sim}X(2)\in\{0\},\varphi(2)=3\mid X(0),\varphi(0))-p(2,0,3)|\end{aligned}\tag{6.11}$$

where $p(2,\ell,j)$ is an approximation to $\mathbb{P}_{sim}(X(2)\in\mathcal{D}_{\ell,j},\varphi(2)=j\mid X(0),\varphi(0))$, $p(2,11,4)$ is an approximation to $\mathbb{P}_{sim}(X(2)\in\{10\},\varphi(2)=4\mid X(0),\varphi(0))$, and $p(2,0,3)$ is an approximation to $\mathbb{P}_{sim}(X(2)\in\{10\},\varphi(2)=3\mid X(0),\varphi(0))$, and $\mathbb{P}_{sim}$ denotes an empirical probability evaluated using the simulations of the fluid queue.

To account for possible Monte-Carlo error, we used a bootstrap with 1,000 bootstrap samples. We sample 5,000,000 realisations of the fluid queue with replacement from the original 5,000,000 samples, then compute error metrics with the resampled data. We resample 1,000 times. Via the bootstrap, we report the 5th and 95th percentile of the sampling distribution of the errors.

To evaluate error metrics, we use a grid of 10,001 evenly spaced points for each phase.

To approximate the point mass initial condition we compute the initial coefficients for each scheme exactly. For the exponential initial condition in (6.10) we compute the initial coefficients via Gauss-Lobatto quadrature for the DG method, by using the mid-point rule for the uniformisation method, and by using a trapezoidal rule with 2,001 points on each cell for the QBD-RAP method.

Model 6.13 with exponential initial condition Figure 6.22 shows the error metrics for the four different spatial discretisation schemes (DG, DG with MUSCL limiter, uniformisation and QBD-RAP). For both error metrics the DG scheme converges rapidly until computational errors become significant. The uniformisation and QBD-RAP schemes converge at a slower rate than the DG method, with the QBD-RAP scheme converging faster than the uniformisation method. The DG scheme with MUSCL limiter does not appear to be converging, which suggests there is at least one iteration during the numerical integration over time at which the numerical solution displays oscillations. However, when the DG approximations for the distribution at time $t = 2$ are plotted, they do not display oscillations (not shown). This suggests that the oscillations which might occur with the DG scheme must be transient, and have dissipated by time $t = 2$. The oscillations which the limiter detects in the DG scheme are likely from the reflecting boundary at $x = 0$. In the early stages of the evolution of the model the majority of the density in Phase 2 near zero will move to the left at rate 1 and hit the boundary at $x = 0$. Upon hitting the boundary, the density is reflected into Phase 1. Meanwhile, the initial density in Phase 1 moves to the right at rate 1 and the density reflected at the boundary from

Phase 2 fills in to the region between $x = 0$ and $x = t$ in Phase 1. Intuitively, in the early evolution of the model, there will be a sharp peak in the transient density at $x = t$ – I suspect that the transient density is continuous at this point, but not differentiable.

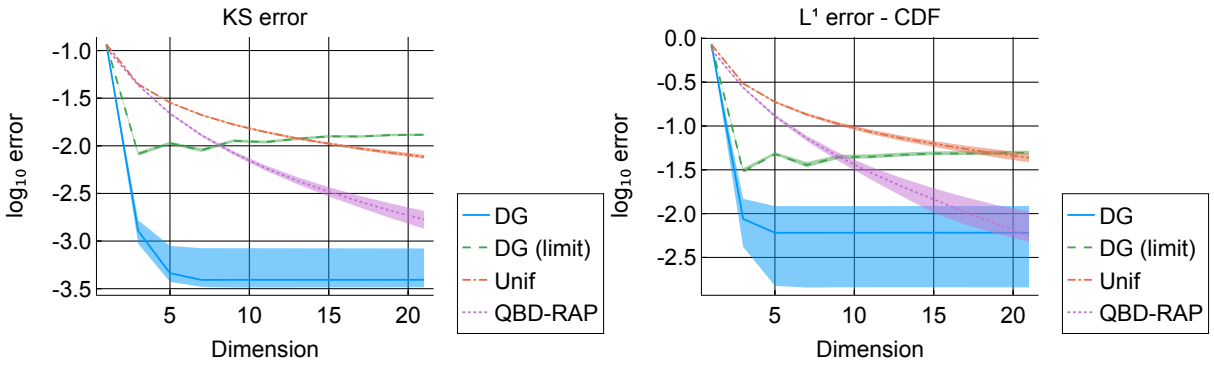

Figure 6.22: KS (left) and L^1 (right) errors between the true transient CDF at time $t = 2$ for Model 6.13 with the exponential initial condition, where the approximations were obtained via the DG method (blue solid line), DG method with Generalised MUSCL limiter (green dashed line), uniformisation method (orange dashed line) and QBD-RAP method (purple dotted line). Bootstrapped 90% confidence intervals are shown by the lighter coloured bars surrounding the lines.

Figure 6.23 plots the cell-wise error metric (6.11) for Model 6.13 with the exponential initial condition. Since the cell-wise errors do not require us to reconstruct the value of the solution within each cell, then this metric allows us to observe the error characteristics of the methods without reconstruction. Figure 6.23 shows similar convergence characteristics to the other error metrics in Figure 6.22.

Model 6.13 with a point-mass initial condition Figure 6.24 shows the error metrics for the four different spatial discretisation schemes (DG, DG with MUSCL limiter, uniformisation and QBD-RAP). Comparing the error metrics in Figure 6.24 for the point mass initial condition with the ones in Figure 6.22 for the exponential initial condition all schemes perform worse for the point mass initial condition. Regarding comparative rates of convergence for this problem, the DG scheme converges fastest, followed by the QBD-RAP scheme, then the uniformisation scheme, while the DG scheme with MUSCL limiter does not appear to converge due to the limiter reducing the scheme to a linear approximation around the discontinuity.

Figure 6.25 plots the cell-wise error metric (6.11) for Model 6.13 with the point mass initial condition. Figure 6.25 suggests that approximating the cell-wise error seems to be a difficult problem. This is likely caused by the discontinuity at $x = 2$ in phase 1, which lies exactly on a cell boundary. To investigate how the position of the discontinuity might

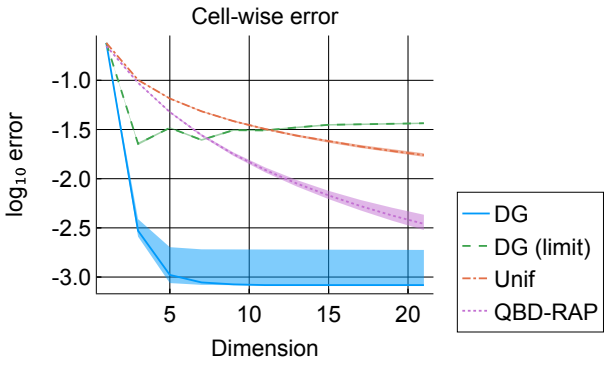

Figure 6.23: Cell-wise error metric from (6.11) for Model 6.13 with the exponential initial condition, where the approximations were obtained via the DG method (blue solid line), DG method with Generalised MUSCL limiter (green dashed line), uniformisation method (orange dashed line) and QBD-RAP method (purple dotted line). Bootstrapped 90% confidence intervals are shown by the lighter coloured bars surrounding the lines.

affect the error metrics we evolved the model to time $t = 2.1$ and computed the KS error, L^1 error between the CDFs and the cell-wise error. Once again, we use simulation and bootstrapping to approximate the *ground truth*. The plots (not shown) of KS error and L^1 error between the CDFs for the model at times $t = 2$ and $t = 2.1$ are relatively similar and not noteworthy. The plot of the cell-wise error metric at time $t = 2.1$ in Figure 6.26 is somewhat more interesting. Figure 6.26 shows that the cell-wise error metric is somewhat volatile for the DG scheme; I suspect that this is due to the oscillations in the DG approximation. In contrast, in Figure 6.26 the uniformisation and QBD-RAP schemes have monotonically decreasing error curves.

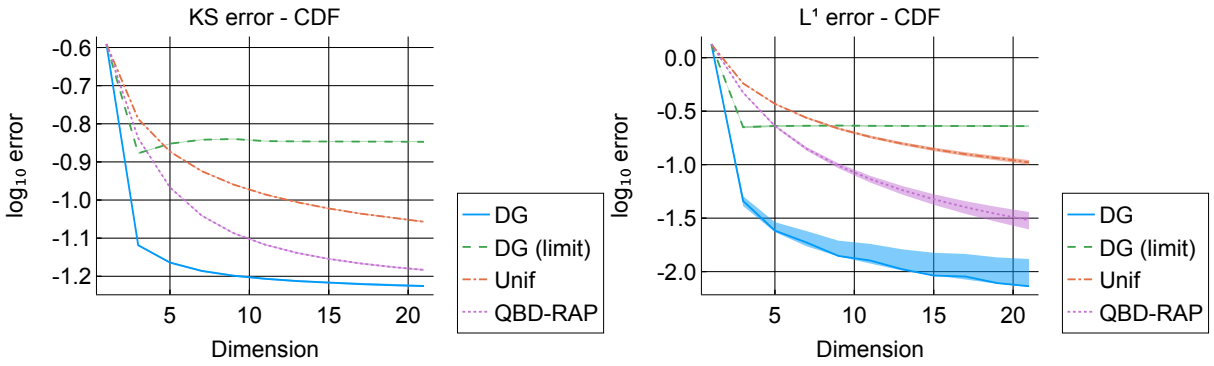

Figure 6.24: KS (left) and L^1 errors between of the CDF (right) at time $t = 2$ for Model 6.13 with the point-mass initial condition, where the approximations were obtained via the DG method (blue solid line), DG method with Generalised MUSCL limiter (green dashed line), uniformisation method (orange dashed line) and QBD-RAP method (purple dotted line). Bootstrapped 90% confidence intervals are shown by the lighter coloured bars surrounding the lines.

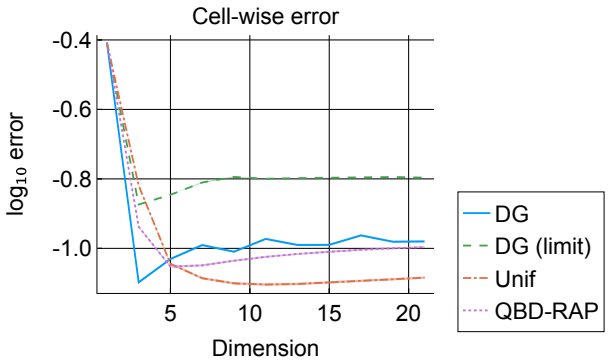

Figure 6.25: Cell-wise errors for Model 6.13 at time $t = 2$ with the point mass initial condition, where the approximations were obtained via the DG method (blue solid line), DG method with Generalised MUSCL limiter (green dashed line), uniformisation method (orange dashed line) and QBD-RAP method (purple dotted line). Bootstrapped 90% confidence intervals are shown by the lighter coloured bars surrounding the lines.

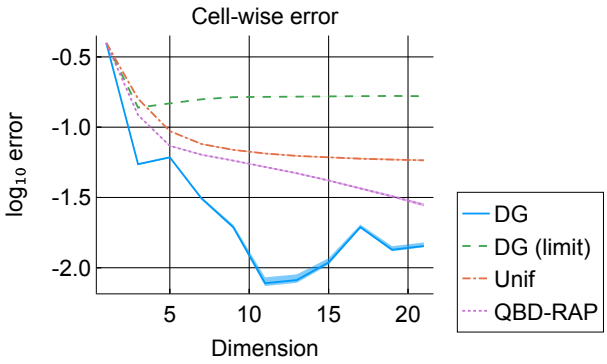

Figure 6.26: L^1 errors between the simulated and approximated cell masses for Model 6.13 at time $t = 2.1$ with the point mass initial condition, and the corresponding approximations obtained via the DG method (blue solid line), DG method with Generalised MUSCL limiter (green dashed line), uniformisation method (orange dashed line) and QBD-RAP method (purple dotted line). Bootstrapped 90% confidence intervals are shown by the lighter coloured bars surrounding the lines.

6.5 Hitting times

Once again we consider Model 6.13. Let $\zeta_X(\{0,1\}) = \{\inf t > 0 \mid X(t) = 0, \text{ or } X(t) = 1\}$, be the first hitting time of $\{X(t)\}$ on the set $\{0,1\}$. The distribution of the hitting time in phase $i \in \{1,2\}$ is

$$\mathbb{P}(\zeta_X(\{0,1\}) < t, \varphi(t) = i \mid \boldsymbol{X}(0) \sim \mu), \tag{6.12}$$

for some initial distribution μ. We look at two initial conditions; an exponential with equal mass in each phase,

$$\mathbb{P}(X(0) \in \mathrm{d}x, \varphi(0) = i) = e^{-x}/(1 - e^{-1})/2,\ i \in \{1,2\},$$

and a point mass at $X(0) = 0$ in phase $\varphi(0) = 1$.

We use the DG, uniformisation and QBD-RAP methods to discretise the fluid queue and partition $[0,1]$ into three intervals of width $1/3$. To capture the mass which has left the interval $[0,1]$, we suppose that when the process hits the boundary it is absorbed forever at the boundary and in the phase in which the process first hit the boundary.

We integrate the schemes until time $t = 10$ using the SSPRK4 method with t-step size $0.005/3$.[‡] We use the DG scheme with and without a slope limiter during the time-integration. At each time-step of the numerical integration, we record the amount of mass at the absorbing boundaries in each phase, which gives us an approximation of the cumulative distribution function of the hitting time in each phase up to time $t = 10$.

As a *ground truth* we simulated 5,000,000 realisations and recorded the hitting time on the boundary of the interval $[0,1]$ and the phase at the time of hitting. We then compute the empirical CDF of the hitting probabilities

$$\mathbb{P}(\zeta_X(\{0,1\}) < t, \varphi(t) = i \mid \boldsymbol{X}(0) \sim \mu),$$

for $t = 0.005/3 \times k$, $k = 0, ..., 6000$.

To account for Monte-Carlo errors we took 1,000 bootstrap resamples of the original 5,000,000 samples and computed the empirical CDF of the hitting probabilities for each bootstrap sample. For each bootstrap sample, we resampled 5,000,000 points with replacement from the original 5,000,000 realisations. For each bootstrap sample we computed the error metrics between the empirical and approximated CDFs and recorded the 5th and 95th percentile of the distribution of the errors.

Exponential initial condition Figure 6.27 shows the error metrics recorded for the four different numerical approximation schemes. The uniformisation and QBD-RAP

[‡]Since we use a smaller cell-width in this example than in previous examples we need to reduce the t-step size accordingly to ensure that numerical integration is stable for schemes up to dimension 21, adhering to a CFL-like condition (Hesthaven & Warburton 2007, Section 4.8).

method both appear to converge, with the QBD-RAP converging at a faster rate. For both error metrics the DG scheme performs the best. For the L^1 error metric the DG scheme converges up to order 5 after which there is no improvement in the error; I believe that this is due to other numerical errors dominating. The DG scheme with MUSCL limiter does not appear to converge, suggesting oscillations in the DG approximation. Intuitively, with this initial condition we suspect that the transient distribution of the fluid queue on the event that it remains in the interval $(0, 1)$ is discontinuous at $x = t$ in Phase 1 and $x = 1 - t$ in Phase 2 for $x < 1$. We also expect there is a discontinuity in the hitting time PDF at time $t = 1$. Indeed, small oscillations are visible in hitting time PDF for both phases, see Figure 6.28.

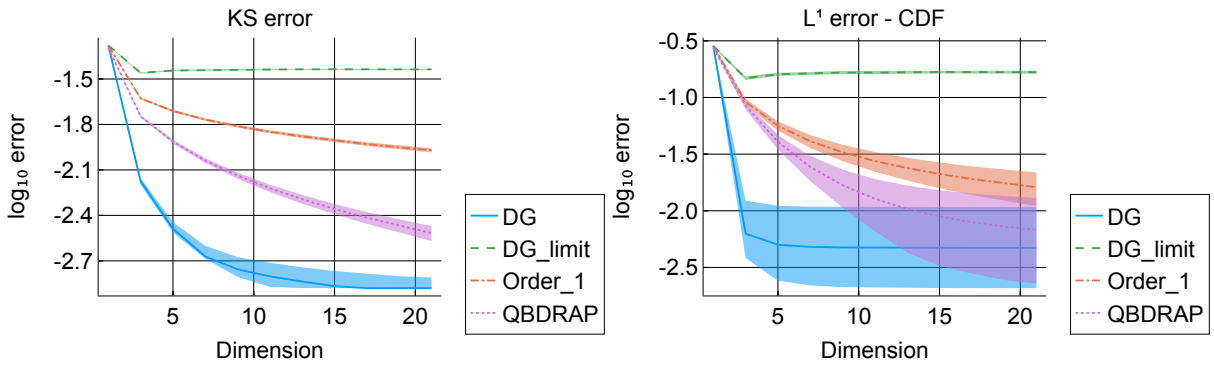

Figure 6.27: KS (left) and L^1 (right) errors between the simulated and approximated first hitting time CDFs in (6.12) for Model 6.13 with the exponential initial condition. The approximations were obtained via the DG method (blue solid line), DG method with Generalised MUSCL limiter (orange dashed line), uniformisation method (green dashed line) and QBD-RAP method (purple dotted line). Bootstrapped 90% confidence intervals are shown by the lighter coloured bars surrounding the lines.

Point mass initial condition Figure 6.29 shows the KS error (left) and L^1 error for the CDF for the four different numerical approximation schemes applied to the hitting time problem with the point mass initial condition. The uniformisation and QBD-RAP method both appear to converge, with the QBD-RAP converging at a faster rate. The DG scheme with MUSCL limiter does not appear to converge, suggesting oscillations in the DG approximation. The DG scheme appears to converge fastest, however, oscillations are present in the DG approximation. In Figure 6.30 we plot the CDFs of the hitting time for Phase 1 obtained via the DG and QBD-RAP schemes, each using a dimension 21 basis. Observing Figure 6.30 the DG approximation clearly displays oscillations around and the discontinuity at $t = 1$.

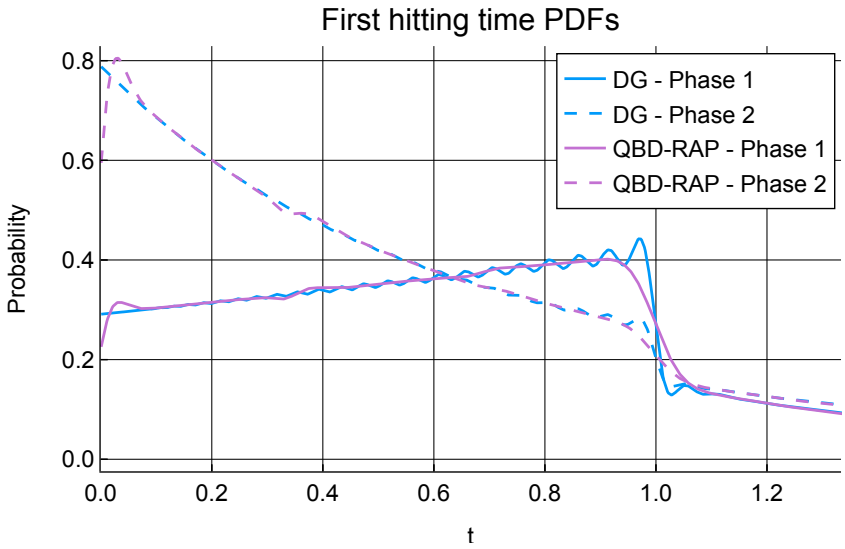

Figure 6.28: Approximations of the PDFs of the first hitting time for Model 6.13 with the exponential initial condition. The blue line were obtained from the dimension-21 DG scheme and the purple lines were obtained from the dimension-21 QBD-RAP scheme. The DG scheme displays oscillations around the discontinuities at $t = 1$.

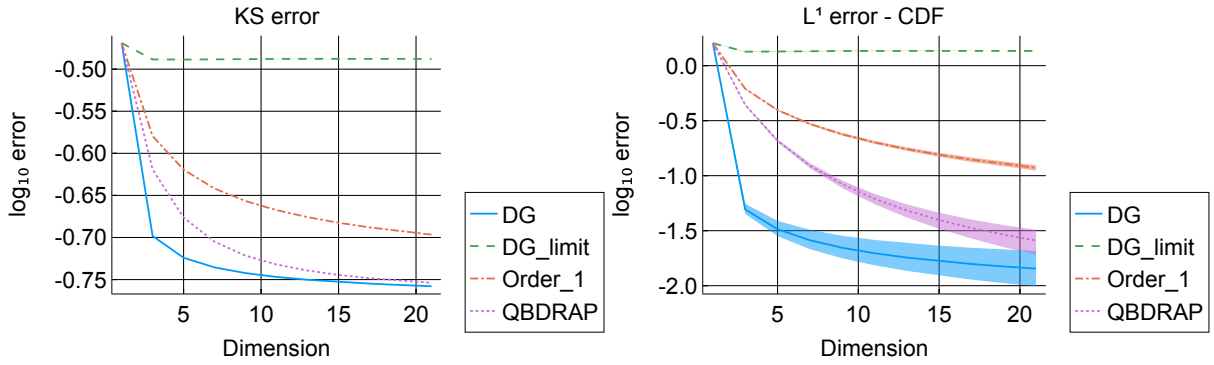

Figure 6.29: KS (left) and L^1 (right) errors between the simulated and approximated first hitting time CDFs in (6.12) for Model 6.13 with the point mass initial condition. The approximations were obtained via the DG method (blue solid line), DG method with Generalised MUSCL limiter (orange dashed line), uniformisation method (green dashed line) and QBD-RAP method (purple dotted line). Bootstrapped 90% confidence intervals are shown by the lighter coloured bars surrounding the lines.

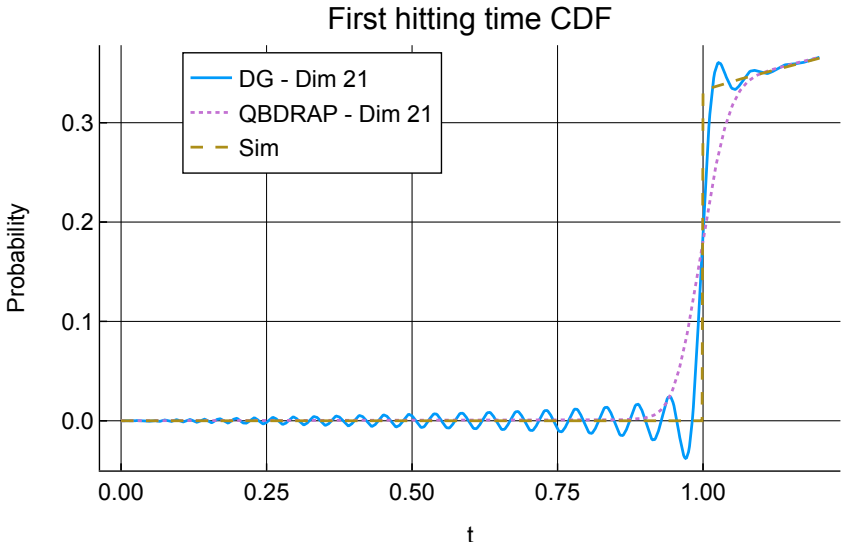

Figure 6.30: Approximations of the CDF of the first hitting time in Phase 1 for Model 6.13 with the point mass initial condition. The blue line was obtained from the dimension-21 DG scheme, the purple dotted line from the dimension-21 QBD-RAP scheme, and the gold dashed line is the empirical CDF obtained via simulation. The DG scheme displays oscillations.

6.6 First-return distributions of fluid-fluid queues

Now consider the fluid-fluid queue model first analysed in Bean et al. (2022) which is a modified version of a model first presented in Latouche et al. (2013). We refer the reader to Bean et al. (2022) for more on the DG method applied to this model.

Model 6.14. *Consider a stochastic fluid-fluid queue* $\{(X(t), Y(t), \varphi(t))\}_{t\geq 0}$, *where* $\{X(t)\}$ *and* $\{Y(t)\}$ *represent the workloads in Buffers 1 and 2 at time* $t \geq 0$, *respectively, both driven by the phase* $\{\varphi(t)\}$, *which is a Markov chain on the state space* $\mathcal{S} = \{11, 10, 01, 00\}$. *Both* $\{X(t)\}$ *and* $\{Y(t)\}$ *have a regulated boundary at 0. Here, the state* 11 *indicates inputs to both buffers being* ON, *the state* 00 *indicates both being* OFF, *the state* 10 *is when only the first input is* ON, *and the state* 01 *is when only the second is* ON. *The input of Buffer* k *is switched from* ON *to* OFF *with rate* γ_k, *and from* OFF *to* ON *with rate* β_k, *for* $k = 1, 2$. *Thus, the infinitesimal generator* T *for* $\varphi(t)$ *is given by*

$$T = \begin{bmatrix} -(\gamma_1+\gamma_2) & \gamma_2 & \gamma_1 & 0 \\ \beta_2 & -(\gamma_1+\beta_2) & 0 & \gamma_1 \\ \beta_1 & 0 & -(\gamma_2+\beta_1) & \gamma_2 \\ 0 & \beta_1 & \beta_2 & -(\beta_1+\beta_2) \end{bmatrix}.$$

The net rates of change for $X(t)$, *denoted* c_i, *are given by*

$$(c_{11}, c_{10}, c_{01}, c_{00}) = \ (\lambda_1 - \theta_1, \ \ \lambda_1 - \theta_1, \ \ -\theta_1, \ \ -\theta_1),$$

and the net rates of change for $Y(t)$, *denoted* r_i, *are as follows*

$$(r_{11}, r_{10}, r_{01}, r_{00}) = \begin{cases} (\lambda_2 - \kappa, & -\kappa, & \lambda_2 - \kappa, & -\kappa) & \text{if } X_t = 0, \\ (\lambda_2 - \theta_2, & -\theta_2, & \lambda_2 - \theta_2, & -\theta_2) & \text{if } X_t \in (0, x^*), \\ (\quad \lambda_2, & 0, & \lambda_2, & 0) & \text{if } X_t \geq x^*. \end{cases}$$

For our numerical experiments, we use the parameter choices given in (Latouche et al. 2013):

$$\gamma_1 = 11, \quad \beta_1 = 1, \quad \lambda_1 = 12.48, \quad \theta_1 = 1.6, \quad \kappa = 2.6, \tag{6.13}$$
$$\gamma_2 = 22, \quad \beta_2 = 1, \quad \lambda_2 = 16.25, \quad \theta_2 = 1.0, \quad x^* = 1.6. \tag{6.14}$$

While the true problem has an unbounded domain $[0, \infty)$, the approximations require the domain of approximation to be a finite interval. Here we choose an upper bound of 48 and place a regulated boundary at the upper boundary. The effect of this truncation can be partly quantified by evaluating $\lim_{t\to\infty} \mathbb{P}(X(t) > 48) \approx 5.83 \times 10^{-9}$, $i \in \mathcal{S}$.

We obtained approximations to the infinitesimal generator of the fluid queue $\{(X(t), \varphi(t))\}_{t\geq 0}$ via the DG method, QBD-RAP method and uniformisation method, all of which used a

cell width of $\Delta = 0.4$. The matrix resulting from the approximation is then used to approximate the first-return operator $\Psi(s)$ as discussed in Section 1.1.2. Due to the stochastic interpretation of the uniformisation and QBD-RAP schemes the approximations to $\Psi(s)$ have a stochastic interpretation as the first-return probabilities of a fluid queue driven by a CTMC and QBD-RAP, respectively (see (Peralta Gutierrez 2019, Chapter 7) and Bean, Nguyen, Nielsen & Peralta (2021) for details on the latter). For the DG method the approximation of $\Psi(s)$ is not as well-understood.[§]

Ultimately, we approximate the first-return distribution

$$\mathbb{P}(X(\zeta_Y(\{0\})) \leq x, \varphi(\zeta_Y(\{0\})) = i \mid \boldsymbol{X}(0) \sim \mu), \tag{6.15}$$

where we recall $\zeta_Y(E) = \inf\{t > 0 \mid Y(t) \in E\}$ is the first hitting time of $\{Y(t)\}$ on the set E. For Model 6.14, it is only possible for the process $Y(t)$ to return to 0 at time t when $(X(t), \varphi(t)) \in [0, 1.6) \times \{10, 00\}$, so we evaluate the approximations over this region only. We use a grid of 10,001 points on which we evaluate the approximations of the CDF in each phase. We consider first the initial distribution which is a point mass at $Y(0) = 0$, $X(0) = 5$, $\varphi(0) = 01$.

For comparison, we simulated 5,000,000 realisations of the fluid-fluid queue and recorded the value of X and φ at the time of first return of the second fluid, Y. The empirical approximation of (6.15) was then constructed, and error metrics for the difference between the empirical CDF and the approximations was computed. To account for Monte-Carlo errors we used a bootstrap with 1,000 bootstrap samples to construct 1,000 bootstrap samples of the error estimates and recorded the 5th and 95th percentiles of the error distribution. Each of the 1,000 bootstrap samples was constructed by resampling the original 5,000,000 realisations 5,000,000 times with replacement.

In Figure 6.31 we plot the error metrics for the approximations to the distribution (6.15). The DG method performs best converging rapidly until the error in the approximation scheme is swamped by other numerical errors. The QBD-RAP method is second best and the uniformisation scheme appears to be the slowest to converge. Here, the first return distribution appears to be smooth, hence we might expect the DG method to perform well. Note that there is a significant number other sources of error here; machine precision errors, errors in solving the matrix Ricatti equation to approximate $\Psi(s)$, errors from approximating error metrics (numerical integration/finding KS statistic), and truncation errors. Furthermore, for the QBD-RAP, since the parameters $\boldsymbol{\alpha}$, $\boldsymbol{S}$, $\boldsymbol{s}$ and $\boldsymbol{D}$ are found numerically, then there is another source of error from this. By modifying slightly Model 6.14, we can construct a first return distribution which is discontinuous.

[§]I believe that the resulting operator is a projection operator which, given an initial distribution, projects the distribution of $X(\zeta_Y(\{0\}))$ on to a set of polynomial basis functions, much like the DG method itself.

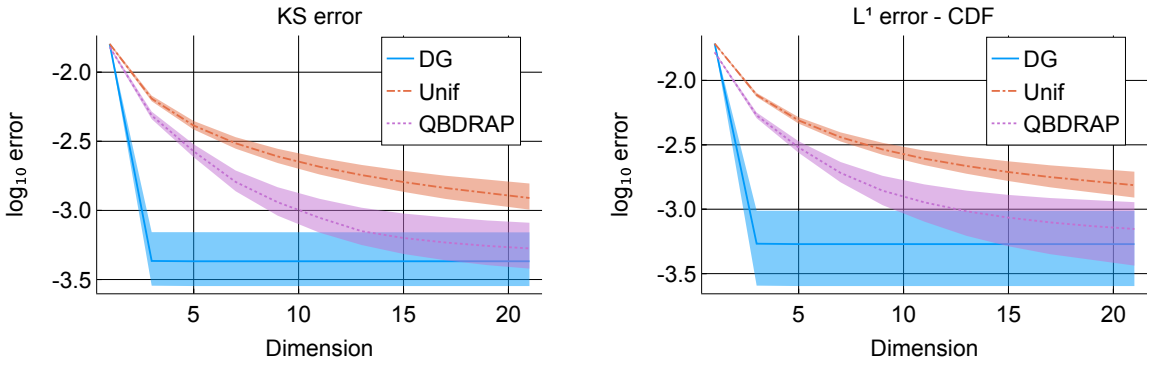

Figure 6.31: KS (left) and L^1 (right) errors between the simulated and approximated CDFs of $X(\zeta_Y(\{0\}))$ in (6.15) for Model 6.14. The approximations were obtained via the DG method (blue solid line), uniformisation method (green dashed line) and QBD-RAP method (purple dotted line). Bootstrapped 90% confidence intervals are shown by the lighter coloured bars surrounding the lines.

Model 6.15. *Consider a fluid-fluid queue which is the same as Model 6.14 except*

$$r_{00}(X(t)) = \begin{cases} -\kappa, & \text{if } X(t) = 0, \\ -\theta_2, & \text{if } X(t) =\in (0, x^*), \\ \theta_2, & \text{if } X(t) \geq x^*, \end{cases} \tag{6.16}$$

with an initial distribution which is a point-mass at $Y(0) = 0$, $X(0) = 2, \varphi(0) = 00$.

As before, we use the DG, uniformisation and QBD-RAP methods to approximate the model, and compare to simulations.

For Model 6.15 there is a point mass at $X(\zeta_Y(\{0\})) = 1.2$ of magnitude $e^{-(\beta_1+\beta_2)} \times 0.5$, which occurs when the phase remains in $\varphi(t) = 00$ for all $t \in [0, \zeta_Y(\{0\})]$.

Figure 6.33 plots the error metrics for the first return distribution. Observing Figure 6.33 we see that the DG method performs well, followed by the QBD-RAP method, then the uniformisation method performs worst. However, the DG method results in an oscillatory solution with the CDF taking impossible values (decreasing at points) as shown in Figure 6.35

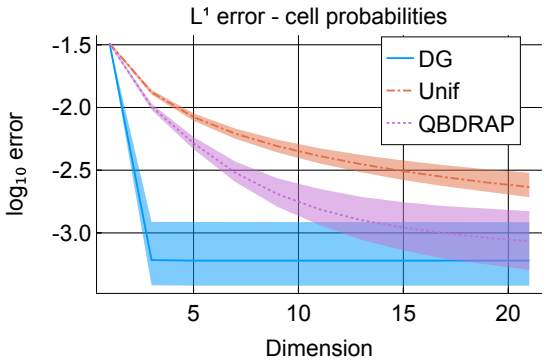

Figure 6.32: Total error between the simulated and approximated probabilities of $X(\zeta_Y(\{0\}))$ residing on each cell $\mathcal{D}_k$ or at the boundary for Model 6.14. The approximations were obtained via the DG method (blue solid line), uniformisation method (green dashed line) and QBD-RAP method (purple dotted line). Bootstrapped 90% confidence intervals are shown by the lighter coloured bars surrounding the lines.

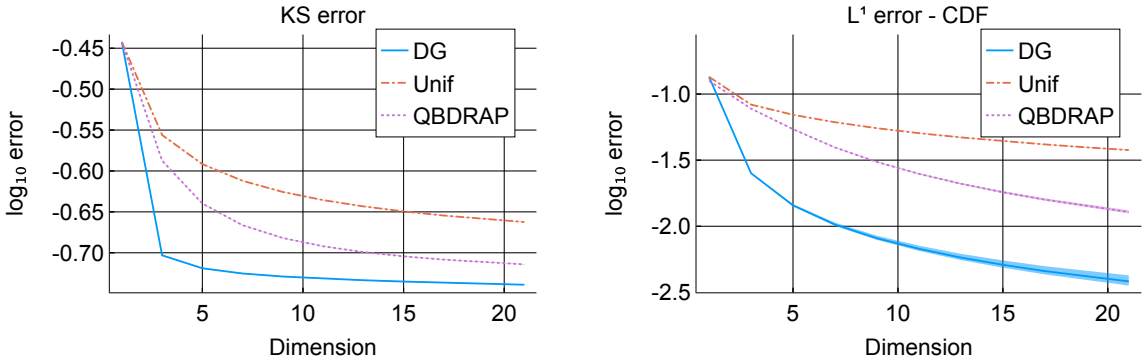

Figure 6.33: KS (left) and L^1 (right) errors between the simulated and approximated CDFs of $X(\zeta_Y(\{0\}))$ (Equation 6.15) for Model 6.15. The approximations were obtained via the DG method (blue solid line), uniformisation method (green dashed line) and QBD-RAP method (purple dotted line). Bootstrapped 90% confidence intervals are shown by the lighter coloured bars surrounding the lines.

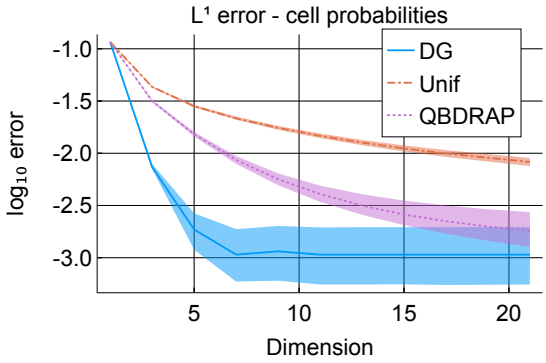

Figure 6.34: Cell-wise error between the simulated and approximated probabilities of $X(\zeta_Y(\{0\}))$ residing in each cell $\mathcal{D}_k$ or at the boundary for Model 6.15. The approximations were obtained via the DG method (blue solid line), uniformisation method (green dashed line) and QBD-RAP method (purple dotted line). Bootstrapped 90% confidence intervals are shown by the lighter coloured bars surrounding the lines.

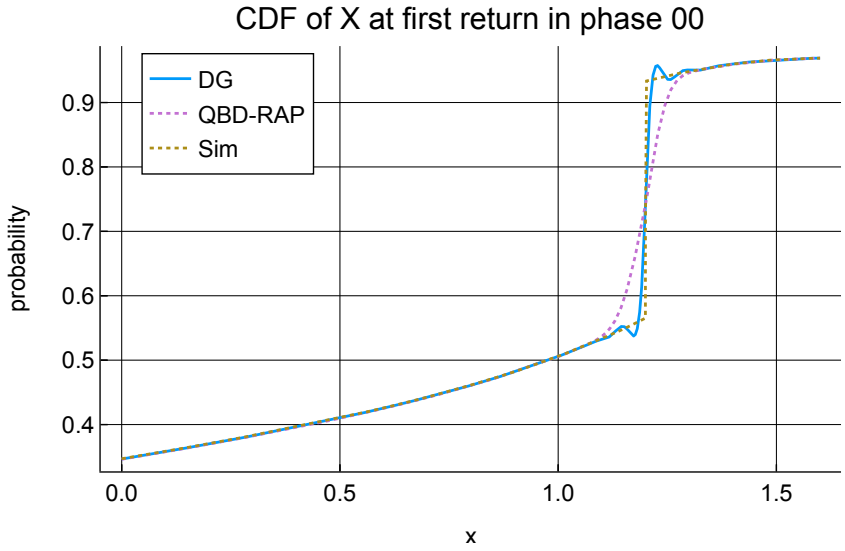

Figure 6.35: Approximations of the CDF of the distribution of X at the time $\zeta_Y(\{0\})$ in Phase 1 for Model 6.15. The blue line was obtained from the dimension-21 DG scheme, the purple dotted line from the dimension-21 QBD-RAP scheme, and the gold dashed line is the empirical CDF obtained via simulation. The DG scheme displays oscillations around the discontinuity.

6.7 Discussion

The structure of this chapter is as follows. In Section 6.1 we compute approximations to various initial conditions for the different methods and observe their performance at approximating the initial condition, which allows us to instrument the performance of the reconstruction methods without considering a specific model or any dynamics of the problem. In Section 6.2 we investigate a simple travelling wave problem with various initial conditions. For this problem the dynamics are deterministic, which allows us to instrument the ability of the schemes to approximate the flow of probability across cells without any stochastic dynamics. Next, we investigate a simple fluid queue with two phases. Section 6.3 investigates the ability of the methods to approximate the stationary distribution of the model, Section 6.4 investigates the ability of the schemes to approximate the transient distribution of the fluid queue for two initial conditions, and Section 6.5 investigates the ability of the methods to approximate the first hitting time of the fluid level on the boundary of the interval $[0, 1]$. Section 6.6 approximates the distribution of $\{(X(t), \varphi(t))\}$ at the time at which $\{Y(t)\}$ first returns to 0 for two simple fluid-fluid queue models.

In this chapter we have numerically investigated some properties of the QBD-RAP approximation scheme and compared it to existing methods; the uniformisation scheme of Bean & O'Reilly (2013) and the discontinuous Galerkin scheme. In general, the numerical experiments show that, for problems with discontinuities, the DG approximation can exhibit oscillations, while the QBD-RAP and uniformisation approximations avoid this and, of the latter two, the QBD-RAP scheme often converges faster. To avoid the problems of oscillations we can sometimes employ a *slope limiter* with the DG scheme, which effectively reduces the scheme to linear in the regions where oscillations are detected. The numerical experiments demonstrate a loss of accuracy in the DG approximation when a slope limiter is used for a purely discontinuous problem. Moreover, for the application of the methods to fluid-fluid queues, there is no obvious way to apply the concept of a slope limiter. In general, we observe that the smoother the problem is the better the performance of the DG method, and it emphatically outperforms the other two methods.

As a first step in the numerical experiments, in Section 6.1, we examined the ability of each method to approximate different initial conditions. For the DG method, this is equivalent to a projection of the initial condition on to a set of basis polynomials. For the uniformisation method this is equivalent to projecting the initial condition on to a basis of constant functions. For the QBD-RAP method the approximation of the initial condition is as described in Sections 3.6 and 3.7. Section 6.1.2 demonstrates that the DG scheme (projection) can result in oscillations and negative regions in the approximation when the initial condition is discontinuous. The uniformisation and QBD-RAP methods avoid this problem, but appear to have higher errors and the QBD-RAP method appears to have the largest errors. For discontinuous initial conditions the rates of convergence are comparable for all three methods. However, when the initial condition to be approximated

is sufficiently smooth, then the DG approximation is superior.

Next, in Section 6.2, we instrumented the performance of approximations for a simple travelling wave problem with various initial conditions. For this problem the solution is given in terms of the initial condition by $f(x,t) = f(x-t,0)$. This model is useful as it allows us to instrument the ability of the methods to capture the flow of probability without stochastic dynamics. Once again, for discontinuous problems, the DG method can display oscillations, while the other methods (DG with slope limiter, uniformisation and QBD-RAP methods) avoid oscillations. Further, for discontinuous problems the rates of convergence of the QBD-RAP and DG methods can be similar. For smooth problems the DG method is superior. Interestingly, even though the QBD-RAP method performed worst for approximating initial conditions in the previous section, it outperformed the uniformisation method for this model, demonstrating that the QBD-RAP method can capture the dynamics of the flow of probability better than the uniformisation method.

We then instrumented the performance of the approximations on a simple fluid queue with two phases. First, in Section 6.3, we looked at the stationary distribution, which is known to be smooth. Since the problem is smooth, then the DG method was superior as expected. Of the uniformisation and QBD-RAP methods, the QBD-RAP method gives more accurate solutions. In Section 6.4 we turned our attention to approximating transient distributions for the same models and consider two different initial conditions, a point-mass and an exponential initial condition. The discontinuous initial condition results in a discontinuous transient distribution. As for the exponential initial condition, this example demonstrates that, even if the initial condition appears 'nice', it can still result in discontinuous, or non-differetiable solutions. The numerical evidence suggests that the DG method can display oscillations, while the other methods do not. The DG method with slope limiter detects the oscillations and reduces the method to linear. Of the uniformisation and QBD-RAP methods, the latter performs better.

Next, Section 6.5 looked at hitting times for the same fluid queue with two initial conditions, an exponential initial condition and a point-mass. We looked at the hitting time of the fluid level on the points $\{0\}$ and $\{1\}$. For this problem there is never any in-flow of mass at the boundaries of the interval and so, for a solution to be continuous, the initial condition needs to be chosen carefully, otherwise discontinuities in the transient distribution may result, as is the case for both initial conditions here. The numerical results suggest that, due to the discontinuities in the problems, the DG method may display oscillations. Since the uniformisation and QBD-RAP methods can handle discontinuities, they perform as expected, with the QBD-RAP method performing better than the uniformisation.

Lastly, we applied the DG, uniformisation and QBD-RAP methods to two simple fluid-fluid queues in Section 6.6. In the first fluid-fluid queue, which appears to have a smooth solution, the DG method performs very well. Of the two positivity preserving schemes the QBD-RAP scheme performs better than the uniformisation scheme. In the

second example, which has a discontinuity, the DG method produces the lowest errors, but exhibits oscillations in the solution. The QBD-RAP and uniformisation schemes do not produce oscillations and, of the two, the QBD-RAP method performs best.

In conclusion, when the problem is known to be smooth, the DG method is very likely to produce excellent results. However, for discontinuous problems, the method can show oscillations and infeasible or negative regions of the solution. The slope limiter overcomes this, but reduces the accuracy of the DG method to linear near discontinuities, sometimes severely affecting the quality of the approximation. The uniformisation and QBD-RAP methods are alternative approximation schemes which exhibit larger errors, but avoid oscillatory solutions and guarantee a non-decreasing approximation of the CDF. Of the uniformisation and QBD-RAP methods, the latter often to produced lower errors.

Appendix A

More mathematical background

A.1 Time-integration schemes

Appendix B

DG applied to a toy example

This appendix has been taken from Appendix 2 of Bean et al. (2022) with only minor changes, such as notations, so that this chapter is consistent with the rest of the thesis. I am a co-author of the paper Bean et al. (2022). The conceptualisation of Bean et al. (2022) was originally by Vikram Sunkara, Nigel Bean and Giang Nguyen, and the original coding was done by Vikram Sunkara. I made significant contributions to Section 3 of the paper, expressing the operator-theoretic expressions to use the same partition as the approximation scheme. I contributed Sections 4.4 and 5.1. I extended the numerical experiments in Section 6 to higher orders and made all the plots in Section 6. Appendix A is also my original work. I did a significant proportion of the writing of the manuscript and addressed the reviewers comments and also developed code for the numerical experiments.

Here we include a small toy example to show how we construct a DG approximation and to help clarify the notation.

Consider a process $\{(\overline{X}_t, Y_t, \varphi_t)\}_{t\geq 0}$ with two phases, $\varphi_t \in \mathcal{S} = \{1, 2\}$ and generator matrix $\boldsymbol{T}$. Let $\mathcal{I} = 1.8$, and partition into two intervals $\mathcal{D}_1 = [0, 1]$ and $\mathcal{D}_2 = [1, 1.8]$, hence $x_1 = 0$, $x_2 = 1$, $x_3 = 1.8$. We choose a basis of Lagrange polynomials of order 1 to define our approximation space. That is,

$$\begin{aligned} &\phi_1^1(x) = 1 - x, && \phi_2^1(x) = x, && x \in \mathcal{D}_1, \\ &\phi_1^2(x) = \frac{1.8 - x}{0.8}, && \phi_2^2(x) = \frac{x - 1}{0.8}, && x \in \mathcal{D}_2. \end{aligned}$$

The mesh and basis functions are shown in Figure 1. We can verify that the matrices $\boldsymbol{M}$

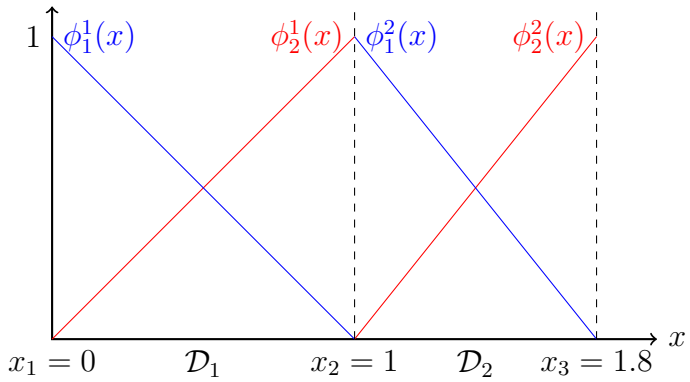

Figure 1: A mesh with nodes $x_1 = 0$, $x_2 = 1$ and $x_3 = 1.8$ and cells $\mathcal{D}_1 = [0, 1]$, $\mathcal{D}_2 = [1, 1.8]$. There are two basis functions on each cell. Point masses are located at $x_1 = 0$ and $x_3 = 1.8$.

and $\boldsymbol{G}$ are given by

$$\boldsymbol{M} = \left[\begin{array}{cc|cc} 1/3 & 1/6 & 0 & 0 \\ 1/6 & 1/3 & 0 & 0 \\ \hline 0 & 0 & 4/15 & 4/30 \\ 0 & 0 & 4/30 & 4/15 \end{array}\right], \quad \boldsymbol{G} = \left[\begin{array}{cc|cc} -1/2 & 1/2 & 0 & 0 \\ -1/2 & 1/2 & 0 & 0 \\ \hline 0 & 0 & -1/2 & 1/2 \\ 0 & 0 & -1/2 & 1/2 \end{array}\right].$$

The matrix $\boldsymbol{P}$ is given by

$$\boldsymbol{P} = \left[\begin{array}{cc|cc} 1/2 & 0 & 0 & 0 \\ 0 & 1/2 & 0 & 0 \\ \hline 0 & 0 & 2/5 & 0 \\ 0 & 0 & 0 & 2/5 \end{array}\right].$$

Let $c_1 = 1$ and $c_2 = -2$. Then the flux matrices are given by

$$\boldsymbol{F}_1 = \left[\begin{array}{cc|cc} 0 & 0 & 0 & 0 \\ 0 & -1 & 1 & 0 \\ \hline 0 & 0 & 0 & 0 \\ 0 & 0 & 0 & -1 \end{array}\right], \quad \boldsymbol{F}_2 = \left[\begin{array}{cc|cc} -1 & 0 & 0 & 0 \\ 0 & 0 & 0 & 0 \\ \hline 0 & 1 & -1 & 0 \\ 0 & 0 & 0 & 0 \end{array}\right].$$

Suppose that $r_1(x) > 0$ on $\mathcal{D}_1 = \mathcal{F}_1^+$ and $r_1(x) < 0$ on $\mathcal{D}_2 \cup \{1\} = \mathcal{F}_1^-$, and further, that $r_2(x) < 0$ on $\{0\} \cup \mathcal{D}_1 = \mathcal{F}_2^-$ and $r_2(x) > 0$ on $\mathcal{D}_2 = \mathcal{F}_2^+$. Specifically, let

$$r_1(x) = \begin{cases} 1 & x \in [0, 1], \\ -1 & x \in [1, 1.8], \end{cases} \quad r_2(x) = \begin{cases} -1 & x = 0, \\ -2 & x \in (0, 1], \\ 1 & x \in [1, 1.8]. \end{cases}$$

Then, constructing $\boldsymbol{B}$ we get

∇	$\mathcal{D}_1$				$\mathcal{D}_2$				Δ
$\mathcal{F}_2^-$	$\mathcal{F}_1^+$		$\mathcal{F}_2^-$		$\mathcal{F}_1^-$		$\mathcal{F}_2^+$		$\mathcal{F}_1^-$
$q_{\nabla,1}$	$a_{1,1}^1$	$a_{1,2}^1$	$a_{2,1}^1$	$a_{2,2}^1$	$a_{1,1}^2$	$a_{1,2}^2$	$a_{2,1}^2$	$a_{2,2}^2$	$q_{\Delta,1}$
T_{22}	$4T_{21}$	$-2T_{21}$	0	0	0	0	0	0	0
0	$T_{11}-3$	3	T_{12}	0	0	0	0	0	0
0	-1	$T_{11}-1$	0	T_{12}	5	-2.5	0	0	0
2	T_{21}	0	$T_{22}-2$	-2	0	0	0	0	0
0	0	T_{21}	6	$T_{22}-6$	0	0	0	0	0
0	0	0	0	0	$T_{11}-\frac{15}{4}$	$\frac{15}{4}$	T_{12}	0	0
0	0	0	0	0	$-\frac{5}{4}$	$T_{11}-\frac{5}{4}$	0	T_{12}	1
0	0	0	-4	8	T_{21}	0	$T_{22}-\frac{5}{2}$	$-\frac{5}{2}$	0
0	0	0	0	0	0	T_{21}	$\frac{15}{2}$	$T_{22}-\frac{15}{2}$	0
0	0	0	0	0	0	0	$-2T_{12}$	$4T_{12}$	T_{11}

We also have sub-matrices

$$\boldsymbol{B}_{11}^{++}=\begin{bmatrix} T_{11}-3 & 3 \\ -1 & T_{11}-1 \end{bmatrix},\ \boldsymbol{B}_{11}^{+-}=\left[\begin{array}{cc|c} 0 & 0 & 0 \\ 5 & -2.5 & 0 \end{array}\right],\ \boldsymbol{B}_{11}^{--}=\left[\begin{array}{cc|c} T_{11}-\frac{15}{2} & \frac{15}{2} & 0 \\ -\frac{5}{2} & T_{11}-\frac{5}{2} & 1 \\ \hline 0 & 0 & T_{11} \end{array}\right],$$

$$\boldsymbol{B}_{12}^{+-}=\left[\begin{array}{c|cc} 0 & T_{12} & 0 \\ 0 & 0 & T_{12} \end{array}\right],\ \boldsymbol{B}_{12}^{-+}=\left[\begin{array}{cc} T_{12} & 0 \\ 0 & T_{12} \\ \hline -2T_{12} & 4T_{12} \end{array}\right],$$

$$\boldsymbol{B}_{21}^{+-}=\left[\begin{array}{cc|c} T_{21} & 0 & 0 \\ 0 & T_{21} & 0 \end{array}\right],\ \boldsymbol{B}_{21}^{-+}=\left[\begin{array}{cc} 4T_{21} & -2T_{21} \\ \hline T_{21} & 0 \\ 0 & T_{21} \end{array}\right],$$

$$\boldsymbol{B}_{22}^{++}=\begin{bmatrix} T_{22}-\frac{5}{2} & -\frac{5}{2} \\ \frac{15}{2} & T_{22}-\frac{15}{2} \end{bmatrix},\ \boldsymbol{B}_{22}^{+-}=\left[\begin{array}{c|cc} 0 & -4 & 8 \\ 0 & 0 & 0 \end{array}\right],\ \boldsymbol{B}_{22}^{--}=\left[\begin{array}{c|cc} T_{22} & 0 & 0 \\ \hline 2 & T_{22}-2 & -2 \\ 0 & 6 & T_{22}-6 \end{array}\right],$$

and $\boldsymbol{B}_{11}^{-+}=\mathbf{0}_{3\times 2}$, $\boldsymbol{B}_{12}^{++}=\mathbf{0}_{2\times 2}$, $\boldsymbol{B}_{12}^{--}=\mathbf{0}_{2\times 3}$, $\boldsymbol{B}_{21}^{++}=\mathbf{0}_{2\times 2}$, $\boldsymbol{B}_{21}^{--}=\mathbf{0}_{3\times 3}$, $\boldsymbol{B}_{22}^{-+}=\mathbf{0}_{3\times 2}$, where $\mathbf{0}_{n\times m}$ denotes an $n\times m$ matrix of zeros. Furthermore,

$$\boldsymbol{B}^{++}=\left[\begin{array}{cc|cc} T_{11}-3 & 3 & 0 & 0 \\ -1 & T_{11}-1 & 0 & 0 \\ \hline 0 & 0 & T_{22}-\frac{5}{2} & -\frac{5}{2} \\ 0 & 0 & \frac{15}{2} & -\frac{15}{2} \end{array}\right],$$

$$\boldsymbol{B}^{+-}=\left[\begin{array}{c|cc|cc|c} 0 & T_{12} & 0 & 0 & 0 & 0 \\ 0 & 0 & T_{12} & 5 & -2.5 & 0 \\ \hline 0 & -4 & 8 & T_{21} & 0 & 0 \\ 0 & 0 & 0 & 0 & T_{21} & 0 \end{array}\right],$$

$$\boldsymbol{B}^{-+} = \left[\begin{array}{cc|cc} 4T_{21} & -2T_{21} & 0 & 0 \\ \hline T_{21} & 0 & 0 & 0 \\ 0 & T_{21} & 0 & 0 \\ \hline 0 & 0 & T_{12} & 0 \\ 0 & 0 & 0 & T_{12} \\ \hline 0 & 0 & -2T_{12} & 4T_{12} \end{array}\right],$$

$$\boldsymbol{B}^{--} = \left[\begin{array}{c|cc|cc|c} T_{22} & 0 & 0 & 0 & 0 & 0 \\ \hline 2 & T_{22}-2 & -2 & 0 & 0 & 0 \\ 0 & 6 & T_{22}-6 & 0 & 0 & 0 \\ \hline 0 & 0 & 0 & T_{11}-\frac{15}{4} & -\frac{15}{4} & 0 \\ 0 & 0 & 0 & -\frac{5}{4} & T_{11}-\frac{5}{4} & 1 \\ \hline 0 & 0 & 0 & 0 & 0 & T_{11} \end{array}\right].$$

Since $r_1(x)$ and $r_2(x)$ are constant on each cell then $\boldsymbol{R}^+$ and $\boldsymbol{R}^-$ take a particularly simple form. We have

$$\boldsymbol{R}^+ = \left[\begin{array}{cc|cc} 1 & 0 & 0 & 0 \\ 0 & 1 & 0 & 0 \\ \hline 0 & 0 & 1 & 0 \\ 0 & 0 & 0 & 1 \end{array}\right], \quad \boldsymbol{R}^- = \left[\begin{array}{c|cc|cc|c} 1 & 0 & 0 & 0 & 0 & 0 \\ \hline 0 & 1/2 & 0 & 0 & 0 & 0 \\ 0 & 0 & 1/2 & 0 & 0 & 0 \\ \hline 0 & 0 & 0 & 1 & 0 & 0 \\ 0 & 0 & 0 & 0 & 1 & 0 \\ \hline 0 & 0 & 0 & 0 & 0 & 1 \end{array}\right].$$

The DG approximations $\boldsymbol{D}^{mn}(s)$, $m, n \in \{+, -\}$ can now be constructed as

$$\boldsymbol{D}^{mn}(s) = \begin{cases} \boldsymbol{R}^m \left(\boldsymbol{B}^{mm} - s\boldsymbol{I}\right) & n = m, \\ \boldsymbol{R}^m \boldsymbol{B}^{mn} & n \neq m. \end{cases}$$

For a given value of s, we construct and solve the matrix Riccati equation,

$$\boldsymbol{D}^{+-}(s) + \boldsymbol{\Psi}(s)\boldsymbol{D}^{-+}(s)\Psi(s) + \boldsymbol{D}^{++}(s)\boldsymbol{\Psi}(s) + \boldsymbol{\Psi}(s)\boldsymbol{D}^{--}(s) = \boldsymbol{0},$$

for the matrix $\boldsymbol{\Psi}(s)$ using, for example, Newtons method (Bean et al. 2009*a*). To obtain the stationary distribution we require $\boldsymbol{\Psi}(0)$.

Now, to find $\boldsymbol{\xi}$, we solve the linear system in Equations (1.11)-(1.12). The result is a vector which we denote,

$$\boldsymbol{\xi} = \left[\begin{array}{c|cc|cc|c} \xi_2^{\nabla} & \xi_{2,1}^1 & \xi_{2,2}^1 & \xi_{1,1}^2 & \xi_{1,2}^2 & \xi_1^{\Delta} \end{array}\right],$$

where ξ_2^{∇} is an approximation to $\lim_{n\to\infty} \mathbb{P}\left(\overline{X}_{\theta_n} = 0, \varphi_{\theta_n} = 2\right)$ and ξ_1^{Δ} is an approximation to the artificial point mass $\lim_{n\to\infty} \mathbb{P}\left(\overline{X}_{\theta_n} = 1.8, \varphi_{\theta_n} = 1\right)$. For $x \in \mathcal{D}_1$ an approximation

to the density of $\lim_{n\to\infty} \mathbb{P}\left(\overline{X}_{\theta_n} \in \mathrm{d}x, \varphi_{\theta_n} = 2\right)$, is constructed as $\xi^1_{2,1}\phi^1_1(x) + \xi^1_{2,2}\phi^1_2(x)$. For $x \in \mathcal{D}_2$ an approximation to the density of $\lim_{n\to\infty} \mathbb{P}\left(\overline{X}_{\theta_n} \in \mathrm{d}x, \varphi_{\theta_n} = 1\right)$, is constructed as $\xi^2_{1,1}\phi^2_1(x) + \xi^2_{1,2}\phi^2_2(x)$.

Next, given a value of y, we solve the system (2.11)-(2.15) to find $\boldsymbol{p} = \boldsymbol{p}^-$ and $\boldsymbol{\pi}(y)$.

For the point masses we have

$$\boldsymbol{p}^- = \left[\ p_2^\nabla \ \middle|\ p^1_{2,1} \quad p^1_{2,2} \ \middle|\ p^2_{1,1} \quad p^2_{1,2} \ \middle|\ p_1^\Delta \ \right],$$

where p_2^∇ is an approximation to $\lim_{t\to\infty} \mathbb{P}\left(\overline{X}_t = 0, Y_t = 0, \varphi_t = 2\right)$ and p_1^Δ is an approximation to the artificial point mass $\lim_{t\to\infty} \mathbb{P}\left(\overline{X}_t = 1.8, Y_t = 0, \varphi_t = 1\right)$. For $x \in \mathcal{D}_1$, an approximation to the density of $\lim_{t\to\infty} \mathbb{P}\left(\overline{X}_t \in \mathrm{d}x, Y_t = 0, \varphi_t = 2\right)$, is constructed as $p^1_{2,1}\phi^1_1(x) + p^1_{2,2}\phi^1_2(x)$. For $x \in \mathcal{D}_2$, an approximation to the density of $\lim_{t\to\infty} \mathbb{P}\left(\overline{X}_t \in \mathrm{d}x, Y_t = 0, \varphi_t = 1\right)$, is constructed as $p^2_{1,1}\phi^2_1(x) + p^2_{1,2}\phi^2_2(x)$.

Similarly, for $\boldsymbol{\pi}^-(y)$, we have

$$\boldsymbol{\pi}^-(y) = \left[\ \pi_2^\nabla(y) \ \middle|\ \pi^1_{2,1}(y) \quad \pi^1_{2,2}(y) \ \middle|\ \pi^2_{1,1}(y) \quad \pi^2_{1,2}(y) \ \middle|\ \pi_1^\Delta(y) \ \right],$$

where $\pi_2^\nabla(y)$ is an approximation to $\lim_{t\to\infty} \mathbb{P}\left(\overline{X}_t = 0, Y_t \in \mathrm{d}y, \varphi_t = 2\right)$ and $\pi_1^\Delta(y)$ is an approximation to the artificial point mass $\lim_{t\to\infty} \mathbb{P}\left(\overline{X}_t = 1.8, Y_t \in \mathrm{d}y, \varphi_t = 1\right)$. For $x \in \mathcal{D}_1$ an approximation to the density of $\lim_{t\to\infty} \mathbb{P}\left(\overline{X}_t \in \mathrm{d}x, Y_t \in \mathrm{d}y, \varphi_t = 2\right)$, is constructed as $\pi^1_{2,1}(y)\phi^1_1(x) + \pi^1_{2,2}(y)\phi^1_2(x)$. For $x \in \mathcal{D}_2$ an approximation to the density of $\lim_{t\to\infty} \mathbb{P}\left(\overline{X}_t \in \mathrm{d}x, Y_t \in \mathrm{d}y, \varphi_t = 1\right)$ is constructed as $\pi^2_{1,1}(y)\phi^2_1(x) + \pi^2_{1,2}(y)\phi^2_2(x)$.

For $\boldsymbol{\pi}^+(y)$, we have

$$\boldsymbol{\pi}^+(y) = \left[\ \pi^1_{1,1}(y) \quad \pi^1_{1,2}(y) \ \middle|\ \pi^2_{2,1}(y) \quad \pi^2_{2,2}(y) \ \right].$$

For $x \in \mathcal{D}_1$ an approximation to the joint density of $\lim_{t\to\infty} \mathbb{P}\left(\overline{X}_t \in \mathrm{d}x, Y_t \in \mathrm{d}y, \varphi_t = 1\right)$ is constructed as $\pi^1_{1,1}(y)\phi^1_1(x) + \pi^1_{1,2}(y)\phi^1_2(x)$. For $x \in \mathcal{D}_2$ an approximation to the density of $\lim_{t\to\infty} \mathbb{P}\left(\overline{X}_t \in \mathrm{d}x, Y_t \in \mathrm{d}y, \varphi_t = 2\right)$ is constructed as $\pi^2_{2,1}(y)\phi^2_1(x) + \pi^2_{2,2}(y)\phi^2_2(x)$.

In summary, for $i \in \mathcal{S}$, a global approximation of the joint stationary distribution is

$$\begin{aligned}
\lim_{t\to\infty} \mathbb{P}\left(\overline{X}_t \in \mathrm{d}x, Y_t \in \mathrm{d}y, \varphi_t = i\right) &\approx \sum_{r\in\{1,2\},k\in\{1,2\}} \pi^k_{i,r}(y)\phi^k_r(x)\,\mathrm{d}x\,\mathrm{d}y, \quad x \in (0, 1.8),\ y > 0,\\
\lim_{t\to\infty} \mathbb{P}\left(\overline{X}_t \in \mathrm{d}x, Y_t = 0, \varphi_t = i\right) &\approx \sum_{r\in\{1,2\},k\in\{1,2\}} p^k_{i,r}\phi^k_r(x)\,\mathrm{d}x, \quad x \in (0, 1.8),\\
\lim_{t\to\infty} \mathbb{P}\left(\overline{X}_t = 0, Y_t \in \mathrm{d}y, \varphi_t = i\right) &\approx \pi_i^\nabla(y)\,\mathrm{d}y, \quad y > 0,\\
\lim_{t\to\infty} \mathbb{P}\left(\overline{X}_t = 0, Y_t = 0, \varphi_t = i\right) &\approx p_i^\nabla,
\end{aligned}$$

$$\lim_{t\to\infty} \mathbb{P}\left(\overline{X}_t = 1.8, Y_t \in \mathrm{d}y, \varphi_t = i\right) \approx \pi_i^{\Delta}(y)\,\mathrm{d}y, \quad y > 0,$$
$$\lim_{t\to\infty} \mathbb{P}\left(\overline{X}_t = 1.8, Y_t = 0, \varphi_t = i\right) \approx p_i^{\Delta}.$$

Appendix C

Properties of DG operator B

This appendix has been taken from Appendix 1 of Bean et al. (2022) with only minor changes, such as notations, so that this chapter is consistent with the rest of the thesis. I am a co-author of the paper Bean et al. (2022). The conceptualisation of Bean et al. (2022) was originally by Vikram Sunkara, Nigel Bean and Giang Nguyen, and the original coding was done by Vikram Sunkara. I made significant contributions to Section 3 of the paper, expressing the operator-theoretic expressions to use the same partition as the approximation scheme. I contributed Sections 4.4 and 5.1. I extended the numerical experiments in Section 6 to higher orders and made all the plots in Section 6. Appendix A is also my original work. I did a significant proportion of the writing of the manuscript and addressed the reviewers comments and also developed code for the numerical experiments.

Recall that the coefficients $\boldsymbol{a}_i^k(t)$ can be used to construct an approximate solution to a differential equation at time t as $u_i^k(x,t) = \boldsymbol{a}_i^k(t)\boldsymbol{\phi}^k(x)'$. For $i \in \mathcal{S}$, $k \in \{\nabla, 1, ..., K, \Delta\}$, $r \in \mathcal{N}_k$, define $\alpha_{i,r}^k(t) := a_{i,r}^k(t) \int_{x\in\mathcal{D}_k} \phi_r^k(x)\,\mathrm{d}x$, and row-vectors $\boldsymbol{\alpha}_i^k(t) = (\alpha_{i,r}^k(t))_{r\in\mathcal{N}_k}$. Motivated by the fact that we may be interested in approximations of the probabilities $\mathbb{P}(X(t) \in \mathcal{D}_k, \varphi(t) = i)$ rather than the function u_i^k itself, we can pose the problem equivalently in terms of the integrals

$$\mathbb{P}\left(X(t) \in \mathcal{D}_k, \varphi(t) = i\right) \approx \boldsymbol{a}_i^k(t) \int_{x\in\mathcal{D}_k} \boldsymbol{\phi}^k(x)'\,\mathrm{d}x = \boldsymbol{\alpha}_i^k(t)\mathbf{1}.$$

Define

$$\boldsymbol{\alpha}^k(t) = (\boldsymbol{\alpha}_i^k(t))_{i\in\mathcal{S}}, \text{ and } \boldsymbol{\alpha}(t) = (\boldsymbol{\alpha}^k(t)))_{k\in\{\nabla,1,...,K,\Delta\}},$$

and matrices

$$\boldsymbol{P}_k = \mathrm{diag}\left(\int_{x\in\mathcal{D}_k} \phi_r^k(x)\,\mathrm{d}x\right)_{r\in\mathcal{N}_k}, \; k \in \{1, ..., K\},$$

$$\boldsymbol{P} = \begin{bmatrix} \boldsymbol{I}_{N_{|\mathcal{S}|}} \otimes \boldsymbol{P}_1 & & \\ & \ddots & \\ & & \boldsymbol{I}_{N_{|\mathcal{S}|}} \otimes \boldsymbol{P}_K \end{bmatrix}.$$

By choosing the basis $\{\phi_r^k\}_{r\in\mathcal{N}_k,k\in\{1,\dots,K\}}$ such that $\int_{x\in\mathcal{D}_k}\phi_r^k(x)\,\mathrm{d}x \neq 0$ for all r,k, then $\boldsymbol{P}$ is invertible. This is the case for the Lagrange polynomials, but not, for example, for the Legendre polynomials. We can (loosely) interpret the new coefficients $\alpha_{i,r}^k(t)$ as representing the amount of probability captured by the basis function $\phi_r^k(x)$ in phase i.

The differential equation (2.9) can be equivalently expressed as $\dfrac{\mathrm{d}}{\mathrm{d}t}\boldsymbol{\alpha}(t) = \boldsymbol{\alpha}(t)\mathfrak{B}$, where

$$\mathfrak{B} = \begin{bmatrix} \boldsymbol{I}_{|\mathcal{S}_\nabla|} & & \\ & \boldsymbol{P}^{-1} & \\ & & \boldsymbol{I}_{|\mathcal{S}_\Delta|} \end{bmatrix} \boldsymbol{B} \begin{bmatrix} \boldsymbol{I}_{|\mathcal{S}_\nabla|} & & \\ & \boldsymbol{P} & \\ & & \boldsymbol{I}_{|\mathcal{S}_\Delta|} \end{bmatrix}.$$

Let

$$\begin{aligned}
\mathfrak{B}^{\nabla 1} &:= \boldsymbol{T}_{\nabla+} \otimes \left(\boldsymbol{\phi}^1(0)\boldsymbol{M}_1^{-1}\boldsymbol{P}_1\right), \\
\mathfrak{B}^{1\nabla} &:= -\mathrm{diag}(c_i\mathbb{1}_{(c_i<0)})_{i\in\mathcal{S}} \otimes \boldsymbol{P}_1^{-1}\boldsymbol{\phi}^1(0)', \\
\mathfrak{B}^{\Delta K} &:= \boldsymbol{T}_{\Delta-} \otimes \left(\boldsymbol{\phi}^K(\mathcal{I})\boldsymbol{M}_K^{-1}\boldsymbol{P}_K\right) \\
\mathfrak{B}^{K,\Delta} &:= \mathrm{diag}(c_i\mathbb{1}_{(c_i>0)})_{i\in\mathcal{S}} \otimes \boldsymbol{P}_K^{-1}\boldsymbol{\phi}^K(\mathcal{I})',
\end{aligned}$$

$$\mathfrak{B}_{ij}^{kk} := \begin{cases} T_{ii}\boldsymbol{I}_{N_k} + c_i\boldsymbol{P}_k^{-1}(\boldsymbol{F}_i^{kk} + \boldsymbol{G}_k)\boldsymbol{M}_k^{-1}\boldsymbol{P}_k & i=j, \\ T_{ij}\boldsymbol{I}_{N_k} & i\neq j, \end{cases} \quad \text{for } k = 1,\dots K,$$

$$\mathfrak{B}_{ij}^{k,k+1} := \begin{cases} c_i\boldsymbol{P}_k^{-1}\boldsymbol{F}_i^{k,k+1}\boldsymbol{M}_{k+1}^{-1}\boldsymbol{P}_{k+1} & i=j, \\ \boldsymbol{0}_{N_k} & i\neq j, \end{cases} \quad \text{for } k = 1,\dots K-1,$$

$$\mathfrak{B}_{ij}^{k-1,k} := \begin{cases} c_i\boldsymbol{P}_k^{-1}\boldsymbol{F}_i^{k,k-1}\boldsymbol{M}_{k-1}^{-1}\boldsymbol{P}_{k-1} & i=j, \\ T_{ij}\boldsymbol{I}_{N_k} & i\neq j, \end{cases}, \quad \text{for } k = 2,\dots K,$$

$$\mathfrak{B}^{kk} =: \begin{bmatrix} \mathfrak{B}_{11}^{kk} & \dots & \mathfrak{B}_{1N_\mathcal{S}}^{kk} \\ \vdots & \ddots & \vdots \\ \mathfrak{B}_{N_\mathcal{S}1}^{kk} & \dots & \mathfrak{B}_{N_\mathcal{S},N_\mathcal{S}}^{kk} \end{bmatrix}, \text{ for } k = 1,\dots K,$$

$$\mathfrak{B}^{k,k+1} =: \begin{bmatrix} \mathfrak{B}_{1,1}^{k,k+1} & \dots & \mathfrak{B}_{1,N_\mathcal{S}}^{k,k+1} \\ \vdots & \ddots & \vdots \\ \mathfrak{B}_{N_\mathcal{S},1}^{k,k+1} & \dots & \mathfrak{B}_{N_\mathcal{S},N_\mathcal{S}}^{k,k+1} \end{bmatrix}, \text{ for } k = 1,\dots K-1,$$

$$\mathfrak{B}^{k,k-1} =: \begin{bmatrix} \mathfrak{B}_{1,1}^{k,k-1} & \dots & \mathfrak{B}_{1,N_\mathcal{S}}^{k,k-1} \\ \vdots & \ddots & \vdots \\ \mathfrak{B}_{N_\mathcal{S},1}^{k,k-1} & \dots & \mathfrak{B}_{N_\mathcal{S},N_\mathcal{S}}^{k,k-1} \end{bmatrix}, \text{ for } k = 2,\dots K.$$

Then

$$\mathfrak{B} = \begin{bmatrix} \boldsymbol{T}_{\nabla\nabla} & \mathfrak{B}^{\nabla 1} & & & & & \\ \mathfrak{B}^{1\nabla} & \mathfrak{B}^{11} & \mathfrak{B}^{12} & & & & \\ & \mathfrak{B}^{21} & \mathfrak{B}^{22} & \mathfrak{B}^{23} & & & \\ & & \ddots & \ddots & \ddots & & \\ & & \mathfrak{B}^{K-1,K-2} & \mathfrak{B}^{K-1,K-1} & \mathfrak{B}^{K-1,K} & & \\ & & & \mathfrak{B}^{K,K-1} & \mathfrak{B}^{K,K} & \mathfrak{B}^{K,\Delta} & \\ & & & & \mathfrak{B}^{\Delta,K} & \boldsymbol{T}_{\Delta\Delta} \end{bmatrix}.$$

Remark C.1. *One may recognise the structure of $\mathfrak{B}$ as the structure of a quasi-birth-and-death process (QBD), with levels $k = 1, ..., K$. This raises the question of whether $\mathfrak{B}$ is indeed a representation of the generator matrix of a QBD, or QBD-like process. In the case of a constant basis function on each cell, i.e. $N_k = 1$ and $\phi_1^k(x) \propto 1$, $k = 1, ..., K$, then $\mathfrak{B}$ is the generator of a QBD: it has zero row-sums, negative diagonal entires, and non-negative off-diagonal entries, the QBD-phase variable is $\{\varphi_t\}$ and the level is $k = \nabla, 1, ..., K, \Delta$. In fact, if h_k is the same for every $k = 1, ..., K$, then this is the same QBD discretisation of a stochastic fluid process analysed by Bean & O'Reilly (2013). However, for higher-degree polynomials $\mathfrak{B}$ is not necessarily the generator of a QBD process. We conjecture that, using polynomial basis functions, then $N_k = 1$ and $\phi_1^k(x) \propto 1$, $k = 1, ..., K$ is the only DG approximation which has an interpretation as a QBD-like process – not even as a QBD-RAP (Bean & Nielsen 2010).*

In the following lemma, we use the following properties of the Lagrange interpolating polynomials defined by the Gauss-Lobatto quadrature nodes.

Property 1 $\displaystyle\sum_{s=1}^{N_k} \phi_s^k(x) = \begin{cases} 1 & x \in \mathcal{D}_k, \\ 0 & x \notin \mathcal{D}_k. \end{cases}$

For $k \in \{1, ..., K\}$, let $\boldsymbol{e}_n^k$ be a row-vector of length N_k with a 1 in the nth position and zeros elsewhere.

Property 2 At the cell edges, $\boldsymbol{\phi}^k(x_k) = \boldsymbol{e}_1^k$ and $\boldsymbol{\phi}^k(x_{k+1}) = \boldsymbol{e}_{N_k}^k$, $k = 1, ..., K$.

Lemma C.2. *If $\{\phi_r^k(x)\}_{r\in\mathcal{N}_k}$, are chosen as the Lagrange interpolating polynomials on $\mathcal{D}_k$, $k \in \{1, \ldots, K\}$, then the matrix $\mathfrak{B}$ has zero row-sums.*

Proof. Let $\mathbf{1}$ and $\mathbf{0}$ be column vectors of ones and zeros, respectively, with an appropriate length depending on the context. Using Property 1, observe that

$$\boldsymbol{M}_k \mathbf{1} = \left(\sum_{s=1}^{N_k} \int_{x\in\mathcal{D}_k} \phi_r^k(x)\phi_s^k(x)\,\mathrm{d}x \right)'_{r\in\mathcal{N}_k}$$

$$
\begin{aligned}
&= \left(\int_{x\in\mathcal{D}_k} \phi_r^k(x) \sum_{s=1}^{N_k} \phi_s^k(x)\,\mathrm{d}x \right)'_{r\in\mathcal{N}_k} \\
&= \left(\int_{x\in\mathcal{D}_k} \phi_r^k(x)\,\mathrm{d}x \right)'_{r\in\mathcal{N}_k} \\
&= \boldsymbol{P}_k\mathbf{1},
\end{aligned}
$$

hence $\boldsymbol{M}_k^{-1}\boldsymbol{P}_k\mathbf{1} = \mathbf{1}$. Also

$$
\begin{aligned}
\boldsymbol{G}_k\mathbf{1} &= \left(\sum_{s=1}^{N_k} \int_{x\in\mathcal{D}_k} \phi_r^k(x) \frac{\mathrm{d}}{\mathrm{d}x}\phi_s^k(x)\,\mathrm{d}x \right)'_{r\in\mathcal{N}_k} \\
&= \left(\int_{x\in\mathcal{D}_k} \phi_r^k(x) \frac{\mathrm{d}}{\mathrm{d}x} \sum_{s=1}^{N_k} \phi_s^k(x)\,\mathrm{d}x \right)'_{r\in\mathcal{N}_k} \\
&= \left(\int_{x\in\mathcal{D}_k} \phi_r^k(x) \frac{\mathrm{d}}{\mathrm{d}x} 1\,\mathrm{d}x \right)'_{r\in\mathcal{N}_k} \\
&= \mathbf{0},
\end{aligned}
$$

where we have again used Property 1.

Consider first $c_i > 0$. Let $\boldsymbol{b}$ and $\boldsymbol{d}$ be arbitrary row-vectors of length N_k and N_{k+1}, respectively. By Property 2, for $k = 1, ..., K-1$,

$$
\begin{aligned}
\boldsymbol{F}_i^{kk}\boldsymbol{b} &= -\boldsymbol{\phi}^k(x_{k+1})'\boldsymbol{\phi}^k(x_{k+1})\boldsymbol{b} \\
&= -(\boldsymbol{e}_{N_k}^k)'\boldsymbol{e}_{N_k}^k\boldsymbol{b} \\
&= -b_{N_k}(\boldsymbol{e}_{N_k}^k)', \\
\boldsymbol{F}_i^{k,k+1}\boldsymbol{d} &= \boldsymbol{\phi}^k(x_{k+1})'\boldsymbol{\phi}^{k+1}(x_{k+1})\boldsymbol{d} \\
&= (\boldsymbol{e}_{N_k}^k)'\boldsymbol{e}_1^{k+1}\boldsymbol{d} \\
&= d_1(\boldsymbol{e}_{N_k}^k)'.
\end{aligned}
$$

Therefore, for $c_i > 0$, we claim

$$
\sum_{j\in\mathcal{S}} T_{ij}\boldsymbol{I}_{N_k}\mathbf{1} + c_i\boldsymbol{P}_k^{-1}(\boldsymbol{F}_i^{kk} + \boldsymbol{G}_k)\boldsymbol{M}_k^{-1}\boldsymbol{P}_k\mathbf{1} + c_i\boldsymbol{P}_k^{-1}\boldsymbol{F}_i^{k,k+1}\boldsymbol{M}_k^{-1}\boldsymbol{P}_k\mathbf{1} = \mathbf{0}.
$$

The first sum is zero since $\boldsymbol{T}$ is a generator of a continuous-time Markov chain. This leaves the other two terms, which, using our previous observations, we get

$$
c_i\boldsymbol{P}_k^{-1}(\boldsymbol{F}_i^{kk} + \boldsymbol{G}_k)\boldsymbol{M}_k^{-1}\boldsymbol{P}_k\mathbf{1} + c_i\boldsymbol{P}_k^{-1}\boldsymbol{F}_i^{k,k+1}\boldsymbol{M}_{k+1}^{-1}\boldsymbol{P}_{k+1}\mathbf{1}
$$

$$
\begin{aligned}
&= c_i \boldsymbol{P}_k^{-1}(\boldsymbol{F}_i^{kk} + \boldsymbol{G}_k)\mathbf{1} + c_i \boldsymbol{P}_k^{-1}\boldsymbol{F}_i^{k,k+1}\mathbf{1} \\
&= c_i \boldsymbol{P}_k^{-1}\boldsymbol{F}_i^{kk}\mathbf{1} + c_i \boldsymbol{P}_k^{-1}\boldsymbol{G}_k\mathbf{1} + c_i \boldsymbol{P}_k^{-1}F_i^{k,k+1}\mathbf{1} \\
&= c_i \boldsymbol{P}_k^{-1}(-\boldsymbol{e}_{N_k}^k)' + \mathbf{0} + c_i \boldsymbol{P}_k^{-1}(\boldsymbol{e}_{N_k}^k)' \\
&= \mathbf{0}.
\end{aligned}
$$

Similarly, for $c_i < 0$, and row-vectors $\boldsymbol{b}$ and $\boldsymbol{d}$ of length N_k and N_{k-1}, respectively,

$$
\begin{aligned}
\boldsymbol{F}_i^{kk}\boldsymbol{b} &= \boldsymbol{\phi}^k(x_k)'\boldsymbol{\phi}^k(x_k)\boldsymbol{b} \\
&= (\boldsymbol{e}_1^k)'\boldsymbol{e}_1^k\boldsymbol{b} \\
&= b_1(\boldsymbol{e}_1^k)' \\
\boldsymbol{F}_i^{k,k-1}\boldsymbol{d} &= -\boldsymbol{\phi}^k(x_k)'\boldsymbol{\phi}^{k-1}(x_k)\boldsymbol{d} \\
&= -(\boldsymbol{e}_1^k)'\boldsymbol{e}_{N_{k-1}}^{k-1}\boldsymbol{d} \\
&= -d_{N_{k-1}}(\boldsymbol{e}_1^k)'.
\end{aligned}
$$

Therefore, for $c_i < 0$ and $k = 2, ..., K$, using the same arguments as before we have

$$
\begin{aligned}
&\sum_{j\in\mathcal{S}} T_{ij}\boldsymbol{I}_{N_k}\mathbf{1} + c_i \boldsymbol{P}_k^{-1}(\boldsymbol{F}_i^{kk} + \boldsymbol{G}_k)\boldsymbol{M}_k^{-1}\boldsymbol{P}_k\mathbf{1} + c_i \boldsymbol{P}_k^{-1}\boldsymbol{F}_i^{k,k-1}\boldsymbol{M}_k^{-1}\boldsymbol{P}_k\mathbf{1} \\
&= \mathbf{0} + c_i \boldsymbol{P}_k^{-1}(\boldsymbol{F}_i^{kk} + \boldsymbol{G}_k)\boldsymbol{M}_k^{-1}\boldsymbol{P}_k\mathbf{1} + c_i \boldsymbol{P}_k^{-1}\boldsymbol{F}_i^{k,k+1}\boldsymbol{M}_{k-1}^{-1}\boldsymbol{P}_{k-1}\mathbf{1} \\
&= c_i \boldsymbol{P}_k^{-1}(\boldsymbol{F}_i^{kk} + \boldsymbol{G}_k)\mathbf{1} + c_i \boldsymbol{P}_k^{-1}\boldsymbol{F}_i^{k,k-1}\mathbf{1} \\
&= c_i \boldsymbol{P}_k^{-1}\boldsymbol{F}_i^{kk}\mathbf{1} + c_i \boldsymbol{P}_k^{-1}\boldsymbol{G}_k\mathbf{1} + c_i \boldsymbol{P}_k^{-1}\boldsymbol{F}_i^{k,k-1}\mathbf{1} \\
&= c_i \boldsymbol{P}_k^{-1}(\boldsymbol{e}_1^k)' + \mathbf{0} + c_i \boldsymbol{P}_k^{-1}(-\boldsymbol{e}_1^k)' \\
&= \mathbf{0}.
\end{aligned}
$$

For the lower boundary,

$$
\boldsymbol{T}_{\nabla\nabla}\mathbf{1} + \mathfrak{B}^{\nabla 1}\mathbf{1} = \boldsymbol{T}_{\nabla\nabla}\mathbf{1} + \left[\boldsymbol{T}_{\nabla+} \otimes \left(\boldsymbol{\phi}^1(0)\boldsymbol{M}_1^{-1}\boldsymbol{P}_1\right)\right]\mathbf{1}.
$$

Swapping the order of summation and recalling $\boldsymbol{M}_k^{-1}\boldsymbol{P}_k\mathbf{1} = \mathbf{1}$ then this is equal to

$$
\begin{aligned}
&\boldsymbol{T}_{\nabla\nabla}\mathbf{1} + \left[\boldsymbol{T}_{\nabla+} \otimes \left(\boldsymbol{\phi}^1(0)\boldsymbol{M}_1^{-1}\boldsymbol{P}_1\right)\mathbf{1}\right]\mathbf{1} \\
&= \boldsymbol{T}_{\nabla\nabla}\mathbf{1} + \left[\boldsymbol{T}_{\nabla+} \otimes \boldsymbol{e}_1^1\mathbf{1}\right]\mathbf{1} \\
&= \boldsymbol{T}_{\nabla\nabla}\mathbf{1} + \left[\boldsymbol{T}_{\nabla+} \otimes \mathbf{1}\right]\mathbf{1} \\
&= \boldsymbol{T}_{\nabla\nabla}\mathbf{1} + \boldsymbol{T}_{\nabla+}\mathbf{1} \\
&= \mathbf{0}.
\end{aligned}
$$

Also, for $c_i < 0$,

$$
-c_i \boldsymbol{P}_1^{-1}\boldsymbol{\phi}^1(0)' + c_i \boldsymbol{P}_1^{-1}(\boldsymbol{F}_i^{1,1} + \boldsymbol{G}_k)\boldsymbol{M}_1^{-1}\boldsymbol{P}_1\mathbf{1} = -c_i \boldsymbol{P}_1^{-1}\boldsymbol{\phi}^1(0)' + c_i \boldsymbol{P}_1^{-1}(\boldsymbol{F}_i^{1,1} + \boldsymbol{G}_k)\mathbf{1}
$$

$$
\begin{aligned}
&= -c_i \boldsymbol{P}_1^{-1} \boldsymbol{\phi}^1(0)' + c_i \boldsymbol{P}_1^{-1} \boldsymbol{F}_i^{1,1} \mathbf{1} \\
&= -c_i \boldsymbol{P}_1^{-1} (\boldsymbol{e}_1^1)' + c_i \boldsymbol{P}_1^{-1} (\boldsymbol{e}_1^1)' \\
&= \mathbf{0}.
\end{aligned}
$$

For the upper boundary,

$$
\boldsymbol{T}_{\Delta\Delta}\mathbf{1} + \mathfrak{B}^{\Delta K}\mathbf{1} = \boldsymbol{T}_{\Delta\Delta}\mathbf{1} + [\boldsymbol{T}_{\Delta-} \otimes (\boldsymbol{\phi}^K(\mathcal{I}) \boldsymbol{M}_K^{-1} \boldsymbol{P}_K)]\mathbf{1}.
$$

Swapping the order of summation and recalling $\boldsymbol{M}_k^{-1}\boldsymbol{P}_k\mathbf{1} = \mathbf{1}$ then this is equal to

$$
\begin{aligned}
\boldsymbol{T}_{\Delta\Delta}\mathbf{1} + [\boldsymbol{T}_{\Delta-} \otimes (\boldsymbol{\phi}^K(\mathcal{I}) \boldsymbol{M}_K^{-1} \boldsymbol{P}_K)\mathbf{1}]\mathbf{1} &= \boldsymbol{T}_{\Delta\Delta}\mathbf{1} + [\boldsymbol{T}_{\Delta-} \otimes \boldsymbol{e}_{N_K}^K \mathbf{1}]\mathbf{1} \\
&= \boldsymbol{T}_{\Delta\Delta}\mathbf{1} + [\boldsymbol{T}_{\Delta-} \otimes \boldsymbol{e}_{N_K}^K]\mathbf{1} \\
&= \boldsymbol{T}_{\Delta\Delta}\mathbf{1} + \boldsymbol{T}_{\Delta-}\mathbf{1} \\
&= \mathbf{0}.
\end{aligned}
$$

Also, for $c_i > 0$,

$$
\begin{aligned}
c_i \boldsymbol{P}_K^{-1} \boldsymbol{\phi}^K(\mathcal{I})' + c_i \boldsymbol{P}_K^{-1} (\boldsymbol{F}_i^{K,K} + \boldsymbol{G}_K) \boldsymbol{M}_K^{-1} \boldsymbol{P}_K \mathbf{1} &= c_i \boldsymbol{P}_K^{-1} \boldsymbol{\phi}^K(\mathcal{I})' + c_i \boldsymbol{P}_K^{-1} (\boldsymbol{F}_i^{K,K} + \boldsymbol{G}_K)\mathbf{1} \\
&= c_i \boldsymbol{P}_K^{-1} \boldsymbol{\phi}^K(\mathcal{I})' + c_i \boldsymbol{P}_K^{-1} \boldsymbol{F}_i^{K,K} \mathbf{1} \\
&= c_i \boldsymbol{P}_K^{-1} (\boldsymbol{e}_{N_K}^K)' + c_i \boldsymbol{P}_K^{-1} (-\boldsymbol{e}_{N_K}^K)' \\
&= \mathbf{0}.
\end{aligned}
$$

Combining all of the above we have shown that the row sums of $\mathfrak{B}$ are zero. □

Corollary C.3. *The DG approximation to the generator $\boldsymbol{B}$ conserves probability. That is, for all $t \geq 0$,*

$$
\begin{aligned}
&\sum_{i \in \mathcal{S}_\nabla} q_{\nabla,i}(t) + \sum_{i \in \mathcal{S}_\Delta} q_{\Delta,i}(t) + \sum_{i \in \mathcal{S}} \int_{x \in [0,\mathcal{I}]} u_i(x,t)\, \mathrm{d}x \\
&= \sum_{i \in \mathcal{S}_\nabla} q_{\nabla,i}(0) + \sum_{i \in \mathcal{S}_\Delta} q_{\Delta,i}(0) + \sum_{i \in \mathcal{S}} \int_{x \in [0,\mathcal{I}]} u_i(x,0)\, \mathrm{d}x.
\end{aligned}
$$

Proof. Let $\{\psi_r^k(x)\}_{r \in \mathcal{N}_k, k \in \{1,\ldots,K\}}$, be a basis for $span(\phi_r^k(x), r \in \mathcal{N}_k, k \in \{1,\ldots,K\})$, where $\{\phi_r^k(x)\}_{r \in \mathcal{N}_k, k \in \{1,\ldots,K\}}$ are the Lagrange polynomials. Also define $\psi_1^\nabla(x) = \delta(x)$ and $\psi_1^\Delta(x) = \delta(x - \mathcal{I})$ to capture the point masses at the boundaries. Let us use the same vector notation for the basis $\psi_r^k(x)$ as we do for $\phi_r^k(x)$. For $k \in \{1,\ldots,K\}$, since $\{\psi_r^k(x)\}_{r \in \mathcal{N}_k}$ and $\{\phi_r^k(x)\}_{r \in \mathcal{N}_k}$ have the same span, then there is a matrix $\boldsymbol{V}^k$ such that $\boldsymbol{\psi}^k(x)' = \boldsymbol{V}^k \boldsymbol{\phi}^k(x)'$. Trivially, this also holds for $k = \nabla, \Delta$.

Let

$$\boldsymbol{W} = \begin{bmatrix} \boldsymbol{I}_{|\mathcal{S}_\nabla|} & & \\ & \boldsymbol{P} & \\ & & \boldsymbol{I}_{|\mathcal{S}_\Delta|} \end{bmatrix} \text{ and } \boldsymbol{V} = \begin{bmatrix} \boldsymbol{I}_{|\mathcal{S}_\nabla|} & & & & \\ & \boldsymbol{V}^1 & & & \\ & & \ddots & & \\ & & & \boldsymbol{V}^K & \\ & & & & \boldsymbol{I}_{|\mathcal{S}_\Delta|} \end{bmatrix}.$$

For a DG approximation, $\boldsymbol{B}$, constructed from $\{\psi_r^k\}_{r\in\mathcal{N}_k,k\in\{\nabla,1,\ldots,K,\Delta\}}$, it can be shown that $\boldsymbol{B}$ is similar to $\mathfrak{B}$ with similarity matrix, $\boldsymbol{VW}$, such that $\boldsymbol{B}_{ij} = \boldsymbol{VW}\mathfrak{B}_{ij}\boldsymbol{W}^{-1}\boldsymbol{V}^{-1}$, $i,j \in \mathcal{S}$. Therefore

$$\begin{aligned} \int_{x\in[0,\mathcal{I}]} \boldsymbol{B}_{ij}\boldsymbol{\psi}(x)'\,\mathrm{d}x &= \boldsymbol{VW}\mathfrak{B}_{ij}\boldsymbol{W}^{-1}\boldsymbol{V}^{-1}\int_{x\in[0,\mathcal{I}]} \boldsymbol{V}\boldsymbol{\phi}(x)'\,\mathrm{d}x \\ &= \boldsymbol{VW}\mathfrak{B}_{ij}\boldsymbol{W}^{-1}\boldsymbol{W}\boldsymbol{1} \\ &= \boldsymbol{VW}\mathfrak{B}_{ij}\boldsymbol{1}, \end{aligned}$$

since $\displaystyle\int_{x\in[0,\mathcal{I}]} \boldsymbol{\phi}(x)'\,\mathrm{d}x = \boldsymbol{W}\boldsymbol{1}$. The row sums of $\mathfrak{B}$ are 0, hence

$$\begin{aligned} \int_{x\in[0,\mathcal{I}]} \sum_{j\in\mathcal{S}} \boldsymbol{B}_{ij}\boldsymbol{\psi}(x)'\,\mathrm{d}x &= \boldsymbol{VW}\sum_{j\in\mathcal{S}}\mathfrak{B}_{ij}\boldsymbol{1} && \text{(C.1)} \\ &= \boldsymbol{VW}\boldsymbol{0} && \text{(C.2)} \\ &= \boldsymbol{0}. && \text{(C.3)} \end{aligned}$$

Let ${}^{\psi}\boldsymbol{a}_i(t)$, $i \in \mathcal{S}$ denote the coefficients related to the DG approximation constructed with the basis $\{\psi_r^k\}_{r\in\mathcal{N}_k,k\in\{\nabla,1,\ldots,K,\Delta\}}$ (to distinguish them from $\boldsymbol{a}$ and $\boldsymbol{\alpha}$ used above). The DE constructed by the DG method is

$$\frac{\mathrm{d}}{\mathrm{d}t}\left({}^{\psi}\boldsymbol{a}_j(t)\right)\boldsymbol{\psi}(x) = \sum_{i\in\mathcal{S}}\left({}^{\psi}\boldsymbol{a}_i(t)\right)\boldsymbol{B}_{ij}\boldsymbol{\psi}(x).$$

Integrating over $x \in [0,\mathcal{I}]$ and summing over $j \in \mathcal{S}$ we get

$$\int_{x\in[0,\mathcal{I}]}\sum_{j\in\mathcal{S}}\frac{\mathrm{d}}{\mathrm{d}t}\left({}^{\psi}\boldsymbol{a}_j(t)\right)\boldsymbol{\psi}(x)\,\mathrm{d}x = \int_{x\in[0,\mathcal{I}]}\sum_{j\in\mathcal{S}}\sum_{i\in\mathcal{S}}\left({}^{\psi}\boldsymbol{a}_i(t)\right)\boldsymbol{B}_{ij}\boldsymbol{\psi}(x).$$

Exchanging the order of operations gives

$$\frac{\mathrm{d}}{\mathrm{d}t}\sum_{j\in\mathcal{S}}\left({}^{\psi}\boldsymbol{a}_j(t)\right)\int_{x\in[0,\mathcal{I}]}\boldsymbol{\psi}(x)\,\mathrm{d}x = \sum_{i\in\mathcal{S}}\left({}^{\psi}\boldsymbol{a}_i(t)\right)\int_{x\in[0,\mathcal{I}]}\sum_{j\in\mathcal{S}}\boldsymbol{B}_{ij}\boldsymbol{\psi}(x)\,\mathrm{d}x = 0, \qquad \text{(C.4)}$$

where the right-hand side is 0 due to Equation (C.1). This holds for all $t \geq 0$. The left-hand side of (C.4) is the rate of change (with respect to time) of the total mass of the system. Since this is 0 for all $t \geq 0$, there is no change in the total mass of the system and thus probability is conserved. □

Appendix D

Properties of closing operators

This appendix is dedicated to proving that the closing operators in (3.20), (3.21), and (3.23) have the Properties 4.2, which we recall below, for convenience.

Properties 4.2. *Let $\{\boldsymbol{v}^{(p)}(x)\}_{p\geq 1}$ be a sequence of closing operators such that they may be decomposed into $\boldsymbol{v}^{(p)}(x) = \boldsymbol{w}^{(p)}(x) + \widetilde{\boldsymbol{w}}^{(p)}(x)$, where;*
(i) for $x \in [0, \Delta), u, v \geq 0$,

$$\boldsymbol{\alpha}^{(p)} e^{\boldsymbol{S}^{(p)}(u+v)} (-\boldsymbol{S}^{(p)})^{-1} \widetilde{\boldsymbol{w}}^{(p)}(x) \leq \boldsymbol{\alpha}^{(p)} e^{\boldsymbol{S}^{(p)}u} (-\boldsymbol{S}^{(p)})^{-1} \widetilde{\boldsymbol{w}}^{(p)}(x).$$

(ii) for $x \in [0, \Delta), u \geq 0$,

$$\boldsymbol{\alpha}^{(p)} e^{\boldsymbol{S}^{(p)}u} (-\boldsymbol{S}^{(p)})^{-1} \widetilde{\boldsymbol{w}}^{(p)}(x) = \widetilde{G}_{\boldsymbol{v}}^{(p)} \to 0, \quad \text{as } p \to \infty.$$

(iii) for $x \in [0, \Delta), u \geq 0$,

$$\boldsymbol{\alpha}^{(p)} e^{\boldsymbol{S}^{(p)}u} (-\boldsymbol{S}^{(p)})^{-1} \boldsymbol{w}^{(p)}(x) \leq \boldsymbol{\alpha}^{(p)} e^{\boldsymbol{S}^{(p)}u} \boldsymbol{e} G_{\boldsymbol{v}},$$

for some $0 \leq G_{\boldsymbol{v}} < \infty$ independent of p for $p > p_0$ where $p_0 < \infty$.
(iv) for $\boldsymbol{a} \in \mathcal{A}$, $u \geq 0$,

$$\int_{x\in[0,\Delta)} \boldsymbol{a}^{(p)} e^{\boldsymbol{S}^{(p)}u} \boldsymbol{v}^{(p)}(x)\, \mathrm{d}x \leq \boldsymbol{a}^{(p)} e^{\boldsymbol{S}^{(p)}u} \boldsymbol{e}.$$

(v) Let g be a function satisfying the Assumptions 4.1. For $u \leq \Delta - \varepsilon^{(p)}$, $v \in [0, \Delta)$, then

$$\left| \int_{x=0}^{\infty} \frac{\boldsymbol{\alpha}^{(p)} e^{\boldsymbol{S}^{(p)}(u+x)}}{\boldsymbol{\alpha}^{(p)} e^{\boldsymbol{S}^{(p)}u} \boldsymbol{e}} \boldsymbol{v}^{(p)}(v) g(x)\, \mathrm{d}x - g(\Delta - u - v) 1(u + v \leq \Delta - \varepsilon^{(p)}) \right| = |r_{\boldsymbol{v}}^{(p)}(u, v)|,$$

where

$$\int_{u=0}^{\Delta} \left| r_{\boldsymbol{v}}^{(p)}(u, v) \right| \, \mathrm{d}u \leq R_{\boldsymbol{v},1}^{(p)} \to 0$$

and

$$\int_{v=0}^{\Delta} \left| r_{\boldsymbol{v}}^{(p)}(u,v) \right| \, \mathrm{d}v \leq R_{\boldsymbol{v},2}^{(p)} \to 0$$

as $\mathrm{Var}(Z^{(p)}) \to 0$.

B.1 The closing operator $\boldsymbol{v}(x) = e^{\boldsymbol{S}x}\boldsymbol{s}$

For the closing operator $\boldsymbol{v}(x) = e^{\boldsymbol{S}x}\boldsymbol{s}$ we may set $\widetilde{\boldsymbol{w}}(x) = \boldsymbol{0}$, so Properties 4.2($i$) and 4.2($ii$) hold trivially.

Lemma B.1. *The closing operator* $\boldsymbol{v}(x) = e^{\boldsymbol{S}x}\boldsymbol{s}$ *has Property 4.2(iii).*

For any valid orbit, $\boldsymbol{a} \in \mathcal{A}$, $x, u \geq 0$,

$$\int_{x_n=0}^{\infty} \boldsymbol{a} e^{\boldsymbol{S}(x_n+u)}\boldsymbol{s} = \boldsymbol{a} e^{\boldsymbol{S}(u)}\boldsymbol{e}.$$

Proof. For any valid orbit, $\boldsymbol{a} \in \mathcal{A}$,

$$\boldsymbol{a} e^{\boldsymbol{S}(x+u)}\boldsymbol{e} = \mathbb{P}(Z > x+u) \leq \mathbb{P}(Z > u) = \boldsymbol{a} e^{\boldsymbol{S}u}\boldsymbol{e}.$$

□

Corollary B.2. *The closing operator* $\boldsymbol{v}(x) = e^{\boldsymbol{S}x}\boldsymbol{s}$ *has Property 4.2(iv).*

For $\boldsymbol{a} \in \mathcal{A}$, $u \geq 0$,

$$\int_{x=0}^{\Delta} \boldsymbol{a} e^{\boldsymbol{S}u} e^{\boldsymbol{S}x}\boldsymbol{v}(x) \, \mathrm{d}x = \int_{x=0}^{\Delta} \boldsymbol{a} e^{\boldsymbol{S}u} e^{\boldsymbol{S}x}\boldsymbol{s} \, \mathrm{d}x \leq \boldsymbol{a} e^{\boldsymbol{S}u}\boldsymbol{e}.$$

Proof.

$$\int_{x=0}^{\Delta} \boldsymbol{a} e^{\boldsymbol{S}u} e^{\boldsymbol{S}x}\boldsymbol{s} \, \mathrm{d}x = \boldsymbol{a} e^{\boldsymbol{S}u}\boldsymbol{e} - \boldsymbol{a} e^{\boldsymbol{S}(u+\Delta)}\boldsymbol{e} \leq \boldsymbol{a} e^{\boldsymbol{S}u}\boldsymbol{e},$$

since $0 \leq \boldsymbol{a} e^{\boldsymbol{S}(u+\Delta)}\boldsymbol{e}$ as it is a probability. □

Corollary B.3. *The closing operator* $\boldsymbol{v}(x) = e^{\boldsymbol{S}x}\boldsymbol{s}$ *has Property 4.2(v).*

Let g *be a function satisfying the Assumptions 4.1 and consider the closing operator* $\boldsymbol{v}(x) = e^{\boldsymbol{S}x}\boldsymbol{s}$. *For* $u \leq \Delta - \varepsilon$, $v \geq 0$,

$$\int_{x=0}^{\infty} \frac{\boldsymbol{\alpha} e^{\boldsymbol{S}(u+x)}}{\boldsymbol{\alpha} e^{\boldsymbol{S}u}\boldsymbol{e}} \boldsymbol{v}(v) g(x) \, \mathrm{d}x = g(\Delta - u - v) 1(u + v \leq \Delta - \varepsilon) + r_{\boldsymbol{v}}(u,v),$$

where

$$R_{\boldsymbol{v},1} = \int_{u=0}^{\Delta-\varepsilon} |r_{\boldsymbol{v}}(u,v)| \, \mathrm{d}u \leq r_2\Delta + 2\varepsilon G + \Delta G \frac{\mathrm{Var}(Z)/\varepsilon^2}{1 - \mathrm{Var}(Z)/\varepsilon^2}$$

and

$$R_{\boldsymbol{v},2} = \int_{u=0}^{\Delta} |r_{\boldsymbol{v}}(u,v)| \, \mathrm{d}u \leq R_{\boldsymbol{v},1} \leq r_2\Delta + 2\varepsilon G + \Delta G \frac{\mathrm{Var}(Z)/\varepsilon^2}{1 - \mathrm{Var}(Z)/\varepsilon^2}.$$

Proof. By Corollary 4.7,

$$\int_{x=0}^{\infty} \frac{\boldsymbol{\alpha} e^{\boldsymbol{S}(u+x)}}{\boldsymbol{\alpha} e^{\boldsymbol{S}u}\boldsymbol{e}} \boldsymbol{v}(v) g(x)\,\mathrm{d}x = g(\Delta - u - v)1(u + v \leq \Delta - \varepsilon) + r_3(u+v),$$

so $r_{\boldsymbol{v}}(u,v) = r_3(u+v)$. All that remains to be shown are the bounds. To this end, observe

$$R_{\boldsymbol{v},1} \leq \int_{u=0}^{\Delta} |r_{\boldsymbol{v}}(u,v)|\,\mathrm{d}u = \int_{u=0}^{\Delta} r_3(u+v)\,\mathrm{d}u \leq r_2\Delta + 2\varepsilon G + \Delta G \frac{\mathrm{Var}(Z)/\varepsilon^2}{1 - \mathrm{Var}(Z)/\varepsilon^2},$$

since $r_3(u,v) \geq 0$ for all $u, v \geq 0$. Similarly,

$$R_{\boldsymbol{v},2} \leq \int_{v=0}^{\Delta} r_{\boldsymbol{v}}(u,v)\,\mathrm{d}v = \int_{v=0}^{\Delta} r_3(u+v)\,\mathrm{d}v \leq r_2\Delta + 2\varepsilon G + \Delta G \frac{\mathrm{Var}(Z)/\varepsilon^2}{1 - \mathrm{Var}(Z)/\varepsilon^2}.$$

□

B.2 The closing operator $\widehat{\boldsymbol{v}}(x) = \left(e^{\boldsymbol{S}x} + e^{\boldsymbol{S}(2\Delta - x)}\right)\boldsymbol{s}$

Let $\widehat{\boldsymbol{v}}(x)$ be the closing operator,

$$\widehat{\boldsymbol{v}}(x) = \left(e^{\boldsymbol{S}x}\boldsymbol{s} + e^{\boldsymbol{S}(2\Delta - x)}\boldsymbol{s}\right),$$

for $x \in [0, \Delta)$.

For the closing operator $\widehat{\boldsymbol{v}}(x)$ we may set $\widetilde{\boldsymbol{w}}(x) = \boldsymbol{0}$, so Properties 4.2(*i*) and 4.2(*ii*) hold trivially.

Lemma B.4. *The closing operator* $\widehat{\boldsymbol{v}}(x)$ *has the Property 4.2(iii).*

For $x \in [0, \Delta), u \geq 0$,

$$\boldsymbol{a} e^{\boldsymbol{S}u}(-\boldsymbol{S})^{-1}\boldsymbol{u}(x) \leq 2\boldsymbol{a} e^{\boldsymbol{S}u}\boldsymbol{e}.$$

Proof. Let $\boldsymbol{a} \in \mathcal{A}$ be arbitrary. By definition

$$\begin{aligned}\boldsymbol{a} e^{\boldsymbol{S}u}(-\boldsymbol{S})^{-1}\boldsymbol{u}(x) &= \boldsymbol{a} e^{\boldsymbol{S}u}(-\boldsymbol{S})^{-1}\left(e^{\boldsymbol{S}x}\boldsymbol{s} + e^{\boldsymbol{S}(2\Delta - x)}\boldsymbol{s}\right) \\ &= \boldsymbol{a} e^{\boldsymbol{S}u}\left(e^{\boldsymbol{S}x}\boldsymbol{e} + e^{\boldsymbol{S}(2\Delta - x)}\boldsymbol{e}\right)\end{aligned}$$

since $(-\boldsymbol{S})^{-1}$ and $e^{\boldsymbol{S}x}$ commute and $\boldsymbol{s} = -\boldsymbol{S}e$. By Lemma B.1 this is less than or equal to,

$$\boldsymbol{a} e^{\boldsymbol{S}u}\left(\boldsymbol{e} + \boldsymbol{e}\right) = 2\boldsymbol{a} e^{\boldsymbol{S}u}\boldsymbol{e}. \tag{B.1}$$

□

Lemma B.5. *The closing operator $\widehat{\boldsymbol{v}}(x)$ has the property 4.2(iv).*

For $\boldsymbol{a} \in \mathcal{A}$, $u \geq 0$,

$$\int_{x=0}^{\Delta} \boldsymbol{a} e^{\boldsymbol{S}u} \widehat{\boldsymbol{v}}(x)\,\mathrm{d}x \leq \boldsymbol{a} e^{\boldsymbol{S}u} \boldsymbol{e}$$

Proof.

$$\int_{x=0}^{\Delta} \boldsymbol{a} e^{\boldsymbol{S}u} \widehat{\boldsymbol{v}}(x)\,\mathrm{d}x = \boldsymbol{a} e^{\boldsymbol{S}u} \boldsymbol{e} - \boldsymbol{a} e^{\boldsymbol{S}(u+2\Delta)} \boldsymbol{e} \leq \boldsymbol{a} e^{\boldsymbol{S}u} \boldsymbol{e}.$$

□

Corollary B.6. *The closing operator $\widehat{\boldsymbol{v}}(x)$ has the Property 4.2(v).*

Let g be a function satisfying the Assumptions 4.1. For $u \leq \Delta - \varepsilon$, $v \in [0, \Delta)$,

$$\int_{x=0}^{\infty} \frac{\boldsymbol{\alpha} e^{\boldsymbol{S}(u+x)}}{\boldsymbol{\alpha} e^{\boldsymbol{S}u} \boldsymbol{e}} \widehat{\boldsymbol{v}}(v) g(x)\,\mathrm{d}x = g(\Delta - u - v) 1(u + v \leq \Delta - \varepsilon) + r_{\widehat{\boldsymbol{v}}}(u, v),$$

where

$$|r_{\widehat{\boldsymbol{v}}}(u, v)| \leq r_3(u + v) + r_3(u + 2\Delta - v).$$

Furthermore,

$$\int_{u=0}^{\Delta} |r_{\widehat{\boldsymbol{v}}}(u, v)|\,\mathrm{d}u \leq R_{\widehat{\boldsymbol{v}},1},$$

and

$$\int_{v=0}^{\Delta} |r_{\widehat{\boldsymbol{v}}}(u, v)|\,\mathrm{d}u \leq R_{\widehat{\boldsymbol{v}},2},$$

where

$$R_{\widehat{\boldsymbol{v}},1},\ R_{\widehat{\boldsymbol{v}},2} \leq 2 \left(\Delta r_2 + 2\varepsilon G + \Delta \frac{\mathrm{Var}(Z)/\varepsilon^2}{1 - \mathrm{Var}(Z)/\varepsilon^2} \right).$$

Proof. By the definition of the operator $\widehat{\boldsymbol{v}}(x)$,

$$\int_{x=0}^{\infty} \frac{\boldsymbol{\alpha} e^{\boldsymbol{S}(u+x)}}{\boldsymbol{\alpha} e^{\boldsymbol{S}u} \boldsymbol{e}} \widehat{\boldsymbol{v}}(v) g(x)\,\mathrm{d}x = \int_{x=0}^{\infty} \frac{\boldsymbol{\alpha} e^{\boldsymbol{S}(u+x)}}{\boldsymbol{\alpha} e^{Su} \boldsymbol{e}} e^{\boldsymbol{S}v} \boldsymbol{s} g(x) + \frac{\boldsymbol{\alpha} e^{\boldsymbol{S}(u+x)}}{\boldsymbol{\alpha} e^{Su} \boldsymbol{e}} e^{\boldsymbol{S}(2\Delta - v)} \boldsymbol{s} g(x)\,\mathrm{d}x. \quad \text{(B.2)}$$

By Corollary 4.7

$$\int_{x=0}^{\infty} \frac{\boldsymbol{\alpha} e^{\boldsymbol{S}(u+x)}}{\boldsymbol{\alpha} e^{Su} \boldsymbol{e}} e^{\boldsymbol{S}v} \boldsymbol{s} g(x)\,\mathrm{d}x = g(\Delta - u - v) 1(u + v \leq \Delta - \varepsilon) + r_3(u + v), \quad \text{(B.3)}$$

$$\int_{x=0}^{\infty} \frac{\boldsymbol{\alpha} e^{\boldsymbol{S}(u+x)}}{\boldsymbol{\alpha} e^{Su} \boldsymbol{e}} e^{\boldsymbol{S}(2\Delta - v)} \boldsymbol{s} g(x)\,\mathrm{d}x = r_3(u + 2\Delta - v). \quad \text{(B.4)}$$

Therefore, (B.2) is,

$$g(\Delta-u-v)1(u+v\leq\Delta-\varepsilon)+r_3(u+v)+r_3(u+2\Delta-v). \tag{B.5}$$

Now,

$$\begin{aligned}
R_{\boldsymbol{u},1} &\leq \int_{u=0}^{\Delta} |r_{\boldsymbol{u}}(u,v)|\,\mathrm{d}u \\
&\leq \int_{u=0}^{\Delta} r_3(u+v)+r_3(u+2\Delta-v)\,\mathrm{d}u \\
&\leq \int_{u=0}^{2\Delta} 2r_3(u+v)\,\mathrm{d}u \\
&\leq 2\left(\Delta r_2+2\varepsilon G+\Delta\frac{\mathrm{Var}(Z)/\varepsilon^2}{1-\mathrm{Var}(Z)/\varepsilon^2}\right).
\end{aligned}$$

Similarly,

$$\begin{aligned}
R_{\boldsymbol{u},2} &\leq \int_{v=0}^{\Delta} |r_{\boldsymbol{u}}(u,v)|\,\mathrm{d}v \\
&= \int_{v=0}^{\Delta} r_3(u+v)+r_3(u+2\Delta-v) \\
&\leq 2\left(\Delta r_2+2\varepsilon G+\Delta\frac{\mathrm{Var}(Z)/\varepsilon^2}{1-\mathrm{Var}(Z)/\varepsilon^2}\right).
\end{aligned}$$

□

B.3 The closing operator $\left(e^{\boldsymbol{S}x}+e^{\boldsymbol{S}(2\Delta-x)}\right)\left[I-e^{\boldsymbol{S}2\Delta}\right]^{-1}\boldsymbol{s}$

Let $\overline{\boldsymbol{v}}(x)$ be the closing operator

$$\overline{\boldsymbol{v}}(x)=\left(e^{\boldsymbol{S}x}+e^{\boldsymbol{S}(2\Delta-x)}\right)\left[I-e^{\boldsymbol{S}2\Delta}\right]^{-1}\boldsymbol{s},$$

for $x\in[0,\Delta)$. Notice that

$$\boldsymbol{a}\overline{\boldsymbol{v}}(x)=\boldsymbol{a}\left(e^{\boldsymbol{S}x}+e^{\boldsymbol{S}(2\Delta-x)}\right)\sum_{n=0}^{\infty}e^{\boldsymbol{S}2n\Delta}\boldsymbol{s}.$$

We decompose the closing operator $\overline{\boldsymbol{v}}(x)=\boldsymbol{w}(x)+\widetilde{\boldsymbol{w}}(x)$, where $\boldsymbol{w}(x)=\widehat{\boldsymbol{v}}(x)$ and

$$\widetilde{\boldsymbol{w}}(x)=\left(e^{\boldsymbol{S}x}+e^{\boldsymbol{S}(2\Delta-x)}\right)\sum_{n=1}^{\infty}e^{\boldsymbol{S}2n\Delta}\boldsymbol{s}.$$

Lemma B.7. *The closing operator $\overline{\boldsymbol{v}}(x)$ has Property 4.2(i).*
For $\boldsymbol{a} \in \mathcal{A}$, $u \geq 0$,

$$\boldsymbol{a}e^{\boldsymbol{S}(u+v)}(-\boldsymbol{S})^{-1}\overline{\boldsymbol{v}}(x) \leq \boldsymbol{a}e^{\boldsymbol{S}u}(-\boldsymbol{S})^{-1}\overline{\boldsymbol{v}}(x).$$

Proof.

$$\begin{aligned}
\boldsymbol{a}e^{\boldsymbol{S}(u+v)}(-\boldsymbol{S})^{-1}\overline{\boldsymbol{v}}(x)\,\mathrm{d}x &= \sum_{n=0}^{\infty} \boldsymbol{a}e^{\boldsymbol{S}(x+u+v+2n\Delta)}\boldsymbol{e} + \boldsymbol{a}e^{\boldsymbol{S}(2\Delta-x+u+v+2n\Delta)}\boldsymbol{e} \\
&\leq \sum_{n=0}^{\infty} \boldsymbol{a}e^{\boldsymbol{S}(x+u+2n\Delta)}\boldsymbol{e} + \boldsymbol{a}e^{\boldsymbol{S}(2\Delta-x+u+2n\Delta)}\boldsymbol{e} \\
&= \boldsymbol{a}e^{\boldsymbol{S}u}(-\boldsymbol{S})^{-1}\overline{\boldsymbol{v}}(x)\,\mathrm{d}x.
\end{aligned}$$

□

Lemma B.8. *The closing operator $\overline{\boldsymbol{v}}(x)$ has Property 4.2(ii).*
For $x \in [0, \Delta), u \geq 0$,

$$\boldsymbol{\alpha}e^{\boldsymbol{S}u}(-\boldsymbol{S})^{-1}\widetilde{\boldsymbol{w}}(x) \leq \frac{\mathrm{Var}(Z)}{\Delta^2}\frac{\pi^2}{4}. \tag{B.6}$$

Proof. The expression on the left-hand side of (B.6) is

$$\begin{aligned}
&\boldsymbol{\alpha}e^{\boldsymbol{S}u}(-\boldsymbol{S})^{-1}\left(e^{\boldsymbol{S}x} + e^{\boldsymbol{S}(2\Delta-x)}\right)\sum_{n=1}^{\infty} e^{\boldsymbol{S}2n\Delta}\boldsymbol{s} \\
&= \boldsymbol{\alpha}e^{\boldsymbol{S}u}\left(e^{\boldsymbol{S}x} + e^{\boldsymbol{S}(2\Delta-x)}\right)\sum_{n=1}^{\infty} e^{\boldsymbol{S}2n\Delta}\boldsymbol{e} \\
&= \sum_{n=1}^{\infty} \mathbb{P}(Z > u + x + 2n\Delta) + \mathbb{P}(Z > u + 2\Delta - x + 2n\Delta) \\
&\leq 2\sum_{n=1}^{\infty} \mathbb{P}(Z > 2n\Delta).
\end{aligned}$$

By Chebyshev's inequality, $\mathbb{P}(Z > 2n\Delta) \leq \dfrac{\mathrm{Var}(Z)}{\Delta^2(1+2(n-1))^2}$. Therefore

$$2\sum_{n=1}^{\infty} \mathbb{P}(Z > 2n\Delta) \leq 2\frac{\mathrm{Var}(Z)}{\Delta^2}\sum_{n=0}^{\infty}\frac{1}{(1+2n)^2}. \tag{B.7}$$

Now, consider the sum

$$\sum_{n=1}^{\infty}\frac{1}{n^2} = \sum_{n=1}^{\infty}\frac{1}{(2n)^2} + \sum_{n=0}^{\infty}\frac{1}{(1+2n)^2} = \frac{1}{4}\sum_{n=1}^{\infty}\frac{1}{n^2} + \sum_{n=0}^{\infty}\frac{1}{(1+2n)^2}. \tag{B.8}$$

The solution to the *Basel problem* states that $\sum_{n=1}^{\infty} 1/n^2 = \pi^2/6$. Hence

$$\frac{\pi^2}{6} = \frac{1}{4}\frac{\pi^2}{6} + \sum_{n=0}^{\infty}\frac{1}{(1+2n)^2}$$

and therefore

$$\sum_{n=0}^{\infty}\frac{1}{(1+2n)^2} = \frac{\pi^2}{8}.$$

Thus, (B.6) is less than or equal to

$$\frac{\mathrm{Var}(Z)}{\Delta^2}\frac{\pi^2}{4}.$$

□

Since $\boldsymbol{w}(x) = \widehat{\boldsymbol{v}}(x)$ then, from the results of the previous section, $\overline{\boldsymbol{v}}(x)$ has Property 4.2(*iii*).

Lemma B.9. *The closing operator* $\overline{\boldsymbol{v}}(x)$ *has Property 4.2(iv).*

For $\boldsymbol{a} \in \mathcal{A}$, $u \geq 0$,

$$\int_{x=0}^{\Delta} \boldsymbol{a}e^{\boldsymbol{S}u}\overline{\boldsymbol{v}}(x)\,\mathrm{d}x = \boldsymbol{a}e^{\boldsymbol{S}u}\boldsymbol{e}.$$

Proof.

$$\begin{aligned}\int_{x=0}^{\Delta} \boldsymbol{a}e^{\boldsymbol{S}u}\overline{\boldsymbol{v}}(x)\,\mathrm{d}x &= \boldsymbol{a}e^{\boldsymbol{S}u}(\boldsymbol{S})^{-1}\left(e^{\boldsymbol{S}\Delta} - I + e^{\boldsymbol{S}2\Delta} - e^{\boldsymbol{S}\Delta}\right)\left[I - e^{\boldsymbol{S}2\Delta}\right]^{-1}\boldsymbol{s} \\ &= \boldsymbol{a}e^{\boldsymbol{S}u}(-\boldsymbol{S})^{-1}\boldsymbol{s} \\ &= \boldsymbol{a}e^{\boldsymbol{S}u}\boldsymbol{e}.\end{aligned}$$

□

Corollary B.10. *The closing operator* $\overline{\boldsymbol{v}}(x)$ *has Property 4.2(v).*

Let g *be a function satisfying the Assumptions 4.1. For* $u \leq \Delta - \varepsilon$, $v \in [0, \Delta)$,

$$\int_{x=0}^{\infty}\frac{\boldsymbol{\alpha}e^{\boldsymbol{S}(u+x)}}{\boldsymbol{\alpha}e^{\boldsymbol{S}u}\boldsymbol{e}}\overline{\boldsymbol{v}}(v)g(x)\,\mathrm{d}x = g(\Delta - u - v)1(u + v \leq \Delta - \varepsilon) + r_{\overline{\boldsymbol{v}}}(u, v),$$

where

$$|r_{\overline{\boldsymbol{v}}}(u, v)| \leq r_{\boldsymbol{u}}(u, v) + \frac{G\varepsilon^2\pi^2}{4\Delta^2}.$$

Furthermore,

$$R_{\overline{\boldsymbol{v}},1} = \int_{u=0}^{\Delta} |r_{\overline{\boldsymbol{v}}}(u,v)|\,\mathrm{d}u \le R_{\widehat{\boldsymbol{v}},1} + \frac{G\varepsilon^2\pi^2}{4\Delta},$$

and

$$R_{\overline{\boldsymbol{v}},2} = \int_{v=0}^{\Delta} |r_{\overline{\boldsymbol{v}}}(u,v)|\,\mathrm{d}u \le R_{\widehat{\boldsymbol{v}},2} + \frac{G\varepsilon^2\pi^2}{4\Delta}.$$

Proof. By the definition of the operator $\overline{\boldsymbol{v}}(v)$,

$$\begin{aligned}&\int_{x=0}^{\infty} \frac{\boldsymbol{\alpha}e^{\boldsymbol{S}(u+x)}}{\boldsymbol{\alpha}e^{\boldsymbol{S}u}\boldsymbol{e}}\overline{\boldsymbol{v}}(v)g(x)\,\mathrm{d}x \\ &= \int_{x=0}^{\infty} \frac{\boldsymbol{\alpha}e^{\boldsymbol{S}(u+x)}}{\boldsymbol{\alpha}e^{\boldsymbol{S}u}\boldsymbol{e}}\widehat{\boldsymbol{v}}(v)g(x)\,\mathrm{d}x + \int_{x=0}^{\infty} \frac{\boldsymbol{\alpha}e^{\boldsymbol{S}(u+x)}}{\boldsymbol{\alpha}e^{\boldsymbol{S}u}\boldsymbol{e}}\left(e^{\boldsymbol{S}v} + e^{\boldsymbol{S}(2\Delta-v)}\right)\sum_{n=1}^{\infty} e^{\boldsymbol{S}2n\Delta}\boldsymbol{s}g(x)\,\mathrm{d}x. \quad \text{(B.9)}\end{aligned}$$

By Lemma B.6 the first term is $g(\Delta-u-v)1(u+v\le\Delta-\varepsilon)+r_{\widehat{\boldsymbol{v}}}(u,v)$, where $|r_{\widehat{\boldsymbol{v}}}(u,v)| \le r_3(u+v)+r_3(u+2\Delta-v)$.

Since $g \le G$, the second term is less than or equal to

$$G\int_{x=0}^{\infty} \frac{\boldsymbol{\alpha}e^{\boldsymbol{S}(u+x)}}{\boldsymbol{\alpha}e^{\boldsymbol{S}u}\boldsymbol{e}}\left(e^{\boldsymbol{S}v} + e^{\boldsymbol{S}(2\Delta-v)}\right)\sum_{n=1}^{\infty} e^{\boldsymbol{S}2n\Delta}\boldsymbol{s}\,\mathrm{d}x = G\frac{\boldsymbol{\alpha}e^{\boldsymbol{S}u}}{\boldsymbol{\alpha}e^{\boldsymbol{S}u}\boldsymbol{e}}\left(e^{\boldsymbol{S}v} + e^{\boldsymbol{S}(2\Delta-v)}\right)\sum_{n=1}^{\infty} e^{\boldsymbol{S}2n\Delta}\boldsymbol{e}.$$

By similar arguments to those used in the proof of Lemma B.8 we can show that this is less than or equal to

$$\frac{G}{\boldsymbol{\alpha}e^{\boldsymbol{S}u}\boldsymbol{e}}\frac{\mathrm{Var}(Z)}{\Delta^2}\frac{\pi^2}{4}.$$

Now, as $u \le \Delta-\varepsilon$, then $\boldsymbol{\alpha}e^{\boldsymbol{S}u}\boldsymbol{e} \ge \mathrm{Var}(Z)/\varepsilon^2$ by Chebyshev's inequality, hence

$$\frac{G}{\boldsymbol{\alpha}e^{\boldsymbol{S}u}\boldsymbol{e}}\frac{\mathrm{Var}(Z)}{\Delta^2}\frac{\pi^2}{4} \le \frac{G}{\mathrm{Var}(Z)/\varepsilon^2}\frac{\mathrm{Var}(Z)}{\Delta^2}\frac{\pi^2}{4} = \frac{G\varepsilon^2\pi^2}{4\Delta^2}.$$

Putting it all together, we have shown

$$\int_{x=0}^{\infty} \frac{\boldsymbol{\alpha}e^{\boldsymbol{S}(u+x)}}{\boldsymbol{\alpha}e^{\boldsymbol{S}u}\boldsymbol{e}}\overline{\boldsymbol{v}}(v)g(x)\,\mathrm{d}x = g(\Delta-u-v)1(u+v\le\Delta-\varepsilon) + r_{\overline{\boldsymbol{v}}}(u,v) \quad \text{(B.10)}$$

where

$$|r_{\overline{\boldsymbol{v}}}(u,v)| \le \left| r_{\widehat{\boldsymbol{v}}}(u,v) + \frac{G\varepsilon^2\pi^2}{4\Delta^2} \right|.$$

Lastly, observe

$$\begin{aligned} R_{\overline{\boldsymbol{v}},1} = \int_{u=0}^{\Delta} |r_{\overline{\boldsymbol{v}}}(u,v)|\,\mathrm{d}u &\leq \int_{u=0}^{\Delta} |r_{\widehat{\boldsymbol{v}}}(u,v)| + \left|\frac{G\varepsilon^2\pi^2}{4\Delta^2}\right| \mathrm{d}u \\ &= R_{\widehat{\boldsymbol{v}},1} + \frac{G\varepsilon^2\pi^2}{4\Delta} \end{aligned}$$

and similarly,

$$R_{\overline{\boldsymbol{v}},2} = \int_{v=0}^{\Delta} |r_{\overline{\boldsymbol{v}}}(u,v)|\,\mathrm{d}v \leq R_{\widehat{\boldsymbol{v}},2} + \frac{G\varepsilon^2\pi^2}{4\Delta}$$

where we have used Lemma B.6. □

Appendix C

Convergence without ephemeral phases

For completeness, we include here results needed to prove a convergence of the QBD-RAP scheme to the fluid queue without the need for the ephemeral initial states. Note that we only need to prove convergence up to, and at, the time of the first change of level of the QBD-RAP, then we can use the results from Chapter 5 to obtain global convergence results.

For $\varphi(0) = k \in \mathcal{S}_{-0}$ (or $\varphi(0) = k \in \mathcal{S}_{+0}$) the added complexity comes from the fact, upon the phase process first leaving $\mathcal{S}_{-0}$ ($\mathcal{S}_{+0}$), that it is possible the phase transitions to a state in $\mathcal{S}_+$ ($\mathcal{S}_-$). Since the orbit of the QBD-RAP is constant on $\varphi(t) \in \mathcal{S}_{-0}$ ($\varphi(t) \in \mathcal{S}_{+0}$), then upon a first transition out of $\mathcal{S}_{-0}$ ($\mathcal{S}_{+0}$) and into $\mathcal{S}_+$ ($\mathcal{S}_-$) the orbit jumps to $\boldsymbol{a}^{(p)}_{\ell_0,i}(x_0)\boldsymbol{D}^{(p)}$. For $k \in \mathcal{S}_{-0}$, $m \geq 0$, the corresponding Laplace transform of the QBD-RAP is

$$\begin{aligned}
&\widehat{f}^{\ell_0,(p)}_{m,-0,+}(\lambda)(x,j;x_0,k)\\
&:= \int_{x_1=0}^{\infty}\cdots\int_{x_{2m+1}=0}^{\infty} \boldsymbol{e}_k[\boldsymbol{I}-\boldsymbol{T}_{00}]^{-1}\boldsymbol{T}_{0+}\boldsymbol{M}^m_{++}(\lambda,x_1,\ldots,x_{2m+1})\boldsymbol{e}_j\\
&\boldsymbol{a}^{(p)}_{\ell_0,k}(x_0)\boldsymbol{D}^{(p)}\boldsymbol{N}^{2m+1,(p)}(\lambda,x_1,\ldots,x_{2m+1})\boldsymbol{v}^{(p)}_{\ell_0,j}(x)\,\mathrm{d}x_{2m+1}\ldots\,\mathrm{d}x_2\,\mathrm{d}x_1\\
&+\int_{x_1=0}^{\infty}\cdots\int_{x_{2m+2}=0}^{\infty} \boldsymbol{e}_k[\boldsymbol{I}-\boldsymbol{T}_{00}]^{-1}\boldsymbol{T}_{0-}\boldsymbol{M}^{m+1}_{-+}(\lambda,x_1,\ldots,x_{2m+2})\boldsymbol{e}_j\\
&\boldsymbol{a}^{(p)}_{\ell_0,k}(x_0)\boldsymbol{N}^{2m+2,(p)}(\lambda,x_1,\ldots,x_{2m+2})\boldsymbol{v}^{(p)}_{\ell_0,j}(x)\,\mathrm{d}x_{2m+2}\ldots\,\mathrm{d}x_2\,\mathrm{d}x_1. \qquad \text{(C.1)}
\end{aligned}$$

The Laplace transform of the fluid queue corresponding to (C.1) is

$$\begin{aligned}
\widehat{\mu}^{\ell_0}_{m,-0,+}(\lambda)(x,j;x_0,k) &:= \sum_{i\in\mathcal{S}_+}\boldsymbol{e}_k\left[\lambda\boldsymbol{I}-\boldsymbol{T}_{00}\right]^{-1}\boldsymbol{T}_{0i}\widehat{\mu}^{\ell_0}_{m,+,+}(\lambda)(x,j;x_0,i)\\
&\quad+\sum_{i\in\mathcal{S}_-}\boldsymbol{e}_k\left[\lambda\boldsymbol{I}-\boldsymbol{T}_{00}\right]^{-1}\boldsymbol{T}_{0i}\widehat{\mu}^{\ell_0}_{m+1,-,+}(\lambda)(x,j;x_0,i), \qquad \text{(C.2)}
\end{aligned}$$

$m \geq 0$.

The second term of (C.1) is a linear combination of $\widehat{f}^{\ell_0,(p)}_{m+1,-,+}(\lambda)(x,j;x_0,k)$ which converges to $\widehat{\mu}^{\ell_0}_{m,-,+}(\lambda)(x,j;x_0,i)$, so there are no issues here. The first term of (C.1) creates significantly more work. Essentially, we need to derive more bounds, analogous to the results from Appendix **??**, but with the initial vector $\boldsymbol{a}_{\ell_0,i}(x_0)\boldsymbol{D}$.

Analogously, for $k \in \mathcal{S}_{-0}$, $m \geq 0$, we also have

$$\begin{aligned}\widehat{f}^{\ell_0,(p)}_{m,-0,-}(\lambda)(x,j;x_0,k) := &\int_{x_1=0}^{\infty}\cdots\int_{x_{2m+2}=0}^{\infty} \boldsymbol{e}_k[\boldsymbol{I}-\boldsymbol{T}_{00}]^{-1}\boldsymbol{T}_{0+}\boldsymbol{M}^{m+1}_{+-}(\lambda,x_1,\ldots,x_{2m+2})\boldsymbol{e}_j\\ &\boldsymbol{a}^{(p)}_{\ell_0,k}(x_0)\boldsymbol{D}^{(p)}\boldsymbol{N}^{2m+2,(p)}(\lambda,x_1,\ldots,x_{2m+2})\boldsymbol{v}^{(p)}_{\ell_0,j}(x)\,\mathrm{d}x_{2m+2}\ldots\,\mathrm{d}x_1\\ &+\int_{x_1=0}^{\infty}\cdots\int_{x_{2m+1}=0}^{\infty} \boldsymbol{e}_k[\boldsymbol{I}-\boldsymbol{T}_{00}]^{-1}\boldsymbol{T}_{0-}\boldsymbol{M}^{m}_{--}(\lambda,x_1,\ldots,x_{2m+1})\boldsymbol{e}_j\\ &\boldsymbol{a}^{(p)}_{\ell_0,k}(x_0)\boldsymbol{N}^{2m+1,(p)}(\lambda,x_1,\ldots,x_{2m+1})\boldsymbol{v}^{(p)}_{\ell_0,j}(x)\,\mathrm{d}x_{2m+1}\ldots\,\mathrm{d}x_1.\end{aligned}$$

For $k \in \mathcal{S}_{+0}$, $m \geq 0$, we have

$$\begin{aligned}\widehat{f}^{\ell_0,(p)}_{m,+0,+}(\lambda)(x,j;x_0,k) := &\int_{x_1=0}^{\infty}\cdots\int_{x_{2m+2}=0}^{\infty} \boldsymbol{e}_k[\boldsymbol{I}-\boldsymbol{T}_{00}]^{-1}\boldsymbol{T}_{0-}\boldsymbol{M}^{m+1}_{-+}(\lambda,x_1,\ldots,x_{2m+2})\boldsymbol{e}_j\\ &\boldsymbol{a}^{(p)}_{\ell_0,k}(x_0)\boldsymbol{D}^{(p)}\boldsymbol{N}^{2m+2,(p)}(\lambda,x_1,\ldots,x_{2m+2})\boldsymbol{v}^{(p)}_{\ell_0,j}(x)\,\mathrm{d}x_{2m+2}\ldots\,\mathrm{d}x_1\\ &+\int_{x_1=0}^{\infty}\cdots\int_{x_{2m+1}=0}^{\infty} \boldsymbol{e}_k[\boldsymbol{I}-\boldsymbol{T}_{00}]^{-1}\boldsymbol{T}_{0+}\boldsymbol{M}^{m}_{++}(\lambda,x_1,\ldots,x_{2m+1})\boldsymbol{e}_j\\ &\boldsymbol{a}^{(p)}_{\ell_0,k}(x_0)\boldsymbol{N}^{2m+1,(p)}(\lambda,x_1,\ldots,x_{2m+1})\boldsymbol{v}^{(p)}_{\ell_0,j}(x)\,\mathrm{d}x_{2m+1}\ldots\,\mathrm{d}x_1,\end{aligned}$$

and

$$\begin{aligned}\widehat{f}^{\ell_0,(p)}_{m,+0,-}(\lambda)(x,j;x_0,k) := &\int_{x_1=0}^{\infty}\cdots\int_{x_{2m+1}=0}^{\infty} \boldsymbol{e}_k[\boldsymbol{I}-\boldsymbol{T}_{00}]^{-1}\boldsymbol{T}_{0-}\boldsymbol{M}^{m}_{--}(\lambda,x_1,\ldots,x_{2m+1})\boldsymbol{e}_j\\ &\boldsymbol{a}^{(p)}_{\ell_0,k}(x_0)\boldsymbol{D}^{(p)}\boldsymbol{N}^{2m+1,(p)}(\lambda,x_1,\ldots,x_{2m+1})\boldsymbol{v}^{(p)}_{\ell_0,j}(x)\,\mathrm{d}x_{2m+1}\ldots\,\mathrm{d}x_1\\ &+\int_{x_1=0}^{\infty}\cdots\int_{x_{2m+2}=0}^{\infty} \boldsymbol{e}_k[\boldsymbol{I}-\boldsymbol{T}_{00}]^{-1}\boldsymbol{T}_{0+}\boldsymbol{M}^{m+1}_{+-}(\lambda,x_1,\ldots,x_{2m+2})\boldsymbol{e}_j\\ &\boldsymbol{a}^{(p)}_{\ell_0,k}(x_0)\boldsymbol{N}^{2m+2,(p)}(\lambda,x_1,\ldots,x_{2m+2})\boldsymbol{v}^{(p)}_{\ell_0,j}(x)\,\mathrm{d}x_{2m+2}\ldots\,\mathrm{d}x_1.\end{aligned}$$

In general, for $q \in \{+,-\}$, $q' \in \{+,-\}$, $m \geq 0$,

$$\widehat{\mu}^{\ell_0}_{m,q0,q'}(\lambda)(x,j;x_0,k) := \sum_{r\in\{+,-\}}\sum_{i\in\mathcal{S}_r} \boldsymbol{e}_k\left[\lambda\boldsymbol{I}-\boldsymbol{T}_{00}\right]^{-1}\boldsymbol{T}_{0i}\widehat{\mu}^{\ell_0}_{m+1(r\neq q'),r,q'}(\lambda)(x,j;x_0,i).$$

Remark C.1. *For technical reasons we should not have point masses at $x_0 \in y_{\ell_0}, y_{\ell_0+1}$ when $\varphi(0) \in \mathcal{S}_{+0} \cup \mathcal{S}_{-0}$. Intuitively, if $\varphi(0) = k \in \mathcal{S}_{+0}$ and $x_0 = y_{\ell_0}$ then, if upon*

exiting $\mathcal{S}_{+0}$ the phase process transitions to $\mathcal{S}_-$ then the fluid queue will instantaneously leave the interval $\mathcal{D}_{\ell_0}$ upon this transition. On the same event, the orbit of the QBD-RAP will be $\boldsymbol{\alpha}^{(p)}\boldsymbol{D}^{(p)}$ at the instant of the transition to $\mathcal{S}_-$. Roughly speaking $\boldsymbol{D}^{(p)}$ maps $\boldsymbol{\alpha}^{(p)}$ to approximately $\dfrac{\boldsymbol{\alpha}^{(p)}e^{\boldsymbol{S}^{(p)}\Delta}}{\boldsymbol{\alpha}^{(p)}e^{\boldsymbol{S}^{(p)}\Delta}\boldsymbol{e}}$ (asymptotically). Our asymptotic arguments rely on Chebyshev's inequality, in the form of a bound in terms of the distance of the random variable $Z^{(p)} \sim ME(\boldsymbol{\alpha}^{(p)}, \boldsymbol{S}^{(p)})$ from its mean Δ. However, we cannot use such a technique to bound terms such as $\dfrac{\boldsymbol{\alpha}^{(p)}e^{\boldsymbol{S}^{(p)}\Delta}}{\boldsymbol{\alpha}^{(p)}e^{\boldsymbol{S}^{(p)}\Delta}\boldsymbol{e}}e^{\boldsymbol{S}^{(p)}z}\boldsymbol{s}^{(p)}$.

In practice, it may be possible to avoid this issue by choosing the intervals $\{\mathcal{D}_\ell\}$ so that the boundaries do not align with any point masses. Another option is to append an ephemeral class of phases to the fluid queue as previously stated.

Theorem C.2 below is analogous to Theorem 4.3 and proves a certain convergence of the QBD-RAP scheme to the fluid queue in the case that $\phi(0) \in \mathcal{S}_{+0} \cup \mathcal{S}_{-0}$. Like the proof of Theorem 4.3, the proof of Theorem C.2 relies on technical bounds which we establish with the remainder of this Appendix.

Theorem C.2. *As $p \to \infty$, for $q \in \{+0, -0\}$, $r \in \{+, -\}$ and $m = 0$,*

$$\int_{x\in\mathcal{D}_{\ell_0}} \widehat{f}^{\ell_0,(p)}_{0,q,r}(\lambda)(x, j; x_0, k)\psi(x)\,\mathrm{d}x \to \int_{x\in\mathcal{D}_{\ell_0}} \widehat{\mu}^{\ell_0}_{0,q,r}(\lambda)(x, j; x_0, k)\psi(x)\,\mathrm{d}x. \tag{C.3}$$

For $q \in \{+0, -0\}, r \in \{+, -\}$ and $m \geq 1$,

$$\int_{x\in\mathcal{D}_{\ell_0}} \widehat{f}^{\ell_0,(p)}_{m,q,r}(\lambda)(x, j; x_0, k)\psi(x)\,\mathrm{d}x \to \int_{x\in\mathcal{D}_{\ell_0}} \widehat{\mu}^{\ell_0}_{m,q,r}(\lambda)(x, j; x_0, k)\psi(x)\,\mathrm{d}x. \tag{C.4}$$

Proof. Cases $(q, r) \in \{(+0, -), (-0, +)\}$, and $m = 0$. First, take $q = -0$ and $r = +$, then

$$\begin{aligned}
&\int_{x\in\mathcal{D}_k} \widehat{f}^{\ell_0,(p)}_{0,-0,+}(\lambda)(x, j; x_0, k)\psi(x)\,\mathrm{d}x \\
&:= \int_{x_1=0}^{\infty}\int_{x\in\mathcal{D}_k} \boldsymbol{e}_k[\boldsymbol{I} - \boldsymbol{T}_{00}]^{-1}\boldsymbol{T}_{0+}\boldsymbol{M}^0_{++}(\lambda, x_1)\boldsymbol{e}_j\boldsymbol{a}^{(p)}_{\ell_0,k}(x_0)\boldsymbol{D}^{(p)}\boldsymbol{N}^{1,(p)}(\lambda, x_1) \\
&\boldsymbol{v}^{(p)}_{\ell_0,j}(x)\psi(x)\,\mathrm{d}x\,\mathrm{d}x_1 \\
&+ \int_{x_1=0}^{\infty}\int_{x_2=0}^{\infty}\int_{x\in\mathcal{D}_k} \boldsymbol{e}_k[\boldsymbol{I} - \boldsymbol{T}_{00}]^{-1}\boldsymbol{T}_{0-}\boldsymbol{M}^1_{-+}(\lambda, x_1, x_2)\boldsymbol{e}_j\boldsymbol{a}^{(p)}_{\ell_0,k}(x_0)\boldsymbol{N}^{2,(p)}(\lambda, x_1, x_2) \\
&\boldsymbol{v}^{(p)}_{\ell_0,j}(x)\psi(x)\,\mathrm{d}x\,\mathrm{d}x_2\,\mathrm{d}x_1.
\end{aligned} \tag{C.5}$$

The second term is a linear combination of $\int_{x\in\mathcal{D}_k} \widehat{f}^{\ell_0,(p)}_{1,-,+}(\lambda)(x, j; x_0, i)\psi(x)\,\mathrm{d}x$ terms, each of which converge to $\int_{x\in\mathcal{D}_k} \widehat{\mu}^{\ell_0,(p)}_{1,-,+}(\lambda)(x, j; x_0, i)\psi(x)\,\mathrm{d}x$, by the case we proved in Theorem 4.3.

As for the first term, it is a linear combination of terms

$$\int_{x_1=0}^{\infty}\int_{x\in\mathcal{D}_k} \boldsymbol{e}_i\boldsymbol{H}^{++}(\lambda,x_1)\boldsymbol{e}_j\boldsymbol{a}^{(p)}_{\ell_0,k}(x_0)\boldsymbol{D}^{(p)}e^{\boldsymbol{S}^{(p)}x_1}\boldsymbol{v}^{(p)}_{\ell_0,j}(x)\psi(x)\,\mathrm{d}x\,\mathrm{d}x_1.$$

Lemma C.3 proves that such terms converge to $\int_{x\in\mathcal{D}_k}\widehat{\mu}^{\ell_0}_{0,+,+}(\lambda)(x,j;x_0,i)\psi(x)\,\mathrm{d}x$. Therefore (C.5) is a finite linear combination of terms, each of which converge, hence (C.5) converges and converges to

$$\begin{aligned}&\int_{x_1=0}^{\infty}\int_{x\in\mathcal{D}_k}\boldsymbol{e}_k\sum_{i\in\mathcal{S}_+}[\boldsymbol{I}-\boldsymbol{T}_{00}]^{-1}\boldsymbol{T}_{0i}\int_{x\in\mathcal{D}_k}\widehat{\mu}^{\ell_0}_{0,+,+}(\lambda)(x,j;x_0,i)\psi(x)\,\mathrm{d}x\\&+\int_{x_1=0}^{\infty}\int_{x_2=0}^{\infty}\int_{x\in\mathcal{D}_k}\sum_{i\in\mathcal{S}_-}\boldsymbol{e}_k[\boldsymbol{I}-\boldsymbol{T}_{00}]^{-1}\boldsymbol{T}_{0i}\int_{x\in\mathcal{D}_k}\widehat{\mu}^{\ell_0}_{1,-,+}(\lambda)(x,j;x_0,i)\psi(x)\,\mathrm{d}x,\end{aligned}\tag{C.6}$$

which is $\widehat{\mu}^{\ell_0}_{0,-0,+}(\lambda)(x,j;x_0,k)$. This proves the result for $r=+$ and $q=-0$. Analogous arguments prove the result for $r=-$ and $q=+0$.

Cases $q\in\{+0,-0\}$, $r\in\{+,-\}$ and $m\geq 1$. First, take $q=+0$ and $r=+$, then

$$\begin{aligned}&\int_{x\in\mathcal{D}_k}\widehat{f}^{\ell_0,(p)}_{m,-0,+}(\lambda)(x,j;x_0,k)\psi(x)\,\mathrm{d}x\\&:=\int_{x\in\mathcal{D}_k}\int_{x_1=0}^{\infty}\cdots\int_{x_{2m+1}=0}^{\infty}\boldsymbol{e}_k[\boldsymbol{I}-\boldsymbol{T}_{00}]^{-1}\boldsymbol{T}_{0+}\boldsymbol{M}^m_{++}(\lambda,x_1,\ldots,x_{2m+1})\boldsymbol{e}_j\\&\boldsymbol{a}^{(p)}_{\ell_0,k}(x_0)\boldsymbol{D}^{(p)}\boldsymbol{N}^{2m+1,(p)}(\lambda,x_1,\ldots,x_{2m+1})\boldsymbol{v}^{(p)}_{\ell_0,j}(x)\psi(x)\,\mathrm{d}x_{2m+1}\ldots\,\mathrm{d}x_2\,\mathrm{d}x_1\,\mathrm{d}x\\&+\int_{x\in\mathcal{D}_k}\int_{x_1=0}^{\infty}\cdots\int_{x_{2m+2}=0}^{\infty}\boldsymbol{e}_k[\boldsymbol{I}-\boldsymbol{T}_{00}]^{-1}\boldsymbol{T}_{0-}\boldsymbol{M}^{m+1}_{-+}(\lambda,x_1,\ldots,x_{2m+2})\boldsymbol{e}_j\\&\boldsymbol{a}^{(p)}_{\ell_0,k}(x_0)\boldsymbol{N}^{2m+2,(p)}(\lambda,x_1,\ldots,x_{2m+2})\boldsymbol{v}^{(p)}_{\ell_0,j}(x)\psi(x)\,\mathrm{d}x_{2m+2}\ldots\,\mathrm{d}x_2\,\mathrm{d}x_1\,\mathrm{d}x.\end{aligned}\tag{C.7}$$

The second term is a linear combination of $\int_{x\in\mathcal{D}_k}\widehat{f}^{\ell_0,(p)}_{m+1,-,+}(\lambda)(x,j;x_0,i)\psi(x)\,\mathrm{d}x$ terms, each of which converge to $\int_{x\in\mathcal{D}_k}\widehat{\mu}^{\ell_0,(p)}_{m+1,-,+}(\lambda)(x,j;x_0,i)\psi(x)\,\mathrm{d}x$. As for the first term, it is a linear combination of terms

$$\begin{aligned}&\int_{x\in\mathcal{D}_k}\int_{x_1=0}^{\infty}\cdots\int_{x_{2m+1}=0}^{\infty}\boldsymbol{e}_i\boldsymbol{M}^m_{++}(\lambda,x_1,\ldots,x_{2m+1})\boldsymbol{e}_j\\&\boldsymbol{a}^{(p)}_{\ell_0,k}(x_0)\boldsymbol{D}^{(p)}\boldsymbol{N}^{2m+1,(p)}(\lambda,x_1,\ldots,x_{2m+1})\boldsymbol{v}^{(p)}_{\ell_0,j}(x)\psi(x)\,\mathrm{d}x_{2m+1}\ldots\,\mathrm{d}x_2\,\mathrm{d}x_1\,\mathrm{d}x\\&=\int_{x\in\mathcal{D}_k}\int_{x_1=0}^{\infty}\cdots\int_{x_{2m+1}=0}^{\infty}\boldsymbol{e}_i\boldsymbol{H}^{+-}(\lambda,x_1)\prod_{r=1}^{m-1}\boldsymbol{H}^{-+}(\lambda,x_{2r})\boldsymbol{H}^{+-}(\lambda,x_{2r+1})\\&\boldsymbol{H}^{-+}(\lambda,x_{2m})\boldsymbol{H}^{++}(\lambda,x_{2m+1})\boldsymbol{e}_j\boldsymbol{a}^{(p)}_{\ell_0,k}(x_0)\prod_{r=1}^{2m}e^{\boldsymbol{S}^{(p)}x_r}\boldsymbol{D}^{(p)}e^{\boldsymbol{S}^{(p)}x_{2m+1}}\end{aligned}$$

$$\boldsymbol{v}_{\ell_0,j}^{(p)}(x)\psi(x)\,\mathrm{d}x_{2m+1}\ldots\,\mathrm{d}x_2\,\mathrm{d}x_1\,\mathrm{d}x,$$

which satisfies the assumptions of Lemma C.8. To see this take $n = 2m+1$, $\boldsymbol{G}_1(x_1) = \boldsymbol{e}_i\boldsymbol{H}^{+-}(\lambda, x_1)$, $\boldsymbol{G}_{2k}(x_{2k}) = \boldsymbol{H}^{-+}(\lambda, x_{2k})$, $\boldsymbol{G}_{2k+1}(x_{2k}) = \boldsymbol{H}^{+-}(\lambda, x_{2k+1})$, $k = 1,\ldots,m-1$, $\boldsymbol{G}_{2m}(x_{2m}) = \boldsymbol{H}^{-+}(x_{2m})$ and $\boldsymbol{G}_{2m+1} = \boldsymbol{H}^{++}(\lambda, x_{2m+1})\boldsymbol{e}_j$ in Equation (C.45). By the remarks following Lemma C.8, this gives the required convergence for this case. Analogous arguments prove the result for the remaining combinations of (q, r). □

C.1 Technical results

As we did in Appendix **??**, we treat the cases of no changes, and $m \geq 1$ changes, of phase from $\mathcal{S}_+$ to $\mathcal{S}_-$ and $\mathcal{S}_-$ to $\mathcal{S}_+$ separately. We start with the *no changes* case. The following result is analogous to Lemma 4.4, though the proof is somewhat more tedious.

Lemma C.3. *Let $\psi : \mathcal{D}_{\ell_0} \to \mathbb{R}$ be bounded $|\psi(x)| \leq F$ and let $\lambda > 0$. For $i \in \mathcal{S}_-, j \in \mathcal{S}_- \cup \mathcal{S}_{-0}$, $x_0 \in (0, \Delta)$,*

$$\int_{x_1=0}^{\infty}\int_{x=0}^{\Delta}\boldsymbol{k}^{(p)}(x_0)\boldsymbol{D}^{(p)}e^{\boldsymbol{S}x_1}\boldsymbol{v}_{\ell_0,j}^{(p)}(x)h_{ij}^{--}(\lambda, x_1)\psi(x)\,\mathrm{d}x\,\mathrm{d}x_1 \to \int_{x=0}^{x_0}h_{ij}^{--}(\lambda, x_0 - x)\psi(x)\,\mathrm{d}x, \tag{C.8}$$

as $p \to \infty$. Similarly, for $i \in \mathcal{S}_+, j \in \mathcal{S}_+ \cup \mathcal{S}_{+0}$

$$\begin{aligned}&\int_{x_1=0}^{\infty}\int_{x=0}^{\Delta}\boldsymbol{k}^{(p)}(x_0)\boldsymbol{D}^{(p)}e^{\boldsymbol{S}^{(p)}x_1}\boldsymbol{v}_{\ell_0,j}^{(p)}(x)h_{ij}^{++}(\lambda, x_1)\psi(\Delta - x)\,\mathrm{d}x\,\mathrm{d}x_1\\ &\to \int_{x=\Delta-x_0}^{\Delta}h_{ij}^{++}(\lambda, x - x_0)\psi(x)\,\mathrm{d}x,\end{aligned} \tag{C.9}$$

Proof. Assume, for simplicity and without loss of generality, that $\ell_0 = 0$ so $\mathcal{D}_{\ell_0} = [0, \Delta]$. In the following we choose $\varepsilon^{(p)} = \mathrm{Var}(Z^{(p)})^{1/3}$ which tends to 0 as $p \to \infty$. Therefore, assume p is sufficiently large so that $x_0 \in (2\varepsilon, \Delta - \varepsilon)$. Such a $p < \infty$ always exists since $x_0 \in (0, \Delta)$.

Now, upon substituting the definition of $\boldsymbol{D}$ and exchanging the order of integration (justified by the Fubini-Tonelli Theorem), the difference between the left and right-hand sides of (C.8) is

$$\begin{aligned}\Bigg|&\int_{u=0}^{\infty}\boldsymbol{k}(x_0)e^{\boldsymbol{S}u}\boldsymbol{s}\int_{x=0}^{\Delta}\int_{x_1=0}^{\infty}\boldsymbol{k}(u)e^{\boldsymbol{S}x_1}\boldsymbol{v}_{\ell_0,j}(x)h_{ij}^{--}(\lambda, x_1)\psi(x)\,\mathrm{d}x_1\,\mathrm{d}x\,\mathrm{d}u\\ &- \int_{x=0}^{x_0}h_{ij}^{--}(\lambda, x_0 - x)\psi(x)\,\mathrm{d}x\Bigg|.\end{aligned} \tag{C.10}$$

We wish to apply Property 4.2(v) to the integral over x_1, however, to do so requires that $u \le \Delta - \varepsilon$. Breaking up the integral with respect to u, then (C.10) is equal to

$$\begin{aligned}
&\left| \int_{u=0}^{\Delta-\varepsilon} \boldsymbol{k}(x_0) e^{\boldsymbol{S}u} \boldsymbol{s} \int_{x=0}^{\Delta} \int_{x_1=0}^{\infty} \boldsymbol{k}(u) e^{\boldsymbol{S}x_1} \boldsymbol{v}_{\ell_0,j}(x) h_{ij}^{--}(\lambda, x_1) \psi(x) \,\mathrm{d}x_1 \,\mathrm{d}x \,\mathrm{d}u + d_1 \right. \\
&\left. - \int_{x=0}^{x_0} h_{ij}^{--}(\lambda, x_0 - x) \psi(x) \,\mathrm{d}x \right| \qquad \text{(C.11)} \\
&\le \left| \int_{u=0}^{\Delta-\varepsilon} \boldsymbol{k}(x_0) e^{\boldsymbol{S}u} \boldsymbol{s} \int_{x=0}^{\Delta} \int_{x_1=0}^{\infty} \boldsymbol{k}(u) e^{\boldsymbol{S}x_1} \boldsymbol{v}_{\ell_0,j}(x) h_{ij}^{--}(\lambda, x_1) \psi(x) \,\mathrm{d}x_1 \,\mathrm{d}x \,\mathrm{d}u \right. \\
&\left. - \int_{x=0}^{x_0} h_{ij}^{--}(\lambda, x_0 - x) \psi(x) \,\mathrm{d}x \right| + |d_1| \qquad \text{(C.12)}
\end{aligned}$$

where

$$|d_1| = \left| \int_{u=\Delta-\varepsilon}^{\infty} \boldsymbol{k}(x_0) e^{\boldsymbol{S}u} \boldsymbol{s} \int_{x=0}^{\Delta} \int_{x_1=0}^{\infty} \boldsymbol{k}(u) e^{\boldsymbol{S}x_1} \boldsymbol{v}_{\ell_0,j}(x) h_{ij}^{--}(\lambda, x_1) \psi(x) \,\mathrm{d}x_1 \,\mathrm{d}x \,\mathrm{d}u \right|.$$

We show later that $|d_1|$ can be made arbitrarily small by choosing Z with sufficiently small variance. For now, let us focus on the first absolute value in (C.12). By Property 4.2(v) and swapping the order of integration (justified by the Fubini-Tonelli Theorem) the first absolute value in (C.12) is

$$\begin{aligned}
&\left| \int_{x=0}^{\Delta} \int_{u=0}^{\Delta-\varepsilon} \boldsymbol{k}(x_0) e^{\boldsymbol{S}u} \boldsymbol{s} \left[h_{ij}^{--}(\lambda, \Delta - u - x) 1(u + x \le \Delta - \varepsilon) + r_{\boldsymbol{v}}(u, x) \right] \psi(x) \,\mathrm{d}u \,\mathrm{d}x \right. \\
&\qquad \left. - \int_{x=0}^{x_0} h_{ij}^{--}(\lambda, x_0 - x) \psi(x) \,\mathrm{d}x \right| \\
&\le \left| \int_{x=0}^{\Delta} \int_{u=0}^{\Delta-\varepsilon} \boldsymbol{k}(x_0) e^{\boldsymbol{S}u} \boldsymbol{s} h_{ij}^{--}(\lambda, \Delta - u - x) 1(u + x \le \Delta - \varepsilon) \psi(x) \,\mathrm{d}u \,\mathrm{d}x \right. \\
&\qquad \left. - \int_{x=0}^{x_0} h_{ij}^{--}(\lambda, x_0 - x) \psi(x) \,\mathrm{d}x \right| + |d_2|, \qquad \text{(C.13)}
\end{aligned}$$

where

$$|d_2| = \left| \int_{x=0}^{\Delta} \int_{u=0}^{\Delta-\varepsilon} \boldsymbol{k}(x_0) e^{\boldsymbol{S}u} \boldsymbol{s} r_{\boldsymbol{v}}(u, x) \psi(x) \,\mathrm{d}u \,\mathrm{d}x \right|.$$

We show later that $|d_2|$ can be made arbitrarily small by choosing Z with sufficiently

small variance. The remaining term in (C.13) can be written as

$$\left| \int_{x=0}^{\Delta-\varepsilon} \int_{u=0}^{\Delta-x-\varepsilon} \boldsymbol{k}(x_0) e^{\boldsymbol{S}u} \boldsymbol{s} h_{ij}^{--}(\lambda, \Delta - u - x)\psi(x)\,\mathrm{d}u\,\mathrm{d}x - \int_{x=0}^{x_0} h_{ij}^{--}(\lambda, x_0 - x)\psi(x)\,\mathrm{d}x \right|. \tag{C.14}$$

Intuitively, when the variance of Z is low, we expect a significant contribution to the integral with respect to u in (C.14) to come from the portion of the integral over the interval $(\Delta - x_0 - \varepsilon, \Delta - x_0 + \varepsilon)$. Although, the integral with respect to u only contains this interval when x is sufficiently small. Breaking up the integral with respect to u in (C.14) into an integral over the interval $(\Delta - x_0 - \varepsilon, \Delta - x_0 + \varepsilon)$ and integrals over the rest, then applying the triangle inequality, (C.14) is less than or equal to

$$\left| \int_{x=0}^{\Delta-\varepsilon} \int_{u=\Delta-x_0-\varepsilon}^{\Delta-x_0+\varepsilon} \boldsymbol{k}(x_0) e^{\boldsymbol{S}u} \boldsymbol{s} h_{ij}^{--}(\lambda, \Delta - u - x)\psi(x)\,\mathrm{d}u 1(x \leq x_0 - 2\varepsilon)\,\mathrm{d}x \right.$$
$$\left. - \int_{x=0}^{x_0} h_{ij}^{--}(\lambda, x_0 - x)\psi(x)\,\mathrm{d}x \right| + |d_3| + |d_4| + |d_5|, \tag{C.15}$$

where

$$|d_3| = \left| \int_{x=0}^{\Delta-\varepsilon} \int_{u=0}^{\Delta-x-\varepsilon} \boldsymbol{k}(x_0) e^{\boldsymbol{S}u} \boldsymbol{s} h_{ij}^{--}(\lambda, \Delta - u - x)\psi(x)\,\mathrm{d}u 1(x \geq x_0)\,\mathrm{d}x \right|,$$
$$|d_4| = \left| \int_{x=0}^{\Delta-\varepsilon} \int_{u=\Delta-x_0+\varepsilon}^{\Delta-x-\varepsilon} \boldsymbol{k}(x_0) e^{\boldsymbol{S}u} \boldsymbol{s} h_{ij}^{--}(\lambda, \Delta - u - x)\psi(x)\,\mathrm{d}u 1(x \leq x_0 - 2\varepsilon)\,\mathrm{d}x \right|,$$
$$|d_5| = \left| \int_{x=0}^{\Delta-\varepsilon} \int_{u=\Delta-x_0-\varepsilon}^{\Delta-x-\varepsilon} \boldsymbol{k}(x_0) e^{\boldsymbol{S}u} \boldsymbol{s} h_{ij}^{--}(\lambda, \Delta - u - x)\psi(x)\,\mathrm{d}u \times 1(x \in [x_0 - 2\varepsilon, x_0))\,\mathrm{d}x \right|.$$

We show later that $|d_3|$, $|d_4|$ and $|d_5|$ can be made arbitrarily small by choosing Z with sufficiently small variance.

In the first integral with respect to x in (C.15), since $x_0 \in (2\varepsilon, \Delta - \varepsilon)$, then we can absorb the indicator function into the limits of the integral which results in

$$\int_{x=0}^{x_0-2\varepsilon} \int_{u=\Delta-x_0-\varepsilon}^{\Delta-x_0+\varepsilon} \boldsymbol{k}(x_0) e^{\boldsymbol{S}u} \boldsymbol{s} h_{ij}^{--}(\lambda, \Delta - u - x)\psi(x)\,\mathrm{d}u\,\mathrm{d}x. \tag{C.16}$$

With this, and breaking up the integral over h_{ij}^{--}, we can write the first absolute value in (C.15) as

$$\left| \int_{x=0}^{x_0-2\varepsilon} \int_{u=\Delta-x_0-\varepsilon}^{\Delta-x_0+\varepsilon} \boldsymbol{k}(x_0) e^{\boldsymbol{S}u} \boldsymbol{s} h_{ij}^{--}(\lambda, \Delta - u - x)\psi(x)\,\mathrm{d}u\,\mathrm{d}x \right.$$

$$
\begin{aligned}
&\quad - \int_{x=0}^{x_0-2\varepsilon} h_{ij}^{--}(\lambda, x_0 - x)\psi(x)\,\mathrm{d}x - \int_{x=x_0-2\varepsilon}^{x_0} h_{ij}^{--}(\lambda, x_0 - x)\psi(x)\,\mathrm{d}x \Bigg| \\
&\leq \Bigg| \int_{x=0}^{x_0-2\varepsilon} \int_{u=\Delta-x_0-\varepsilon}^{\Delta-x_0+\varepsilon} \boldsymbol{k}(x_0) e^{\boldsymbol{S}u} \boldsymbol{s} h_{ij}^{--}(\lambda, \Delta - u - x)\psi(x)\,\mathrm{d}u\,\mathrm{d}x \\
&\quad - \int_{x=0}^{x_0-2\varepsilon} h_{ij}^{--}(\lambda, x_0 - x)\psi(x)\,\mathrm{d}x \Bigg| + |d_6|, \qquad \text{(C.17)}
\end{aligned}
$$

where

$$
|d_6| = \left| \int_{x=x_0-2\varepsilon}^{x_0} h_{ij}^{--}(\lambda, x_0 - x)\psi(x)\,\mathrm{d}x \right|.
$$

We show later that $|d_6|$ can be made arbitrarily small by choosing Z with sufficiently small variance.

Now, since probability densities integrate to 1, then we can write

$$
\begin{aligned}
\int_{x=0}^{x_0-2\varepsilon} h_{ij}^{--}(\lambda, x_0 - x)\psi(x)\,\mathrm{d}x &= \int_{x=0}^{x_0-2\varepsilon} h_{ij}^{--}(\lambda, x_0 - x)\psi(x)\,\mathrm{d}x \mathbb{P}(|Z - \Delta| \leq \varepsilon \mid Z > x_0) \\
&\quad + \int_{x=0}^{x_0-2\varepsilon} h_{ij}^{--}(\lambda, x_0 - x)\psi(x)\,\mathrm{d}x \mathbb{P}(|Z - \Delta| > \varepsilon \mid Z > x_0) \\
&= \int_{x=0}^{x_0-2\varepsilon} \int_{u=\Delta-x_0-\varepsilon}^{\Delta-x_0+\varepsilon} \boldsymbol{k}(x_0) e^{\boldsymbol{S}u} \boldsymbol{s} h_{ij}^{--}(\lambda, x_0 - x)\psi(x)\,\mathrm{d}u\,\mathrm{d}x \\
&\quad + \int_{x=0}^{x_0-2\varepsilon} h_{ij}^{--}(\lambda, x_0 - x)\psi(x)\,\mathrm{d}x \mathbb{P}(|Z - \Delta| > \varepsilon \mid Z > x_0).
\end{aligned}
$$

Therefore, the first absolute value in (C.17) can be written as

$$
\begin{aligned}
&\Bigg| \int_{x=0}^{x_0-2\varepsilon} \int_{u=\Delta-x_0-\varepsilon}^{\Delta-x_0+\varepsilon} \boldsymbol{k}(x_0) e^{\boldsymbol{S}u} \boldsymbol{s} h_{ij}^{--}(\lambda, \Delta - u - x)\psi(x)\,\mathrm{d}u\,\mathrm{d}x \\
&\quad - \int_{x=0}^{x_0-2\varepsilon} \int_{u=\Delta-x_0-\varepsilon}^{\Delta-x_0+\varepsilon} \boldsymbol{k}(x_0) e^{\boldsymbol{S}u} \boldsymbol{s} h_{ij}^{--}(\lambda, x_0 - x)\psi(x)\,\mathrm{d}u\,\mathrm{d}x \\
&\quad - \int_{x=0}^{x_0-2\varepsilon} h_{ij}^{--}(\lambda, x_0 - x)\psi(x)\,\mathrm{d}x \mathbb{P}(|Z - \Delta| > \varepsilon \mid Z > x_0) \Bigg| \\
&= \Bigg| \int_{x=0}^{x_0-2\varepsilon} \int_{u=\Delta-x_0-\varepsilon}^{\Delta-x_0+\varepsilon} \boldsymbol{k}(x_0) e^{\boldsymbol{S}u} \boldsymbol{s} \left[h_{ij}^{--}(\lambda, \Delta - u - x) - h_{ij}^{--}(\lambda, x_0 - x)\psi(x) \right] \mathrm{d}u\,\mathrm{d}x \\
&\quad - \int_{x=0}^{x_0-2\varepsilon} h_{ij}^{--}(\lambda, x_0 - x)\psi(x)\,\mathrm{d}x \mathbb{P}(|Z - \Delta| > \varepsilon \mid Z > x_0) \Bigg|
\end{aligned}
$$

$$\leq \left| \int_{x=0}^{x_0-2\varepsilon} \int_{u=\Delta-x_0-\varepsilon}^{\Delta-x_0+\varepsilon} \boldsymbol{k}(x_0) e^{\boldsymbol{S}u} \boldsymbol{s} \left[h_{ij}^{--}(\lambda, \Delta - u - x) - h_{ij}^{--}(\lambda, x_0 - x)\psi(x) \right] \mathrm{d}u \, \mathrm{d}x \right| + |d_7|$$
$$\leq \int_{x=0}^{x_0-2\varepsilon} \int_{u=\Delta-x_0-\varepsilon}^{\Delta-x_0+\varepsilon} \boldsymbol{k}(x_0) e^{\boldsymbol{S}u} \boldsymbol{s} \left| h_{ij}^{--}(\lambda, \Delta - u - x) - h_{ij}^{--}(\lambda, x_0 - x) \, || \, \psi(x) \right| \mathrm{d}u \, \mathrm{d}x + |d_7|, \tag{C.18}$$

where

$$|d_7| = \left| \int_{x=0}^{x_0-2\varepsilon} h_{ij}^{--}(\lambda, x_0 - x)\psi(x) \, \mathrm{d}x \mathbb{P}(|Z - \Delta| > \varepsilon \mid Z > x_0) \right|.$$

We show later that $|d_7|$ can be made arbitrarily small by choosing Z with sufficiently small variance.

Since h_{ij}^{--} is Lipschitz and $|(\Delta - u - x) - (x_0 - x)| \leq 2\varepsilon$ for all $u \in (\Delta - x_0 - \varepsilon, \Delta - x_0 + \varepsilon)$, then the first absolute value of (C.18) is less than or equal to

$$\int_{u=\Delta-x_0-\varepsilon}^{\Delta-x_0+\varepsilon} \boldsymbol{k}(x_0) e^{\boldsymbol{S}u} \boldsymbol{s} \, \mathrm{d}u 2L\varepsilon \int_{x=0}^{x_0-2\varepsilon} |\psi(x)| \, \mathrm{d}x. \tag{C.19}$$

Now, $\int_{u=\Delta-x_0-\varepsilon}^{\Delta-x_0+\varepsilon} \boldsymbol{k}(x_0) e^{\boldsymbol{S}u} \boldsymbol{s} \, \mathrm{d}u \leq 1$ as it is a probability, and $\int_{x=0}^{x_0-2\varepsilon} |\psi(x)| \, \mathrm{d}x \leq F\Delta$ as $|\psi| \leq F$ and $x_0 \in (2\varepsilon, \Delta - \varepsilon)$. Therefore, (C.19) is less than or equal to $2\varepsilon LF\Delta$.

What remains is to bound the terms $|d_\ell|$, $\ell = 1, \ldots, 7$.

Since $|\psi| \leq F$ then

$$|d_1| \leq \left| \int_{u=\Delta-\varepsilon}^{\infty} \boldsymbol{k}(x_0) e^{\boldsymbol{S}u} \boldsymbol{s} \int_{x=0}^{\Delta} \int_{x_1=0}^{\infty} \boldsymbol{k}(u) e^{\boldsymbol{S}x_1} \boldsymbol{v}(x) h_{ij}^{--}(\lambda, x_1) \, \mathrm{d}x_1 \, \mathrm{d}x \, \mathrm{d}u \right| F. \tag{C.20}$$

From Property 4.2(iv), (C.20) is less than or equal to

$$\begin{aligned} &\left| \int_{u=\Delta-\varepsilon}^{\infty} \boldsymbol{k}(x_0) e^{\boldsymbol{S}u} \boldsymbol{s} \int_{x_1=0}^{\infty} \boldsymbol{k}(u) e^{\boldsymbol{S}x_1} \boldsymbol{e} h_{ij}^{--}(\lambda, x_1) \, \mathrm{d}x_1 \, \mathrm{d}u \right| F \\ &\leq \left| \int_{u=\Delta-\varepsilon}^{\infty} \boldsymbol{k}(x_0) e^{\boldsymbol{S}u} \boldsymbol{s} \int_{x_1=0}^{\infty} \boldsymbol{k}(u) \boldsymbol{e} h_{ij}^{--}(\lambda, x_1) \, \mathrm{d}x_1 \, \mathrm{d}u \right| F \\ &= \left| \int_{u=\Delta-\varepsilon}^{\infty} \boldsymbol{k}(x_0) e^{\boldsymbol{S}u} \boldsymbol{s} \int_{x_1=0}^{\infty} h_{ij}^{--}(\lambda, x_1) \, \mathrm{d}x_1 \, \mathrm{d}u \right| F, \end{aligned} \tag{C.21}$$

since $\boldsymbol{k}(u) e^{\boldsymbol{S}x_1} \boldsymbol{e}$ is decreasing in x_1 and $\boldsymbol{k}(u)\boldsymbol{e} = 1$. Now, as $h_{ij}^{--}(\lambda, x_1)$ is integrable with $\int_{x_1=0}^{\infty} h_{ij}^{--}(\lambda, x_1) \, \mathrm{d}x_1 \leq \widehat{G}$, then (C.21) is less than or equal to

$$\left| \int_{u=\Delta-\varepsilon}^{\infty} \boldsymbol{k}(x_0) e^{\boldsymbol{S}u} \boldsymbol{s} \, \mathrm{d}u \right| \widehat{G}F = \mathbb{P}(Z > x_0 + \Delta - \varepsilon \mid Z > x_0) \widehat{G}F$$

$$\leq \frac{\mathrm{Var}(Z)/\varepsilon^2}{1-\mathrm{Var}(Z)/\varepsilon^2}\widehat{G}F,$$

by Chebyshev's inequality, since $x_0 \in (2\varepsilon, \Delta-\varepsilon)$.

Since $|\psi(x)| \leq F$, then

$$|d_2| \leq \left|\int_{x=0}^{\Delta}\int_{u=0}^{\Delta-\varepsilon} \boldsymbol{k}(x_0)e^{\boldsymbol{S}u}\boldsymbol{s}r_{\boldsymbol{v}}(u,x)\,\mathrm{d}u\,\mathrm{d}x\right| F \tag{C.22}$$

$$\leq \left|\int_{u=0}^{\Delta-\varepsilon} \boldsymbol{k}(x_0)e^{\boldsymbol{S}u}\boldsymbol{s}\,\mathrm{d}u\right| R_{\boldsymbol{v},2}F \tag{C.23}$$

$$\leq R_{\boldsymbol{v},2}F, \tag{C.24}$$

where the first inequality holds from Property 4.2(v), and the last inequality holds since $\int_{u=0}^{\Delta-\varepsilon} \boldsymbol{k}(x_0)e^{\boldsymbol{S}u}\boldsymbol{s}\,\mathrm{d}u = \mathbb{P}(Z \in (x_0, x_0+\Delta-\varepsilon) \mid Z > x_0) \leq 1$.

Since $|\psi(x)| \leq F$ and $h_{ij}^{--}(\lambda, \Delta-u-x) \leq G$, then

$$\begin{aligned}|d_3| &\leq \int_{u=0}^{\min(\Delta-x_0-\varepsilon,\Delta-x-\varepsilon)} \boldsymbol{k}(x_0)e^{\boldsymbol{S}u}\boldsymbol{s}\,\mathrm{d}u\Delta GF \\ &\leq \mathbb{P}(Z \leq \Delta-\varepsilon \mid Z > x_0)\,\mathrm{d}u\Delta GF \\ &\leq \frac{\mathrm{Var}(Z)/\varepsilon^2}{1-\mathrm{Var}(Z)/\varepsilon^2}\Delta GF,\end{aligned} \tag{C.25}$$

where the last inequality holds from Chebyshev's inequality.

Similarly, since $|\psi(x)| \leq F$ and $h_{ij}^{--}(\lambda, \Delta-u-x) \leq G$, then

$$\begin{aligned}|d_4| &\leq \int_{x=0}^{x_0-2\varepsilon}\int_{u=\Delta-x_0+\varepsilon}^{\Delta-x-\varepsilon} \boldsymbol{k}(x_0)e^{\boldsymbol{S}u}\boldsymbol{s}\,\mathrm{d}u\,\mathrm{d}xGF \\ &= \int_{x=0}^{x_0-2\varepsilon} \mathbb{P}(Z \in [\Delta+\varepsilon, \Delta-x-\varepsilon+x_0] \mid Z > x_0)\,\mathrm{d}xGF \\ &\leq \int_{x=0}^{x_0-2\varepsilon} \mathbb{P}(Z \in [\Delta+\varepsilon, \Delta-\varepsilon+x_0] \mid Z > x_0)\,\mathrm{d}xGF \\ &\leq \mathbb{P}(Z \in [\Delta+\varepsilon, \Delta-\varepsilon+x_0] \mid Z > x_0)\Delta GF \\ &\leq \frac{\mathrm{Var}(Z)/\varepsilon^2}{1-\mathrm{Var}(Z)/\varepsilon^2}\Delta GF.\end{aligned}$$

Since $|\psi(x)| \leq F$ and $h_{ij}^{--}(\lambda, \Delta-u-x) \leq G$, then

$$|d_5| \leq \int_{x=0}^{\Delta-\varepsilon}\int_{u=\Delta-x_0-\varepsilon}^{\Delta-x-\varepsilon} \boldsymbol{k}(x_0)e^{\boldsymbol{S}u}\boldsymbol{s}\,\mathrm{d}u1(x \in [x_0-2\varepsilon, x_0))\,\mathrm{d}xGF \tag{C.26}$$

$$\leq \int_{x=0}^{\Delta-\varepsilon} 1(x \in [x_0 - 2\varepsilon, x_0))\,\mathrm{d}xGF$$
$$= 2\varepsilon GF,$$

where the second inequality holds since $\int_{u=\Delta-x_0-\varepsilon}^{\Delta-x-\varepsilon} \boldsymbol{k}(x_0)e^{\boldsymbol{S}u}\boldsymbol{s}\,\mathrm{d}u \leq 1$.

Since $|\psi(x)| \leq F$ and $h_{ij}^{--}(\lambda, \Delta - u - x) \leq G$, then

$$|d_6| \leq \int_{x=x_0-2\varepsilon}^{x_0} \mathrm{d}xGF$$
$$= 2\varepsilon GF. \tag{C.27}$$

Since $|\psi(x)| \leq F$ and $h_{ij}^{--}(\lambda, \Delta - u - x) \leq G$ then

$$|d_7| \leq \mathbb{P}(|Z - \Delta| > \varepsilon \mid Z > x_0)\Delta GF \tag{C.28}$$
$$\leq \frac{\mathrm{Var}(Z)/\varepsilon^2}{1 - \mathrm{Var}(Z)/\varepsilon^2}\Delta GF \tag{C.29}$$

Convergence follows after setting $\varepsilon^{(p)} = \mathrm{Var}(Z^{(p)})^{1/3}$ and observing that all the bounds $|d_1|, \ldots, |d_7|$ tend to 0, as does the bound on (C.19), given by $2\varepsilon^{(p)}LF\Delta$, as $p \to \infty$. □

Now we show bounds for certain Laplace transform expressions which arise when the QBD-RAP starts in phases in $\mathcal{S}_{+0} \cup \mathcal{S}_{-0}$ and there is more than one change from $\mathcal{S}_+$ to $\mathcal{S}_-$ or $\mathcal{S}_-$ to $\mathcal{S}_+$ before the first change of level. These expressions have the form

$$\int_{x_1=0}^{\infty} g_1(x_1)\boldsymbol{k}(x_0)\boldsymbol{D}e^{\boldsymbol{S}x_1}\,\mathrm{d}x_1\boldsymbol{D}\left[\prod_{n=2}^{k-1}\int_{x_n=0}^{\infty} g_n(x_n)e^{\boldsymbol{S}x_n}\,\mathrm{d}x_n\boldsymbol{D}\right]\int_{x_n=0}^{\infty} g_n(x_n)e^{\boldsymbol{S}x_n}\,\mathrm{d}x_n\boldsymbol{v}(x). \tag{C.30}$$

Here, we ultimately wish to show that (C.30) converges to $g_{1,n}^*(\Delta - x_0, x)$. We do not do this directly, instead, we show that (C.30) is 'close' to $w_n(\Delta - x_0, x)$, then rely on the results from Appendix **??** to get the desired convergence.

Observe that by substituting the first matrix $\boldsymbol{D}$ in the expression above for its integral expression, then (C.30) is equal to

$$\int_{x_1=0}^{\infty} g_1(x_1)\boldsymbol{k}(x_0)\int_{z_0=0}^{\infty} e^{\boldsymbol{S}z_0}\boldsymbol{s}\frac{\boldsymbol{\alpha}e^{\boldsymbol{S}z_0}}{\boldsymbol{\alpha}e^{\boldsymbol{S}z_0}\boldsymbol{e}}\mathrm{d}z_0 e^{\boldsymbol{S}x_1}\,\mathrm{d}x_1\boldsymbol{D}\left[\prod_{n=2}^{k-1}\int_{x_n=0}^{\infty} g_n(x_n)e^{\boldsymbol{S}x_n}\,\mathrm{d}x_n\boldsymbol{D}\right] \tag{C.31}$$
$$\times \int_{x_n=0}^{\infty} g_n(x_n)e^{\boldsymbol{S}x_n}\,\mathrm{d}x_n\boldsymbol{v}(x)$$
$$= \boldsymbol{k}(x_0)\int_{z_0=0}^{\infty} e^{\boldsymbol{S}z_0}\boldsymbol{s}w_n(z_0, x)\,\mathrm{d}z_0. \tag{C.32}$$

Intuitively, when the variance of Z is low, we expect that the integral in (C.32) above will be approximately equal to $w_n(\Delta - x_0, x)$. Indeed, we proved in Lemma 4.6 that this is the case for functions g satisfying the Assumptions 4.1. However, here we do not immediately have that $w_n(x_0, x)$ is Lipschitz in x_0, which we would need for it to satisfy Assumptions 4.1. Instead, we can show a Lipschitz-like condition in x_0 for $w_n(x_0, x)$, which suffices.

For later use, observe that

$$\begin{aligned} g^*_{2,n}(u_1, x) &= \int_{u_2=0}^{\Delta-u_1} g_2(\Delta - u_2 - u_1)\,\mathrm{d}u_1 \ldots \int_{u_{n-1}=0}^{\Delta-u_{n-2}} g_{n-1}(\Delta - u_{n-1} - u_{n-2})\,\mathrm{d}u_{n-2} \\ &\qquad g_n(\Delta - x - u_{n-1})1(\Delta - x - u_{n-1} \geq 0)\,\mathrm{d}u_{n-1} \\ &\leq G^{n-1} \int_{u_2=0}^{\Delta-u_1} \mathrm{d}u_1 \ldots \int_{u_{n-1}=0}^{\Delta-u_{n-2}} \mathrm{d}u_{n-1} \\ &\leq G^{n-1}\Delta^{n-2} := G^*_n. \end{aligned} \tag{C.33}$$

Corollary C.4. *For $x_0, x \in [0, \Delta)$, $n \geq 2$,*

$$|w_n(x_0, x) - w_n(z_0, x)| \leq 2|r_5(n)| + 2|r_6(n)| + 2(n-1)|r_4(n)| + |x_0 - z_0|G^*_n(G + L\Delta). \tag{C.34}$$

Proof. By adding and subtracting both $\int_{u_1=0}^{\Delta-x_0} g_1(\Delta - u_1 - x_0)g^*_{2,n}(u_1, x)\,\mathrm{d}u_1$ and $\int_{u_1=0}^{\Delta-z_0} g_1(\Delta - u_1 - z_0)g^*_{2,n}(u_1, x)\,\mathrm{d}u_1$, we can write the left-hand side of (C.34) as

$$\begin{aligned} \Bigg| & w_n(x_0, x) - \int_{u_1=0}^{\Delta-x_0} g_1(\Delta - u_1 - x_0)g^*_{2,n}(u_1, x)\,\mathrm{d}u_1 \\ & - w_n(z_0, x) + \int_{u_1=0}^{\Delta-z_0} g_1(\Delta - u_1 - z_0)g^*_{2,n}(u_1, x)\,\mathrm{d}u_1 \\ & + \int_{u_1=0}^{\Delta-x_0} g_1(\Delta - u_1 - x_0)g^*_{2,n}(u_1, x)\,\mathrm{d}u_1 - \int_{u_1=0}^{\Delta-z_0} g_1(\Delta - u_1 - z_0)g^*_{2,n}(u_1, x)\,\mathrm{d}u_1 \Bigg| \end{aligned}$$

which, by the triangle inequality, is less than or equal to

$$\begin{aligned} & \left| w_n(x_0, x) - \int_{u_1=0}^{\Delta-x_0} g_1(\Delta - u_1 - x_0)g^*_{2,n}(u_1, x)\,\mathrm{d}u_1 \right| \\ & \quad + \left| w_n(z_0, x) - \int_{u_1=0}^{\Delta-z_0} g_1(\Delta - u_1 - z_0)g^*_{2,n}(u_1, x)\,\mathrm{d}u_1 \right| \end{aligned}$$

$$+\left|\int_{u_1=0}^{\Delta-x_0} g_1(\Delta-u_1-x_0)g^*_{2,n}(u_1,x)\,\mathrm{d}u_1-\int_{u_1=0}^{\Delta-z_0} g_1(\Delta-u_1-z_0)g^*_{2,n}(u_1,x)\,\mathrm{d}u_1\right|. \tag{C.35}$$

By Corollary 4.9, the first two terms of (C.35) are less than or equal to $|r_5(n)|+|r_6(n)|+(n-1)|r_4(n)|$. As for the last term, adding and subtracting $\int_{u_1=0}^{\Delta-z_0} g_1(\Delta-u_1-x_0)g^*_{2,n}(u_1,x)\,\mathrm{d}u_1$ gives

$$\begin{aligned}
&= \left|\int_{u_1=0}^{\Delta-x_0} g_1(\Delta-u_1-x_0)g^*_{2,n}(u_1,x)\,\mathrm{d}u_1-\int_{u_1=0}^{\Delta-z_0} g_1(\Delta-u_1-x_0)g^*_{2,n}(u_1,x)\,\mathrm{d}u_1\right.\\
&\qquad\left.-\int_{u_1=0}^{\Delta-z_0}(g_1(\Delta-u_1-z_0)-g_1(\Delta-u_1-x_0))g^*_{2,n}(u_1,x)\,\mathrm{d}u_1\right|\\
&\le \left|\int_{u_1=\Delta-z_0}^{\Delta-x_0} g_1(\Delta-u_1-x_0)g^*_{2,n}(u_1,x)\,\mathrm{d}u_1\right|\\
&\qquad+\int_{u_1=0}^{\Delta-z_0}|g_1(\Delta-u_1-z_0)-g_1(\Delta-u_1-x_0)|g^*_{2,n}(u_1,x)\,\mathrm{d}u_1\\
&\le GG^*_n|x_0-z_0|+\int_{u_1=0}^{\Delta-z_0} L|x_0-z_0|G^*_n\,\mathrm{d}u_1,
\end{aligned} \tag{C.36}$$

since g_1 is Lipschitz by Assumption 4.1(iv) and $g^*_{2,n}\le G^*_n$. Bounding the integral over u_1 by Δ, then (C.36) is less than or equal to

$$GG^*_n|x_0-z_0|+\Delta L|x_0-z_0|G^*_n. \tag{C.37}$$

□

Corollary C.5. *Let $g_1,g_2,\ldots,$ be functions satisfying Assumptions 4.1 and let $\boldsymbol{v}(x)$, $x\in[0,\Delta)$, be a closing operator with Properties 4.2. For $x_0,x\in[0,\Delta)$, $n\ge 2$,*

$$\left|\boldsymbol{k}(x_0)\int_{z_0=0}^{\infty} e^{\boldsymbol{S}z_0}\boldsymbol{s}w_n(z_0,x)\,\mathrm{d}z_0-w_n(\Delta-x_0,x)\right|=r_8(n),$$

where

$$\begin{aligned}
|r_8(n)|\le{}&(2|r_5(n)|+2|r_6(n)|+2(n-1)|r_4(n)|+\varepsilon G^*_n(G+L\Delta))\\
&+2\widehat{G}^{n-2}GG_{\boldsymbol{v}}\frac{\mathrm{Var}(Z)/\varepsilon^2}{1-\mathrm{Var}(Z)/(\Delta-x_0)^2}.
\end{aligned}$$

Proof. Now

$$\left|\boldsymbol{k}(x_0)\int_{z_0=0}^{\infty} e^{\boldsymbol{S}z_0}\boldsymbol{s}w_n(z_0,x)\,\mathrm{d}z_0-w_n(\Delta-x_0,x)\right|$$

$$
\begin{aligned}
&= \left| \boldsymbol{k}(x_0) \int_{z_0=0}^{\infty} e^{\boldsymbol{S}z_0} \boldsymbol{s} (w_n(z_0, x) - w_n(\Delta - x_0, x)) \, \mathrm{d}z_0 \right| \\
&\leq \boldsymbol{k}(x_0) \int_{z_0=0}^{\infty} e^{\boldsymbol{S}z_0} \boldsymbol{s} \, |w_n(z_0, x) - w_n(\Delta - x_0, x)| \, \mathrm{d}z_0 \\
&= \boldsymbol{k}(x_0) \int_{z_0=0}^{\Delta-\varepsilon-x_0} e^{\boldsymbol{S}z_0} \boldsymbol{s} \, |w_n(z_0, x) - w_n(\Delta - x_0, x)| \, \mathrm{d}z_0 \\
&\quad + \boldsymbol{k}(x_0) \int_{z_0=\Delta+\varepsilon-x_0}^{\infty} e^{\boldsymbol{S}z_0} \boldsymbol{s} \, |w_n(z_0, x) - w_n(\Delta - x_0, x)| \, \mathrm{d}z_0 \\
&\quad + \boldsymbol{k}(x_0) \int_{z_0=\Delta-\varepsilon-x_0}^{\Delta+\varepsilon-x_0} e^{\boldsymbol{S}z_0} \boldsymbol{s} \, |w_n(z_0, x) - w_n(\Delta - x_0, x)| \, \mathrm{d}z_0. \qquad \text{(C.38)}
\end{aligned}
$$

Using Equations (4.52), (4.60) and (4.72) we can claim

$$
\begin{aligned}
|w_n(x_0, x)| &\leq \frac{1}{\boldsymbol{\alpha} e^{\boldsymbol{S}x_0} \boldsymbol{e}} G^2 \widehat{G}^{n-2} \int_{u_k=0}^{\infty} \boldsymbol{\alpha} e^{\boldsymbol{S}u_k} \boldsymbol{e} \, \mathrm{d}u_k G_{\boldsymbol{v}} + \frac{1}{\boldsymbol{\alpha} e^{\boldsymbol{S}x_0} \boldsymbol{e}} G \widehat{G}^n \widetilde{G}_{\boldsymbol{v}} \\
&= \frac{1}{\boldsymbol{\alpha} e^{\boldsymbol{S}x_0} \boldsymbol{e}} G^2 \widehat{G}^{n-2} G_{\boldsymbol{v}} + \frac{1}{\boldsymbol{\alpha} e^{\boldsymbol{S}x_0} \boldsymbol{e}} G \widehat{G}^n \widetilde{G}_{\boldsymbol{v}} \\
&=: W_n. \qquad \text{(C.39)}
\end{aligned}
$$

Therefore, the sum of the first two terms in (C.38) is less than or equal to

$$
\begin{aligned}
&2W_n \left(\int_{z_0=0}^{\Delta-\varepsilon-x_0} \boldsymbol{k}(x_0) e^{\boldsymbol{S}z_0} \boldsymbol{s} \, \mathrm{d}z_0 + \int_{z_0=\Delta+\varepsilon-x_0}^{\infty} \boldsymbol{k}(x_0) e^{\boldsymbol{S}z_0} \boldsymbol{s} \, \mathrm{d}z_0 \right) \\
&= 2W \frac{\mathbb{P}(|Z - \Delta| > \varepsilon)}{\mathbb{P}(Z > x_0)} \\
&\leq 2W_n \frac{\mathrm{Var}(Z)/\varepsilon^2}{1 - \mathrm{Var}(Z)/(\Delta - x_0)^2} \qquad \text{(C.40)}
\end{aligned}
$$

by Chebyshev's inequality. As for the last term in (C.38), we can use Corollary C.4 to bound the integrand so that the last term is less than or equal to

$$
\begin{aligned}
&\boldsymbol{k}(x_0) \int_{z_0=\Delta-\varepsilon-x_0}^{\Delta+\varepsilon-x_0} e^{\boldsymbol{S}z_0} \boldsymbol{s} \left(2|r_5(n)| + 2|r_6(n)| + 2(n-1)|r_4(n)| + \varepsilon G^{n-1} \Delta^{n-2} (G + L\Delta) \right) \mathrm{d}z_0 \\
&\leq \left(2|r_5(n)| + 2|r_6(n)| + 2(n-1)|r_4(n)| + \varepsilon G^{n-1} \Delta^{n-2} (G + L\Delta) \right) \\
&\quad + 2W_n \frac{\mathrm{Var}(Z)/\varepsilon^2}{1 - \mathrm{Var}(Z)/(\Delta - x_0)^2}, \qquad \text{(C.41)}
\end{aligned}
$$

since $\boldsymbol{k}(x_0) \int_{z_0=\Delta-\varepsilon-x_0}^{\Delta+\varepsilon-x_0} e^{\boldsymbol{S}z_0} \boldsymbol{s} \, \mathrm{d}z_0 \leq 1$. □

Corollary C.6. *Let $g_1, g_2, \ldots,$ be functions satisfying Assumptions 4.1 and let $\boldsymbol{v}(x)$, $x \in (0, \Delta)$, be a closing operator with Properties 4.2. For $x_0, x \in (0, \Delta)$, $n \geq 2$*

$$\begin{aligned}&\left|\boldsymbol{k}(x_0)\int_{z_0=0}^{\infty} e^{\boldsymbol{S}z_0}\boldsymbol{s}w_n(z_0,x)\,\mathrm{d}z_0 - g^*_{1,n}(\Delta - x_0, x)\right| \\ &\leq |r_8(n)| + |r_5(n)| + |r_6(n)| + (n-1)|r_4(n)|. \end{aligned} \tag{C.42}$$

Proof. Adding and subtracting $w_n(\Delta - x_0, x)$ within the absolute value on the left-hand side of (C.42)

$$\begin{aligned}&\left|\boldsymbol{k}(x_0)\int_{z_0=0}^{\infty} e^{\boldsymbol{S}z_0}\boldsymbol{s}w_n(z_0,x)\,\mathrm{d}z_0 - w_n(\Delta - x_0, x) + w_n(\Delta - x_0, x) - g^*_{1,n}(\Delta - x_0, x)\right| \\ &\leq \left|\boldsymbol{k}(x_0)\int_{z_0=0}^{\infty} e^{\boldsymbol{S}z_0}\boldsymbol{s}w_n(z_0,x)\,\mathrm{d}z_0 - w_n(\Delta - x_0, x)\right| + \left|w_n(\Delta - x_0, x) - g^*_{1,n}(\Delta - x_0, x)\right|\end{aligned}$$

where the first absolute value is less than or equal to $|r_8(n)|$ by Corollary C.5 and the second absolute value is less than or equal to $|r_5(n)| + |r_6(n)| + (n-1)|r_4(n)|$ by Corollary 4.9. □

Corollary C.7. *Let ψ be bounded and Lipschitz, let $g_1, g_2, \ldots,$ be functions satisfying Assumptions 4.1 and let $\boldsymbol{v}(x)$, $x \in (0, \Delta)$, be a closing operator with Properties 4.2. For $x_0, x \in (0, \Delta)$, $n \geq 2$*

$$\begin{aligned}&\left|\int_{x\in[0,\Delta)} \boldsymbol{k}(x_0)\int_{z_0=0}^{\infty} e^{\boldsymbol{S}z_0}\boldsymbol{s}w_n(z_0,x)\,\mathrm{d}z_0\psi(x)\,\mathrm{d}x - \int_{x\in[0,\Delta)} g^*_{1,n}(\Delta - x_0, x)\psi(x)\,\mathrm{d}x\right| \\ &\leq \left(|r_8(n)| + |r_5(n)| + |r_6(n)| + (n-1)|r_4(n)|\right) F\Delta. \end{aligned} \tag{C.43}$$

Proof. The left-hand side of (C.43) is less than or equal to

$$\int_{x\in[0,\Delta)} \left|\boldsymbol{k}(x_0)\int_{z_0=0}^{\infty} e^{\boldsymbol{S}z_0}\boldsymbol{s}w_n(z_0,x)\,\mathrm{d}z_0 - g^*_{1,n}(\Delta - x_0, x)\right| |\psi(x)|\,\mathrm{d}x. \tag{C.44}$$

Now, using $|\psi(x)| \leq F$ and Corollary C.6 then (C.44) is less than or equal to

$$\left(|r_8(n)| + |r_5(n)| + |r_6(n)| + (n-1)|r_4(n)|\right)\Delta F.$$

□

We now extend the previous results to the matrix case.

Lemma C.8. *Let $\boldsymbol{G}_k(x)$, $k \in \{1, 2, ...\}$, be matrix functions with dimensions $N_k \times N_{k+1}$. Further, suppose $[\boldsymbol{G}_k(x)]_{ij}$, $k \in \{1, 2, ...\}$ satisfy Assumptions 4.1. Then,*

$$\left|\int_{x\in[0,\Delta)}\int_{x_1=0}^{\infty} \boldsymbol{G}_1(x_1)\otimes\boldsymbol{k}(x_0)\boldsymbol{D}e^{\boldsymbol{S}x_1}\,\mathrm{d}x_1\boldsymbol{D}\left[\prod_{k=2}^{n-1}\int_{x_k=0}^{\infty}\boldsymbol{G}_k(x_k)\otimes e^{\boldsymbol{S}x_k}\,\mathrm{d}x_k\boldsymbol{D}\right]\right.$$

$$\times \int_{x_n=0}^{\infty} \boldsymbol{G}_n(x_n) \otimes e^{\boldsymbol{S}x_n} \,\mathrm{d}x_n \boldsymbol{v}(x)\psi(x)\,\mathrm{d}x$$
$$- \int_{x\in[0,\Delta)} \int_{u_1=0}^{x_0} \boldsymbol{G}_1(x_0-u_1) \left[\prod_{k=2}^{n-1} \int_{u_k=0}^{\Delta-u_{k-1}} \boldsymbol{G}_k(\Delta-u_k-u_{k-1})\,\mathrm{d}u_{k-1}\right]$$
$$\boldsymbol{G}_n(\Delta-x-u_{n-1}) \times 1(\Delta-x-u_{n-1}\geq 0)\,\mathrm{d}u_{n-1}\psi(x)\,\mathrm{d}x\Bigg|$$
$$\leq (|r_8(n)| + |r_5(n)| + |r_6(n)| + (n-1)|r_4(n)|)\, F\Delta \prod_{k=2}^{n} N_k. \tag{C.45}$$

Moreover, choosing $\varepsilon = \mathrm{Var}(Z)$, then, for fixed n, the bound is $\mathcal{O}(\mathrm{Var}(Z)^{1/3})$.

Proof. The proof is the same as the proof of Lemma 4.11. □

Lemma 4.11 effectively shows that, as $p \to \infty$, then

$$\int_{x\in[0,\Delta)} \int_{x_1=0}^{\infty} \boldsymbol{G}_1(x_1) \otimes \boldsymbol{k}^{(p)}(x_0)\boldsymbol{D}^{(p)} e^{\boldsymbol{S}^{(p)}x_1}\,\mathrm{d}x_1 \boldsymbol{D}^{(p)} \left[\prod_{k=2}^{n-1} \int_{x_k=0}^{\infty} \boldsymbol{G}_k(x_k) \otimes e^{\boldsymbol{S}^{(p)}x_k}\,\mathrm{d}x_k \boldsymbol{D}^{(p)}\right]$$
$$\times \int_{x_n=0}^{\infty} \boldsymbol{G}_n(x_n) \otimes e^{\boldsymbol{S}^{(p)}x_n}\,\mathrm{d}x_n \boldsymbol{v}^{(p)}(x)\psi(x)\,\mathrm{d}x$$
$$\to \int_{x\in[0,\Delta)} \int_{u_1=0}^{x_0} \boldsymbol{G}_1(x_0-u_1) \left[\prod_{k=2}^{n-1} \int_{u_k=0}^{\Delta-u_{k-1}} \boldsymbol{G}_k(\Delta-u_k-u_{k-1})\,\mathrm{d}u_{k-1}\right]$$
$$\boldsymbol{G}_n(\Delta-x-u_{n-1}) \times 1(\Delta-x-u_{n-1}\geq 0)\,\mathrm{d}u_{n-1}\psi(x)\,\mathrm{d}x.$$

Thus, we have established a type of convergence of the QBD-RAP scheme to the fluid queue on the event that the phase is initially in $\mathcal{S}_{+0} \cup \mathcal{S}_{-0}$, and before the first change of level. However, we are not quite done yet. The last thing we need to prove is convergence at the first change of level. Since the result in Corollary C.6 is pointwise in x, choosing the closing operator as $e^{\boldsymbol{S}x}\boldsymbol{s}$ and setting $x = 0$, then we get convergence at the first change of level, on the event that there is one or more phase transition from $\mathcal{S}_+$ to $\mathcal{S}_-$ or $\mathcal{S}_-$ to $\mathcal{S}_+$. The only thing that remains is to show convergence at the first change of level on the event that there is no phase transition from $\mathcal{S}_+$ to $\mathcal{S}_-$ or $\mathcal{S}_-$ to $\mathcal{S}_+$.

Lemma C.9. *Let g satisfy the Assumptions 4.1 and $x_0 \in (2\varepsilon, \Delta-\varepsilon)$. Then*

$$\left|\int_{x=0}^{\infty} \boldsymbol{k}(x_0)\boldsymbol{D}e^{\boldsymbol{S}x} g(x)\boldsymbol{s}\,\mathrm{d}x - g(x_0)\right| \leq \frac{\mathrm{Var}(Z)/\varepsilon^2}{1-\mathrm{Var}(Z)/(\Delta-x_0)^2} 4G + 3L\varepsilon + 6G\frac{\mathrm{Var}(Z)}{\varepsilon^2}. \tag{C.46}$$

Proof. First rewrite the left-hand side as

$$\left|\int_{x=0}^{\infty} \boldsymbol{k}(x_0)\boldsymbol{D}e^{\boldsymbol{S}x}(g(x)-g(x_0))\boldsymbol{s}\,\mathrm{d}x\right| \leq \int_{x=0}^{\infty} \boldsymbol{k}(x_0)\boldsymbol{D}e^{\boldsymbol{S}x}|g(x)-g(x_0)|\boldsymbol{s}\,\mathrm{d}x. \tag{C.47}$$

Substituting in the expression for $\boldsymbol{D}$ gives,

$$\begin{aligned}
&\int_{x=0}^{\infty} \boldsymbol{k}(x_0) \int_{u=0}^{\infty} e^{\boldsymbol{S}u}\boldsymbol{s}\frac{\boldsymbol{\alpha}e^{\boldsymbol{S}u}}{\boldsymbol{\alpha}e^{\boldsymbol{S}u}\boldsymbol{e}}\mathrm{d}ue^{\boldsymbol{S}x}|g(x)-g(x_0)|\boldsymbol{s}\,\mathrm{d}x \\
&= \int_{x=0}^{\infty} \boldsymbol{k}(x_0) \int_{u=0}^{\Delta-\varepsilon} e^{\boldsymbol{S}u}\boldsymbol{s}\frac{\boldsymbol{\alpha}e^{\boldsymbol{S}u}}{\boldsymbol{\alpha}e^{\boldsymbol{S}u}\boldsymbol{e}}\mathrm{d}ue^{\boldsymbol{S}x}|g(x)-g(x_0)|\boldsymbol{s}\,\mathrm{d}x \\
&\quad + \int_{x=0}^{\infty} \boldsymbol{k}(x_0) \int_{u=\Delta-\varepsilon}^{\infty} e^{\boldsymbol{S}u}\boldsymbol{s}\frac{\boldsymbol{\alpha}e^{\boldsymbol{S}u}}{\boldsymbol{\alpha}e^{\boldsymbol{S}u}\boldsymbol{e}}\mathrm{d}ue^{\boldsymbol{S}x}|g(x)-g(x_0)|\boldsymbol{s}\,\mathrm{d}x.
\end{aligned} \tag{C.48}$$

Since g is bounded, the second term is less than or equal to

$$\begin{aligned}
\int_{x=0}^{\infty} \boldsymbol{k}(x_0) \int_{u=\Delta-\varepsilon}^{\infty} e^{\boldsymbol{S}u}\boldsymbol{s}\frac{\boldsymbol{\alpha}e^{\boldsymbol{S}u}}{\boldsymbol{\alpha}e^{\boldsymbol{S}u}\boldsymbol{e}}\mathrm{d}ue^{\boldsymbol{S}x}\boldsymbol{s}\,\mathrm{d}x2G &= \boldsymbol{k}(x_0) \int_{u=\Delta-\varepsilon}^{\infty} e^{\boldsymbol{S}u}\boldsymbol{s}\frac{\boldsymbol{\alpha}e^{\boldsymbol{S}u}}{\boldsymbol{\alpha}e^{\boldsymbol{S}u}\boldsymbol{e}}\mathrm{d}u\boldsymbol{e}2G \\
&= \boldsymbol{k}(x_0) \int_{u=\Delta-\varepsilon}^{\infty} e^{\boldsymbol{S}u}\boldsymbol{s}\,\mathrm{d}u2G \\
&= \frac{\mathbb{P}(Z \geq x_0+\Delta-\varepsilon)}{\mathbb{P}(Z > x_0)}2G.
\end{aligned} \tag{C.49}$$

For $x_0 \in (2\varepsilon, \Delta-\varepsilon)$, then (C.49) is less than or equal to

$$\frac{\mathrm{Var}(Z)/\varepsilon^2}{1-\mathrm{Var}(Z)/(\Delta-x_0)^2}2G.$$

As for the first term in (C.48), it can be written as

$$\begin{aligned}
&\int_{x=0}^{\infty} \boldsymbol{k}(x_0) \int_{u=\Delta-x_0-\varepsilon}^{u=\Delta-x_0+\varepsilon} e^{\boldsymbol{S}u}\boldsymbol{s}\frac{\boldsymbol{\alpha}e^{\boldsymbol{S}u}}{\boldsymbol{\alpha}e^{\boldsymbol{S}u}\boldsymbol{e}}\mathrm{d}ue^{\boldsymbol{S}x}|g(x)-g(x_0)|\boldsymbol{s}\,\mathrm{d}x \\
&\quad + \int_{x=0}^{\infty} \boldsymbol{k}(x_0) \int_{u=0}^{\Delta-x_0-\varepsilon} e^{\boldsymbol{S}u}\boldsymbol{s}\frac{\boldsymbol{\alpha}e^{\boldsymbol{S}u}}{\boldsymbol{\alpha}e^{\boldsymbol{S}u}\boldsymbol{e}}\mathrm{d}ue^{\boldsymbol{S}x}|g(x)-g(x_0)|\boldsymbol{s}\,\mathrm{d}x \\
&\quad + \int_{x=0}^{\infty} \boldsymbol{k}(x_0) \int_{u=\Delta-x_0+\varepsilon}^{\Delta-\varepsilon} e^{\boldsymbol{S}u}\boldsymbol{s}\frac{\boldsymbol{\alpha}e^{\boldsymbol{S}u}}{\boldsymbol{\alpha}e^{\boldsymbol{S}u}\boldsymbol{e}}\mathrm{d}ue^{\boldsymbol{S}x}|g(x)-g(x_0)|\boldsymbol{s}\,\mathrm{d}x.
\end{aligned} \tag{C.50}$$

Since g is bounded, then the last two terms in (C.50) are

$$2G\left(\int_{x=0}^{\infty} \boldsymbol{k}(x_0) \int_{u=0}^{\Delta-x_0-\varepsilon} e^{\boldsymbol{S}u}\boldsymbol{s}\frac{\boldsymbol{\alpha}e^{\boldsymbol{S}u}}{\boldsymbol{\alpha}e^{\boldsymbol{S}u}\boldsymbol{e}}\mathrm{d}ue^{\boldsymbol{S}x}\boldsymbol{s}\,\mathrm{d}x\right.$$

$$
\begin{aligned}
&\quad + \int_{x=0}^{\infty} \boldsymbol{k}(x_0) \int_{u=\Delta-x_0+\varepsilon}^{\Delta-\varepsilon} e^{\boldsymbol{S}u}\boldsymbol{s}\frac{\boldsymbol{\alpha}e^{\boldsymbol{S}u}}{\boldsymbol{\alpha}e^{\boldsymbol{S}u}\boldsymbol{e}}\mathrm{d}u e^{\boldsymbol{S}x}\boldsymbol{s}\,\mathrm{d}x\Bigg) \\
&= 2G\left(\boldsymbol{k}(x_0)\int_{u=0}^{\Delta-x_0-\varepsilon} e^{\boldsymbol{S}u}\boldsymbol{s}\frac{\boldsymbol{\alpha}e^{\boldsymbol{S}u}}{\boldsymbol{\alpha}e^{\boldsymbol{S}u}\boldsymbol{e}}\boldsymbol{e}\,\mathrm{d}u + \boldsymbol{k}(x_0)\int_{u=\Delta-x_0+\varepsilon}^{\Delta-\varepsilon} e^{\boldsymbol{S}u}\boldsymbol{s}\frac{\boldsymbol{\alpha}e^{\boldsymbol{S}u}}{\boldsymbol{\alpha}e^{\boldsymbol{S}u}\boldsymbol{e}}\boldsymbol{e}\,\mathrm{d}u\right) \\
&= 2G\frac{\mathbb{P}(Z > x_0, Z \notin (\Delta-\varepsilon, \Delta+\varepsilon))}{\mathbb{P}(Z > x_0)} \\
&\leq 2G\frac{\mathrm{Var}(Z)/\varepsilon^2}{1-\mathrm{Var}(Z)/(\Delta-x_0)^2}. \qquad \text{(C.51)}
\end{aligned}
$$

Exchanging the order of integration for the first term in (C.50) (justified by the Fubini-Tonelli Theorem)

$$
\int_{u=\Delta-x_0-\varepsilon}^{u=\Delta-x_0+\varepsilon} \boldsymbol{k}(x_0)e^{\boldsymbol{S}u}\boldsymbol{s}\int_{x=0}^{\infty}\frac{\boldsymbol{\alpha}e^{\boldsymbol{S}u}}{\boldsymbol{\alpha}e^{\boldsymbol{S}u}\boldsymbol{e}}e^{\boldsymbol{S}x}|g(x)-g(x_0)|\boldsymbol{s}\,\mathrm{d}x\,\mathrm{d}u, \qquad \text{(C.52)}
$$

from which we see that we can apply Corollary 4.7 with $v = 0$ to the integral over x, implying that (C.52) is less than or equal to

$$
\int_{u=\Delta-x_0-\varepsilon}^{u=\Delta-x_0+\varepsilon} \boldsymbol{k}(x_0)e^{\boldsymbol{S}u}\boldsymbol{s}\left(|g(\Delta-u)-g(x_0)| + r_3(u)\right)\,\mathrm{d}u. \qquad \text{(C.53)}
$$

Noting that $\sup|r_3(u)| \leq |r_2|$ for $u \leq \Delta - \varepsilon$, and since g is Lipschitz, then (C.53) is less than or equal to

$$
\int_{u=\Delta-x_0-\varepsilon}^{u=\Delta-x_0+\varepsilon} \boldsymbol{k}(x_0)e^{\boldsymbol{S}u}\boldsymbol{s}\left(L\varepsilon + |r_2|\right)\,\mathrm{d}u \leq L\varepsilon + |r_2|. \qquad \text{(C.54)}
$$

Putting all the bounds together proves the result. □

Lastly, the geometric domination results in Lemma 4.12 follow by the same arguments as in the proof of Lemma 4.12, except with the initial vector $\boldsymbol{a}_{\ell_0,i}(x_0)$ replaced by $\boldsymbol{a}_{\ell_0,i}(x_0)\boldsymbol{D}$. Similarly, an anologue of the domination condition required in the proof of Lemma 4.15 can be established by the same arguments except with the initial vector $\boldsymbol{a}_{\ell_0,i}(x_0)$ replaced by $\boldsymbol{a}_{\ell_0,i}(x_0)\boldsymbol{D}$.

Appendix D

Kronecker properties

Here we detail some properties of Kronecker sums, products, and exponential (see (Bladt & Nielsen 2017), Appendix A.4).

Let

$$\boldsymbol{A} = \begin{bmatrix} a_{11} & \dots & a_{1m} \\ \dots & & \dots \\ a_{n1} & \dots & a_{nm} \end{bmatrix} \qquad \boldsymbol{B} = \begin{bmatrix} b_{11} & \dots & b_{1m'} \\ \dots & & \dots \\ b_{n'1} & \dots & b_{n'm'} \end{bmatrix}$$

be matrices with dimensions $n \times m$ and $n' \times m'$, respectively. The operator $\otimes$ is the Kronecker product of two matrices;

$$\boldsymbol{A} \otimes \boldsymbol{B} = \begin{bmatrix} a_{11}\boldsymbol{B} & \dots & a_{1m}\boldsymbol{B} \\ \dots & & \dots \\ a_{n1}\boldsymbol{B} & \dots & a_{nm}\boldsymbol{B} \end{bmatrix},$$

which is an $nn' \times mm'$ matrix.

Let $\boldsymbol{C}, \boldsymbol{D}$ be matrices with dimensions $m \times k$ and $m' \times k'$. A property of the Kronecker Product is

$$(\boldsymbol{A} \otimes \boldsymbol{B})(\boldsymbol{C} \otimes \boldsymbol{D}) = \boldsymbol{AC} \otimes \boldsymbol{BD}. \qquad \text{(Mixed Product Rule)}$$

Proof. The proof follows from

$$\begin{bmatrix} a_{i1}\boldsymbol{B} & a_{i2}\boldsymbol{B} & \dots & a_{in}\boldsymbol{B} \end{bmatrix} \begin{bmatrix} c_{1j}\boldsymbol{D} \\ c_{2j} \\ \vdots \\ c_{nj}\boldsymbol{D} \end{bmatrix} = \left(\sum_{\ell} a_{i\ell} c_{\ell j} \right) \boldsymbol{BD}$$
$$= (\boldsymbol{AC})_{ij}\, \boldsymbol{BD}.$$

□

If $\boldsymbol{A}$ and $\boldsymbol{B}$ are invertible matrices, then

$$(\boldsymbol{A} \otimes \boldsymbol{B})^{-1} = \boldsymbol{A}^{-1} \otimes \boldsymbol{B}^{-1}. \tag{D.1}$$

Let $\boldsymbol{A}$ and $\boldsymbol{B}$ be $n \times n$ and $m \times m$ matrices, respectively. The Kronecker sum of $\boldsymbol{A}$ and $\boldsymbol{B}$ is denoted by $\oplus$ and defined as

$$\boldsymbol{A} \oplus \boldsymbol{B} := \boldsymbol{A} \otimes \boldsymbol{I}_m + \boldsymbol{I}_n \otimes \boldsymbol{B}.$$

The exponential of a square matrix $\boldsymbol{B}$ is

$$e^{\boldsymbol{B}} := \sum_{n=0}^{\infty} \frac{1}{n!} \boldsymbol{B}^n.$$

A property of the Kronecker sum is

$$e^{\boldsymbol{A} \oplus \boldsymbol{B}} = e^{\boldsymbol{A}} \otimes e^{\boldsymbol{B}}. \tag{D.2}$$

Proof. First, the matrices $\boldsymbol{A} \otimes \boldsymbol{I}_m$ and $\boldsymbol{I}_n \otimes \boldsymbol{B}$ commute; from the mixed product rule their product is $\boldsymbol{A} \otimes \boldsymbol{B}$. Hence

$$e^{\boldsymbol{A} \oplus \boldsymbol{B}} = e^{\boldsymbol{A} \otimes \boldsymbol{I}_m} e^{\boldsymbol{I}_n \otimes \boldsymbol{B}}.$$

We now show that $e^{\boldsymbol{A} \otimes \boldsymbol{I}_m} = e^{\boldsymbol{A}} \otimes \boldsymbol{I}_m$ and $e^{\boldsymbol{I}_n \otimes \boldsymbol{B}} = \boldsymbol{I}_n \otimes e^{\boldsymbol{B}}$. The latter follows from the fact that $\boldsymbol{I}_n \otimes \boldsymbol{B}$ is a block diagonal matrix with blocks $\boldsymbol{B}$, hence its exponential is also block diagonal with blocks equal to the exponential of $\boldsymbol{B}$. The former follows from

$$\begin{aligned} e^{\boldsymbol{A} \otimes \boldsymbol{I}_m} &= \sum_{n=0}^{\infty} \frac{1}{n!} (\boldsymbol{A} \otimes \boldsymbol{I}_m)^n \\ &= \sum_{n=0}^{\infty} \frac{1}{n!} (\boldsymbol{A}^n \otimes \boldsymbol{I}_m) \\ &= \left(\sum_{n=0}^{\infty} \frac{1}{n!} \boldsymbol{A} \otimes \boldsymbol{I}_m \right) \\ &= e^{\boldsymbol{A}} \otimes \boldsymbol{I}_m. \end{aligned} \tag{D.3}$$

Therefore

$$e^{\boldsymbol{A} \oplus \boldsymbol{B}} = \left(e^{\boldsymbol{A}} \otimes \boldsymbol{I}_m \right) \left(\boldsymbol{I}_n \otimes e^{\boldsymbol{B}} \right),$$

and the result follows by the mixed product rule. □

Lemma D.1. *Let $\boldsymbol{T}$ and $\boldsymbol{C}$ be $n \times n$, square matrices with $\boldsymbol{C}$ diagonal and invertible; let $\boldsymbol{S}$ be a $p \times p$ matrix. Further, suppose $[\boldsymbol{T} \otimes \boldsymbol{I} + \boldsymbol{C} \otimes \boldsymbol{S} - \lambda \boldsymbol{I}]$ is invertible for $\lambda > 0$. Then*

$$\int_{t=0}^{\infty} e^{-\lambda t} e^{(\boldsymbol{T} \otimes \boldsymbol{I} + \boldsymbol{C} \otimes \boldsymbol{S})t} \, \mathrm{d}t = \int_{x=0}^{\infty} e^{\boldsymbol{C}^{-1}(\boldsymbol{T} - \lambda \boldsymbol{I})x} \otimes e^{\boldsymbol{S}x} \, \mathrm{d}x \, (\boldsymbol{C} \otimes \boldsymbol{I})^{-1}. \tag{D.4}$$

Proof. Computing the integral on the left-hand side and then factorising the result and using the Mixed Product Rule multiple times gives

$$\begin{aligned}\int_{t=0}^{\infty} e^{-\lambda t} e^{(\boldsymbol{T}\otimes\boldsymbol{I}+\boldsymbol{C}\otimes\boldsymbol{S})t}\,\mathrm{d}t &= -\left[\boldsymbol{T}\otimes\boldsymbol{I}+\boldsymbol{C}\otimes\boldsymbol{S}-\lambda\boldsymbol{I}\right]^{-1}\\ &= -\left[\boldsymbol{T}\otimes\boldsymbol{I}+(\boldsymbol{C}\otimes\boldsymbol{I})(\boldsymbol{I}\otimes\boldsymbol{S})-\lambda\boldsymbol{I}\right]^{-1}\\ &= -\left[(\boldsymbol{C}\otimes\boldsymbol{I})\left((\boldsymbol{C}\otimes\boldsymbol{I})^{-1}(\boldsymbol{T}\otimes\boldsymbol{I})+\boldsymbol{I}\otimes\boldsymbol{S}-(\boldsymbol{C}\otimes\boldsymbol{I})^{-1}\lambda\boldsymbol{I}\right)\right]^{-1}.\end{aligned} \tag{D.5}$$

By Equation (D.1) and since $\boldsymbol{C}$ is invertible, (D.5) is equal to

$$-\left[(\boldsymbol{C}\otimes\boldsymbol{I})\left(\left(\boldsymbol{C}^{-1}\otimes\boldsymbol{I}\right)(\boldsymbol{T}\otimes\boldsymbol{I})+\boldsymbol{I}\otimes\boldsymbol{S}-\left(\boldsymbol{C}^{-1}\otimes\boldsymbol{I}\right)\lambda\boldsymbol{I}\right)\right]^{-1}. \tag{D.6}$$

Using the Mixed Product Rule and algebraic manipulation, (D.6) is equal to

$$\begin{aligned}&-\left[(\boldsymbol{C}\otimes\boldsymbol{I})\left(\left(\boldsymbol{C}^{-1}\boldsymbol{T}\right)\otimes\boldsymbol{I}+\boldsymbol{I}\otimes\boldsymbol{S}-\left(\boldsymbol{C}^{-1}\lambda\boldsymbol{I}\right)\otimes\boldsymbol{I}\right)\right]^{-1}\\ &=-\left[(\boldsymbol{C}\otimes\boldsymbol{I})\left(\left(\boldsymbol{C}^{-1}(\boldsymbol{T}-\lambda\boldsymbol{I})\right)\otimes\boldsymbol{I}+\boldsymbol{I}\otimes\boldsymbol{S}\right)\right]^{-1}\\ &=-\left[\left(\boldsymbol{C}^{-1}(\boldsymbol{T}-\lambda\boldsymbol{I})\right)\otimes\boldsymbol{I}+\boldsymbol{I}\otimes\boldsymbol{S}\right]^{-1}(\boldsymbol{C}\otimes\boldsymbol{I})^{-1}\\ &=-\left[\left(\boldsymbol{C}^{-1}(\boldsymbol{T}-\lambda\boldsymbol{I})\right)\oplus\boldsymbol{S}\right]^{-1}(\boldsymbol{C}\otimes\boldsymbol{I})^{-1},\end{aligned} \tag{D.7}$$

by definition of the Kronecker sum.

Now, for an invertible matrix $\boldsymbol{A}$ we can write $-\boldsymbol{A}^{-1}=\int_{x=0}^{\infty} e^{\boldsymbol{A}x}\,\mathrm{d}x$. Therefore (D.7) is

$$-\left[\left(\boldsymbol{C}^{-1}(\boldsymbol{T}-\lambda\boldsymbol{I})\right)\oplus\boldsymbol{S}\right]^{-1}(\boldsymbol{C}\otimes\boldsymbol{I})^{-1}=\int_{x=0}^{\infty} e^{\left(\boldsymbol{C}^{-1}(\boldsymbol{T}-\lambda\boldsymbol{I})x\right)\oplus\boldsymbol{S}x}\,\mathrm{d}x\,(\boldsymbol{C}\otimes\boldsymbol{I})^{-1}.$$

Using the rule in Equation (D.2) gives

$$\int_{x=0}^{\infty} e^{\left(\boldsymbol{C}^{-1}(\boldsymbol{T}-\lambda\boldsymbol{I})\right)x}\otimes e^{\boldsymbol{S}x}\,\mathrm{d}x\,(\boldsymbol{C}\otimes\boldsymbol{I})^{-1},$$

which is the result. □

Lemma D.2 (Latouche & Nguyen (2015))**.** *Let $\boldsymbol{B}$ be the block-partitioned matrix*

$$\boldsymbol{B}=\begin{bmatrix}\boldsymbol{B}_{11} & \boldsymbol{B}_{12}\\ \boldsymbol{B}_{21} & \boldsymbol{B}_{22}\end{bmatrix}$$

where $\boldsymbol{B}_{11}$ and $\boldsymbol{B}_{22}$ are matrices of order m_1 and m_2, respectively. Denote by $\boldsymbol{H}_{11}(t)$ the top-left quadrant of order m_1 of $e^{\boldsymbol{B}t}$:

$$\boldsymbol{H}_{11}(t)=\begin{bmatrix}\boldsymbol{I}_{m_1\times m_1} & \boldsymbol{0}\end{bmatrix}e^{\boldsymbol{B}t}\begin{bmatrix}\boldsymbol{I}_{m_1\times m_1}\\ \boldsymbol{0}\end{bmatrix}.$$

The matrix $\boldsymbol{H}_{11}(t)$ *is the solution of*

$$\boldsymbol{H}_{11}(t) = e^{\boldsymbol{B}_{11}t} + \int_{v=0}^{t}\int_{u=v}^{t} e^{\boldsymbol{B}_{11}(t-u)}\boldsymbol{B}_{12}e^{\boldsymbol{B}_{22}(u-v)}\boldsymbol{B}_{21}\boldsymbol{H}_{11}(v)\,\mathrm{d}u\,\mathrm{d}v. \tag{D.8}$$

Proof. See Latouche & Nguyen (2015). □

Let $\boldsymbol{H}_{12}(t)$ be the top-right quadrant of $e^{\boldsymbol{B}t}$ of size $m_1 \times m_2$, i.e.

$$\boldsymbol{H}_{12}(t) = \begin{bmatrix}\boldsymbol{I}_{m_1\times m_1} & \boldsymbol{0}\end{bmatrix} e^{\boldsymbol{B}t}\begin{bmatrix}\boldsymbol{0}\\ \boldsymbol{I}_{m_2\times m_2}\end{bmatrix}. \tag{D.9}$$

Denote by $\widehat{\boldsymbol{H}}_{11}(\lambda) := \int_{t=0}^{\infty} e^{-\lambda t}\boldsymbol{H}_{11}(t)\,\mathrm{d}t$ and by $\widehat{\boldsymbol{H}}_{12}(\lambda) := \int_{t=0}^{\infty} e^{-\lambda t}\boldsymbol{H}_{12}(t)\,\mathrm{d}t$, the Laplace transforms of $\boldsymbol{H}_{11}(t)$ and $\boldsymbol{H}_{12}(t)$, respectively. Using Lemma D.2 we can show the following result.

Lemma D.3.

$$\widehat{\boldsymbol{H}}_{11}(\lambda) = \int_{x=0}^{\infty} e^{\left(\boldsymbol{B}_{11}-\lambda\boldsymbol{I}_{m_1\times m_1}+\boldsymbol{B}_{12}(\lambda\boldsymbol{I}_{m_2\times m_2}-\boldsymbol{B}_{22})^{-1}\boldsymbol{B}_{21}\right)x}\,\mathrm{d}x, \tag{D.10}$$

$$\widehat{\boldsymbol{H}}_{12}(\lambda) = \int_{x=0}^{\infty} e^{\left(\boldsymbol{B}_{11}-\lambda\boldsymbol{I}_{m_1\times m_1}+\boldsymbol{B}_{12}(\lambda\boldsymbol{I}_{m_2\times m_2}-\boldsymbol{B}_{22})^{-1}\boldsymbol{B}_{21}\right)x}\boldsymbol{B}_{12}(\lambda\boldsymbol{I}_{m_2\times m_2}-\boldsymbol{B}_{22})^{-1}\,\mathrm{d}x. \tag{D.11}$$

Proof. First we show the result for $\widehat{\boldsymbol{H}}_{11}(\lambda)$. Taking the Laplace transform of (D.8) shows that $\widehat{\boldsymbol{H}}_{11}(\lambda)$ is equal to

$$\begin{aligned}&\int_{t=0}^{\infty}\int_{v=0}^{t}\int_{u=v}^{t} e^{-\lambda(t-u)}e^{\boldsymbol{B}_{11}(t-u)}\boldsymbol{B}_{12}e^{-\lambda(u-v)}e^{\boldsymbol{B}_{22}(u-v)}\boldsymbol{B}_{21}e^{-\lambda v}\boldsymbol{H}_{11}(v)\,\mathrm{d}u\,\mathrm{d}v\\ &\qquad + (\lambda\boldsymbol{I}_{m_1\times m_1}-\boldsymbol{B}_{11})^{-1}\\ &= (\lambda\boldsymbol{I}_{m_1\times m_1}-\boldsymbol{B}_{11})^{-1} + (\lambda\boldsymbol{I}_{m_1\times m_1}-\boldsymbol{B}_{11})^{-1}\boldsymbol{B}_{12}(\lambda\boldsymbol{I}_{m_2\times m_2}-\boldsymbol{B}_{22})^{-1}\boldsymbol{B}_{21}\widehat{\boldsymbol{H}}_{11}(\lambda),\end{aligned} \tag{D.12}$$

by the convolution theorem for Laplace transforms. This implies

$$\begin{aligned}&\left[\boldsymbol{I}_{m_1\times m_1} - (\lambda\boldsymbol{I}_{m_1\times m_1}-\boldsymbol{B}_{11})^{-1}\boldsymbol{B}_{12}(\lambda\boldsymbol{I}_{m_2\times m_2}-\boldsymbol{B}_{22})^{-1}\boldsymbol{B}_{21}\right]\widehat{\boldsymbol{H}}_{11}(\lambda)\\ &= (\lambda\boldsymbol{I}_{m_1\times m_1}-\boldsymbol{B}_{11})^{-1},\end{aligned}$$

and therefore

$$\begin{aligned}&\widehat{\boldsymbol{H}}_{11}(\lambda)\\ &= \left[\boldsymbol{I}_{m_1\times m_1} - (\lambda\boldsymbol{I}_{m_1\times m_1}-\boldsymbol{B}_{11})^{-1}\boldsymbol{B}_{12}(\lambda\boldsymbol{I}_{m_2\times m_2}-\boldsymbol{B}_{22})^{-1}\boldsymbol{B}_{21}\right]^{-1}(\lambda\boldsymbol{I}_{m_1\times m_1}-\boldsymbol{B}_{11})^{-1}\\ &= \left[(\lambda\boldsymbol{I}_{m_1\times m_1}-\boldsymbol{B}_{11})\left(\boldsymbol{I}_{m_1\times m_1} - (\lambda\boldsymbol{I}_{m_1\times m_1}-\boldsymbol{B}_{11})^{-1}\boldsymbol{B}_{12}(\lambda\boldsymbol{I}_{m_2\times m_2}-\boldsymbol{B}_{22})^{-1}\boldsymbol{B}_{21}\right)\right]^{-1}\end{aligned}$$

$$= \left[\lambda \boldsymbol{I}_{m_1\times m_1} - \boldsymbol{B}_{11} - \boldsymbol{B}_{12}(\lambda \boldsymbol{I}_{m_2\times m_2} - \boldsymbol{B}_{22})^{-1}\boldsymbol{B}_{21}\right]^{-1}$$
$$= \int_{t=0}^{\infty} e^{\left(\boldsymbol{B}_{11}-\lambda \boldsymbol{I}_{m_1\times m_1}+\boldsymbol{B}_{12}(\lambda \boldsymbol{I}_{m_2\times m_2}-\boldsymbol{B}_{22})^{-1}\boldsymbol{B}_{21}\right)t}\,\mathrm{d}t,$$

which is (D.10).

Now, to show (D.11), differentiate (D.9)

$$\begin{aligned}\frac{\mathrm{d}}{\mathrm{d}t}\boldsymbol{H}_{12}(t) &= \begin{bmatrix}\boldsymbol{I}_{m_1\times m_1} & \boldsymbol{0}\end{bmatrix} e^{\boldsymbol{B}t}\begin{bmatrix}\boldsymbol{B}_{11} & \boldsymbol{B}_{12}\\ \boldsymbol{B}_{21} & \boldsymbol{B}_{22}\end{bmatrix}\begin{bmatrix}\boldsymbol{0}\\ \boldsymbol{I}_{m_2\times m_2}\end{bmatrix}\\ &= \begin{bmatrix}\boldsymbol{I}_{m_1\times m_1} & \boldsymbol{0}\end{bmatrix} e^{\boldsymbol{B}t}\begin{bmatrix}\boldsymbol{B}_{12}\\ \boldsymbol{B}_{22}\end{bmatrix}\\ &= \boldsymbol{H}_{11}(t)\boldsymbol{B}_{12} + \boldsymbol{H}_{12}(t)\boldsymbol{B}_{22}. \end{aligned} \tag{D.13}$$

Now take the Laplace transform

$$\lambda\widehat{\boldsymbol{H}}_{12}(\lambda) - \boldsymbol{H}_{12}(0) = \widehat{\boldsymbol{H}}_{11}(\lambda)\boldsymbol{B}_{12} + \widehat{\boldsymbol{H}}_{12}(\lambda)\boldsymbol{B}_{22}. \tag{D.14}$$

Since $\boldsymbol{H}_{12}(0) = \boldsymbol{0}$ and after rearranging we get

$$\widehat{\boldsymbol{H}}_{12}(\lambda) = \widehat{\boldsymbol{H}}_{11}(\lambda)\boldsymbol{B}_{12}(\lambda \boldsymbol{I}_{m_2\times m_2} - \boldsymbol{B}_{22})^{-1}, \tag{D.15}$$

which gives (D.11) upon substituting (D.10). □

Now, recall the matrix-functions

$$\begin{aligned}\boldsymbol{Q}_{++}(\lambda) &= \boldsymbol{C}_{+}^{-1}\left(\boldsymbol{T}_{++} - \lambda\boldsymbol{I} + \boldsymbol{T}_{+0}\left[\lambda\boldsymbol{I} - \boldsymbol{T}_{00}\right]^{-1}\boldsymbol{T}_{0+}\right),\\ \boldsymbol{Q}_{+-}(\lambda) &= \boldsymbol{C}_{+}^{-1}\left(\boldsymbol{T}_{+-} + \boldsymbol{T}_{+0}\left[\lambda\boldsymbol{I} - \boldsymbol{T}_{00}\right]^{-1}\boldsymbol{T}_{0-}\right),\\ \boldsymbol{Q}_{--}(\lambda) &= \boldsymbol{C}_{-}^{-1}\left(\boldsymbol{T}_{--} - \lambda\boldsymbol{I} + \boldsymbol{T}_{-0}\left[\lambda\boldsymbol{I} - \boldsymbol{T}_{00}\right]^{-1}\boldsymbol{T}_{0-}\right),\\ \boldsymbol{Q}_{-+}(\lambda) &= \boldsymbol{C}_{-}^{-1}\left(\boldsymbol{T}_{-+} + \boldsymbol{T}_{-0}\left[\lambda\boldsymbol{I} - \boldsymbol{T}_{00}\right]^{-1}\boldsymbol{T}_{0+}\right),\end{aligned}$$

from Chapter 4.

Corollary D.4. *For $m \in \{+,-\}$ the top-left quadrant of size $m_1\times m_1 = |\mathcal{S}_m|\cdot p \times |\mathcal{S}_m|\cdot p$ of $e^{\boldsymbol{B}_{mm}t}$,*

$$\begin{bmatrix}\boldsymbol{I} & \boldsymbol{0}\end{bmatrix}\int_{t=0}^{\infty} e^{-\lambda t}\exp\left\{\begin{bmatrix}\boldsymbol{T}_{mm}\otimes\boldsymbol{I} + \boldsymbol{C}_m\otimes\boldsymbol{S} & \boldsymbol{T}_{m0}\otimes\boldsymbol{I}\\ \boldsymbol{T}_{0m}\otimes\boldsymbol{I} & \boldsymbol{T}_{00}\otimes\boldsymbol{I}\end{bmatrix}t\right\}\mathrm{d}t\begin{bmatrix}\boldsymbol{I}\\ \boldsymbol{0}\end{bmatrix},$$

is given by

$$\int_{x=0}^{\infty} e^{\boldsymbol{Q}_{mm}(\lambda)x}\otimes e^{\boldsymbol{S}x}\,\mathrm{d}x(\boldsymbol{C}_m^{-1}\otimes\boldsymbol{I}). \tag{D.16}$$

For $m \in \{+,-\}$ the top-right quadrant of size $m_1 \times m_2 = |\mathcal{S}_m| \cdot p \times |\mathcal{S}_0| \cdot p$ of $e^{\boldsymbol{B}_{mm}t}$,

$$\begin{bmatrix} \boldsymbol{I} & \boldsymbol{0} \end{bmatrix} \int_{t=0}^{\infty} e^{-\lambda t} \exp\left\{ \begin{bmatrix} \boldsymbol{T}_{mm} \otimes \boldsymbol{I} + \boldsymbol{C}_m \otimes \boldsymbol{S} & \boldsymbol{T}_{m0} \otimes \boldsymbol{I} \\ \boldsymbol{T}_{0m} \otimes \boldsymbol{I} & \boldsymbol{T}_{00} \otimes \boldsymbol{I} \end{bmatrix} t \right\} \mathrm{d}t \begin{bmatrix} \boldsymbol{0} \\ \boldsymbol{I} \end{bmatrix},$$

is given by

$$\int_{x=0}^{\infty} e^{\boldsymbol{Q}_{mm}(\lambda)x} \otimes e^{\boldsymbol{S}x} \, \mathrm{d}x((\boldsymbol{C}_m^{-1}\boldsymbol{T}_{m0}(\lambda\boldsymbol{I} - \boldsymbol{T}_{00})^{-1}) \otimes \boldsymbol{I}). \tag{D.17}$$

Also,

$$\begin{bmatrix} \boldsymbol{I} & \boldsymbol{0} \end{bmatrix} \int_{t=0}^{\infty} e^{-\lambda t} e^{\boldsymbol{B}_{mm}t} \, \mathrm{d}t \boldsymbol{B}_{mn} = \int_{x=0}^{\infty} \boldsymbol{H}^{mn}(\lambda, x) \otimes e^{\boldsymbol{S}x} \boldsymbol{D} \, \mathrm{d}x \left(\begin{bmatrix} \boldsymbol{I}_{pn} & \boldsymbol{0}_{pn \times p|\mathcal{S}_0|} \end{bmatrix} \right), \tag{D.18}$$

for $m, n \in \{+,-\}$, $m \neq n$.

Proof. From Lemma D.2 the top-left quadrant of size $m_1 \times m_1 = |\mathcal{S}_m| \cdot p \times |\mathcal{S}_m| \cdot p$ of the integral with respect to t on the left-hand side of (D.16) is

$$\int_{t=0}^{\infty} e^{\left(\boldsymbol{T}_{mm} \otimes \boldsymbol{I} + \boldsymbol{C}_m \otimes \boldsymbol{S} - \lambda \boldsymbol{I} + (\boldsymbol{T}_{m0} \otimes \boldsymbol{I})(\lambda \boldsymbol{I} - \boldsymbol{T}_{00} \otimes \boldsymbol{I})^{-1}(\boldsymbol{T}_{0m} \otimes \boldsymbol{I})\right)t} \, \mathrm{d}t. \tag{D.19}$$

By Lemma D.1, (D.19) is equal to

$$\begin{aligned} &\int_{x=0}^{\infty} e^{\boldsymbol{C}_m^{-1}\left(\boldsymbol{T}_{mm} - \lambda \boldsymbol{I} + \boldsymbol{T}_{m0}(\lambda \boldsymbol{I} - \boldsymbol{T}_{00})^{-1}\boldsymbol{T}_{0m}\right)x} \otimes e^{\boldsymbol{S}x} \, \mathrm{d}x (\boldsymbol{C}_m \otimes \boldsymbol{I})^{-1} \\ &= \int_{x=0}^{\infty} e^{\boldsymbol{Q}_{mm}(\lambda)x} \otimes e^{\boldsymbol{S}x} \, \mathrm{d}x (\boldsymbol{C}_m \otimes \boldsymbol{I})^{-1}, \end{aligned} \tag{D.20}$$

from the definition of $\boldsymbol{Q}_{mm}(\lambda)$. This proves (D.16).

Now, from Lemma D.2 the top-right quadrant of size $m_1 \times m_2 = |\mathcal{S}_m| \cdot p \times |\mathcal{S}_0| \cdot p$ of the integral with respect to t on the left-hand side of (D.17) is

$$\begin{aligned} &\int_{t=0}^{\infty} e^{\left(\boldsymbol{T}_{mm} \otimes \boldsymbol{I} + \boldsymbol{C}_m \otimes \boldsymbol{S} - \lambda \boldsymbol{I} + (\boldsymbol{T}_{m0} \otimes \boldsymbol{I})(\lambda \boldsymbol{I} - \boldsymbol{T}_{00} \otimes \boldsymbol{I})^{-1}(\boldsymbol{T}_{0m} \otimes \boldsymbol{I})\right)t} (\boldsymbol{T}_{m0} \otimes \boldsymbol{I})(\lambda \boldsymbol{I} - \boldsymbol{T}_{00} \otimes \boldsymbol{I})^{-1} \\ &\qquad \times (\boldsymbol{T}_{0m} \otimes \boldsymbol{I}) \, \mathrm{d}t. \end{aligned} \tag{D.21}$$

By Lemma D.1, (D.21) is equal to

$$\int_{x=0}^{\infty} e^{\boldsymbol{Q}_{mm}(\lambda)x} \otimes e^{\boldsymbol{S}x} \, \mathrm{d}x (\boldsymbol{C}_m \otimes \boldsymbol{I})^{-1} (\boldsymbol{T}_{m0} \otimes \boldsymbol{I})(\lambda \boldsymbol{I} - \boldsymbol{T}_{00} \otimes \boldsymbol{I})^{-1} (\boldsymbol{T}_{0m} \otimes \boldsymbol{I}). \tag{D.22}$$

Now,

$$(\lambda \boldsymbol{I} - \boldsymbol{T}_{00} \otimes \boldsymbol{I})^{-1} = \int_{u=0}^{\infty} e^{-(\lambda \boldsymbol{I} - \boldsymbol{T}_{00} \otimes \boldsymbol{I})u} \, \mathrm{d}u$$

$$
\begin{aligned}
&= \int_{u=0}^{\infty} e^{-\lambda u} e^{(\boldsymbol{T}_{00}\otimes\boldsymbol{I})u}\,\mathrm{d}u \\
&= \int_{u=0}^{\infty} e^{-\lambda u} e^{\boldsymbol{T}_{00}u}\otimes\boldsymbol{I}\,\mathrm{d}u,
\end{aligned}
$$

by (D.3). Using this and the Mixed Product Rule we can write

$$
\begin{aligned}
&(\boldsymbol{C}_m\otimes\boldsymbol{I})^{-1}(\boldsymbol{T}_{m0}\otimes\boldsymbol{I})(\lambda\boldsymbol{I}-\boldsymbol{T}_{00}\otimes\boldsymbol{I})^{-1}(\boldsymbol{T}_{0m}\otimes\boldsymbol{I}) \\
&= (\boldsymbol{C}_m^{-1}\otimes\boldsymbol{I})(\boldsymbol{T}_{m0}\otimes\boldsymbol{I})\int_{u=0}^{\infty} e^{-\lambda u}e^{\boldsymbol{T}_{00}u}\otimes\boldsymbol{I}\,\mathrm{d}u(\boldsymbol{T}_{0m}\otimes\boldsymbol{I}) \\
&= \left(\boldsymbol{C}_m^{-1}\boldsymbol{T}_{m0}(\lambda\boldsymbol{I}-\boldsymbol{T}_{00}u)^{-1}\boldsymbol{T}_{0m}\right)\otimes\boldsymbol{I}). \qquad \text{(D.23)}
\end{aligned}
$$

Substituting (D.23) into (D.22) completes the proof of (D.17).

Now, using (D.16) and (D.17) we can write

$$
\begin{aligned}
&\begin{bmatrix}\boldsymbol{I} & \boldsymbol{0}\end{bmatrix}\int_{t=0}^{\infty} e^{-\lambda t}e^{\boldsymbol{B}_{mm}t}\,\mathrm{d}t\boldsymbol{B}_{mn} = \begin{bmatrix}\boldsymbol{I} & \boldsymbol{0}\end{bmatrix}\int_{t=0}^{\infty} e^{-\lambda t}e^{\boldsymbol{B}_{mm}t}\,\mathrm{d}t\begin{bmatrix}\boldsymbol{T}_{mn}\otimes\boldsymbol{D} & \boldsymbol{0}\\ \boldsymbol{T}_{0n}\otimes\boldsymbol{D} & \boldsymbol{0}\end{bmatrix} \\
&= \int_{x=0}^{\infty} e^{\boldsymbol{Q}_{mm}(\lambda)x}\otimes e^{\boldsymbol{S}x}\,\mathrm{d}x(\boldsymbol{C}_m^{-1}(\boldsymbol{T}_{mn}+\boldsymbol{T}_{m0}(\lambda\boldsymbol{I}-\boldsymbol{T}_{00})^{-1}\boldsymbol{T}_{0n})\begin{bmatrix}\boldsymbol{I}_n & \boldsymbol{0}_{n\times|\mathcal{S}_0|}\end{bmatrix}\otimes\boldsymbol{D}) \\
&= \int_{x=0}^{\infty} e^{\boldsymbol{Q}_{mm}(\lambda)x}\otimes e^{\boldsymbol{S}x}\,\mathrm{d}x\left(\left(\boldsymbol{Q}_{mn}(\lambda)\begin{bmatrix}\boldsymbol{I}_n & \boldsymbol{0}_{n\times|\mathcal{S}_0|}\end{bmatrix}\right)\otimes\boldsymbol{D}\right) \\
&= \int_{x=0}^{\infty} \left(\boldsymbol{H}^{mn}(\lambda,x)\begin{bmatrix}\boldsymbol{I}_n & \boldsymbol{0}_{n\times|\mathcal{S}_0|}\end{bmatrix}\right)\otimes e^{\boldsymbol{S}x}\boldsymbol{D}\,\mathrm{d}x, \\
&= \int_{x=0}^{\infty} \boldsymbol{H}^{mn}(\lambda,x)\otimes e^{\boldsymbol{S}x}\boldsymbol{D}\,\mathrm{d}x,\begin{bmatrix}\boldsymbol{I}_{pn} & \boldsymbol{0}_{pn\times p|\mathcal{S}_0|}\end{bmatrix}, \qquad \text{(D.24)}
\end{aligned}
$$

for $m,n\in\{+,-\}$, $m\neq n$ which is (D.18), where the last line holds from the Mixed Product Rule. □

Bibliography

Ahn, S., Jeon, J. & Ramaswami, V. (20035), 'Steady state analysis of finite fluid flow models using finite QBDs', *Queueing Syst.* **49**, 223–259.

Ahn, S. & Ramaswami, V. (2003), 'Fluid flow models and queues—a connection by stochastic coupling', *Stochastic Models* **19**(3), 325–348.
URL: *https://doi.org/10.1081/STM-120023564*

Ahn, S. & Ramaswami, V. (2004), 'Transient analysis of fluid flow models via stochastic coupling to a queue', *Stochastic Models* **20**(1), 71–101.
URL: *https://doi.org/10.1081/STM-120028392*

Aldous, D. & Shepp, L. (1987), 'The least variable phase type distribution is Erlang', *Stochastic Models* **3**(3), 467–473.
URL: *https://doi.org/10.1080/15326348708807067*

Anick, D., Mitra, D. & Sondhi, M. (1982), 'Stochastic theory of a data-handling system with multiple sources', *The Bell System Technical Journal* **61**(8), 1871–1894.

Asmussen, S. (2008), *Applied probability and queues*, Vol. 51, Springer Science & Business Media.

Badescu, A., Breuer, L., Soares, A. D. S., Latouche, G., Remiche, M.-A. & Stanford, D. (2005), 'Risk processes analyzed as fluid queues', *Scandinavian Actuarial Journal* **2005**(2), 127–141.

Bean, N. G., Lewis, A., Nguyen, G., O'Reilly, M. M. & Sunkara, V. (2022), 'A discontinuous Galerkin method for approximating the stationary distribution of stochastic fluid-fluid processes', *arXiv preprint ARXIV TICKER* .

Bean, N. G., Nguyen, G. T., Nielsen, B. F. & Peralta, O. (2021), 'Rap-modulated fluid processes: First passages and the stationary distribution', *arXiv preprint arXiv:2101.03242* .

Bean, N. G. & Nielsen, B. F. (2010), 'Quasi-birth-and-death processes with rational arrival process components', *Stochastic Models* **26**(3), 309–334.

Bean, N. G. & O'Reilly, M. M. (2013), 'Spatially-coherent uniformization of a stochastic fluid model to a quasi-birth-and-death process', *Performance Evaluation* **70**(9), 578 – 592.

Bean, N. G. & O'Reilly, M. M. (2014), 'The stochastic fluid-fluid model: A stochastic fluid model driven by an uncountable-state process, which is a stochastic fluid itself', *Stochastic Processes and their Applications* **124**, 1741–1772.

Bean, N. G., O'Reilly, M. M. & Palmowski, Z. (2020), 'Matrix-analytic methods for the analysis of stochastic fluid-fluid models'.

Bean, N. G., O'Reilly, M. M. & Sargison, J. (2010), 'A stochastic fluid flow model of the operation and maintenance of power generation systems', *IEEE Transactions on Power Systems* **25**(3), 1361–1374.

Bean, N. G., O'Reilly, M. M. & Taylor, P. G. (2005*a*), 'Algorithms for return probabilities for stochastic fluid flows', *Stochastic Models* **21**(1), 149–184.
URL: *https://doi.org/10.1081/STM-200046511*

Bean, N. G., O'Reilly, M. M. & Taylor, P. G. (2005*b*), 'Hitting probabilities and hitting times for stochastic fluid flows', *Stochastic Processes and their Applications* **115**(9), 1530–1556.

Bean, N. G., O'Reilly, M. M. & Taylor, P. G. (2009*a*), 'Algorithms for the Laplace-Stieltjes transforms of first return times for stochastic fluid flows', *Methodology and Computing in Applied Probability* **10**, 381–408.

Bean, N. G., O'Reilly, M. M. & Taylor, P. G. (2009*b*), 'Hitting probabilities and hitting times for stochastic fluid flows: the bounded model', *Probability in the Engineering and Informational Sciences* **23**(1), 121–147.

Bean, N. G. & O'Reilly, M. M. (2008), 'Performance measures of a multi-layer Markovian fluid model', *Annals of Operations Research* **160**(1), 99–120.

Bean, N., Lewis, A., Nguyen, G. T., O'Reilly, M. M. & Sunkara, V. (2021), 'A discontinuous Galerkin method for approximating the stationary distribution of stochastic fluid-fluid processes', *arXiv preprint arXiv:1901.10635* .

Billingsley, P. (1999), *Convergence of probability measures*, Wiley series in probability and statistics. Probability and statistics section, 2nd ed. edn, Wiley, New York ;.

Bladt, M. & Nielsen, B. (2017), *Matrix-Exponential Distributions in Applied Probability*, Springer.

Cockburn, B. (1999), Discontinous Garlekin methods for convection-dominated problems, *in* T. Barth & H. Deconink, eds, 'Higher-Order Methods for Computational Physics', Vol. 9 of *Lecture Notes in Computational Science and Engineering*, Springer Verlag, Berlin, pp. 69–224.

da Silva Soares, A. (2005), Fluid queues: building upon the analogy with QBD processes, PhD thesis, Université Libre de Bruxelles.

Élteto, T., Ŕacz, S. & Telek, M. (2006), Minimal coefficient of variation of matrix exponential distributions, *in* '2nd Madrid Conference on Queueing Theory'.

Feller, W. (1957), *An introduction to probability theory and its applications*, Wiley series in probability and mathematical statistics, 2nd ed. edn, Wiley, New York.

Hautphenne, S., Massaro, M. & Taylor, P. (2017), 'How old is this bird? The age distribution under some phase sampling schemes', *Journal of Mathematical Biology* **75**(6), 1319–1347.

Hesthaven, J. S. & Warburton, T. (2007), *Nodal discontinuous Galerkin methods: algorithms, analysis, and applications*, Springer Science & Business Media.

Horváth, I., Sáfár, O., Telek, M. & Zambó, B. (2016), Concentrated matrix exponential distributions, *in* 'In proceedings of European Performance Evaluation Workshop'.

Horváth, G., Horváth, I. & Telek, M. (2020), 'High order concentrated matrix-exponential distributions', *Stochastic Models* **36**(2), 176–192.

Karandikar, R. L. & Kulkarni, V. G. (1995), 'Second-order fluid flow models: Reflected Brownian motion in a random environment', *Operations Research* **43**(1), 77–88.

Koltai, P. (2011), *Efficient approximation methods for the global long-term behavior of dynamical systems: theory, algorithms and examples*, Logos Verlag Berlin GmbH.

Latouche, G. & Nguyen, G. T. (2015), 'The morphing of fluid queues into Markov-modulated Brownian motion', *Stochastic Systems* **5**(1), 62–86.

Latouche, G. & Nguyen, G. T. (2019), 'Analysis of fluid flow models', *arXiv preprint arXiv:1901.10635* .

Latouche, G., Nguyen, G. T. & Palmowski, Z. (2013), Two-dimensional fluid queues with temporary assistance, *in* G. Latouche, V. Ramaswami, J. Sethuraman, K. Sigman, M. Squillante & D. Yao, eds, 'Matrix-Analytic Methods in Stochastic Models', Vol. 27 of *Springer Proceedings in Mathematics & Statistics*, Springer Science, New York, NY, chapter 9, pp. 187–207.

Mészáros, A. & Telek, M. (2021), 'Concentrated matrix exponential distributions with real eigenvalues', *Probability in the Engineering and Informational Sciences* p. 1–17.

Peralta Gutierrez, O. (2019), Advances of matrix–analytic methods in risk modelling, PhD thesis.

Sonenberg, N. (2017), Networks of interacting stochastic fluid models, PhD thesis.

Spiteri, R. J. & Ruuth, S. J. (2002), 'A new class of optimal high-order strong-stability-preserving time discretization methods', *SIAM Journal on Numerical Analysis* **40**(2), 469–23. Copyright - Copyright] © 2002 Society for Industrial and Applied Mathematics; Last updated - 2021-09-11.
URL: *http://proxy.library.adelaide.edu.au/login?url=https://www.proquest.com/scholarly-journals/new-class-optimal-high-order-strong-stability/docview/922330952/se-2?accountid=8203*

Wurm, M. (2020), Stochastic modelling of coral-algal symbiosis on the Great Barrier Reef, Master's thesis, The University of Adelaide.